![USGS logo]

USGS
science for a changing world

Assessment of Metallic Mineral Resources in the Humboldt River Basin, Northern Nevada

With a section on
Platinum-Group-Element (PGE) Potential of the Humboldt Mafic Complex

Bulletin 2218

Assessment of Metallic Mineral Resources in the Humboldt River Basin, Northern Nevada

By Alan R. Wallace, Steve Ludington, Mark J. Mihalasky, Stephen G. Peters, Ted G. Theodore, David A. Ponce, David A. John, and Byron R. Berger

With a section on
Platinum-Group-Element (PGE) Potential of the Humboldt Mafic Complex

By Michael L. Zientek, Gary B. Sidder, and Robert A. Zierenberg

Bulletin 2218

U.S. Department of the Interior
U.S. Geological Survey

U.S. Department of the Interior
Gale A. Norton, Secretary

U.S. Geological Survey
Charles G. Groat, Director

Any use of trade, product, or firm names in this publication is for descriptive purposes only and does not imply endorsement of the U.S. Government.

Contents

Tables

Figures

Executive Summary

By Alan R. Wallace, Steve Ludington, Mark J. Mihalasky, Stephen G. Peters, Ted G. Theodore,
David A. Ponce, David A. John, Byron R. Berger, with contributions from Michael L. Zientek,
Gary B. Sidder, and Robert A. Zierenberg

Introduction

The Humboldt River Basin is an arid to semiarid, internally drained basin that covers approximately 43,000 km^2 in northern Nevada (fig. E-1). The basin contains a wide variety of metallic and nonmetallic mineral deposits and occurrences, and, at various times, the area has been one of the Nation's leading or important producers of gold, silver, copper, mercury, and tungsten. Nevada currently (2003) is the third largest producer of gold in the world and the largest producer of silver in the United States. Current exploration for additional mineral deposits focuses on many areas in northern Nevada, including the Humboldt River Basin.

Much of the land in the Humboldt River Basin is publicly owned and administered by the U.S. Bureau of Land Management (BLM). Minerals-related activities, including exploration and mining, are among the multiple uses of these lands. Most metallic minerals are produced from open-pit mines of various sizes, although production from underground mining has increased in the last few years. The dimensions of some of the open-pit mines are on the order of kilometers, and mining-related heap-leach and waste-rock piles, mills, and roads can cover large areas near the mines. Dewatering of large open-pit and deep underground gold-silver mines has modified water tables near those mines, and the water is diverted to agriculture uses, recharged into the aquifers, or discharged directly into the Humboldt River and its tributaries. Exploration for new metallic mineral deposits takes place throughout the Humboldt River Basin, in part near known mineral deposits and in part in other areas that industry, for various geological, geochemical and geophysical reasons, deems worthy of more detailed investigations.

In 1996, the Nevada State Office of BLM requested a mineral resource assessment of the Humboldt River Basin to aid their land-use planning, including the future possible locations of mine dewatering. A U.S. Geological Survey (USGS) mineral-resource assessment of the BLM Winnemucca District in northwestern Nevada and the Surprise Resource area in northeastern California, published in 1996, included the western third of the Humboldt River Basin. In its 1996 request, BLM asked that the USGS expand its assessment to include the entire Humboldt River Basin, which extends east into north-central and northeastern Nevada (fig. E-1). To that end,

the USGS evaluated the mineral resource potential of much of northern Nevada, including the Humboldt River Basin, to (1) provide continuity with the Winnemucca-Surprise report, which included areas outside of the basin, and (2) place the Humboldt River Basin in a geologically broader context. The focus of the assessment, however, was on the area covered by the basin.

The Humboldt River Basin mineral assessment used geological, geochemical, geophysical, and mineral-deposit data to predict where undiscovered metallic mineral resources might be present in the Humboldt River Basin. From a present and near-future economic standpoint, gold and silver are the important metal commodities in the Humboldt River Basin study area, and deposits that contain those elements are the most likely to be explored for and mined in the foreseeable future. These deposits fall into three broad categories: pluton-related polymetallic deposits, sedimentary rock-hosted gold-silver deposits, and epithermal gold-silver deposits. The assessment focused on these types of deposits, and the results are summarized here. The prices for platinum and palladium have been high in recent years, and industry may continue to explore geologic environments, including those in the Humboldt River Basin, that may contain economic concentrations of these elements. A brief description of these deposits is provided in the summary of pluton-related polymetallic deposits. Placer gold deposits are present in the Basin, but they are small relative to the sizes of the hydrothermal deposits that currently are mined in the region. A summary of known placer gold deposits was published in 1973 by the USGS, and placer gold deposits were not evaluated further in this assessment.

Northern Nevada contains deposits of many other metallic and nonmetallic elements. With the exception of barium, exploration for these types of deposits that contain little or no gold and (or) silver is unlikely in the near future, and deposits of these other elements were not considered in this assessment. Nonetheless, some of these elements are recovered as by-products during mining of gold and (or) silver deposits. Northern Nevada also contains a wide variety of industrial minerals, some of which are being mined in and near the Humboldt River Basin. However, this assessment focused on metallic mineral deposits and did not address industrial minerals.

Geologic and Mineral Deposit Setting

The geologic history of northern Nevada, including the Humboldt River Basin, spans more than 2 billion years, ranging from Precambrian rocks in the East Humboldt Range to modern alluvial deposits in valleys and along streams (fig. E-2). A regional blanket of sediments was deposited on the ocean floor during the Paleozoic Era and by streams and on the ocean floor during the Mesozoic Era. During both Paleozoic and Mesozoic times, continental-scale tectonic activity thrust the sedimentary rocks eastward, creating a complexly interleaved stratigraphic sequence. For mineral deposits, especially sedimentary rock-hosted gold-silver deposits, the middle Paleozoic Antler orogeny was the most important of these tectonic events. This orogeny took place in the late Devonian to Mississippian and produced the Roberts Mountains thrust (fig. E-2). The thrust placed fine-grained, deep-ocean sedimentary rocks over shallow-water carbonate rocks to form favorable sites for gold-silver mineralization in the Cretaceous and early Tertiary Periods.

Igneous activity produced plutons and volcanic rocks throughout much of the Humboldt River Basin. Jurassic magmatism was widespread throughout northern Nevada, but it did not produce notable concentrations of metals except near Yerington. Major plutonic activity during the Cretaceous Period, however, generated numerous multi-element mineral deposits in and around the plutons. Widespread volcanic activity at various times in the Cenozoic Era created favorable environments for the formation of shallow, epithermal deposits (fig. E-2).

Throughout the geologic history of the region, both erosion and deposition of additional sediments and volcanic units have variably destroyed or concealed mineral deposits. This is readily apparent today: erosion has stripped away parts or all of some mineral deposits in mountain ranges and deposited the eroded rocks as sediments in adjacent basins, concealing large areas of possibly mineralized rock. These processes, when combined with the complex geologic events over a period of 2 billion years, make exploration for and discovery and assessment of mineral deposits a challenging endeavor.

Assessment Concepts and Methodology

Methods of Assessment

The mineral resource assessment used a combination of expert (knowledge-based) and data-driven methods to evaluate the potential for major, undiscovered gold- and silver-bearing deposits in the Humboldt River Basin. Deposits of these precious metals form in a wide variety of mineralizing environments that are subsets of three major classes of mineral deposits: (1) multi-element deposits related to plutonic rocks, (2) gold-silver deposits in sedimentary rocks (including Carlin-type and distal-disseminated gold-silver deposits),

and (3) gold-silver deposits that formed in relatively shallow, epithermal environments. Examples of deposits in the Humboldt River Basin that fall into each class of deposit are given in table E-1.

Mineral deposits form when optimal combinations of geological processes converge in time and space to produce a deposit. Thus, a mineral assessment must consider a wide variety of geologic processes and evaluate their interactions. Using their knowledge of the geology and mineral deposits of the Humboldt River Basin, the assessment team created specific geological, geophysical, geochemical, and mineral-deposit data and converted this information into digital layers ("predictor layers"). For the assessment, the data were analyzed and modeled in a Geographic Information System (GIS) using weights-of-evidence and weighted logistic regression techniques to produce maps that show varying degrees of likelihood for the occurrence of undiscovered deposits of the class being assessed. The areas with the highest likelihood of containing undiscovered deposits were classified as "prospective," and those with the next-highest likelihood were classified as "favorable." "Permissive" areas are the broadest and most general category; all undiscovered deposits are likely to occur in these areas, although many parts of these areas may not contain mineral deposits. "Nonpermissive" areas are those outside of the permissive areas, and they represent areas in which mineral deposits are almost certain to be absent or buried beneath thick deposits of young sediments. The permissive and nonpermissive areas were delineated in a 1996 USGS mineral assessment of the State of Nevada, and those areas were incorporated into the final assessment maps for this study.

To be consistent with the earlier assessment of the Winnemucca District, this assessment was done at a regional scale to delineate broad areas in northern Nevada and the Humboldt River Basin that are likely to contain undiscovered mineral deposits. The data used for the assessment were created at a wide range of scales, and the effective scale of the assessment maps is 1:1,000,000. This regional scale should be kept in mind when using this assessment and the GIS-based mineral-resource assessment maps. The use of the maps at larger scales to examine small areas in detail, such as a specific mining district or mountain range, is inappropriate: this use diverges from the purpose of and the concepts utilized in the assessment.

Data Used in the Assessment

Using its expertise in the geology and mineral deposits of the region, the members of the assessment team evaluated geologic data from a wide variety of sources, including considerable new data collected by the assessment team. The geological, geochemical, geophysical, and mineral deposit-related data used for the assessment were chosen both for their relevancy to mineral-deposit formation and for use in a GIS system. Some information could not be converted into predictor layers, but the concepts and ideas were used qualitatively

while generating the digital layers and during the assessment process. Other data were evaluated but not used because they either were not directly relevant to the formation of mineral deposits or did not apply to the entire study area. The final data layers that were used in assessing each class of mineral deposits are described briefly below and listed in Table E-2.

Rock units and structures that are represented on geologic maps reflect some of the geologic events that formed mineral deposits. Maps showing the regional distributions of various types of rocks and structures known to host or have had an influence on mineralization were a fundamental component of this mineral assessment. Of particular importance were the distributions of volcanic and sedimentary units related to epithermal mineralization, the presence of and proximity to plutonic rocks, and the relative lithologic diversity throughout the study area. Structural data included the locations of various thrust terranes (such as that related to the Roberts Mountains thrust), proximities to the thrust faults, and northeast-striking structural zones that may have played a role in the formation of sedimentary rock-hosted mineral deposits. With the exception of the northeast-striking structural zones, most of the data for these layers were derived from the 1:500,000-scale state geologic map, with modifications by the assessment team on the basis of newly acquired data.

Some trace elements are guides to mineral deposits, and the regional distributions of some of these elements may indicate areas when mineralization took place. Geochemical data used for this assessment were derived from multi-element analyses of stream-sediment samples collected during the National Uranium Resource Evaluation (NURE) program in the 1970s. The original analyses of those samples for the NURE program were done by multiple laboratories that used different element suites, analytical methods, and detection limits. The samples were reanalyzed for this project to provide a broader, consistent suite of elements, consistent analytical methods, and lower detection limits. Although many elements were evaluated for the final assessments, arsenic, copper, lead, zinc, and the barium/sodium ratio were considered to be the most valuable at a regional scale. The data were gridded, and then, using a series of band-pass frequency filters, resolved into distinct textural components. The component used for the assessments shows anomalies related to mineralized areas.

Geophysical data provide information on geological units and structures that are not visible at the surface, including certain types of igneous rocks, the thickness of alluvial cover, and major faults. The geophysical predictor maps used for this assessment were derived from a variety of gravity and magnetic anomaly datasets. These included basement gravity terranes and lineaments and magnetic terranes. A subset of the magnetic terranes data focused on features that specifically are associated with epithermal deposits. Gravity data also indicate the depth of basement rocks beneath young sediments in Quaternary basins, as most mineral deposits that are concealed beneath a kilometer or more of sediments are considered to be unlikely exploration targets.

Any search for undiscovered mineral deposits relies on knowledge of the locations and characteristics of the deposits that occur in the area. This assessment used USGS databases that provide mineral-deposit data on the locations, types, and characteristics of known mineral deposits, occurrences, and prospects in the Humboldt River Basin and northern Nevada. These databases were updated and subsets used for the assessment. For the data-driven part of the assessment (see description above), the subsets ("training sites") include deposits that are known, on the basis of various production data and industry property evaluations, to contain significant concentrations of gold and (or) silver. The training sites for pluton-related, sedimentary rock-hosted, and epithermal deposits are shown in figure E-3.

Results of Assessment

For the reasons described above, the focus of the mineral assessment was on undiscovered pluton-related polymetallic, sedimentary rock-hosted gold-silver, and epithermal gold-silver mineral deposits in the Humboldt River Basin and surrounding areas in northern Nevada. The relationships between the training site locations and the various geological, geochemical, and geophysical data identified geologic characteristics common to the known economic and subeconomic deposits in the region. These characteristics were applied to the entire study area, and the resulting assessment maps show the locations of areas that contain features common to these mineral deposits. These areas, of course, include those that contain known deposits and mines, and exploration undoubtedly will continue in these areas. Areas that do not contain known deposits are considered to be favorable or prospective for undiscovered mineral deposits, and future mineral exploration likely will focus on these areas as well.

Pluton-related Polymetallic Deposits

Pluton-related deposits form during the intrusion of small to large bodies of magma into rocks in the upper crust. Pluton-related deposits of various types around the world contain copper, molybdenum, tungsten, tin, gold, silver, lead, zinc, iron, platinum, and palladium, as well as other elements of economic interest. In general, these types of mineralizing systems are large, and they form several kinds of mineral deposits that, singly or in aggregate, comprise some of the largest concentrations of economic minerals on the planet.

Mesozoic and Tertiary plutons are related to a large number of pluton-related deposits and occurrences in the Humboldt River Basin and surrounding areas. The metallic mineral deposit types include porphyry deposits (porphyry copper-(molybdenum), low-fluorine porphyry molybdenum, Climax-type molybdenum, porphyry copper–gold, intrusion-related gold), base- and precious-metal skarn deposits (porphyry-related copper skarns, copper skarn, zinc–lead skarn,

iron skarn, gold skarn, tungsten skarn), polymetallic vein and replacement deposits, and replacement manganese deposits. Distal-disseminated silver–gold deposits, which are discussed in the following section on sedimentary rock-hosted deposits, are products of plutonic activity but formed well away from the related plutons, generally as oxidized parts of gold-bearing pyrite haloes that surround the porphyry plutons. Porphyry deposits, skarn deposits, some polymetallic vein deposits, and distal-disseminated silver–gold deposits form a continuum, with the porphyry copper deposits typically at the core of the plutonic and mineralizing system. In addition, the magmatic processes that formed igneous rocks of the Humboldt mafic complex east of Lovelock also formed iron deposits, and parts of the complex may contain deposits of platinum and palladium. Weathering and erosion of many of the gold-bearing, pluton-related deposits in the region created placer gold deposits, which were some of earliest indications to prospectors of the presence of the larger pluton-related deposits.

In northern Nevada, the Battle Mountain Mining District contains several large pluton-related systems of different ages, including those in the Copper Canyon and Copper Basin areas, and other large systems of various types are present elsewhere in the Humboldt River Basin and surrounding regions (table E-1). None of the pluton-related deposits at Copper Canyon and Copper Basin currently are being mined, although several in the Battle Mountain, McCoy-Cove, and Ruth areas were active into the mid-to-late 1990s. Pluton-related deposits in the region have been mined by both open-pit and underground operations.

The formation of pluton-related mineral deposits involves a complex variety of factors, and the many different types of deposits produced by pluton-related mineralizing systems (see above) are a testament to that complexity. Given adequate data, some of these factors can be represented by spatial data layers, whereas other factors are not as easy to portray spatially. The assessment criteria that were used for pluton-related deposits in the Humboldt River Basin included (1) skarn proximity buffers around plutons, (2) combined regional distributions of copper, lead, and zinc from geochemical data, (3) regional arsenic concentrations from geochemical data, (4) proximity to plutons, (5) lithodiversity of the geologic map of Nevada, (6) buffers around interpreted basement gravity lineaments, (7) regional gravity terranes, (8) depth to basement, and (9) pluton-related training sites (table E-2).

As shown in figure E-4, the assessment of pluton-related deposits demonstrates that seven northeast- and northwest-trending belts are favorable to prospective for undiscovered pluton-related deposits. These belts include the Battle Mountain–Eureka, Humboldt–Toulon, Stillwater, Toiyabe, Osgood, Ruby, and Adobe–Piñon plutonic belts. All of the belts have known pluton-related deposits of various types, and many areas in these belts will continue to draw significant attention from the mining industry during the next 10 to 15 years.

Brief summaries of the plutonic and related mineral belts, which are shown in figure E-4, are given below:

- **Battle Mountain–Eureka plutonic belt.** The Battle Mountain-Eureka mineral belt is the premier locus of pluton-related deposits in the Humboldt River Basin. The belt mainly is a Late Cretaceous and Tertiary porphyry trend, and it contains the large Battle Mountain Mining District near the central part of the basin. The belt is defined by clusters of deposits in a zone extending southeast from the general area of the Battle Mountain Mining District to the general area of Eureka. Metals produced from this belt include copper, gold, silver, molybdenum, lead, and zinc. Although this belt has been recognized since the 1960s, an alignment of prospective tracts in the mountain ranges reaffirms the major importance of the Battle Mountain-Eureka mineral belt. The McCoy Mining District, due south of the Battle Mountain Mining District, might reflect a predominantly Tertiary southward protrusion of the belt.

- **Humboldt–Toulon plutonic belt.** A broad zone of generally northeast-trending areas that are prospective and favorable for pluton-related deposits define the Humboldt-Toulon belt. The belt extends northeast from the southern Trinity Range and broadens in an east-west direction near Lovelock to include the Humboldt Range and the Unionville Mining District. The belt includes numerous clusters of pluton-related mineral occurrences and deposits that have many characteristics compatible with porphyry-related copper, tungsten, and molybdenum deposits, skarns, and polymetallic veins.

- **Stillwater plutonic belt.** The Stillwater belt is defined by an almost continuous band of favorable and prospective areas for pluton-related deposits that extend from the general area of the East Range on the northeast to the Stillwater Range on the southwest. The largest known mineralized system is in the Kennedy Mining District and peripheral areas in the southern East Range, which have characteristics of a middle Tertiary porphyry copper-(molybdenum) plutonic system.

- **Osgood plutonic belt.** As defined, the Osgood belt is a relatively short, northeast-trending zone of prospective areas that coincides largely with the Osgood Mountains. Tungsten skarn deposits are present along the western and eastern contacts of northeast-trending Cretaceous plutons in the Osgood Mountains. Further, a number of fairly well explored porphyry copper and stockwork molebdenum systems are present near the broad junction of the Osgood belt with the Stillwater and Battle Mountain-Eureka belts.

- **Toiyabe plutonic belt.** The Toiyabe belt is an almost continuous zone of favorable and prospective areas that extends along the entire length of the north-north-east-trending Toiyabe Range. Plutons of various ages are present along the range, and these plutons generally are associated with polymetallic vein occurrences in

numerous mining districts, including the large Austin Mining District. In addition, the belt largely coincides with a northeast-trending zone of anomalously high arsenic contents in NURE stream-sediment samples. Several other metals common in pluton-related environments, including bismuth and tin, also appear to be concentrated preferentially along the Toiyabe belt.

- **Ruby plutonic belt.** The Ruby belt of favorable areas largely is coincident with the northeast-trending Ruby Mountains near the east edge of the Humboldt River Basin. At least two phases of mineralized skarn are present in the Ruby Mountains, and they are associated with Jurassic and Tertiary magmatic events. These skarns have produced generally small amounts of base and precious metals and tungsten.

- **Adobe–Piñon plutonic belt.** The Adobe-Piñon belt of largely favorable areas extends in a southwest direction from the Independence Mountains, through the Adobe Range, to the Piñon Range and some parts of the northern Cortez Range. The belt includes the gold-silver–producing Railroad and Cortez Mining Districts. The belt parallels a prominent northeast-trending set of linear features, and the favorable areas reflect several overlapping predictor patterns.

The localization of mineral deposits along these belts likely reflects upper crustal zones of weakness that are inferred to coincide with deep-crustal flaws and boundaries. Magmas generated deep in the crust used these crustal flaws to penetrate higher levels of the crust and form large mineralizing systems. Thus, areas away from these zones of weakness are less likely to have pluton-related mineral deposits. Areas shown in figure E-4 as being favorable or prospective outside of these belts may reflect data combinations that are not indicative of mineralization. The data-driven methodology and lithodiversity layer used for the assessment suggest that virtually all of the mountain ranges in the assessment area are favorable to prospective for pluton-related deposits, and that adjacent sediment-filled basins are much less likely to contain these deposits. This likely is not true in most cases, as the lithodiversity of bedrock units beneath the sediments, and thus perhaps the mineral resource potential, undoubtedly is much higher than shown and possibly as high as in the ranges. Only where the bedrock beneath basins is concealed by more than a kilometer of sediment can the potential for undiscovered pluton-related deposits be considered to be nonpermissive.

The Humboldt mafic igneous complex east of Lovelock bears some similarities, including size, to other mafic complexes in the world that contain platinum-group elements (PGE), such as platinum and palladium. However, a thorough assessment of the Humboldt complex is not possible at this time. Because of the variable natures and general rarity of mafic complexes, an adequate general model for mineralization in mafic complexes is not available for use in evaluating other complexes. Adding to this is the general lack of detailed knowledge about the Humboldt complex in particular, which limits comparison with better-studied complexes. Our current understanding of PGE–enriched magmatic ore deposits reasonably suggests that high-grade PGE deposits would not be expected in these rocks. However, a level of uncertainty still remains. Someone willing to accept high risk could explore for unconventional deposit types, such as hydrothermal PGE, or some new or variant styles of mineralized magmatic rocks in the Humboldt mafic complex.

Sedimentary Rock-hosted Gold-Silver Deposits

Sedimentary rock-hosted gold-silver deposits in the Humboldt River Basin contribute the vast majority of the gold mined in the region, and economically they are the most important types of gold-bearing deposits in northern Nevada and the United States. The deposits currently are being mined along five belts ("trends") of mineral deposits: Carlin, Getchell, Battle Mountain-Eureka, Independence, and Bald Mountain-Alligator (fig. E-5, table E-1). Many of the deposits are mined from deep, extremely large open pits, and recent mining activity has exploited high-grade orebodies from underground operations below and near the open-pit mines. Exploitation of these deep ores has required extensive dewatering of adjacent aquifers. The economic significance of these deposits and their accompanying potential hydrologic impact are important reasons for estimating the potential for and location of future discoveries in the Humboldt River Basin.

Sedimentary rock-hosted gold-silver deposits formed in sedimentary rocks, largely of Paleozoic age and commonly with carbonate-bearing horizons, although a variety of rock types host these deposits. The deposits fall into two categories: distal-disseminated deposits and Carlin-type deposits (fig. E-5). The distal-disseminated deposits clearly are related to igneous activity, but, as the name implies, the deposits formed in environments distant from the igneous centers. They tend to have higher silver-gold ratios than the Carlin-type deposits, and their trace-element and isotopic signatures indicate a genetic relation to igneous systems. Although distal-disseminated and pluton-related deposits are related genetically, these deposits were assessed separately from pluton-related deposits because of (1) their strict association with sedimentary rocks, and (2) some shared geologic characteristics with Carlin-type deposits.

In contrast, and despite several decades of research, the formation of the Carlin-type deposits remains controversial. Ongoing disputes include the age(s) of mineralization, the role of igneous activity, the sources of the gold and fluids, and the mechanisms that transported large volumes of gold-bearing fluids to the sites of mineralization. Recent studies show that the large majority of the Carlin-type mineralization took place in the late Eocene (roughly 43-35 million years ago). Carlin-type deposits tend to have higher gold-silver ratios than distal-disseminated deposits, have abundant arsenic and

antimony, and have few geochemical and isotopic attributes that would suggest a direct igneous association. Carlin-type deposits can be divided into north and south types (fig. E-5). North Carlin-type deposits, found in the northern part of the study area, are larger than those in the southern part, have a greater abundance of arsenic minerals, and generally, but not always, are hosted in middle Paleozoic sedimentary rocks. The south Carlin-type deposits are smaller with lesser gold grades, and they formed in both lower Paleozoic or upper Paleozoic rocks. Both north and south types share many general characteristics.

As a result of the differences within and between the two types of sedimentary rock-hosted deposits, the assessment of undiscovered deposits of both types of deposits involved a complex group of assessment criteria. As shown in table E-2, 11 evidence layers were used for the overall assessment: lithologic units, lithotectonic terranes, northeast linear features, proximity to thrusts and plutons, lithodiversity, basement gravity lineaments, arsenic and the barium/sodium ratio from geochemical data, sedimentary rock-hosted training sites, and depth to basement.

As shown in figure E-6, the assessment of the Humboldt River Basin indicates that undiscovered sedimentary rock-hosted gold-silver deposits may be present along extensions of the five known mineral trends, as well as in five broad areas in and near the western, southern, and northeastern parts of the basin. Ongoing exploration along the known mineral trends (Carlin, Getchell, Battle Mountain-Cortez/Pipeline-Eureka, Independence, and Bald Mountain-Alligator), continues to identify new orebodies, either as extensions of known deposits or as separate deposits that formed from the same or different mineralizing systems. New discoveries along these trends may be within a kilometer or two of known deposits or separated from known deposits by several to tens of kilometers. Because distal-disseminated deposits are the direct products of magmatic activity, the prospective areas in and around the Battle Mountain Mining District reflect, in part, the influence of the magmatic systems that are some distance from the site of mineralization.

In addition to the known mineral trends, five additional areas (A-E in fig. E-6) are prospective to favorable for undiscovered sedimentary rock-hosted deposits; none contain known deposits of this type. Each area has a somewhat different combination of favorable assessment criteria, but all criteria are characteristic of sedimentary rock-hosted gold-silver deposits. These areas may be candidates for future mineral exploration. Briefly, these areas include:

- **Sonoma-East and Tobin Range area (Area A).** This area lies to the southwest of the extension of the Getchell trend and includes several gold-silver±antimony occurrences in the Sonoma Range, East, and Tobin Ranges. The favorable and prospective areas are defined by geochemistry, lithologies, and proximity to plutons and structures. These characteristics are suggestive of distal-disseminated silver-gold deposits, although few occurrences are known.

- **Northumberland, north Monitor, and Toquima Range area (Area B), including the northernmost part of the Antelope Range.** The favorable and prospective areas reflect geochemistry, lithology, and proximity to major thrusts and plutons. These characteristics may be favorable for both Carlin-type deposits and for distal-disseminated Ag-Au deposits.

- **Bull Run, Copper, and Jarbidge Mountains area (Area C).** Geochemistry, lithology, structure, and proximity to plutons define the favorable and prospective domains in this area. The most likely deposit type present is distal-disseminated silver-gold deposits in favorable lithologic horizons. Proximity to the Independence Mountains mineral belt to the south may imply that Carlin-type deposits also could be present.

- **North Adobe Range (Area D).** This area contains the Coal Mine District and the Garamendi Mine and Canyon Property, and it has potential for future discoveries of polymetallic deposits, oil shale, barite, and phosphate deposits. The tracts were constructed on the basis of geochemistry, lithology, and proximity to plutons and thrusts. The lithostratigraphic terrane in the area includes the upper and lower plates of the Roberts Mountains thrust and thus has potential for Carlin-type and distal-disseminated deposits.

- **North Pequop Mountains area (Area E).** The area contains the Pequop polymetallic district. All favorable evidence layers except the northeast-striking lineaments contributed to defining the favorable and prospective tracts. This area has potential for both Carlin-type and distal-disseminated deposits.

A sixth area, in the Hot Springs Range west of the Getchell trend, has criteria favorable for Carlin-type, distal-disseminated, pluton-related, and, to a lesser degree, epithermal deposits.

Epithermal Gold-Silver Deposits

Epithermal mineral deposits form at depths generally within 1 to 2 kilometers of the Earth's surface. They commonly occur as deposits in veins, but a number of deposits formed by replacement of or dissemination of metals into permeable sedimentary and volcanic rocks. Epithermal deposits, such as those along the Comstock Lode in western Nevada, were among the first significant nonplacer mineral deposits to be mined in Nevada, and gold and silver currently are being produced from several other deposits in northern Nevada. Gold, silver, mercury, sulfur, fluorine, lithium, uranium, and manganese have been recovered from epithermal deposits in northern Nevada, although only gold and silver currently are being produced. These mineralizing systems vary in size and grade, and the deposits are mined using either open-pit or underground methods, depending on the characteristics of

the deposit being mined. Epithermal deposits in or adjacent to the Humboldt River Basin that currently or very recently have been mined include those at Midas, Mule Canyon, Florida Canyon, Rosebud, and Sleeper (table E-1).

Extensive research on epithermal deposits in northern Nevada has shown that almost all of the deposits are related to regional volcanic systems that variously were active from about 43 million years ago to the present. Volcanic rocks that formed from these systems are common throughout the western three-quarters of the Humboldt River Basin. Heat from these systems induced deep circulation of ground water, and faults and volcanic-related structures provided conduits through which the water circulated. Thus, proximity to a volcanic center is an extremely important criterion for mineralization. The epithermal deposits formed where the fluids neared the surface, commonly in volcanic rocks, but also in virtually any rock type of any age that was present at the site of mineralization.

The assessment criteria for epithermal deposits in the Humboldt River Basin included (1) the type of and proximity to volcanic and volcaniclastic rocks, (2) magnetic anomalies that suggest the presence of mafic intrusive rocks that were emplaced along deep crustal structures and that fed mafic volcanic flows, (3) arsenic anomalies that suggest that mineralization took place, (4) epithermal training sites, and (5) depth to basement (table E-2). The assessment shows that much of the western three-quarters of the basin permissively contain undiscovered epithermal gold-silver deposits (fig. E-7). Less-extensive favorable areas throughout the basin reflect the presence of rhyolite and mafic volcanic systems that formed in the middle Miocene, roughly between about 17 and 13 million years ago. These areas contain the vast majority of known epithermal deposits and occurrences in the area, and field evidence indicates that additional favorable mineralizing environments are present in these areas. Fairly restricted areas along north-northwest-trending magnetic anomalies are prospective for epithermal deposits. These zones may have served as long-lived conduits for hydrothermal fluids in the late Cenozoic, and various lines of evidence suggest that multiple episodes of mineralization took place along these zones. The nature of the epithermal assessment gave additional weight (i.e., higher potential) to areas that contained both favorable volcanic lithologies and magnetic anomalies. However, the areas shown as favorable probably have mineral-resource potentials comparable to the areas shown as prospective, and exploration for epithermal deposits could take place in all favorable and prospective areas.

Several young (less than 6 million years old) epithermal deposits, as well as modern geothermal systems, have formed in response to continued high heat flow throughout northern Nevada. These systems can occur anywhere that high heat flow, high-angle (generally late Cenozoic in age) faults, and adequate groundwater are available. Examples of young epithermal deposits include Hycroft near Sulphur, Dixie Comstock northeast of Fallon, and Relief Canyon, Standard, and parts of Florida Canyon between Lovelock and Winnemucca;

geothermal areas include Beowawe, Golconda, and Desert Peak/Brady. These high-heat-flow environments are not specifically portrayed on the assessment maps, but the extensive high heat flow makes most of the central and western parts of the Humboldt River Basin favorable for young epithermal and geothermal-related deposits.

Epithermal deposits formed near the paleosurface present at the time of mineralization. Post-mineralization erosion, volcanism, and sedimentation in the Humboldt River Basin have unevenly preserved, destroyed, and (or) concealed the paleosurface and related epithermal deposits. These different levels of exposure are shown in figure E-7. As a result, many areas in the basin and northern Nevada may contain epithermal deposits that are concealed by a few tens of meters to less than a kilometer of younger rocks. Many areas are shown as permissive on the assessment map, largely on the basis of the absence of favorable criteria. In some cases, this absence is a result of post-mineralization concealment, and these areas actually may contain economic, shallowly concealed epithermal deposits. Although concealment makes exploration more difficult, shallowly concealed epithermal deposits such as Sleeper have been discovered and mined. Therefore, permissive areas may be targets for future exploration. Gravity data showing a depth to basement of more than a kilometer are, in part, misleading because the nonbasement cover used in the gravity modeling includes favorable volcanic rocks. Therefore, some areas identified as nonpermissive may be more permissive for undiscovered deposits than shown, especially along their fringes where cover is thin.

Conclusions

Past and present mining activity throughout the Humboldt River Basin demonstrate that the area has a world-class endowment of metals, especially gold and silver. This regional mineral-resource assessment indicates that undiscovered deposits belonging to three major classes may be present in many parts of the basin. New discoveries, albeit in a time of limited exploration activity, are continuing to this date (2002), and new geologic environments are being examined or reexamined as exploration methods and concepts of mineral deposit genesis evolve.

Favorable and prospective areas identified by this assessment are present both in areas that have had little or no mining and in known mining districts. "Grassroots" exploration outside of known mineralized areas has, in the past, resulted in the discovery of numerous mineral deposits, some of which have been mined. However, "grassroots" exploration has been curtailed severely for a number of years in northern Nevada. Many newly discovered deposits also have been found in established mining districts, either as extensions of previously mined deposits or as separate deposits that formed from the same mineralizing system. Therefore, although new areas outside of mining districts will be explored, areas in and around

mining districts will continue to remain attractive targets for future exploration simply because the processes that led to the formation of economic deposits are known to have occurred there.

Although economics are critically important, this assessment did not consider the economic factors associated with exploring for and mining a mineral deposit. Instead, this report defines areas that have various geological characteristics of known mineralized areas and may contain targets for future mineral exploration. Within very optimal economic and technological constraints, these areas may or may not contain the locations of future mines. Economics and corporate philosophies play a significant role in where exploration for and mining of new deposits takes place, even in regions such as northern Nevada that have a significant potential for undiscovered mineral deposits. Guidelines for some large companies require that only multi-million-ounce gold deposits be considered for further drilling and evaluation, thereby eliminating smaller but economically viable deposits from company consideration. In contrast, ore from some small, high-grade deposits has been mined and trucked to processing facilities, where it is mixed with subeconomic ore from large, low-grade deposits to produce a net economic mill output.

As demonstrated over the last 50 years in the Humboldt River Basin, mining in any particular area may last continuously or episodically for a year to several decades. This wide variation in the duration of mining depends on many variables, including the size of the deposit(s) being mined, discovery of

new deposits or satellite orebodies in the area, and fluctuations in economic conditions. For example, the most recent mining in the large Copper Canyon area of the Battle Mountain Mining District continued episodically from the late 1960s to the middle 1990s as deposits were mined out, new ones were discovered, and the economics (metal prices, interest rates) fluctuated. Similarly, mining along the world-class Carlin trend has been continuous since the early 1960s. At a smaller scale, mining at the Mule Canyon Mine east of Battle Mountain started in 1996, ceased due to depressed metal prices in 2000, and restarted on a limited scale in 2002. Other deposits, such as Relief Canyon and Hog Ranch, had finite metal resources and were mined out, and low metal prices have precluded renewed exploration in those areas. Thus, activity in a particular mining area or district can vary significantly over the years, and mining-related activity can take place at different times and places throughout the Humboldt River Basin. Consequently, the role of mining-related activities in land-use planning and impact on hydrology is dynamic and not restricted in time and place.

The Humboldt River Basin and northern Nevada contain numerous deposits and occurrences of elements and commodities that currently are not attractive economically and were not evaluated in this report. Changes in the economics related to many of these elements and commodities could induce exploration for and mining of those types of deposits. If and when that becomes the case, a separate assessment should be made of those types of deposits.
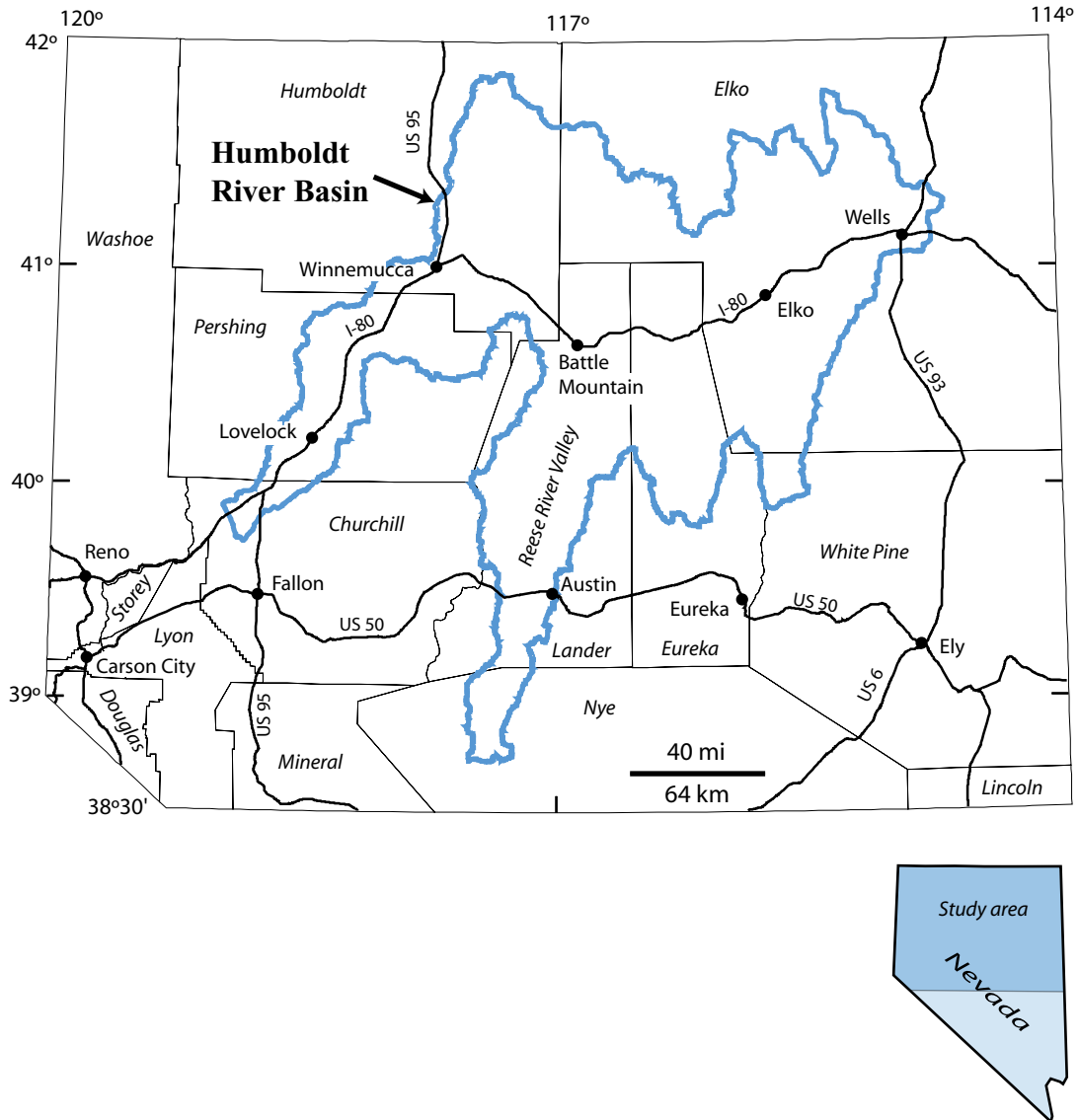
Figure E-1. Location map of northern Nevada, showing the outline of the Humboldt River Basin (blue line) and towns, cities, counties (italics), and major roads. This part of Nevada, shown in the darker blue at right, represents the "study area," which is described throughout the mineral assessment report and in figures E-2, E-3, and E-4.

Geologic Events in Northern Nevada

Era	Period	Age (Ma)	Tectonic events	Sedimentation/igneous activity	Mineralization
Cenozoic	Quaternary			Alluvial, lacustrine sedimentation	Epithermal
Cenozoic	Tertiary	1.6	Extension; uplift begins	Volcanism (bimodal, western andesite)	
Cenozoic	Tertiary		Extension	Volcanism (interior andesite-rhyolite)	Sedimentary rock-hosted
Mesozoic	Cretaceous	66		Plutonism (felsic)	
Mesozoic	Jurassic	138	Nevadan/Sevier/ Elko orogenies	Plutonism (mafic), volcanism (mafic)	Pluton
Mesozoic	Triassic	205		Shelf, basinal sedimentation	
Paleozoic	Permian	240	Sonoma orogeny (Golconda thrust)	Volcanism (felsic)	
Paleozoic	Pennsylvanian	290		Antler sequence, craton-margin sedimentation	
Paleozoic	Mississippian	330	Antler orogeny (Roberts Mtns. thrust)		
Paleozoic	Devonian	360			
Paleozoic	Silurian	410			
Paleozoic	Ordovician	435		Craton-margin (shelf, slope, deep basin) sedimentation	
Paleozoic	Cambrian	500			
Pre-cambrian	Proterozoic	570	Craton-margin rifting Archean/Proterozoic suturing		
Pre-cambrian	Archean	2500			

Figure E-2.   Geologic time scale showing major geologic events in northern Nevada.
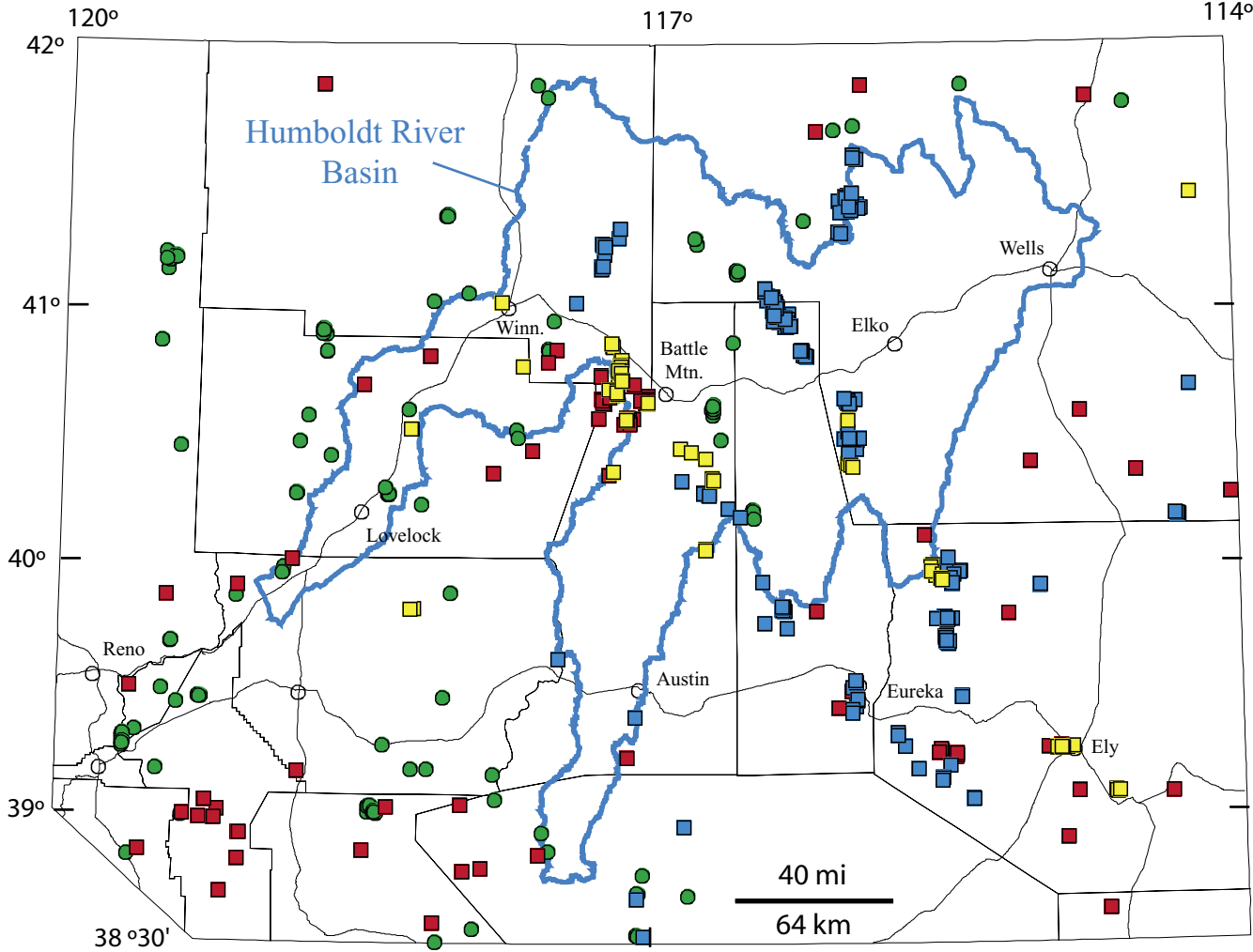
Figure E-3. Locations of significant pluton-related, sedimentary rock-hosted, and epithermal mineral deposits ("training sites") in northern Nevada and the Humboldt River Basin. Base map as in figure E-1; Humboldt River Basin outlined in blue.
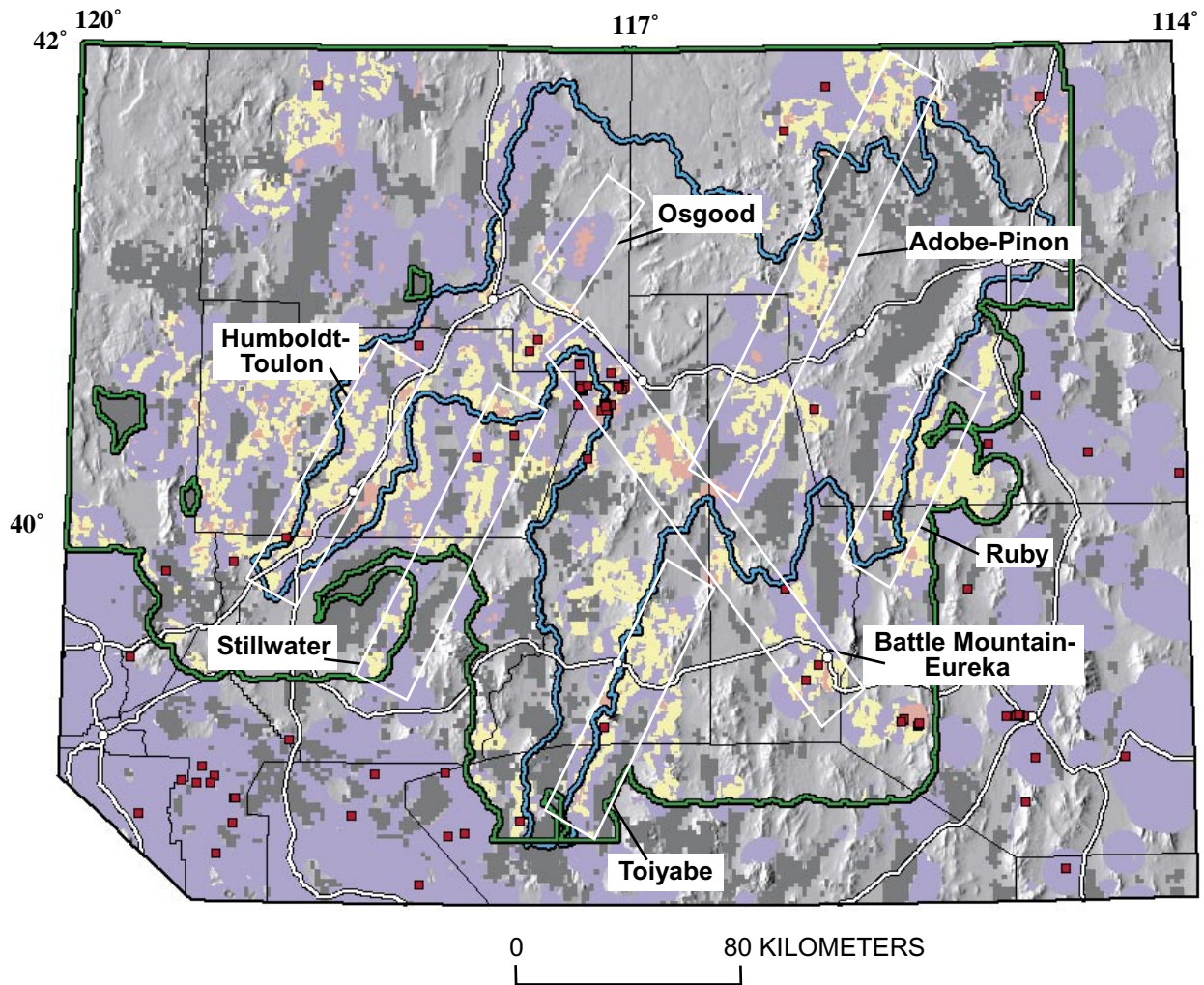
Figure E-4.   Pluton-related mineral resource assessment map of northern Nevada showing selected mineral belts(outline in white) discussed in text. Training sites are shown as red squares. Prospective and favorable tracts were delineated only where geochemical data are available (within the light green line). Humboldt River Basin shown as pale blue outline. Occurrence favorability: red, prospective; yellow, favorable; pale purple, permissive; uncolored, nonpermissive. Dark gray areas represent Cenozoic cover deposits that are greater than 1 km thick. Area of map same as in figure E-1.
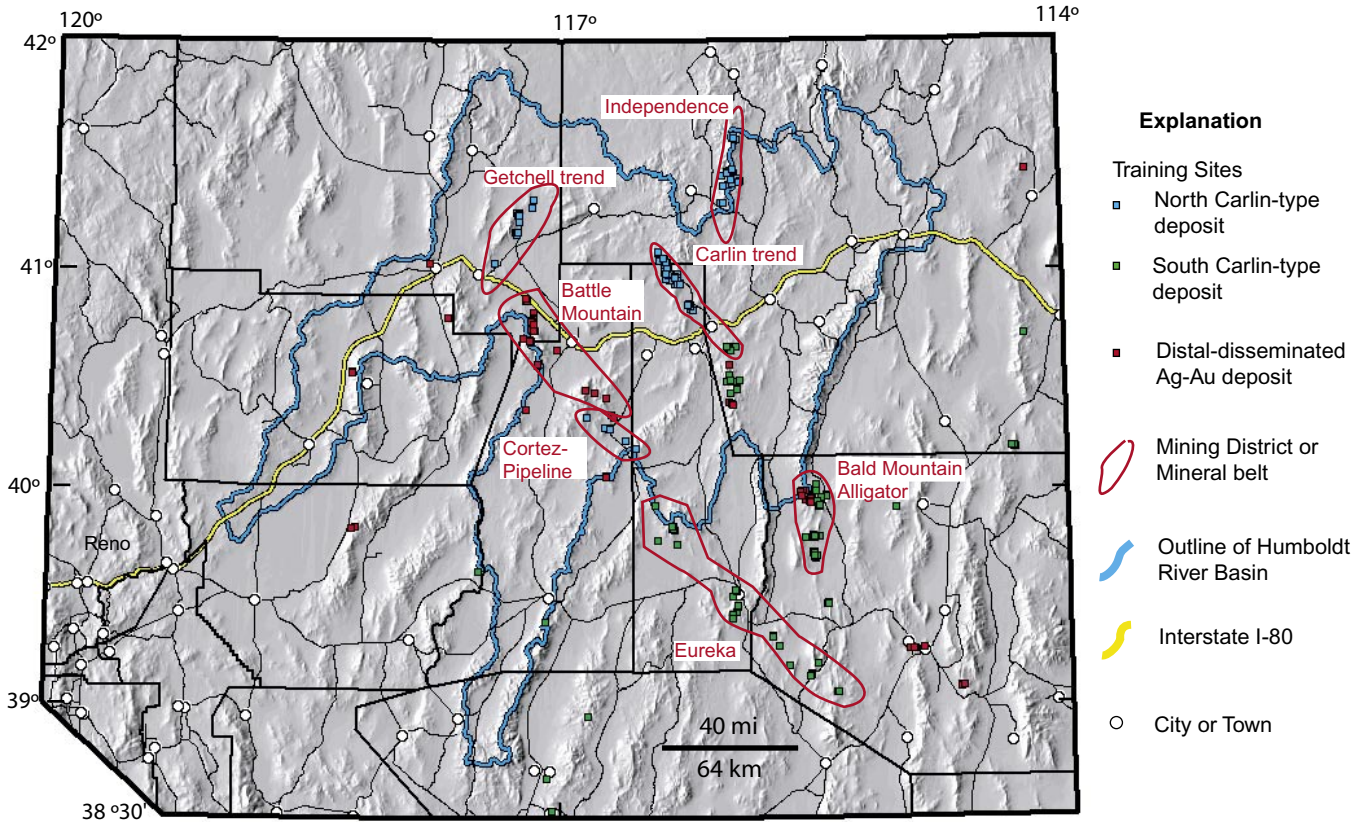
Figure E-5.   Index map showing the locations of sedimentary rock-hosted gold-silver deposits and major mineral trends in northern Nevada, including Carlin-type and distal-disseminated deposits. Outline of Humboldt River Basin shown in light blue. Area of map same as in figure E-1.
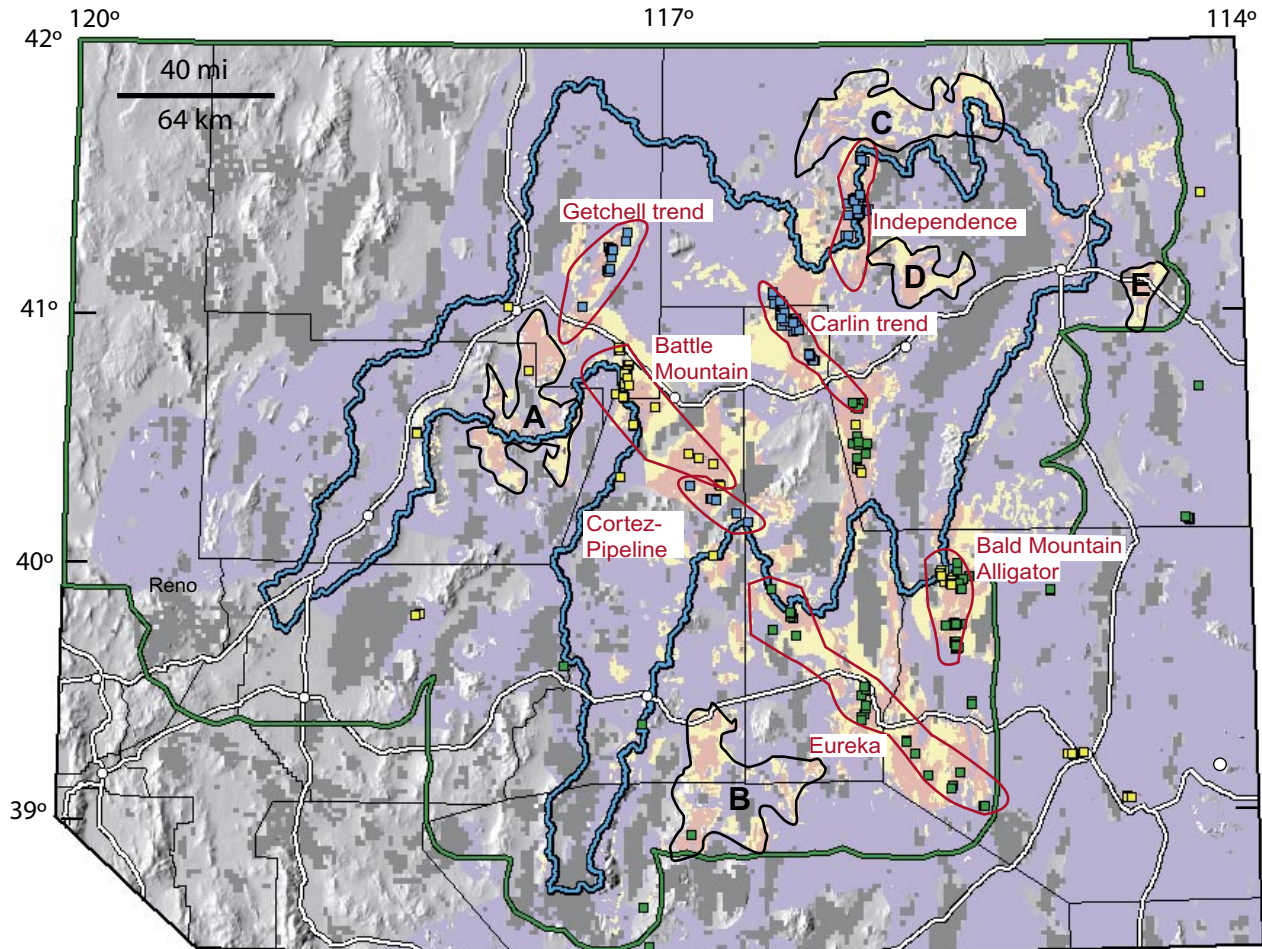
Figure E-6. Sedimentary rock-hosted gold-silver deposit mineral resource assessment map for northern Nevada, showing prospective (red), favorable (yellow), permissive (blue), and nonpermissive (uncolored) tracts. Prospective and favorable tracts were delineated only where geochemical data are available (within the light green line). Darker gray areas represent Cenozoic cover deposits that are more than 1 km thick. Sedimentary rock-hosted gold-silver sites shown as blue (north Carlin-type), green (south Carlin-type), and yellow (distal disseminated) squares. The Humboldt River Basin is outlined in light blue. Major cities and roads are shown in white. Features are plotted on a background of shaded relief of topography. Main mining districts are outlined in red. Areas outlined in black are discussed in text: *A*, Sonoma-East and Tobin Range area; *B*, Northumberland, north Monitor, and Toquima Range area; *C*, Bull Run, Copper, and Jarbidge Mountains area; *D*, North Adobe Range; and *E*, North Pequop Mountains area. Area of map same as in figure E-1.
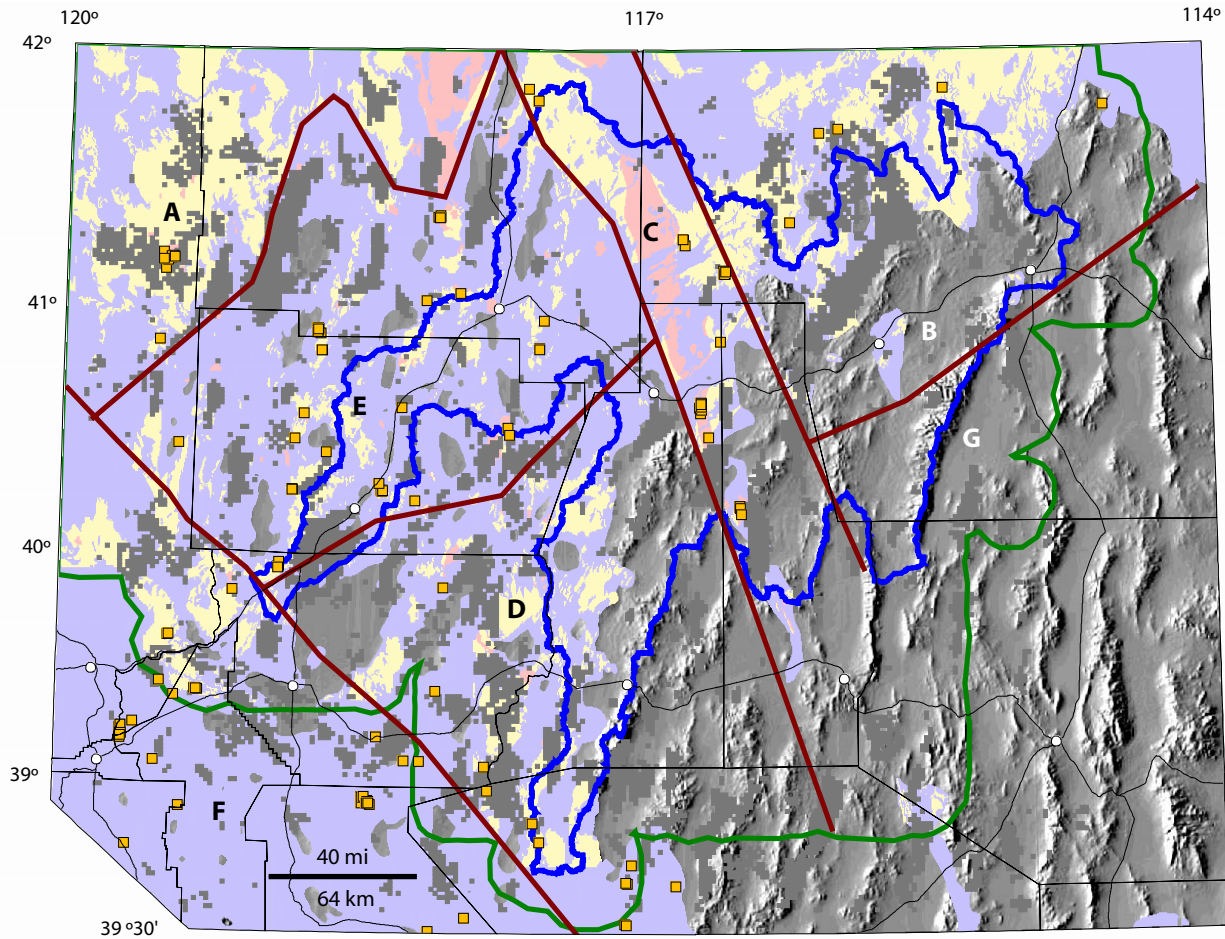
Figure E-7.   Epithermal gold-silver deposit mineral-resource assessment map for northern Nevada, showing prospective (red), favorable (yellow), permissive (blue), and nonpermissive (uncolored) tracts. Prospective and favorable tracts were delineated only where geochemical data are available (within the light green line). Darker gray areas represent Cenozoic cover deposits that are greater than 1 km thick. Epithermal deposit training sites are shown as orange squares. Areas of differing exposure levels are shown in brown lines; letters A-G refer to subregions described in assessment report. The Humboldt River Basin is outlined in blue. Features are plotted on a background of shaded relief of topography. Area of map same as in figure E-1.

Table E-1.   Examples of pluton-related, sedimentary rock-hosted gold-silver, and epithermal gold-silver deposits in the Humboldt River Basin and nearby areas, northern Nevada.

Type of Mineral Deposit	Examples
Pluton-related polymetallic	Battle Mountain (Fortitude, Copper Canyon, Copper Basin), Ruth, Majuba Hill, Kennedy, Yerington, McCoy-Cove (in part)
Sedimentary rock-hosted gold-silver: Carlin-type	Carlin Trend (Post-Betze, Meikle, Gold Quarry, Rain), Getchell Trend (Twin Creeks, Getchell, Pinson), Independence (Jerritt Canyon, Big Springs), Alligator Ridge, Pipeline, Cortez
Sedimentary rock-hosted gold-silver: distal-disseminated	Lone Tree, Marigold, Trenton Canyon, Bald Mountain, Bullion, McCoy-Cove (in part), Toiyabe
Epithermal gold-silver	Midas, Mule Canyon, Tuscarora, Sleeper, Florida Canyon, Buckskin-National, Adelaide Crown, Goldbanks, Rosebud, Hycroft, Ivanhoe

Table E-2.   Evidence (data) layers used for data-driven component of mineral resource assessments of pluton-related, sedimentary rock-hosted gold-silver, and epithermal gold-silver deposits, Humboldt River Basin, Nevada.

Evidence Layer	Pluton-Related Polymetallic	Sedimentary Rock-Hosted Gold-Silver	Epithermal Gold-Silver
Geology			
Lithologic Units		X	
Lithotectonic Terranes		X	
Tertiary Volcanic Lithologies			X
Northeast Linear Features		X	
Thrust Proximity		X	
Pluton Proximity	X	X	
Lithodiversity	X	X	
Geophysics			
Basement Gravity Lineaments	X	X	
Basement Gravity Terranes	X		
Magnetic Terranes			X
Depth to Basement (Gravity)	X	X	X
Geochemistry			
Arsenic	X	X	X
Barium/Sodium Ratio		X	
Copper-lead-zinc Signature	X		
Mineral Deposits			
Training Sites	X	X	X
Skarn Proximity	X		

Chapter 1

Introduction to the Humboldt River Basin Mineral Resource Assessment

By Alan R. Wallace

Introduction

Northern Nevada has a rich endowment of metallic mineral deposits, and, at various times, it has been one of the nation's leading producers of gold, silver, copper, mercury, and tungsten. Currently, Nevada is the third largest producer of gold in the world, and the area is the site of active exploration for other deposits. The Humboldt River Basin (HRB) in northern Nevada includes many of the large open-pit and underground gold mines in northern Nevada. Roughly 70 percent of Nevada is composed of Federal lands; in northern Nevada, these lands largely are under the stewardship of the U.S. Bureau of Land Management (BLM) and the U.S. Forest Service. Many of the known mineral deposits in northern Nevada underlie these areas.

The Humboldt River and its many tributaries form a 43,000-km², internally drained hydrologic basin that covers a large part of northern Nevada (fig. 1-1). The main stem of the Humboldt River starts in northeastern Nevada near the town of Wells, and it flows west and then south to the Humboldt Sink southwest of Lovelock, where the water evaporates. The Reese River subbasin, which forms the largest subbasin in the Humboldt River drainage system, drains north from north of Tonopah and joins the Humboldt River at Battle Mountain (fig. 1-1). Water in the basin is used for agriculture, municipalities, livestock, mining, and recreation (fishing, boating). Dewatering of large open-pit and deep underground mines has modified water tables near those mines, and the water is diverted to agriculture uses, recharged into the aquifers, or discharged directly into the Humboldt River and its tributaries.

An earlier mineral assessment of the Winnemucca-Surprise Resource Areas in northwestern Nevada and northeasternmost California included the western third of the HRB (Peters and others, 1996). In 1996, in order to facilitate long-term land-use planning in the region, and the HRB in particular, BLM requested that the U.S. Geological Survey (USGS) "extend [the] Winnemucca-Surprise type minerals project for the remaining Humboldt River Basin" (T. Leshendock, BLM, written commun., 1996). To that end, this study of the entire HRB provides data that suggest where exploration and mining activity might occur outside of known mining districts and other areas of known mineral deposits. These areas may include future locations of mine dewatering.

This report provides an assessment of undiscovered deposits of Au, Ag, Cu, Pb, and Zn (see list of abbreviations in table 1-1) in Nevada north of latitude 38°30', an area that includes the Humboldt River Basin (fig. 1-1). These elements were chosen because they likely will be the elements of greatest economic interest in the next ten or so years. The assessment focused on three types of mineralizing systems that contain one or more of those elements: pluton-related (chapter 7), sedimentary rock-hosted Au-Ag (chapter 8), and epithermal Au-Ag deposits (chapter 9). Northern Nevada contains more than 40 different types of metallic mineral deposits, on the basis of the taxonomy of Cox and Singer (1986). Many deposits formed in one of the three types of mineralizing systems, and mineral exploration in northern Nevada traditionally has focused on systems rather than on individual deposit types. Platinum-group elements, such as Pt and Pd, have not been mined in northern Nevada. However, continued and projected high prices for these elements, and the presence of favorable plutonic environments for their occurrence, suggests that these environments may become targets for mineral exploration. As such, these types of deposits are discussed, but not specifically assessed, in the chapter on pluton-related mineral deposits (chapter 7).

This interdisciplinary mineral assessment included geology, geophysics, geochemistry, and computer modeling. Significant new data were acquired through parallel projects in the USGS Mineral Resources Program, including the Northern Nevada Gold Project and the Surveys and Analysis Project, and those data were used in the assessment. As a result, many existing databases were updated and revised using the new results. These databases are discussed in ensuing chapters in this report.

By assessing the entire northern half of the State (fig. 1-1), the assessment was able to consider geologic and mineral deposit features outside of the HRB that potentially could point to undiscovered mineral deposits within the basin. This broader area includes the Winnemucca-Surprise Resource Area of northwestern Nevada (Peters and others, 1996). The present assessment updates the assessment of the Winnemucca-Surprise area, thereby permitting a consistent, regional mineral evaluation.

The results of this mineral assessment reflect our current (2001) knowledge and understanding of the geology, geophysics, geochemistry, and mineral deposits of northern Nevada. New data acquired during the course of this project modestly

to significantly changed our understanding of some of these concepts, and ongoing exploration by industry continues to identify new mineralized areas and mineral deposits. This evolution of thought and acquisition of new data will not diminish, and the results of this assessment should be used with evolving concepts in mind.

The organization of this report builds towards the final three assessment chapters. Chapter 2 (Assessment Methodology) describes the methods and databases used for this assessment, and chapter 3 (Use of the Assessment) guides the user on the best way to use the assessment. Chapters 4 through 6 supply background information on the geology, geochemical data, and geophysical data, respectively, that were used for this assessment. Chapters 7, 8, and 9 provide the mineral resource assessments for undiscovered pluton-related, sedimentary rock-hosted Au-Ag, and epithermal mineral deposits, respectively, in northern Nevada and the HRB.

Definition of Terms Used in This Report

The definitions and concepts used in this report are adopted from those used in the Winnemucca-Surprise mineral assessment (Peters and others, 1996). Terms and concepts used to describe and define the rankings of undiscovered mineral-resource potential are defined in chapter 2. Additional definitions and concepts are described elsewhere (Cox and others, 1986; John and others, 1993). Geologic terms can be found in common geologic glossaries, such as the Glossary of Geology (Bates and Jackson, 1987).

- A **mineral occurrence** is "… a concentration of a mineral … that is considered valuable by someone somewhere or that is of scientific or technical interest" (Cox and others, 1986). Occurrences are useful to identify areas where mineralizing processes took place, regardless of economic value.

- A **mineral deposit** is "… a mineral occurrence of sufficient size and grade that it might, under the most favorable of circumstances, be considered to have economic potential" (Cox and others, 1986). This includes those mineral occurrences that have been tested through drilling in the third dimension to the point that a **grade** (amount of metal per unit of rock) and **tonnage** (total weight of mineralized rock) can be assigned to the volume of rock with some level of confidence.

- An **ore deposit** is "… a mineral deposit that has been tested and is known to be of sufficient size, grade, and accessibility to be producible to yield a profit" (Cox and others, 1986). "Profit" applies to conventional supply-demand economics, yet national needs at times might require mining at a financial loss when it is in the Nation's best economic and societal interests. In addition, the economic viability of a mineral deposit can vary with time, depending on the value of the con-

tained metals and the costs related to extracting them from the ground. An ore deposit generally includes the **geologic reserve**, which is mineable within economic constraints, and the **geologic resource**, which includes the grade and tonnage of all the mineralized volume of rock, regardless of economic factors. The mineralized volume of rock, including the ore deposit itself, commonly is broken down by variable grades, some economic and some not, as well as the current price of the sought-for commodity.

- A **mining district** is an area that includes a few to many mines and prospects. Mining districts were organized by the miners as a mechanism to govern mining and related regulations in those areas. Districts can include one or more different mineral deposit types, and a single mineral deposit can be part of more than one district, depending on how and why the districts were established. This assessment generally used the names and locations of Nevada mining districts described by Tingley (1992). In some instances, however, the extent of a mining district was modified somewhat to include a number of similarly formed deposits.

- A mineral deposit **trend** is a generally linear array of mineral deposits. The deposits in a trend may or may not be geologically related. Examples in the HRB include the Carlin, Getchell, and Battle Mountain-Eureka trends, which include a variety of mineral deposit types, and the northern Nevada rift (John and others, 2000), which includes a linear belt of genetically related epithermal mineral deposits.

The names of various mining, milling, and mineral exploration methods are mentioned in this report to help describe the different shapes, sizes, and depths of ore bodies. Readers interested in these methods are referred to Peters (1978) or other mining- and mining-engineering-related books for more information on these topics.

Previous Work

Innumerable geologic studies have focused on northern Nevada and the HRB area. This work dates back to the mid 1800s, when studies of newly discovered mineral deposits led to reports on the geology of the important mining camps of the day. Geologists even studied the geology along the route of the Transcontinental Railroad (Lee and others, 1915), both to understand the potential for undiscovered mineral resources along the railroad and to provide popular "in-transit" guides for travelers (and potential investors) during their journeys.

The State geologic map of Nevada (Stewart and Carlson, 1978; Stewart, 1980) provides the best overall geologic setting of northern Nevada and the HRB. This map in large part was derived from county geologic reports that, in northern Nevada, include Elko (Coats, 1987; LaPointe and others, 1991), Humboldt (Will-

den, 1964), Lander (Stewart and McKee, 1977), Eureka (Roberts and others, 1967), Pershing (Johnson, 1977), Churchill (Willden and Speed, 1974), northern Nye (Kleinhampl and Ziony, 1984), Lyon, Douglas, and Ormsby [Carson City] (Moore, 1969), White Pine (Hose and others, 1976), and Washoe and Storey (Bonham, 1969) counties. In addition, the published literature is replete with detailed studies on virtually all aspects of the geology, geochemistry, and geophysics of northern Nevada.

Many reports, a number of which are cited in other chapters in this report, define the regional metallogeny, the geology and mineral deposits of mining districts, and specific mines in northern Nevada. These studies range from the early work in the 1800s to very recent work that was published in 2000 in the Geological Society of Nevada's symposium proceedings volumes (Cluer and others, 2000).

A number of studies focused on the mineral resources and the potential for undiscovered resources in northern Nevada. Bonham and others (1985) conducted a mineral inventory in the Paradise-Denio and Sonoma-Gerlach BLM Resource Areas of northwestern Nevada, and Garside and Davis (1992) inventoried mineral resources in the Nevada part of the Susanville Resource Area in westernmost Nevada. At the request of the BLM and the U.S. Forest Service, the USGS assessed the mineral resources of many wilderness and wilderness study areas in northern Nevada. These and related investigations by the U.S. Bureau of Mines were summarized by Marsh and others (1984) and Conrad (1990). In 1996, the USGS published the results of a mineral resource assessment of the Winnemucca BLM district of northwestern Nevada and the Surprise Resource Area of northeastern California (Peters and others, 1996). The present assessment includes and updates the Nevada part of the Winnemucca-Surprise study area.

General studies that relate specifically to Wilderness Study Areas in northwestern Nevada were conducted for the BLM and were summarized by Barringer Resources, Inc., (1982) and Connors and others (1982). Miller (1993) conducted an inventory of mineral occurrences and a study of mineral-resource potential in the proposed High Rock National Conservation Area. Reports by Greene (1976, 1984) and Greene and Plouff (1981) described the resource potential for precious opal, uranium, mercury, and gold in the Charles Sheldon Antelope Range and Sheldon National Antelope Refuge in northwestern Nevada. A study of the mineral-resource potential of Nevada (Ludington and others, 1993; Singer, 1996) provides substantial data that have been incorporated into parts of this assessment.

Acknowledgments

Figure 1-1. Location map of northern Nevada, showing the outline of the Humboldt River Basin (blue line) and towns, cities, counties (italics), and major roads. This part of Nevada represents the "study area" described in this mineral assessment report and is shown in many figures throughout this report. Specific locations described in the various chapters of this report are shown in figures accompanying those chapters.

Table 1-1. List of abbreviations used in the Humboldt River Basin mineral assessment report.

Chemical elements

Ag	Silver	Na	Sodium
As	Arsenic	Ni	Nickel
Ba	Barium	Pb	Lead
Bi	Bismuth	Pd	Palladium
Au	Gold	Pt	Platinum
Co	Cobalt	S	Sulfur
Cu	Copper	Sb	Antimony
F	Fluorine	Se	Selenium
Fe	Iron	Te	Tellurium
Hg	Mercury	Tl	Thallium
K	Potassium	U	Uranium
Mo	Molybdenum	W	Tungsten
Mn	Manganese	Zn	Zinc

Grade, tonnage, concentration

t	Ton (2,000 pounds)
oz/ton	Ounces per ton (of element listed)
tonne	Metric tons (0.91 English tons)
kg	Kilogram
km	Kilometer
ppm	Parts per million
ppb	Parts per billion

Miscellaneous

BLM	U.S. Bureau of Land Management
GIS	Geographical Information System
HRB	Humboldt River Basin
MRDS	Mineral Resources Data System
NURE	National Uranium Resource Evaluation
Ma	millions of years
m.y.	million years
USGS	U.S. Geological Survey
WLR	Weighted Logistic Regression
WofE	Weights of Evidence

[1] Some specific abbreviations are defined where they are used in the text.

Chapter 2

Assessment Concepts and Methodology

By Mark J. Mihalasky and Alan R. Wallace

Inroduction

The purpose of this mineral-resource assessment was to (1) assess the favorability for undiscovered pluton-related, sedimentary rock-hosted, and epithermal metallic mineral occurrences and deposits in the Humboldt River Basin (HRB) and adjacent areas, (2) provide an analysis of the mineral-resource favorability (Bonham-Carter, 1994) that can be reproduced on the basis of the data and defined assumptions, and (3) present that assessment in a digital format, using a geographic information system (GIS). The assessment was carried out for the whole of northern Nevada north of latitude 38°30', which is referred to as the "study area" (fig. 2–1). Previous small-scale U.S. Geological Survey (USGS) mineral-resource assessments in northern Nevada include the Nevada assessment (Singer, 1996), the Winnemucca-Surprise Resource Areas (Peters and others, 1996), and the Reno 1° x 2° quadrangle (John and others, 1993). These assessments used qualitative, expert-based approaches to determine the favorability for undiscovered mineral deposits. The HRB assessment used digital data and an initial phase of knowledge-driven (expert) analysis, followed by data-driven analysis and modeling techniques to create a number of mineral-resource assessment maps. The assessment was conducted by a team of USGS mineral-resource experts, and it consists of (1) new research and up-to-date reviews of the geology, mineral resources, and data for northern Nevada, (2) mineral-resource assessment maps, and (3) discussions on land classification and how to interpret and use the assessment maps. An ancillary part of the HRB mineral-resource assessment was to reproduce the results of previous assessments, specifically the Winnemucca-Surprise and Nevada assessments.

The following sections provide an overview of how the assessment was carried out, as well as discussions on mineral deposits, analysis and modeling techniques, and data.

Mineral Deposits and Models

Mineral deposits form in a wide variety of mineralizing environments. Cox and Singer (1986) compiled a taxonomy for these mineral deposit "types." In some cases, one mineralizing system or process may produce only one mineral deposit type, such as placer deposits along streams. In other cases, a single mineralizing system can form several different types of deposits, such as skarn, polymetallic vein and replacement, and various porphyry-type deposits related to a single intrusive body. In the Winnemucca-Surprise mineral-resource assessment (Peters and others, 1996), mineral deposits were assigned to specific deposit types of Cox and Singer (1986), and a separate assessment was made for each of the 28 metallic mineral deposit types in the study area (table 2 of Peters and others, 1996).

This mineral-resource study of the HRB assessed the potential for undiscovered mineralizing systems (pluton-related, sedimentary rock-hosted Au-Ag, and epithermal Au-Ag) and contained mineral deposits and occurrences, instead of the specific deposit types related to those systems. Thus, the resulting assessment tracts for deposits and occurrences that formed from a pluton-related mineralizing system, for example, can contain more than one of the pluton-related deposit types defined by Cox and Singer (1986). The rationale for this approach was that (1) mineralizing systems are larger than individual mineral deposits, (2) mineralizing systems can form more than one individual deposit type, and (3) the presence of one mineral deposit type might indicate the presence of a larger system. In some locations, the various deposit types in a mineralizing system represent a continuum of site-specific processes of mineral deposition. As a result, the economic viability of any part(s) of the mineralizing system is a function of its metal endowment. Thus, the approach that was taken in the HRB assessment addresses areas where mineralizing processes took place over relatively large areas to form concentrations of metallic minerals.

Three fundamental types of mineralizing systems are addressed in the HRB mineral-resource assessment: (1) pluton-related, (2) sedimentary rock-hosted Au–Ag, and (3) epithermal. Although these three systems can have some genetic and spatial overlap, their features and origins are sufficiently distinct to allow them to be evaluated separately. These three types of mineralizing systems account for most important lode metallic mineral deposits discovered in northern Nevada since the middle of the Nineteenth Century. They are important sources of gold, silver, copper, lead, zinc, and molybdenum. Pluton-related systems also have potential for producing platinum-group elements (PGE). Descriptions of these systems and the geologic criteria used for their assessment are detailed in chapters 7, 8, and 9.

Land Management, Classification, and Mineral-resource Assessment Tracts

USGS mineral-resource assessments of public lands recognize that land-managing agencies, in this case the BLM, require judgments about differing levels of mineral-resource favorability to aid in land-use planning activities. Thus, the purpose of a mineral-resource assessment is to estimate the relative favorability for undiscovered mineral deposits for a given region. It can be used to identify where minerals exploration and development activity may occur in the future. The assessment and its products can facilitate decision-making processes by extending the possible options for future land use and stewardship.

In previous mineral-resource assessments, such as the BLM Wilderness Study Areas (Conrad, 1990), relative levels of favorability for undiscovered deposits were described in qualitative terms like "high," "moderate," and "low," as well as "no mineral potential" and "unknown mineral potential." More recent studies, such as the Nevada (Singer, 1996) and Winnemucca-Surprise (Peters and others, 1996) assessments, used the concepts of "permissive terranes" and "favorable tracts," in combination with estimates of numbers and size of undiscovered deposits, in order to quantify predicted resources (Menzie and Singer, 1990; Singer, 1993). Prior to the HRB assessment, all USGS mineral-resource assessments in Nevada (see Peters and others, 1996; Cox and others, 1996; John and others, 1993; Conrad, 1990) used exclusively knowledge-driven methods to define areas of relative favorability for undiscovered deposits.

The HRB mineral-resource assessment adopted the terminology used in the Winnemucca-Surprise assessment, including the terms "nonpermissive," "permissive," "favorable," and "prospective" tracts, as introduced by Peters and others (1996). As defined here, a "mineral-resource assessment tract" is a geographic region (a tract of land) that has been determined to possess geologic attributes that allow for the occurrence of mineral resources of a particular type(s). For the HRB mineral-resource assessment, tracts have been delineated that show favorability for pluton-related, sedimentary rock-hosted, and epithermal mineralized systems and contained occurrences and deposits.

Because the techniques used to delineate mineral-resource assessment tracts for the HRB assessment are different from those used in the Winnemucca-Surprise assessment, the terms as used here do not have the same meaning. The nonpermissive and permissive tracts delineated in the HRB mineral-resource assessment are similar to those used and defined in the Nevada assessment (Cox and others, 1996), differing only in the depth-to-basement maps used to define areas of thick Cenozoic volcanic or sedimentary deposits. In general, permissive areas are regions that might contain a mineralized system within a depth of 1 km beneath the surface. These tracts may or may not contain mineral deposits or occurrences, and their designation as permissive does not necessarily imply that any resources, if they are present, will be discovered. This designation is based on the presence of one or more geologic

factors that the assessment team considered to be important, some of which may be widespread, and that are known to have been involved with the formation of mineral deposits and occurrences elsewhere in the assessment area. By definition, permissive tracts include favorable and prospective areas and thus are considered to contain virtually all undiscovered deposits of a certain type or group. Nonpermissive tracts are those areas judged to have a negligible probability of containing a mineral deposit or occurrence, or that are covered by more than 1 km of Cenozoic rocks or alluvial sediments. As described by Singer (1993), these areas have roughly less than a 1 in 100,000 to 1,000,000 chance of containing undiscovered deposits of the type being assessed. The nonpermissive designation is based on absence of geologic environments and (or) known mineralizing processes that are understood to be necessary for formation of the type of mineral occurrence or deposit under consideration.

The favorable and prospective tracts delineated in the HRB mineral-resource assessment, although derived in a manner different from the Winnemucca-Surprise assessment, convey roughly similar concepts in terms of resource favorability because they both represent "moderate" and "high" levels, respectively. The HRB assessment team created and (or) selected datasets for mineral-resource analysis and modeling that represent a number of important regional processes believed to be related to formation of mineral deposits and occurrences. The relative rankings of the tracts reflect the combination of these datasets for each type of mineralizing system assessed. For a given combination, the contribution of each dataset to the level of favorability is derived mathematically from the spatial association between the distribution pattern of the known mineral occurrences and deposits and the geoscientific phenomena represented in the dataset. For example, if the mathematical calculations determine that mineral occurrences and deposits have a greater spatial association with geochemical anomalies than with a geophysical anomalies, then the geochemical anomalies contribute more to the level of favorability than do the geophysical anomalies. The implication is that certain dataset combinations represent a greater likelihood that mineralizing processes took place in a given area than other combinations. Thus, a prospective area represents the optimum combination of the datasets, whereas a favorable area consists of a somewhat less optimum, but still relatively significant, combination. Combining the datasets and determining the threshold between prospective and favorable also is done mathematically. The shape and distribution of the prospective and favorable tracts is determined by the overlap intersections among the patterns of geoscientific phenomena represented in each of the datasets.

The following sections describe in detail the various concepts, methods, and datasets used in the assessment process. Knowledge- and data-driven analysis and modeling methods are described immediately below. The datasets used for data-driven modeling are described later in this chapter and discussed in greater detail in each of the respective mineral deposit type assessment chapters (chapters 7-9).

Analysis and Modeling Methodologies

The HRB mineral-resource assessment delineated nonpermissive, permissive, favorable, and prospective assessment tracts using a combination of knowledge- and data-driven analyses and modeling techniques. This hybrid approach, illustrated in figure 2–2, was used to maximize the use of expert knowledge, and to analyze and integrate the data in a reproducible manner.

Expert knowledge was used to (1) create, select, and appraise datasets for data-driven modeling, (2) delineate permissive and nonpermissive assessment tracts (Cox and others, 1996), and (3) evaluate and revise preliminary mineral-resource assessment maps derived from data-driven modeling. In addition, expert knowledge was used to evaluate the final assessment maps produced by data-driven modeling, including discrepancies between the models and known geologic and mineral deposit relations. These evaluations are presented in the three assessment chapters (chapters 7-9). Given the available data, the assessment team concluded that the nonpermissive–permissive tract boundary was best delineated by the knowledge-driven Nevada assessment (Cox and others, 1996), rather than by data-driven means.

Data-driven modeling, including weights-of-evidence (WofE) and weighted logistic regression (WLR), was used to delineate the preliminary and final prospective and favorable assessment tracts. The WofE technique was used to analyze the bivariate spatial associations among the datasets. In some cases, the databases selected by the assessment team had a high conditional dependence. WLR avoids bias caused by combining datasets that are conditionally dependent (mutually interrelated; Agterberg, 1992, Agterberg and others, 1993, Bonham-Carter, 1994, and Singer and Kouda, 1999). Thus, the WLR technique was then used to model (combine) the datasets and delineate the prospective and favorable assessment tracts.

WofE and WLR modeling were carried out using the ArcView® GIS extension "Arc–SDM" (Spatial Data Modeller), developed by the USGS and the Geological Survey of Canada (Kemp and others, 2001). The WofE method is based on a technique originally developed for nonspatial medical diagnosis (Spiegelhalter and Knill-Jones, 1984). Bonham-Carter and others (1989) and Agterberg and others (1990) modified the original technique to deal with spatial prediction—"diagnosing" mineral occurrences and deposits using the "symptoms" of various geoscientific phenomena. Wright and Bonham-Carter (1996) applied WofE to mineral-resource exploration and they predicted the location of a new discovery in Canada that was made in a favorable area. In Nevada, using mineral deposits and occurrences that represent mineralizing systems similar to those considered in this assessment, Raines (1999) and Mihalasky (2001) demonstrated that WofE yields assessment tracts that are comparable to expert-delineated tracts of the Nevada assessment (Cox and others, 1996).

The WLR method was derived from a suggestion by Tukey (1972) that logistic regression techniques could be applied to resource analysis. Mineral-resource studies that applied logistic regression using unweighted, equal-area, cell-base datasets were first carried out by Agterberg (1974), Chung (1978), and Chung and Agterberg (1980). The application of WLR, using unequal-area, polygon-based datasets that are weighted according to polygon size, was introduced by Agterberg (1992) and Agterberg and others (1993) and studied further by Wright (1996). Regression techniques generally seek to establish a relationship between a response variable (mineral deposits and occurrences) and one or more predictor variables (geoscientific phenomena). The logistic regression technique is applied when the response variable is binary, such as the presence or absence of a deposit or occurrence. In terms of regression, the response variable is affected by (or perhaps "caused by") the predictor variable (McGrew and Monroe, 1993). The algorithm and methodology used here is described in Agterberg (1989, 1992) and Agterberg and others (1993).

Data-driven modeling was performed by the senior author, with assistance from Gary L. Raines; other assessment team members provided advice during the early stages of the modeling. The mineral-resource tract maps that resulted from the final modeling were then furnished to the assessment team members for inclusion and evaluation in the pluton-related, sedimentary rock-hosted, and epithermal assessment chapters (chapters 7–9). A review of the knowledge- and data-driven concepts, terminology, and techniques is given below.

Knowledge-Driven Component

The knowledge-driven component of the HRB mineral-resource assessment is composed of a large body of conceptual and qualitative data, information, and experience. This expert knowledge derives from field-based studies of the geology and mineral resources in northern Nevada conducted by assessment team members and from various publications and communications by other researchers. An essential aspect of this knowledge base was ongoing interaction of the assessment team with the mining industry in northern Nevada, which provided important information on exploration and ore-genesis concepts and access to many active mines and mineralized properties in the area.

Expert knowledge was used directly and indirectly throughout the assessment process and construction and interpretation of the WofE–WLR-based mineral-resource tract maps. Experience and expert-based information were used to select and modify datasets used for data-driven analysis and modeling, as well as to evaluate and interpret the results. In keeping with the BLM request that the assessment team "extend [the] Winnemucca-Surprise type minerals project for the remaining Humboldt River Basin" (T. Leshendock, BLM, written commun., 1996), many of the geologic criteria and concepts used for that assessment (shown in table 5 of Peters and others, 1996) were used for the HRB assessment. In contrast to the HRB assessment, the various assessment tracts for Winnemucca-Surprise were drawn empirically by hand using the various available data and expertise of the assessment team. Data-driven methods were not used.

Beginning in 1999, the HRB assessment team, with the goal of producing a digital, reproducible assessment, created, selected, and evaluated a wide variety of individual digital datasets (or various combinations thereof) in an attempt to replicate both the concepts and the tracts defined for Winnemucca-Surprise. Using a GIS and qualitative support from published information and team expertise, these digital maps ("preliminary mineral-resource tract maps") were compared iteratively against the Winnemucca-Surprise assessment tract maps. The team ultimately was satisfied that the digital maps chosen (the "evidence maps" defined below) showed reasonable, but admittedly not precise, agreement with the Winnemucca-Surprise tract maps. This inconsistency in part came from (1) the use of somewhat different databases or database combinations, (2) the ability of the Winnemucca-Surprise team to modify tract boundaries on the basis of local geologic information, and (3) the increased knowledge of the geology and mineral deposits of the region since the Winnemucca-Surprise assessment was conducted. Similarly, the concepts regarding regional metallogeny that were used for Winnemucca-Surprise generally, but not exactly, were reproduced for the overlapping HRB area. Overall, the HRB assessment team concluded that the Winnemucca-Surprise assessment was reproducible using digital data, and that these data could be applied consistently throughout the HRB study area. On the basis of these knowledge-driven preliminary assessments, the assessment team created, selected, and (or) modified the final datasets used for the subsequent data-driven analysis and modeling of pluton-related, sedimentary rock-hosted Au–Ag, and epithermal Au-Ag deposits in northern Nevada and the HRB. As much as possible, the rationale for making such decisions is provided in each of the respective mineral deposit type assessment chapters (chapters 7–9).

Data-Driven Component

The data-driven modeling component of the HRB assessment used (1) WofE to measure the spatial association between point-objects and patterns, and (2) WLR to mathematically combine the patterns to predict the distribution of the point-objects (see Agterberg and others, 1993). As applied to mineral-resource assessment, the patterns represent maps of geoscientific phenomena that are likely to be useful predictors and are referred to as "evidence maps." These typically include maps of lithology, structure, geochemical and geophysical anomalies, as well as remotely sensed images and other earth-observation data. The point-objects represent known mineral occurrences and deposits, and are referred to as "training sites." Training sites are used to identify and weight the importance of predictor patterns on the evidence maps. Training sites collectively possess characteristics that are common to a particular deposit type or mineralizing system, such as those evaluated for the HRB assessment. It is presumed that the presence and locations of the training sites enable prediction by identifying evidence map patterns that cover areas where

sites may be present but not yet discovered. A single "favorability map" is output from the data-driven modeling procedure. It consists of integrated predictor patterns and represents the spatial distribution of training sites in terms of the spatial distribution of predictor patterns. The favorability map highlights areas that have combinations of evidence map characteristics similar to those at the training sites. These highlighted areas comprise only the favorable and prospective areas on the HRB mineral-resource tract maps. The complete assessment tract map was created by merging favorable and prospective tracts, which were defined using data-driven methods, with the permissive and nonpermissive tracts, which were defined using knowledge-driven methods.

The data-driven modeling component of the HRB mineral-resource assessment has three parts: (1) measurement of spatial association between the training sites and the evidence maps, (2) optimization of the evidence maps for prediction, and (3) combination of the optimized evidence maps. Parts one and two used WofE analysis; part three used WLR (fig. 2–3).

In part one, conditional probabilities that involve area proportions were used to determine the spatial association between the training sites and an evidence map. Each evidence map unit was treated individually as a binary pattern (evidence map unit present or absent), and is composed of the area of the particular evidence map unit being evaluated and the combined total area of the remaining evidence map units. A training site likewise was regarded as present or absent. Each training site has equal importance, and the training sites were not classified or weighted in WofE with regard to the size, grade, or tonnage. A training site was assumed to occupy a small unit-cell area, which for this assessment is 1 km^2.

Two weights of spatial association were calculated with respect to the training sites: W$^+$ for a particular evidence map unit present, W$^-$ for absent. The value of the weights were calculated from the ratio of training sites that fall on a particular evidence map unit to the total number of training sites, which is divided by the ratio of the particular evidence map unit area to the total evidence map area. Where no spatial association exists, the weights are both zero. Where there are more training sites in a particular evidence map unit than would be expected due to chance, W$^+$ is positive and W$^-$ is negative. Where data is unknown or missing due to incomplete evidence map coverage, the weights are assigned the value zero. The weights can be combined into a single coefficient called the contrast (C), where C = W$^+$ – W$^-$. C provides a useful measure of the strength of the spatial association between the training sites and the individual evidence map units. C is zero when the training sites and an individual evidence map unit overlap by the expected amount due to chance. C is greater than zero for positive spatial associations and less than zero for negative associations. The significance of C is estimated by calculating its Student value, or "Studentized C," which is the ratio of C to its standard deviation.

In part two, the evidence maps were reclassified into two units (absence or presence of a predictor pattern), such that the spatial association between the training sites and an evidence

map is optimized (as discussed below). Although reclassification to more than two or three units is possible, evidence maps of just a few units yield more stable and meaningful weights of spatial association and facilitate interpretation of the favorability map. As a result of reclassification, the strongest predictor patterns are grouped and preserved, which in turn, when combined with other evidence map predictor patterns, yields a mineral resource assessment tract that is conservatively delineated.

The reclassification of the evidence maps involved both objective and subjective methods. For each evidence map, an individual evidence map unit that is highly correlated (spatially) with the training sites may be selected as predictive evidence, or multiple evidence map units may be grouped in such a way as to maximize the spatial association between the training sites and the evidence map. The weight estimates, the value of C, the variances of the weights and C, and the significance of C, are used to identify and evaluate evidence map units that are optimal for prediction.

Nominal (categorical) scale evidence maps, such as geological maps, were reclassified by grouping individual units that show strong spatial associations with the training sites. This reclassification was guided in part by expert knowledge and in part by combinations that produced the strongest and most geologically and (or) statistically significant spatial associations.

Ordinal (or ranked), interval, and ratio scale evidence maps, such as geophysical or geochemical anomaly maps, or distance buffer maps, were reclassified by grouping successive cumulative evidence map unit areas. The optimum threshold was determined by the number of successively combined units that collectively demonstrated the strongest spatial association. The grouping of evidence map units and the determination of optimum threshold was performed using a graph that plots area-cumulative C along the y-axis and distance buffers or anomaly intensities along the x–axis, as shown in figure 2–4. In this example, the peak of the area-cumulative C curve occurs at the 3rd interval on the x–axis. The evidence map is optimized by reclassifying into two units, 0–3 and 3–10. For the HRB mineral-resource assessment, all evidence map optimization was performed in this manner, except where the C peak was determined to be an edge-effect artifact of the study area boundary. In such instances, the next highest C peak was chosen. Using the C peak to determine the optimum threshold is the traditional approach (Bonham-Carter, 1994), but alternative approaches that use of maximum significance of C (Cheng and others, 1994; Smailbegovic, 2002) or the weights-crossover (Leonard and others, 2002) have been implemented. Generally speaking, the traditional, maximum C approach serves to exclude areas unlikely to host training sites, and is characterized by large, broadly defined predictor patterns with W^+ magnitudes that are significantly smaller than W^-. The maximum significance of C approach serves to include smaller areas more likely or favorable to contain deposits, and is characterized by small, narrowly defined predictor patterns with W^+ magnitudes that are significantly larger than W^-. The weights-crossover approach yields a balance between the maximum C and maximum significance of C approaches.

The optimized evidence maps served as the prediction criteria for the occurrence of pluton-related, sedimentary rock-hosted Au–Ag, and epithermal mineralizing systems. These criteria were solely derived from the spatial association between the training sites and the evidence maps (as discussed above). In some cases, these criteria do not agree with expert knowledge that is based on known field relations or geologic processes in northern Nevada. The criteria, the disagreements, and how they were used to evaluate and revise the mineral-resource tract maps, are described and discussed in each of the respective mineral deposit type assessment chapters (chapters 7-9).

In part three, the WofE-optimized evidence maps were combined using WLR to produce the favorability map, which represents only prospective and favorable mineral-resource tracts. In the WLR approach, predictive evidence was weighted according to the combined area of a particular unique overlap condition among various evidence maps and by the number of training sites that fell within the unique overlap condition. The absence or presence of the training sites was first determined, and then a simultaneous solution, using an inverted matrix technique, was performed to estimate the degree of spatial association between the training sites and predictor patterns on the evidence maps (the method of estimation used is maximum likelihood; see Chung, 1978; Agterberg, 1989, 1992; Agterberg and others, 1993; and Wright, 1996). Unlike WofE, only one coefficient of spatial association, β, was calculated. The coefficient β represents the information conveyed by W^+ and W^- and is comparable to C, but β affects the favorability map only where evidence map patterns are present (in the WLR approach, the WofE term W^- does not have an equivalent). The coefficients are confined to values between 0 and 1, which can be interpreted as the conditional probabilities (the conditional probability that a unit-cell area of the favorability map contains a training site). Where evidence map coverage was incomplete (data are unknown or missing), the missing data area was assigned an area-weighted mean of the known values in the study area.

The favorability map was produced by applying a ranking scheme, defined by the HRB assessment team and reviewed later in this chapter, to the conditional probabilities (here termed "favorabilities"). The favorabilities were ranked into "favorable" and "prospective" based upon break-points and population groups on cumulative area versus favorability plots. The permissive–favorable boundary was delineated using the "prior favorability" value, which is a simple, or non-conditional probability (given no geoscientific information), and equal to the number of known training sites per unit area (Bonham-Carter, 1994). The favorable–prospective boundary was defined by the most prominent break-point in the cumulative area versus favorability above the prior favorability. Only favorabilities with a statistical significance of ≥ 90 percent (Studentized C ≥ 1.282) were considered; areas of the favorability map below this significance level were masked out. Studentized C is an informal test to determine whether the relative certainty of the calculated favorabilities is greater than zero (Bonham-Carter and others, 1989; Agterberg and others, 1993), and insures that

areas with low confidence (< 90%) are not included in favorable or prospective tracts. A cut-off of 90 percent is not uncommon for WofE and WLR modeling, and it was considered by the HRB assessment team to be a reasonable, conservative level of confidence for delineating the favorable and prospective mineral resources assessment tracts. By comparison, a minerals exploration company, which may be more aggressive and willing to take greater risks, might consider using a much lower level of confidence, such as 50 percent (as well as using multi-class predictor patterns rather than binary).

Construction of the Mineral-Resource Tract Maps

The mineral-resource tract maps were created by merging the knowledge-driven-derived tracts (nonpermissive and permissive) and the data-driven-derived tracts (favorable and prospective). The assessment team made certain revisions to the favorable and prospective tracts (the favorability map) that reflect incomplete data coverage and that address some, but not all, of the expert-based exceptions to the data-driven-derived prediction criteria. These revisions and the overall construction of the tract maps is discussed below. Detailed discussions about the expert-based exceptions are presented in each of the respective mineral deposit type assessment chapters (chapters 7-9).

Construction of the mineral-resource tract maps consisted of four steps: (1) clipping of the favorable and prospective tracts to the extent of geochemistry evidence map coverage, (2) clipping of the favorable and prospective tracts to knowledge-driven-delineated permissive tract, (3) merging of the clipped favorable and prospective tracts with the knowledge-driven-delineated permissive tract, and (4) masking out of areas where the depth to basement is greater than 1 km. These four operations were performed to construct each of the pluton-related, sedimentary rock-hosted Au–Ag, and epithermal mineral-resource tract maps.

In the first part, the extents of the favorable and prospective tracts were truncated to the areal coverage of the geochemistry evidence map. This was done because geochemistry is the strongest predictor where National Uranium Resource Evaluation (NURE) data are available, and absence of NURE geochemical data in some parts of northern Nevada adversely affected the favorability estimates in those areas. In many cases, these regions of missing data are characterized by favorabilities with Student t values < 90 percent. This principally affected the eastern and southeastern parts of the northern Nevada study area, which, although having similar geology and mineral deposits, did not impact the assessment within the HRB (see fig. 2–1, regions outside of green boundary).

In the second part, the favorable and prospective tracts were truncated to the extent of the permissive tract, as delineated in the Nevada assessment (Singer, 1996). The digital datasets available for the data-driven modeling procedure did not allow for acceptable estimation of the nonpermissive–permissive tract boundary. The expert-delineated permissive

tracts in Cox and others (1996) were considered by the HRB assessment team to be the best regional-scale representation of areas permissive for pluton-related deposits, sedimentary rock-hosted Au–Ag deposits, and epithermal deposits available for the whole of northern Nevada. Cox and others (1996) describe the rationale for delineating these permissive tracts.

In the third part, the truncated favorable and prospective tracts were merged with the permissive tract by simply overlaying them onto the permissive tracts. The merged favorable and prospective tracts represent data-driven refinements to the previously delineated knowledge-driven permissive tract.

Finally, in the fourth part, areas of thick cover were masked out and classified as nonpermissive. Cenozoic volcanic and sedimentary deposits that are more than 1 km thick conceal pre-Tertiary basement rocks in many areas of northern Nevada. As discussed in previous assessments (Singer, 1996; Peters and others, 1996), exploration for and mining of deposits in deeply buried (typically greater than 1 km) basement rocks currently are uneconomic. However, this rationale is less applicable to most epithermal deposit types, which largely formed in the Cenozoic units, or to areas within active mining districts, such as the Carlin trend, where exploration and milling infrastructure already are present. A map showing areas of thick Cenozoic cover, as defined by the geophysical data (see chapter 6), was overlain on the mineral-resource tract maps to mask out areas of deeply buried basement. The depth-to-basement map used here differs somewhat from that used to define nonpermissive tracts in the Nevada assessment (Cox and others, 1996). As a result, the boundaries between the nonpermissive and permissive tracts shown on the final maps for this assessment in part reflect both the previously and currently defined depths to basement. Regardless of the depth-to-basement map used, the areas defined by one or both methods indicate thick Cenozoic cover above the older basement rocks.

Databases

The datasets used for the HRB mineral-resource assessment represent many different aspects of geology, geophysics, geochemistry, and metallogeny for northern Nevada. They come in a wide variety of formats and from various published and unpublished sources in government, academia, and industry. The HRB assessment team selected datasets that provide information about the formation and distribution of the mineral systems being assessed, and evaluated their suitability for data-driven modeling. In some instances, assessment team members created the datasets that were used for data-driven modeling. Some datasets, such as gravity and magnetic anomalies and NURE geochemistry, were applicable to both knowledge- and data-driven analysis and modeling. Other data sources, such as informative large- and small-scale schematic figures in the published literature, were not suitable for data-driven modeling because they lacked necessary resolution, accuracy, or areal coverage. However, the information from those figures conceptu-

ally and qualitatively aided the knowledge-driven component of the assessment process. The following sections review datasets used for data-driven modeling (see fig. 2–3).

The digital datasets used for the assessment were portrayed and used at a regional scale, consistent with the regional scale of the assessment. The information contained in those datasets represents a variety of scales of location and concept. For example, the training sites represent very specific geographic locations of economic or subeconomic mineral deposits. In contrast, the 1:500,000-scale state geologic map (Stewart and Carlson, 1978) is an accurate but somewhat generalized portrayal of the actual rock units present: the age-lithology units on the map are combinations of one or more geologic units that originally were identified by larger-scale mapping. Similarly, data layers derived from that map (such as volcanic terranes, lithotectonic terranes, thrust faults and windows) are generalized from the larger-scale geologic data. Thus, the various datasets used for the assessment were not necessarily created with the same original scale and concept in mind. An example of this is the use of site-specific training sites with maps showing generalized Tertiary volcanic units and magnetic terranes in the assessment of epithermal deposits (see chapter 9).

In addition, the team recognized during the course of the assessment that some datasets were incomplete, such as comprehensive data on the ages and compositions of the plutons, biostratigraphic data on Paleozoic sedimentary rocks, magnetic properties of igneous rocks, and the ages of many volcanic rocks. Some of the needed data were collected during the course of other parallel projects and used for this assessment, but comprehensive acquisition of these data over such a large region was beyond the scope of this assessment. Some potentially very useful evidence layers, such as pluton chemistry, could not be used because of incomplete information across the entire study area. The assessment team felt that a more comprehensive database could have led to a more refined mineral-resource assessment, even at a regional scale, and it recommends that acquisition of these data be a focus for future geologic studies in the region.

Training Sites

A training site dataset for northern Nevada (see study area, fig. 2–1) was created by selecting, modifying, and updating mineral sites from the Nevada Bureau of Mines and Geology (NBMG) database of gold and silver resources in Nevada (Davis and Tingley, 1999). The NBMG database contains precious- and base-metal mineral deposits and occurrences with a noted or implied gold and (or) silver resource or reserve discovered since 1930, and includes industrial-mineral deposits and occurrences that contain a significant amount of gold or silver. All mineral site locations were determined from locations on 1:24,000 or larger scale maps or by making GPS determinations at the sites (J. V. Tingley, oral commun., 2000). The HRB assessment team checked the site locations for overall positional accuracy and discarded duplicates. The team

then classified the NBMG mineral sites into three deposit-type subsets—pluton-related, sedimentary rock-hosted Au–Ag, and epithermal—and added 40 pluton-related and 4 epithermal sites (the sedimentary rock-hosted sites were considered to be complete). A total of 519 training sites were used for data-driven modeling, and classified and subdivided as follows:

- Pluton-related deposit-type training sites, consisting of 92 occurrences and deposits (fig. 2–5) that include porphyry (Cu, Mo (Climax, low–F), and Au), skarn (Au, Ag, Cu, Fe, Pb, Zn), and polymetallic replacement and vein (see chapter 7 and table 7–1).

- Sedimentary rock-hosted Au–Ag deposit-type training sites, consisting of 293 occurrences and deposits (fig. 2–6) that include Carlin-type (northern and southern subtypes) and distal-disseminated type deposits (see chapter 8 and table 8–1).

- Epithermal deposit-type training sites, consisting of 134 occurrences and deposits (fig. 2–7) that include low-sulfidation and hot-spring type deposits (see chapter 9 and table 9–1).

The training sites represent orebodies that have been mined, either by open pit or underground methods, or that have been identified with exploration drilling. The sites are size independent, but they reflect concentrations of metals that are considered to be large enough to warrant mining or closer scrutiny. Depending upon the mineralized system and the type and amount of mining and exploration, some mineralized systems are represented by multiple training sites, whereas others may have only one site. Many pluton-related systems, such as at Battle Mountain, have multiple training sites that, in part, reflect different mineral deposits and mines (porphyry, skarn) related to the same mineralizing system. Further, some epithermal deposits, such as Hog Ranch, Mule Canyon, and Willard, have several identified orebodies, each represented by a training site although they all formed in the same mineralizing system; Willard, as noted in chapter 9, is a very small epithermal deposit. In contrast, only one training site represents the Ken Snyder Au-Ag deposit at Midas, which is much larger than the Hog Ranch, Mule Canyon, and Willard deposits.

For the purposes of data-driven modeling, training sites that occur within 1 km of one another are considered one site. This is because the modeling is carried out for a discrete unit cell area of 1 km^2 (see discussion in "Data Driven Component" section earlier in this chapter). When considered in this manner, the number of sites that remain for a given mineralized system can be regarded as a proxy for its size and (or) importance. The rationale for this approximation is that, under ideal conditions, a larger and (or) longer-lived system would generate more and (or) larger and (or) richer orebodies; hence, the greater the number of sites, the greater the size and (or) importance of the system. An obvious scenario that illustrates the break down of this rationale is where a large, cylindrical ore body is oriented perpendicular to the surface and is mined top-down along its length. The same orebody, if oriented hori-

zontally, would likely be mined from multiple sites. As such, this proxy is a gross, first-order approximation for system size and (or) importance. Nonetheless, while not perfect, it is not an unreasonable measure of size and (or) importance given the dearth of production, reserve, or other endowment data for training sites. Additionally, it was beyond the scope of this assessment for team members to visit each individual site to determine or collect such information.

Evidence Maps

Fourteen evidence maps were prepared from datasets chosen by the HRB assessment team. A number of the datasets were suitable for creating evidence maps that could be applied to assessment of all three broad deposit classes, whereas others could only be applied to one or two of classes. For example, the reanalyzed NURE geochemical samples, particularly the arsenic analyses, were used in all assessments. The Nevada state geologic map (Stewart and Carlson, 1978) and its derivative products were used in the assessment of all three systems, but in different ways. Some geologic units and structures are more appropriately used for assessing one type of system than another. As such, certain rock types and structures were isolated and extracted from the Nevada state geologic map for the purpose of assessing the different mineralizing systems. Volcanic rocks are related specifically to the epithermal deposit types, and plutonic rocks to the pluton-related and some sedimentary rock-hosted Au–Ag deposit types. Structural windows and lithotectonic terranes are particularly important as evidence for the occurrence of sedimentary rock-hosted Au–Ag deposit types. All datasets that were used by the assessment team for knowledge- and data-driven analysis and modeling were complete for the scale at which they were applied.

The evidence maps are reviewed below. They are listed in bullet form under subheadings that reflect the source data-type from which they were created. Shortened names, which appear in italics, have been given to the evidence maps and are used in tables and text throughout the subsequent chapters of this report. Basic information about data processing is provided, as well as references where additional details are discussed. The rationale for selection, application, and interpretation of the evidence maps used for each of the three mineralizing system assessments are described in more detail in ensuing sections and in the respective assessment sections (chapters 7-9).

Lithology

The lithology-related evidence maps were all prepared or derived from the 1:500,000 geologic map of Nevada (Stewart and Carlson, 1978). The dataset was obtained from Raines and others (1996) in vector format and converted to raster with 500-m cell size.

- Geologic units (fig. 2–8). The geologic map of Nevada consists of 101 map units. As described in Stewart and Carlson (1978) and Stewart (1980), the map units are

combinations of one or more formations or geologic units of similar age and geologic context that were identified during larger-scale geologic mapping. In some cases, such as map units that consist entirely of Tertiary basalts, the map units are good proxies for lithologic units. In many cases, however, the inclusion of several disparate lithologies into one map unit, such as shale, sandstone, and limestone in some Paleozoic-age map units, limits a direct comparison to lithology (see discussion in chapter 8). For analysis and modeling, this dataset is considered to have a resolution of 500–1,000 m.

- Epithermal-lithologic units (fig. 2–9). The 101 geologic map units were reclassified to five, expert-ranked lithologic host units for epithermal deposits and occurrences, as defined in chapter 9. For analysis and modeling, this dataset is considered to have a resolution of 500–1,000 m.

- Lithodiversity (fig. 2–10). Lithodiversity for the geologic map of Nevada was generated by counting the number of unique map units in a square moving window that is 2.5–by–2.5 km in dimension. Lithodiversity was calculated by centering the window on each cell, counting the number of unique geologic map units within the neighborhood, assigning the number to the center cell, and then incrementing the window by one cell. The lithodiversity map was reclassified such that each map class value (an integer) represents diversity. For example, lithodiversity map class 5 represents five geologic units within a sample neighborhood. Mihalasky (2001) and Mihalasky and Bonham-Carter (1999; 2001) discuss methods of preparation and processing of lithodiversity. For analysis and modeling, this dataset is considered to have a resolution of 1,000 m.

- Pluton proximity (fig. 2–11). The plutonic rocks, represented in terms of unit abbreviations from the geologic map of Nevada, include Tri, Tmi, Ti, Tr2, Tr1, TJgr, Tgr, Mzgr, Kgr, KJd, Jgr, TRgr, and TRlgr. These units range in age from Middle-Late Triassic to late Miocene, but with respect to total area covered, the units predominantly are Mesozoic. Plutonic and intrusive bodies were buffered with a distance interval of 1 km. The plutons were included as part of the first buffer. For analysis and modeling, this dataset is considered to have a resolution of 1,000 meters.

Structure and tectonics

The structure- and tectonic-related evidence maps were all prepared or derived from (1) the 1:750,000 preliminary map of allochthonous tectonic ("lithotectonic terrane") units in Nevada and eastern California (Lahren and others, in press) or (2) interpreted from digital elevation and remotely sensed

data. The preliminary map of allochthonous tectonic units was obtained in vector format from K.A. Connors (written commun., 1999) and converted to raster with 500–m cell size. Interpreted datasets were processed as described below.

- Lithotectonic-terrane units (fig. 2–12). The lithotectonic-terrane units map shows geologic map units that, in combination, represent specific allochthonous terranes in Nevada. These terranes include, but are not limited to, the Roberts Mountains, Golconda, and Fencemaker allochthons. The definitions of the allochthonous terranes were based on many studies reported in the published literature. The locations of the units and the terranes that they define are based on the geologic units shown in the geologic map of Nevada (Stewart and Carlson, 1978). For analysis and modeling, this dataset is considered to have a resolution of 1,000 m.

- Thrust proximity (fig. 2–13), defined as the proximity to thrust faults between upper- and lower-plate tectonic units and structural windows of the Roberts Mountains thrust fault. As described in chapter 8, this thrust was instrumental in the localization of many sedimentary rock-hosted Au-Ag deposits. Thrust faults related to other allochthons were not considered in this assessment. The thrust faults were extracted and buffered with a distance interval of 1 km. The faults were included as part of the first buffer. For analysis and modeling, this dataset is considered to have a resolution of 1,000 m.

- NE (northeast) linear features (fig. 2–14), consisting of the Crescent Valley-Independence (CVIL) and Getchell (GLF) lineaments. Two corridor regions that envelop the CVIL (Peters, 1998; Theodore and Peters, 1998) and the Getchell mineral trend were interpreted by the assessment team from LANDSAT MSS imagery (60–m resolution) and shaded relief of topography (30 arc-second, ~ 1-km resolution). The corridor regions were outlined in vector format and converted to raster with 2,000–m cell size. For analysis and modeling, this dataset is considered to have a resolution of 2,000 m.

Geochemistry

The geochemical-related evidence maps were derived from newly reanalyzed NURE geochemical samples (chapter 5). The data were acquired as point-sample concentrations, which were preprocessed in various ways and converted to continuous raster surfaces, as outlined below.

- As–frequency (fig. 2–15), representing As concentration (partial digestion) that was processed in the frequency domain. The concentration values were log transformed (base-10) and converted to a continuous

raster surface with 1,000–m cell size using a minimum-curvature spatial interpolator. The data were resolved into several textural components by computing the spatial frequency structure of the surface, then deriving a series of band-pass frequency filters to decompose the surface in the frequency domain into distinct layers, each with varying degrees of smoothness. The residual As anomaly evidence map corresponds to subtraction of the long- and medium-wavelength components of the signal. The rationale for this method, and the preparation and processing of this dataset, are discussed in greater detail in chapter 5 and in Ludington and others (2000). For analysis and modeling, this dataset is considered to have a resolution of 500–1,000 m.

- As–spatial (fig. 2–16), representing As concentration (partial digestion) that was processed in the spatial domain. The concentration values were log transformed (base-10) and converted to two continuous raster surfaces, "local" and "regional", with 1,000–m cell size using an inverse distance spatial interpolator. The local surface was interpolated using a fixed sampling radius of 15 km and a distance-decay rate that diminishes with the square of the distance, and represents the local-scale variation of As. The regional surface was interpolated using a fixed sampling radius of 100 km and a distance-decay rate that diminishes with square of the distance, and represents the broad, regional-scale variation of arsenic. The regional surface was subtracted from the local to yield a third surface, the residual local-scale anomaly, which represents departure from the background variation. The residual local-scale anomaly is used as the evidence map. In essence, a nonlinear filter was applied to the data to remove the regional-scale background variation and reveal the local-scale anomaly. The rationale for this method is discussed in Cheng and others (1996) and Cheng (1999). For analysis and modeling, this dataset is considered to have a resolution of 500–1,000 m.

- Ba/Na (fig. 2–17), calculated from Ba and Na concentrations (total digestion). The ratio values were converted to a continuous raster surface with 1,000–m cell size using an inverse distance spatial interpolator. The surface was interpolated using a fixed sampling radius of 15 km and a distance-decay rate that diminishes with the square of the distance. Ba/Na is thought to provide a reasonable overall relative measure of regional-scale alteration activity associated with formation of Carlin-type sedimentary rock-hosted deposits, particularly north Carlin-type (Mihalasky, 2001). For analysis and modeling, this dataset is considered to have a resolution of 500–1,000 m.

- Cu–Pb–Zn signature (fig. 2–18), calculated from Cu, Pb, and Zn concentrations (total digestion). The concentration values were (1) log transformed (base

10), (2) normalized to a unitless, standardized scale (a "z–score"; see McGrew and Monroe, 1993, and Theodore and others, 2000), and (3) converted to three continuous raster surfaces with 1,000–meter cell size using an inverse distance spatial interpolator. For surface interpolation, a fixed sampling radius of 15 km and a distance-decay rate that diminishes with the square of the distance was used. The three datasets were then re-scaled between zero and one, where the z–score value of zero was set to 0.5. After the re-scaling, any values greater than one or less than zero were set to 1 and 0, respectively. Processed in this way, z-score value of zero, which represents the mean log value of a given element concentration, is assigned a fuzzy membership score of 0.5. The datasets were then mathematically combined using a fuzzy logic "OR" operator (Bonham-Carter, 1994), which selects the maximum value at a given cell when the rasters are combined, yielding an elevated Cu–Pb–Zn signature value wherever a high value in any one of the three elements is present. The output of the fuzzy operator is the evidence map. For analysis and modeling, this dataset is considered to have a resolution of 500–1,000 m.

Geophysics

The geophysical-related evidence maps are all derivative products, interpreted from a variety of gravity and magnetic anomaly datasets and maps. They contribute subsurface evidence for modeling by providing information about local- and regional-scale crustal structures and rocks at depth that are important to mineralization and ore formation, and ultimately to the delineation of mineral resource assessment tracts. The preparation and processing of these datasets is discussed in greater detail in chapter 6. The interpretive datasets, provided in vector format, were converted to raster surfaces as described below.

- Basement gravity terranes (fig. 2–19), reflecting regions of similar anomaly features or geophysical fabric. The terranes were derived from the inspection of isostatic and basement gravity maps, and maximum horizontal gradients of basement gravity anomalies. The terranes were outlined in vector format and converted to raster with a 500–m cell size. For analysis and modeling, this dataset is considered to have a resolution of 1,000 m.

- Basement gravity lineaments (fig. 2–20), reflecting abrupt lateral variations in the density of basement rocks. The lineaments were derived from basement gravity anomalies and their maximum horizontal gradients. The linear features were buffered at a distance interval of 2 km. The features were included as part of the first buffer. For analysis and modeling, this dataset is considered to have a resolution of 2,000 m.

- Magnetic terranes (fig. 2–21), reflecting regions of similar anomaly features or geophysical fabric. The terranes were derived from the inspection of a total intensity aeromagnetic map, derivative magnetic maps, and maximum horizontal gradients of magnetic potential anomalies. The regions were outlined in vector format and converted to raster with a 500–m cell size. For analysis and modeling, this dataset is considered to have a resolution of 1,000 m. A subset of this evidence map, showing the magnetic terranes related to middle Miocene mafic intrusive zones, was created and used for the epithermal assessment (see chapters 6, 9).

Mineral

A mineral-related evidence map was prepared from the USGS Mineral Resources Data System database (MRDS; McFaul and others, 2000). This evidence map was used only for the pluton-related mineral-resource tract map.

- Skarn proximity (fig. 2–22). As an extension of the classification of mineral deposits done in the Winnemucca-Surprise assessment (Peters and others, 1996), the HRB mineral-resource assessment team classified 550 MRDS mineral sites as skarn related, based on Cox and Singer (1986) deposit model types 14a, 18a, 18b, 18c, 18d, 18e, and 18f. The mineral sites were buffered at distance interval of 1 km. The sites were included as part of the first buffer. For analysis and modeling, this dataset is considered to have a resolution of 1,000 m.

Other

- Depth to basement (fig. 2–23), reflecting thickness of Cenozoic cover deposits. Isostatic residual gravity data were used to produce a map of the thickness of Cenozoic deposits based on assumed variations of density with depth in these deposits (chapter 6; Jachens and others, 1996). Computations were carried out using continuous raster surfaces with 2,000–m cell size. The depth to basement map does not serve as an evidence map proper. Rather, it is used as an overlay on the mineral-resource tract maps to mask out areas that are covered by Cenozoic deposits that are more than 1 km thick. For analysis and modeling, this dataset is considered to have a resolution of 2,000 m.
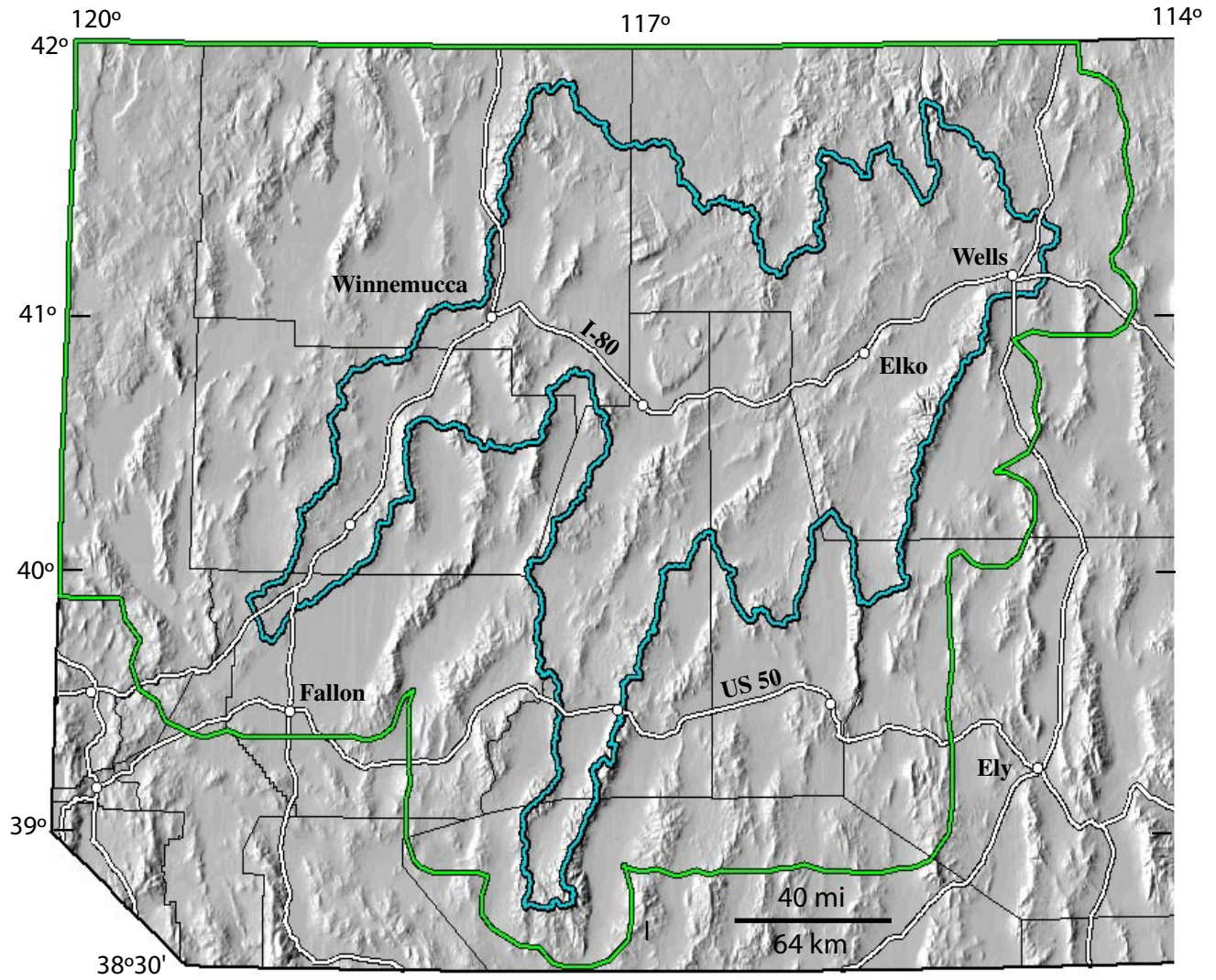
Figure 2-1.   Mineral resource assessment region, northern Nevada, shown on background of shaded relief with a southern boundary of 38°30′ north latitude. The area outlined in green represents a 15-km distance buffer around all National Uranium Resource Evaluation (NURE) geochemical samples used for the Humboldt River Basin (HRB) assessment, clipped to the north and west by the state boundary. Mineral resource assessment maps for pluton-related, sedimentary rock-hosted, and epithermal deposit-types are provided for this area in chapters 7-9. HRB outlined in light blue.

Modeling Procedure	*Procedure Description*	*Modeling Technique*

Mineral Occurrences And Deposits

Maps of Geoscientific Phenomena

Data Selected By Experts

Weights of Evidence

Measurement of spatial association between occurrences and deposits and maps

Optimization of maps for prediction

Weighted Logistic Regression

Combination of maps for prediction

DATA-DRIVEN

WLR Favorability Ranking Scheme

Break-points between prospective-favorable and favorable-permissive determined

Favorable and prospective tracts delineated

Geochemistry Coverage

Permissive Tract

Favorable and prospective tracts clipped to extent of geochemistry data and to expert-delineated permissive tract

EXPERT-DRIVEN

Favorable and prospective tracts combined with expert-delineated permissive tract, and areas of thick cover masked out

Mineral Resource Assessment Map

Figure 2-2. Flow chart illustrating the construction of the mineral resource tract maps. The procedure consists of data-driven and knowledge-driven components.
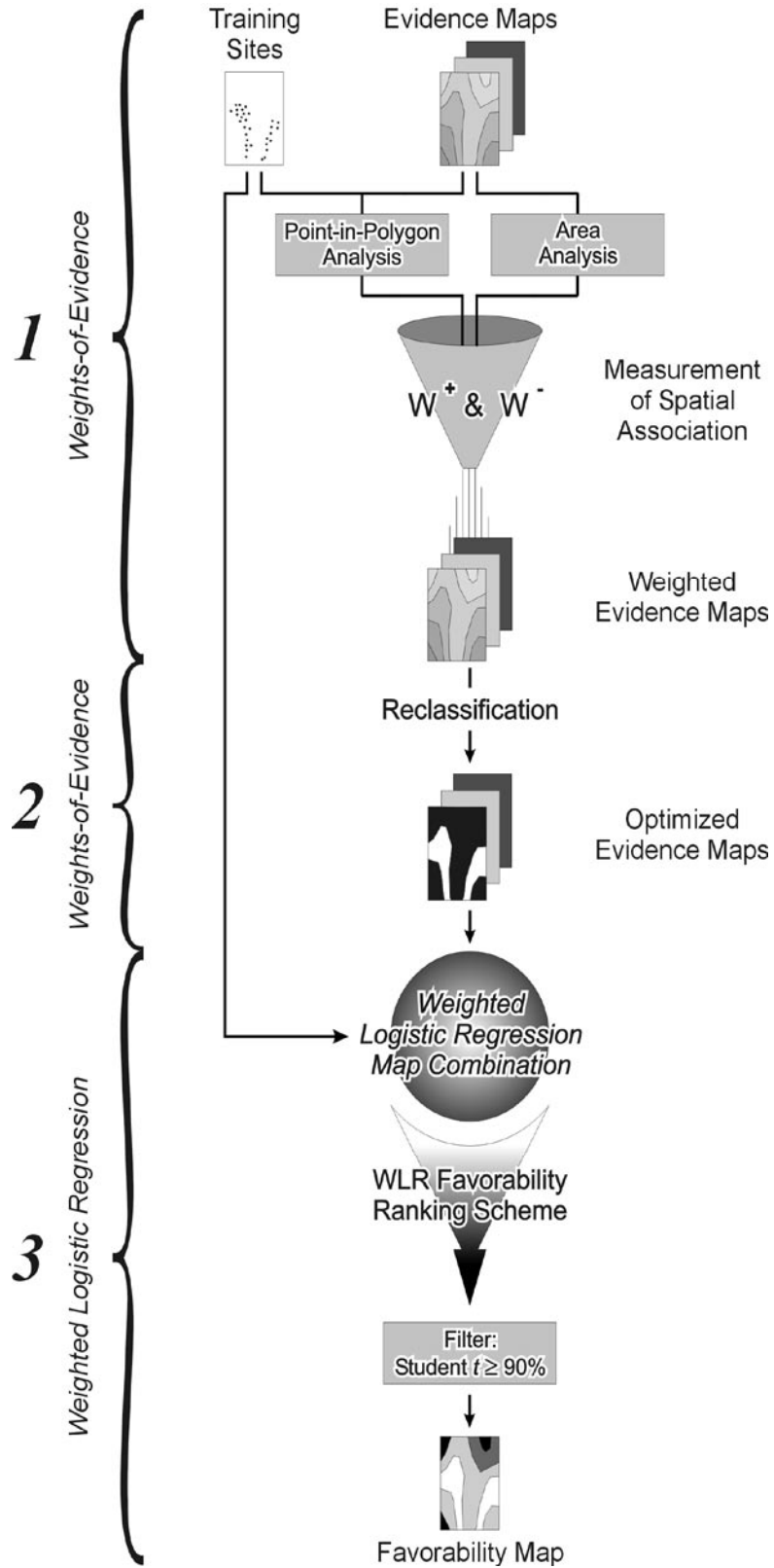
Figure 2-3. Flow chart illustrating the data-driven modeling component of the construction of the mineral resource tract maps (see fig. 2-2). It is subdivided into three main parts, as indicated by the numbered brackets on the left, and was used to delineate prospective and favorable assessment tracts.

Map Unit Grouping	0 - 3	3 - 10
Proximity:	Pattern Present (W$^+$)	Pattern Absent (W$^-$)
Intensity:	Pattern Absent (W$^-$)	Pattern Present (W$^+$)
Concetration:	Pattern Absent (W$^-$)	Pattern Present (W$^+$)
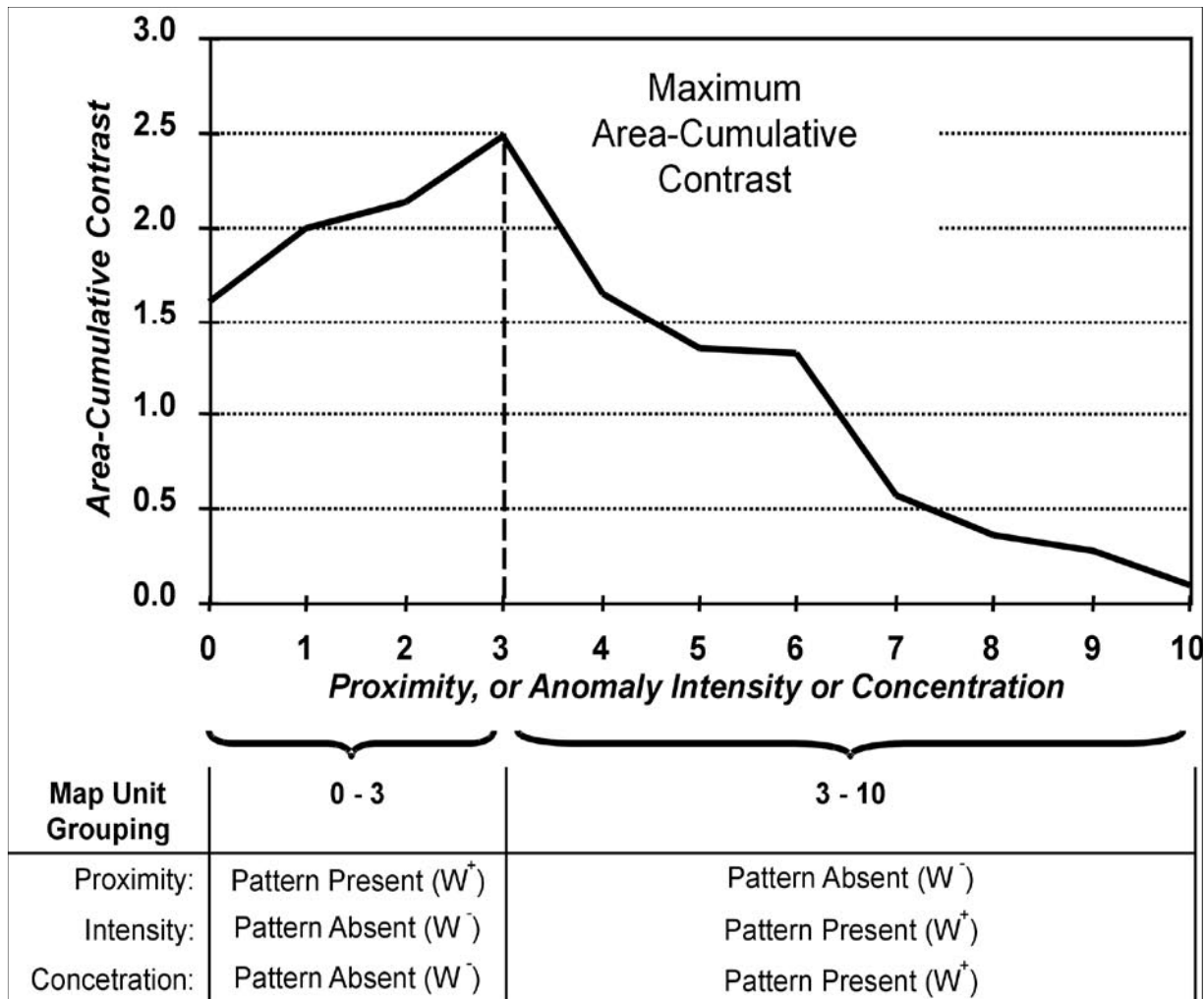
Figure 2-4.   Area-cumulative contrast curve for an evidence map that has 10 classes. This curve is used to help determine the optimum threshold between absence and presence of a predictor pattern for ordinal (or ranked), interval, or ratio scaled data. The table in the lower part of the figure shows examples of how the classes would be grouped into predictor pattern present or absent for measurements of proximity (0 = close; 10 = far), intensity (0 = low; 10 = high), and concentration (0 = low; 10 = high).
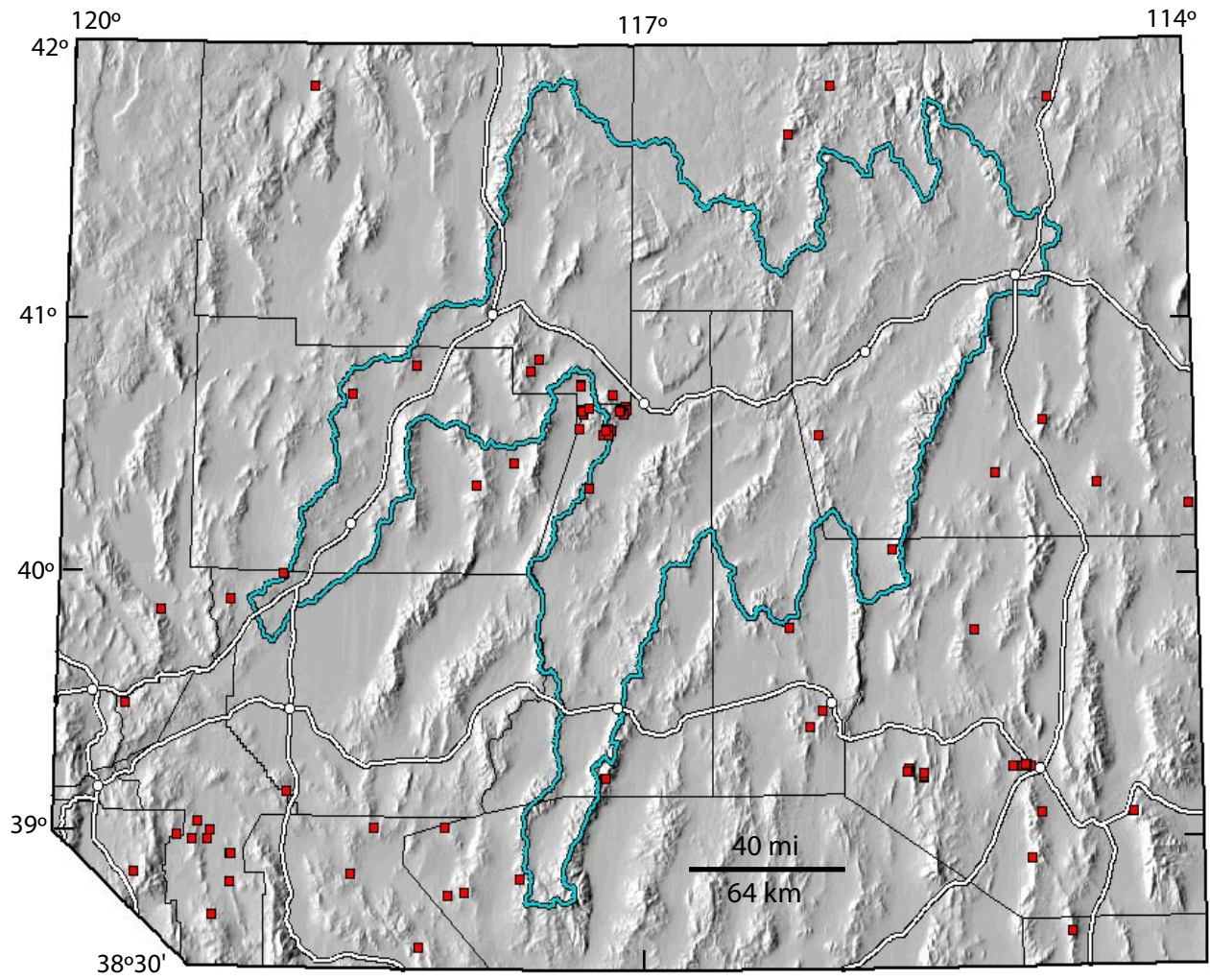
Figure 2-5.   Pluton-related deposit training sites (red squares). Humboldt River Basin outlined in blue. Roads and towns the same as shown in figure 2-1.
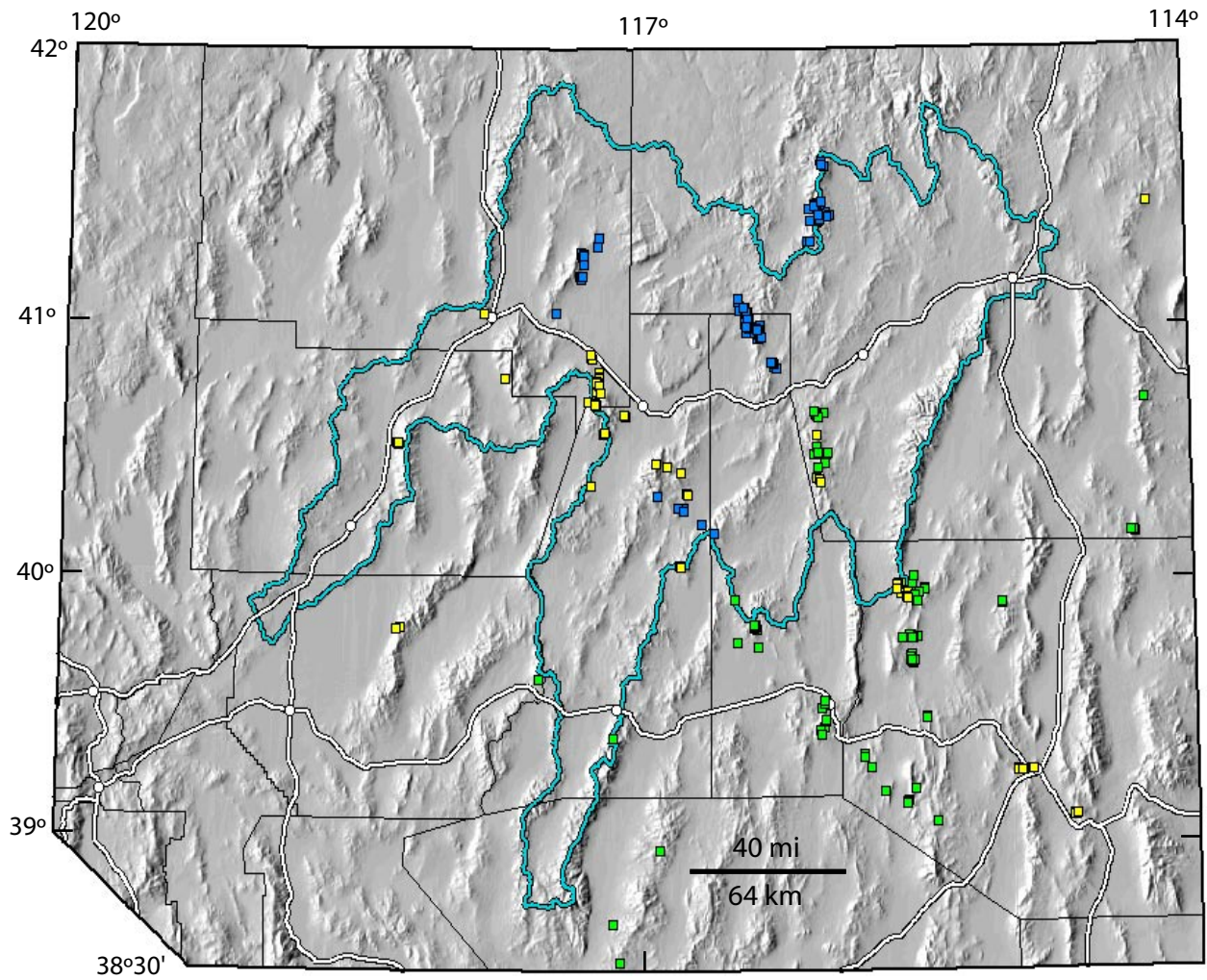
Figure 2-6.   Sedimentary rock-hosted deposit training sites. Blue squares represent northern Carlin-type, green squares southern Carlin-type, and yellow squares distal-disseminated Ag-Au sites. Humboldt River Basin outlined in blue. Roads and towns the same as shown in figure 2-1.
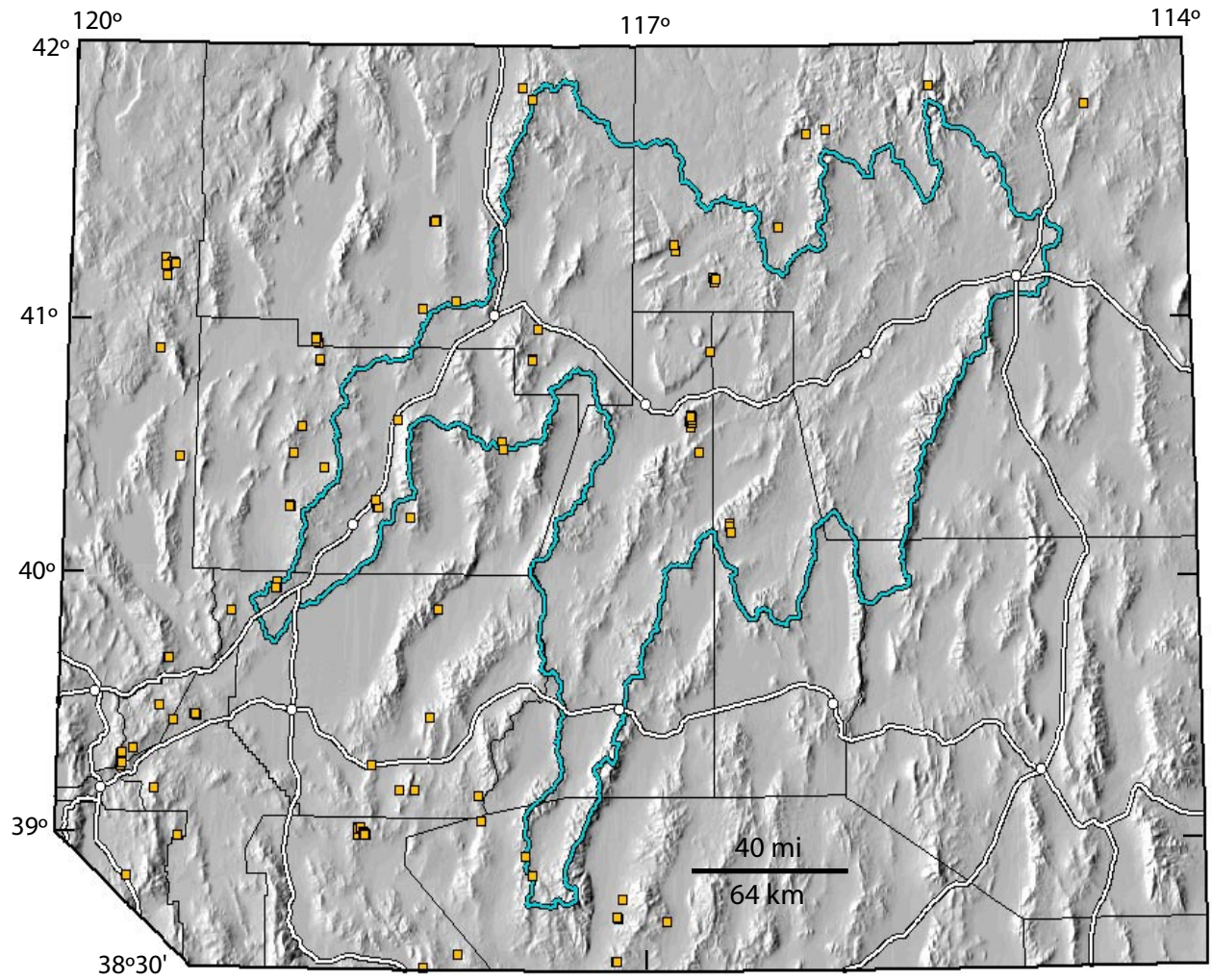
Figure 2-7. Epithermal deposit training sites (orange squares). Humboldt River Basin outlined in blue. Roads and towns the same as shown in figure 2-1.
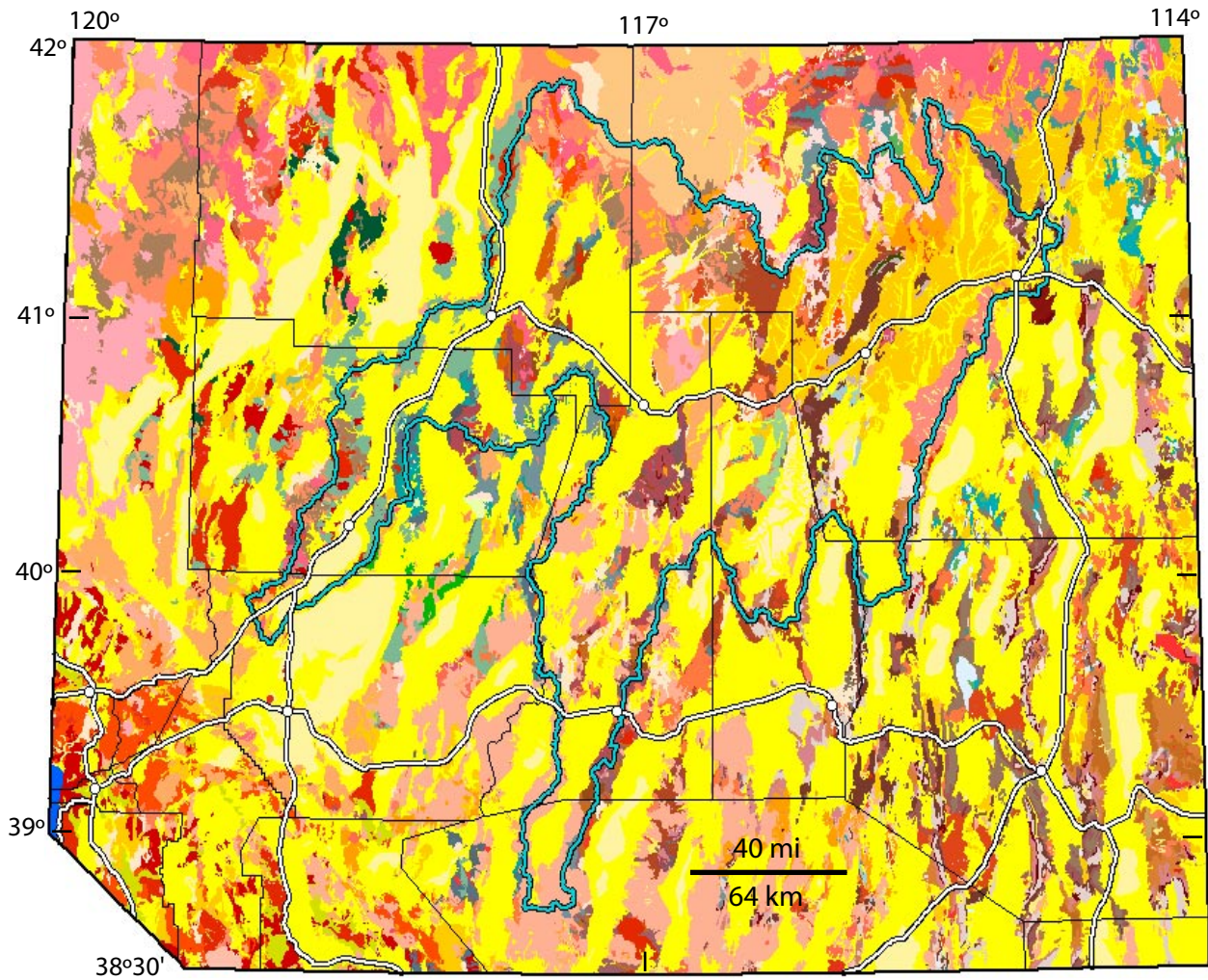
Figure 2-8.   Geologic map of northern Nevada (from Stewart and Carlson, 1978). In general, yellows and oranges are unconsolidated Pliocene and Quaternary sedimentary units; reds and pinks are Phanerozoic plutonic and Tertiary volcanic rocks; and blues, grays, greens, and browns are Phanerozoic sedimentary rocks. Humboldt River Basin outlined in blue. Roads and towns the same as shown in figure 2-1.
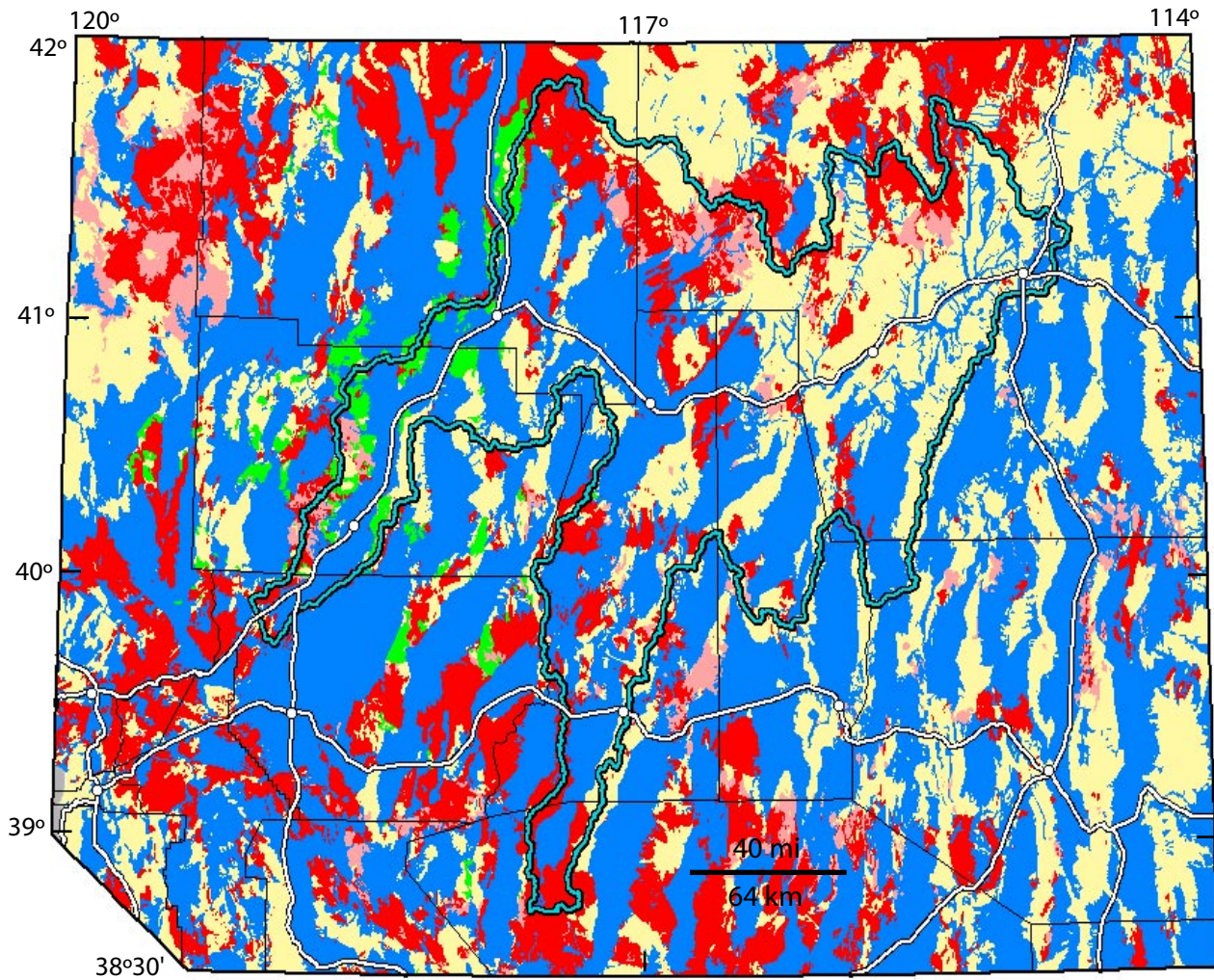
Figure 2-9.   Epithermal-lithologic units evidence map. Expert favorability ranks: prospective-high (red), permissive-medium (light red), permissive-Jungo (green), permissive-low (light yellow), and permissive-Quaternary (blue). See chapter 9 for more details. Humboldt River Basin outlined in blue. Roads and towns the same as shown in figure 1.
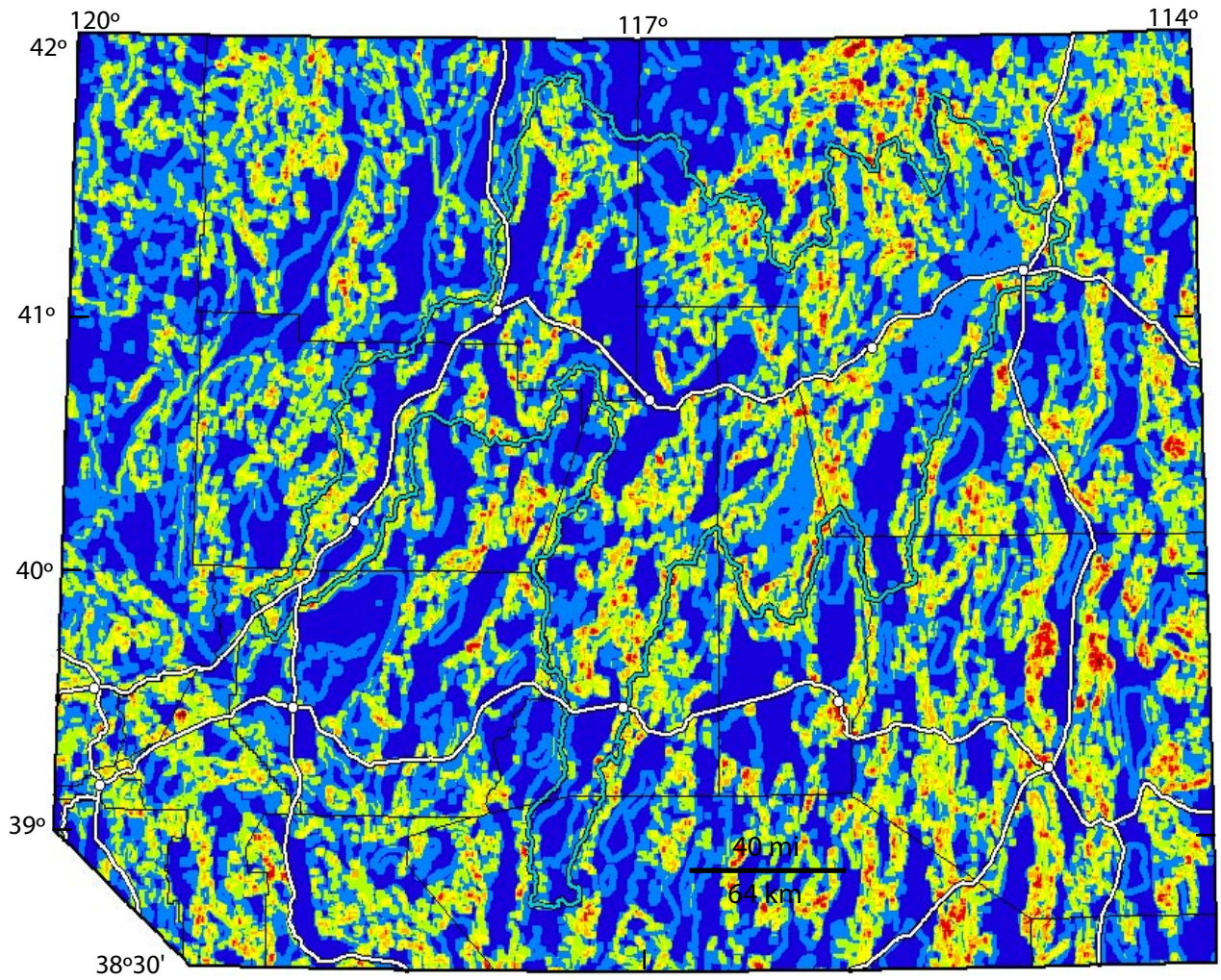
Figure 2-10. Lithodiversity evidence map. Lithodiveristy ranges from 1 to 11. Lower lithodiversity is represented by cooler colors (blues) and higher lithodiversity by warmer colors (green to dark red). Humboldt River Basin outlined in blue. Roads and towns the same as shown in figure 2-1.
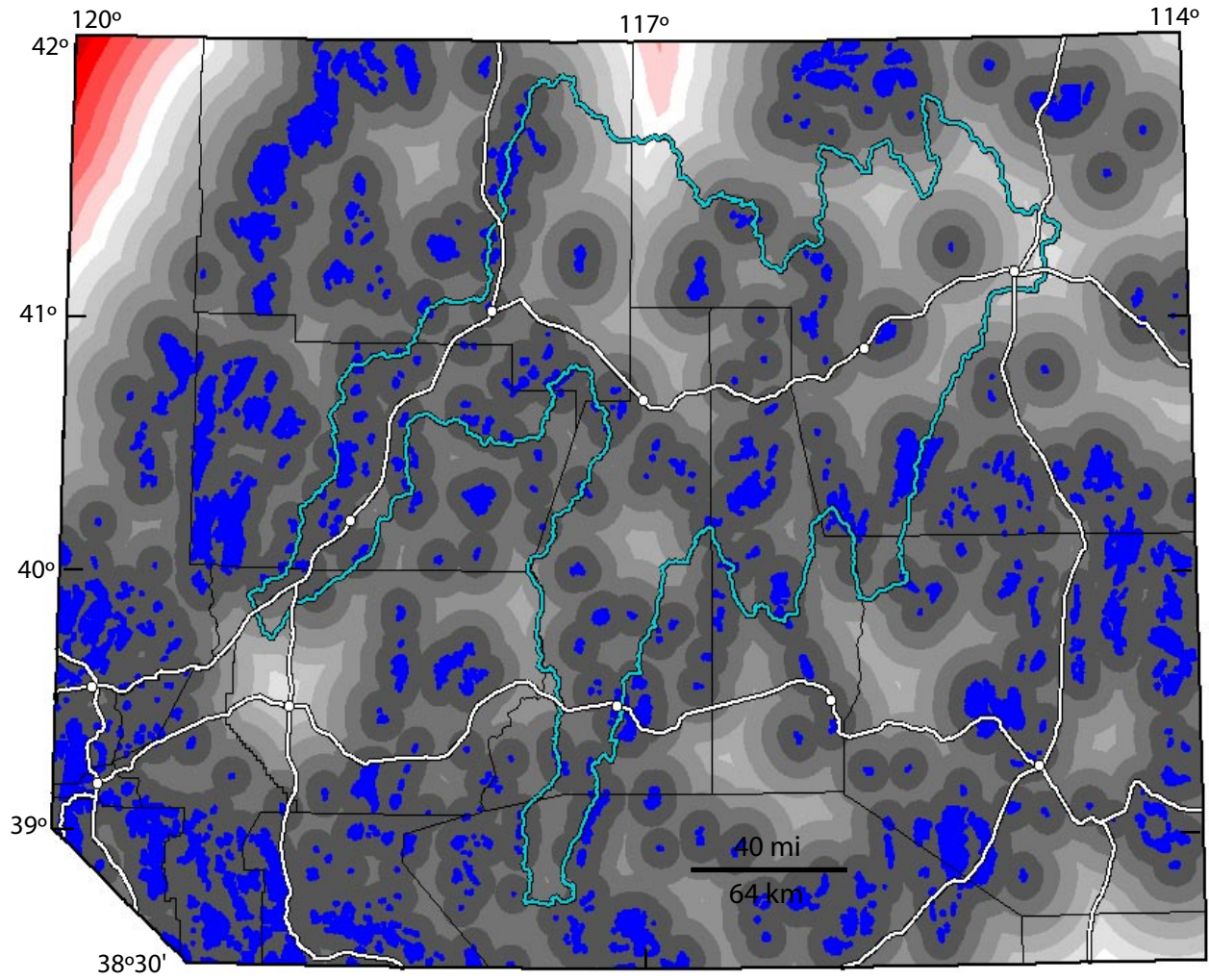
Figure 2-11. Pluton proximity evidence map. Plutons shown in dark blue. The plutons were buffered at 1-km distance intervals. These intervals are too narrow to be visually resolved, and the figure is represents the buffers by showing 10-km buffer widths. Humboldt River Basin outlined in blue. Roads and towns the same as shown in figure 2-1.
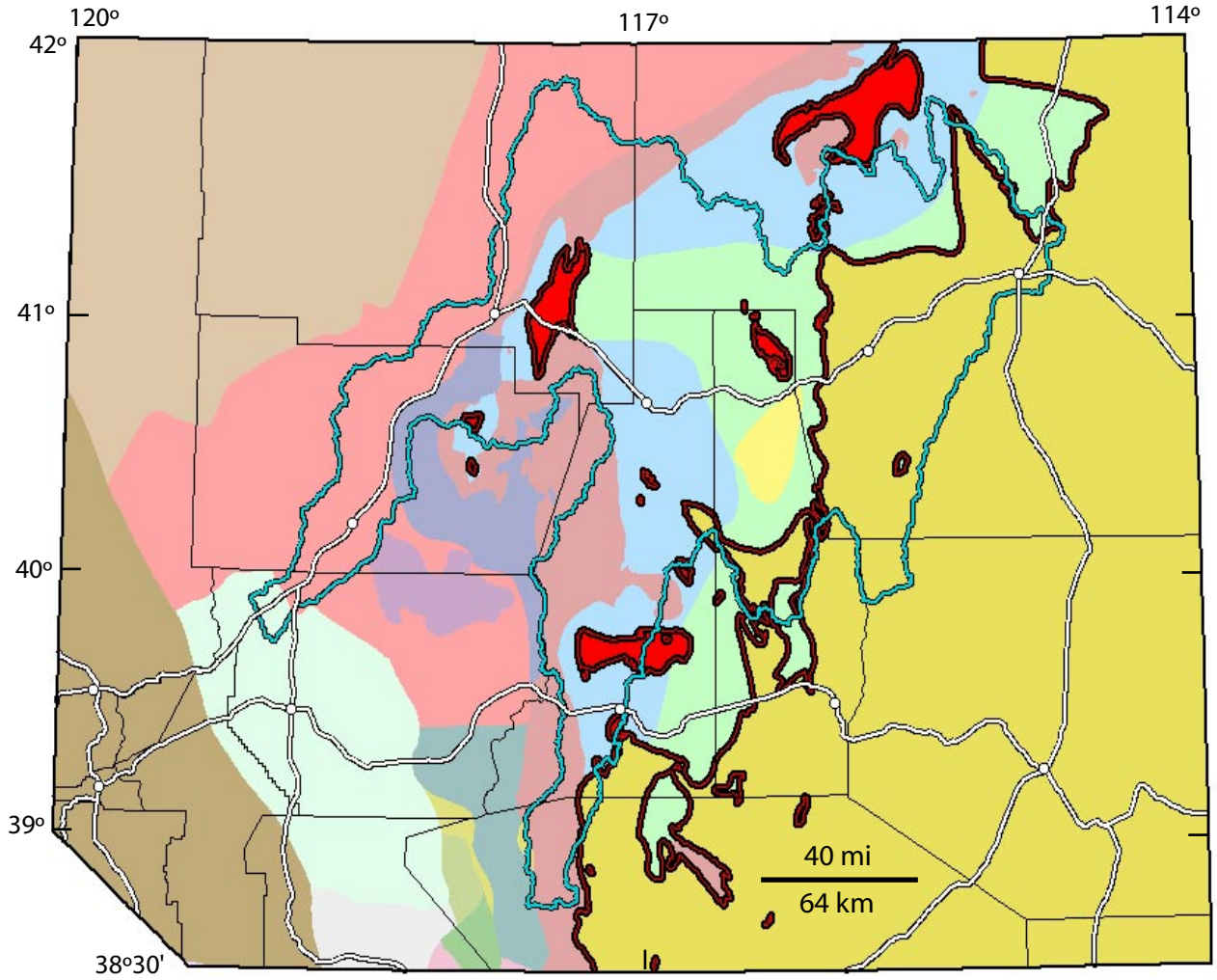
Figure 2-12. Lithotectonic-terrane units evidence map derived from Lahren and others (in press). Dark red line delineates allochthonous-autochthonous terrane thrust contact. Structural windows through allochthonous terranes are shown in red. Humboldt River Basin outlined in blue. Roads and towns the same as shown in figure 2-1.
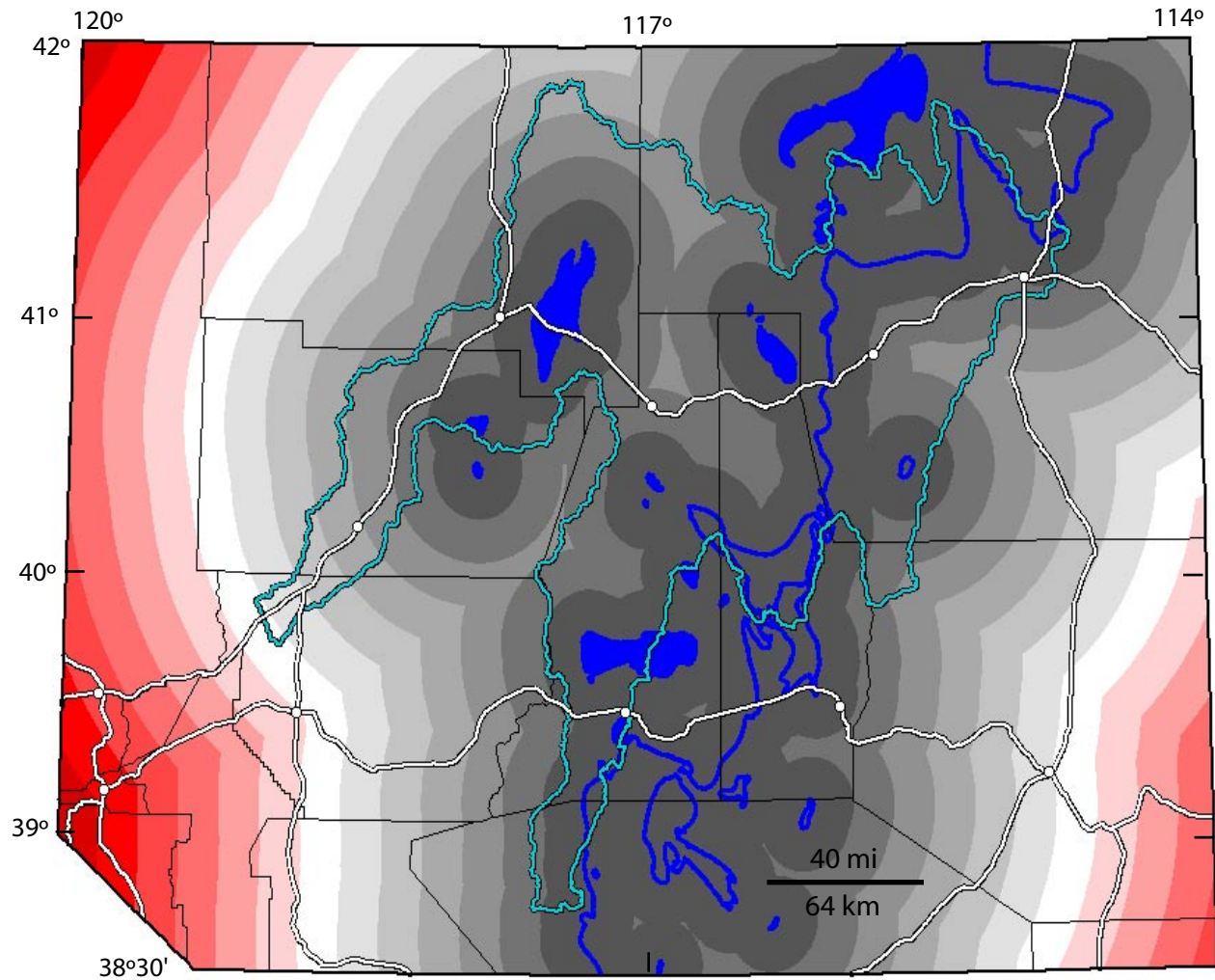
Figure 2-13. Thrust proximity evidence map derived from Lahren and others (in press). Thrust faults and structural windows shown in dark blue. Humboldt River Basin outlined in blue. Roads and towns the same as shown in figure 2-1.
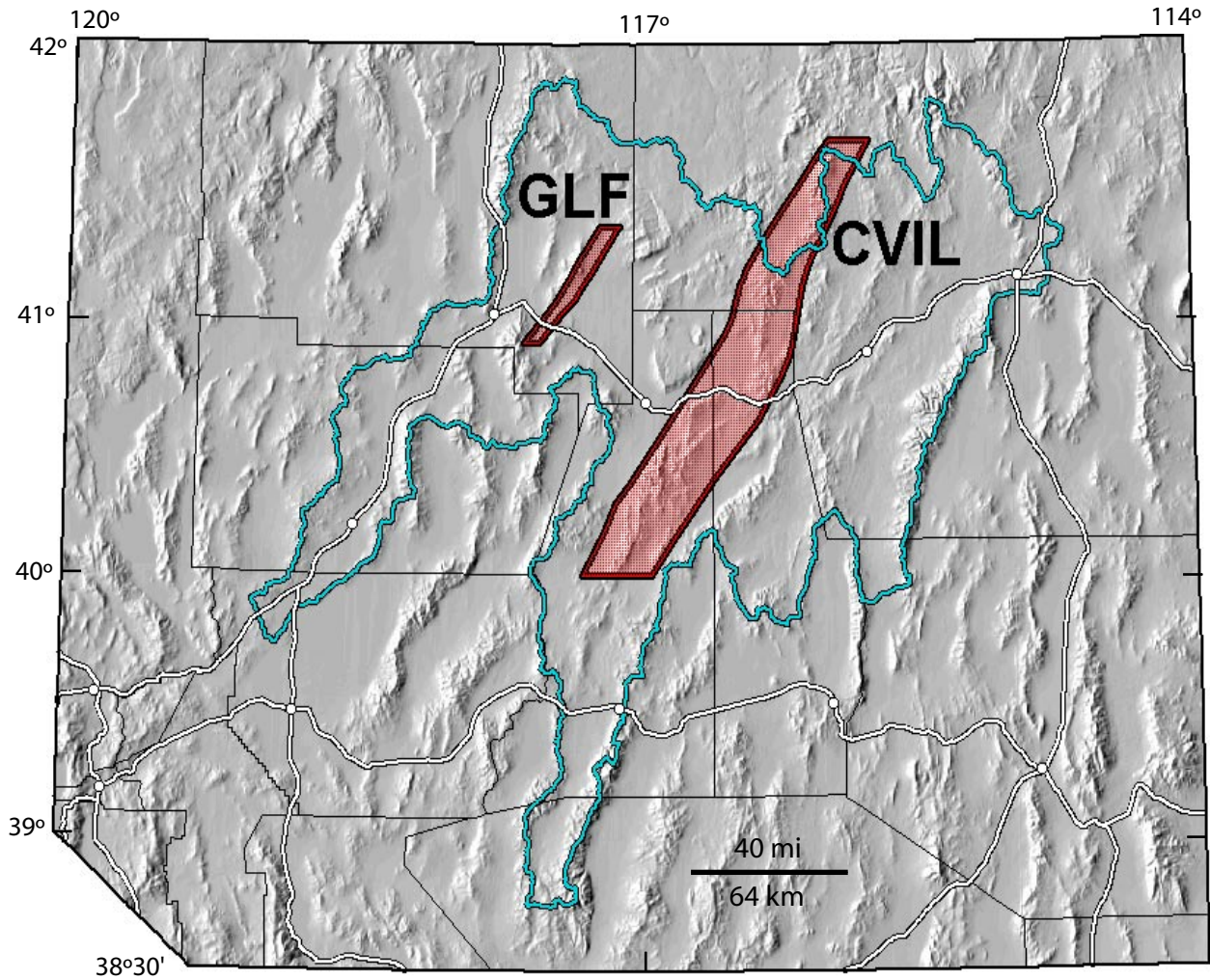
Figure 2-14.   Northeast linear features evidence map, showing the Crescent Valley-Independence (CVIL) and Getchell (GLF) lineaments. Humboldt River Basin outlined in blue. Roads and towns the same as shown in figure 2-1.
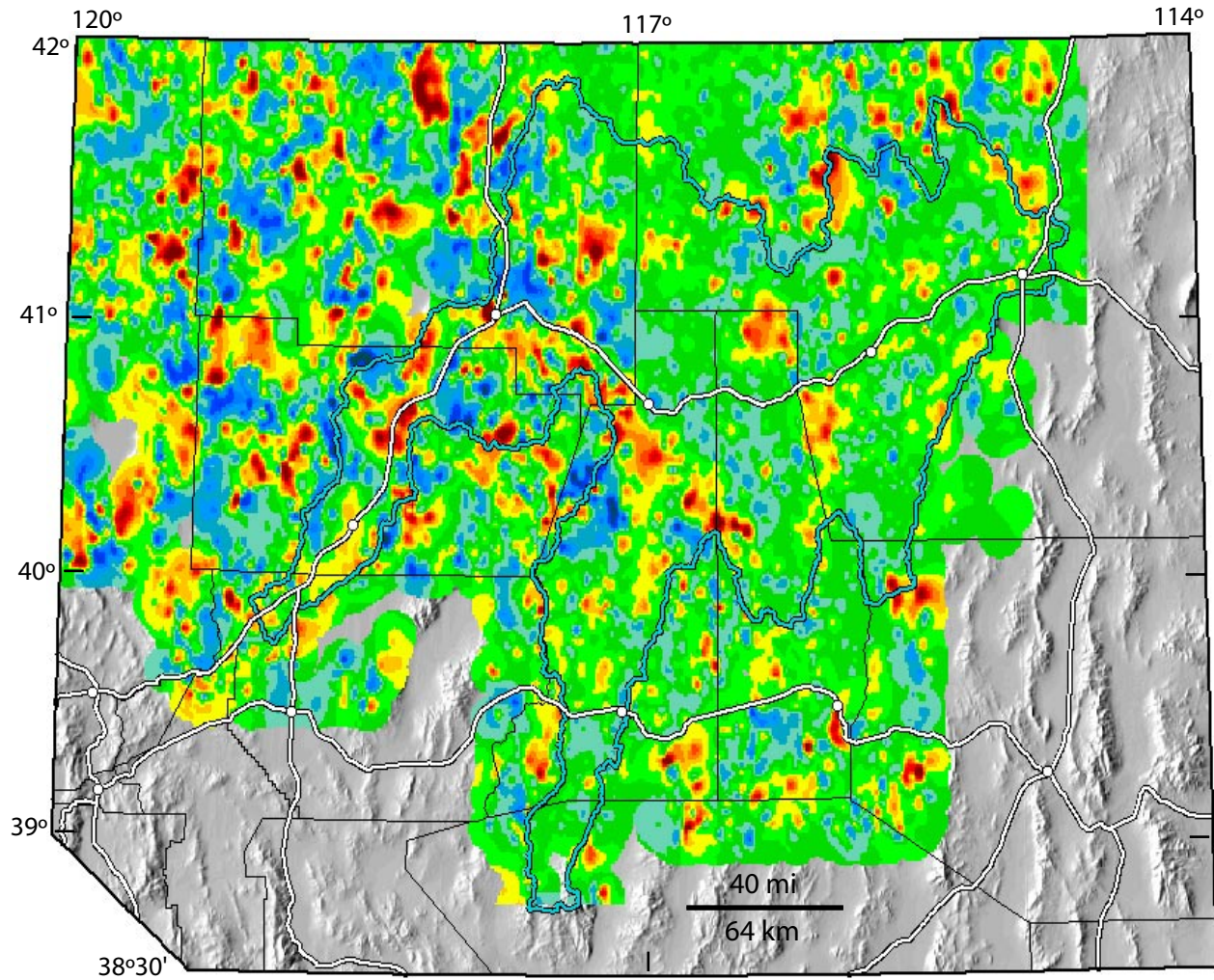
Figure 2-15.   As-frequency evidence map. Lower concentrations are represented by cooler colors (blue to green) and higher concentrations by warmer colors (yellow to dark red). Dark red areas represent 10 ppm and higher. Humboldt River Basin outlined in blue. Roads and towns the same as shown in figure 2-1.
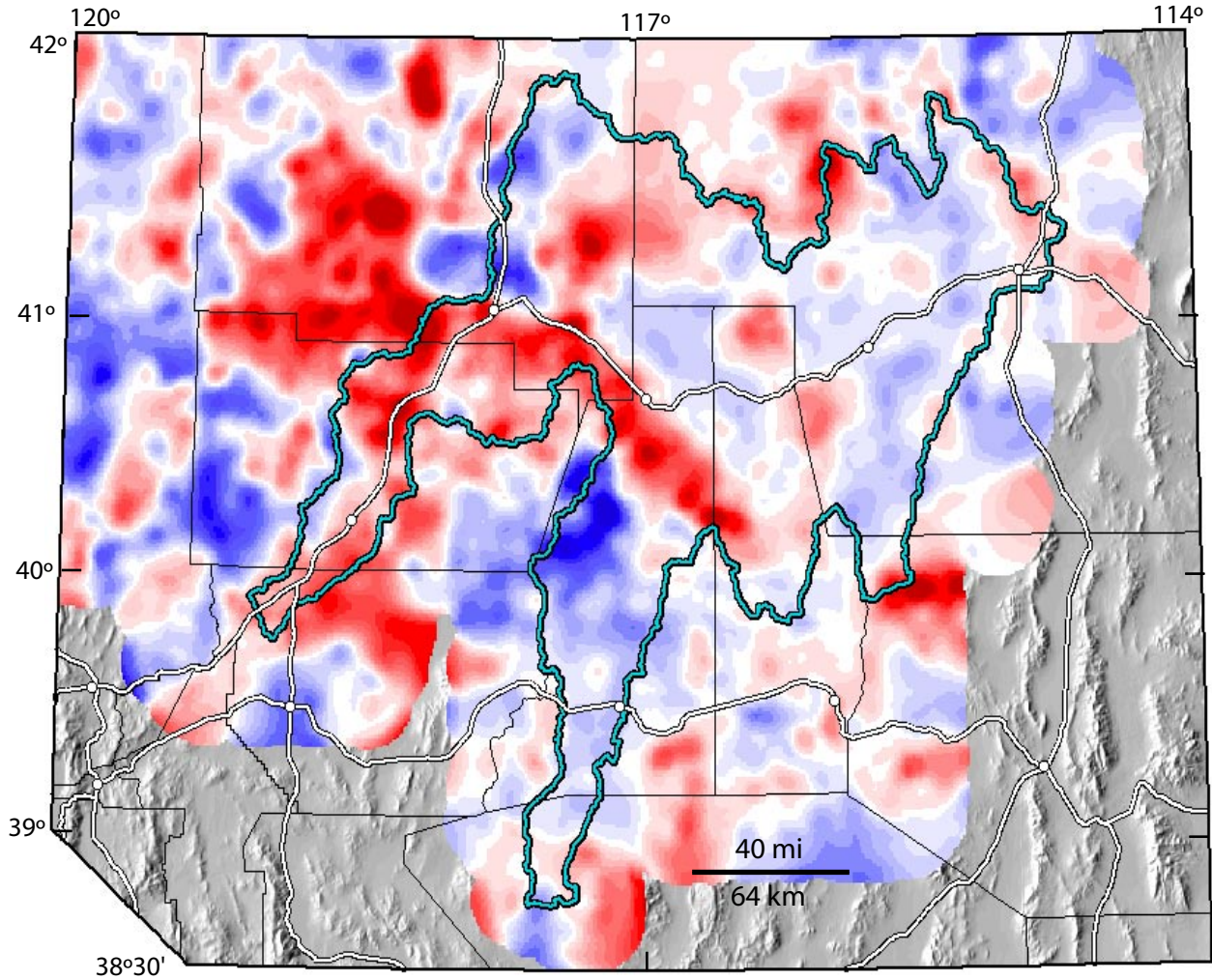
Figure 2-16.   As-spatial evidence map. As concentrations below the mean (1 ppm) are represented by blue colors and concentrations above the mean by red colors. Dark red areas represent 3.5 ppm and higher. Humboldt River Basin outlined in blue. Roads and towns the same as shown in figure 2-1.
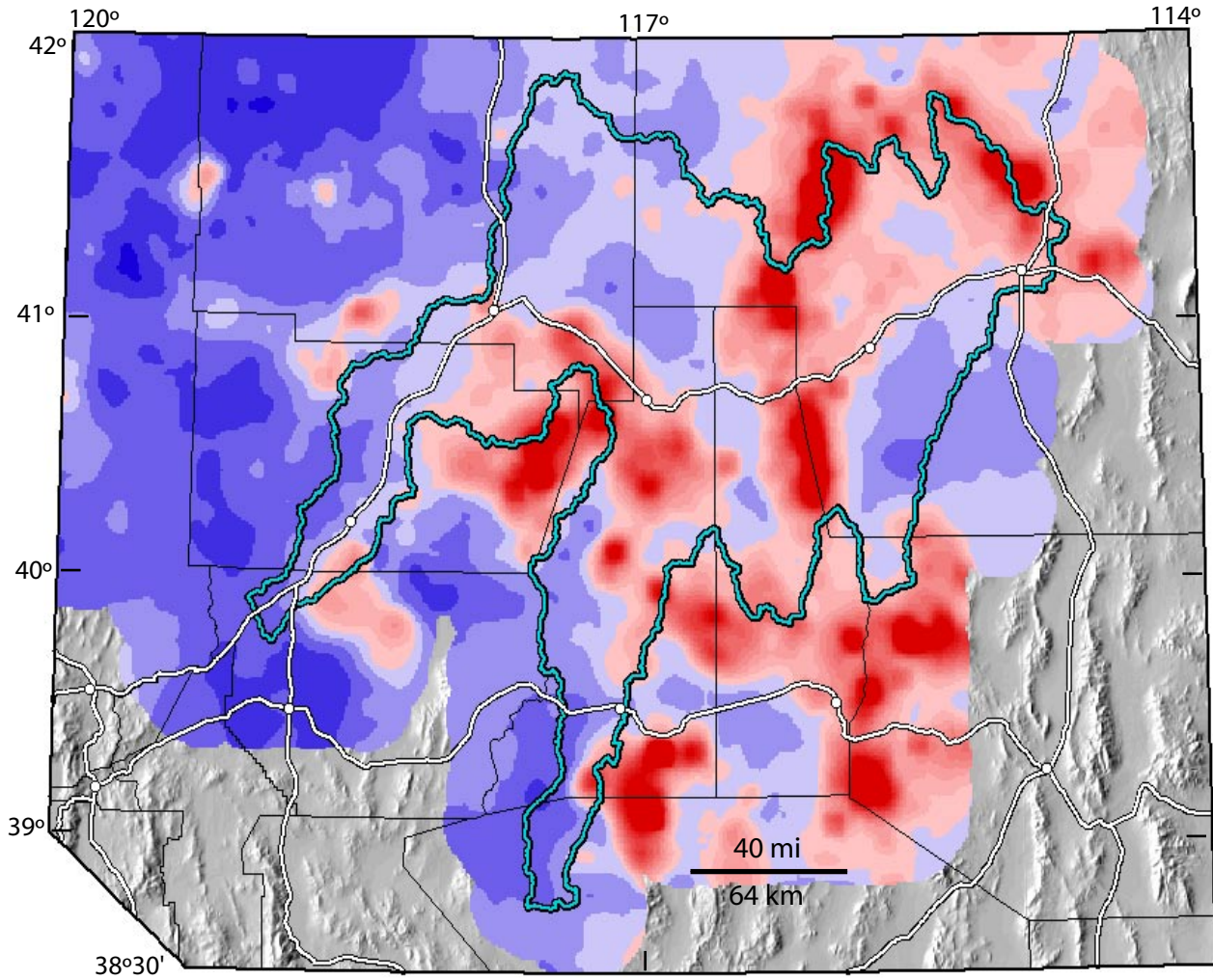
Figure 2-17.   Ba/Na evidence map. Ba/Na values below the mean (1.2) are represented by blue colors and concentra-tions above the mean by red colors. Dark red areas represent a Ba/Na value of 1.6 and higher. Humboldt River Basin outlined in blue. Roads and towns the same as shown in figure 2-1.
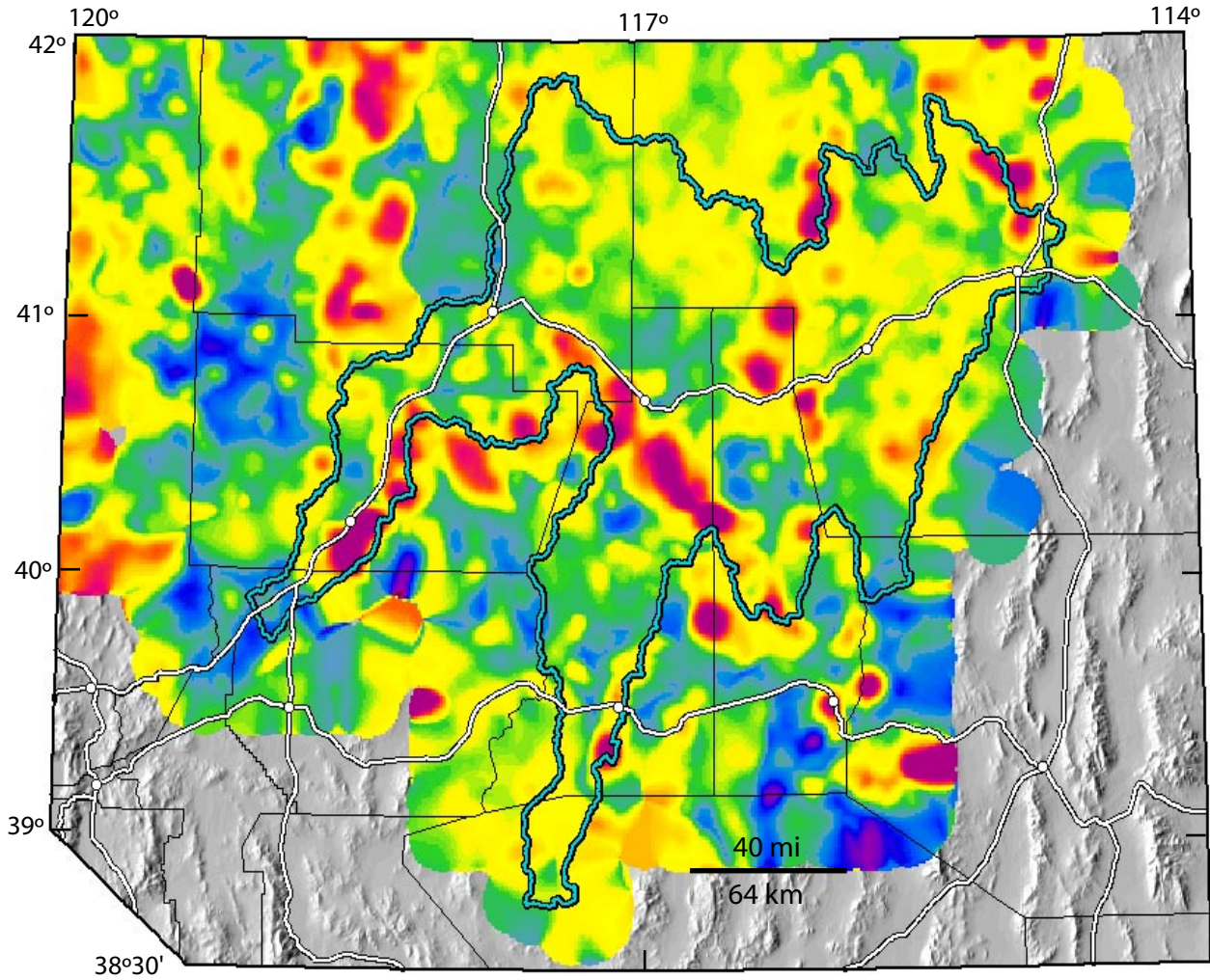
Figure 2-18. Cu-Pb-Zn signature evidence map. Lower Cu-Pb-Zn signature fuzzy membership values are represented by cooler colors and higher values by warmer colors. Green areas represent a fuzzy membership value of 0.5. Dark red areas represent membership values of 0.9 and greater. Humboldt River Basin outlined in blue. Roads and towns the same as shown in figure 2-1.
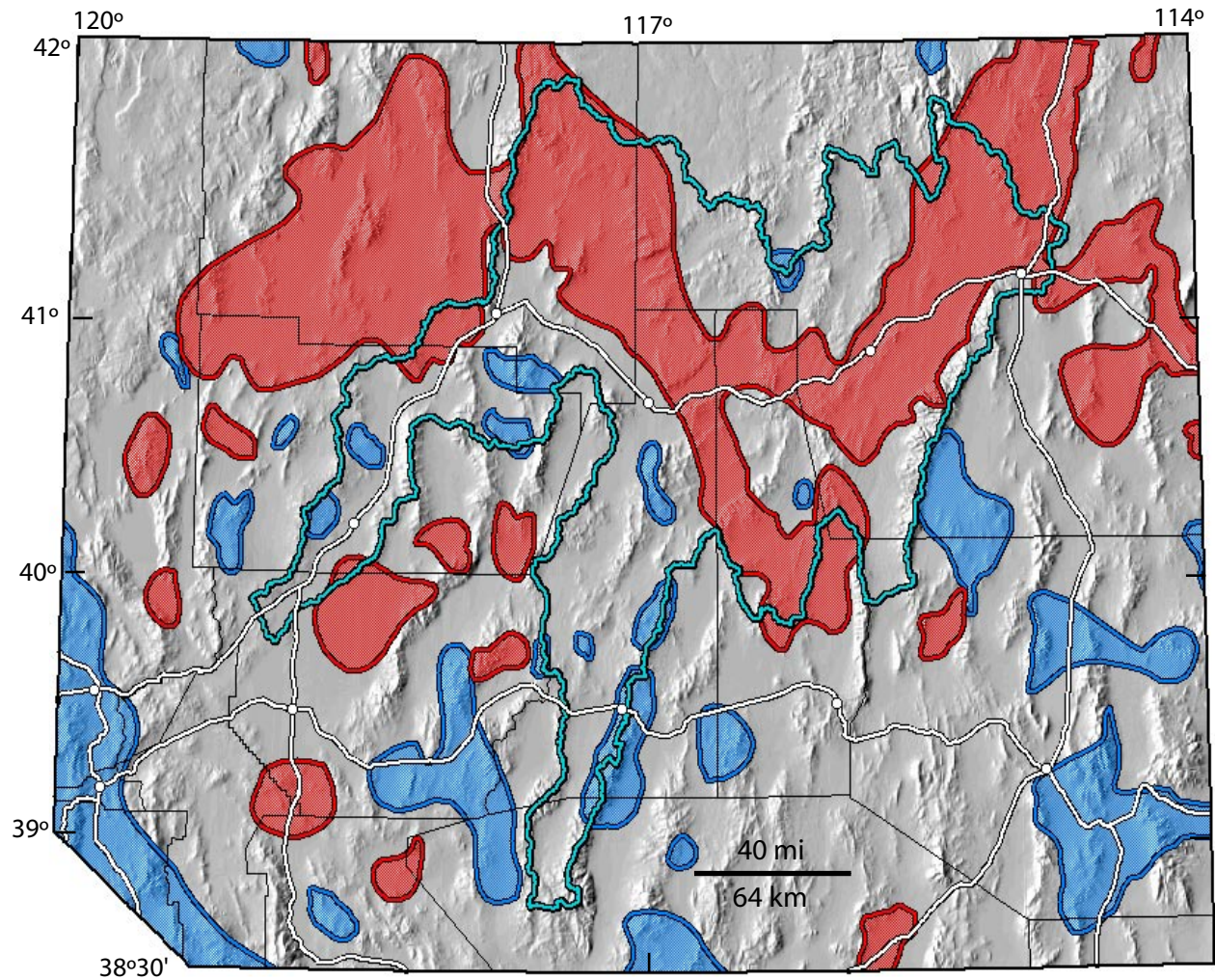
Figure 2-19.   Basement gravity terranes evidence map, showing terranes of anomaly highs (red) and lows (blue). See text in Chapter 6 for more details. Humboldt River Basin outlined in blue. Roads and towns the same as shown in figure 2-1.
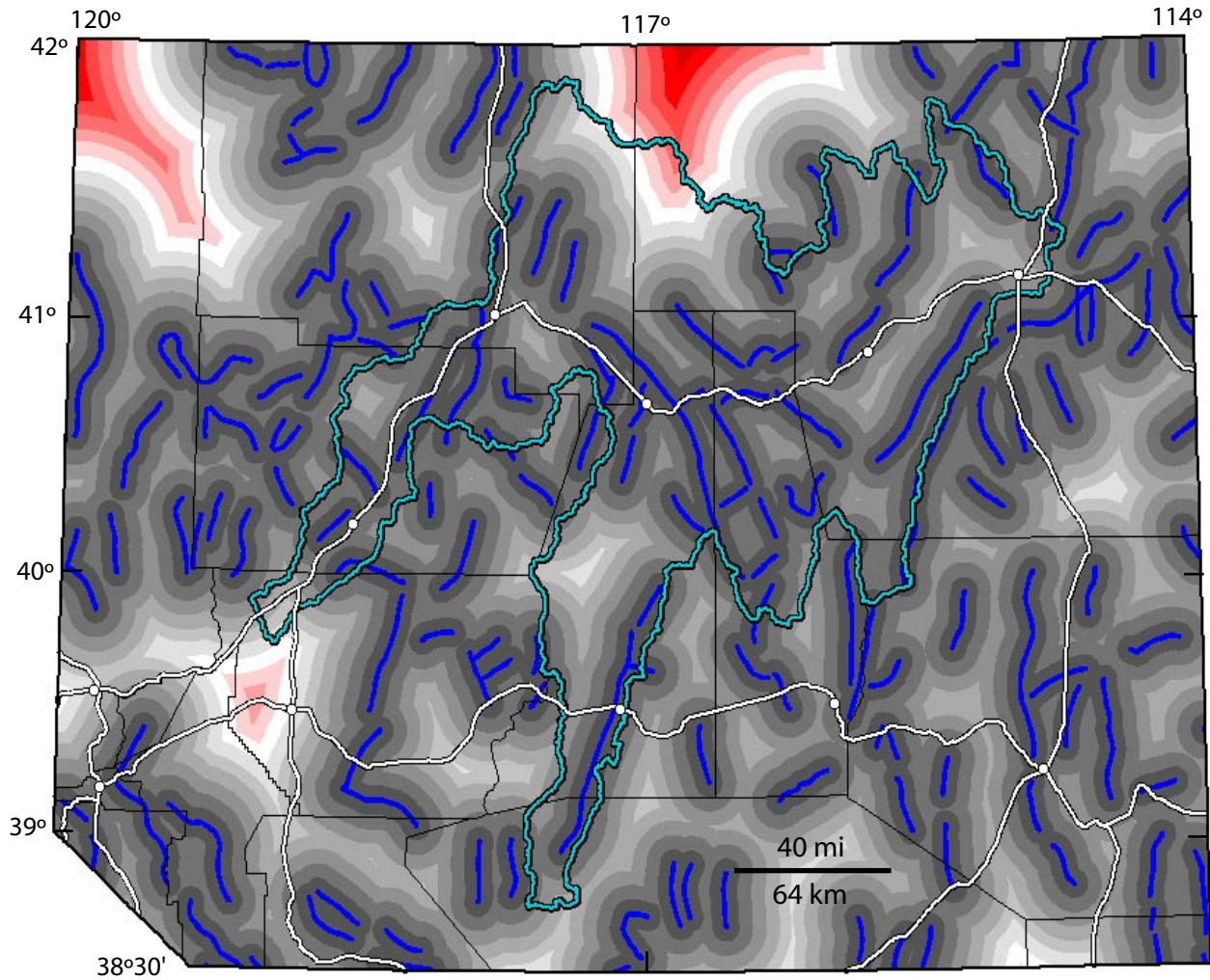
Figure 2-20.   Basement gravity lineaments evidence map. Linear features shown in dark blue. See text in chapter 6 for more details. Humboldt River Basin outlined in blue. Roads and towns the same as shown in figure 2-1.
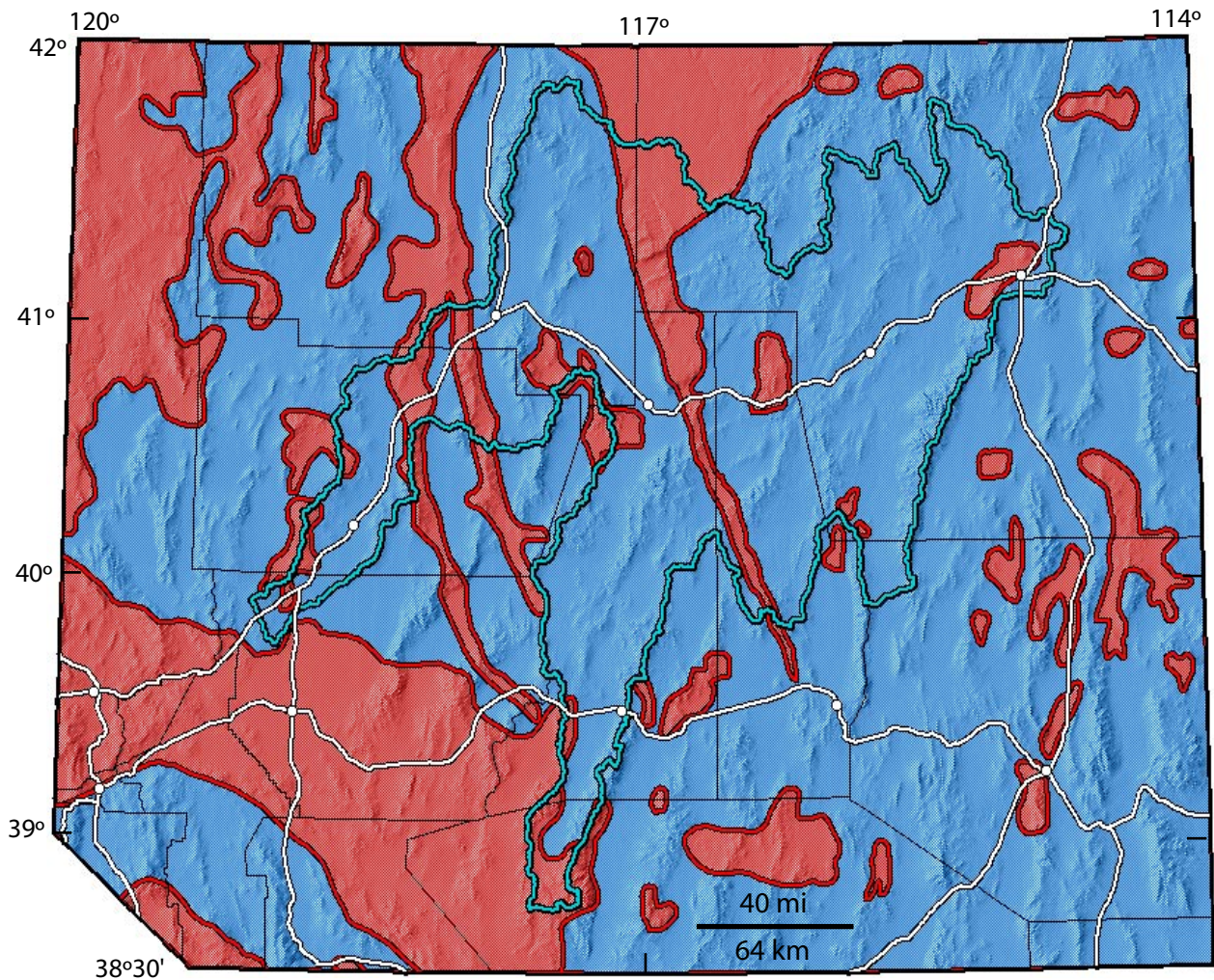
Figure 2-21. Magnetic terranes evidence map, showing presence of a terrane (red) and absence (blue). See text in chapter 6 for more details. For data-driven modeling, only a subset of this dataset was used (see chapter 9). Humboldt River Basin outlined in blue. Roads and towns the same as shown in figure 2-1.
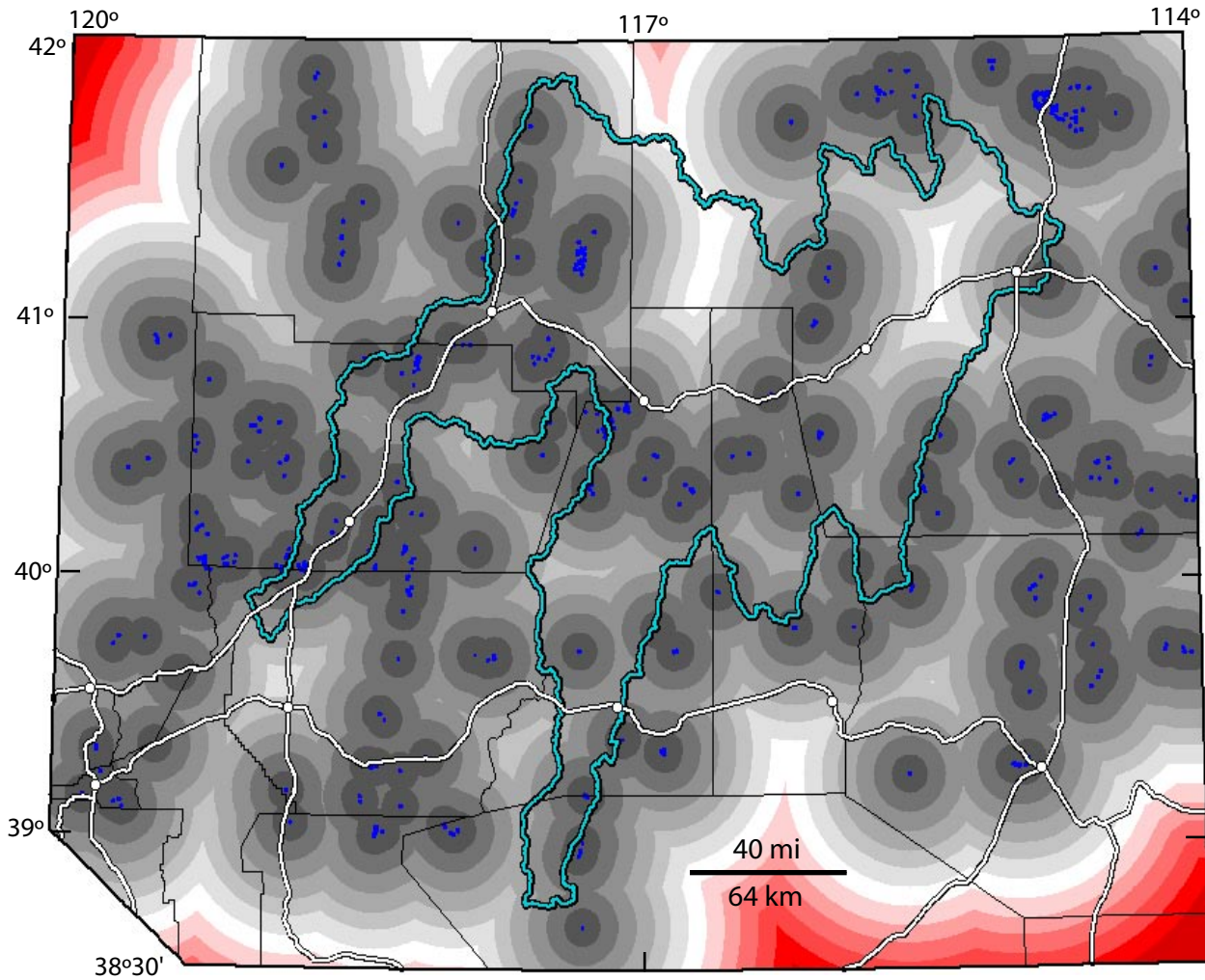
Figure 2-22.   Skarn proximity evidence map. Skarn occurrences and deposits are shown in dark blue. The occurrences and deposits are buffered at 1-km distance intervals, which are too narrow to be individually resolved. This figure is a diagrammatic representation of the buffers and shows 10-km buffer widths. Humboldt River Basin outlined in blue. Roads and towns the same as shown in figure 2-1.
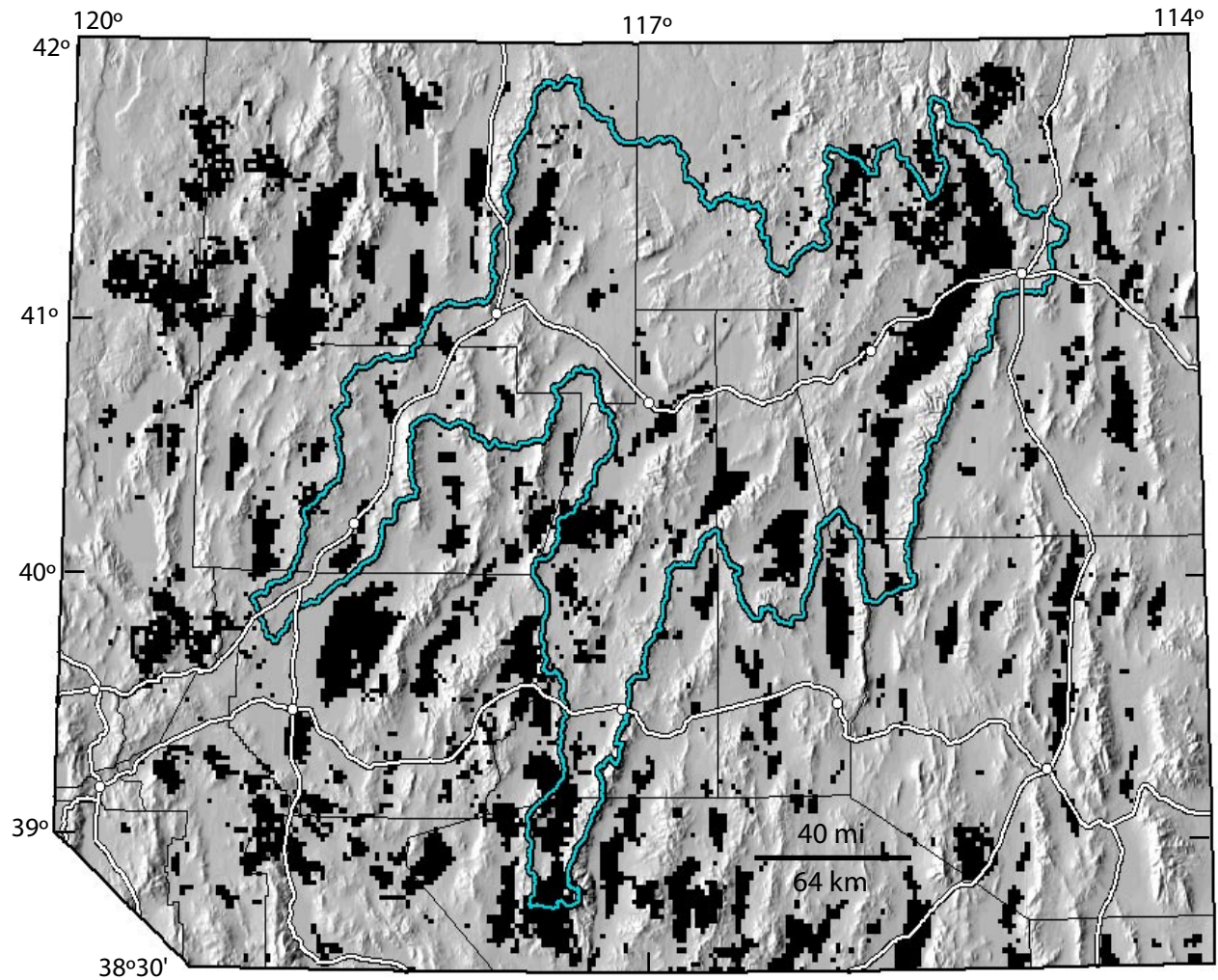
Figure 2-23.   Depth to basement map. Black areas show where Cenozoic deposits are greater than 1 km in thickness. See text in chapter 6 for more details. Humboldt River Basin outlined in blue. Roads and towns the same as shown in figure 2-1.

Chapter 3

Use of the Mineral Resource Assessment Report

By Mark J. Mihalasky and Alan R. Wallace

Introduction

This report provides a regional-scale assessment of metallic mineral resources of northern Nevada, which includes the Humboldt River Basin (HRB). It builds and expands upon other regional assessments of the state of Nevada (Singer, 1996) and the Winnemucca-Surprise Bureau of Land Management (BLM) Resource Areas (Peters and others, 1996). Unlike those assessments, the HRB assessment was conducted using digital databases and a combination of expert and data-driven modeling techniques. The resulting assessment maps, figures, tables, and text are provided in digital format for use with various commercially available software. Chapter 2 describes the data and methods that were used in the assessment. We strongly recommended that the user consult chapter 2 for information about the expert analysis, modeling techniques, and the vocabulary used in this mineral resource assessment, as that information is essential for properly interpreting and applying the assessment tract maps.

This chapter briefly outlines the conceptual and digital manner in which the assessment report and accompanying tract maps should be used. More specific comments pertaining to the data and their application to the assessment of the three deposit groups are noted throughout the report.

Scale of Assessment

Both the expert and data-driven components of the HRB mineral resource assessment were conducted using data that range in scale from 1:250,000 to about 1:1,000,000 (see chapter 2, sections "Training Sites" and "Evidence Layers"). These scales were chosen because many of the data sets used in the assessment were at those scales, most notably the geologic map of Nevada (Stewart and Carlson, 1978) and various derivative maps. As noted in chapter 2, many other sources of data at larger and smaller scales were available. These data were used as guides during the assessment, and some are reproduced in this report as page-size figures, but they were not used for the data-driven component of the assessment. Manipulation of these data as part of the expert analysis and data-driven modeling processes, as well as the combination of these different scale data,

has further decreased their collective resolution and accuracy to nearer 1:1,000,000. As such, the mineral resource assessment tract maps should not be used at a scale larger than 1:1,000,000. In practical terms, the ground resolution of the assessment maps is about 2 km. Therefore, any boundary between two assessment tracts has no greater resolution than 2 km. In keeping with the regional concept of this assessment, and the possible use of the maps for land-use planning purposes, any small areas of interest that lie along or near a tract boundary should be evaluated with care and with supplementary data that are consistent with the large scale and resolution of the area being examined. Similar considerations should be applied when working with small, isolated assessment tract areas, as they are less reliably classified, as discussed further below.

The purpose of the assessment was to delineate broad areas in northern Nevada and the HRB that are relatively more or less likely to contain undiscovered mineral deposits, similar to the purpose of the Winnemucca-Surprise assessment. This purpose, and the regional scale of the data used to achieve it, should be kept in mind when using this assessment and the digital mineral-resource assessment maps. Use of maps at larger scales to examine small areas in detail diverges from the concept and purpose of the assessment and the assessment maps.

Prospective and Favorable Tracts

The data used for data-driven modeling were selected because they reflect geological, geochemical, and geophysical attributes common to known pluton-related, sedimentary rock-hosted Au-Ag, and epithermal mineral deposits and mineralizing processes in the assessment area. The resulting prospective and favorable tracts are areas in which the data have an optimal combination of attributes found at known deposits. This does not mean that mineralizing processes took place in those areas, but rather that the models identify areas that may warrant further, more detailed evaluation before land-use or mining-related decisions are made. Conversely, it does not mean that a mineralizing process did not take place outside of that area.

The assessment tract maps show the more optimal data combinations, from the standpoint of the possible presence of a mineralized system, as "prospective" or "favorable." These

areas range in size from small to large. The smallest areas (less than or equal to about 2 km^2) are artifacts of the data-driven modeling process; these should be considered "noise" and thus warrant little or no further scrutiny. Some prospective and favorable areas are extensive and represent relatively large areas that have many attributes common to known deposits. Many of these areas have known mineral deposits of the type being assessed, and these broad areas are those that are most likely to contain undiscovered mineral deposits. The certainty that these areas have been correctly classified as favorable or prospective is 90 percent or greater, as discussed in chapter 2 (sections "Data-Driven Component" and "Modifications During Data-Driven Modeling").

The assessment tract maps do not define the specific locations of potential deposits within the broad prospective and favorable areas. Given the scale and nature of the data used for the assessment, it is possible that the data do not reflect isolated mineralizing systems and mineral deposits that are outside of prospective or favorable areas. The surface expression of the largest known mineralizing systems in northern Nevada, such as the cluster of large pluton-related systems at Battle Mountain, is several tens of square kilometers. The surface expressions of other known, in some cases large, mineral deposits in the region are somewhat to substantially smaller than that. In addition, the vertical dimension of some deposits, such as the Meikle deposit in the Carlin trend or the Ken Snyder deposit in Midas, is equal to or greater than their horizontal dimension at the surface. Therefore, more detailed studies of small areas within prospective and favorable tracts require data and concepts relevant to that scale of assessment, similar to the methods employed by the mining industry to evaluate specific properties.

Finally, it should be noted that the assessment area contains numerous deposits unrelated to pluton-related, sedimentary rock-hosted Au-Ag, and epithermal mineralizing systems. The assessment area also may contain undiscovered mineral deposit types that do not have the attributes used for this assessment and are not yet known to occur in the area.

Use of Digital Products

Three digital products are provided with the HRB mineral resource assessment: (1) a pluton-related polymetallic tract map, (2) a sedimentary rock-hosted Au-Ag tract map, and (3) an epithermal Au-Ag tract map. These maps classify tracts of land in northern Nevada according to mineral-resource favorability and are intended to facilitate land-use planning activities and decision-making. The tract maps represent the results of data- and knowledge-driven analysis and modeling carried out by the HRB assessment team (see Chapter 2 for methodology, and chapters 7, 8, and 9 for interpretations of the maps).

The three tract maps are provided in raster format as ESRI™ integer grid coverages (Mihalasky and Moyer, 2004). Associated with each map is an ArcInfo™ attribute table that

details (1) grid class and related characteristics, (2) the specific combinations of data (unique spatial overlap conditions among evidence map patterns) that comprise a given mineral-resource assessment tract, (3) the number of mineral occurrences and deposits (training sites) that fall within a given tract, (4) mineral-resource favorability estimates and related measures of error and uncertainty, and (5) a categorical classification of land tracts.

The land tract classification, which appears in the column named "tracts" (last column of the attribute table), categorizes regions of northern Nevada into areas that are considered to be "nonpermissive," "permissive," "favorable," or "prospective" for pluton-related polymetallic, sedimentary rock-hosted Au-Ag, or epithermal Au-Ag mineralized systems and contained occurrences and deposits. These categories represent relative levels of favorability for undiscovered occurrences and deposits, as determined by the HRB mineral resource assessment team in chapters 7, 8, and 9; these are defined and described in chapter 2, as well as in the metadata that accompanies the digital tract maps (Mihalasky and Moyer, 2004). It is important to note that the classification of land tracts as "favorable" or "prospective" is valid only for the area of northern Nevada where National Uranium Resource Evaluation (NURE) geochemical data are available (Figs. 2-1 and 5-1), whereas tracts classified as "nonpermissive" or "permissive" are valid for the whole of the study area (Fig. 2-1; see chapter 2 for details).

The tract classification will be of greatest utility to land-use planners and other end-users, and it can be used to symbolize and display the maps (for an example of proper display, see Figures 7-35, 8-31, and 9-15). Other information contained in the attribute table, such as evidence map presence-absence combinations and the measures of uncertainty, can provide addition insight into a given tract's classification (see the "Analysis and Modeling Methodologies" section of chapter 2 for guidance). A particularly useful measure is the "Studentized favorability," which is calculated by dividing the Weights of Evidence (WofE) favorability ("post_prob" in the attribute table) by the total uncertainty ("tot_uncrty"); in ArcView™, using the legend editor for a given grid, the tract map can be symbolized according to Studentized favorability by selecting "Graduated Color" for Legend Type, "post_prob" for Classification Field, and "tot_uncrty" for Normalize by. Regions with Student-values greater than about 1.28 have a high degree of confidence (~90 percent) with respect to variances of weights and variance due to missing data (see chapter 2). A Studentized favorability map is useful in a relative sense for highlighting regions with low or high confidence for the WofE-derived favorability estimate. For the confidence of the WLR-derived favorability estimate, which is the estimate that was used to determine the relative levels of favorability of land tract classification ("tract" in the attribute table), the tract map can be symbolized directly using the field "lrtvalue" in the attribute table (there is no need to normalize WLR-derived favorability estimate by the total uncertainty). For additional information on the use and interpretation of the analysis and modeling values contained in the attribute table, see chapter 2, Bonham-Carter (1994), and Kemp and others (2001).

Chapter 4

Geologic Setting of the Humboldt River Basin

By Alan R. Wallace

Introduction

The geologic history of northern Nevada, including the Humboldt River Basin (HRB), spans more than a billion years, ranging from Precambrian rocks in the East Humboldt Range to Quaternary alluvial deposits and active faults. The mineral deposits and occurrences in the region result from the geologic events during this protracted period of time. Thus, a mineral-resource assessment of the area must take into account the complex geologic history and the distribution of rocks types and geologic environments. This chapter briefly summarizes the geologic history of the region as it pertains to the mineral deposits that are being assessed. Specific geologic details of those deposits can be found in the three assessment chapters in this report (chapters 7–9). Stewart (1980) provides an excellent summary of the geology of Nevada, and Dickinson (2001) places the geology in a regional time-tectonic framework. Doebrich (1996) focuses in more detail on the geologic events in the Winnemucca-Surprise Resource Area in northwestern Nevada, and many of those events pertain to the entire HRB study area. The general geology of the region is shown in figure 4-1, which is a simplified geologic map of Nevada (Stewart and Carlson, 1977) based on the 1:500,000-scale geologic map of Nevada (Stewart and Carlson, 1978). Geologic time scales showing major geologic events are provided in figures 4-2 and 4-3.

Pre-Tertiary Geology

Stable continental shelf sedimentation, with periodic accretion of allochthonous geologic terranes from the west, characterized the period from the Late Proterozoic through early Mesozoic (fig. 4-2). A late Proterozoic continental rifting event produced the continental margin and set the stage for subsequent continent-margin sedimentation (Stewart, 1972). This rifting event also created major crustal breaks that were important in Phanerozoic igneous, structural, and metallogenic processes. Little is known about earlier geologic events except for isotopic data that indicate the presence of Archean and Proterozoic crystalline rocks at depth beneath eastern Nevada (Wooden and others, 1998; Kistler and Peterman, 1976). The

shelf environment in the early Paleozoic (Cambrian through Devonian) produced regionally extensive carbonate, quartzite, and shale deposits along the edge of the North American craton, which, at the time, formed a general north-south line that bisected Nevada. In general, carbonate rocks are more common to the east and shales predominate to the west, consistent with deposition in progressive shelf, slope, and deep basin environments from east to west (Stewart and Poole, 1974).

Starting in the late Devonian, allochthonous deep-basin rocks of the Roberts Mountains allochthon were thrust eastward over the autochthonous shelf-slope deposits along the Roberts Mountains thrust (Roberts and others, 1958). The deep-basin rocks originally formed just to the west of the North American craton, based on studies of sediment sources (Gehrels and others, 2000; Stewart and others, 2001). This event, termed the Antler orogeny, continued episodically into the Permian. Sediments shed to the east and west from the resulting Antler orogenic high formed the Pennsylvanian and Permian Antler sequence (also known as the overlap assemblage; Roberts, 1964), which covered both the allochthonous and autochthonous rocks. Shelf sedimentation resumed to the east, again generating widespread carbonate units that in part interfingered with the sediments of the Antler sequence, which was forming just to the west. The Humboldt phase of the Antler orogeny disrupted the central part of the region in the late Pennsylvanian (Ketner, 1977; Theodore and others, 1998), creating north-south shortening and significant unconformities in late Paleozoic stratigraphic sections. In northern Nevada, many sedimentary rock-hosted Au deposits formed in the late Eocene in carbonate rocks beneath the Roberts Mountains thrust, and in Mississippian rocks of the overlap assemblage (see chapter 8). The overlap assemblage also hosts some Tertiary distal-disseminated Ag-Au and sedimentary rock-hosted Au deposits. As a result, the Paleozoic sedimentary environments and the Antler orogeny were essential to the formation of these mineral deposits during the Tertiary.

A second allochthonous terrane, the Golconda allochthon, was emplaced along the Golconda thrust during the late Permian-early Triassic Sonoma orogeny (Silberling and Roberts, 1962). The Sonoma orogeny carried deep basinal upper Paleozoic sediments eastward over upper-plate rocks of the Roberts Mountains thrust, as well as the overlap and upper and lower Paleozoic shelf units. The basinal units

formed just west of the craton margin (Riley and others, 2000) and contained scattered volcanogenic massive sulfide and manganese deposits that formed before the orogeny (Snyder, 1977). Volcanism at the end of and following this orogenic event produced volcanic, volcaniclastic, and intrusive rocks of the Late Permian and Early Triassic Koipato Group, which is exposed generally east of Lovelock and south of Winnemucca (Silberling and Wallace, 1969; Kistler and Speed, 2000). With the exception of a few precious-metal veins in the southern East Range (Wallace, 1977), mineralization was not associated with this igneous event. During the Triassic, central Nevada was a broad, gentle highland traversed by west-flowing streams (Manuszak and others, 2000). To the west, widespread platform carbonate rocks and subsequent fine-grained clastic sediments of the Jungo terrane were deposited on the Koipato and other older rocks (Oldow, 1984). This shelf environment merged westward the back-arc environment of the Black Rock terrane (Wyld, 2000). Triassic sedimentation east of the central Nevada highland largely was in shallow-marine to locally terrestrial environments.

Starting in the Middle Jurassic, perhaps as early as the Late Triassic, and extending into at least the Late Cretaceous, the entire width of northern Nevada was compressed in a general west to east direction. In northwestern Nevada, southeast-directed thrusting carried the Triassic and Early Jurassic rocks of the Jungo and Black Rock terranes over the Triassic platform carbonate units and the Koipato Group (Oldow, 1984). The Jungo terrane rocks were carried along the Fencemaker thrust, and the volcanic arc rocks of the Black Rock terrane were thrust eastward over the Jungo terrane along the Black Rock thrust. In northeastern Nevada, east-directed thrusting began in the Jurassic and continued through the Cretaceous. In some areas, the thrusting overthickened the crust, and the deep rocks were metamorphosed to upper amphibolite grade facies. Regionally, this compressional event ended in the Paleocene (early Tertiary). This tectonic event produced metamorphic gold-silver deposits, primarily in Jungo terrane rocks (Cheong, 1999).

During roughly the same period of time, widespread and compositionally diverse igneous rocks were emplaced throughout northern Nevada, most abundantly in the western half of the area. Satellitic igneous activity related to emplacement of the Sierra Nevada batholith to the west produced widespread Jurassic and Cretaceous granitic to dioritic plutons (Kistler and Peterman, 1978). These intrusions produced numerous W, Cu, and Mo deposits in northern Nevada, including those in the Battle Mountain area and the Osgood and Eugene Mountains (see chapter 7), and Ag-rich deposits at Rochester northeast of Lovelock (Vikre, 1981). Some distal-disseminated Ag-Au deposits also formed during this magmatic event (Bald Mountain, in part; see chapter 8). Middle Jurassic back-arc mafic igneous activity produced the 165–Ma Humboldt gabbroic complex (Speed, 1976; Johnson and Barton, 2000), a thick sill-like intrusion east of Lovelock, and mafic volcanic and subvolcanic rocks in the Jackson Mountains (Happy Creek igneous complex; Maher, 1989) and eastern Cortez Range (Frenchie Creek volcanics; Muffler,

1964). The Humboldt complex produced iron deposits, and it potentially is a source of platinum-group elements (see chapter 7). In eastern Nevada, Cretaceous anorogenic, two-mica granitic plutons were emplaced during and after thrusting (Lee and others, 1981). These plutons largely are devoid of metallic mineral deposits, although some contain elevated amounts of U, Be, F, Th, and Ti.

Tertiary Geology

The geologic record for events from the Late Cretaceous (~70 Ma) to the middle Eocene (~46 Ma) in northern Nevada largely is missing. Arc-related magmatism had ceased, and the region was a broad topographic high due to the late Mesozoic thrusting and overthickening. Starting in the middle to late Eocene, with some of the first recorded events at about 46 Ma, northern Nevada became the site of extensional and magmatic events that characterized the rest of the Tertiary. The major Tertiary geologic events, including igneous activity, tectonic events, and periods of uplift and erosion, are shown in figure 4-3.

Tertiary magmatism in the region formed three igneous assemblages: the interior andesite-rhyolite (IAR), the western andesite (WA), and bimodal basalt-rhyolite (BM) assemblages (Ludington and others, 1996; see also chapter 9). The IAR and WA assemblages were related to arc volcanism; the BM assemblage was related to regional extension. The IAR assemblage began to form at about 43 Ma as a south-sweeping belt of intrusive and volcanic activity entered the northeastern corner of the state. This sweep of igneous activity migrated south-southwestward across northern Nevada between about 43 Ma and 19 Ma, producing plutons, calderas, and widespread ash-flow tuff sheets. Mineral deposits associated with this magmatic suite include porphyry-related deposits (porphyry Cu, skarn, veins at Battle Mountain), distal-disseminated Ag–Au deposits (Lone Tree, Trenton Canyon), sedimentary rock-hosted Au-Ag deposits along several major trends, and epithermal Au-Ag deposits (Tuscarora, Wonder, and Round Mountain) (see further discussion in chapters 7–9).

Between approximately 20 Ma and 4 Ma, volcanic and subvolcanic rocks associated with the WA assemblage were emplaced in western Nevada. These represent early igneous activity related to the Cascade volcanic arc (Christiansen and Yeats, 1992). Most mineral deposits associated with this assemblage are epithermal deposits, including the world-class Ag-Au deposits at Virginia City (Comstock Lode), as well as deposits at Rawhide, Bodie, Aurora, and Tonopah. None of these deposits, though, are in the Humboldt River Basin.

The bimodal basalt-rhyolite assemblage began to form at about 17 Ma and continues to the present. These volcanic rocks are the most extensive, although not necessarily the most voluminous, of the three volcanic assemblages in northern Nevada. The magmas were erupted from a variety of sources during crustal extension, forming widespread basalt and rhyolite flows and local calderas and silicic domes. These volcanic

rocks interfingered with lacustrine deposits in numerous small to extensive shallow lakes. Almost all mineral deposits associated with the bimodal assemblage are epithermal, including Au-Ag veins (Midas, Sleeper) and hot-spring deposits (Ivanhoe and Goldbanks Hg-Au, McDermitt U-Hg) (see chapter 9).

Northern Nevada experienced varying amounts of extension throughout the Tertiary (Christiansen and Yeats, 1992). Middle to late Tertiary extension produced large low-angle detachment faults in the Ruby Mountains and East Humboldt Range (Snoke and Miller, 1988) and differential tilting and uplift throughout the region (Seedorff, 1991; John and others, 2000). West-southwest-directed extension began in the middle Miocene and continued to about 6-8 Ma. Extension then shifted to a northwest direction and began to create the modern basin-and-range physiography. High-angle faults produced during both extensional periods provided fluid flow paths for the related epithermal mineralizing systems. During the most recent period of extension, deep-seated magmas underplated the extending crust beneath northern Nevada. High heat flow related to this magmatic underplating has produced numerous hot springs and geothermal areas in the region (Shevenell and others, 2000), including late Tertiary and Quaternary Au deposits at Dixie Comstock, Sulphur/Hycroft, and Wind Mountain and Mn-W deposits at Golconda.

Late Tertiary and Quaternary unconsolidated sediments blanket at least half of northern Nevada, filling the broad, intermontane basins that formed during late Tertiary and Quaternary crustal extension (fig. 4-2). Widespread Quaternary lakes, such as Pleistocene Lake Lahontan, deposited fine-grained sediments in western and central Nevada, further adding to the young sedimentary cover. While these deposits host placer gold and titanium deposits along the original lake margins, their most significant economic impact is that they conceal vast areas of bedrock that undoubtedly contain mineral deposits such as those described elsewhere in this report.

GENERALIZED
GEOLOGIC MAP OF NEVADA

Legend:

- County boundaries
- Quaternary and suspected Quaternary faults, less than 1.6 Ma (million years old), dashed where age uncertain
- Lakes and reservoirs
- Alluvial and playa deposits
- Volcanic rocks, less than 6 Ma
- Upper volcanic rocks, 6–17 Ma
- Tuffaceous sedimentary rocks, 6–17 Ma
- Lower volcanic rocks, mostly 17–43 Ma
- Intrusive rocks, Mesozoic and Tertiary
- Igneous and metamorphic complex, Jurassic or Cretaceous
- Sedimentary, volcanic, and intrusive rocks, Mesozoic
- Sedimentary and volcanic assemblage, upper Paleozoic
- Carbonate and other sedimentary rocks, upper Paleozoic
- Sedimentary and volcanic assemblage, lower Paleozoic
- Carbonate and other sedimentary rocks, lower Paleozoic and Late Proterozoic
- Metamorphic and intrusive rocks, Early and Middle Proterozoic

0 10 20 30 40 50 miles
0 20 40 60 80 kilometers

Figure 4-1. Generalized geologic map of northern Nevada, showing the major geologic units. Geology based on Stewart and Carlson (1977); figure from digital geologic map provided by Nevada Bureau of Mines and Geology. Dark blue line shows the approximate outline of the Humboldt River Basin.

Geologic Events in Northern Nevada

Era	Period	Age (Ma)	Tectonic events	Sedimentation/igneous activity	Mineralization
Cenozoic	Quaternary			Alluvial, lacustrine sedimentation	Epithermal
		1.6			
	Tertiary		Extension; uplift begins	Volcanism (bimodal, western andesite)	
			Extension	Volcanism (interior andesite-rhyolite)	
		66			
Mesozoic	Cretaceous			Plutonism (felsic)	Sedimentary rock-hosted / Pluton-related
		138	Nevadan/Sevier/ Elko orogenies	Plutonism (mafic), volcanism (mafic)	
	Jurassic				
		205			
	Triassic			Shelf, basinal sedimentation	
		240	Sonoma orogeny (Golconda thrust)	Volcanism (felsic)	
Paleozoic	Permian				
		290		Antler sequence, craton-margin sedimentation	
	Pennsylvanian				
		330			
	Mississippian		Antler orogeny (Roberts Mtns. thrust)		
		360			
	Devonian				
		410			
	Silurian				
		435		Craton-margin (shelf, slope, deep basin) sedimentation	
	Ordovician				
		500			
	Cambrian				
		570	Craton-margin rifting		
Pre-cambrian	Proterozoic		Archean/Proterozoic suturing		
		2500			
	Archean				

Figure 4-2. Geologic time scale showing major geologic events in northern Nevada.

Cenozoic Events in Northern Nevada

Figure 4-3. Cenozoic (Tertiary and Quaternary) igneous, tectonic, and mineralizing events in northern Nevada.

Chapter 5

Geochemical Data for the Humboldt River Basin

By Steve Ludington

Introduction

The chemical composition of stream-sediment samples reflects the overall chemistry of rocks contained within the drainage basins upstream from the samples. This information can be used to identify those basins that contain anomalous concentrations of elements that may be related to mineral deposits or other geologic features. Soil samples have a similar use, and they also may reflect the chemistry of underlying rocks. However, the area of influence of any particular sample is more restricted than for stream-sediment samples because the materials are more locally derived. Nevertheless, they are sometimes the only samples available for an area, and can still be of value for mineral exploration and assessments.

Geochemical data for several elements have been used in the present mineral resource assessment of the Humboldt River Basin (HRB). The purpose of this chapter is to catalogue the available data, and to indicate some of the ways these data could be used to enhance the present assessment.

Data

A significant existing data set of stream-sediment and soil samples covers nearly all of the HRB. Figure 5-1 shows the geographic distribution of the two distinct data sets that cover the study area. The two data sets contain a total of 7,589 individual samples and provide nearly complete coverage of the northern half of Nevada and a small area in the northeastern corner of California. Both data sets represent samples that were collected in the 1970s under the National Uranium Resource Evaluation program (NURE) and that were reanalyzed in the 1990s. These NURE samples are now curated by the U.S. Geological Survey (USGS). Details of the program can be found in Smith (2000).

Sources of Data

In 1993 through 1995, the USGS conducted a mineral resource assessment of the Winnemucca and Surprise resource areas for the Bureau of Land Management (BLM) in northwest Nevada and northeast California (fig. 5-1; Doebrich and others, 1994; Peters and others, 1996). To support that assessment, more than 3,000 NURE samples were reanalyzed by USGS laboratories, a few hundred new samples were collected, primarily in the California part of the study area. Those results are reported in USGS Open-file Report 96-062 (King and others, 1996).

In 1995, as part of the present mineral resource assessment of the HRB, the reanalysis of an additional group of samples in north-central and northeastern Nevada was begun (fig. 5-1). Those analyses were performed by private-sector laboratories, in cooperation with the Nevada Bureau of Mines and Geology, and analyses were completed in 2000. The results have been released as USGS Open-file Report 2000-421 (Folger, 2000).

Methods

In both studies, the original, archived samples, were obtained from USGS storage in a Denver, Colo., warehouse, and splits were taken for analysis. The splits were sieved, when necessary, to pass an 80-mesh (0.18-mm) sieve, and the finer-grained fraction was used for analysis. Samples were analyzed for about 40 elements by inductively coupled plasma-atomic emission spectrometry (ICP-AES) (Briggs, 1990, or similar method). The samples also were analyzed by a partial extraction ICP-AES method (Motooka, 1990, or similar method) to obtain lower limits of determination for selected elements. This second method utilizes a partial solution method, using concentrated hydrochloric acid and hydrogen peroxide, followed by extraction into an organic solvent, and it is designed to measure the metals not bound in silicate minerals. Gold contents of the samples were determined by atomic absorption spectrophotometry (AA) with a graphite furnace (O'Leary and Meier, 1990), providing a distinctly lower limit of determination. A small number of samples (55 samples) collected by the USGS in the Reno 1°x2° quadrangle was analyzed for Hg by cold vapor atomic absorption spectrophotometry (CVAA) (O'Leary and others, 1990). Additional samples were analyzed for As, Se, Te, and Tl by a

hydride-generation atomic-adsorption spectrometry method. The elements analyzed in both studies and their lower limits of determination are given in table 5-1.

Discussion

Analysis and interpretation of a comprehensive data set that covers a large geographic area, like the one available for the HRB, requires a few special precautions and considerations.

The area spans a wide variety of geologic and tectonic environments, as described in chapter 4. In the east, the area consists of primarily carbonate and quartzite sedimentary rocks that overlie the stable North American craton. In the far northwest, all rocks exposed at the surface are Miocene volcanic rocks and their clastic derivatives. These rocks overlie a basement that is completely hidden but which may be composed entirely of Jurassic oceanic crust. In between these two regions lie several lithologically varied terranes that were accreted to North America in a complex series of events throughout Phanerozoic time (see chapter 4), and that now overlie a complexly fragmented cratonal margin. It is unrealistic to expect any element to exhibit a single background concentration or value over such a varied spectrum of rocks. As a result, users of these data would do well to model the geochemical background carefully, in order to distinguish between residual anomalies that may be related to mineral deposits and regional anomalies that are related to varied lithology and structure.

Once background values are carefully established, their removal should result in a series of residual anomalies, that may, or may not, be related to known or undiscovered mineral deposits. Residual anomalies for individual elements may, or may not, be useful in distinguishing between different mineral deposit types, and many of them may correspond to little-known or insignificant mineral deposits. Finally, the pattern of such anomalies may reveal important information about the location, nature, and history of large basement structural features.

An example of application of the methods discussed above was described by Ludington and others (2000). In that study, the data for As were gridded, and then, using a series of band-pass frequency filters, the entire map was resolved into distinct textural components. Each of the three maps used for interpretation emphasized features of differing wavelengths, from hundreds of kilometers for a map that shows one feature—the margin of the pre-Cretaceous craton—to 5 to 20 km for a residual map that shows anomalies related to mineralized areas. This residual map was used in the data-driven component of the mineral resource assessment described in chapters 7-9 (see also, chapter 2).
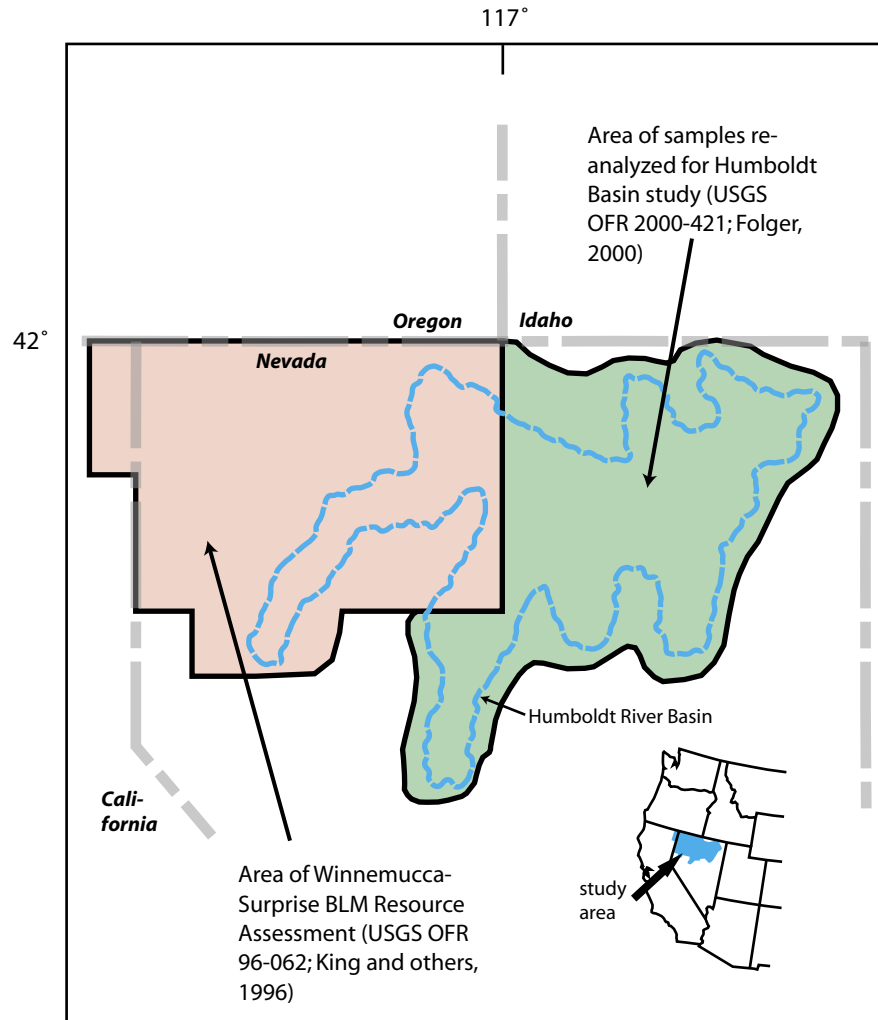
Figure 5-1.   Location of major stream-sediment and soil-sample surveys, northern Nevada, used for Humboldt River Basin mineral assessment. Humboldt River Basin outlined in blue.

Table 5-1.   Elements analyzed and detection limits for NURE samples used for Humboldt River Basin mineral resource assessment.

Element	Symbol	Method	DL (or minimum value) Humboldt	DL (or minimum value) Winnemucca-Surprise	Units
silver	Ag	ICP-total	0.5	2	ppm
aluminum	Al	ICP-total	0.82	0.69	percent
arsenic	As	ICP-total	5	10	ppm
gold	Au	ICP-total	4	8	ppm
barium	Ba	ICP-total	92	26	ppm
beryllium	Be	ICP-total	1	1	ppm
bismuth	Bi	ICP-total	5	10	ppm
calcium	Ca	ICP-total	0.13	0.2	percent
cadmium	Cd	ICP-total	0.4	2	ppm
cerium	Ce	ICP-total	10	4	ppm
cobalt	Co	ICP-total	2	2	ppm
chromium	Cr	ICP-total	6	1	ppm
cesium	Cs	ICP-total	5	n.d.	ppm
copper	Cu	ICP-total	2	3	ppm
europium	Eu	ICP-total	n.d.	2	ppm
iron	Fe	ICP-total	0.38	0.21	percent
gallium	Ga	ICP-total	1	4	ppm
holmium	Ho	ICP-total	n.d.	4	ppm
potassium	K	ICP-total	0.34	0.17	percent
lanthanum	La	ICP-total	5	4	ppm
lithium	Li	ICP-total	5	6	ppm
magnesium	Mg	ICP-total	0.03	0.12	percent
manganese	Mn	ICP-total	82	130	ppm
molybdenum	Mo	ICP-total	2	2	ppm
sodium	Na	ICP-total	0.07	0.1	percent
niobium	Nb	ICP-total	2	4	ppm
neodymium	Nd	ICP-total	n.d.	5	ppm
nickel	Ni	ICP-total	2	2	ppm
phosphorous	P	ICP-total	0.012	0.008	percent
lead	Pb	ICP-total	5	4	ppm
rubidium	Rb	ICP-total	19	n.d.	ppm
antimony	Sb	ICP-total	1 (5)	n.d.	ppm
scandium	Sc	ICP-total	1	2	ppm
tin	Sn	ICP-total	2	5	ppm
strontium	Sr	ICP-total	33	29	ppm
tantalum	Ta	ICP-total	n.d.	40	ppm
thorium	Th	ICP-total	2	4	ppm
titanium	Ti	ICP-total	0.04	0.03	percent
uranium	U	ICP-total	10	100	ppm
vanadium	V	ICP-total	4	6	ppm
tungsten	W	ICP-total	4	n.d.	ppm
yttrium	Y	ICP-total	4	4	ppm
ytterbium	Yb	ICP-total	n.d.	1	ppm
zinc	Zn	ICP-total	18	5	ppm
zirconium	Zr	ICP-total	10	n.d.	ppm

Table 5-1.   Elements analyzed and detection limits for NURE samples used for Humboldt River Basin mineral resource assessment.—Continued

Element	Symbol	Method	DL (or minimum value) Humboldt	DL (or minimum value) Winnemucca-Surprise	Units
silver	Ag	Partial	0.012	0.067	ppm
arsenic	As	Partial	0.86	.67 (1)	ppm
gold	Au	Partial	n.d.	0.1	ppm
bismuth	Bi	Partial	0.019	1	ppm
cadmium	Cd	Partial	0.019	.05 (.5)	ppm
copper	Cu	Partial	1.28	1	ppm
gallium	Ga	Partial	0.733	n.d.	ppm
mercury	Hg	Partial	0.00001	n.d.	ppm
molybdenum	Mo	Partial	0.204	0.08	ppm
lead	Pb	Partial	3.11	1.1	ppm
antimony	Sb	Partial	0.095	.67 (1)	ppm
selenium	Se	Partial	0.0002	n.d.	ppm
tellurium	Te	Partial	0.0005	n.d.	ppm
thallium	Tl	Partial	0.084	n.d.	ppm
zinc	Zn	Partial	10	1.7	ppm
gold	Au	Graphite furnace AA	0.00001	0.002	ppm
arsenic	As	hydride	0.6	n.d.	ppm
selenium	Se	hydride	0.1	n.d.	ppm
tellurium	Te	hydride	0.1	n.d.	ppm
thallium	Tl	hydride	0.2	n.d.	ppm

Abbreviations: n.d., no data; DL, detection limit.

Chapter 6

Geophysical Methods and Application

By D.A. Ponce

Introduction

Geophysical investigations of the Humboldt River Basin (HRB) (fig. 6–1) are part of an interagency effort by the U.S. Geological Survey (USGS) and Bureau of Land Management (BLM) to help characterize the geology, mineral resources, and hydrology of northern Nevada. This report describes the geophysical data and methods used to aid in the present mineral-resource assessment of the HRB. Basic gravity and magnetic data sets available for the study area are described in this chapter. The interpretation of these geophysical data were aided by the use of simplified geologic map of northern Nevada and the HRB, derived from a digital version of Stewart and Carlson's (1978) geologic map of Nevada (fig. 6–2).

Geophysical Data and Maps

Gravity

An isostatic gravity map (fig. 6–3) of the HRB was compiled from data from more than 30,000 gravity stations, most of which are publicly available and described on a CD–ROM of gravity data of Nevada (Ponce, 1997). This data set, which in part includes gravity data recently collected by the USGS (Ponce and others, unpub. data, 2000), resulted in publication of the final two remaining gravity maps of Nevada—the Lovelock and Vya 1 x 2 degree quadrangles (Ponce and others, 1999; Ponce and Plouff, 2001). In addition, an isostatic gravity map of the central part of the HRB that covers the Battle Mountain 30 x 60 minute quadrangle was described by Ponce and Morin (1999). Gravity data coverage varies from one area to another and averages about 1 to 2 stations per 4 km^2 (fig. 6–4).

All gravity data were reduced using standard gravity methods (for example, Dobrin and Savat, 1988; and Blakely, 1995). Gravity data processing included the following corrections: (1) the earth-tide correction, which corrects for tidal effects of the moon and sun; (2) instrument drift correction, which compensates for drift in the instrument's spring; (3) the latitude correction, which incorporates the variation of the Earth's gravity with latitude; (4) the free-air correction, which accounts for the variation in gravity due to elevation relative

to sea-level; (5) the Bouguer correction, which corrects for the attraction of material between the station and sea-level; (6) the curvature correction, which corrects the Bouguer correction for the effect of the Earth's curvature; (7) the terrain correction, which removes the effect of topography to a radial distance of 166.7 km; and (8) the isostatic correction, which removes long-wavelength variations in the gravity field arising from isostatic compensation of crustal roots that are inversely related to topography.

Observed gravity values were referenced to the International Gravity Standardization Net 1971 (IGSN 71) gravity datum (Morelli, 1974). Free-air gravity anomalies were calculated using the Geodetic Reference System 1967 formula for the theoretical gravity on the ellipsoid (International Union of Geodesy and Geophysics, 1971) and Swick's formula (1942) for the free-air correction. Bouguer, curvature, and terrain corrections were added to the free-air correction to determine the complete Bouguer anomaly at a standard reduction density of 2,670 kg/m^3. Finally, a regional isostatic gravity field was removed from the Bouguer gravity field assuming an Airy-Heiskanen model for isostatic compensation of topographic loads (Jachens and Roberts, 1981) with an assumed crustal thickness of 25 km, a crustal density of 2,670 kg/m^3, and a density contrast across the base of the model of 400 kg/m^3.

Terrain corrections, which account for variation of topography near a gravity station, were computed using manual methods for older data and digital methods for recent data. Terrain corrections consist of a three-part process: (1) the innermost or field terrain correction, (2) inner-zone terrain correction, and (3) outer-zone terrain correction. Terrain corrections nearest the gravity station, that is the innermost or field terrain corrections, were estimated in the field and typically extend to a radial distance of 53 to 68 m. Inner-zone terrain corrections were made using either Hayford and Bowie (1912) or Hammer (1939) systems that divide the terrain surrounding a gravity station into zones and equal-area compartments. Average elevations for each compartment were manually estimated from the largest-scale topographic maps available, usually USGS 1:24,000-scale maps. The terrain corrections were then calculated on the basis of the average estimated elevation of each compartment. Inner-zone terrain corrections typically extend to a radial distance of 0.59 to 2.29 km. With the advent of computer processing and

the availability of detailed digital elevation models (DEMs), modern-day inner-zone terrain corrections were computed using USGS 7.5' DEMs with a resolution of 30 m derived from USGS 1:24,000–scale topographic maps. Outer-zone terrain corrections, to a radial distance of 166.7 km, were computed using a DEM derived from USGS 1:250,000-scale topographic maps and an automated procedure (Plouff, 1966; Godson and Plouff, 1988). Digital terrain corrections were calculated by computing the gravity effect of each grid cell using the distance and difference in elevation of each grid cell from the gravity station.

The resulting isostatic gravity digital data set was gridded at an interval of 800 m using a computer program (Webring, 1981) based on a minimum curvature algorithm by Briggs (1974). The resulting grid was then interpolated to a 1-km grid and color contoured.

Magnetics

A residual total intensity aeromagnetic map (fig. 6–5) of the study area was derived from a statewide compilation by Hildenbrand and Kucks (1988). Aeromagnetic surveys were flown at various flight-line spacings and altitudes (fig. 6–6). Most of the study area was flown at a flight-line spacing of 0.6–1.2 km (1–2 mi) and a barometric flight-line altitude greater than or equal to 2.7 km (9,000 ft). The northeastern part the map is covered by NURE (National Uranium Resource Evaluation) aeromagnetic surveys flown at a coarse flight-line spacing of 4.8 km (3 mi) and a nominal flight-line elevation of 120 m (400 ft) above the ground. Other parts of the maps were flown at a flight-line spacing of 1.2 km (1 mi) and a nominal flight-line elevation of 152–610 m (500–2,000 ft) above the ground. Residual magnetic anomalies were computed by subtracting an International Geomagnetic Reference Field (Langel, 1992) appropriate for the year of the survey. Individual aeromagnetic surveys were upward or downward continued, if necessary, to a flight-line elevation of 305 m (1,000 ft) above the ground, adjusted to a common datum, and merged to produce a uniform map that allows interpretations across survey boundaries. Because of the coarse flight-line spacing and, in general, high flight-line elevation, the resulting magnetic map may not resolve magnetic sources lying at shallow depths beneath the surface. In addition, because of the poor quality of some surveys, caution should be exercised when interpreting short-wavelength anomalies that cross the original survey boundaries. The digital data set was gridded at an interval of 1 km using a computer program (Webring, 1981) based on a minimum curvature algorithm by Briggs (1974) and color contoured.

Physical-Property Data

Physical-property data from rocks within the study area are essential for understanding the relation between geophysical anomalies and their causative sources. For purposes of this study, rock samples were collected at newly acquired gravity stations when a rock outcrop was nearby and at other locations when time permitted. More than 480 physical property measurements are available from within the study area (fig. 6–7, table 6–1). Rock densities within the study area can be separated into several broad groups: (1) pre-Cenozoic rocks that have an average density of about 2,700 kg/m³, (2) felsic granitic rocks that have an average density of about 2,650 kg/m³, (3) mafic volcanic rocks that have an average density of about 2,800 kg/m³, (4) felsic volcanic rocks that have a density of about 2,200 to 2,400 kg/m³, and (5) low-density alluvial deposits that are inferred to have a range in density of about 1,800 to 2,200 kg/m³.

Magnetic rock properties may have a wide range in values that span several orders of magnitude. Magnetic properties also can be separated into several broad groups for geophysical analyses, including essentially nonmagnetic pre-Cenozoic carbonate rocks, granitic rocks with moderately variable magnetic properties, volcanic rocks that may have highly variable induced and remanent magnetizations, and essentially nonmagnetic alluvial deposits. Granitic rocks are moderately magnetic, and about 60 samples in northern Nevada have an average susceptibility of 0.51 cgs units and a range in susceptibility of 0.00 to 1.97 cgs units. In general, felsic volcanic rocks are moderately magnetic, and 24 samples of felsic volcanic rocks have an average susceptibility of 0.21 cgs units and a range in susceptibility of 0.00 to 0.60 cgs units. Mafic dikes, in the vicinity of the Northern Nevada Rift and the two similar features to the west (NNRW, NNRC, NNE, fig. 6–1), are strongly magnetic, and 35 sites (81 samples) have an average susceptibility of 1.87 cgs units and a range in susceptibility of 0.24 to 5.30 cgs units.

On the basis of their aeromagnetic expression, magnetic properties of mapped Jurassic, Cretaceous, and Eocene plutons were inferred for the central part of the HRB (fig. 6–8). The area is bounded by latitudes 40° 00' and 41° 45'N., and longitudes 115° 45' and 117° 30'W. Only one third of the 23 Jurassic plutons are associated with magnetic highs; 4 out of 5 Cretaceous plutons are associated with magnetic highs; and only about a third of the 34 Eocene plutons in this area are associated with magnetic highs. Although Cretaceous plutons are more commonly associated with magnetic highs than other granitic rocks of either Jurassic or Eocene age, there are probably an insufficient number of Cretaceous plutons in the study area for this inference to be statistically significant. Overall, the results indicate that one age group is not preferentially more commonly magnetic than another age group. Thus, for example, aeromagnetic data alone do not support the notion that circular magnetic highs usually reflect plutons of Eocene age.

Derivative Geophysical Maps

Depth to Basement Map

An iterative gravity inversion method (Jachens and Moring, 1990) was used to determine the thickness of Cenozoic basin deposits in northern Nevada shown in figure 6–9.

Gravity data used in this process were reduced using standard techniques that include terrain and isostatic gravity corrections. Isostatic gravity anomalies (Simpson and others, 1986) were used during the inversion process because they enhance or reflect shallow- to mid-crustal sources within the Earth.

The depth-to-basement method separates the gravity field into two components—the field caused by pre-Tertiary basement and the field caused by overlying younger basin deposits. An initial basement gravity field is determined by using just those stations located on pre-Cenozoic basement outcrops. The initial basement gravity field is only approximate because stations located on basement are influenced by the gravity effect of low-density deposits in nearby basins, especially for those stations near the edge of the basins. The difference between the isostatic gravity and basement gravity fields provides the first estimate of the basin gravity field, which is inverted to provide the first estimate of the basin depth and shape. The gravitational effects of the basins are subtracted from each station located on basement, and a new and improved basement gravity field is determined. This process is repeated until successive iterations converge. Inversion of the final basin gravity field constrained with a density-depth function (table 2), geology, and drill-hole information yields an estimate of the depth to pre-Tertiary basement. The density of basement rocks is allowed to vary horizontally, whereas the density of basin-filling deposits increases with depth according to the density-depth relationships shown in table 2. The density-depth function is based on density information from rock samples, geophysical well logs, and borehole gravity data. A density-depth profile representative for the entire state of Nevada (Jachens and Moring, 1990) was used for sedimentary and volcanic deposits. Drill-hole data were used as independent constraints for the Winnemucca quadrangle (Ponce and Moring, 1998) in the central part of the study area. The digital data sets used in the depth-to-basement process were gridded at an interval of 2 km using a computer program (Webring, 1982) based on a minimum curvature algorithm by Briggs (1974). The resulting grid was then interpolated to a 1-km grid to minimize pixel size and color-contoured.

A number of limitations are inherent in the gravity data themselves, as well as in the inversion process. Some uncertainties are related to the gravity data coverage, especially for stations on basement outcrops, the density-depth function, accuracy or scale of the geologic mapping, simplifying assumptions regarding concealed geology, and the distribution of basement outcrops. The depth-to-basement process itself is regional in scope and caution should be exercised when using these results at a scale greater than about 1:250,000. A more detailed discussion of the limitations and accuracy of the method are provided by Jachens and Moring (1990).

Basement Gravity Map

One of the by-products produced during the depth-to-basement process described above is a basement gravity map (fig. 6–10). The basement gravity map is the isostatic gravity map with the effects of Cenozoic basins removed and reflects lateral density variations in pre-Cenozoic basement rocks. The basement gravity map is particularly useful for defining pre-Cenozoic structures and crustal geophysical domains.

Reduction-to-the-magnetic-pole Map

Because the regional magnetic field and the direction of magnetizations are seldom vertical, magnetic anomalies are commonly laterally displaced from their sources and may have distorted, asymmetrical shapes. This effect often increases the complexity and difficulty of magnetic anomaly interpretation. A reduction-to-the-magnetic-pole (RTP) transformation and resulting map (fig. 6–11) removes the effect of the direction of the earth's magnetic field and the direction of magnetization by transforming the data to their expression at a vertical field and magnetization as if measured at the north magnetic pole. Remanent magnetization is assumed to be either negligible or in the same direction as the Earth's magnetic field. This transformation approximately centers magnetic anomalies over their sources and will produce a symmetrical anomaly over a symmetrical source. A more detailed discussion of reduction to the pole can be found in Baranov and Naudy (1964) and Blakely (1995).

Magnetic-Potential (or Pseudogravity) Map

The magnetic and gravity potentials are related by a directional derivative, thus the total magnetic field can be transformed into an equivalent gravity field. Magnetic-potential, or pseudogravity, maps (fig. 6–12) are produced by the transformation of the magnetic field into the equivalent gravity field assuming a density distribution equal to the magnetization distribution (Baranov, 1957). The ratio between magnetization and density is held constant, and, in this application, the ratio is a magnetization contrast of 0.001 cgs units to a density contrast of 0.10 g/cm^3. This process amplifies long wavelengths (deeper sources) at the expense of short wavelengths (shallow sources). The pseudogravity transformation is a useful geophysical tool because interpretations of magnetic maps are often more complex than interpretations of gravity maps. In addition, because gravity anomalies have their steepest gradients approximately over the edges of their causative sources, especially for shallow sources, the magnetic potential map can be used to approximate the edges of magnetic sources (Blakely, 1995).

To illustrate differences between total magnetic field, reduction to the pole, and magnetic potential, two theoretical models were constructed across idealized sources. A theoretical profile across a buried slab along east-west and north-south trending lines is shown in figure 6–13. The slab is 2-km thick, 100 km in length, and buried at a depth of 2 km. The relative ratio of the magnetization and density distribution during the transformation to pseudogravity anomalies is as

described above. The model reveals that the total magnetic field is asymmetrical and that the edge of the source does not correlate with the inflection point of the magnetic profile. In contrast, the RTP and magnetic potential anomalies are centered over the source and their maximum horizontal gradients align with the edges of the buried slab. In addition, these profiles reveal that the magnetic potential anomaly has a simple (gravimetric) form and removes the complexity of interpreting total field or RTP anomalies. Another example illustrating the differences between these derivative magnetic maps is a theoretical model in contour form over a cube 2 km on a side and buried at a depth of 2 km (fig. 6–14). Especially noticeable is the transformation of the total field anomaly to the RTP anomaly where the anomaly becomes centered over the symmetrical source.

Maximum Horizontal Gradients

To better define the edges of geophysical sources and to help derive geophysical lineaments and terranes, the maximum horizontal gradients of both gravity and magnetic data were computer generated. A technique described by Blakely and Simpson (1986) was used to calculate the maximum horizontal gradients. Maximum horizontal gradients were derived for both previously described basement gravity and magnetic-potential maps, and their locations are shown on the isostatic-gravity and total-field aeromagnetic maps, respectively (figs. 6–3 and 6–5). These maxima reflect abrupt lateral changes in the density or magnetization of the underlying rocks.

Geophysical Lineaments and Terrane Maps

To facilitate integration of geophysical interpretations into the mineral assessment of the HRB, geophysical features were converted to lineaments and similar structural fabrics or crustal terranes. Gravity and magnetic lineations (figs. 6–15 and 6–16) were derived from the basic data sets with the aid of a physical boundary enhancing technique to determine the maximum horizontal gradients (Blakely and Simpson, 1986). Terrane maps, on the other hand, reflect regions with similar features or crustal blocks of similar physical properties or sources. Gravity and magnetic terrane maps (figs. 6–17 and 6–18) were created by visual inspection of gravity, magnetic, and derivative geophysical maps; by drawing polygons around similar geophysical areas; and by using lineaments as a guide to locating terrane boundaries.

These techniques resulted in production of four interpretive maps that include basement-gravity lineaments, magnetic lineaments, basement gravity terranes, and magnetic terranes. These maps were derived from the aforementioned geophysical data and derivative products including isostatic gravity, basement gravity, aeromagnetics, reduction-to-the-pole magnetics, magnetic potential, and the maximum horizontal gradients of gravity and magnetic data. The utilization of

these four digital products in the data-driven part of the HRB mineral resource assessment of pluton-related, sedimentary rock-hosted Au–Ag, and epithermal deposits are described in chapter 2.

Application to Data-Driven Modeling Methods

The data-driven modeling process used in the mineral assessment is geographic information system- (GIS-) driven and utilized both weights-of-evidence and weighted-logistic-regression processes. These two methods were ultimately integrated with expert knowledge to derive the final mineral resource assessment (see Chapter 2). The data-driven modeling component of the mineral assessment utilized a representative training set for a particular deposit type, determined the weights of spatial association between specific GIS layers and the training set, and then, using a weighted-logistic-regression process, predicted the probability of undiscovered mineral deposits (see chapter 2). These data-driven methods are particularly well suited to utilizing categorical data, such as geologic terranes, and ratio data, such as proximity to linear features. Although geophysical contours in themselves also are easily incorporated into a data-driven modeling process, they can lead to erroneous results for the following reasons:

- Datums are arbitrary—compounded by numerous individual surveys merged together and datum shifted to match one another.

- Contour intervals have no absolute or physical meaning.

- Contour levels from one place to another may not reflect the same source or feature. A simple horizontal sheet, for example, that may not have any significance to mineral resource potential could shift anomaly values from one place to another.

- For total intensity magnetic maps, the dipole nature of magnetic anomalies and the remanent magnetization properties of rocks are not taken into account.

- Alteration may have destroyed the magnetic properties of the causative rocks and thus altered the magnetic anomaly from one place to another.

- Physical properties can be highly variable within a single lithologic unit, especially magnetic properties that can vary by several orders of magnitude.

Because of these limitations, direct use of geophysical contours should be avoided in the data-driven modeling process and, thus, contour information was not used in the HRB mineral resource assessment. To facilitate the use of geophysical information, geophysical maps were converted

to interpretive causative features such as lineaments, physical property boundaries, similar geophysical fabrics, and geophysical terranes. Filtered geophysical maps were used as an aid in determining the location and physical boundaries of these features. When using a particular layer in the modeling process, it is also important to verify that the physical model on which the data are based is honored in the modeling process. For example, suppose high values of limonite anomalies (iron-oxide staining that may reflect hydrothermal alteration) correlate to epithermal gold deposits—can we develop a physical model to account for the relationship, can the model be verified in the field, and is it properly represented in the modeling process? In addition to these caveats, Singer and Kouda (1999) compared the weights-of-evidence method to probabilistic neural networks and described some of the limitations involved in using the weights-of-evidence method. In particular, results can be biased if the target area is not uniformly explored, and adverse effects may result even when there is small to moderate correlation between data layers (non-independent layers). These caveats were mitigated in the mineral assessment of the HRB by using expert opinion and by combining evidence layers using weighted logistic regression (Chapter 2).

Discussion

General

In general, isostatic gravity anomalies reflect lateral (horizontal) density variations in the middle to upper crust. Thus, gravity anomalies can be used to infer the subsurface structure of known or unknown geologic features. In general, gravity anomalies within the HRB reflect carbonate rocks, calderas, deep sedimentary basins, plutons, and linear geologic features such as faults. Many of these features play an important role in assessing the mineral resource potential of the HRB. These features may also play an important role as aquifers or confining units in the region, and their distribution is important to understand the hydrogeologic framework of the area. Pre-Cenozoic carbonate and crystalline rocks underlie most of the region, and their subsurface distribution is especially important in evaluating the hydrogeology of the area. Thick accumulations of Tertiary volcanic rocks are present in the central and northwestern part of the HRB. These volcanic rocks also play a significant role in the extensional history of the area. Quaternary alluvial deposits are present throughout the study area and are composed of nonmarine sedimentary and volcanic rocks. These deposits and their thickness affect the depth of mineral exploration and may play an important role in the saturated-zone hydrology of the deep alluvial basins within the study area.

Geologic features commonly produce small magnetic fields that perturb the main field of the Earth and can be enhanced by the removal of a regional magnetic field. These measurements reflect lateral changes in rock magnetic properties and can be analyzed to gain insights into the three-dimensional nature of the causative source. In general, aeromagnetic anomalies within the HRB reflect volcanic rocks, calderas, granitic intrusions, and linear geologic features such as faults. Many of these features play an important role in ore formation, and their distribution is important to the understanding of the mineral resource framework of the area. In this region, the use of magnetic methods is critical to the understanding of the geologic, tectonic, and hydrogeologic framework. The diverse physical properties of rock units that underlie this region are well suited to geophysical investigations. The contrast in magnetic properties between pre-Cenozoic rocks, volcanic rocks, and alluvium produces a distinctive pattern of anomalies that can be used to determine the sources of the anomalies and their subsurface extent.

Most Paleozoic rocks are relatively non-magnetic within the study area. Intrusive rocks are, in general, moderately magnetic and are associated with magnetic highs. Tertiary volcanic rocks are strongly magnetic with variable magnetic properties, and they play significant roles in assessing the mineral resource potential and extensional history of the area. Thick accumulations of these volcanic rocks are present throughout the study area. Alluvial deposits within the study area are essentially nonmagnetic and most basins have subdued magnetic anomalies with the exception of those basins that may contain volcanic centers, buried volcanic rocks, or buried granitic rocks.

Depth to Basement

In general, the depth-to-basement within basins in the study area (fig. 6–9) is similar to that of other basins in Nevada, where most basins are less than about 2 km thick. Several basins within the HRB study area are greater than about 5 km in thickness, including Pine Valley, one of the deepest basins in Nevada. Most basins are characterized by the presence of multiple subbasins and steep gravity gradients along their margins.

Many basins within the study area veer northward as they approach the Northern Nevada Rift (NNR), as observed by Blakely and Jachens (1991b). This is particularly evident for the following basins that, from south to north, include: Railroad Valley, Antelope Valley-Monitor Valleys, Little Smoky Valley, Carico Lake-Crescent Valleys, Pine Valley, and Reese River Valley (figs. 6–9 and 6–1). This phenomenon is probably related to the basement feature described below rather than the NNR that is itself contained within the basement gravity high.

As a general guide to mineral exploration, Cenozoic basins that are greater than about 1 km thick are uneconomical to exploit, and these areas were excluded in the mineral resource assessment of the HRB. Although 80 percent of the bedrock in Nevada is covered by basin-fill deposits, these

deposits are thicker than 1 km in only about 20 percent of the State (Blakely and Jachens, 1991a). Thus, a large portion of the potentially favorable source rocks that are present below basin-fill deposits in Nevada are within reach of current exploration models.

Basement Gravity

A prominent "V-shaped" basement gravity high transects northern Nevada (fig. 6–10). In the middle part of the HRB, this high is characterized by a steep basement gravity gradient trending N20°W that parallels the NNR, especially from Eureka to north of Battle Mountain. Gravity modeling suggests that this feature is not caused by mafic volcanic rocks because the associated magnetic anomaly would be too large. Rather, the feature probably is related to lateral density contrasts within basement rocks. This basement feature is about 40 km wide and includes the NNR. The western margin of the western leg of this feature lies near the western edge of the NNR. The eastern edge of the western leg of this feature is parallel to and lies near the Carlin mineral trend. This basement gravity feature probably reflects a deep crustal structure that may have been reactivated by the NNR and Basin and Range normal faulting (Ponce and Glen, 2000).

A crustal feature along the Battle Mountain-Eureka mineral trend (BME) was described in detail by Grauch and others (1995, 1998) and Rodriguez (1998) on the basis of gravity, magnetic, and electrical data. The BME (Roberts, 1966) is defined as an alignment of a wide range of gold deposits that includes sediment-hosted disseminated and pluton-related gold deposits in north-central Nevada. The Battle Mountain-Eureka crustal feature diverges from the trend of the NNR and the basement gravity feature described above, and it appears to be a second-order feature and possibly could be related to the NNR basement gravity feature. These regional crustal features are of critical importance to mineral exploration in northern Nevada as they may serve as the structural controls on mineralizing fluids and ore deposition.

Northern Nevada Rift and Related Features

Some of the most prominent magnetic anomalies in the study area are the Northern Nevada Rift (NNRE, fig. 6-5), described in great detail by Zoback (1978) and Zoback and others (1995) and the two similar and parallel features to the west (NNRW, NNRC; fig. 6-5). These features are here called the western, central, and eastern Northern Nevada Rifts (NNRW, NNRC, and NNRE, respectively). Recent studies of the NNRE by John and others (2000) and John and Wallace (2000) indicate that the NNRE is a much broader rift feature than previously thought and correlates to mid-Miocene epithermal Au–Ag deposits. They indicate that the rift formed in the mid-Miocene between 16.5 and 15 Ma. Within the HRB, the NNRE is defined by an arcuate aeromagnetic high

that reflects mafic rocks that extend to depths of about 15 km. Recent geophysical and paleomagnetic studies by Ponce and Glen (2000) and Glen and Ponce (2000) suggest that the NNRE and the two parallel features to the west are genetically related, arcuate, and extend well to the north beyond the Nevada-Oregon border. Furthermore, they suggest that these features converge and probably reflect the impact of the Yellowstone hot spot on the crust, not at the McDermitt caldera along the Nevada-Oregon border (lat 42°N.) as previously suggested (e.g., Pierce and Morgan, 1992; Zoback and others, 1994; John and others, 2000), but much further to the north along the Oregon-Idaho border at about lat 44°N. Field investigations of these two anomalies indicate they also may be related to possible Miocene mafic dikes (Glen and Ponce, unpub. data, 2000), as well as to rhyolite porphyry domes (see Chapter 9). Prominent isostatic gravity highs also correlate to the western and central Northern Nevada Rifts as noted by Blakely (1988). Magnetic data and their correlation with known epithermal deposits (fig. 6–11) along these features suggest that these sites are favorable locations for mid-Miocene epithermal Au–Ag deposits.

Other Geophysical Lineaments and Terranes

Geophysical terranes defined by basement gravity highs probably reflect lateral density variations in pre-Cenozoic sedimentary, carbonate, or mafic igneous rocks. For example, the basement gravity high at Emigrant Pass (fig. 6–1) that also correlates to a large elliptical magnetic high may be related to a possible mafic plutonic complex or possibly a metamorphic core complex. Terranes defined by basement gravity lows may reflect lower density pre-Cenozoic rocks or relatively less dense plutons surrounded by more dense pre-Cenozoic rocks. Geophysical terranes derived from magnetic data reveal three major terranes that include the eastern Northern Nevada Rift (NNRE) and the two similar anomalies to the west (NNRW, NNRC), the Modoc Plateau in the northwest corner of the study area, and the Walker Lane geophysical terrane. Other small magnetic terranes probably reflect local accumulations of magnetite-bearing rocks throughout the area, some of which are pluton related.

The geophysical terranes associated with the Northern Nevada Rifts are defined by the extent of associated arcuate aeromagnetic anomalies that reflect mafic intrusions, isostatic gravity anomalies, basement gravity anomalies, and by the western leg portion of the prominent "V-shaped" basement gravity anomaly along the NNRE. This terrane is also associated with mid-Miocene felsic rhyolite flows and domes and graben-filling sedimentary deposits along the NNRE. Presumably, these fractures reflect the effects of the Yellowstone hot spot on the crust that caused partial melting of the crust.

The Modoc Plateau, in the northwest corner of the study area, is characterized by high-amplitude, short-wavelength aeromagnetic anomalies and an associated gravity low. These

anomalies primarily result from a thick sequence of volcanic rocks that probably have relatively low densities and highly variable induced and remanent magnetizations.

The Walker Lane belt, defined on the basis of a complex zone of strike-slip faults and irregular topography, is about 100 km wide and extends about 700 km along the southwest margin of Nevada (Stewart, 1988). The Walker Lane belt is partly composed of Jurassic and Triassic granitic and volcanic rocks that correlate to a northwest-trending geophysical fabric of high-amplitude aeromagnetic anomalies in the southwest corner of the study area (fig. 6–18). However, Blakely (1988) noted that the associated geophysical terrane extends much further to the northeast than the eastern edge of the physio-graphic Walker Lane belt by as much as 150 km and probably reflects an underlying, but similar, tectonic fabric. Cox and others (1991) described patterns of mineralized occurrences in the Great Basin and noted a correlation of volcanic-hosted epithermal gold-silver deposits to the Walker Lane belt (com-pare figs. 6–11 and 6–18). For these reasons, the geophysi-cal expression and extension of the Walker Lane belt was considered as a separate terrane during the mineral-resource analysis.

Conclusions

Gravity and magnetic studies of the HRB and their appli-cation to a knowledge- and data-driven mineral assessment reveal that the data from such studies are easily imported into the mineral assessment process and provide new insights into the mineral resource potential of the area. Gravity and mag-netic lineaments and terranes, defined on the basis of a number of derivative geophysical maps, suggest that these features reflect geologic structures, some of which may be associated with gold mineralization in northern Nevada. These features include well-defined lineaments, such as the Northern Nevada Rift and related features to the west, terranes associated with the Northern Nevada Rift and related features to the west, a basement crustal feature in north-central Nevada, and the Walker Lane geophysical terrane.
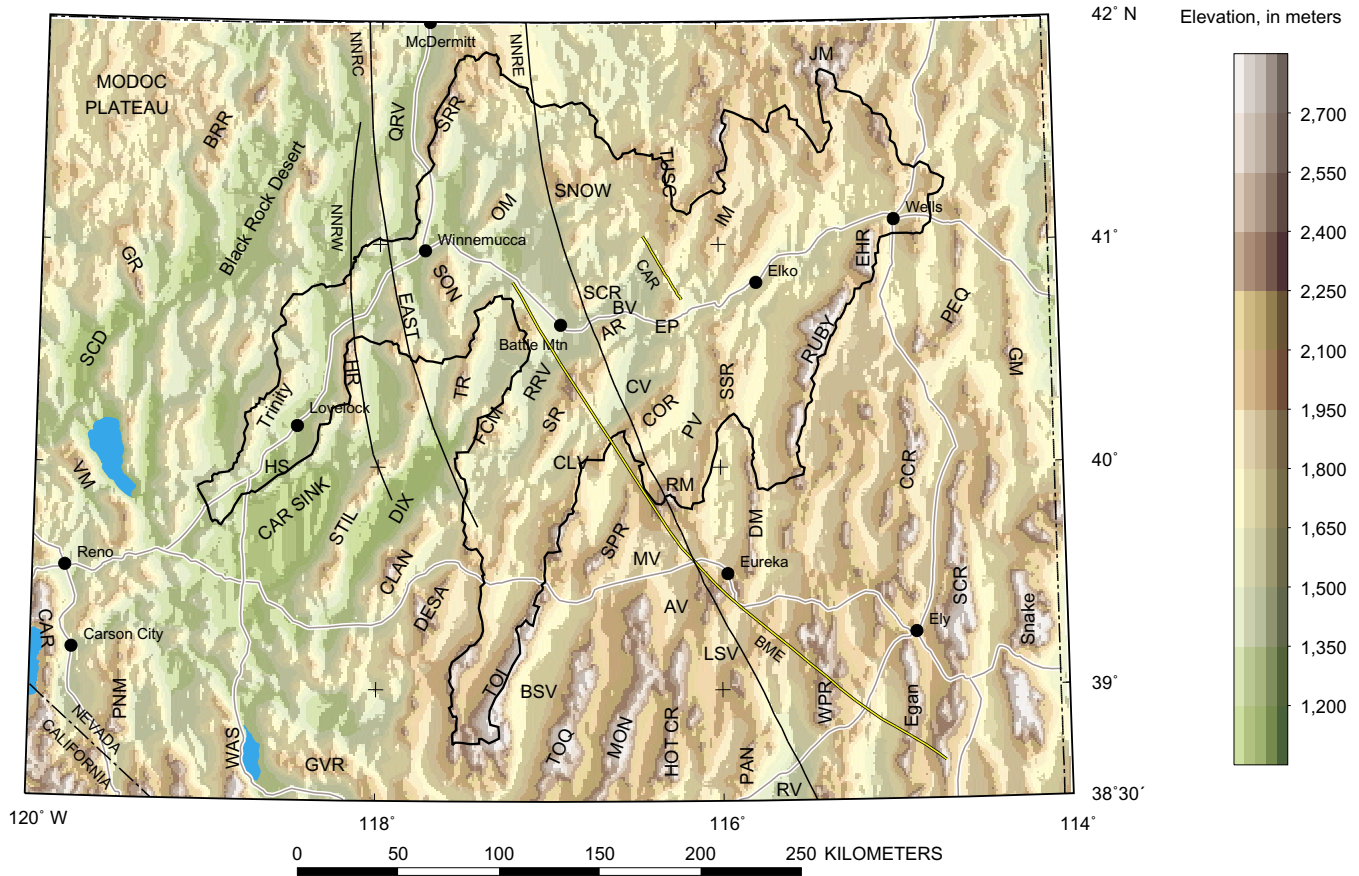
Figure 6-1. Shaded-relief topographic map of northern Nevada showing the outline of the Humboldt River Basin. Geologic features: BME, Battle Mountain-Eureka mineral trend; CAR, Carlin mineral trend; NNRC, central NNR; NNRE, eastern NNR; NNRW, western NNR. Geographic features: AR, Argenta Rim; AV, Antelope Valley; BRR, Black Rock Range; BSV, Big Smokey Valley; BV, Boulder Valley; CCR, Cherry Creek Range; CLAN, Clan Alpine Mts; CLV, Carico Lake Valley; COR, Cortez Mts; CAR, Carson Range; CAR SINK, Carson Sink; CV, Crescent Valley; DESA, Desatoya Mts; DM, Diamond Mts; EAST, East Range; Egan, Egan Range; EGH, East Humboldt Range; EP, Emmigrant Pass; FCM, Fish Creek Mts; GM, Granite Mts; GR, Granite Range; GVR, Gabbs Valley Range; HOT CR, Hot Creek Range; HR, Humboldt Range; HS, Humboldt Sink; IM, Independence Mts; JM, Jarbidge Mountains; LSV, Little Smokey Valley; MON, Monitor Range; MV, Monitor Valley; OM, Osgood Mts; PAN, Pancake Range; PEQ, Pequop Mts; PNM, Pine Nut Mts; PV, Pine Valley; QRV, Quinn River Valley; RV, Railroad Valley; RRV, Reese River Valley; RM, Roberts Mountain; RUBY, Ruby Mts; SCD, Smoke Creek Desert SCR, Schell Cr Range; Snake, Snake Range; SNOW, Snow Storm Mts; SON, Sonoma Range; SPR, Simpson Park Range; SSR, Sulphur Spring Range; STIL, Stillwater Range; TOI, Toiyabe Range; TOQ, Toquima Range; TR, Tobin Range; TUSC, Tuscarora Mts; SRR, Santa Rosa Range; Trinity, Trinity Range; VM, Virginia Mts; WAS, Wassuk Range; and WPR, White Pine Range.
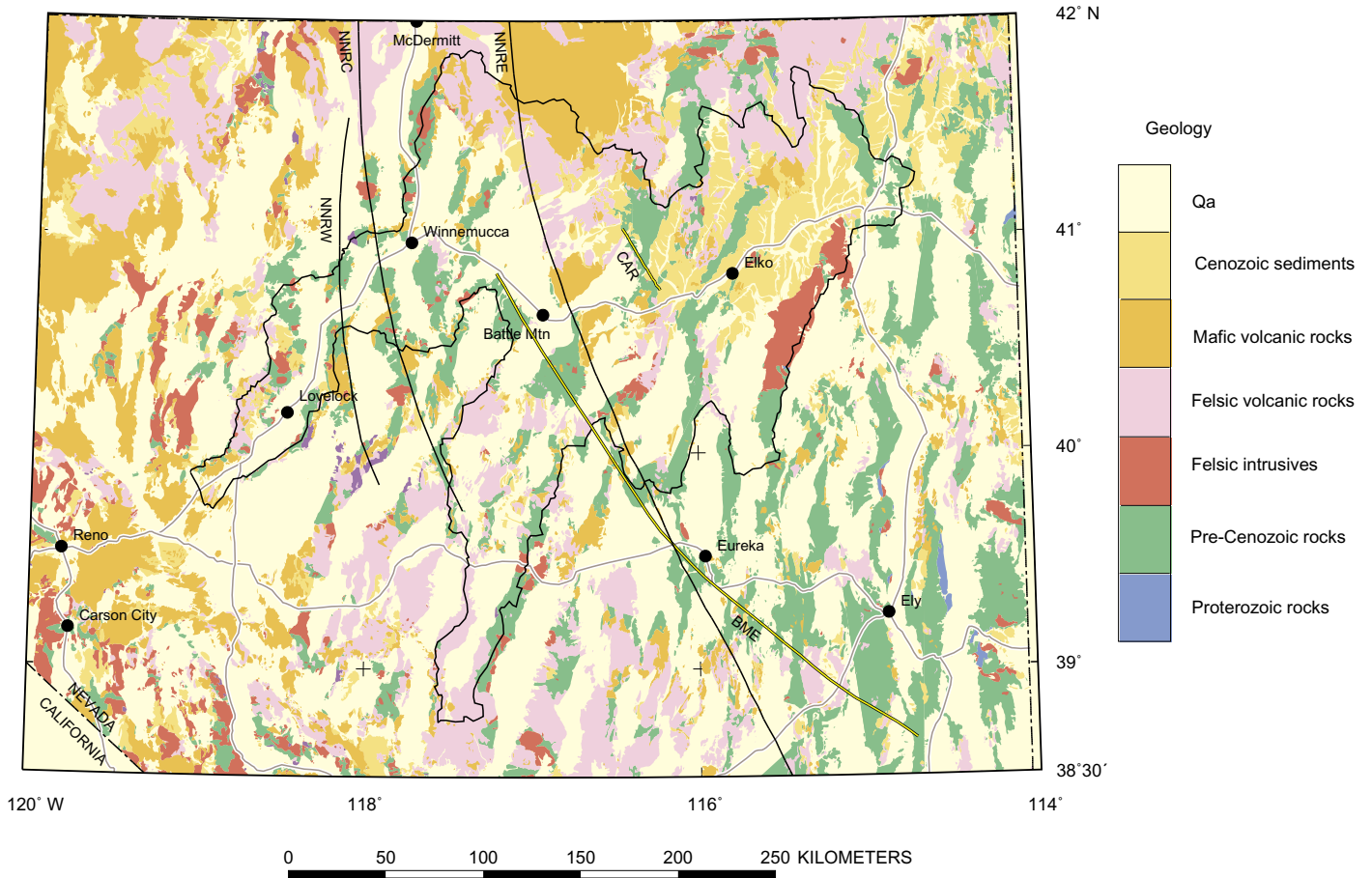
Figure 6-2. Simplified geologic map of northern Nevada modified from Stewart and Carlson (1978). Explanation as in figure 6-1.
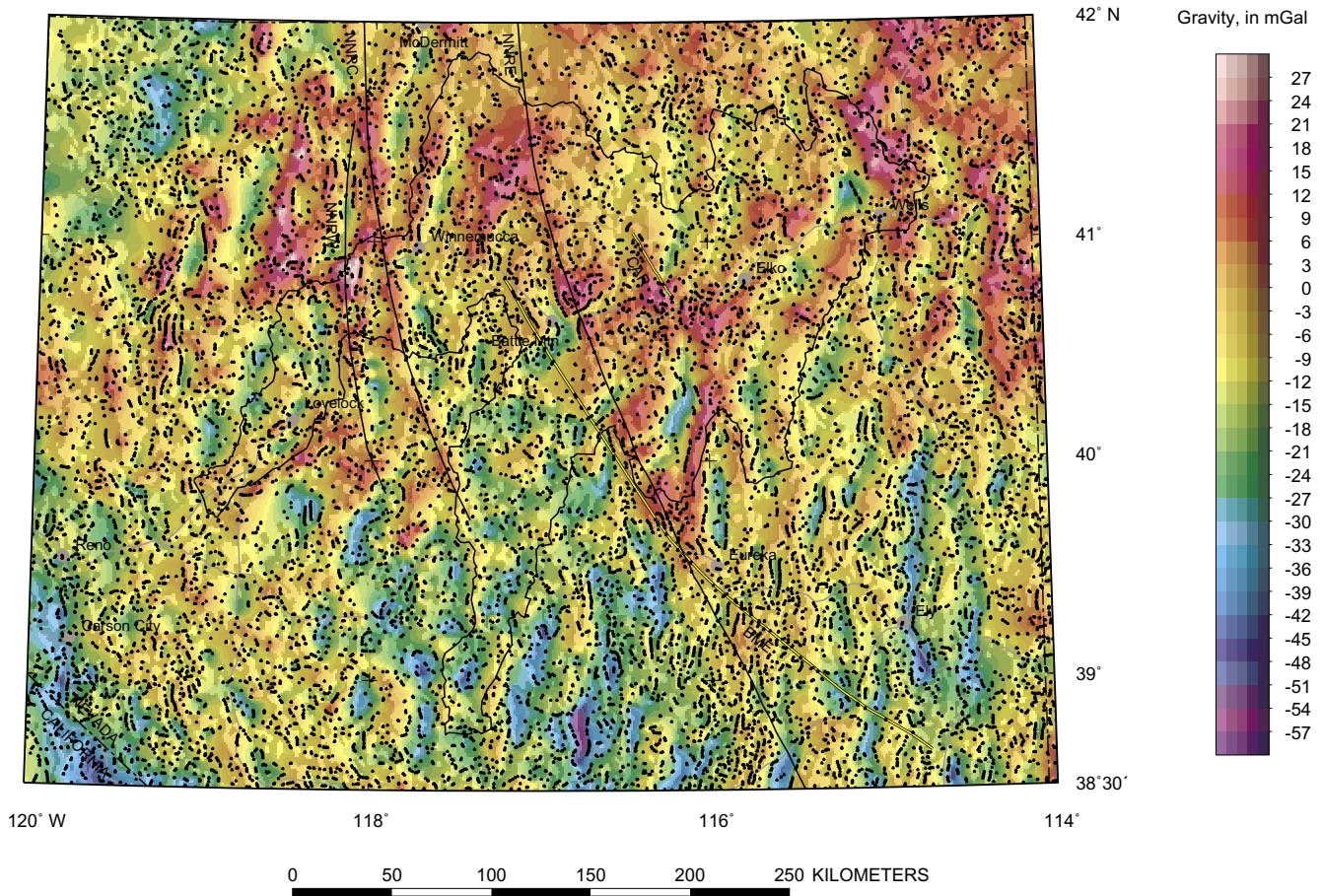
Figure 6-3.   Isostatic gravity map of northern Nevada. Small dots, maximum horizontal gradients derived from basement gravity data. Explanation as in figure 6-1.
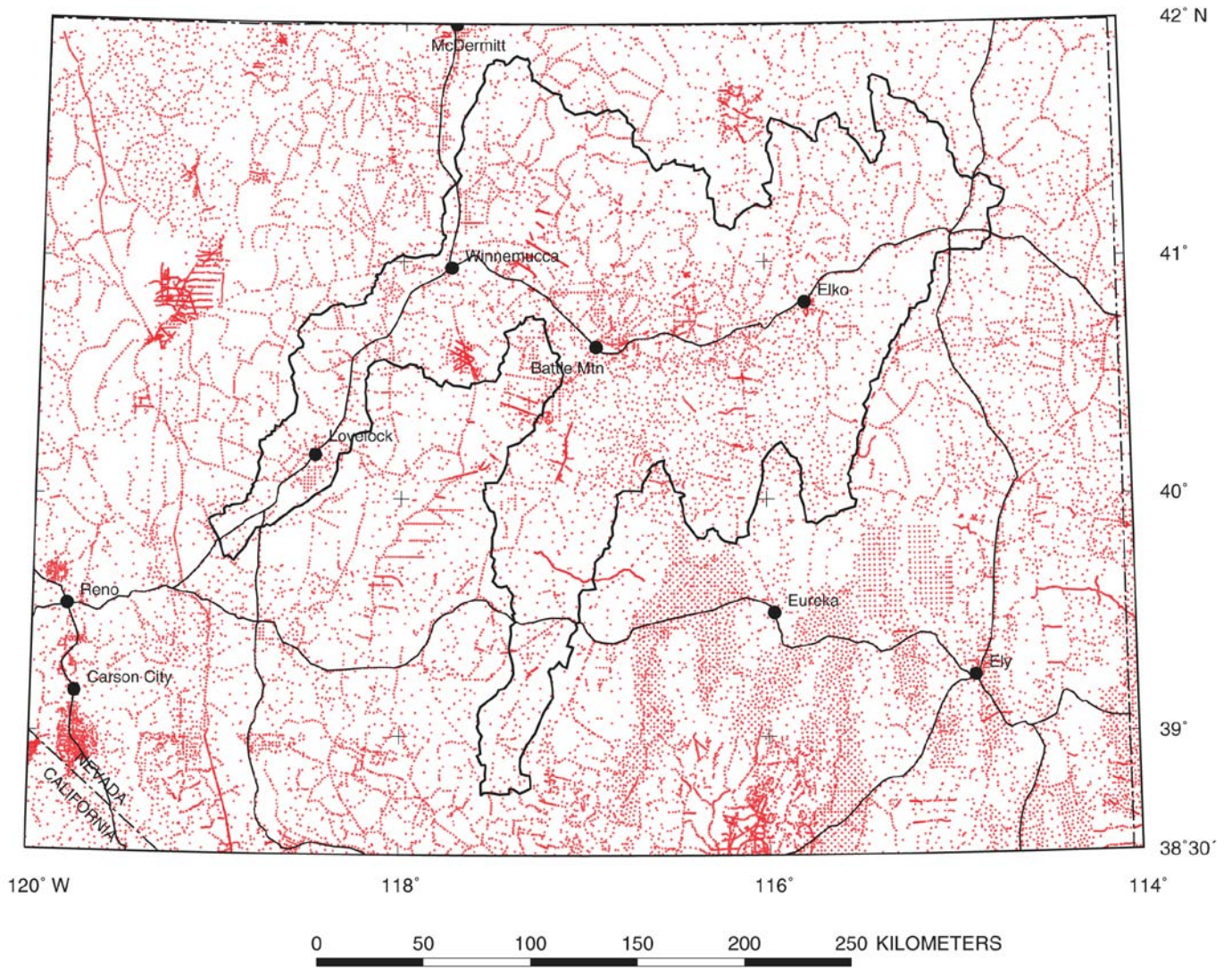
Figure 6-4. Gravity station location map of northern Nevada.
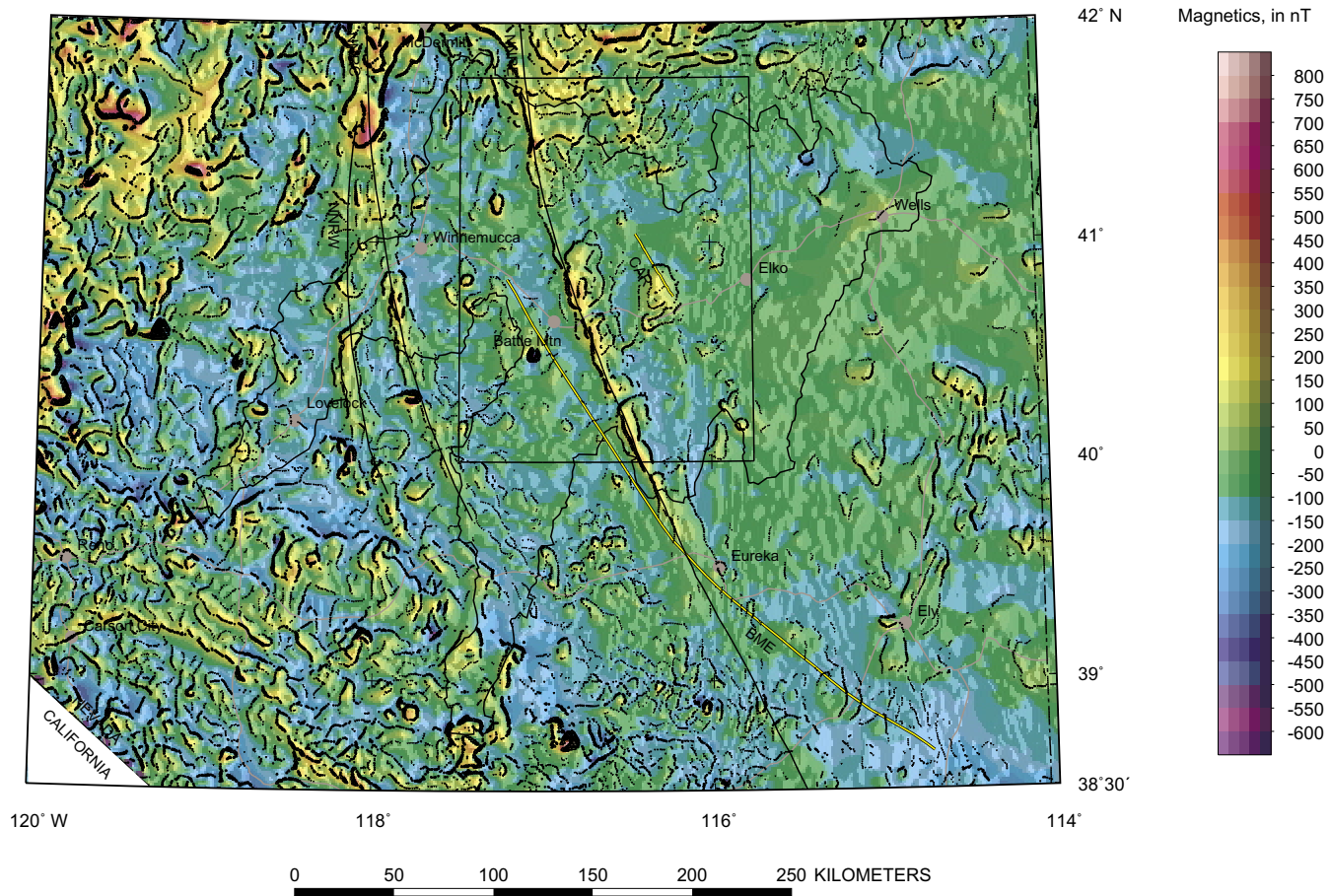
Figure 6-5.   Aeromagnetic map of northern Nevada. Small dots, maximum horizontal gradients derived from magnetic potential data (some dots may coalesce and appear as lines). Explanation as in figure 6-1. An expanded view of the area delimited by the bold rectangular outline is shown in figure 6-8.
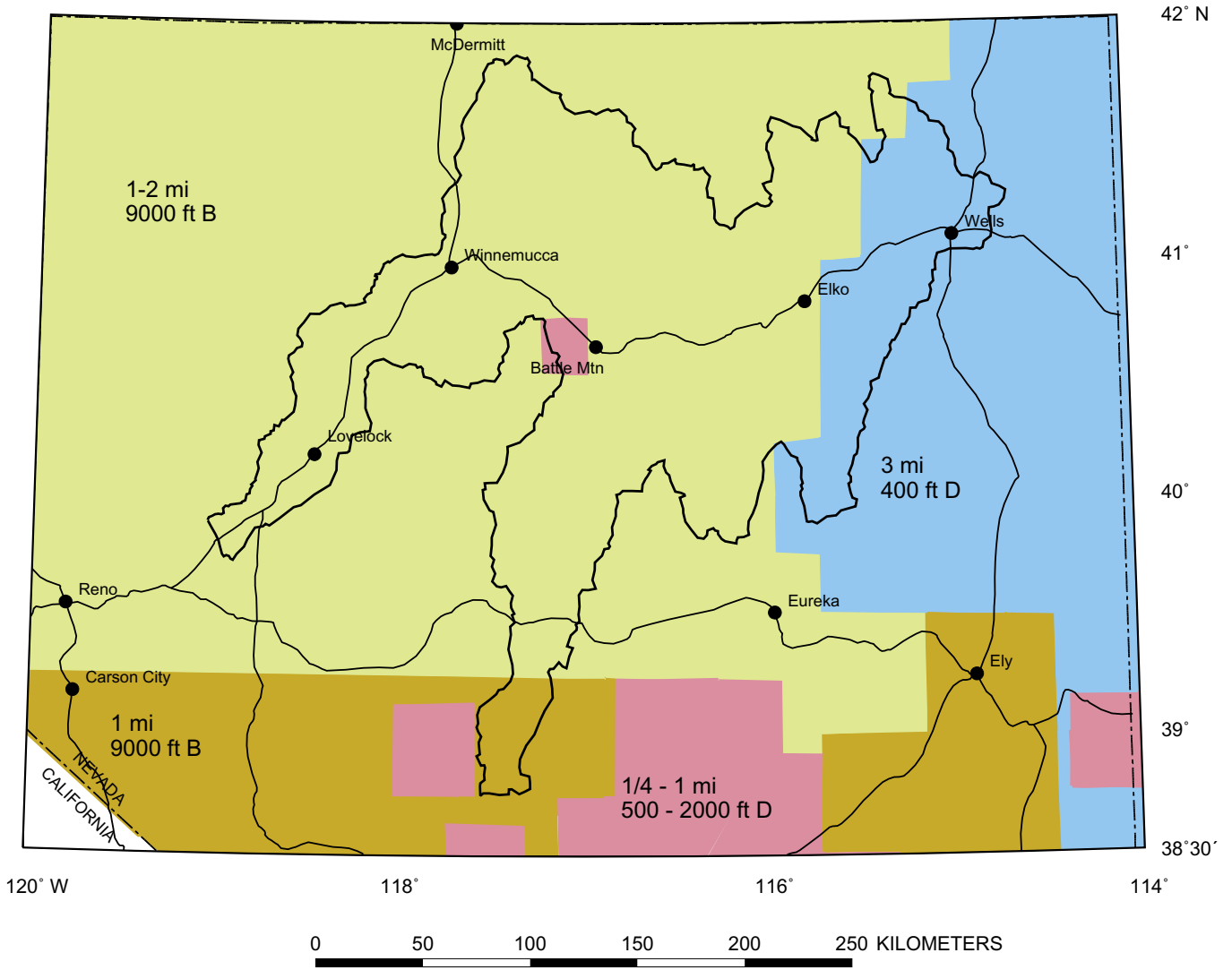
Figure 6-6. Aeromagnetic flight-line specifications. Blue, flight-lines spaced at 3 mi and elevation at 400 ft drape (or constant terrain clearance); Green, flight-lines spaced at 1 to 2 mi and elevation at 9,000 ft barometric; Orange, flight-lines spaced at 1 mi and elevation at 9,000 barometric; Red, flight-lines spaced at 1/4 to 1 mi and elevations at 500 to 2,000 ft drape. B, barometric; D, drape.
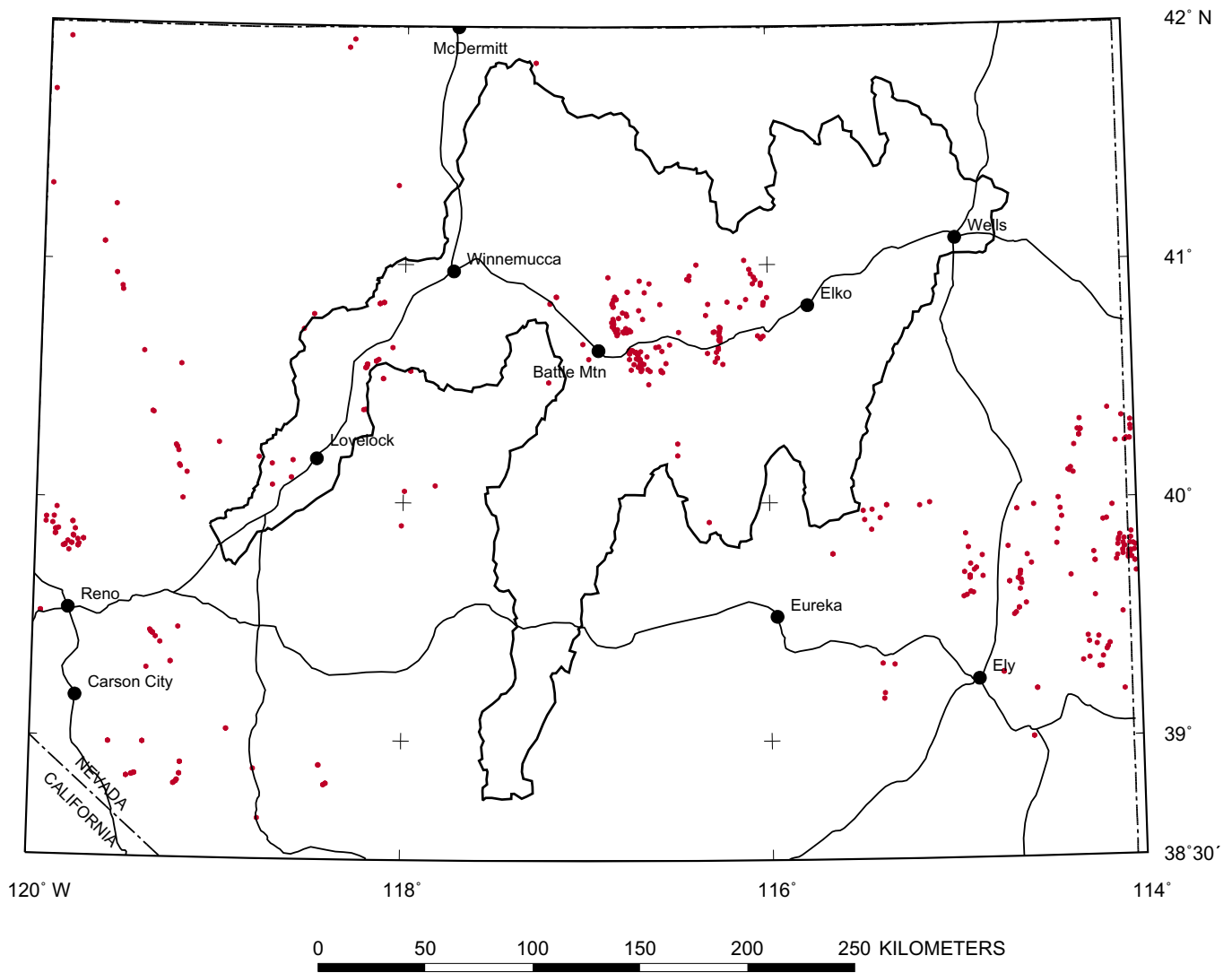
Figure 6-7.   Rock sample locations (red dots) in northern Nevada.
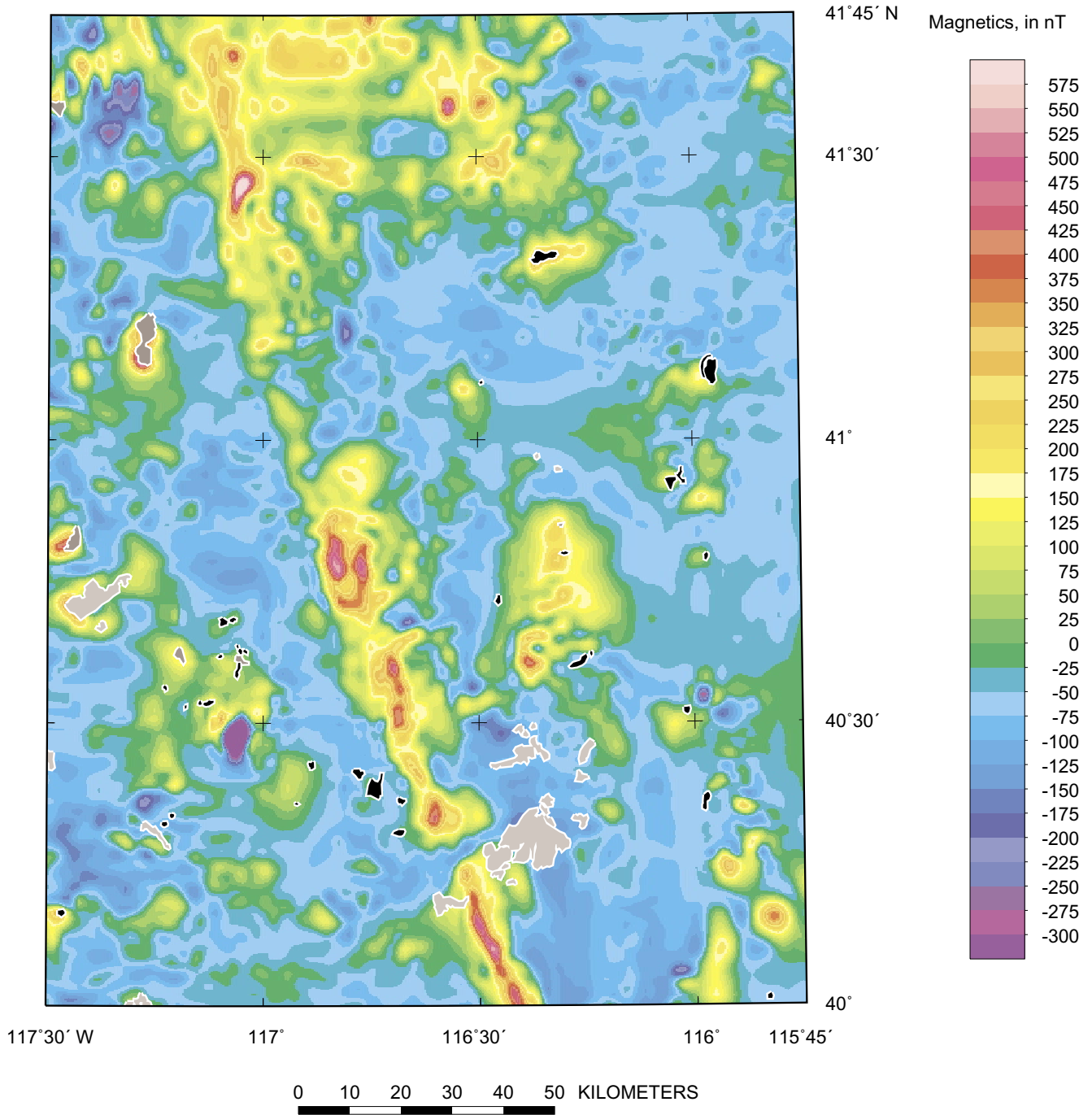
Figure 6-8. Aeromagnetic map showing the distribution of Jurassic, Cretaceous, and Eocene plutons in the central part of the Humboldt River basin (see fig. 6-5). Light gray, Jurassic plutons; Gray, Cretaceous plutons; Black, Eocene plutons. Geology modified from Stewart and Carlson (1978) and Henry and Ressel (2000). Explanation as in figure 6-1.
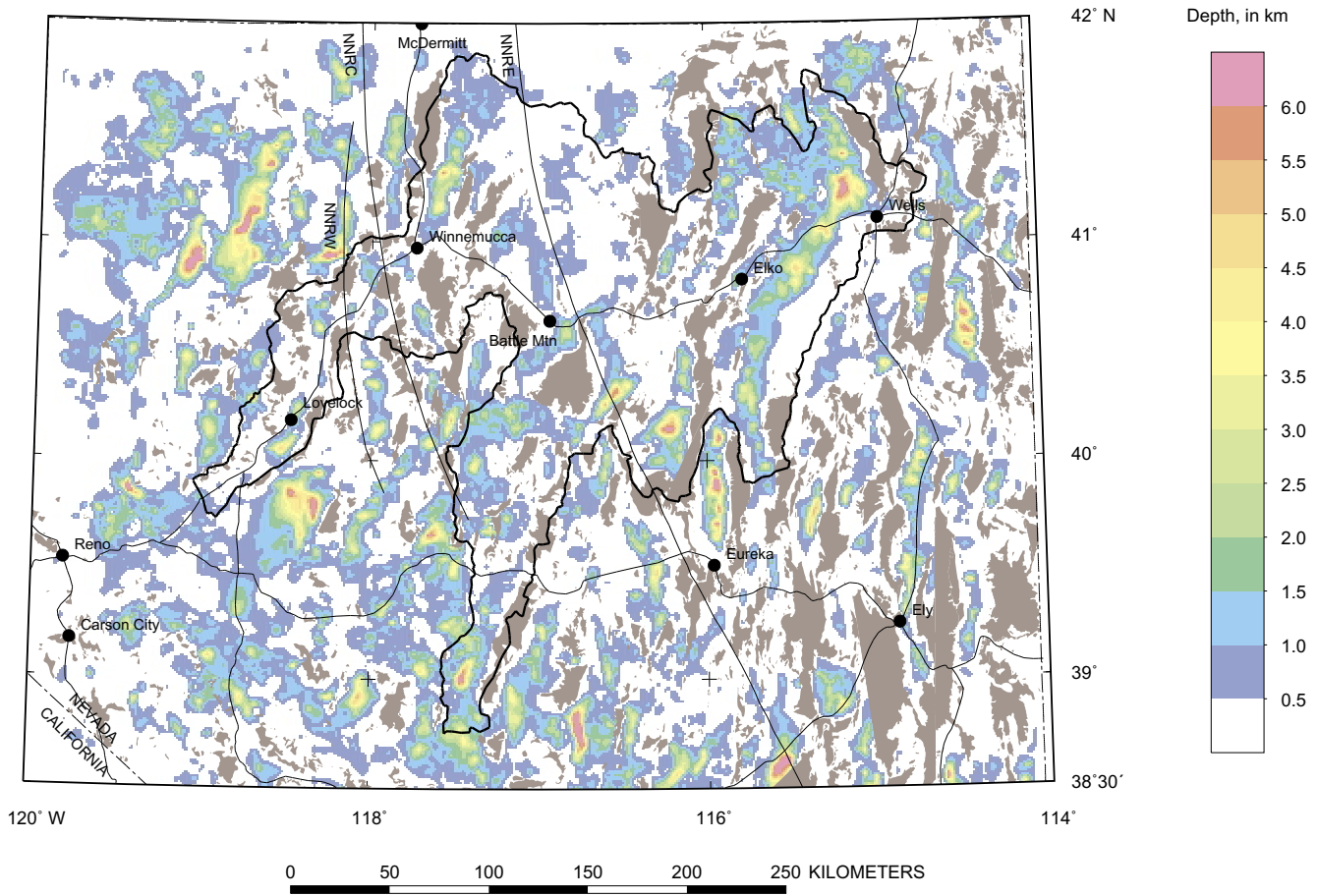
Figure 6-9.   Depth to pre-Cenozoic basement map of northern Nevada. Gray, pre-Cenozoic basement rocks modified from Stewart and Carlson (1978). Explanation as in figure 6-1.
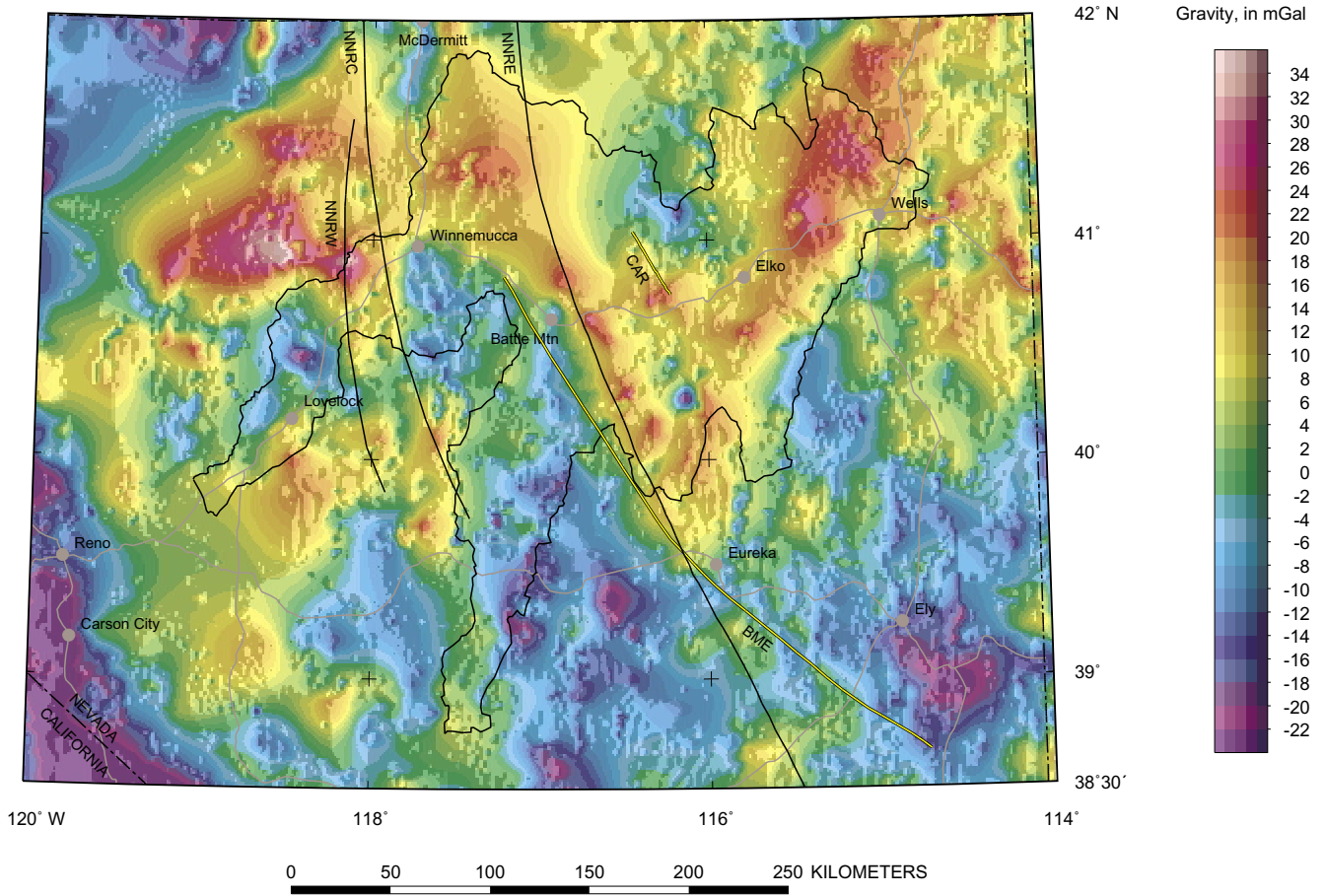
Figure 6-10. Basement gravity map of northern Nevada. Prominent 'V-shaped' anomaly transverses the entire study area. Explanation as in figure 6-1.
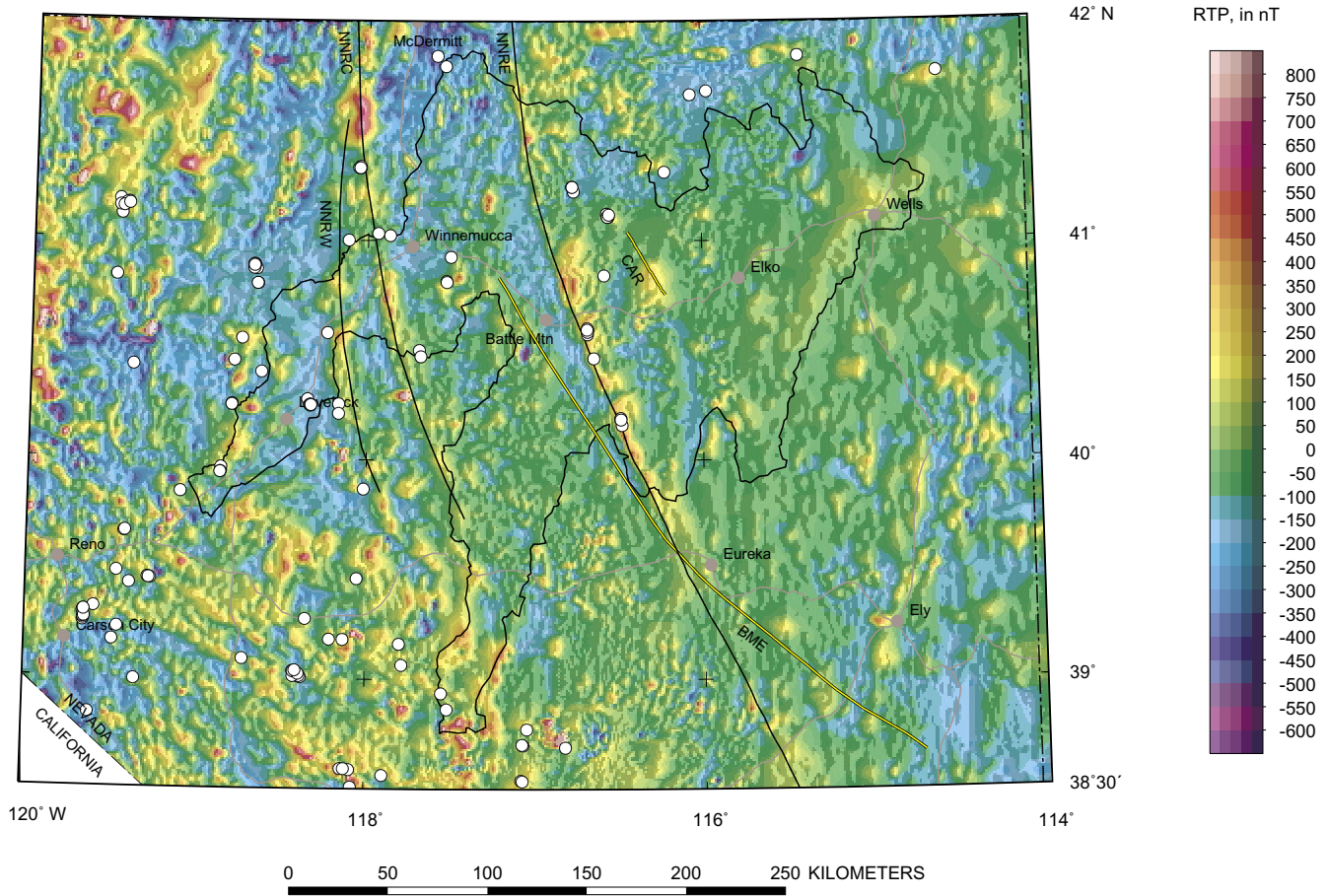
Figure 6-11.   Reduction–to-the-pole magnetic map of northern Nevada derived from the transformation of total field magnetic anomalies. Magnetic data indicate that epithermal gold-silver deposits (white circles) correlate to the northern Nevada rift and the two parallel features to the west. Explanation as in figure 6-1.
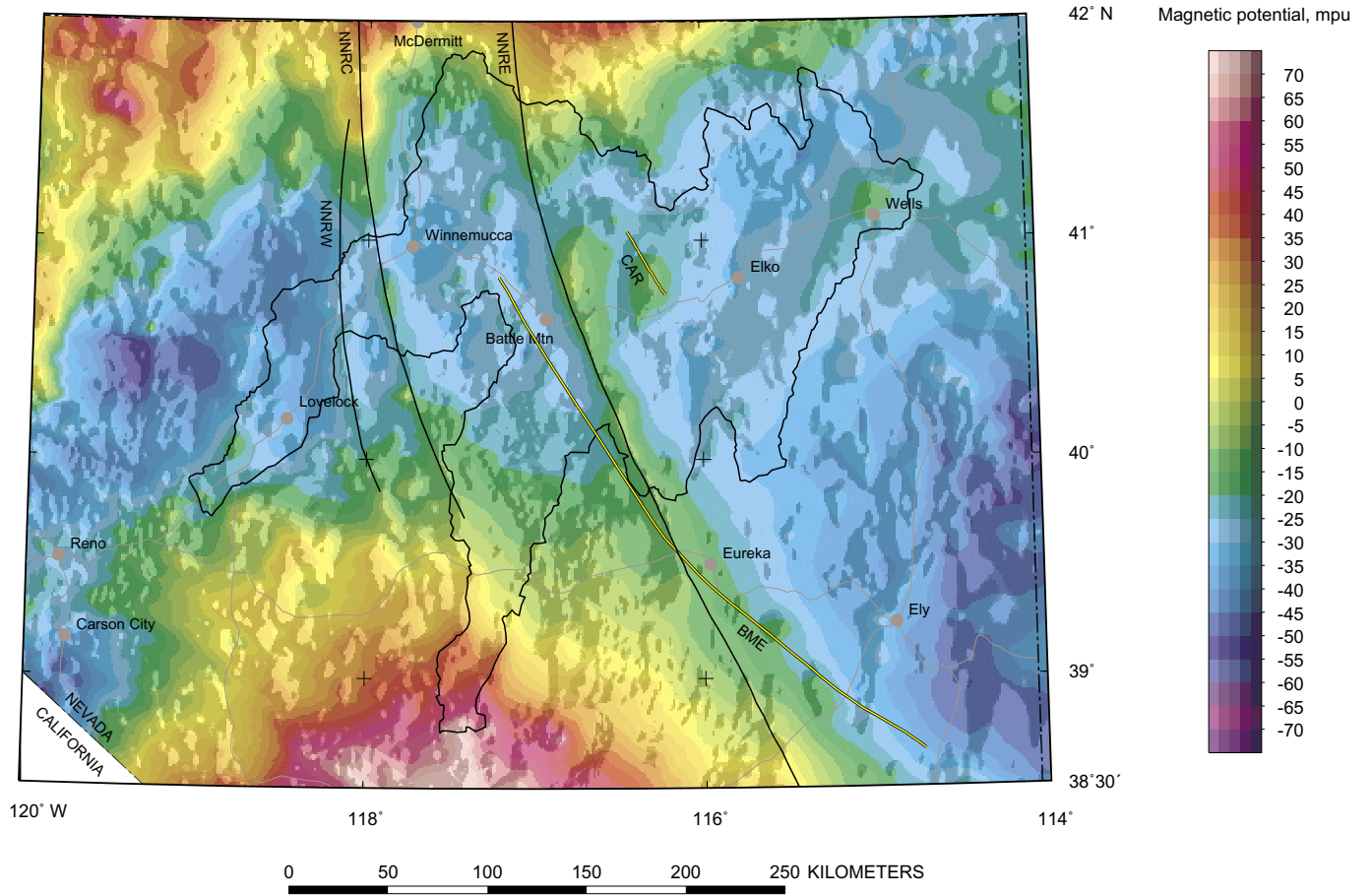
Figure 6-12.   Magnetic potential map of northern Nevada derived from the transformation of magnetic anomalies; mpu, magnetic potential units (dimensionally amperes). Explanation as in figure 6-1.
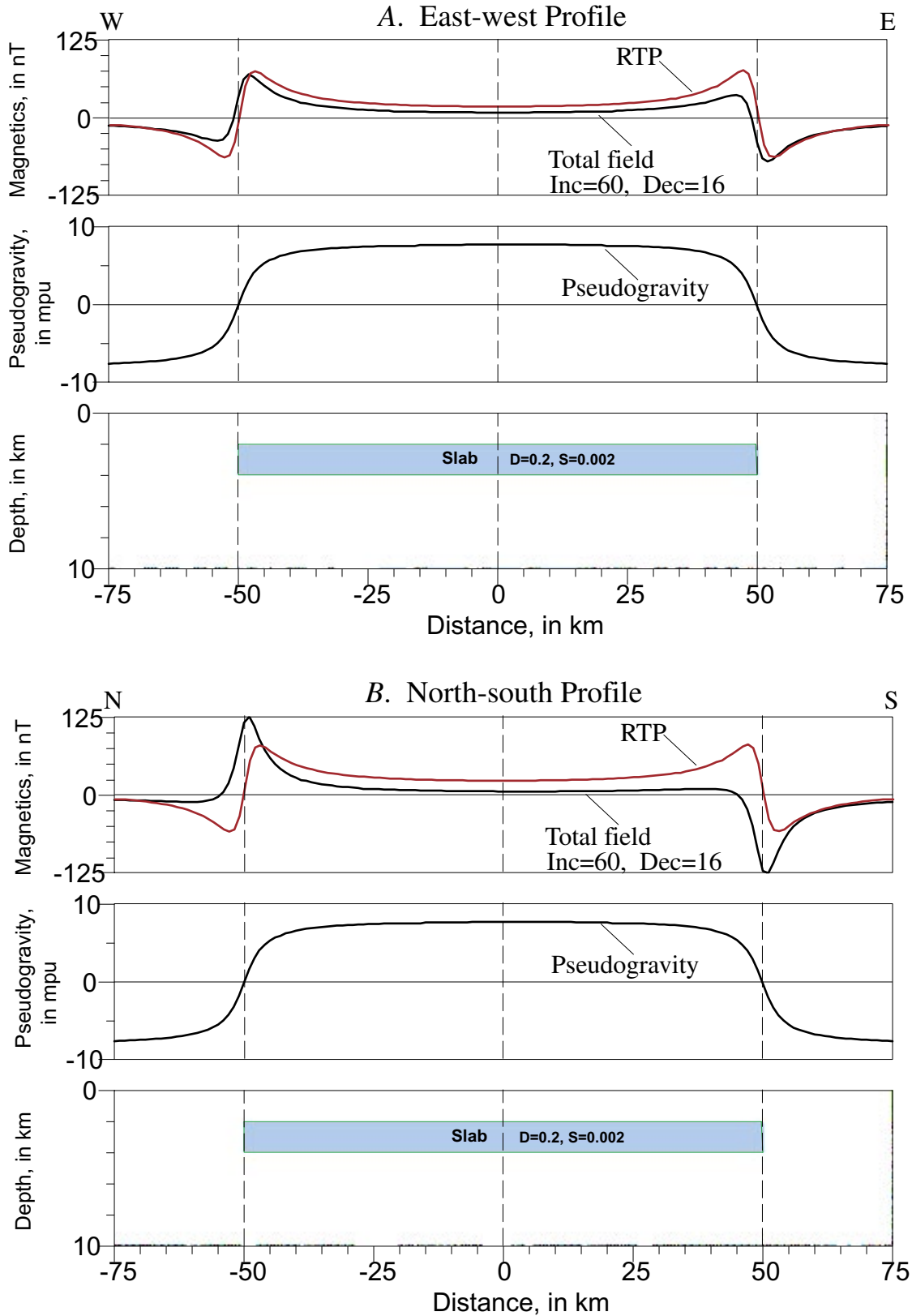
Figure 6-13. Theoretical model illustrating the differences between total magnetic field, reduced to the pole (RTP), and magnetic potential (or pseudogravity) across a buried slab 2 km thick, 100 km in length, and buried at a depth of 2 km. D, density in g/cm^3; Dec, declination in degrees; Inc, inclination in degrees; S, susceptibility in cgs units. A, east-west profile. B, north-south profile.
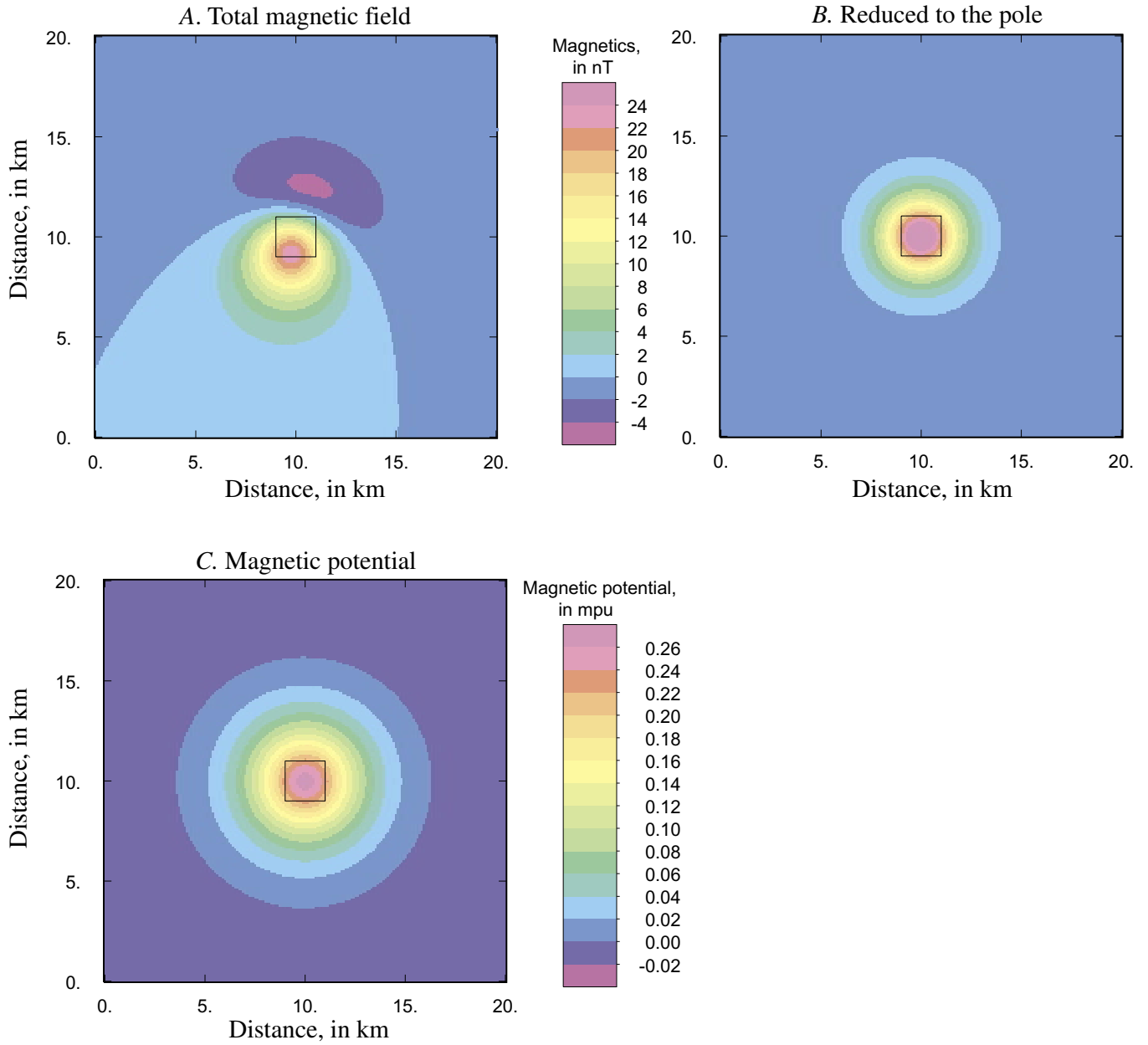
Figure 6-14. Theoretical contour map model over a 2-km cube buried 2 km in depth illustrating the differences between (a) total magnetic field, (b) reduced to the pole, and (c) magnetic potential. Source body, outlined in black, has an inclination of 60°, declination of 16° and a magnetization of 0.0005 cgs units. Total magnetic field also has an inclination of 60° and declination of 16° mpu, magnetic potential units (dimensionally amperes).
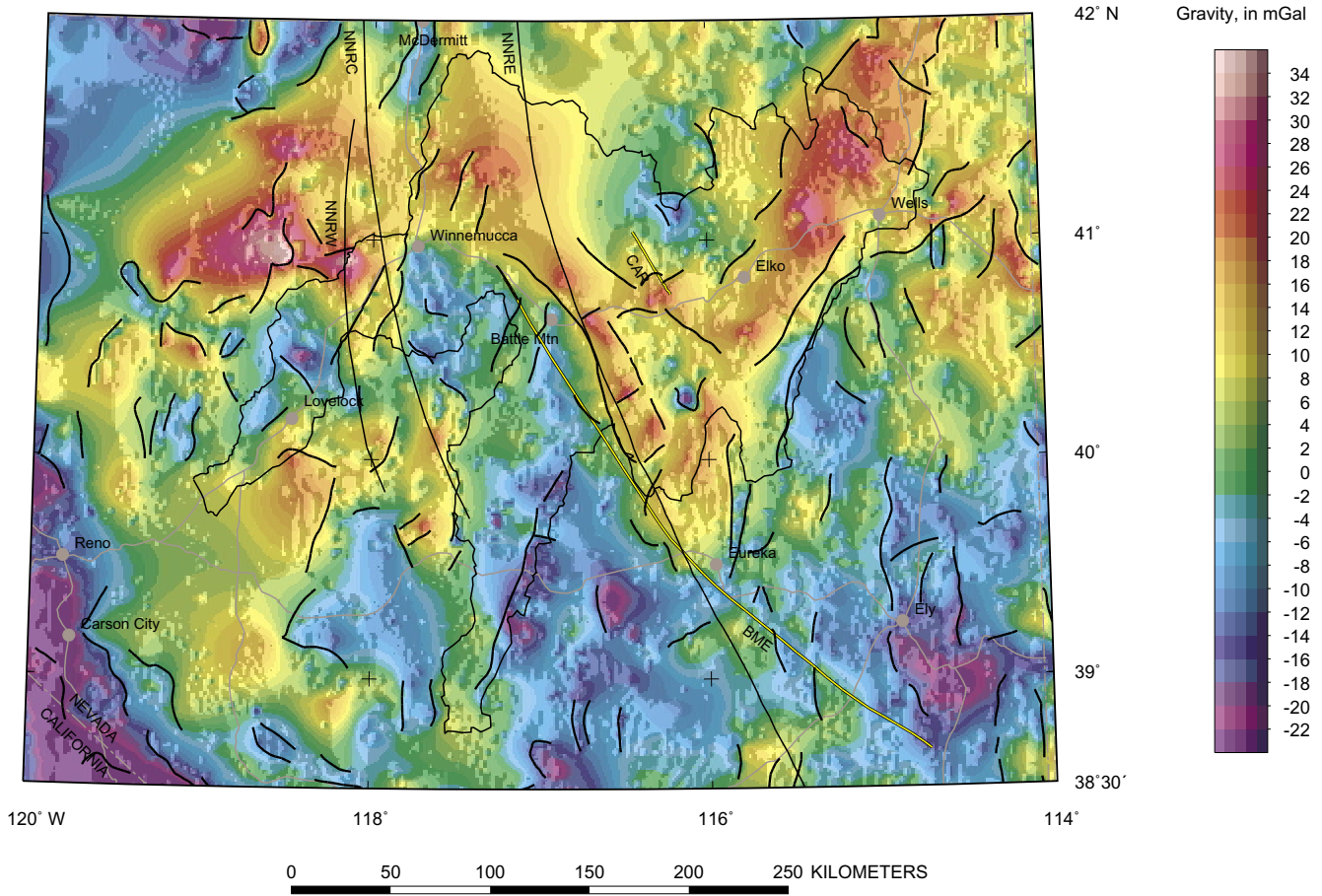
Figure 6-15. Gravity lineaments derived from and superimposed on basement gravity map. Explanation as in figure 6-1.
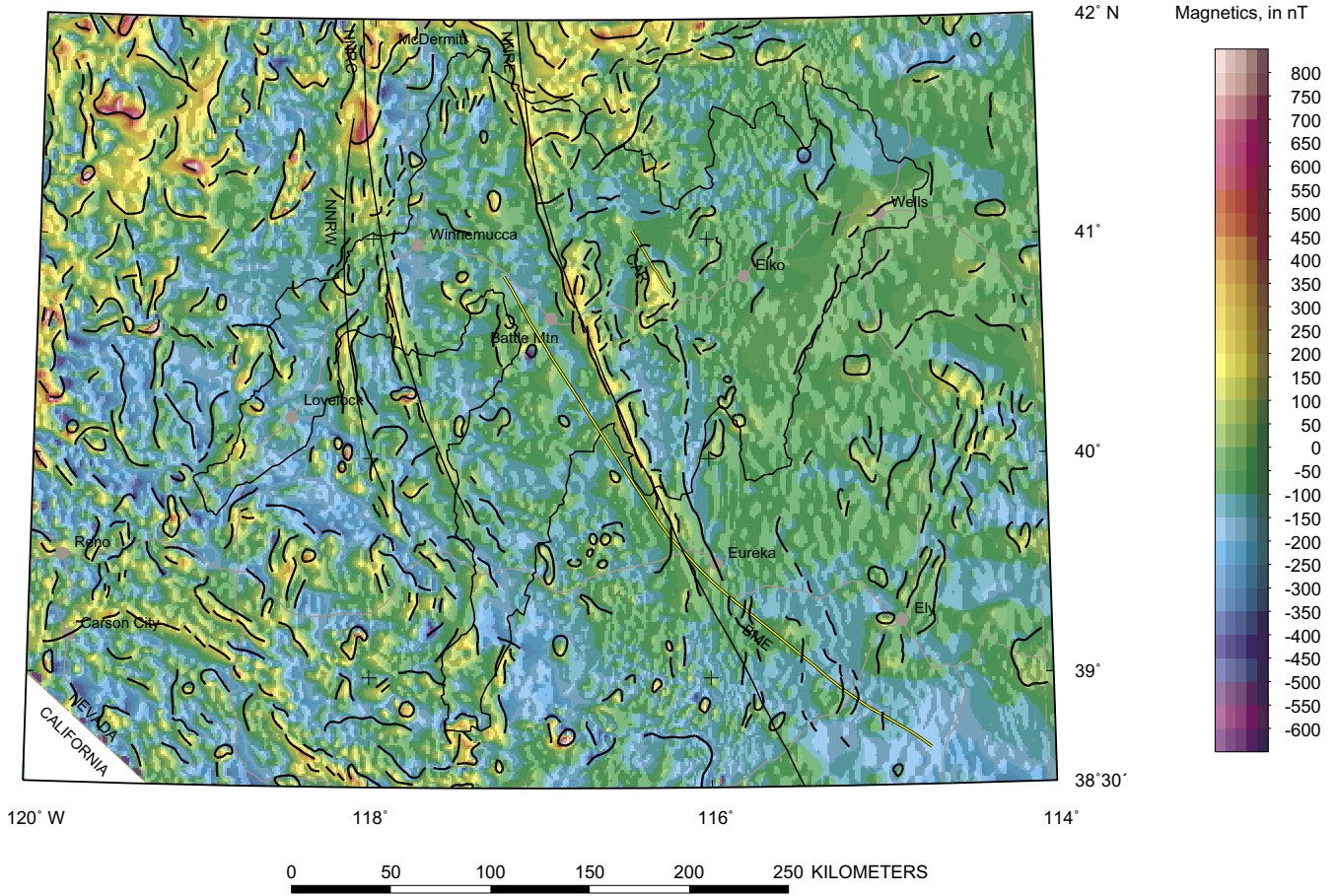
Figure 6-16. Magnetic lineaments derived from magnetic potential anomalies and superimposed on total field aeromagnetic map. Explanation as in figure 6-1.
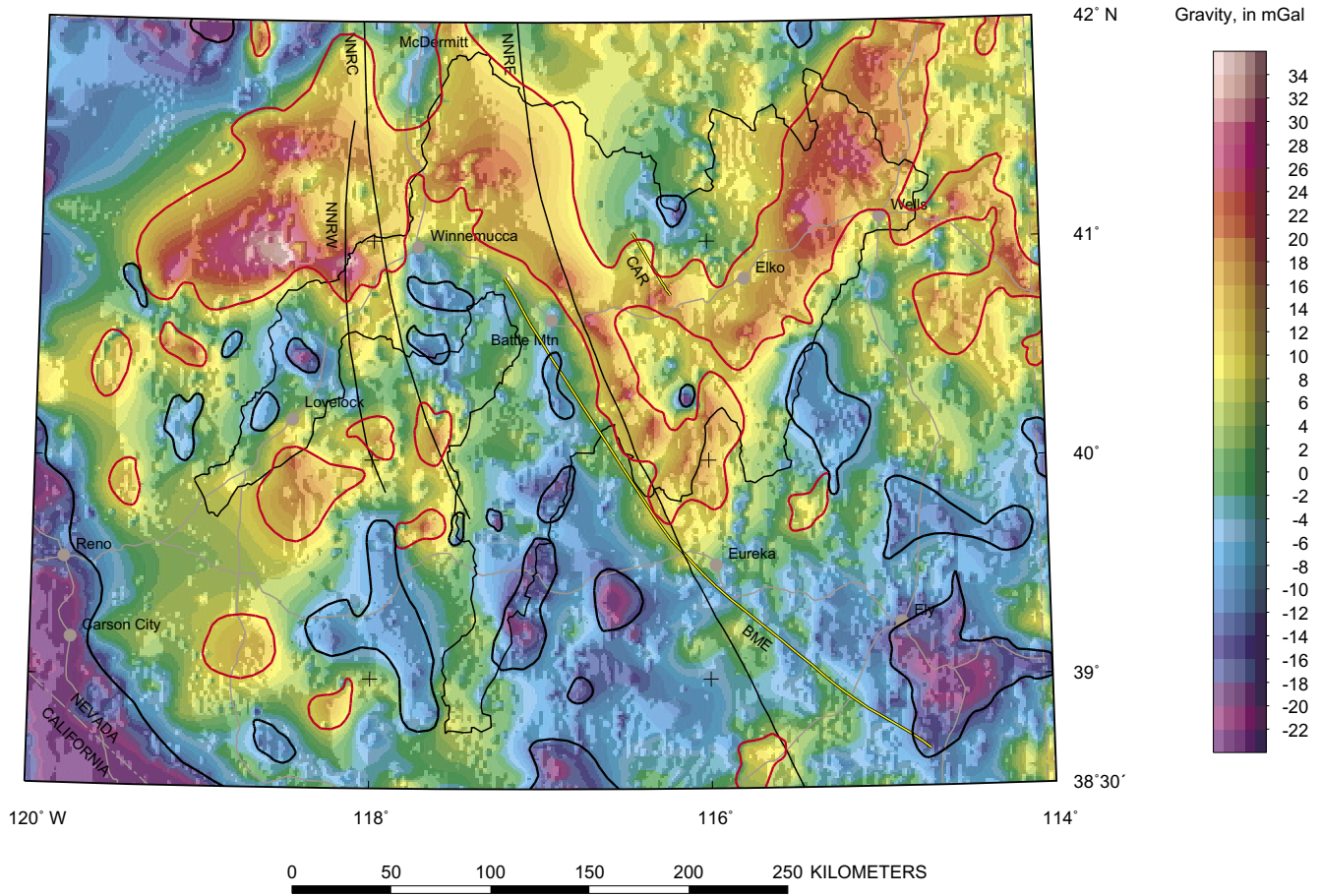
Figure 6-17.   Gravity terranes derived from and superimposed on basement gravity map. Red lines, gravity highs; black lines, gravity lows. Explanation as in figure 6-1.
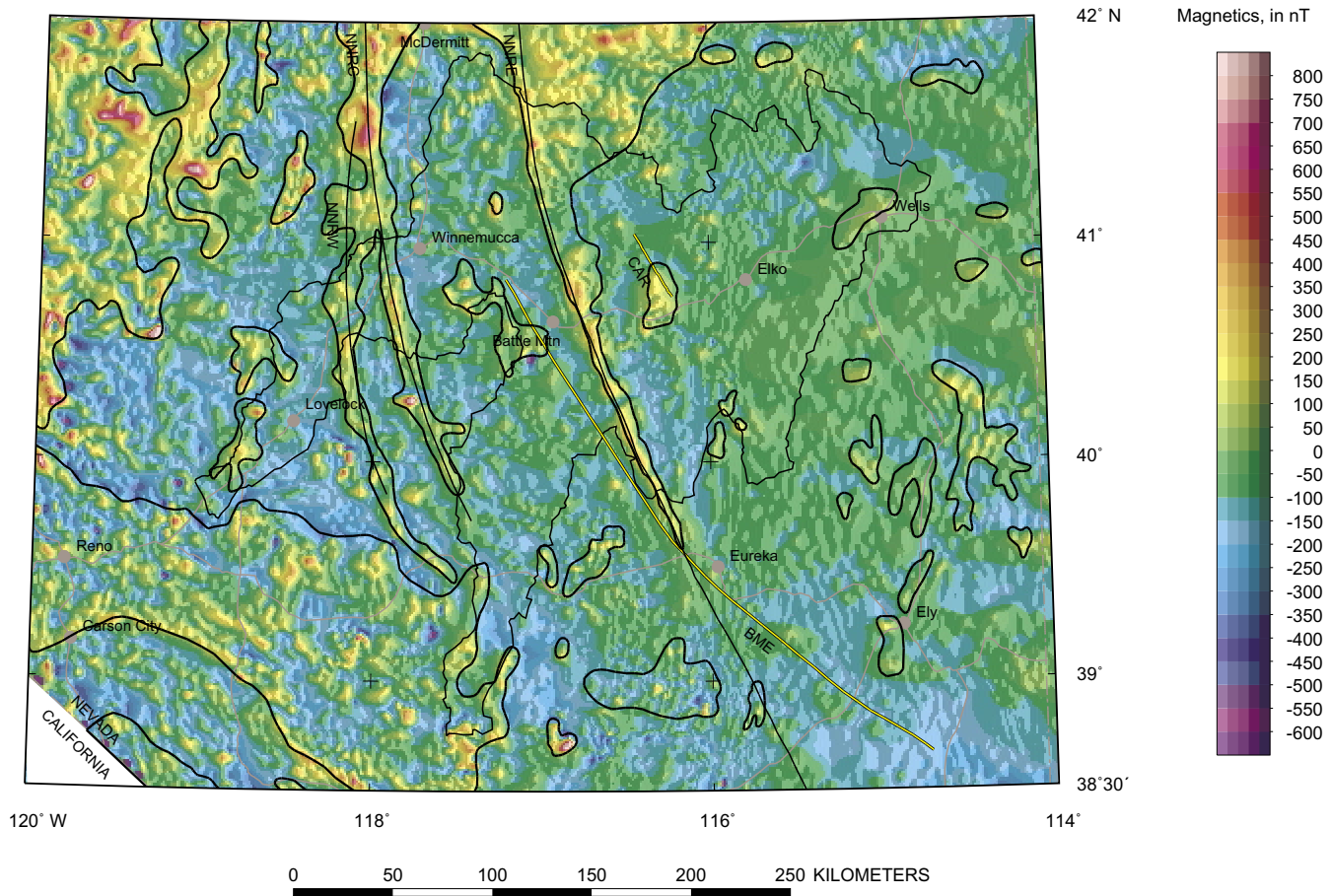
Figure 6-18. Magnetic terranes derived from and superimposed on total field magnetic map. Explanation as in figure 6-1.

Table 6-1. Physical property measurements of selected rock types.

[DBD, dry bulk density; GD, grain density; SBD, saturated bulk density; Susc, volume magnetic susceptibility]

Rock type	No. of samples	GD g/cm3	SBD g/cm3	DBD g/cm3	Susc 10-3 cgs
Volcanic rocks					
Andesite	22	2.61	2.57	2.55	0.61
Basalt	68	2.65	2.60	2.57	0.47
Dacite	14	2.48	2.48	2.47	0.72
Mafic dike	81	2.83	2.81	2.80	1.87
Rhyodacite	1	2.41	---	---	---
Rhyolite	24	2.41	2.35	2.29	0.21
Rhyolite porphyry	1	2.47	2.41	2.36	0.25
Trachydacite	7	2.59	2.56	2.55	0.63
Tuff	3	2.50	2.33	2.20	0.26
Undifferentiated volcanic	28	2.47	2.39	2.33	0.21
Volcanic breccia	4	2.39	2.35	2.32	0.08
Granitic rocks					
Aplite	1	2.59	2.58	2.58	0.00
Diorite	3	2.84	2.82	2.81	4.23
Gabbro	2	2.55	2.53	2.50	1.06
Granodiorite	4	2.65	2.63	2.61	0.50
Granite	13	2.65	2.63	2.62	0.52
Quartz diorite	2	2.69	2.68	2.67	0.11
Quartz monzonite	5	2.46	---	---	---
Granitic rocks	60	2.64	2.63	2.61	0.51
Sedimentary and other rocks					
Chert	3	2.60	2.56	2.53	0.03
Conglomerate	2	2.42	2.34	2.27	0.08
Dolomite	10	2.73	---	---	---
Gneiss	2	2.37	---	---	---
Greywacke	1	2.58	2.57	2.56	0.00
Limestone	69	2.66	2.62	2.60	0.01
Mudstone	2	2.71	2.54	2.52	0.00
Quartzite	21	2.61	2.63	2.62	0.00
Shale	3	2.73	2.69	2.67	0.01
Slate	2	2.70	2.70	2.69	0.00
Sandstone	7	2.46	2.50	2.48	0.00
Siltstone	7	2.59	2.56	2.55	0.63
Ultramafic	1	3.00	2.97	2.96	0.01

Table 6-2. Density-depth function for Cenozoic sedimentary and volcanic deposits.

Depth range (m)	Density for sedimentary deposits kg/m³	Density for volcanic deposits kg/m³
0-200	2020	2220
200-600	2120	2270
600-1,200	2320	2320
>1,200	2420	2420

Chapter 7

Assessment for Pluton-Related Mineral Deposits and Occurences

By Ted G. Theodore, Mark J. Mihalasky, Stephen G. Peters, and Barry C. Moring

with a section on

PGE Potential of the Humboldt Mafic Complex

By Michael L. Zientek, Gary B. Sidder[1], and Robert A. Zierenberg[2]

Introduction

Pluton-related mineral deposits and occurrences in the Humboldt River Basin (HRB) were among the first exploited during the late 1860s by miners attracted primarily to Cu–stained rocks and Au–bearing placers in and near mountain ranges close to the then recently completed Central Pacific rail line. However, somewhat earlier, the 49ers on their way to the goldfields of California probably panned most major stream drainages near the Emigrant Trail, which closely follows the Humboldt River through much of northern Nevada (Coope, 1991). Tracing of placer Au upstream to its lode sources by streambed panning steered the prospectors to many early discoveries of metal deposits. After the Civil War, railroads replaced inland waterways as the primary mode of transportation in the States and Territories comprising the western United States, and pressure mounted for expanded knowledge about the mineral resources of the West (National Research Council, 2001). Over the next 100 years, lode mining of pluton-related deposits in the HRB was widespread but generally inconsequential from a present-day national standpoint. This mining concentrated mostly on small Au– and Ag–bearing quartz veins and high-grade Cu occurrences, and it resulted in a large number of boomtowns that sprang up almost overnight and then disappeared almost as quickly as ores either were depleted or metal markets crashed. Initiation of large-scale mining of Cu ores at Ely (Robinson Mining District) (fig. 7–1), Nev., in 1908, and at Yerington, Nev., in the early 1950s, however, added substantially to national Cu production, as did large-scale mining of Cu–Au–Ag ores from Battle Mountain, Nev., in the middle 1960s. However, Cu production from these three mining camps eventually

declined, and it currently (2002) has been curtailed for a variety of reasons. Renewed mining of Cu began at Ely in 1995 (Maher, 1996) and continued through 1998; the renewed production of Cu was anticipated at that time to amount to approximately 135 million lbs Cu per year (Tingley, 1995). Thus, the pluton-related deposits generally accounted for progressively decreasing amounts of base (Cu+Pb+Zn) and precious (Au+Ag) metals over time from a national standpoint. This production decrease from pluton-related deposits in Nevada was more than counterbalanced monetarily by production increases from pluton-related systems elsewhere in the West, and by mining and exploration shifts in the 1960s to highly profitable Au ores in Carlin-type deposits that, at that time, were thought to be clustered only in northeastern Nevada and western Utah (see chapter 8 entitled "Assessment of Sedimentary Rock-hosted Au–Ag Deposits").

Early production of base and precious metals from pluton-related deposits in Nevada is minor when viewed retrospectively in light of the current national economy. However, the economic significance of these deposits should be considered relative to local economies and national priorities during the westward-expansive Nation-building and Nation-consolidation eras of the late 1800s and early 1900s for a reasoned perspective of its overall historic importance. Nonetheless, although well recognized for more than 100 years, all pluton-related deposits and occurrences in northern Nevada still (2002) have not been thoroughly evaluated by modern exploration techniques. This mineral environment in the HRB contains a large number of base- and precious-metal targets, as well as a small number of Pt–group-element (PGE) targets, that continue to attract considerable attention from exploration companies. Post-mineralization rocks and unconsolidated gravel deposits cover many of these targets, rendering them extremely difficult to evaluate fully regardless of modern advances in exploration methodologies.

---

[1]Littleton, CO.
[2]University of California, Davis, Davis, CA.

A relatively large number of deposits and types of Mesozoic and Tertiary pluton-related deposits and occurrences are present in the HRB. They contain Cu, Mo, Au, Ag, Pb, Zn, W, and Fe and also are referred to as intrusion-related, magma-related, granitoid-related, or granite-related (sensu lato) (fig. 7–1). In other parts of the world, sizeable granitoid bodies that contain a large number of pluton-related deposits have had at least some of their metal zonation attributed to sequential precipitation of metals from a single parental fluid that evolved from the associated granitoids (Audétat and others, 2000). As applied in the present report, the pluton-related deposits and occurrences include the following broad categories of mineral deposits: (1) several kinds of porphyry Cu–(Mo) deposits; (2) two types of porphyry Mo deposits—also referred to as stockwork Mo deposits; (3) various types of skarn deposits; and (4) two types of polymetallic deposits, many of which cluster into a number of mining districts in northern Nevada (fig. 7–2). In addition, a number of Au deposits primarily hosted by intrusive rocks and associated with elevated contents of Bi, W, As, Mo, Te, and (or) Sb recently have been referred to as intrusion-related Au systems (Lang and Baker, 2001). Further, another type of deposit in the HRB, the distal-disseminated Ag–Au deposits, is pluton-related, but this deposit type will be discussed in chapter 8. A relatively small number of Fe, Ni, Co, and Cu deposits and occurrences are associated with the Humboldt gabbroic mafic complex in and near the western part of the HRB. As will be discussed below, the Humboldt mafic complex and its nearby surrounding areas have some potential for the presence of PGE. In the HRB, the most important pluton-related deposits from an economic standpoint are best concentrated along a northwest-trending alignment of mineral districts termed the Battle Mountain-Eureka mineral belt (Roberts, 1966; see also, Madrid and Roberts, 1991) that extends roughly between those two respective mining districts (fig. 7–2). The northwest orientation of the Battle Mountain-Eureka mineral belt is parallel to inferred paleotransforms through Idaho and southern California that bound the Cordilleran miogeocline on the northeast and southwest, respectively (Dickinson, 2001). Thus, the underlying root of the Battle Mountain-Eureka mineral belt may be a subsidiary zone of weakness related to these features (see also, chapter 6, wherein the northern segment of the Battle Mountain-Eureka mineral belt is suggested to have at one time been part of the northern Nevada rift system).

Two fundamental, continental-scale phenomena controlled formation and regional distribution of long-lived geologic processes that affect the pluton-related environment in the HRB: (1) continental-margin Jurassic and Cretaceous magmatism (fig. 7–3) associated with dehydration of a subducted slab and its metal-rich oceanic sediments, which generated metal-bearing granitoids and fluids that rose high into the crust during a largely compressional tectonic event (Sillitoe, 2000a; see also, Hildenbrand and others, 2000, 2001); and (2) mostly middle Tertiary (43– to 34–Ma) magmatism associated with probable flat-slab subduction and onset of extensional breakup of the crust in the Great Basin (Hofstra and Cline, 2000). Most of the HRB and the immediately surrounding Basin and Range Province presently is underlain by a low-density anomaly that (1) appears to reside mostly in the upper mantle, and (2) may be due to emplacement of low-density basalt into the upper mantle (Kaban and Mooney, 2001; see also, Hildenbrand and others, 2001). In company with the first two phenomena listed above, a number of other relatively large-scale metallotects influenced the distribution of pluton-related mineral deposits and occurrences. These metallotects will be described below. Moreover, recent advances in application of tectonic models at the mining district scale to emplacement of magmas associated with porphyry Cu systems have shown that some of these metallotects are likely to be related to transtensional strains associated with strike-slip duplexes that create zones of extension into which porphyry Cu–related magmas may be intruded (Drew and Berger, 2001).

Porphyry Cu–(Mo) systems are by far the most important economically of the pluton-related deposits and occurrences in the HRB. Further, these deposits and their numerous satellitic metal occurrences dominate three of the major mining districts in northern Nevada (see also, Hildenbrand and others, 2001). These three mining districts have recorded significant base and precious metal production from porphyry Cu–(Mo) systems in the past and they include: (1) Yerington (Dilles and Proffett, 1995; Dilles and others, 2000a,b); (2) Robinson near Ely (Fournier, 1967; James, 1976; Maher, 1996); and (3) Battle Mountain (Roberts and Arnold, 1965; Doebrich and Theodore, 1996; Theodore, 2000) (fig. 7–1). The latter mining district is partially within the HRB, whereas the two former ones are peripheral. Throughout this report, the term "Battle Mountain Mining District" is used in a geographic manner somewhat larger than that proposed by Tingley (1992). As applied herein, we include the Buffalo Valley Mining District and the area near Lone Tree as part of the Battle Mountain Mining District.

The Yerington and Robinson Mining Districts have been important producers of base and precious metals at one time. Ores at Yerington are associated with the Jurassic Yerington batholith that, in aggregate, contained a total geologic resource of 6 million t Cu in mineralized sulfide rock as well as >100 million t Fe in mineralized oxide rock (Dilles and Proffett, 1995). A geologic resource, however, is not necessarily equivalent to an economic resource (Peters, 1978). The MacArthur Cu deposit, an oxide Cu deposit, is part of the cluster of Cu deposits at Yerington, and it is estimated to contain reserves of approximately 97 million t at 0.21 weight percent Cu (Tingley, 1995). The Robinson Mining District is associated with a 10–km-long, east-west elongate, 109– to 111–Ma Cretaceous porphyry Cu–(Mo) system; between 1908 and 1978 more than 3.5 million t Cu were produced from the district (Benedetto and others, 1991; Shaver and Jeanne, 1996). The total value of metal production between 1908 and 1978 was more than $1 billion (Benedetto and others, 1991). This production included approximately 2.7 million oz Au as a byproduct of the Cu ores from the Robinson Mining District. Fifteen satellitic Au deposits surround the central Cu ores in the Robinson Mining District (Shaver and Jeanne, 1996).

The porphyry Cu–(Mo) systems in the Battle Mountain Mining District are more complex than those in either the

Yerington or Robinson Mining Districts because they are localized in at least ten widespread centers across the mining district (fig. 7–4), and because they are of two ages, Late Cretaceous (approximately 90 Ma) or middle Tertiary (41 to 35 Ma; late Eocene and (or) early Oligocene) (Theodore and others, 1973; Doebrich and Theodore, 1996; Theodore, 2000). Most extension and crustal thinning in north-central Nevada must have taken place during the late Eocene and (or) early Oligocene (Muntean and others, 2001). Further, the Battle Mountain Mining District contains well-developed geologic and geochemical zoning in these mineralized systems that include a number of relatively deep porphyry Cu and stock-work Mo systems, Au skarns, and a number of geologically shallow distal-disseminated Ag–Au deposits (Theodore, 2000; see also, Cox and Singer, 1990, 1992; Hofstra and Cline, 2000; chapter 8).

Some pluton-related deposits and occurrences in the HRB currently (2002) are producing mostly Au and Ag, and many of these, as well as their enclosing mineralized systems, are more likely than others to continue in production during the next 15 years. Mineralized areas that are likely to continue their production, or are likely to be brought into production during the next 15 years, are indicated in the various sections of this chapter below.

The area of the HRB (fig. 7–1) has been included in a number of broad regional mineral assessments previously completed by the USGS. The potential presence of many types of undiscovered pluton-related mineral deposits throughout the HRB, including those that might be concealed to depths of 1 km in the valleys under Tertiary and Quaternary gravel deposits, was evaluated in a statewide mineral assessment (fig. 7–5) for Nevada that included within its permissive domain rocks within a 10–km radial buffer of all plutons shown on the geologic map of Nevada by Stewart and Carlson (1978; see also, Cox and others, 1996). Similarly, the western parts of the HRB were assessed in a study of the Winnemucca-Surprise BLM Resource Area (Peters and others, 1996).

Much of this chapter has been modified and updated significantly from Peters and others (1996), but it includes discussion of the implications of newly acquired, regionally extensive geochemical data from sediments, including stream sediments and soils (Folger, 2000; see also, chapter 5). Some geochemical data—in particular, Cu, Pb, Zn, and As concentrations—systematically have been considered during preparation of the pluton-related mineral assessment map. This chapter also includes a section describing the PGE implications of reconnaissance geochemical studies conducted in the Humboldt mafic complex (see section below entitled "PGE Potential of the Humboldt Mafic Complex").

Specific Types of Pluton-Related Deposits

The following specific types of mineral deposits are considered to belong under the pluton-related classification in this chapter: (1) porphyry Cu–(Mo) deposits (models 17, 21a of Cox and Singer, 1986); (2) porphyry Mo, low–F deposits (model 21b of Cox and Singer, 1986); (3) Climax Mo deposits (model 16 of Cox and Singer, 1986); (4) porphyry Cu–Au deposits (model 20c of Cox and Singer, 1986); (5) tungsten-skarn deposits (model 14a of Cox and Singer, 1986); (6) tungsten vein deposits (model 15a of Cox and Singer, 1986); (7) porphyry Cu, skarn-related deposits (model 18a of Cox and Singer, 1986); (8) Cu skarn deposits (model 18b of Cox and Singer, 1986); (9) Zn–Pb skarn deposits and polymetallic replacement deposits (models 18c and 19a of Cox and Singer, 1986); (10) Fe skarn deposits, including widespread Fe endoskarn at the Humboldt mafic complex (model 18d of Cox and Singer, 1986); and (11) Au skarn deposits (model of Theodore and others, 1991; see also, Meinert, 1998, 2000). Additional pluton-related deposits in the HRB include polymetallic vein deposits (model 22c of Cox and Singer, 1986), replacement manganese deposits (model 19b of Cox and Singer, 1986), and possibly the intrusion-related Au systems of Lang and Baker (2001), but they are not directly assessed in this report. The worldwide grade and tonnage distributions for these pluton-related deposit models are included in the references cited above. Although some authors (Henry and Ressel, 2000; Ressel and others, 2000; Theodore, 2000) rigorously regard the distal-disseminated Ag–Au and Carlin-type or sedimentary rock-hosted Au–Ag deposits as being pluton- or magma-related deposits, they have been assessed separately in chapter 8 with other sedimentary rock-hosted deposits.

In addition, we also have carefully considered the possible presence in the HRB of a newly recognized class of mineral deposits—Au deposits related to reduced granitic intrusions (Thompson and Newberry, 2000; Lang and Baker, 2001). This particular class of deposits—best exemplified by the Fort Knox, Alaska, deposit that includes a geologic resource of approximately 215 metric t Au—commonly is associated with an intrusive suite of igneous rocks that typically (1) lack porphyritic textures common to most porphyry Cu–(Mo) systems; (2) lack widespread high concentrations of genetically associated Cu, Mo, Sn, and W; and (3) are associated with elevated concentrations of Bi, As, Sb, and Te. Further, the deposits are envisioned to have formed in a petrochemical environment wherein oxygen fugacities are significantly depleted relative to the much more widespread porphyry Cu–(Mo) systems (Thompson and Newberry, 2000). However, a worldwide map of metallogenic belts of reduced intrusion-related Au deposits does not include the HRB (Thompson and Newberry, 2000). Nonetheless, future mineral evaluations of pluton-related deposits and mineral occurrences in the HRB—in particular those occurrences that contain sparse concentrations of associated base-metal sulfide minerals—may result in reclassification of some of these occurrences to Au deposits related to reduced granitic intrusions, such as some Au–skarn occurrences (see section below entitled "Gold Skarn Deposits (Model of Theodore and others, 1991)") as well as some deposits in the Bald Mountain Mining District (Nutt and others, 2000).

Uncertainty still (2002) remains in classification of many known occurrences of presumably pluton-related occurrences

and deposits in the HRB. These uncertainties primarily involve a lack of critical geologic information in Mineral Resource Data System (MRDS) records of the USGS. The MRDS locations of a large number of occurrences throughout northern Nevada are shown in figure 7–6. As a comparison, in the state-wide study of Nevada, enough information was available only to classify approximately 1,500 of 5,500 MRDS records into appropriate models (Cox, 1993), and, in the study of the Reno 1° x 2° quadrangle of western Nevada, approximately 300 of 400 occurrences were classified (John and others, 1993). In the Winnemucca-Surprise mineral-resource assessment, approximately 1,032 of 1,168 mineral occurrences were classified provisionally (Peters and others, 1996). The overall geologic environments of the pluton-related deposits in the HRB are quite similar, in most cases, to the respective environments documented in the worldwide models described by Cox and Singer (1986). Some exceptions, however, are noted throughout the descriptions for the HRB that follow. Each model is outlined briefly in the sections below, and a description and discussion of representative deposits that closely fit the parameters of that model in the HRB then follow it. Many deposits cluster in mining districts or groups of districts (fig. 7–6), and this clustering usually is evident on the data-driven favorability map as prospective or favorable tracts to be described below (see also, fig. 7–2). Finally, although we have archived and tabulated information concerning mineralized occurrences and deposits from throughout northern Nevada for a data-driven evaluation (see chapter 2), our descriptions of mineralized areas will focus on those that are present in or near the HRB.

In the sections of this chapter that follow, we describe geologically those deposits present in the HRB that are most closely allied genetically to igneous rocks of various ages and their associated hydrothermal fluids. These hydrothermal fluids generally followed complex structural pathways and were influenced by diverse histories of water-rock interactions after they initially evolved from magmas during emplacement and crystallization of the parent igneous rocks. Porphyry deposits (fig. 7–7), their related skarn and vein deposits, and broad halos of altered rock are all closely allied to magma. As depicted, the breadth of alteration associated with these systems emphasizes how widespread the overall effects associated with them can be.

The Battle Mountain Mining District includes 28 of the 92 mineralized occurrences used as training sites for the pluton-related assessment and, because of this, many deposits from this district are described in somewhat more detail than others. Copper, Zn, Pb, and Au skarns, as well as polymetallic veins and replacement Mn deposits, also are present in the Battle Mountain area and elsewhere in the HRB as well. Although 92 pluton-related training sites (table 7–1) are used in the data-driven assessment method, only seven of these pluton-related training sites are present in the HRB outside the Battle Mountain Mining District (fig. 7–8). Nonetheless, many types of pluton-related mineral occurrences are widespread in the HRB (fig. 7–1). For example, approximately 150 pluton-related mineralized sites, mostly polymetallic veins (see section below entitled "Other Pluton-related Deposits"), are present in the Shoshone Range in

the central part of the HRB (fig. 7–1). None of these 150 sites is included in the pluton-related training set. Approximately 15 of the 150 polymetallic veins in the Shoshone Range, however, are included in the MRDS database. Finally, a large number of the remaining pluton-related training sites in northern Nevada are clustered near (1) the Jurassic porphyry Cu system near Yerington, and (2) the Cretaceous porphyry Cu system near Ely (fig. 7–1). Distal-disseminated Ag–Au deposits that are concentrated near the northern margin of the Battle Mountain Mining District represent the upper parts—that is, they are close to the paleo-surface at the time of their formation—of the overall porphyry-related family of deposit models (fig. 7–4; Theodore, 2000). However, as discussed previously, the largely sedimentary-rock hosted distal-disseminated Ag–Au deposits in this district are best addressed later in the report with other carbonate- or sediment-hosted Au deposits (see chapter 8).

Additional Pluton- and Metamorphism-Related Deposits

Several other types of economically prominent and geologically significant pluton-related deposits and occurrences also are present in the HRB—they are described in detail in subsections below. Many W skarn deposits (fig. 7–9), for example, are present in a confined metallogenic area in the western and northern parts of the HRB that is an apparently deep geologic paleoenvironment (>3 km) relative to many of the exposed porphyry Cu and (or) low–F, stockwork Mo deposits in the central parts of the HRB. Although a number of the past-producing W deposits and occurrences are present in the HRB (Kerr, 1934, 1940, 1946; Stager and Tingley, 1988; John and Bliss, 1994), some of them might again warrant added exploration activity if a national emergency or requirement were to arise because of the critical need of W to our economy and the absence of current (2002) domestic production.

Although most pluton-related deposits and occurrences in the HRB are associated with Cretaceous and Tertiary felsic plutons, some Fe deposits instead are associated with Jurassic gabbroic plutons or Jurassic felsic volcanic complexes. For example, a cluster of previously productive Fe deposits at the Buena Vista Mines is associated with the Middle Jurassic (approximately 170–Ma) Humboldt mafic igneous complex that extends from the West Humboldt Range near Lovelock, Nev., across several mountain ranges to the southeast (fig. 7–1; Speed, 1962; Johnson and Barton, 2000). Total geologic resource estimates, including past production, probably aggregate >500 million t at an average grade of approximately 33 weight percent Fe (Johnson and Barton, 2000). Additional minor mineral occurrences—mostly Cu, Ni, Co, and PGE—associated with the Humboldt mafic complex are addressed in the section below entitled "PGE Potential of the Humboldt Mafic Complex." Nonetheless, those small numbers of Fe deposits of this type elsewhere in the HRB, because of their association with plutonic units on the State of Nevada geologic map (Stewart and

Carlson, 1978; Stewart, 1980), are necessarily included in the mineral-resource assessment of pluton-related deposits.

Several types of regional metamorphism-related and magma-related deposits also are present in the HRB and merit some mention. A large number of mineral occurrences throughout the western part of the HRB have been reclassified as low-sulfide Au–quartz veins (Peters and others, 1996; Cheong, 1999; Cheong and others, 2000) that apparently are related to Late Cretaceous metamorphism and docking of the Jungo terrane of Silberling and others (1984, 1987) along the western margin of North America. The low-sulfide Au–quartz veins individually yielded small production in the past, mostly 1,000 oz Au or less, yet regionally they delineate a dismembered north-trending mineral belt of deposits that are concentrated west of the Sonoma Range in the western part of the HRB (fig. 7–10). Some of the largest cumulative production has been from the Sierra (13,899 oz Au), Rochester (778,018 oz Au), Awakening (26,000 oz Au), and the Winnemucca-Antelope (13,553 oz Au) mining Districts (Cheong and others, 2000). The Rochester Mining District is in the footwall of the regionally extensive Luning-Fencemaker thrust fault system. The Fencemaker thrust makes up the sole structure of the Jungo terrane (Oldow, 1984), whereas Triassic shelf rocks and the Triassic Koipato Group comprise the footwall of the Fencemaker thrust (see chapter 4). Some mineral occurrences within these districts also may be related, in part, to plutons. These low-sulfide Au–quartz veins are distinct and separate from the polymetallic vein deposits to be described below (Peters and others, 1996).

Some other types of mineral deposits are present in the HRB, and they may be either directly or indirectly associated with plutons. Massive sulfide deposits, potential exhalative sedimentary Pb–Zn deposits, volcanic-hosted magnetite-hematite Fe deposits, and volcanogenic Mn deposits are associated with specific lithologies—mostly Paleozoic siliceous ocean-basin varieties of rock—of the various allochthons in the eastern and central part of the HRB (fig. 4–1).

Two types of Au deposits have been excluded from this evaluation. We specifically exclude from our discussion those Au deposits—either shallow level or deep seated—that are related to alkaline magmatism (Jensen and Barton, 2000), primarily because these types of deposits apparently are not present in the general region of the HRB. In addition, Au–placer deposits are excluded as well. The Au–placer deposits mostly appear to be associated spatially with low-sulfide Au–quartz veins, and porphyry Cu environments to a lesser degree. The Au–placer deposits are concentrated along the margins of many late Tertiary and Quaternary basins that make up many valleys of the HRB (Peters and others, 1996).

General Description of Porphyry Deposits

Porphyry systems represent generally large volumes of rock characterized by chalcopyrite, bornite, molybdenite, or Au—as well as a number of other prograde and secondary sul-

fide minerals—in intensely fractured rocks filled by stockwork veins or disseminated grains in hydrothermally altered porphyritic intrusions and (or) in their hydrothermally altered adjacent wall rock. In fact, the Bingham, Utah, porphyry Cu system contains the seventh largest concentration of Au in the world— it has approximately 50 million oz Au as a combined total of its past production, economic reserve, and inferred resource (Sillitoe, 2000b). Much of the mineralized rock in these types of systems owes its origin to magmatic fluids that were expelled during crystallization of the genetically associated magma, typically present locally in composite intrusive centers. Supergene-altered equivalents of these deposits also may be important because supergene enrichment processes can enhance the Cu grades in a substrate beneath oxidizing parts of the deposits. Porphyry mineralized systems tend to form preferentially in some shallow-level granitoid intrusions (Titley, 1993). Further, porphyry deposits, skarn deposits, some polymetallic vein deposits, and distal-disseminated Ag–Au deposits form a continuum, with the porphyry Cu deposits typically at the center (see also, Carten and others, 1993; Titley, 1993; Sillitoe, 2000b). The main types of porphyry deposits considered in the HRB are: (1) porphyry Cu and porphyry Cu–(Mo) deposits; (2) porphyry Mo, low–F deposits; (3) Climax Mo deposits; and (4) porphyry Cu–(Au) deposits. These types of deposit commonly are mined by open-pit methods because of the large volume of mineralized rocks that they involve.

A small number of porphyry Cu and porphyry Cu–(Au) deposits in the HRB have been significant sites of base-metal mineral production in the past, and a number of additional sites contain significant volumes of rock that were mineralized by porphyry-style processes. Moreover, numerous sites have recorded significant base- and precious-metal production from widespread porphyry systems in the Battle Mountain Mining District (Roberts and Arnold, 1965; Blake, 1992; Doebrich and Theodore, 1996). However, the polymetallic veins that surround the centers of porphyry-style mineralized rock in the mining district have generally small production (Roberts and Arnold, 1965). Moreover, the southeast part of that mining district contains seven exposed porphyry systems (Theodore and others, 1992; Theodore, 2000), from which significant metal production has occurred from two (fig. 7–4). The most productive areas at Battle Mountain in terms of Cu, Au, and Ag include the porphyry Cu system at Copper Canyon and the Cu–(Mo) system at Buckingham and Copper Basin. Gold and minor Ag currently (2002) are being produced in the northern part of the district from the Marigold and Lone Tree complexes that are discussed in chapter 8.

The presence of several additional occurrences of porphyry Cu and porphyry Cu–(Mo) in the general area of the HRB (Schilling, 1980; Wendt and Albino, 1992) intuitively suggests that some level of potential exists for these types of deposit throughout much of the HRB (see below). As examples, a porphyry Cu prospect is present in the Kennedy Mining District (fig. 7–2), south of the HRB in the southern part of the East Range and some other mineral occurrences as well in the Truckee and Copper Valley areas have suggestions of por-

phyry affinities (Wendt and Albino, 1992). Further, the Mike Au–Cu–Zn deposit, approximately 16 km west-northwest of Elko, Nev., along the Carlin trend of Au deposits in the central part of the HRB (chapter 8), appears to have many base-metal characteristics of a large porphyry Cu system, including large concentrations of Zn on its periphery (see also, Kotlyar and others, 1998b). The Mike Au–Cu–Zn deposit also contains overlapping Au– and Cu–enriched zones largely coincident with rock flooded by secondary K–feldspar and quartz, thereby further suggesting a genetic association with a concealed felsic intrusion (Branham and Arkell, 1995). The Mike deposit hosts a 1998 drill-indicated mineral inventory of approximately 370,000 metric tones Zn, all as sphalerite (Norby and Orobono, 2000). One large Cretaceous stockwork Mo deposit of the low–F type (Buckingham, approximately 1.4 billion tonnes at 0.05 weight percent Mo), and two other major occurrences belonging to the same model, are present in the Battle Mountain Mining District (fig. 7–4), but they have had no production of Mo from their molybdenite–enriched cores (Theodore and others, 1992). This deposit type is described in somewhat more detail below in the section entitled "Porphyry Mo, Low–F Deposits (Model 21b of Cox and Singer, 1986)." However, some of the secondary-enriched Cu shell of the Buckingham system, specifically that present in the Copper Basin area (Blake, 1992), recorded significant production of Cu during 1966–1981 (Doebrich and Theodore, 1996). As noted by Doebrich and Theodore (1996), this metal production included approximately 44,000 metric tonnes Cu. Somewhat less production—approximately 13,055 metric tonnes Cu—has been recorded during 1917–1951 from the Copper Queen secondarily-enriched Cu deposit on the north flank of the Buckingham stockwork Mo system (Doebrich and Theodore, 1996). Several other stockwork Mo systems are known to be present in the Sonoma Range in the central part of the HRB (fig. 7–8) and are included as part of the pluton-related data set (table 7–1).

Elsewhere in Nevada, stockwork Mo occurrences of the low–F type, which are related to Mesozoic compressional tectonism along the paleocontinental margin, are associated with (1) W skarns that are widespread in northern Nevada (John and Bliss, 1994), and (2) disseminated scheelite—a W–bearing mineral—in the Mo–rich central parts of quartz stockworks (Theodore and others, 1992). Thus, exposed occurrences of W skarn may be linked genetically at depth to stockwork Mo deposits of the low–F type in the HRB. Climax-type Mo deposits, however, differ from the low–F type in that they have a genetic association with high-silica rhyolite and with regionally widespread zones of extension in areas of thick continental crust (Carten and others, 1993).

Porphyry Cu–(Mo) Deposits (Models 17, 21a of Cox and Singer, 1986)

Porphyry Cu–(Mo) deposits (Cox, 1986c, 1986d, 1986e; McMillan and Panteleyev, 1986; Titley, 1993) contain Cu–Fe sulfide minerals and molybdenite in quartz stockworks, in and adjacent to porphyritic intrusions emplaced to shallow levels in the crust. These typically are large deposits—the median tonnage of the worldwide general porphyry Cu model is 140 million tonnes (Singer and others, 1986a). These types of deposits generally are mined by open-pit methods because of their enormous tonnages of ore. Associated rocks are small stocks or dike sets of quartz-feldspar porphyritic quartz monzonite to granodiorite that have intruded cogenetic intermediate-composition volcanic rocks or preintrusive wall rocks. In the HRB, Cenozoic examples are most important (Titley and Beane, 1981).

Associated types of deposit are Cu skarn, Au skarn, polymetallic replacement, distal-disseminated Ag–Au, polymetallic vein, high-sulfidation state epithermal vein, and Au placer deposits. Some Fe (magnetite) skarn also is associated with a number of productive porphyry Cu deposits, exemplified as well by the Cretaceous porphyry Cu system at Ely, Nev. (Einaudi, 1982), and distal replacement of carbonate rocks by magnetite and less abundant chalcopyrite-pyrite assemblages yields as much as 200 million tonnes at a grade of 40 weight percent Fe at the Pumpkin Hollow (Lyon) Mine at Yerington (Dilles and Proffett, 1995).

Ore minerals typically include chalcopyrite, bornite, and (or) molybdenite in central zones of representative porphyry Cu systems, and these zones are surrounded peripherally by chalcopyrite-pyrite and local magnetite (Beane and Titley, 1981; Titley, 1993). Peripheral zones also are the sites of elevated concentrations of galena, sphalerite, and sulfosalt minerals. Supergene processes can produce enhanced concentrations of chalcocite, digenite, chrysocolla, malachite, azurite, and Cu–oxide minerals in rocks beneath a leached capping.

Alteration typically consists of a central, early K–feldspar-secondary biotite±anhydrite zone, mantled in the deep parts of the system by a peripheral propylitic zone dominated by chlorite±epidote±calcite mineral assemblages. In many known deposits, a well-developed phyllic (quartz-sericite-pyrite) overprint is present, generally concentrated at the original potassic-propylitic boundary, although the Yerington, Nev., deposit south of the HRB (fig. 7–1) has deep Ca–Na alteration (Dilles and others, 1995; Dilles and others, 2000a). In many deposits, however, phyllic alteration also may be concentrated irregularly in the central, upper parts of the system, generally close to some of the igneous rocks associated genetically with the system (fig. 7–11). Upper parts of many porphyry Cu systems are characterized by advanced argillic mineral assemblages that may be difficult to discriminate from supergene acid-sulfate altered rocks (Lipske and Dilles, 2000). Hydrothermally altered rocks in many of these systems can be extremely widespread—they affect as much as several tens of square kilometers in the Battle Mountain Mining District. The distribution or type of alteration was not used in the regional-scale HRB assessment.

Many of these porphyry systems are extremely complex geologically and they have been tilted, disrupted, and (or) extended significantly by post-mineral faults. Some systems also have been affected by synmineral faults or fault systems that were at times important concentrators of large volumes of mineralized rock (see this section below; see also, Tosdal and

Richards, 2001). Nonetheless, the original overall configuration of ore shells and alteration assemblages in many porphyry Cu–(Mo) systems (fig. 7–11) can be reconstructed if relevant data are available (see for example, Maher, 1996). Fractures are strongly developed episodically in many porphyry systems as the systems evolve (Tosdal and Richards, 2001), and they preferentially are filled by quartz-sulfide mineral stockwork veins, showing multiple veinlet sets, commonly with preferred orientations (Titley, 1993).

The fundamental ore controls essentially involve proximity to a mineralizing intrusion, which may have been emplaced at the intersections of regionally extensive faults and fractures or along prominent zones of dilation (Doebrich and Theodore, 1996; Drew and Berger, 2001; Hildenbrand and others, 2001). As we discuss below, we use a 19–km radius from all felsic igneous bodies shown on the geologic map of Nevada (Stewart and Carlson, 1978) as one of seven fundamental layers for our evaluation (see below). This radius was chosen on the basis of statistical conventions and does not reflect adequately the known extent of geologic processes in the porphyry Cu (Mo) environment. For example, in the Copper Canyon area of the Battle Mountain Mining District—one of the most intensely mineralized porphyry systems in the HRB—the surrounding alteration halo encompasses approximately 13 km2 as opposed to an area of 1,100 km2 that is encompassed by a 19–km radius around a point source. However, polymetallic veins at Copper Canyon extend at the surface well beyond the outer limits of the alteration halo (Kotlyar and others, 1998). Further, at Battle Mountain, emplacement of at least four, and probably as many as seven, porphyry systems of various categories occurred in conjunction with the earliest onset of extension documented in the Tertiary (Theodore, 2000). Local ore controls are a function both of wall rock composition and structure, as well as morphology of the associated intrusions, some of which are notably laccolithic in configuration (Theodore and Blake, 1975; Doebrich and others, 1995; Kotlyar and others, 1998b). A spatial and genetic continuum is present between porphyry Cu deposits and porphyry Cu–related skarns in some systems (Cox, 1986f); this is particularly evident in the Battle Mountain Mining District (Theodore and Blake, 1975, 1978).

Weathering of these systems typically results in a well-developed Fe–oxide-stained "leached" capping that shows the presence of phyllic zones of alteration (Cox, 1986d, 1986e; Titley, 1993). The geochemical signature in the weathered, oxidized zone of these systems includes anomalous Cu, Mo, Ag, as well as variable Au and peripheral Zn, Pb±Ag±Au. It is noteworthy that anomalous concentrations of Cu, Pb, and Zn are widespread in stream sediments and soils throughout much of the HRB (fig. 7–12). Arsenic is contained in arsenopyrite around many porphyry Cu systems in northern Nevada. Aresnic in rock and stream sediments from these areas also provides a regional indicator element to the extent and orientation of the mineralized regional trends along which many porphyry Cu systems are concentrated (fig. 7–13; see also, Kotlyar and others, 1998a). Much of the As in stream sediments apparently is adsorbed as As(V) onto various Al–bear-

ing phases, including gibbsite, amorphous Al oxyhydroxide, or aluminosilicate minerals (Andrea L. Foster, written commun., 2001). The Yerington porphyry Cu deposit (fig. 7–14), however, has essentially only Cu as an oxidation signature as well as a surrounding zone of advanced argillic alteration assemblages (Lipske and Dulles, 2000).

Four occurrences are present in or near the HRB that we classify as either generic porphyry Cu occurrences (Cox, 1986d, model 17) or as porphyry Cu–Mo occurrences (Cox, 1986e, model 21a). These porphyry Cu occurrences are in the Fireball Ridge area of the Truckee Mining District, in the Granite Mountain area of the Kennedy Mining District (Wallace, 1977, 1978; Thurber, 1982), and at Elder Creek (Theodore, 1996b; Gostyayeva and others, 1996). The latter occurrence is at the range front along the northeast flank of the Battle Mountain Mining District (fig. 7–4). We have no data on either the size or the grade of these three occurrences, although some of them have been drilled extensively for their porphyry Cu–style mineralized rock during the last 30 years. The likelihood that they will be brought into production during the next 15 years is low. The last of the four occurrences is the Contact, Nev., prospect of Golden Phoenix Minerals, Inc., Reno, Nev., located in northeastern Nevada

Drilling completed during 1998–1999 by Golden Phoenix Minerals, Inc., in the Contact Mining District (fig. 7–1), as well as drilling completed earlier by previous exploration efforts, suggests that a measured and indicated resource of approximately 953 million lbs Cu—named the Banner deposit—is contained in a Jurassic (155– to 157–Ma) porphyry Cu system associated with an albitic-altered composite granodiorite complex (S.D. Craig, oral commun., 2000). This Cu resource is contained in approximately 61.5 million t of mineralized rock that grades approximately 0.77 weight percent Cu (Golden Phoenix Minerals Inc., Press Release, June 20, 2000). The newly defined Cu resource is in the general area of the Marshall, Palo Alto, Brooklyn, and Bellevue (Nevada Bellevue) Mines, near the old town site of Contact and along an approximately 1.6–km strike length of the granodiorite's contact with Paleozoic sedimentary rocks (LaPointe and others, 1991). Apparently, mineralizing fluids were released from the intrusive complex in conjunction with district-scale, left-lateral wrench faulting during the Jurassic (S.D. Craig, oral commun., 2000). In addition, K–rich mineral assemblages replace early-stage albitic assemblages as the porphyry system evolved. The Banner deposit apparently has considerable potential for (1) expansion of near-surface Cu resources suitable for open-pit operations, and (2) expansion of relatively high–Cu–grade mineralized rock suitable for underground operations.

Porphyry Mo, Low–F Deposits (Model 21b of Cox and Singer, 1986)

Porphyry Mo, low–F deposits—also termed quartz monzonite or calc-alkaline Mo stockwork deposits by others—are

spatially and genetically associated with quartz monzonite and monzogranite stocks that are comprised of multiple intrusive phases. In this part of Nevada, these deposits are generally Late Cretaceous in age, and they were emplaced during compressional tectonic regimes. Porphyry Mo, low–F deposits can be extremely large systems—for example, the Buckingham deposit at Battle Mountain (see below). This type of deposit is characterized by molybdenite-quartz stockwork veinlets that typically cut calc-alkaline porphyritic intrusive rocks and significant volumes of the adjacent country rock. As much as 50 volume percent of intensely mineralized rock may be present in the wall rocks of the multiphase intrusive systems associated with the deposits (fig. 7–15; see also, Theodore and others, 1992). In addition, the Buckingham system, as well as some satellitic Tertiary porphyry systems superposed on its flanks, has a combined area of altered rock that is approximately 25 km2 (fig. 7–15). Copper typically is relatively abundant compared to Climax-type Mo deposits, and, in some deposits related to the porphyry Mo, low–F deposits, such as those at Copper Basin in the Battle Mountain Mining District (fig. 7–16; see above), Cu was mined from highly oxidized supergene-enriched orebodies marginal to the Mo–enriched core of the large system (Blake, 1992). However, at Buckingham, precious metals are concentrated preferentially near the east (top) end of the system, and only through superposition of a Au–Ag enriched outer shell from the nearby Tertiary Paiute Gulch porphyry system do Au–Ag grades locally reach ore-grade concentrations (fig. 7–15; see also, Ivosevic and Theodore, 1996). Gold-skarn deposits resulting from these superposed events are thought to be those at the Surprise Mine. Tin is usually absent or is present in extremely low concentrations in the porphyry Mo, low–F deposits. However, Sn may be concentrated to as much as 100–200 ppm along some of the young Tertiary veins that cut porphyry Mo, low–F deposits (Theodore and others, 1992). Some of these veins continued to be explored by drilling for their precious metal content well into 2000.

Alteration in the porphyry Mo, low–F deposits includes secondary K–feldspar with areally restricted phyllic envelopes, and intermediate-argillic assemblages may be pervasive. Topaz and fluorite are relatively common in some deposits (for example, Hall, Nev., and Big Hunch, Calif.) that comprise the grade-tonnage model, and extremely rare to absent in others (Buckingham). As mentioned above, alteration was not used in this assessment. Stockwork veinlets typically are concentrated in umbrella-shaped volumes of rock that are draped over the genetically associated pulses of magma (Loucks and Johnson, 1992). Compared to Climax-type deposits, however, these deposits, as a whole, are deficient in F, have significantly lower Mo grades, and are associated genetically with metaluminous intrusive rocks that have lower silica content than the Climax-type Mo deposits (Theodore and Menzie, 1984; Theodore, 1986). The deposits form during the late stages of intrusion with paleodepths of mineralization at 1 to 2 km for stocks and 3 to 5 km for plutons.

The largest and best explored of porphyry Mo, low–F occurrences is Buckingham (Theodore and others, 1992; Carten and others, 1993; Theodore, 2000), which contains more than 1 billion tonnes of rock mineralized at grades of approximately of 0.05 weight percent Mo, as well as substantial amounts of Cu, Ag, and W. However, median tonnage of this type of deposit is much smaller—approximately 100 million tonnes (Menzie and Theodore, 1986; see also, Theodore, 2000). The Buckingham deposit is within the boundaries of the HRB, and the two others in the Battle Mountain Mining District—Trenton Canyon and Buffalo Valley Mo—also are within the HRB as well (Theodore and others, 1992; Doebrich and others, 1995; Doebrich and Theodore, 1996). All of the porphyry Mo, low–F occurrences in the Battle Mountain Mining District are Late Cretaceous in age (McKee, 1992). The Buckingham deposit is the only one for which reserve data are available from near and (or) in the HRB (Theodore and others, 1992). The Buckingham stockwork molybdenum deposit also contains as much as 100 million oz Ag (see also, Carten and others, 1993). Unlike the Tertiary deposits in the Copper Canyon part of the Battle Mountain Mining District, the Buckingham deposit is Late Cretaceous in age and is related to a composite quartz monzonite porphyry stock emplaced at approximately 86 Ma (McKee, 1992). In addition, as described above, the supergene-enriched Cu orebodies at Copper Basin are part of a Cu shell that surrounds the Buckingham system (Blake, 1992). The central Mo orebodies have been extended structurally by a number of Tertiary low-angle faults. The orebodies are composed of stockworks of quartz-molybdenite-pyrite veinlets, with lesser amounts of Cu, Ag, and W accompanying Mo. The orebodies are especially well developed where ore shells have been superposed onto each other as a result of emplacement of loci of magmatic pulses into two separate intrusive centers (Loucks and Johnson, 1992). Superposition of these quartz stockwork shells onto each other resulted in generation of a 300– to 400–million-t deposit grading close to 0.1 weight percent Mo between the East and West stocks of the Buckingham Mo system. This is the deposit that would most likely be brought initially into production if the decision were made to exploit the system for its Mo content.

A number of additional sites are classified as porphyry Mo, low–F occurrences (Theodore, 1986) in and near the HRB. One is in the Leonard Creek Mining District, west of Quinn River Crossing, that is associated with Cretaceous or Tertiary porphyritic granodiorite. Wendt and Albino (1992) have identified a porphyry Mo, low–F occurrence in a Cretaceous granodiorite at Granite Point southwest of Lovelock, Nev., near Interstate 80. Two other occurrences, also classified as porphyry Mo, low–F occurrences, are near the south end of the Gold Run Mining District (fig. 7–9), where the genetically associated intrusions are apparently Cretaceous in age.

The most important indication in outcrop for the likelihood of porphyry Mo, low–F deposits is the presence of intensely silicified zones, including both vein and replacement quartz, that are present near the roofs of the intrusive cupolas. These features are associated with many porphyry Mo, low–F occurrences in the HRB and elsewhere, and they are diagnostic of these systems as described by Theodore (1986) and

Theodore and Menzie (1984). Although digital spatial data-bases were not available to treat these features in the current assessment, most exposed outcrops of silicified rock in the HRB probably have been evaluated already as potential targets for occurrence of a porphyry Mo, low–F system during the height of exploration for these types of mineralized system in the late 1970s and early 1980s.

Among the various sites enumerated above, the Buckingham system has the strongest possibility for production of large amounts of Mo during the next 15 years. However, the likelihood even for this system to be brought into production for its Mo content is doubtful because of the generally low Mo grades it contains relative to high-grade Climax-type Mo systems present in Colorado.

Climax Molybdenum Deposits (Model 16 of Cox and Singer, 1986)

Climax molybdenum deposits are characterized by stockworks of molybdenite and quartz associated with fluorite in high-silica rhyolite and granite porphyry typically containing more than 75 weight percent $SiO2$ (White and others, 1981; Ludington, 1986; Carten and others, 1993). Numerous intrusive phases associated with these systems have (1) zoned, shell-like, alteration patterns, and (2) ore zones that are draped over the apex of the systems and down the steep sides of the complexes (Mutschler and others, 1981; Carten and others, 1988; Carten and others, 1993). Ore shells in these systems typically are related to successively deep pulses of magma—the last mineralizing magma usually is the one deepest in the system. These deposits form at paleodepths of 1 to 3 km and may be indicated at the surface by the presence of topaz-bearing rhyolite (Christiansen and others, 1986). Igneous complexes associated with these deposits contain dikes, breccias, and multistage, subvolcanic porphyritic intrusive rocks, as well as zoned alteration patterns. Molybdenite-quartz stockwork veins commonly are related to aplitic quartz porphyry, and they usually are present in the middle stage of several rhyolite porphyry phases. Low-grade mineralized rocks may be present in deep, and slightly younger, coarser-grained igneous phases (Lowe and others, 1985). Lead, Zn, Ag, Sn, Cu, F, and Mo are anomalous in alteration zones around these plutons (Westra and Keith, 1981).

Majuba Hill in the Antelope Mining District, near the western boundary of the HRB (figs. 7–2, 7–9), has been classified provisionally as a Climax Mo occurrence (Ludington, 1986) (table 7–1). This occurrence is one of 92 training sites used for the pluton-related evaluation (see below). The relatively large amount of Cu at this locality, however, does not compare well with the abundance of Cu usually ascribed to this type of deposit. The Majuba Hill occurrence (MacKenzie and Bookstrom, 1976) is associated with 24– to 25–Ma rhyolitic rock emplaced during multiple pulses into Triassic basinal rocks of the allocthonous Jungo terrane. In addition, the Majuba Hill occurrence is not one of the nine depos-

its used to construct the grade and tonnage models for the Climax Mo deposits (Singer and others, 1986b). On the basis of available surface and subsurface information (MacKenzie and Bookstrom, 1976), Majuba Hill appears to lack some key aspects of an ideal Climax deposit, such as amount of F, quartz veining, and Mo enrichment. Regardless of its classification, it is doubtful, because of relatively low Mo grades compared to the Climax-type Mo deposits in Colorado, that Majuba Hill will be brought into production primarily for its Mo content anytime during the next 15 years.

Porphyry Cu–Au Deposits (Model 20c of Cox and Singer, 1986)

Porphyry Cu–Au deposits (Cox, 1986f), also termed porphyry Au deposits by some (Vila and Sillitoe, 1991; Muntean and Einaudi, 2000) and high-sulfidation epithermal deposits by others (Sillitoe, 2000b), consist of disseminated and stockwork Cu–Fe sulfide minerals and magnetite with Au in sub-volcanic intrusions and (or) their coeval volcanic rocks emplaced into weakly extended calc-alkaline arcs or bimodal island arcs (see also, Sillitoe, 1988; Rytuba and Cox, 1991). Three of these types of deposits (Yanacocha, Peru; Pascua-Lama, Chile-Argentina; and Pueblo Viego, Dominican Republic) are among the 28 largest Au deposits in the world (Sillitoe, 2000b). They respectively contain 48.9, 20.7, and 34.5 million oz Au. The porphyry Au deposits of the Refugio Mining District, Chile, contain approximately 180 million t of mineralized rock in two orebodies that average 1.02 and 0.85 g Au/t (Muntean and Einaudi, 2000). Rock types associated with many of these types of deposits include early gabbro or quartz diorite, synmineral diorite porphyry, and generally andesitic country rocks, as well as local marine carbonate rocks and other sedimentary rocks. Associated deposit types are Cu skarn, Au skarn, massive pyrite-enargite replacement deposits, and polymetallic replacements and veins. Ore mineralogy consists of chalcopyrite, bornite, magnetite, Au, and Pt–group-element telluride minerals and arsenide minerals. Disseminated Cu–Fe sulfide minerals are usually early phases and are followed by dense stockwork veins of quartz and additional sulfide minerals. Alteration is typically early K–feldspar–Fe–Mg silicate minerals such as biotite, amphibole, or pyroxene, as well as anhydrite. Banded quartz veins are one of the diagnostic mineralized fabrics associated with these deposits (Muntean and Einaudi, 2000). Subsequent stages of intermediate argillic alteration are common, and advanced argillic alteration forms the upper parts of some deposits. Ore controls are proximity to late-stage, porphyritic, sub-volcanic intrusions. Geochemical signature includes elevated concentrations of Cu, Au, and Ag, as well as As. Porphyry Au deposits formed at paleodepths less than 1 km, as opposed to 1.5 to 4.0 km depths for most porphyry Cu–(Mo) deposits (Muntean and Einaudi, 2000).

We have assigned no mineral occurrences in the HRB to the igneous-hosted porphyry Cu–Au category of deposits (fig.

7–1; table 7–1). Nonetheless, some Au deposits in the Battle Mountain Mining District and the McCoy Mining District, south of Battle Mountain (fig. 7–4), superficially may appear to belong to this class of deposits because of widespread presence of precious-metal bearing skarn and other similarities as described below. The geologic environment of Au metallogeny in these mining districts—rifted cratonal flat slab magmatism (Severinghaus and Atwater, 1990) possibly involving the Yellowstone "plume" (Oppliger and others, 1997; see also, Pierce and others, 2000)—does not precisely fit that model. Furthermore, there are no volcanic rocks present in these two mining districts that are coeval with the 38– to 40–Ma magmatic event that is responsible for the abundant precious metal-mineralized rocks (Doebrich, 1995; Doebrich and Theodore, 1995, 1996; see also, Henry and Ressel, 2000). However, the shallow seated (see also, chapter 8) distal-disseminated Ag–Au deposits in the Battle Mounrtain Mining District may be sedimentary-rock hosted counterparts of the porphyry Au deposits of Muntean and Einaudi (2000), primarily because of the former's inferred presence near the tops of columns of buried porphyry Cu–(Mo)-mineralized rock (Theodore, 2000). This geologic relation resembles the geologic setting of the porphyry Au deposits. However, because of a relative lack of widespread silicification in the distal-disseminated Ag–Au deposits in the HRB compared to most porphyry Au deposits, the former probably formed at depths more shallow than the latter. Moreover, farther to the east in the general area of the northern Tuscarora Mountains and southern Independence Range near the north-central border of the HRB, 38– to 40–Ma andesitic volcanic rocks are widespread and they are roughly coeval with intrusive rhyolitic rocks that are now (2002) considered by some geologists (Henry and Ressel, 2000; Ressel and others, 2000) to be genetically associated with at least some of the Au–mineralized rock present along the Carlin trend Au deposits (see chapter 8). As is described in chapter 8, this trend of currently (2002) producing Au deposits hosts one of the premier clusters of Au deposits in the world (fig. 7–2)—approximately 25 million oz Au were produced from this concentration of deposits up to 1996. If we grant some reasonable assumptions, a geologic environment favorable for presence of buried porphyry Cu–Au occurrences may exist at depth in the general region of these Au deposits. If such occurrences are eventually found and determined to be of a quality suitable for mining—most likely by underground methods—it is entirely possible that high Au–grade parts of the buried porphyry Cu–Au systems could be brought into production within a time frame of 10 to 15 years.

Base- and Precious-Metal Skarn Deposits

Various types of fairly isolated skarn deposits, as well as some mining districts made up almost entirely of skarn occurrences, are widespread throughout the HRB (fig. 7–17).

We follow the generic definition of skarn formulated by Einaudi (2000): "coarse-grained calc-silicate rocks rich in Fe and (or) Mg formed in dominantly calcareous wall rocks...a metasomatic product formed by import of exotic components by hydrothermal fluids." However, some skarns are composite, including parts hosted by the mineralizing intrusion (endoskarn) as well as parts hosted by the intruded host rock (exoskarn)—each part is dominated by a characteristic set of alteration assemblages. The geology of most skarn-bearing mining districts and the descriptions of their included deposits suggest that several types of skarn or replacement deposits are present, including porphyry Cu, skarn-related deposits; Cu skarn deposits; Zn–Pb skarns; polymetallic replacement deposits; Fe skarn deposits; Au skarn deposits; W skarn; and replacement Mn deposits (Peters and others, 1996). Precious metals as byproducts are not uniformly present in all of these types of skarn deposits.

Permissive areas for skarn occurrences other than W skarn are similar to those delineated for pluton-related deposits (Cox and others, 1996). Skarn or replacement deposits are known to be present in the Gold Run, Jackson Mountains, Iron Hat, Antelope, Harmony, and Trinity Mining Districts (fig. 7–9; see also, Jones, 1984a, 1985), as well as in a large number of other mining districts (fig. 7–17). However, an unusual concentration of highly productive skarn deposits is present in the Battle Mountain Mining District near the central part of the HRB (fig. 7–17; Doebrich and others, 1995; Doebrich and Theodore, 1996).

Porphyry Cu, Skarn-Related Deposits (Model 18a of Cox and Singer, 1986)

Porphyry Cu, skarn-related deposits usually are characterized by chalcopyrite-bearing quartz-sulfide mineral stockwork veinlets in porphyritic intrusive rock and adjacent altered rocks, including skarn (Cox, 1986e). Typically, these types of deposit in the general region of the HRB are generated by Mesozoic- to Tertiary-age granitic stocks intruded into carbonate rocks. Associated deposit types are Zn–Pb skarn, distal-disseminated Ag–Au (see chapter 8), and polymetallic vein and replacement deposits. Copper skarn, as defined by Einaudi and others (1981) and Cox and Theodore (1986), generally is restricted to occurrences that are associated genetically with intrusive stocks barren of metals, and are thereby excluded from being classified with porphyry Cu, skarn-related deposits. Alteration usually is K–silicate in barren intrusive rock associated with Cu skarn, and skarn minerals such as andradite, diopside, wollastonite, and tremolite are present in the adjoining carbonate wall rocks (Einaudi and others, 1981).

A number of porphyry Cu, skarn-related occurrences are present in the HRB. Specifically, most deposits in the Copper Canyon area of the Battle Mountain Mining District are included in this type of deposit, including the East and West orebodies, which produced Cu, Au, and Ag in the late 1960s through the late 1970s (Theodore and Blake, 1975,

1978; Doebrich and Theodore, 1996; Cary and others, 2000). These deposits are associated with a Tertiary (38–Ma), potassic-altered porphyritic granodiorite that contains about 0.25 weight percent Cu in its protore as chalcopyrite. Copper, Au, and Ag ore was produced in the late 1960s and early 1970s from those two orebodies in the Copper Canyon area predominantly from Paleozoic metasedimentary rocks which contained pyrrhotite, chalcopyrite, pyrite, and marcasite, as well as calc-silicate minerals in some places (Theodore and Blake, 1975, 1978). The original East Orebody, now (2002) mined out (Doebrich and others, 1995), contained K–silicate mineral assemblages without any prograde anhydrous calc-silicate minerals, even though ore formed in previously calcareous strata. Historic production from the Copper Canyon area is shown in table 7–2. Some mineralized rock remaining in the general area of the East Orebody (fig. 7–18) is projected to be included within the outer limit of the Phoenix open pit (Cary and others, 2000). The eventual outer limit of the Phoenix open pit includes the surface projection of the Fortitude (Lower and Upper) (fig. 7–19), West, and Northeast Extension orebodies, and the Phoenix open pit is one of the four pits currently (2002) in the process of being permitted for mining through a Plan of Operation from BLM. The other three pits are the Greater Midas, Iron Canyon, and Reona (fig. 7–20). Inasmuch as most ore scheduled to be mined from the Copper Canyon area is classified as Au skarn (Cary and others, 2000; Johnson, 2000), the ore there will be discussed as well in the section below entitled "Gold Skarn Deposits (Model of Theodore and others, 1991)."

The most likely location for undiscovered porphyry Cu, skarn-related deposits is in, and around, previously identified porphyry Cu systems, especially if carbonate wall rocks are affected by any alteration assemblages associated with the mineralizing porphyry systems. However, these features are not represented in the data sets used in this assessment and, therefore, the potential for these deposits cannot be depicted well. Near many of these systems, the rocks are extremely complex structurally because of the large number of protracted structural events to which the rocks have been subjected. Relatively small, but economic, targets require substantial drilling to prove or disprove, and young gravels that fill the valleys may cover some of these systems. An example of the latter relation is the Redline (Converse) mineralized system that is present under Tertiary and Quaternary gravel near the middle of Buffalo Valley northwest of the main Battle Mountain Mining District (fig. 7–3; Cleveland, 2000). This mineralized system is described below in the subsection entitled "Gold Skarn Deposits (Model of Theodore and others, 1991)."

Copper Skarn Deposits (Model 18b of Cox and Singer, 1986)

Copper skarn deposits are characterized by chalcopyrite associated with magnetite and pyrrhotite and a variety of other sulfide and oxide minerals (Cox and Theodore, 1986). These deposits are associated with barren stocks (Einaudi and others, 1981). Most of approximately 20 known Cu skarn occurrences near the western part of the HRB are spatially associated with Jurassic intrusive rocks, but Cretaceous and Tertiary deposits also are present (fig. 7–9). According to Einaudi and others (1981), Cu skarns form in less-dynamic magmatic-hydrothermal environments and at greater depths than the porphyry-related skarns, so fluid flow apparently is restricted while crystal growth is retarded. Therefore, development of widespread, disseminated mineralized rocks—including large tonnages of mineralized rock—is less likely, and Cu skarns typically are relatively small deposits. Permissive and favorable tracts for Cu skarn occurrences are similar to those in Peters and others (1996) for Fe skarn and Zn–Pb skarn, all of which share many geologic and geochemical characteristics (Einaudi and others, 1981; Meinert, 1993).

Zinc–Pb Skarn Deposits and Polymetallic Replacement Deposits (Models 18c and 19a of Cox and Singer, 1986)

Zinc–Pb skarn deposits also are found where carbonate rocks are intruded by granitic rocks and typically are formed farther away from the mineralizing intrusive rocks than are Cu and Fe skarns. Zinc–Pb skarn deposits generally are more common in the eastern part of the HRB than in the western part, although their overall number of occurrences is rather small. Their geologic environment of formation and geographic distribution is similar to those of polymetallic replacement deposits (Cox, 1986g; Morris, 1986). Zinc–Pb skarns are characterized by sphalerite and galena in metasomatic calc-silicate rocks derived from carbonate and calcareous clastic sedimentary rocks. Zinc–Pb skarns typically contain a number of minerals rich in Mn and Fe as opposed to other varieties of skarn (Zharikov, 1970; Burt, 1972, 1977; Einaudi and others, 1981). Pyroxenes commonly are enriched in the Mn end member, whereas garnets are commonly Fe–rich andradite. Calc-silicate mineralogy typically includes garnet, diopside, epidote, and tremolite.

Polymetallic replacement deposits (Morris, 1986) typically form tabular, pod-like, and pipe-like ore bodies, which are localized by faults or bedding in sedimentary rocks. The deposits are in sedimentary rocks, chiefly carbonate strata, which were intruded by porphyritic calc-alkalic or alkali-calcic plutons. Thick carbonate beds may fracture during magma intrusion and deformation and act as good host rocks. Polymetallic replacement ores contain galena, sphalerite, tetrahedrite, and Ag–sulfosalt minerals. Mineral zoning is common so that inner zones are rich in chalcopyrite or enargite, and outer zones contain sphalerite and rhodochrosite. In many mining districts, polymetallic replacement deposits are several to many tens of meters outboard from the Zn–Pb skarn interface (Einaudi and others, 1981). Jasperoid is common as well. One locality in the Dutch Flat Mining District (fig. 7–2), in the southern part of the Hot Springs Range, has been classified

provisionally as a Zn–Pb skarn, and there are a number of localities that have been classified as a polymetallic replacement occurrences—two of the latter are in the Gold Run Mining District (Peters and others, 1996; see also, Jones, 1983, 1984a), and nine are in the Humboldt Range (Cameron, 1939).

Although Pb and Zn are present as minor commodities in many other types of skarn in the HRB, Zn–Pb skarn and polymetallic replacement deposits generally are not important in this region. Nonetheless, two exceptions to this generalization are present in the HRB. First, the Tomboy-Minnie Au skarn in the Copper Canyon area of the Battle Mountain Mining District was mined from 1978 to 1982 and yielded approximately 7,902 kg Au from approximately 3.28 million t ore (table 7–2). The Tomboy-Minnie also contained abundant sphalerite and galena, but was mined only for its precious-metal content (Theodore and others, 1986), and is therefore classified as a Au skarn (see section below entitled "Gold Skarn Deposits (Model of Theodore and others, 1991)." An exception may be the large geologic resource of Zn in sphalerite associated with the Mike Au deposit along the Carlin trend (see above).

Iron Skarn Deposits (Model 18d of Cox and Singer, 1986)

Iron skarn deposits typically are related to intermediate-composition intrusions that were emplaced into carbonate strata or other mafic igneous rocks (Cox, 1986b). The deposits contain magnetite or hematite with calc-silicate minerals in contact metasomatic rocks. The most important Fe skarns near the HRB have formed where Mesozoic plutons intruded Triassic and Jurassic carbonate rocks—22 sites in the general area of the western part of the HRB have been classified as Fe skarn occurrences (Peters and others, 1996).

Iron endoskarns near the southwestern boundary of the HRB near Lovelock in the Mineral Basin Mining District are associated with the Middle Jurassic Humboldt mafic complex (Reeves and Kral, 1955; Shawe and others, 1962; Speed, 1962; Johnson, 1977; John and Sherlock, 1991; Johnson and Barton, 2000). This complex forms part of a Jurassic continental magmatic arc (Dilek and Moores, 1995). The broad expanse of Jurassic plutons in the Great Basin also has been referred to as a backarc magmatic event that may owe its origins to a slab collapse with attendant upwelling of the asthenosphere (Dickinson, 2001). Jurassic Fe endoskarns consist of massive magnetite replacement of gabbroic rocks and magnetite stockworks in both plutonic and coeval volcanic rocks accompanied by scapolite and albite alteration. These deposits are analogous to the island-arc calcic magnetite skarn model type described by Einaudi and others (1981). Such igneous-related Fe–oxide systems are relatively common in Jurassic rocks throughout western North America (Barton and others, 1988; Barton, 1996; Johnson and Barton, 2000). Two major occurrences are in or near the HRB: the one near Lovelock and several in the Cortez Mountains near Elko. In

the Humboldt mafic complex near Lovelock, the Buena Vista Mine is the largest deposit with reserves of 18 million t at 32.7 weight percent Fe (Lowe and others, 1985). Total production to 1971 is at least 4 million t ore (Johnson and Barton, 2000). The ore mainly is in replacement veins of magnetite and hematite in scapolitized gabbro. The Humboldt mafic complex has an enormous volume, approximately 7,900 cubic kilometers, that was pervasively altered by Na–enriched fluids that likely were derived largely from nonmagmatic sources (Johnson and Barton, 2000). The Humboldt mafic complex and its wall rocks also contain small oxidized Cu deposits and some occurrences of amygdaloidal Cu, as well as some occurrences of Ni and Co near the easternmost part of the complex in the Stillwater Range (Ferguson, 1939). In Fe occurrences in the Cortez Mountains, a number of Fe–oxide deposits, hosted by Mesozoic felsic volcanic rocks, comprise the Modarelli-Frenchie Creek Mining District (fig. 7–2; Roberts and others, 1967). The Modarelli Mine is the largest of these deposits, and total production through 1961 is approximately 0.4 million long t (that is, 2,240 lbs per long t) of ore probably averaging approximately 57 weight percent Fe (Roberts and others, 1967).

In addition to the two major clusters of Fe–endoskarn occurrences described above, a small number of Fe–skarns in the McCoy Mining District in the Fish Creek Mountains (fig. 7–17) are recorded as having minor production during 1943, 1951, and 1954, as well as 1961 through 1964 (Stager, 1977). The Fe deposit at the McCoy Mine is known as the Uhalde-New World, and is not to be confused with the nearby McCoy Au skarn (Kuyper, 1988; Brooks and others, 1991). The Uhalde-New World Fe deposit consists of three lensoid magnetite-rich orebodies that dip shallowly to the south as replacement of a dolomitic protolith (Stager, 1977) belonging to the Triassic Star Peak Group of Nichols and Silberling (1977). The Hancock, at the east edge of the district at the range front, is smaller than those at Uhalde-New World. In all, approximately 40,000 long t of about 60 weight percent Fe were mined from these deposits that are all related genetically to intrusion of a nearby, east-trending Jurassic diorite into the Triassic Augusta sequence (Stewart and McKee, 1977).

Permissive areas reported by Peters and others (1996) for Fe skarn deposits are similar to those for other skarn deposits in the general area of the HRB where the two areas overlap. Known Fe skarn deposits, and areas of strongly positive aeromagnetic anomalies from both plutons and Buena Vista-type deposits, are considered the most likely areas for their occurrence. Aeromagnetic data was not used in the present assessment, and these deposits are contained in the generic pluton-related tracts. However, it is possible that some magnetite-bearing skarn deposits that have been converted to hematite during protracted periods of oxidation in the Tertiary and Quaternary may not have a strong magnetic anomaly and they may be covered by young gravels in the valleys. Such covered oxidized magnetite skarn deposits probably could best be detected by closely-spaced magnetic surveys that attempt to find the similarly covered plutons associated with the deposits.

Gold Skarn Deposits (Model of Theodore and Others, 1991)

Gold skarn deposits form in contact metasomatic rocks, generally in shallow-level paleoenvironments, formed at or distal to contacts with intrusive rocks that range in composition from diorite to quartz monzonite. Meinert (1989, 1993, 1999; see also, 2000) suggests that most large Au skarn deposits are associated with reduced rather than oxidized plutons. Rock textures in Au skarns typically are coarse-grained granoblastic (Meinert, 1989; Theodore and others, 1991). Deposits associated with Au skarn include porphyry Cu, skarn related; Cu skarn; Zn–Pb skarn; polymetallic replacement; polymetallic vein; distal-disseminated Ag–Au; Au placer deposits, and Carlin-type Au deposits. Recent studies by Johnson (2000a) in the McCoy Mining District have concluded that a continuum of mineralized environments exists from the Au skarn environment through the Carlin-type environment (see also, chapter 8). In addition, many skarn deposits mined in the past for base metals would be most valuable today for their contained Au (Theodore and others, 1991).

The mineralogy of Au skarns includes Au and electrum, arsenopyrite, pyrrhotite, pyrite, high–Fe sphalerite, chalcopyrite, magnetite, native Bi, hedleyite, tetradymite, and other telluride minerals. Altered rocks surrounding Au skarns are typically converted to early K–feldspar-biotite, local intermediate-stage grandite, andradite garnet, and hedenbergitic or diopsidic pyroxene, as well as locally abundant retrograde alteration minerals—the latter can include chlorite, hematite, epidote, actinolite, sericite, and calcite. Limestone beyond the metasomatic silicate front typically is still within the contact aureole of the associated pluton, and, as such, has been converted to marble. Some marble beyond the metasomatized silicate front may contain concentrations of carbonaceous material along narrow seams or fractures. This carbonaceous material probably is expelled from those parts of the system undergoing conversion to calc-silicate minerals.

Ore controls of Au skarn deposits may include mining district-scale faults or fault intersections (Doebrich and others, 1995; Doebrich and Theodore, 1996), as well as district-scale regimes of dilatancy resulting from transpressional shear couples operating during the time of magma emplacement and its associated mineralization (Hildenbrand and others, 2001). Ore may be distal to source intrusive rocks, near the marble line, or it may form in apical parts of the intrusive complex (Ray and Dawson, 1994). Geochemical signature is typically Au, Ag, Cu, As, Pb, Zn, and Bi, as well as Te with local W. Many of these metals form well-organized stacked mushroom-shaped and pillar-shaped haloes that envelope ore in the system (Kotlyar and others, 1998b). These ore controls are not specifically addressed in the present mineral assessment of the HRB.

In the central part of the HRB, a number of mineralized occurrences in the Battle Mountain Mining District (Doebrich and others, 1995) have been classified as Au skarn. Among these occurrences is the Fortitude Au skarn, which is one of the most economically important Au skarns worldwide (figs.

7–18, 7–19). These types of deposit also are present in the McCoy Mining District (Brooks and others, 1991; see also, Johnson, 2000), where they have 38– to 40–Ma ages of mineralization—these ages are the same as the ages of mineralization of Au skarns in the Battle Mountain Mining District (Theodore and others, 1973; McKee, 1992; McKee, 2000).

Gold skarn comprises the dominant orebodies in the Copper Canyon area of the Battle Mountain Mining District. A number of these orebodies were mined from 1978 through 1994 (fig. 7–18; see also, Blake and others, 1984; Theodore and others, 1986; Wotruba and others, 1988; Myers and Meinert, 1991; Myers, 1994). The Fortitude Au skarn deposit at Copper Canyon produced approximately 1.9 million oz Au between 1984 and 1993—it also contained approximately 0.2 weight percent Cu (Wotruba and others, 1988). The Phoenix project (Doebrich and others, 1995; Cary and others, 2000; Johnson, 2000b) presently (2002) includes a number of economically important unmined Au skarn deposits at Copper Canyon (fig. 7–20). A geologic resource of as much as 12 million oz Au eventually may be attributed to the Copper Canyon area (Kotlyar and others, 1998b), with an economic resource of approximately 6 million oz Au remaining to be mined as of late 2001 (table 7–3; see also, Cary and others, 2000; Johnson, 2000b). All Au deposits at Copper Canyon lie closer to a central granodiorite stock than a well-developed surrounding zone of Pb–Zn–Ag polymetallic veins (Roberts and Arnold, 1965; Kotlyar and others, 1998b). However, the Tomboy-Minnie Au skarn (deposit nos. 8–9, fig. 7–18), which also is mined out (Doebrich and others, 1995), contained high Pb and Zn concentrations in a retrograde-altered pyroxene skarn (Theodore and others, 1986).

Advanced exploration activities and resource evaluations by Battle Mountain Gold Co. (BMGC) primarily were focused on the Copper Canyon area of the Battle Mountain Mining District during 2000 even though actual mining operations had been curtailed in late 1999. These activities included a 20,000 t test of Au ore from four separate ore zones at Copper Canyon as throughput for the autoclave at the Twin Creek mining facilities. The Twin Creek facilities belong to Newmont Mining Corporation. On November 22, 2000, the Securities and Exchange Comission approved a merger between BMGC and Newmont Mining Corporation—BMGC stockholders approved the merger January 5, 2001, and the merger was completed January 10, 2001. A draft Plan of Operations, including the proposed processing of Au ore from Copper Canyon in the autoclave at Lone Tree approximately 25 km north of Copper Canyon and also belonging to Newmont Mining Corporation, was being processed by BLM during 2001. This plan includes open-pit mining at Copper Canyon to proceed for 13 years at a rate of approximately 30,000 t of ore per day from the Phoenix, Greater Midas, Iron Canyon, and Reona open pits (fig. 7–20). Such production would include most of the in-place proven and probable 176,633 kg Au (5.9 million oz Au) and 1,328,854 kg Ag (44.3 million oz Ag) reserves as of year-end 1999 (table 7–3; see also, Cary and others, 2000). However, the likelihood is quite good that additional reserves of Au and Ag could be

found in the immediate area of Copper Canyon during that proposed 13–year-long span of mining, thereby extending the projected mine life of the area even further. In addition, the likelihood is quite good that as much as 2 million oz Au will be added to the overall inventory of Au reserves from the Copper Basin part of the district. Further, as many as five or six structurally-controlled, relatively small orebodies—each measuring approximately 100,000 to 200,000 t ore—from elsewhere in the areas of either Copper Canyon or Copper Basin should progress to an economic ore reserve category over the next ten years on the basis of past discovery rates of similarly-sized deposits during the previous 30–year mining history at Copper Canyon. Therefore, all of these reasonable projections should extend duration of mining at Copper Canyon to approximately 20 years once it commences. Certainly, this overall scenario for mining is contingent highly upon a reasonable future price for Au and a decision to begin mining again.

The shallow bedrock areas of the pediments surrounding the southern and southeastern parts of the Battle Mountain Mining District are exceptionally good target areas for discovery of additional Au orebodies. However, several companies apparently have encountered only large volumes of low-grade Au–mineralized rock after they have drilled as many as 50 holes. The appropriateness of exploration programs focusing on shallow-bedrock pediment areas in the region, nevertheless, is emphasized by the recent discovery of the Redline Au–skarn deposits in Buffalo Valley (fig. 7–3). Post-mineral unconsolidated valley-fill alluvial gravels cover the Redline deposits (fig. 7–21). These Au skarn deposits at year-end 1998 include an in-place indicated geologic resource of 48 million t at a grade of 0.024 oz Au/t or approximately 1.2 million oz Au, and an in-place inferred geologic resource of 35 million t at a grade of 0.023 oz Au/t or approximately 0.8 million oz Au (Cleveland, 2000). In contrast to the high-sulfide mineral content of the Au–skarn orebodies at Copper Canyon (Cary and others, 2000; Johnson, 2000b), mineralized rock in the Redline deposits contains approximately 0.5 volume percent sulfide minerals (Cleveland, 2000). The Redline deposits are related to a 41–42 Ma (R.J. Fleck, oral commun., 2001) Tertiary porphyry stock and dikes that were emplaced into calcareous sandstone of the Mississippian, Pennsylvanian, and Permian Havallah sequence—the stock and dikes are present at the intersection of north- and northwest-striking structures. A cross-section through the system shows the relation of the central porphyry stock to the two adjoining deposits, South Redline and North Redline, as well as the fact that the mineralized system is covered by gravel deposits younger than the mineralized rocks (fig. 7–21). The mineralized system is covered by 8.5–m- to as much as >240–m-thick gravels. As a result, discovery of the South Redline deposit occurred roughly six years after initial exploration efforts began to be focused on the property (Cleveland, 2000).

Favorable areas for Au skarn in the western part of the HRB coincide with favorable tracts for porphyry-related deposits in Peters and others (1996), but Au skarn also may be found elsewhere where contact metasomatic or skarn occur-

rences or porphyry-related districts containing Au production or anomalous concentrations of Au have been reported. On the basis of the recent discovery of a continuum of deposits from the Au skarn environment through Carlin-like Au–mineralized rock (Johnson, 2000a), Carlin-type Au deposits also could be considered as indicator deposits for skarn-type mineralized rock at depth (see chapter 8).

Tungsten Deposits

Tungsten skarn deposits are common in Nevada, but W vein deposits are not (fig. 7–9; Hess, 1911; Hess, 1917; Kerr, 1946; Lemmon and Tweto, 1962; Kornhauser and Stafford, 1978; Stager and Tingley, 1988; John and Bliss, 1994). Tungsten skarn deposits are particularly widespread in the HRB (Schilling, 1963, 1964; Johnson and Benson, 1963), where two of the previously largest W–producing areas in the United States, the Mill City and Potosi Mining Districts, are present (fig. 7–17). There has been no significant W production in the HRB since 1957 when funding of the U.S. Stockpile Program was suspended (J. Tingley, written commun., 2002).

The geologic setting of W skarns and minor W–bearing quartz veins is consistent in the region, and the deposits generally are present at or near the contacts of limestone-bearing strata and granitic plutons (Cox, 1986a, and many others previously). The tungsten mineral in skarns generally is a variety of scheelite, whereas in quartz veins the mineral generally is wolframite. The plutons are Early Cretaceous in the Imlay (Vikre and McKee, 1985) and Hooker Mining Districts (fig. 7–2; Smith and others, 1971), but Late Cretaceous in the large Mill City Mining District and in the Potosi Mining District (Silberman and McKee, 1971; Silberman and others, 1974) (fig. 7–17). Tungsten mostly is contained in scheelite-bearing quartz veins that cut altered Triassic limestone in the Imlay Mining District (Johnson, 1977). Tungsten deposits also are associated with Late Cretaceous granitic rocks in the Nightingale Mining District near the south westernmost lobe of the HRB (fig. 7–17). In contrast to porphyry Cu deposits, hot-spring Au deposits, and sedimentary rock-hosted Au–Ag deposits, which have mainly been mined by open-pit methods, most W production in the general region of the HRB has come from underground mines. In addition, W is associated with hot-spring Mn deposits in the Golconda Mining District (fig. 7–2), in the north-central part of the HRB (Penrose, 1893; Kerr, 1940; see also, section below entitled "Other Tungsten Deposits").

Tungsten-Skarn Deposits (Model 14a of Cox and Singer, 1986)

Tungsten-skarn occurrences are present at or near contacts of mesozonal quartz monzonite plutons with carbonate wall rocks. Many of these plutons are weakly peraluminous. An association with aplite and (or) pegmatite bodies is common. These occurrences have many similarities and commonly are

associated spatially with base-metal skarns (fig. 7–17; see also, Einaudi and others, 1981; Einaudi and Burt, 1982). Tungsten-bearing skarns commonly form in roof pendants or thermal aureoles of relatively deep-seated mesozonal plutons that have been emplaced at depths where ambient pressures are 1 kb or greater. Skarn mineralogy is dominated by grandite garnet and hedenbergitic pyroxene. Mineralized rocks generally contain molybdenite, pyrrhotite, sphalerite, bismuthinite, chalcopyrite, and scheelite, as well as magnetite (Barton and others, 1988). Large areas of early-formed, Fe–poor calc-silicate rock, which are formed by isochemical recrystallization, generally extend significant distances from the centers of metasomatism at the sites of the W skarns. Ore controls for W skarns are both stratigraphic and structural, and they include the three dimensional configuration of contacts between igneous intrusions and wall rock. These contacts influenced profoundly the channeling and the ponding of ore-forming fluids. Tungsten-skarn occurrences range in size from small showings (<1 tonne) or trace byproducts to major deposits (>1 million tonnes), and they are present in many areas of the western part of the HRB where Late Cretaceous plutons, ranging in composition from diorite—as little as 62 weight percent SiO_2 (see table in John and Bliss, 1994)—to granite, intrude limestone, dolomite, or other chemically reactive rocks (Hess and Larson, 1921; Cox, 1986a; Stager and Tingley, 1988). Approximately 150 mineral occurrences in the HRB have been classified as W skarn. Base metals, Mo, and Ag accompany W in trace amounts in many of these occurrences. John and Bliss (1994) indicate that the size of W–skarn deposits mined in Nevada is unusually small because they were mainly exploited during times of war when government subsidies were used to stimulate production.

Although the districts are relatively minor economically, the Corral Creek, Lee, and Harrison Pass Mining Districts in the Ruby Mountains, approximately 40 km southeast of Elko, Nev., and near the east border of the HRB (fig. 7–17), contain some importanr relations between W and base metals. Mineralized rock at the American Beauty and Summit View Mines in the Corral Creek and Lee Mining Districts contains Pb, Zn, Cu, and Ag sulfide minerals, as well as Ba (barite ± celsian) and minor W and Au (Berger and others, 2000). Polymetallic quartz-sulfide mineral (chalcopyrite ± galena ± sphalerite) veins represent the final retrograde stages of mineralization at the deposits following a predominantly pyroxene-rich, anhydrous early alteration stage. Copper–Pb–Zn ± Au ± Ag ore from the late-stage veins is dominant at approximately 8,200–ft elevations at these occurrences. However, just to the east in the Harrison Pass Mining District, which is at a much lower elevation, approximately 15,000 units WO_3 were produced from W–skarn occurrences during 1941–1944, 1953–1957, and 1978–1979 (LaPointe and others, 1991). These relations suggest a vertical metal zonation from deep W skarn to relatively shallow Cu–Pb–Zn polymetallic veins across a vertical interval of about 500 m in this area.

The broad W metallogenic province outlined by Stager and Tingley (1988) in Nevada contains many clusters of National Uranium Resource Evaluation (NURE) stream-sedi-ment and soil samples that also have anomalous concentrations of Mo (King, 1996; King and others, 1996). The only other strong clustering of anomalous concentrations of Mo is in the general area of the Battle Mountain Mining District. In addition, the W province appears to have relatively low concentrations of Ba when Ba concentrations within it are compared with those in the surrounding region (King, 1996).

Permissive tracts for both W–skarn and W–vein deposits are defined by presence of granitoid plutons within the HRB and should be similar to permissive tracts for porphyry-related deposits. However, only Cretaceous intrusive centers are known to be associated with significant concentrations of W in the HRB—exemplified by those in the Mill City and Potosi Mining District. Limited age data on plutons in the HRB prevented the separation of Cretaceous intrusive centers from other plutons in the present mineral assessment of the HRB. Nonetheless, some minor amounts of W have been mobilized by fluids as young as approximately 1 Ma—probably even younger than this—in the Golconda Mining District (see section below entitled "Other Tungsten Deposits"). Stager and Tingley (1988) have defined a northeast-trending tungsten belt through the southwest part of the HRB.

The Mill City (Kerr, 1934) and Potosi Mining Districts (Klepper, 1943) are located at the east margin of the Cretaceous Lovelock granitoid batholith belt, which is interpreted as the northeast extension of the Sierra Nevada batholith by Smith and others (1971). The largest W–skarn deposit is the Springer Mine (previously known as the Sutton Number 1 and 2 deposits) in the Nevada Massachusetts group (King and Holmes, 1950; Johnson and Keith, 1991), where a small granodiorite stock intruded and metamorphosed a thick clastic sequence of Triassic shale, quartzite, and minor limestone. The Riley Mine in the Potosi (or Getchell) Mining District in the Osgood Mountains has the third largest recorded production of W in Nevada (Neuerburg, 1966; Taylor, 1976), whereas the Getchell Mining District has third largest W production in Nevada after Mill City and Tempiute Mining District in eastern Nevada. Mineralized rocks at the Riley Mine are associated with the 92–Ma granodioritic Osgood Mountains stock, which intruded Cambrian shale and limestone. Tungsten skarn clusters near the contact between the stock and adjacent limestone strata. Wollastonite is the most abundant contact metamorphic mineral (Hobbs and Clabaugh, 1946; Hobbs and Elliott, 1973; Joraleman, 1975). Skarn minerals, associated with ore in both the Mill City and Potosi Mining Districts, include quartz, epidote, garnet, and diopside, as well as minor retrograde tremolite. In addition, scheelite, pyrrhotite, molybdenite, chalcopyrite, arsenopyrite, pyrite, sphene, and apatite are present.

In the event that some type of national emergency takes place wherein newly mined W is needed to supplement that existing in the national stockpile, several deposits in the HRB are likely candidates for further development. The underground Springer Mine in the Imlay Mining District (fig. 7–2) contains approximately 1 million units of WO_3 at a grade sufficient to sustain significant production (J.V. Tingley, oral commun., 2000). However, the existing shaft at the Springer

Mine probably would need dewatering and rehabilitation if production of W is to recommence. In the Potosi Mining District, near the east flank of the Osgood Mountains, undeveloped W–skarn mineralized rock is present below the workings at the Moly-Tonopah Mine. However, these W resources are not fully explored and further development would require significant additional in-fill drilling (J.V. Tingley, oral commun., 2000). Further, the entire remaining W resource, if present, at the Moly-Tonopah Mine may have been removed during stripping associated with westward advance of open-pit operations associated with nearby open-pit Au mining at the Getchell Mine (see also, Chevillon and others, 2000).

Tungsten Vein Deposits (Model 15a of Cox and Singer, 1986)

Tungsten vein deposits are present as quartz-wolframite veins that contain molybdenite and minor base-metal sulfide minerals (Kelly and Rye, 1979; Cox and Bagby, 1986). They usually form in monzogranite to peraluminous granite stocks or in the contact aureoles of these bodies in surrounding siliciclastic sedimentary rocks and metasedimentary rocks, rather than in carbonate rocks (Ludington and Johnson, 1986; Barton, 1990). Other minerals present include bismuthinite, pyrite, pyrrhotite, arsenopyrite, bornite, scheelite, beryl, fluorite, and tourmaline. The ore typically includes massive quartz veins with minor vugs, parallel walls for the veins themselves, and local breccia. The W vein deposits have produced significantly less than W skarn deposits in the in the general region of the HRB (see also, John and Bliss, 1994). Known occurrences are located in New York Canyon (Ludington and Johnson, 1986; Johnson and others, 1986), in the Imlay Mining District, and in the West Humboldt Range, south of Lovelock. Most occurrences in the HRB contain scheelite, rather than wolframite, and, therefore, such occurrences are not directly compatible with the deposit model. In addition, they are apparently much smaller than the tonnages shown in the model. Tungsten deposits in the Humboldt Range (Peters and others, 1996) include veins and pegmatites containing quartz, fluorite, beryl and anomalous U (Cameron, 1939; Klepper, 1943)—these are mineral and elemental associations generally not associated with hornblende-bearing granitic (sensu lato) rocks. This association suggests that the areas near W vein deposits may represent mineralized rocks formed from a magma type different from that associated with W skarn found elsewhere throughout the HRB. Tungsten skarn generally is associated with hornblende-bearing granitic rocks (John and Bliss, 1994).

Other Tungsten Deposits

Other areas in the HRB that are considered to lie within favorable or prospective W domains include mining districts that have either minor production of W or known occurrences of W minerals (Peters and others, 1996). These W localities have many characteristics similar to those in the large mining districts, but they also may be associated with porphyry-related mineralized rocks (Erickson and Marsh, 1974a, 1974b, 1974c), or they may be associated with epithermal deposits (Willden and Hotz, 1955). Tungsten, as scheelite, is present in some of the low–F porphyry Mo deposits in the Battle Mountain Mining District (Theodore and others, 1992) as we described above.

Tungsten deposits in the Golconda Mining District, near Interstate 80 approximately 25 km east of Winnemucca (fig. 7–17), have characteristics different from those listed above. These deposits contain MnO_2 minerals in lacustrine beds associated with Pleistocene Lake Lahontan (Penrose, 1893; Palmer, 1918). The deposits are hosted in fanglomerate under a caliche-like cap, and W is contained within psilomelane and limonite (Pardee and Jones, 1920; Buttl, 1945). These characteristics are not compatible with either the W–skarn or the W vein models, but represent another type of W resource. Kerr (1940, 1946) suggested that these deposits in the Golconda Mining District are associated with recent hot springs—which are still (2002) active in the area—and it is likely that these deposits closely have a close genetic alliance to epithermal (hot-spring) Mn deposits described by Mosier (1986a; see also, Mosier, 1986b). Some have suggested that W at Golconda may have been remobilized during the Holocene from Cretaceous skarn deposits at depth.

Other Pluton-Related Deposits

Other types of deposits that are related to the plutonic geologic environment include polymetallic vein and replacement deposits, and replacement Mn deposits. Polymetallic occurrences are widely distributed throughout northern Nevada and the HRB (fig. 7–22). Many of these mining districts contained economically and geologically significant deposits—these include Battle Mountain, McCoy, Lewis-Hilltop, Bullion, and Kennedy Mining Districts (fig. 7–22), as well as a number of mining districts near Austin, Nev., and elsewhere in the northern part of the State. Mining districts near Austin include the Reese River, Ravenswood, Skookum, New Pass, Big Creek, and Kingston (Victorine). Silver ore was discovered in polymetallic quartz veins in the Reese River Mining District in 1862, and probably as much as $26 million was produced between 1863 and 1908 (Stager, 1977). In the Ravenswood Mining District, Ag–Pb–Cu quartz veins yielded less than $10,000 worth of production (Stager, 1977). However, this mining district includes a structural window through the allochthon of the Roberts Mountains thrust (Stewart and McKee, 1977), which has some potential for presence of sedimentary rock-hosted Au–Ag occurrences (see below). Base metal veins are part of the geologic signature of some of the largest Carlin-type Au deposits in Nevada (see chapter 8). The Skookum Mining District also contains some Au–Ag polymetallic quartz veins that contain tetrahedrite and Cu– and Pb–oxide minerals—at most, production during 1908 had a value of about $100,000 (Stager, 1977). A similar quantity

of production was obtained from the mining of Ag–(Cu–Sb) quartz veins from the Big Creek Mining District. The Kingston (Victorine) Mining District contained Au–Ag quartz veins formed in silicified zones in lower Paleozoic limestone—these veins geochemically zone to Pb–Zn–bearing quartz veins at depth. Most of these polymetallic veins near Austin are related to intrusion of Jurassic and (or) Cretaceous granitioid rocks. In contrast to the Mesozoic age for polymetallic vein deposits in the mining districts near Austin, polymetallic veins in the Battle Mountain, Kennedy, Lewis-Hilltop, and Bullion Mining Districts probably are mostly middle Tertiary (Roberts and Arnold, 1965; Gilluly and Gates, 1965; Johnson, 1977; Kotlyar and others, 1998b; Theodore, 2000).

Polymetallic occurrences have been important past producers of base and precious metals in the Bullion, Hilltop, and Lewis Mining Districts which are located in the Shoshone Range, approximately 35 km southeast of the town of Battle Mountain (fig. 7–22). However, the bulk of the Au in these districts has come from Carlin-type Au systems at Gold Acres and Pipeline and will be discussed below in chapter 8. The Bullion, Hilltop, and Lewis Mining Districts have a cumulative production from the 1870s to about 1950 of 180 metric tonnes Ag, 600 metric tonnes Cu, and 600 metric tonnes Pb from as many as 150 sites (Stager, 1977). Although most mineralized occurrences in the Hilltop district are associated with Pb and Zn, one prominent Au occurrence at the promontory known as Hilltop is on the margins of a 41.2–Ma cluster of diorite-granodiorite intrusions and is associated with Sb and As (Kelson and others, 2000). At Hilltop (fig. 7–22), mineral assemblages containing precious metals overprint base metal-mineralized rock (Kelson and others, 2000). The Au occurrence at Hilltop contains 10.35 million tons of mineralized rock grading 0.073 oz Au/t (Adams and others, 1991) and has been classified as a distal disseminated Au–Ag deposit by Theodore (2000; see also, chapter 8). All of these mineralized occurrences in the Shoshone Range provide a convincing anchor point for preferred clustering of mineralized systems along the northwest alignment of mineral occurrences (fig. 7–22) termed the Battle Mountain-Eureka mineral belt by Roberts (1966), and also referred to as the "Battle Mountain gold belt " by Madrid and Roberts (1991).

Polymetallic veins are the predominant types of mineral deposit in the Contact Mining District, which is near Ellen D Mountain near the northeast corner of the HRB approximately 80 km north of Wells, Nev. (fig. 7–22). Between 1908 and 1965, this mining district produced approximately 260 metric tonnes Cu, 35 kg Au, 16 metric tonnes Pb, 3,600 kg Ag, and 8,300 kg Zn from about 60 mineralized sites (LaPointe and others, 1991). Further, in 1972–1973 Coralta Mines drilled out 8 million t mineralized rock grading approximately 2.3 weight percent Cu (Banner deposit, table 1; see also, LaPointe and others, 1991). In June, 2000, Golden Phoenix Minerals, Inc., announced the results of an evaluation that found a measured and indicated resource of approximately 432,000 metric tonnes Cu that is contained in 61 million metric tonnes ore grading 0.77 wt percent Cu (Golden Phoenix Minerals, Inc., Reno, Nev., Press Release, June 20, 2000).

In addition, the base-metal vein part of the Cove distal disseminated Au–Ag deposit in the McCoy Mining District (fig. 7–22)—premining reserves included 1.0 million kg Au and 4.7 million kg Ag—is economically important and includes galena, sphalerite, and a Ag–sulphosalt-carbonate mineral stage (Johnson, 2000a; see also, Kuyper and others, 1991). The polymetallic mineral assemblage at Cove apparently has been superposed on an earlier Au–bearing Carlin-like mineral assemblage that includes Au–bearing arsenical pyrite and (or) marcasite as narrow rims on early-formed Fe sulfide minerals.

Manganese replacement deposits also are considered under this overall family of polymetallic mineral deposits, but they are not widely distributed in the HRB. All of these types of deposit are considered to be related to, but distant from, centers of porphyry Cu and other types of porphyry systems. Because fluids associated with the generation of polymetallic vein and replacement and replacement Mn occurrences can migrate far from their magmatic source, permissive areas for porphyry Cu tracts in the western part of the HRB previously were expanded somewhat by Peters and others (1996) to include some Cenozoic rocks and deeply eroded Tertiary rocks that may host polymetallic vein and replacement occurrences.

Finally, reference also should be made to the economically significant polymetallic replacement deposits in the Eureka Mining District, even though this district is far to the south of the HRB (fig. 7–22). Recorded production during 1866–1994 from the district includes approximately 0.3 million tonnes Pb., 7,000 metric tonnes Zn, 48 metric tonnes Au, and about 1,000 metric tonnes Ag (Vikre, 1998). However, these production figures are grossly understated because much of the early metal production from the district went unrecorded. The bulk of the metal production in the district is from structurally dismembered pods of oxidized carbonate replacement deposits that formed distal to a composite 107–Ma intrusion that includes well-developed skarn assemblages proximal to the intrusion (Vikre, 1998). Although the polymetallic replacement ores have not generated much production in the recent past, the important point to bear in mind is that exploration interest continues in the mining district to this date (2002) because of possible economic viability of relatively small tonnage, but high grade, underground targets that would not cause much surface disturbance. In addition, recent discoveries of large-tonnage Au deposits have added to overall production from the district (see chapter 8).

Platinum-Group-Element (PGE) Potential of the Humboldt Mafic Complex, Nevada

By Michael L. Zientek, Gary B. Sidder, and Robert A. Zierenberg

Introduction

The Humboldt mafic complex is a Jurassic suite of mafic plutons and volcanic rocks exposed in the Stillwater, West Humboldt, and Clan Alpine Ranges in west-central

Nevada (fig. 7–23). The complex was mapped and described by Page (1965) and Speed (1962, 1976), who considered that the complex was emplaced as a single lopolithic mass. This comagmatic suite of volcanic and intrusive rocks is now (2002) thought to have evolved from subduction-derived magmas in a volcanoplutonic setting (Dilek and Moores, 1995). These rocks show intense Na–rich alteration related to circulation of non-magmatic external brines driven by the heat generated during emplacement of the magmatic rocks (Johnson and Barton, 2000; Kistler and Speed, 2000). Iron deposits and prospects, as described above, are the predominant resource that is related to this event (Reeves and Kral, 1955; Moore, 1971; Johnson, 1977). The ore is present as massive magnetite, as bodies that replace mafic volcanic and gabbroic or dioritic rocks, as veins and dikes, and as cement in breccia bodies. Alteration related to young, epithermal deposits, such those at the Dixie Comstock Mine (Vikre, 1994), also affects the mafic complex.

Processes that Form PGE–Enriched Ore Deposits

Mafic intrusions have potential for the occurrence of deposits that may be enriched in Pt–group elements (PGE), Ni, and Cu. However, the type of deposit and likelihood of occurrence depend on the geologic environment in which the mafic rocks were formed. This section discusses the potential for PGE–enriched deposits in the Humboldt mafic complex. The processes that form magmatic ore deposits are described in the context of how this knowledge would be used to evaluate the PGE potential of these rocks. In addition, magmatic ore deposits that are present in mafic rocks similar to those that comprise the Humboldt mafic complex are reviewed briefly. Finally, the limited PGE information on the Humboldt mafic complex is summarized.

Mineral deposits enriched in PGE commonly are associated with mafic to ultramafic igneous rocks. Most commonly, these are magmatic ore deposits, which represent concentrations of crystals of metallic oxides, such as chromite, or immiscible sulfide or oxide liquids that formed during the cooling and crystallization of magma. In some instances, hydrothermally mineralized rocks that formed near mafic to ultramafic igneous rocks also can be enriched in PGE (McCallum and others, 1975; Hulbert and others, 1988; Rowell and Edgar, 1986).

Deposits that represent the crystallization products of an immiscible sulfide liquid are the most likely type of magmatic ore deposit to be found in rocks like those that make up the Humboldt mafic complex. If droplets of immiscible sulfide liquid form in mafic or ultramafic magmas, they will act as "collectors" for Cu, Ni, and PGE as a result of the high partition coefficient for these elements between sulfide and silicate liquids (Naldrett, 1989; Barnes and Maier, 1999). One strategy to evaluate the PGE potential of mafic rocks is to determine if any indication is present that processes that cause sulfide exsolution may have occurred.

Processes that change magma composition also may cause exsolution of an immiscible sulfide liquid from a mafic magma

(Haughton and others, 1974; Naldrett, 1989; Ripley, 1999). Magma composition can be changed by assimilating sulfur, assimilating country rocks, mixing magmas, or fractionational crystallization. Sulfur assimilation has been documented for deposits that are present near the margins of intrusions that are emplaced into country rocks that are enriched in S; for example, evaporites and sulfidic black shales. Sulfur isotope studies show that the S in these magmatic deposits was derived largely from the sedimentary rocks (Godlevsky and Grinenko, 1963; Ripley and others, 1999). Some deposits near the margins of intrusions do not show evidence for S assimilation. However, presence of inclusions of country rock in various stages of reaction, variable modes and textures, and changes in mineral and isotopic compositions may indicate that magma composition was changed by assimilation of country rock. Mixing of magmas takes place during emplacement and recharge of large magma chambers (which may form cyclic units found in cumulates) or during co-mingling of magmas in upper level magma chambers (mixed rocks, mutually intrusive relations, magmatic breccias). Exsolution also can be triggered by fractional crystallization of magmas; immiscible sulfide liquids are typically found in the Fe–rich differentiates that represent some of the last material to crystallize.

The immiscible sulfide liquids that form magmatic sulfide deposits are variably enriched in Ni, Cu, Co, and the PGE. PGE composition of ore should reflect the initial concentration of these metals in the silicate magma and the value of the partition coefficient of these metals between the silicate and sulfide liquids. However, composition variability of magmatic ores indicates that other factors influence metal contents of these deposits as well. In particular, the relative amount of available sulfide versus silicate liquid and the extent to which they interact is an important control on metal content (Naldrett, 1989). This relation is expressed in the following equation:

$$Y_i = D_i * C^\circ_i R + 1 R + D_i$$

where R is the mass ratio of silicate to sulfide liquid; C°_i is the initial concentration of metal i in the silicate magma; D_i is the Nernst partition coefficient; and Y_i is the concentration of any metal i in the sulfide melt. For equilibria between sulfide melts and silicate magmas, the Nernst partition coefficient is defined as:

$$D_i = \text{wt percent of metal i in sulfide melt} \text{wt percent of metal i in silicate melt}$$

Values of the Nernst partition coefficient have been calculated from experimentally determined exchange partition coefficients and estimated from studies of deposits. Values of D range between 315 to 1,070 for Ni, 913 to 1,383 for Cu, and thousands to hundreds of thousands for the PGE (Barnes and Maier, 1999).

In order to get a magmatic deposit enriched in PGE, large mass ratio of silicate to sulfide liquid must be achieved. This can be accomplished by mixing magmas, migrating interstitial melts and "fluids" upward through crystal mush, or streaming magma over sulfide minerals as in a flow, sill, or feeder dike. Field and laboratory studies can provide evidence for the presence of these processes.

Crystallization processes for immiscible liquids also can affect composition of deposits (Zientek and others, 1994; Barnes and Maier, 1999). These liquids as well can fractionally crystallize. In most natural sulfide melts, the first phase to crystallize is monosulfide solid solution (MSS). Constituents such as Cu, Pt, and Pd, which are less compatible in the MSS structure than in the melt, become enriched in the melt. Ores that consist of MSS cumulates have lower Pd and Pt contents than would be expected of ores that represent liquid compositions. The differentiates of this process are enriched in Cu, Pt, and Pd. Examples of such compositional variability are seen in Sudbury and Noril'sk-Talnakh ores (Naldrett, Asif, and others, 1994; Naldrett, Pessaran, and others, 1994; Zientek and others, 1994).

Magmatic ore deposits have two endmembers—those in which the amount of sulfide minerals is small relative to the overall size of the intrusion versus those in which the amount of sulfide minerals is large. Most deposits are of the first type; the size of the deposit is related roughly to the size of the intrusion. However, several world-class deposits are present in small intrusions. These latter deposits appear to have formed in conduits or feeder zones through which large volumes of magma passed. Exsolution of sulfide minerals occurred in the conduit, and sulfide liquids migrated into physical traps (Lightfoot and Naldrett, 1999; Naldrett and Lightfoot, 1999). The resulting sulfide deposits became enriched in metals as magma flowed over the sulfide liquids. The deposits at Noril'sk-Talnakh and Voisey's Bay may have been produced in a conduit or feeder zone. Even though this mechanism has formed large deposits, our understanding of the processes is limited; we only can speculate on specific processes that control the locations of these conduits and deposits that may form in them.

Geologic Settings and Mineral Deposit Types

Various types of magmatic sulfide deposits can be distinguished by the amount of sulfide minerals present; the relative enrichment of PGE, Cu, and Ni in the sulfide minerals; the tonnage of rock that is mineralized; associated rock types; and, finally, the geometry of the mineralized rocks relative to the mafic-ultramafic igneous rocks. Some types of magmatic ore deposits can be found in any ultramafic-to-mafic rock; others are restricted to rocks that form in particular geologic settings and age, or they were derived from magmas of a particular composition.

Classification schemes for magmatic ore deposits integrate rock associations and magma type, tectonic setting, principal mineral associations (for example, sulfide minerals versus oxide minerals), as well as setting and (or) geometry within an intrusion. Many schemes have been proposed for classifying mafic and ultramafic rocks and their associated ore deposits (Naldrett, 1981; Page and others, 1982; Naldrett, 1989; Capri and Naldrett, 1984; Hulbert and others, 1988). Table 7–4 summarizes information on ultramafic mafic rocks associations and various types of PGE–enriched magmatic processes of mineralization. The rock associations reflect the

different geologic settings within which mafic and ultramafic rock can be present. However, the geologic environment determines the size of the pluton, the emplacement style, the composition of magma, rates of magma discharge, and the likelihood of preservation. All these factors influence the kind, size, and grade of magmatic deposits that may be found. The different types of mineralized rocks reflect the underlying ore-forming processes that, in turn, determine the geometry of the mineralized rocks and their rock associations, as well as the tonnage and grade of the deposits.

Humboldt Mafic Complex—Geologic Setting and Expected Deposits

Rocks of the Humboldt mafic complex have been interpreted to be the upper part of an arc-marginal basin ophiolitic sequence (Dilek and others, 1988), part of a backarc complex (Gleason and others, 1994), or possibly part of a rift complex (John and others, 1993). However, the complex is now (2002) interpreted to be part of a continental volcanic arc (Dilek and Moores, 1995). This arc is considered to be the northern continuation of a Jurassic continental margin arc that extended from the Sonora Desert region in the south to northern California in the north (Dilek and Moores, 1995). Trace and rare-earth element geochemical data collected in this study complement the work by Dilek and Moores (1995) and Johnson and Barton (2000), and they support the interpretation that the Humboldt complex formed in an arc setting. Ternary, trace-element, and trace-element ratio discrimination diagrams such as Zr–Nb–Y, Cr–Y, and Cr–Ce/Sr plots, respectively, and chondrite-normalized spider plots classify rocks of the Humboldt complex as volcanic arc (fig. 7–24).

The work by Dilek and Moores (1995) and Johnson and Barton (2000) provide evidence that the gabbroic rocks of the Humboldt mafic complex are an example of a magmatic association, known world-wide, that includes synorogenic mafic complexes that formed in and near calc-alkaline batholiths in subduction-related magmatic arcs (Pitcher, 1982; Regan, 1985). In general, this association consists of small mafic-ultramafic plutons in calc-alkaline volcano-plutonic complexes that formed as a result of subduction-related magmatism at convergent plate margins. The intrusions display a close temporal and spatial association with calc-alkaline plutonic rocks. The setting may be analogous to the Early Cretaceous Andean continental margin, in which similar gabbro-diorite intrusions, coeval mafic volcanic rocks, and associated Fe and Cu–Fe deposits were formed prior to emplacement of the Coastal Batholith of Peru (Pitcher and others, 1985; Vidal and others, 1990).

Characteristics of Other Synorogenic Mafic Complexes

Synorogenic mafic plutons rarely exceed a few hundred square kilometers in areal extent. Equidimensional plutons are generally less than 10 km in diameter; elongate plutons

rarely exceed 5 km in width but may be more than 40 km long (Regan, 1985, Brew and Morrell, 1983; Espenshade, 1972; Thompson, 1984).

The mode of occurrence varies tremendously (Regan, 1985). Mafic plutonic rocks can be present as small sill-, dike-, or plug-like bodies or as large plutonic complexes. Depth of emplacement ranges from epizonal intrusions emplaced into generally coeval volcanic rocks to mesozonal plutons that are part of composite batholiths. The plutonic complexes also can take the form of flat-topped, steep-sided plutons; arcuate screens that lie between younger, commonly more silicic plutons; or steep-sided lenticular or tabular masses. Mafic plutons commonly appear to be clustered. The mafic intrusions can be massive or homogeneous, layered, compositionally zoned, or composite. Layered complexes in this setting may have over 10,000 m of layered cumulates (Thy, 1983).

Cumulates and rocks formed by nonaccumulative crystallization may be present in mafic plutons. Layered intrusions are not common, but plutons with modal layering, cryptic layering, and cyclic units have been described (Thy 1983; Boyd and Nixon, 1985; Wilson and Larsen, 1985). Other intrusions contain considerable tracts of unlayered cumulates. Rocks with porphyritic or diabasic texture and orbicular rocks are some examples of textures that may result from nonaccumulative solidification. Rock types include peridotite, pyroxenite, olivine gabbro, gabbro, gabbronorite, norite, diorites, and ferrodiorite, as well as quartz-bearing norite, ferrodiorite, and ferrosyenite.

Ore deposits in other synorogenic mafic complexes

Three types of magmatic deposits have been described from mafic-ultramafic rock associations in synorogenic settings. The most common deposit type consists of disseminated to massive sulfide minerals that are present near the intrusive margins of a mafic-ultramafic pluton. Rare examples of other styles of mineralized rock also have been reported. Stratiform PGE–enriched layers have been reported from the Lake Owen Complex in Wyoming. Disseminated, discordant PGE–enriched sulfide-mineralized rocks are being mined from the Lac des Iles Complex in Ontario. Further, hydrothermal PGE–mineralized rock is associated with the Mullen Creek Complex in Wyoming.

Marginal Sulfide Deposits

Marginal sulfide deposits typically form irregular zones of disseminated to massive Fe–Ni–Cu sulfide minerals that are present near the base or margins of intrusions (Page, 1986c; Eckstrand, 1984). Pipe-like discordant bodies and veins of Fe–Ni–Cu sulfide minerals, representing remobilized or late-stage magmatic sulfide minerals, also have been described. Tonnage and grade deposit models indicate a median tonnage of 2.1 million metric tons with median grades of 0.77 weight percent Ni and 0.47 weight percent Cu (Singer and others, 1986b). Low PGE tenors in magmatic sulfide minerals are

characteristic for many deposits of this type. For the deposits considered by Singer and others (1986b), only 10 percent of the deposits have Pt, Pd, and Au greater than 16 ppb, 63 ppb, and 35 ppb respectively. Low PGE concentrations also have been reported in sulfide deposits that are present near the margins of the St. Stephen, Portage Brook, and Goodwin Lake intrusions, New Brunswick (Paktunc, 1989; 1990), as well as those for Skjaekerdalen and Bruvann, Norway (Boyd and others, 1987; Boyd and others, 1988).

Some sulfide deposits associated with synorogenic intrusions have slightly elevated PGE concentrations. Disseminated sulfide concentrations in the Mechanic intrusion, New Brunswick have as much as 2.4 ppm PGE (Paktunc, 1990). Mineralized sulfide-rich rock—approximately 100 million tons of ore grading 0.5 weight percent Ni and 0.3 weight percent Cu—near the base of the LaPerouse layered gabbro in Alaska has average Pt+Pd+Rh concentrations of 0.18 ppm in ultramafic and gabbroic rocks and 1.2 to 1.5 ppm in massive sulfide and floatation concentrates (Czamanske and others, 1981).

Stratiform Disseminated Sulfide Minerals in Layered Cumulates

Stratiform layers of PGE–Au-bearing minerals are concentrated in thin intervals of disseminated sulfide minerals that are present in layered gabbroic cumulate rocks that comprise the Lake Owen Complex in Wyoming (Louckes, 1991). This intrusion is associated with a Proterozoic accreted arc terrane along the Cheyenne Belt (Houston and others, 1989). Four laterally persistent cumulus sulfide-enriched layers in this intrusion have Au+Pt+Pd concentrations in the range of several hundred to several thousand ppb. Mineralized intervals range from less than 1 m to 3 m thick and have been traced along strike for more than 9 km. Mineralized rocks contain disseminated sulfide minerals; however, maximum concentrations of Au and PGE are offset below one sulfide-enriched layer by 1 to 3 m. Generally, Au to Pt ratios are >1. Numerous PGE minerals have been identified, including platinum arsenide, Pt–Pd tellurides, PGE selenotellurides, and malanite (Pt_2CuS_4).

Discordant, PGE–Enriched Mineralized Rocks

The Lac des Iles mafic and ultramafic complex in northwestern Ontario, Canada, contains bulk-mineable PGE–enriched mineralized rocks that are present in three specific associations (Macdonald, 1988 ,1989): (1) low-grade sulfide mineralized rocks (<1 ppm Pt+Pd+Au) associated with locally pegmatoidal gabbro, anorthositic phases and complex heterolithic breccias; (2) high-grade sulfide-mineralized rocks (as much as 15 ppm Pt+Pd+Au) associated in an intrusive, PGE–rich pyroxenitic dike; and (3) highest grade sulfide mineralized rocks (locally as much as 37 ppm Pt+Pd+Au) that are associated with crosscutting, pematoidal gabbroic dikes. Proven and probable reserves (Jan. 1, 2000) in the Lac des Iles complex are estimated to be 71.9 million metric tons containing 1.76 ppm Pd, 0.19 ppm Pt, 0.14 ppm Au, 0.065 weight percent Cu, and 0.055 weight percent Ni

(http://www.napalladium.com/mineopset.html; March 16, 2001). The complex is a composite synorogenic intrusion. The PGE–mineralized rocks are associated with a melano-gabbro that invades and brecciates pyroxenite, gabbronorite and gabbro; pegmatoidal gabbro is abundant. The ore typically contains from zero to 5 volume percent pyrrhotite, chalcopyrite, pyrite, and pentlandite.

Hydrothermal PGE–Enriched Mineralized Rocks Associated With Mafic Rocks

The Mullen Creek Complex, Wyoming, is one example of a hydrothermal PGE–enriched environment associated with mafic rocks. The Mullen Creek Complex comprises a deformed, synorogenic gabbroic complex that is truncated by the Mullen Creek-Nash Fork shear zone (McCallum and Orback, 1968; McCallum and others, 1975). Along the north flank of the complex, quartz-pyrite-chalcopyrite veins with minor sperrylite were developed at the New Rambler Mine. The veins are present in hydrothermally altered metapyroxenite and metagabbro in shear-zone tectonites and mylonitic gneiss. Coarsely crystalline, sheared, epidotized granite, metadiorite and metaperidotite also are present. Near the surface, the veins are oxidized and supergene-enriched. A porous spongy limonite and jaspilite gossan overlies a 25–m-thick oxidized zone that is characterized by presence of malachite and azurite with lesser cuprite, tenorite, chalcotrichite, and chalcopyrite. The underlying supergene-enriched zone contains Pt–bearing covellite and chalcocite. After the mine closed in 1918, probable reserves were estimated to be 7,000 tons of 7 to 8 weight percent Cu, 0.25 oz Pt/t, with some Au and Ag (Needham, 1942). The last ore shipped from the mine showed concentrations ranging from 3.24 to 61.37 weight percent Cu, 0.0007 to 1.4 oz Au/t, 1.01 to 7.5 oz Ag/t, 0.047 to 3.2 oz Pt/t, and 0.33 to 12.3 oz Pd/t (U S Bureau of Mines, 1942). Total metal production was reported to be 1,753,924 lbs Cu; 171.35 oz Au; 7,346 oz Ag; 170.16 oz Pt; and 451.4 oz Pd (Needham, 1942). McCallum and others (1975) report that ore samples average 75 ppm Pd and 4 ppm Pt.

Deposits and Prospects of the Humboldt Mafic Complex

Fieldwork was conducted in 1986 to assess the PGE potential of the Humboldt mafic complex. Our field work focussed on previously mapped areas of layered mafic rocks, contacts of the mafic complex with sulfur-rich wall rocks, and identified mines and prospects. Many samples analyzed for PGE concentration came from known mineralized areas, which are described below. Polished thin sections of mineralized rocks were examined in reflected and transmitted light to determine ore and alteration mineralogy. Selected samples were analyzed for sulfur isotopes (table 7–5) to evaluate sources of sulfur and the potential for assimilation of crustal sulfur and sulfide saturation during emplacement of mafic magmas.

PGE Analyses

We analyzed 267 samples for PGE and associated trace and major elements (fig. 7–23). PGE were analyzed using NiS fire assay. Detection limits were typically around 1 ppb, and results are available in Baedecker and others (1998; job numbers LS33, LY62 through LY64, LY67, and MA83 through 86). Our strategy was to analyze: (1) a variety of igneous rock types that contain visible sulfide minerals and (or) are variably altered, (2) plutonic rocks that crop out near the intrusive contact with S–bearing sedimentary rocks, and (3) hydrothermally-mineralized rocks that cut the complex. The hydrothermally altered rocks in the Humboldt mafic complex comprise an unconventional PGE target and could provide a further guide to primary magmatic-mineralized rocks in the complex.

Sixty-six samples of hydrothermally altered and mineralized rocks were sampled and analyzed for PGE from the Humboldt mafic complex. The mineral deposits included: Cu–mineralized rocks in mafic volcanic rocks (Wilden and Speed, 1974); Ni–Co–Ag–As-mineralized rocks (Ferguson, 1939); Fe deposits associated with the pervasive sodic alteration (Reeves and Kral, 1955; Moore, 1971; Johnson, 1977); a semi-massive pyrite–pyrrhotite-magnetite deposit near the margin of the complex (Tule deposits; Moore, 1971); epithermal Sb deposits (Green Mine and Muttleberry Mine; Johnson, 1977); and epithermal Au–(Ag, Hg) deposits (Dixie Comstock deposit, Vikre, 1994). Description of the most important mineralized areas follows below. The deposits are grouped according to the dominant sulfur source in table 7-6, which summarizes the dominant ore and alteration mineralogy of each deposit type.

Copper Mineralization in Mafic Volcanic Rocks

Numerous shows and prospects of Cu are present in the mafic volcanic rocks that overlie the intrusive rocks of the Humboldt complex. These prospects primarily reflect concentrations of chalcopyrite and other Cu sulfide minerals in narrow fractures and amygdule fillings in the Jurassic mafic volcanic rocks (Willden and Speed, 1974). Prospects such as Boyer Copper and Bradshaw Copper in the Table Mountain Mining District in the Stillwater Range are typical of such Cu occurrences. These types of mineralized rocks were sampled at the Bradshaw Copper prospect and in Cottonwood Canyon near the Lovelock and Nickel Mines.

Cottonwood Canyon

One of the two samples collected in the Cottonwood Canyon area is the PGE anomalous sample listed in table 7–7. The second sample did not have anomalous PGE contents, but it contained elevated As and Co, similar to the PGE–enriched sample. The second sample also had an elevated Ni concentration.

Bradshaw Copper

The Bradshaw Copper prospect hosts disseminated and fracture-controlled chalcopyrite and pyrite in intensely altered porphyritic volcanic rocks, breccias, and finely to

coarsely crystalline diorite and gabbro. The host rocks are strongly fractured and faulted. Pink albite veins and (or) dikes and veins and veinlets of hematite cut the rocks. Albite and hematite replace the matrix and rock fragments in the breccias and phenocrysts and groundmass in the volcanic rocks. Thin, irregular quartz seams also contain pyrite and chalcopyrite (Willden and Speed, 1974). Hematitization, silicification, albitization, and chloritization are the dominant types of alteration; carbonate alteration also is present, but is less pervasive, and colorless, non-pleochroic tourmaline (dravite) is a minor alteration product.

Pyrite in altered volcanic rocks from the Bradshaw Copper prospect has S isotopic compositions that are in the range mostly from 2.5 to 4.3‰—one sample has a high value of 7.3‰ (table 7–6). The light S isotope values, the alteration assemblage, and location near a fault suggest that these mineralized rocks formed from an igneous-dominated hydrothermal system with neutral to acidic hydrothermal fluids. Mineralization at this prospect may be related to Tertiary volcanic activity, perhaps the widespread Miocene volcanic event in the region (Dilek and Moores, 1995), although it is just as likely that mineralization is associated with the Jurassic Humboldt mafic complex (see below).

The geochemistry of mineralized rocks at the Bradshaw Copper prospect differs from that in the samples from Cottonwood Canyon. Although Cu concentrations are similar, only one sample had PGE reported at the detection limit; all other samples have PGE concentrations below their respective detection limits. Whereas the Cottonwood Canyon samples are enriched in As and Co, the samples from the Bradshaw Copper prospect have elevated concentrations of B and Hg. Some samples also have detectable Ag and Au.

Hydrothermal Ni-Co Mineralized Rocks in Cottonwood Canyon

Minor amounts of Ni and Co were produced from the Lovelock and Nickel Mines in Cottonwood Canyon in the late nineteenth Century (Ferguson, 1939; Willden and Speed, 1974; Lechler and Desilets, 1987). Nickel- and Co–bearing sulfide, arsenide, and sulfarsenide minerals are disseminated and in veinlets in brecciated and altered quartzite along a fault that juxtaposes gabbro of the Humboldt complex with quartzite of the Middle Jurassic Boyer Ranch Formation. The quartzite in the Cottonwood Canyon area also contains pyrite, which was deposited in at least two stages. Earliest pyrite is extensively crushed and has been completely replaced by Fe–oxide minerals. Later pyrite shows minor brittle fracturing, but is generally unoxidized. Near the Nickel and Lovelock Mines, veins of green Ni–bearing minerals cut carbonate breccia that consists dominantly of coarse-grained ankeritic carbonate minerals with less abundant late pore-filling calcite. Euhedral quartz and brownish microcrystalline quartz and chalcedony are present in the carbonate matrix. Chalcopyrite is disseminated in

the carbonate breccia, and it is partly replaced by minor amounts of covellite and as well overgrown by Fe–oxide minerals. Traces of marcasite are the only other sulfide mineral in the carbonate breccia. The sulfur isotope ratios of the Ni–bearing mineral veins, pyrite in gabbro and quartzite, and chalcopyrite in the carbonate are all enriched in ^{34}S relative to Bradshaw Copper, and all fall within the narrow range of 9.3‰ to 11.0‰.

A grab sample collected near the Nickel Mine contains 4.6 and 3.0 weight percent Ni and Co, respectively (table 7–7). PGE concentrations are below detection limit or low. This style of mineralization may be similar to the hydrothermal deposits at Bou Azzer, Morocco. Average PGE concentrations in Co–arsenide, Ni–arsenide, and Fe–arsenide ores from Bou Azzer are 582 ppb, 225 ppb, and 134 ppb respectively (LeBlanc and Fisher, 1990).

Iron Oxide Mineralization

The Tule Iron prospect is present near the contact between the Humboldt mafic complex and underlying sedimentary rocks (Moore, 1971). The sedimentary rocks consist of shale and minor limestone; these rocks are altered and contact metamorphosed. Magnetite- and pyrite- mineralized rocks are present in the limestone and hornfels. The prospect is deeply weathered at the surface and is characterized by prominent, brilliantly colored gossans. Core drilling below the gossans encountered concentrations of magnetite and pyrite in hornfels and pyrite in the limestone (Moore, 1971).

In an area northeast of the Tule Iron prospect, reclaimed trenches exposed pods of massive sulfide minerals that are present as segregations in altered igneous rock. The concentrations of massive-sulfide minerals appear to be developed in coarse-grained gabbro, which is present as highly fractured and replaced fragments in the concentrations of sulfide minerals, predominantly pyrrhotite. Chalcopyrite is abundant in some samples as grains interstitial to pyrrhotite, or as late veinlets that cut pyrrhotite. Some coarse-grained pyrite is intergrown with pyrrhotite. Fine-grained "birds-eye" replacement of pyrrhotite by interbanded pyrite-marcasite is present in some samples. Euhedral sphene crystals, some intergrown with crystalline rutile, are present as inclusions in the sulfide minerals. The gangue to the massive sulfide minerals is dominantly albite, tremolite, and sphene that contain some coarse-grained scapolite locally.

None of the samples collected from this area contained anomalous PGE concentrations (table 7–8). Even though the PGE concentrations are low, we nonetheless considered the possibility that the concentrations of massive sulfide minerals in the igneous rocks are magmatic. Although poorly exposed, field relations suggest this prospect is present along an intrusive contact with sedimentary rocks. A mineral assemblage dominated by pyrrhotite is what would be expected in a magmatic sulfide deposit.

Sulfur isotope values of the sulfide minerals range from 11.4 to 17.7‰, overlapping the range of Lower to Middle

Jurassic seawater sulfate (Strauss, 1999). The heavy S isotopic composition in the massive sulfide minerals could reflect assimilation of Lower to Middle Jurassic evaporates of the Lovelock Formation (Speed, 1974), which are intruded by the Humboldt Complex. This raises the possibility that the gabbroic intrusion reached sulfur saturation due to the assimilation of crustal S. However, the composition of the mineralization is not consistent with a magmatic origin (table 7–5). The samples have slightly elevated Cu contents; however Ni contents are low. If the sulfide minerals originated as an immiscible sulfide liquid, Ni, as well as Cu, would have partitioned into the melt. Cu/Ni ratios for magmatic ores formed from basaltic magmas should be approximately 3 to 1; the low Ni contents and high Cu/Ni ratios suggest that the massive sulfide minerals did not form from an immiscible sulfide liquid.

Epithermal Gold and Antimony Mineralization

Quartz-rich alteration and cation leaching are well developed in cross-cutting ore assemblages such as the Dixie Comstock low sulfidation Ag–Au deposit and the Green Mine Pb–Sb–Ag deposit.

Dixie Comstock Mine

Gabbroic rocks of the Humboldt complex are crushed along the range-bounding Dixie Comstock Mine fault that separates the Stillwater Range from Dixie Valley at the Dixie Comstock Mine. Drilling has defined a potentially bulk-mineable resource of about 1.7 million metric tonnes of ore that grades 0.058 oz Au/t in a mullion within the fault (Vikre, 1994). Vikre (1994) proposed a mid-Pleistocene age for the mineralization and demonstrated that the ore is structurally controlled by the range-bounding normal fault that cuts the gabbro.

The gabbroic rocks in the Dixie Comstock Mine area are typically coarse grained with abundant titanomagnetite. Titanomagnetite generally shows moderate amounts of early oxidative exsolution of ilmenite, later partial replacement of ilmenite lamellae by TiO_2 and Fe–oxide minerals, and variable degrees of oxidation and replacement of magnetite by hematite. Most samples are relatively unaltered with generally fresh feldspar dusted with clay; moderate amounts of chlorite, amphibole, epidote, sphene, and calcite partially replace the mafic minerals. Quartz generally is not present as a secondary mineral except in samples of jasperoid that represent extensively silicified gabbro that is altered to quartz plus kaolinite with only traces of epidote and without carbonate minerals. Disseminated euhedral pyrite and pyrite plus hematite in carbonate veins are the dominant metallic minerals, and most pyrite is heavily oxidized and replaced by Fe–oxide minerals.

Gold in grab samples collected from the fault zone in this study ranges in concentration from about 50 ppb to 20 ppm, and Ag ranges from about 1.5 to 7 ppm. Twenty-six rock samples were analyzed for PGE from this area. For most samples, PGE concentrations were at or below detection limit. The highest value was 2.9 ppb Pt.

A sample of jasperoid from the Dixie Comstock area has a $\delta^{34}S$ value of 5.1‰, typical of a hydrothermal system dominated by an igneous-related source. The rock is a highly silicified gabbro with sericitic alteration indicative of low pH alteration and cation leaching. Pyrite sampled from drill core from the Dixie Comstock Mine ranges from -7.5‰ to 3.9‰ (Vikre, 1994), which is distinctly lighter than disseminated pyrite in the altered gabbro wall rocks.

Green Mine

Rocks in the vicinity of the Green Mine (fig. 7–23) are altered plagioclase-rich diabasic or gabbroic rocks, although Triassic limestone and shale hosts the predominantly Pb–Ag–Sb ore at the mine (Lawrence, 1963). The extensively altered gabbros contain albite, carbonate minerals, muscovite, quartz, apatite, and tourmaline. Quartz veins in these rocks contain abundant tourmaline. Pyrite is the dominant sulfide mineral, but some samples contain minor amounts of a sulfosalt mineral tentatively identified as boulangerite. Relative to other analyzed rocks, the quartz vein samples are enriched in B, Ag, Au, As, Pb, Sb, and Tl. Twenty rock samples were analyzed for PGE from this area. For most samples, PGE concentrations were at or below detection limit. The highest value was 6.7 ppb Pd.

Sulfur isotopes from samples of the quartz veins range from 9.4‰ to 10.1‰; the associated altered diabase samples gave values of 5.5‰ and 7.8‰. The ore and alteration assemblages are characteristic of volcanic-related epithermal systems, but the intermediate sulfur isotope ratios may indicate a mixed igneous and sedimentary source of S.

Discussion of PGE Potential of the Humboldt Mafic Complex

Assessment of the PGE potential of the Humboldt mafic complex sought to address several questions. First, are the rocks that make up the complex or hydrothermal deposits that formed within or near the complex enriched in PGE? Second, is the type and style of igneous layering like that associated with reef-type or stratabound mineralization in other mafic intrusions? Third, is evidence present for processes that could result in the exsolution of an immiscible sulfide liquid? Specifically, is there evidence for assimilation of crustal S, extensive interaction with country rocks, or co-mingling of magmas?

The PGE content in unaltered and altered rocks of the Humboldt complex is low. About 50 samples of relatively unaltered plutonic rocks were analyzed. Only 11 samples have detectable PGE; the maximum value was about 30 ppb. Copper concentrations are low—generally less than 50 ppm. As expected, samples of picrite have higher concentrations of Cr and Ni than gabbroic samples. About 60 samples of altered igneous rocks also were analyzed; only nine samples have PGE contents above detection limits; total Pt+Pd is less than 24 ppb.

High PGE concentrations would not be expected in unmineralized gabbroic rocks from synorogenic plutons. These results for the Humboldt mafic complex are similar to those for other synorogenic gabbroic intrusions. For example, approximately 90 percent of the PGE analyses for 90 samples of synorogenic gabbroic rocks from the Southern Peninsula batholith were below detection limit (Baedecker and others, 1998; jobs LZ81, LZ82, and UD54). The highest concentrations of Pd and Pt of these gabbroic rocks from the Southern Peninsula batholith were 7.5 ppb and 5 ppb respectively.

Only 27 samples of the 66 hydrothermally altered and mineralized rock samples had PGE above detection limit; 10 samples were above 5 ppb. Two samples were anomalously enriched in PGE (table 7–7). The sample from Cottonwood Creek is a mafic volcanic rock with abundant secondary Cu minerals. The other PGE–enriched sample is from the Buena Vista Hills and is a scapolitite with no conspicuous sulfide or oxide mineral concentrations. No other samples of Fe ores or rocks showing sodic alteration had elevated PGE contents. Anomalous concentrations of PGE were surprising because elevated PGE concentrations have not been previously reported in either style of mineralization.

Although this work significantly extends the available data on PGE abundance in the Humboldt Complex, we do not contend that PGE enrichment in Cu–mineralized rocks associated with the mafic volcanic rocks has been adequately tested. Mineralized rocks in the Bradshaw Copper prospect do not appear to be enriched in PGE, perhaps because they are related to a subsequent alteration event. Only one sample, from Cottonwood Creek, is enriched in PGE. More samples should be collected from Cottonwood Creek to validate the anomalous sample. In addition, PGE concentrations should be determined for Cu–mineralized rocks at the Boyer Copper and Copper Kettle deposits (Wilden and Speed, 1974).

Layering Characteristics and Potential for Stratiform-Mineralized Rocks

Speed (1963, 1976) described the gabbroic rocks that make up the complex as cumulates. He also described layering, ranging from 1 cm to 100 m thick. Igneous layering can form by a variety of mechanisms (Irvine, 1987); some of these processes also can lead to formation of magmatic ore deposits. Specifically, igneous layering that forms cyclic or rhythmic units is commonly associated with stratiform chromitite or reef-type PGE deposits. We examined areas indicated on the map published by Speed (1976) as containing layered mafic rocks to determine if the layering characteristics of various map units are comprised of cumulates similar to those associated with stratiform or reef-type mineralization.

Our observations suggest the dominant style of layering in mafic rocks in the Humboldt complex is modal layering or foliation (layering characterized by parallel alignment of nonequant mineral grains). We did not observe cyclic units or meter-scale layering features that could be traced for signifi-

cant distances. The mapping published by Speed (1976) also indicates that the gabbroic cumulates are present in composite intrusions. If stratiform concentration of sulfide minerals is present in the gabbroic cumulates, the layers will have limited continuity relative to stratiform complexes like the Bushveld Complex or the Stillwater Complex.

Source of Sulfur in Mineralized Rocks

The intrusive contact between the Humboldt mafic complex and older sedimentary rocks was examined in two places in the West Humboldt Range (near the Tule Iron prospects and near exposures of microgabbro south of Muttlebury Canyon) to assess the possibility that assimilation of sediments may have lead to saturation with an immiscible sulfide liquid. The igneous intrusive rocks were finer grained near the contacts than in the interior of the complex, and a xenolith of sedimentary rock was noted near the Tule Iron prospects. However, we did not observe vari-textured gabbros or other evidence for extensive interaction with wall rocks.

Assimilation of S from country rocks also could cause exsolution of sulfide liquids in the Humboldt mafic complex. The complex intruded Early to Middle Jurassic marine sedimentary rocks that contain gypsum (Speed, 1974). To determine if the mafic complex interacted with these S–rich sediments, the isotopic composition of S was determined for samples of the marine evaporites and sulfide-bearing rocks associated with the Humboldt mafic complex. The data are presented in table 7–5 and the results are summarized in table 7–6.

Seawater sulfate $\delta^{34}S$ values increased from approximately 12‰ to 17‰ from Early to Middle Jurassic (Strauss, 1999). Sulfates in marine evaporites deposited in that time interval have a broader range (~10-22‰; Claypool and others, 1980; Strauss, 1997) due to processes, such as mineral precipitation and bacterial sulfate reduction, that result in isotopic fractionation of dissolved sulfate in evaporite basins (Raab and Spiro, 1991). Gypsum from the Early to Middle Jurassic Muttlebury Formation analyzed in this study ranges from 11.4‰ to 22.3‰, which overlaps the values for Jurassic marine evaporites.

Elevated S isotope values from several of the mineralized areas in the Humboldt Complex are a clear indication of incorporation of Jurassic seawater sulfate, or sulfate derived from evaporitic facies of the Lovelock or Muttlebury Formations. However, ore mineralogy, alteration assemblages, and Cu/Ni all indicate a hydrothermal origin for the heavy S. Samples with isotopic compositions that suggest derivation of S from the Jurassic sedimentary rocks (table 7–6) are affected by the pervasive Na and Na+Ca metasomatic alteration (Battles and Barton, 1989; Johnson and Barton, 2000). The early pervasive Na and Na–Ca alteration is consistent with water-rock interaction at low water-to-rock ratios that forms mineral assemblages typical of low greenschist metamorphism (albitization and epidote-amphibole alteration of gabbroic and mafic volcanic rocks). The regional abundance of marialitic scapolite

in the Humboldt complex provides mineralogic and geochemical evidence of extensive circulation of high temperature, high salinity fluids (Vanko and Bishop, 1982).

This alteration appears to be related to large-scale hydrothermal circulation of fluids in response to intrusion of the Humboldt complex. The heavy S isotope signature of pyrite associated with this alteration event suggests that hydrothermal circulation driven by intrusion of the Humboldt complex leached evaporitic S from the Muttlebury and Lovelock Formations. This S was totally reduced—approximately a closed system—during interaction with gabbroic rocks of the Humboldt complex, which resulted in $\delta^{34}S$ values for sulfide minerals that approximate the S isotope value for Jurassic seawater sulfate.

Altered gabbro from near the Tule Iron prospects and from the Bradshaw Copper Mine area have alteration assemblages and heavy S isotope values that suggest they are part of this widespread alteration event. The elevated $\delta^{34}S$ of the sulfide minerals and the Na–rich, hydrous alteration assemblage in rocks from these areas are consistent with hydrothermal circulation of fluids that interacted with evaporites of the Lovelock Formation.

Other samples of hydrothermally altered rock that were analyzed have isotopic compositions that reflect a magmatic or volcanic source of S or a mixed magmatic and sedimentary source. The light S isotope values in mineralized rocks from the Bradshaw Copper Mine are consistent with an igneous-dominated hydrothermal system with neutral to acidic hydrothermal fluids. A sample of jasperoid from the Dixie Comstock area has a $\delta^{34}S$ value of 5.1‰, typical of a hydrothermal system dominated by an igneous-related source (table 7–6). The isotopic composition of mineralized rocks in Cottonwood Canyon suggests a hydrothermal circulation system that derived S from either late Tertiary and (or) Pleistocene heat sources ($\delta^{34}S$ ~ 2–5‰, as exemplified by the Dixie Comstock, see above) and the regionally altered Jurassic rocks ($\delta^{34}S$ ~ 16‰).

Summary

Exposures of mafic intrusive rocks of the Humboldt mafic complex are extensive enough to be associated with a large PGE ore deposit. Has the potential for magmatic mineralization in the complex been adequately evaluated? For an unequivocal answer, we would need information from outcrop-scale mapping, stream-sediment and soil sampling, and geophysical surveys.

An alternate approach is to use analogous occurrences to build models that describe the geologic characteristics of the deposit as well as the distribution of grade and tonnage. Further, well-explored terranes can give us an idea about the expected density of deposits. This approach also works well for certain types of deposit that are present in mafic and ultramafic rocks; enough examples are available in the literature to construct descriptive, grade, and tonnage models for a number of deposits. These deposits include komatiitic

Ni deposits found in komatiites (Page, 1986b; Singer and others, 1986c); Ni–Cu deposits found in synorogenic intrusions (Page, 1986c; Singer and others, 1986b); and podiform chromitites in ophiolites (Albers, 1986; Singer and Page, 1986; Singer and others, 1986a).

However, some important types of world-class magmatic deposits are quite uncommon. Thus, quantitative grade-tonnage models cannot be constructed because too few deposits comprise the models. Descriptive models that could guide exploration efforts also are difficult to construct; not enough examples are available with shared characteristics to build a model that does not include a large amount of uncertainty in its application to unexplored terranes. For example, enough examples of reef-type PGE deposits and occurrences are known to describe generally their setting in a layered intrusion. All the known deposits are in stratiform-layered intrusions that are associated with intraplate magmatism. We do not know if reef-type deposits are restricted to rocks formed in that setting, or if they also could form in layered mafic rocks formed in other tectonic settings. The PGE–enriched sulfide deposit being mined at Lac des Iles, an Archean synorogenic intrusion, is the only example of this type of deposit. Although it has been described adequately, a comprehensive model that would predict where other similar deposits could be expected would have a large degree of uncertainty.

We can apply our knowledge about deposit models to the Humboldt mafic complex, but we also should expect the unexpected. Our current understanding of PGE–enriched magmatic ore deposits reasonably suggests that high-grade PGE deposits would not be expected in these rocks. However, a level of uncertainty still remains. Someone willing to accept high risk could explore for unconventional deposit types, such as hydrothermal PGE, or some new or variant styles of mineralized magmatic rocks in the Humboldt mafic complex.

The geologic setting inferred for the Humboldt mafic complex limits what may be expected for PGE–mineralized rocks. World-class reef-type deposits have not been found in synorogenic complexes. Stratiform or reef-type sulfide-enriched layers, exemplified by the Merensky Reef and J–M Reef, are associated with large, cyclically-layered mafic-ultramafic intrusions that formed in large igneous provinces (Mahoney and Coffin, 1997). Cyclically-layered rocks do not appear to have formed in the Humboldt mafic complex— emplacement of multiple plutons in the complex also limits lateral continuity of any layering features that may be present. Limited lateral continuity would affect the tonnage of a deposit, if a stratiform deposit were present.

Massive sulfide deposits that are present in dikes or sills that provide feeders to large mafic-ultramafic igneous systems, however, are an important, but uncommon, deposit type. Examples of these deposits include those at Noril'sk-Talnakh and Voisey's Bay. Nonetheless, the probability for occurrence of one of these deposits near the Humboldt mafic complex is not high simply because they are so rare. In addition, feeder zones in which magma flow may have been focussed have not been identified for the Humboldt mafic complex.

Disseminated to massive sulfide minerals that might be present near the intrusive contact with older, S–bearing sedimentary rocks is the most likely deposit type to be found in the Humboldt mafic complex. Rocks near the contact are exposed in the West Humboldt Range; S isotopic data indicate that S–bearing rocks were near the complex at the time it was emplaced. No magmatic mineralized rocks or varitextured rocks typically associated with this type of mineralization have been found. Deposits in other synorogenic intrusions are characterized by low PGE concentrations, indicating inefficient mixing of sulfide liquid and magma. Geophysical surveys that identify conductive rocks would be the most effective way to search for these deposits. Nickel depletion in olivine may provide indirect evidence for the existence of a deposit (Thompson and Naldrett, 1984).

The Humboldt mafic complex has not been evaluated, however, for the type of mineralized rocks that are present at Lac des Iles. We would need to look for places where magmas intermingled at time of emplacement forming magmatic breccias and mafic pegmatoids and causing a sulfide-liquid exsolution event. Relatively large-scale mapping could identify such geologic relations—PGE anomalies could be detected by sampling stream sediments or soils. Nonetheless, no pegmatoids or igneous breccias similar to those at Lac des Iles have been described.

The effect of subsequent alteration on the distribution of PGE has not been tested fully. Two samples of hydrothermally altered rocks with elevated PGE were found in this study. The elevated PGE associated with mineralized mafic volcanic rocks in the Cottonwood Canyon area suggests that more work should be done at this locality, as well as at the prospects near the Boyer Copper and Copper Kettle prospects. However, the elevated PGE concentration found in the scapolitite is problematic. No other rocks sampled during our study that show this type of alteration were anomalous. Further, the worldwide literature on PGE does not report PGE concentrations in similar rocks from similar geologic settings. A split of the scapolitite sample should be re-analyzed to determine whether the reported PGE concentrations can be duplicated. If so, then additional work should be done in the field near the anomalous sample to find material similarly enriched in PGE.

Results of Assessment

Combined Knowledge-Driven and Data-Driven Model

The mineral-resource assessment map for pluton-related deposits was created using a combination of knowledge- and data-driven modeling techniques (chapter 2). Expert knowledge was used to identify permissive and non-permissive areas as well as to assemble and build the various databases used in the assessment. The permissive versus nonpermissive tracts used are those defined by Cox and others (1996) (fig. 7–5).

Expert knowledge also was used to select evidence maps for a preliminary data-driven weights-of-evidence (WofE) analysis that was reviewed by the entire team writing the present report—this review resulted in a number of problems, as discussed above, if WofE were to constitute the end product of the assessment effort. Nonetheless, WofE analysis was used to analyze spatial associations among the training sites and evidence maps and to optimize the evidence maps for prediction. Subsequently, Mihalasky and Gary L. Raines (USGS, Reno, Nev.) independently conducted WLR modeling whereby the optimized evidence maps were combined to delineate prospective and favorable areas within the overall permissive area. The evidence map criteria used for prediction were determined by data-driven means (chapter 2).

From pluton-related sites of mineralized rock in the Mineral Resource Data System (MRDS; McFaul and others, 2000) of the USGS, as well as a number of recently discovered occurrences tabulated for the present report, 92 representative deposits and occurrences from northern Nevada were assembled to construct a "training set" for the data-driven mineral-resource assessment of pluton-related mineral deposits in the HRB (chapter 2). The deposits compiled in this assessment are listed in table 7–1 and their locations shown on figure 7–8. However, as discussed below, only 58 of the 92 training sites fall within the area actually assessed, because of the areal limitations of the National Uranium Resource Evaluation (NURE) geochemistry. Tabulations in table 7–1 are more up-to-date than material archived in MRDS during the final stages of the assessment in late 2001, and this tabulation represents those economically important mineralized sites that we judge to demonstrate relevance to the pluton-related environment in the HRB. Classification of pluton-related deposits is complex, and includes some subjective interpretation(s). In this report, a data-driven favorability map was prepared on the basis that the applicable training set reflects all types of pluton-related deposits regardless of numerous classifications of the various types of deposits that belong to the entire pluton-related group. The result of this approach is a highly generalized representation of actual areas of favorability for undiscovered pluton-related deposits and occurrences. At a scale larger than this present assessment, favorability maps specific for individual deposit types could be prepared by taking into account specific differences among the deposits—for example, the spatial association of mineralized skarn deposits with their enclosing carbonate host rocks. Buffers around all skarn occurrences in the HRB are shown in figure 7–25.

The prospective and favorable tracts were modeled using eight evidence maps (figs. 7–26 to 7–32; table 7–9), a unit cell size of 1 km^2, and a significance level of 1.282 (90 percent confidence, tabled Student–t value). The eight evidence maps used in the assessment are: (1) skarn proximity spatial buffers around intrusive igneous rocks shown on the geologic map of Nevada; (2) combined regional distributions of Cu, Pb, and Zn in sediment data; (3) regional sediment data of As concentrations; (4) pluton proximity; (5) buffers

around intrusive igneous rocks shown on the geologic map of Nevada; (6) lithodiversity of the geologic map of Nevada; (7) buffers around interpreted basement gravity lineaments; and (8) regional gravity terrane map. Proximity to mineralized skarns and presence of plutonic rocks are the two strongest predictors, followed by geochemical then geophysical evidence. The skarn proximity and geochemical evidence maps serve to include areas likely to host pluton-related ore deposits, and are characterized by narrowly defined predictor patterns with W^+ magnitudes (see chapter 2) that are significantly larger than W^- where the pattern is present. Conversely, the pluton proximity and geophysical evidence maps serve to exclude areas unlikely to host pluton-related ore deposits, and are characterized by broadly-defined predictor patterns with W^- magnitudes that are significantly larger than W^+ where the predictor pattern is absent. The lithodiversity predictor pattern provides nearly equal amounts of inclusive and exclusive evidence, as indicated by approximately equal W^+ and W^- magnitudes.

The pluton-proximity-predictor pattern provides exclusive evidence, which seems counterintuitive, given the wide range of deposit types included in the pluton-related category. However, insufficient data are available to classify the plutons individually according to some scheme that might relate them to pluton-related deposit ore-forming processes, and as such, all plutons within the study area were chosen as positive evidence for an association with a pluton-related ore-forming process. However, if such ore-discriminating data were available, the number of plutons used as positive evidence could be reduced significantly, resulting in a more inclusive predictor pattern. For example, an informal inspection carried out within the greater HRB area reveals that only about 5 percent of the approximately 300 individual plutonic units identified on the geologic map (Stewart and Carlson, 1978) have a training site nearby, which is defined arbitrarily as within 10 km for the purpose of this cursory examination.

The seven evidence layers will now be discussed in order of declining values of contrast strength (see chapter 2).

Buffers Around Skarn Deposits Excluded from Training Set

A 1–km radial buffer was used around all skarn occurrences in MRDS for the data-driven assessment (figs. 7–25, 7–26). Radial buffers shown in decreasing intensities of red contrast MRDS sites of skarn in northern Nevada versus sites of the training set used for the pluton-related deposits (fig. 7–25). A 1–km radial buffer around these occurrences shows a highly positive correlation with the deposits that make up the training set, and only 11 of the 92 training sites are far distant from occurrences of skarn in the MRDS database. The skarn proximity and geochemical evidence maps serve to include areas likely to host pluton-related occurrences and deposits, and are characterized by narrowly-defined predictor patterns with W+ (see chapter 2) magnitudes that are significantly larger than W.

Combined Cu, Pb, and Zn Contents in Sediments

Copper, Pb, and Zn regional geochemical data for sediments (Folger, 2000) were combined together into a single synoptic base-metal signature for the assessment (fig. 7–27). The Cu–Pb–Zn signature evidence map shows a number of relatively small, isolated areas where the predictor pattern is present. Some of these small areas near the south-central part of the HRB are concentrated along the trace of the Battle Mountain-Eureka mineral belt. However, although the Cu–Pb–Zn signature evidence map shows that the predictor pattern is present and overlaps some of the known porphyry-related deposits at Copper Canyon in the southern part of the Battle Mountain Mining District, the predictor pattern is not present in the rest of the district where Cu–mineralized rock is quite widespread. This includes the Copper Basin area in the northern part of the district that includes widespread, well-exposed secondarily-enriched Cu orebodies (Theodore and others, 1992).

Arsenic Contents in Sediments

Concentrations of As $\geq$ 18 ppm in the regional sediment data set (Folger, 2000) are considered to be the third strongest positive predictor for presence of pluton-related deposits (table 7–9). However, the As frequency map for northern Nevada shows that small areas indicating presence of the predictor are widespread throughout the northern quadrant of the State and are most common in the western part of the HRB (fig. 7–28). Furthermore, these patterns do not outline satisfactorily the Battle Mountain-Eureka mineral belt (fig. 7–28), although quartile standard deviations from the mean of log concentrations of the As data define it quite well (fig. 7–13A). Arsenic, as arsenopyrite, is quite common throughout the skarn-related porphyry Cu system at Copper Canyon in the southern part of the Battle Mountain Mining District (Theodore and Blake, 1975), and As has been shown as well to be present as arsenopyrite epitaxial growths on pyrite in a non-porphyry environment in the northern Carlin trend (T.G. Theodore, unpub. data, 2001). Where zonation in porphyry systems has been well defined as in the Kuskokwim region, Alaska, As is usually present in association with arsenopyrite-pyrite-scheelite–Au–sulfosalt veins or chalcopyrite–Bi–Au skarns that formed somewhat deeper than Hg–dominated epithermal occurrences in the upper parts of the porphyry systems (Szumigala, 1996). High sulfidation rocks in the upper parts of porphyry Cu systems typically form at paleodepths of <500 m (Sillitoe, 1999).

Buffers Around Intrusive Igneous Rocks

A 19–km radial buffer (fig. 7–29) was used around all plutons shown on the geologic map of Nevada (Stewart and Carlson, 1978). The 13 intrusive units that comprise the pluton suite of map units are listed in table 7–9. The 19–km size of this radial buffer was selected using conventional statistical

constants that are derived from the spatial association between the plutons and the pluton-related deposit training sites (see chapter 2). The spatial association steadily increases to a maximum at 19 km, after which it rapidly decreases. In conceptual terms, the optimum training-site density, with respect to buffer area, is reached at a distance of 19 km. Beyond 19 km, the area of each successive buffer is increasing at a greater relative rate than the number of training sites. However, usage of even the 19–km radial buffer probably does not include all areas of the HRB that, from a strictly geologic standpoint, have some unknown but probably overall limited potential for presence of pluton-related deposits. An example of one of these areas involves the south end of the Sheep Creek Range, roughly 10 km northeast of the town of Battle Mountain, where mostly Ag– and Pb–bearing polymetallic veins at the Snowstorm (Mountain View) Mine produced ore valued between $5,000 and $100,000 during 1910–1928 (Stager, 1977). The location of this mine is within a part of the HRB that is classified as nonpermissive (fig. 7–5) for pluton-related deposits on the basis of a 10–km radial buffer applied by Cox and others (1996) to all of the plutonic units shown on the map by Stewart and Carlson (1978). The mine is barely within the 19–km buffer applied to the plutons (fig. 7–29). In addition, one of the 92 training sites—Washington Hill, site no. 90, a low–F stockwork Mo system—is located within a nonpermissive domain (table 7–1). Further, from precise comparisons of map patterns resulting from usage of 10–km versus 19–km buffers, it becomes readily apparent that the same data base of pluton units was not used for the respective plots of each buffer. Apparently, the 10–km buffer used by Cox and others (1996), in fact, includes some plutonic data layers showing presence of intrusive rock supplementary to that actually shown on the map of Stewart and Carlson (1978) as well as expert judgments concerning inferred distances of polymetallic occurrences from their generative intrusive centers. Thus, areas in the HRB classified as nonpermissive at the scale of our evaluation may in fact be shown to have some potential for occurrence of pluton-related deposits if evaluated at a scale larger than the present investigation.

Finally, we recognize the problem in logic involving usage of a 10–km buffer to define permissive versus non-permissive tracts as opposed to a 19–km buffer that results statistically from the spatial associations among geographic locations of plutonic units relative to locations of the 92 training sites (see above). The value of this buffer is strictly an artifact of calculations involving locations of training sites and plutons on the State geologic map. It really has no geologic meaning. However, if other sets of geographically different pluton-related deposits were selected as training sites as well as areas of different sizes, then the value of the statistical buffer would change dramatically. For example, if we restricted our assessment area to the Battle Mountain Mining District and used only those 30 pluton-related deposits within the district as a training set, then the optimal buffered distance would be 2 km. If we restricted the assessment area to the area sampled during the NURE program and 60 of the 92 sites within the

sampled area, then the optimal buffer would be 11 km. Further, a test involving 92 training sites arbitrarily placed within the HRB results in a typical random noise pattern, wherein a plot of spatial association contrast versus proximity to a pluton oscillates around zero, indicating no particular spatial association. Random points that make up a large segment of the plot account for 94.5 percent of the total number of points (n total = 92). The peaks are not statistically significant and in effect represent "noise" within which there is no "optimum" to pick from and no apparent spatial association with the distribution of the plutons. If the modeling is working correctly, this is what we should expect and should observe.

Lithodiversity in the Geologic Map of Nevada

In the Great Basin, lithologic complexity or lithodiversity, at least in the plan view of the State geologic map (Stewart and Carlson, 1978), results from superposed structural, stratigraphic, and intrusive relations within a given domain of measurement (Mihalasky and Bonham-Carter, 1999). This is particularly true in the HRB. For example, faults can distort, dismember, and rotate structural blocks—they can, as well, disrupt continuity of units, juxtapose unrelated rocks, and possibly expose now steeply dipping, but previously horizontal strata. The greater the number and more intricate these relations, the more spatially complex an area should appear in a geologic map thereby emphasizing an enhanced structural preparation in the area—such geologically complex relations are requisite for generation of most epigenetic ore deposits. The purpose of considering a map showing lithologic diversity as one assessment layer for pluton-related occurrences is to determine the degree of spatial association between the mineral occurrences and such areas. The rationale is that structure, stratigraphy, and intrusive activity all are important factors that control eventual areal distribution of mineralized rocks and (or) orebodies. Lithologically diverse terranes should show some degree of spatial association with the bulk of the epigenetic mineral occurrences in and near the HRB. The positive prediction criteria used is ≥ 3 lithologic units present per 6.25 km^2 of the Stewart and Carlson (1978) geologic map of Nevada (table 7–9; fig. 7–30). Griffiths and Smith (1992) demonstrated that a simple linear relationship exists between geologic diversity and mineral-resource diversity in support of this proposition. They found that domains that have relatively high diversity are favorable hosts for metal-bearing ores, as demonstrated by most counties in Nevada (12 of 17) which have a high diversity and also are prolific producers of base and precious metals. Geologically, Griffiths and Smith (1992) interpreted this relation as reflecting a complex mixture of igneous, metamorphic, and sedimentary rocks that accompany metal-bearing ores which, in turn, serves to emphasize the inherent complexity of protracted geologic processes necessary to provide a good potential for metal-bearing ores as well as the pre-mineralization structural preparation required at the district scale for development of significant orebodies.

However, as applied to the geologic map of Nevada (fig. 7–30), these predictive criteria using lithodiversity have a tendency to emphasize inordinately the bedrock areas of the State versus the valleys that have a relatively small number of geologic map units compared to the mountain ranges. Usage of this relation in the preliminary WofE assessment in effect enhances variability in the final pattern for favorability in the mountain ranges to the point that all of the mountain ranges are uniformly classified as prospective.

Buffers Around Interpreted Basement Gravity Lineaments

Distances from gravity lineaments, interpreted from D. Ponce (written commun., 2000), were considered ideally to have a 29–km buffer (table 7–9; fig. 7–31). No known geologic process has been recognized to require a buffer as wide as this.

Gravity Terrane

Those areas outside of domains wherein high gravity is present are considered to be a positive predictor for presence of pluton-related deposits (table 7–9; fig. 7–32). The Great Basin is situated in a regional gravity low (Eaton and others, 1978). Regional Bouguer gravity at wavelengths greater than 1,000 km indicate that the dominant, first-order feature in the Great Basin and adjacent regions to the east, is an enormous anomalous low (less than –200 mGals), and reflect sources within the pre-Tertiary basement (Kane and Godson, 1989; Blakely and Jachens, 1991). Gravity-anomaly lows in Nevada are related to rocks of lower density, or attributes which effectively lower the density of rocks, such as widespread fractures related to fault and shear zones (Telford and others, 1976; see also, Jachens and others, 1989). In Nevada, isostatic gravity lows generally correlate with sediment- and volcanic rock-filled inter-range basins, as well as with the presence of felsic intrusions (Mabey and others, 1983; Saltus, 1988; Blakely and Jachens, 1991). The dominant feature, visible in both the isostatic and Bouguer anomalies, is a regionally extensive gravity low that stretches from the Nevada-Utah border across the center of the State into the Walker Lane region. This low, flanked to the north and south by gravity highs, reflects sources in the pre-Tertiary basement, but its strongest correlation is with distribution of thick accumulations of Cenozoic volcanic rocks (Blakely and Jachens, 1991; Mabey and others, 1983). The isostatic gravity lows are reasonably well correlated with (1) volcanic rocks erupted during the 34– to 17–Ma interval and (2) a possible east–west-trending structural zone that extends across south-central Nevada—for the south-central Nevada structural zone, see Kepper and others (1991). The isostatic gravity low also is visible in the Bouguer gravity anomaly, where it is characterized by gross bilateral symmetry that is best developed in east-central Nevada. The axis of symmetry trends northwest and is generally coincident with the northern Nevada rift zone. The Nevada gravity low may actu-ally be part of a large alternating pattern of northwest-south-east-trending high-low anomalies that stretches from California, across the Great Basin and into Utah (see also, Jachens and others, 1989, pl. 1; Kane and Godson, 1989). This large gravity pattern is probably related to features at the crust-mantle boundary, and may represent areas of igneous underplating (Mutschler and others, 1992; Parsons and others, 1994).

Description of Tracts for Pluton-Related Deposits

The data-driven pluton-related deposit mineral-assessment map, which only delineates prospective and favorable tracts, is shown in figure 7–33. However, the four assessment ranks shown below—nonpermissive, permissive, favorable, prospective—are derived from two sources: (1) the former two from the Nevada assessment by Cox and others (1996); and (2) the latter two from the data-driven modeling on the basis of break-points in the cumulative assessment area curve (fig. 7–34). As noted on this figure, only 58 of the 92 pluton-related training sites are within the NURE–sampled domain of figure 33. The amount of the area of each assessment rank, in relation to the total assessed area of the greater HRB, and the number of training sites in each rank, are given in table 7–10. For example, approximately 2 areal percent of the NURE–sampled domain has been classified as prospective. The most prominent break-point in the curve above the prior favorability was used to delineate the favorable–prospective rank boundary (see dotted red line on fig. 7–34).

The pluton-related deposit mineral-resource assessment map was created by combining the data-driven favorable-prospective map with the expert-delineated permissive tract and masking out areas with Cenozoic cover greater than 1 km (fig. 7–35; see also, fig. 7–5 and chapter 2). The area of each assessment tract, the number of training sites in each tract, and the rank of each training site are given in tables 7–10 and 7–1. Within the greater HRB area, the largest cluster and most important ore deposits, which are located in the Battle Mountain Mining District, are present mostly within prospective and favorable areas. The Battle Mountain–Eureka mineral trend also is well defined by a linear alignment of prospective areas. In the western part of the HRB, in Pershing County, a weak, linear alignment of prospective and favorable areas appears to be present, and it trends northeast from the West Humboldt Range, along the western flank of the Humboldt Range, to the eastern flank of the Eugene Mountains. This alignment is one of many that apparently are present in the greater HRB region (see below).

A number of areas showing various levels of favorability for pluton-related deposits have been delineated in the HRB (fig. 7–35). The favorable tracts in the greater HRB area also appear to coalesce into broad and areally extensive coherent patterns that might represent belts of magmatic activity and their attendent fluid flow deep in the crust and, therefore, areas favorable for pluton-related deposits. Most of the broad favorable areas and less areally extensive prospective areas used to

define the belts all contain variable numbers of mineral occurrences classifiable as pluton-related. However, many features that might be used to document these inferred belts precisely are not directly measurable in outcrop, including presence of faults parallel to the long axes of the delineated belts. Nonetheless, six northeast-trending belts have been delineated in the general area of the HRB for further discussion—including three on either side of the Battle Mountain-Eureka mineral belt. What is most striking is the fact that the easternmost belts on either side of the Battle Mountain-Eureka mineral belt apparently are offset approximately 80 km from each other in a right lateral sense along the trace of the Battle Mountain-Eureka mineral belt. If these offsets are real, then they must result from deep zones of crustal weakness, such as major faults, linked to the supracrustal rocks only by the alignment of the prospective and favorable tracts. These, in turn, probably track magmas that are associated with enhanced capacities for generating pluton-related deposits—the magmas are inferred to have been emplaced along the zones of weakness. The latter appear to be parallel to the edge of the craton.

Battle Mountain-Eureka Mineral Belt

The Battle Mountain-Eureka mineral belt is the premier subcontinental-scale metallotect for pluton-related deposits in the HRB (fig. 7–35). As described above, it partly may have inherited its northwest orientation from a zone of weakness that parallels paleotransforms that bound the northeastern and southwestern margins of the Cordilleran miogeocline (Dickinson, 2001). Numerous stream-sediment and soil samples from the Battle Mountain-Gold Run segment of the Battle Mountain-Eureka mineral belt also contain anomalous concentrations of As, Sb, Au, Ag, Cu, Pb, Mo, and Zn (King, 1996; see also, Kotlyar and others, 1998a). These anomalies are especially concentrated in the Battle Mountain part of the trend (see also, figs. 7–12, 7–13). The Battle Mountain-Eureka mineral belt mainly is a Late Cretaceous and Tertiary porphyry trend and contains the Battle Mountain Mining District near the central part of the HRB. The belt is defined by clusters of deposits in a zone extending southeast from the general area of the Battle Mountain Mining District to the general area of Eureka (fig. 7–35). Although recognized for a number of years (Roberts, 1966), our study has reaffirmed distribution of the Battle Mountain-Eureka mineral belt through an alignment of prospective tracts in the mountain ranges. This alignment of prospective tracts also includes the Buffalo Mountain and Iron Hat Mining Districts of Tingley (1992). However, the central axis of the Battle Mountain-Eureka mineral belt is parallel to, but approximately 20 km west of, an isostatic gravity gradient that marks the boundary of rocks in the middle and upper crust that are quite dense relative to surrounding ones (Kotlyar and others, 1998a; see also, Grauch, 1998). The northwest part of the trend at Battle Mountain—in effect the generally accepted northern terminus of the Battle Mountain-Eureka mineral belt—contains as many as 10 exposed and inferred porphyry Cu and stockwork Mo systems as we described previously

above. However, it should be emphasized that current overall prospectivity of the Battle Mountain Mining District—particularly its pediment areas—is still (2002) locally much higher than other adjoining mountain ranges that generally are classified as favorable.

The McCoy Mining District, due south of the Battle Mountain Mining District, possibly is controlled by an inferred deep north-striking crustal structure, originally suggested by Bloomstein and others (1991), that intersects the northwest-trending Battle Mountain-Eureka mineral belt. Thus, widespread mineralized rock at McCoy might reflect a predominantly Tertiary southward protrusion of mineralized rock near the intersection of the two crustal structures.

Humboldt-Toulon Belt

The Humboldt-Toulon belt—also referred to as the Humboldt porphyry tract by Peters and others (1996)—is defined by a broad zone of generally northeast-trending areas that are prospective and favorable for pluton-related deposits. This belt is located generally north of Lovelock and it is centered on the Humboldt River (fig. 7–35)—the belt is part of a much more wide-ranging W belt defined by Stager and Tingley (1988). The Humboldt-Toulon belt also is envisioned to broaden in an east-west direction near Lovelock to include the Humboldt Range and the Unionville Mining District. The Mo occurrence at Majuba Hill also is present near the northeast terminus of the belt (fig. 7–9). Further, the belt includes numerous clusters of pluton-related mineral occurrences that have many characteristics compatible with a porphyry Cu–related-environment—these include occurrences at Fireball Ridge and at Granite Point (fig. 7–9). Near its south end, the Humboldt-Toulon belt also includes the Ragged Top Mining District (fig. 7–9), which district contains Triassic to Jurassic metasedimentary rocks that have been intruded by Cretaceous granodiorite that produced Cu– and W–bearing skarn, some of which contains Mo (Lincoln, 1923; Johnson, 1977; Schilling, 1980; Stager and Tingley, 1988). Southeast of Lovelock, the Wildhorse and Muttlebury Mining Districts contain many polymetallic veins (Lawrence, 1963; Johnson, 1977), and W skarns, which also contain Cu, Au, and Ag (Stager and Tingley, 1988). Many mineralized rocks are associated with early-stage thermal metamorphism, and are veined by quartz—they as well contain aplite dikes, such as those at the Long Lease Mine, which also include Mo (Schilling, 1980).

A number of other mineral occurrences in the general area of Lovelock also are pluton-related. Deposits in the Gold Butte and Trinity Mining Districts, west-northwest of Lovelock, include polymetallic veins which contain W, Ag, Pb, Zn, and Mo in zones of hornfels, in skarn, and in aplite sills (Lincoln, 1923; Johnson, 1977; Schilling, 1980). In the Rye Patch Mining District, Cretaceous granitic rocks have intruded Triassic metasedimentary rocks and produced quartz and pegmatite veins in a surrounding zone within which the veins contain W, fluorite, muscovite, and beryl (Wallace and others, 1969a, 1969b). The quartz and pegmatite veins are associated

spatially with polymetallic metal assemblages that are rich in Ag, Sb, Pb, Zn, and Au (Lawrence, 1963; Johnson, 1977), as well as with the Empire Mo occurrence (Schilling, 1980). However, a group of W deposits in the Humboldt Range, east of Lovelock, clearly is related to two-mica granite (Peters and others, 1996).

Another small area just to the north of the Humboldt-Toulon belt merits mention. In the Mill City Mining District (fig. 7–9), Triassic sedimentary rocks were intruded by Cretaceous granodiorite stocks and quartz monzonite aplite dikes and pegmatites; associated hornfels, W skarn, and Cu and W skarn are anomalous in Mo, Ag, Sb, Pb, and Zn (Lincoln, 1923; Johnson, 1977). The Springer W skarn locality, which is discussed at some length above, also contains Mo (Schilling, 1980), and it has been classified as a porphyry Mo, low–F deposit by Wendt and Albino (1992). The Mill City Mining District also shows numerous stream-sediment and soil samples that have anomalous concentrations of Sb, As, Au, Ag, and Pb (King, 1996).

Stillwater Belt

The Stillwater belt is defined by an almost continuous band of favorable and prospective areas for pluton-related deposits that extend from the general area of the East Range on the northeast to the Stillwater Range on the southwest (fig. 7–35). In the northern part of the Stillwater belt, the Kennedy Mining District contains Mo– and Cu–mineralized rocks in an Oligocene intrusive complex that includes gabbro-diorite and monzonite-quartz monzonite phases (Johnson, 1977; Juhas, 1982). These rocks have intruded Paleozoic rocks on the north and Triassic leucogranite on the south (Whitebread and Sorensen, 1980). Alteration consists of K–silicate assemblages together with phyllic and propylitic alteration (Bowes and others, 1982). Mineralized rocks include disseminated and stockwork chalcopyrite and molybdenite (Thurber, 1982). Polymetallic veins surround the central district—particularly near the east end of the mining district—and contain Cu, Pb, Zn, As, Ag, and Au (Klopstock, 1913; Muller and others, 1951; Wallace, 1977). The eastern end of the mining district also contains numerous stream-sediment and soil samples that have anomalous concentrations of Ag (King, 1996). The Kennedy Mining District also lies along an east-west regional structural trend that is interpreted to be the westward extension of an Oligocene and Miocene trough of volcanic rocks (Wallace, 1978; Kutina and Bowes, 1982; Burke and McKee, 1979). The Oligocene intrusive complex in the Kennedy Mining District represents probably some of the geologically deepest parts of this trough, which also contains a circular magnetic signature at the surface (Hallof, 1982). The trough is regionally composite in that it is filled with early Oligocene Caetano Tuff near its eastern terminus near Cortez, Nev. (Gilluly and Masursky, 1965)—that is, near the east-central part of the HRB—and it contains younger 20–Ma tuff in the general area of the Fish Creek Mountains (McKee, 1970). Many of these features are consistent with the porphyry Cu–(Mo) type of deposit described by Cox (1986c).

Osgood Belt

As defined, the Osgood belt is a relatively short, northeast-trending belt of prospective areas for pluton-related deposits that coincide largely with the Osgood Mountains (fig. 7–35). Tungsten skarn deposits are present along the western and eastern contacts of northeast-trending Cretaceous plutons in the Osgood Mountains. The economically important sedimentary rock-hosted Au–Ag deposits that are present generally near the eastern range front of the Osgood Mountains are discussed in chapter 8. Further, a number of fairly well explored porphyry Cu and stockwork Mo systems are present near the broad junction of the Osgood belt with the Stillwater and Battle Mountain-Eureka belts. The general area of this "triple" junction remains unassigned as to belt affiliation because all three inferred belts may have contributed substantially to structural controls that localized the delineated favorable and prospective tracts (fig. 7–35). These systems are in the Sonoma Range as well as near the south end of the Edna Mountains.

Toiyabe Belt

The Toiyabe belt is defined by an almost continuous belt of favorable and prospective areas for pluton-related deposits that extends along the entire length of the Toiyabe Range in a north-northeast direction (fig. 7–35). A number of plutons of various ages are present along the range, and these plutons generally are associated with polymetallic vein occurrences that are clustered together into a number of mining districts. The belt includes all of the mostly polymetallic mining districts in the general area of Austin that were discussed at some length above. In addition, as shown, the belt largely coincides with a northeast-trending zone of anomalously high As contents in sediment samples (Kotlyar and others, 1998a). Several other metals common in pluton-related environments, including Bi and Sn, also appear to be preferentially concentrated along the Toiyabe belt on the basis of an evaluation by B.B. Kotlyar (oral commun., 2001) of the recently-released NURE regional geochemical data base (Folger, 2000).

Ruby Belt

The Ruby belt of favorable areas, which also is elongated in a northeasterly direction, is a relatively short belt near the east edge of the HRB. It is largely coincident with the Ruby Mountains (fig. 7–35). The Ruby Mountains contain widespread exposures of Jurassic pegmatitic granite, Cretaceous two-mica granite, and Oligocene granite-monzonite of the Harrison Pass pluton, as well as a number of areally restricted occurrences of Miocene basalt dikes (Howard, 1966; Howard and others, 1979; Howard, 1980). All of these plutonic units were emplaced into an extensive migmatitic complex—including components of a metamorphic core complex—in the range. This core complex largely reflects migmatization of

Paleozoic platformal sequences, probably drawing to a close sometime in the Tertiary. At least two phases of mineralized skarn are present in the Ruby Mountains, and they are associated with Jurassic and Tertiary magmatic events (Berger and others, 2000). These skarns have produced generally small amounts of base and precious metals and W (see discussion above for a summary of the metal production history from this mountain range). The mineralized occurrences in the Ruby belt are inferred to reflect mineralization processes that occurred somewhat deeper in the crust than those in the companion Toiyabe belt offset to the southwest across the Battle Mountain-Eureka mineral belt (fig. 7–35).

Adobe-Piñon Belt

The Adobe-Piñon belt of largely favorable areas for pluton-related deposits extends in a southwest direction from the Independence Mountains, through the Adobe Range, to the Piñon Range (fig. 7–35). The belt also includes some parts of the northern Cortez Range, and apparently is anchored at its southwest terminus by favorable areas in the general area of Jurassic magmatism and associated polymetallic vein deposits in the Cortez Mining District (fig. 7–35). As currently defined, the belt is parallel with, but slightly offset to the east, from the prominent set of linear features that define the Crescent Valley-Independence lineament (see fig. 7–13). The belt is delineated by a number of more or less continuous prospective areas that are the result of a number of overlapping predictor patterns, including: (1) gravity terrane (fig. 7–32), (2) gravity linears (fig. 7–31), (3) lithodiversity (fig. 7–30), and (4) pluton proximity (fig. 7–29). The belt includes prominent plutons at Lone Mountain along the east flank of the Adobe Range, and a large number of Jurassic plutonic bodies in the northern part of the Cortez Range in the southern part of the belt (Stewart and Carlson, 1978). Between 1868 and 1988, the Railroad Mining District, approximately 10 km southeast of the inferred trace of the Adobe-Piñon belt (fig. 7–35), produced approximately 7 million lbs Cu, 36,000 oz Au, 25 million lbs Pb, 1.3 million oz Ag, and 0.4 million lbs Zn (LaPointe and others, 1991). The large number of mineral occurrences present in the northern part of the Cortez Range (fig. 7–6) represents Fe deposits associated with Jurassic felsic magmatism (see above for discussion of the relatively minor amounts of Fe produced from these occurrences).

Summary of Pluton-Related Assessment

Evaluation of the HRB for pluton-related deposits resulted in variable proportions of many mountain ranges being classified as favorable (12 areal percent of the entire area of northern Nevada covered by the NURE geochemical data) and prospective (2 areal percent) (table 7–10). The generally nonuniform distribution of favorable and prospective tracts across the HRB must be a consequence primarily of numerous interrelated geologic phenomena. In addition, many outlined tracts seem to define narrow north-northeast trending belts that may reflect upper crustal zones of weakness that are inferred to coincide with major rifts deep in the crust—the generally northeast trends appear to parallel roughly the margin of the craton (Wooden and others, 1998; see also, Theodore, 2000, fig. 5). Such deep-seated rifts in continental crust, if present, probably are largely decoupled rheologically from supracrustal rocks presently exposed in the mountain ranges. We further envision that the belts must reflect supracrustal zones that were reactivated repeatedly through geologic time—though reactivation in the region of the HRB apparently was concentrated especially during the Mesozoic and middle Tertiary—as various continental-scale processes became operative. Repeated reactivation along the roots of the belts periodically thereby allowed a rise into the supracrustal rocks of magmas and their associated pluton-related fluids and metals. Massingill (2001) suggests that north-northwest striking faults in north-central Nevada invariably have dextral-normal offsets whereas north-northeast ones have sinistral-normal offsets. This sense of dextral offset also applies to the northwest-trending Battle Mountain-Eureka mineral belt as a whole on the basis of an interpretation of the 0.706 isopleth for the ratio of 87Sr to 86Sr (Massingill, 2001). Nonetheless, some further discussion of the predictor layers used in our evaluation that led to delineation of the belts is warranted.

First, use of lithodiversity as a predictor layer, as well as all other data layers that are derived specifically from the mountain ranges, contributed to a "more favorable" status for pluton-related deposits preferentially in the mountain ranges as opposed to the valleys. The geologic map of Stewart and Carlson (1978) shows a small number of areally expansive geologic units, mostly unconsolidated surficial deposits of various kinds, to be present in the valleys. These relations thus weight positively the mountain ranges more heavily than the covered areas. However, the inverse may in fact be true today from an explorationist's viewpoint. Covered pediment areas near the fronts of the mountain ranges are probably the most coveted areas to explore for undiscovered deposits. Most easily recognized targets in the mountain ranges have been tested and evaluated for their viability as metal-producing systems. However, small-footprint deposits that have high metal grades in the mountain ranges are extremely difficult to find even with the most modern of exploration methodologies. For example, some recently discovered deposits in the mountain ranges have undergone roughly 10 years of continuous exploration by drilling before ore was eventually discovered.

As a further example of obstacles facing the modern explorationist, the section above concerning PGE in the Humboldt mafic complex emphasizes how important subtle textural changes in gabbroic fabrics might be during evaluation of the possible presence of these metals in such geologic environments. However, it would be at least several orders of magnitude more difficult to evaluate such textural relations in gravel-covered pediment areas than in mountain ranges, assuming that the textural changes could be found in gravel-covered areas.

Second, our evaluation clearly showed a glaring need for much better data on the igneous rocks in the region. Certainly, igneous rocks have a widespread geographic distribution and wide-ranging ages throughout the HRB. However, even at the small scale of our investigation, the ages of these plutons are far from adequate for metallogenic purposes. As a corollary, a further complicating factor is that we cannot discriminate uniformly across the HRB as to the relative degree and type(s) of alteration, if any, that may be present in igneous rocks represented by the 13 intrusive map units of the geologic map of Stewart and Carlson (1978). Therefore, all igneous occurrences in the HRB have been ranked the same as to potential association with pluton-related deposits. If the requisite alteration and age data were available, then those igneous bodies that show no signs of widespread hydrothermal alteration could be ranked lower than altered ones as to potential genetic association with many types of pluton-related deposits. The number of plutons used as evidence for a particular type of pluton-related deposit could be reduced, resulting in a more inclusive predictor pattern. Further, only about 5 percent of the approximately 300 mapped igneous bodies on the geologic map of Stewart and Carlson (1978) within the greater HRB area have a training site within 10 km. Usage of large-scale geologic maps showing additional intrusive bodies present in the HRB would have improved the results of the assessment, but these maps are not available at a uniform large scale across the entire HRB. In addition, the statistically valid buffer chosen for the plutons in the present assessment—19 km (see above)—must be recognized solely for what it represents; that is, a statistical fall out from the location of the plutons, the locations of the selected training sites, and the size of the overall area. We do not mean to infer that we consider all plutons mapped in the HRB to have a potential to generate deposits out to a radius of 19 km. For example, one of the most intensely mineralized areas in the HRB, Copper Canyon in the southern part of the Battle Mountain Mining District, has an alteration halo that incorporates only 13 km2 of altered rock. A 19–km radius is equal to a circular area of 1,133 km2. However, entire mining districts that host porphyry Cu systems typically are on the order of 40 km2 (Gustafson and others, 1999). The largest area of altered rock in the Babine Lake, British Columbia, porphyry systems, for instance, is approximately 6.5 km2 (Sheets and Nesbitt, 1996). At the Frieda River igneous complex, Papua New Guinea, a cluster of seven porphyry Cu and skarn deposits is present within an area of approximately 16 km2 that makes up only 16 percent of the entire igneous complex (Morrison and others, 1999).

In porphyry Cu–(Mo) systems, the lateral extent of distal polymetallic Pb–Zn–Ag zones that are present outside their proximal Cu–rich cores typically also is much less than 19 km. However, because of structural and (or) lithologic controls, the polymetallic zones of many of these systems commonly continue well beyond the widespread Fe–sulfide-altered haloes that encompass the systems. These haloes are the result of disseminated pyrite and (or) pyrrhotite in the rocks. For example, at Copper Canyon, mostly Pb–Zn–Ag polymetallic veins associated with the large porphyry Cu, skarn-related system are present, at most, 4 km from the core of the system whereas, in the same area, the Fe–sulfide halo extends approximately 1 km from its core (Roberts and Arnold, 1965; Kotlyar and others, 1998). At Bingham, Utah, the outer limit of Pb–Zn replacement ores is approximately 3 km from the core of the system (Einaudi, 1982). At Bisbee, Arizona, and Cananea, Sonora, Mexico, the outer limit of Pb–Zn relacement ores is about 2 km from the respective cores of each of these two large porphyry Cu systems (Einaudi, 1982). On the one hand, usage of a 19–km buffer far exceeds the extent of genetically related ores that one might expect to surround a mineralizing granitoid body. On the other hand, usage of a 19–km buffer tends to eradicate any areal deficiencies in the pluton-related assessment that may result from presence of small granitoid bodies that can be shown only on geologic maps that are at much larger scale than the geologic map of Stewart and Carlson (1978).

In conclusion, as we have indicated throughout this chapter, many areas in the HRB that are assessed primarily as having a superior potential for undiscovered pluton-related deposits will continue to draw significant attention from the mining industry during the next 10 to 15 years. Moreover, even considering all of the caveats noted throughout this chapter with regards to qualifications intrinsic in the modus operandi of the assessment, our assessment for pluton-related deposits in the HRB nonetheless is state-of-the-art for the data available to us. A better geographic specificity in the response map for pluton-related deposits in the HRB currently is not possible considering the largely small-scale data available for the combined expert and WLR evaluation. Lastly, the recent surge during late 2000 and early 2001 in PGE market price unquestionably has resulted in the Humboldt mafic complex, which is present in the western part of the HRB, becoming an exploration target of some interest for PGE as described above; however, the economic consequence, if any, of these exploration efforts will not be known for a number of years.
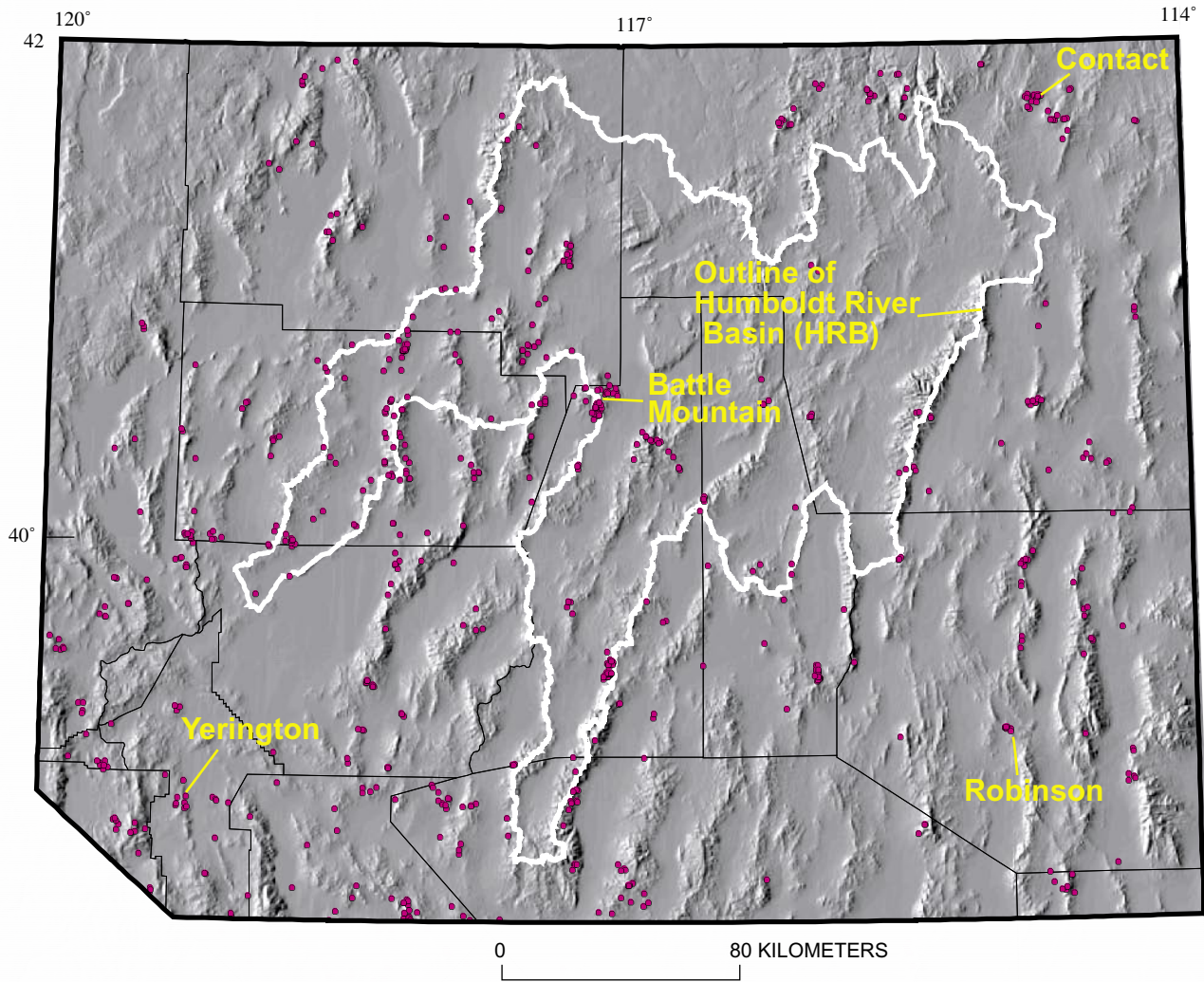
Figure 7-1.   Digital elevation model of northern Nevada showing locations of pluton-related (see text) mineral occurrences (red circles) from Mineral Resources Data System (MRDS) of U.S. Geological Survey and outline of Humboldt River Basin (HRB). Includes occurrences in MRDS having general characters of porphyry Cu; porphyry Cu–(Mo); porphyry Mo, low F; and Climax Mo as described in MRDS. Locations of Yerington, Robinson, Battle Mountain, and Contact Mining Districts also shown.
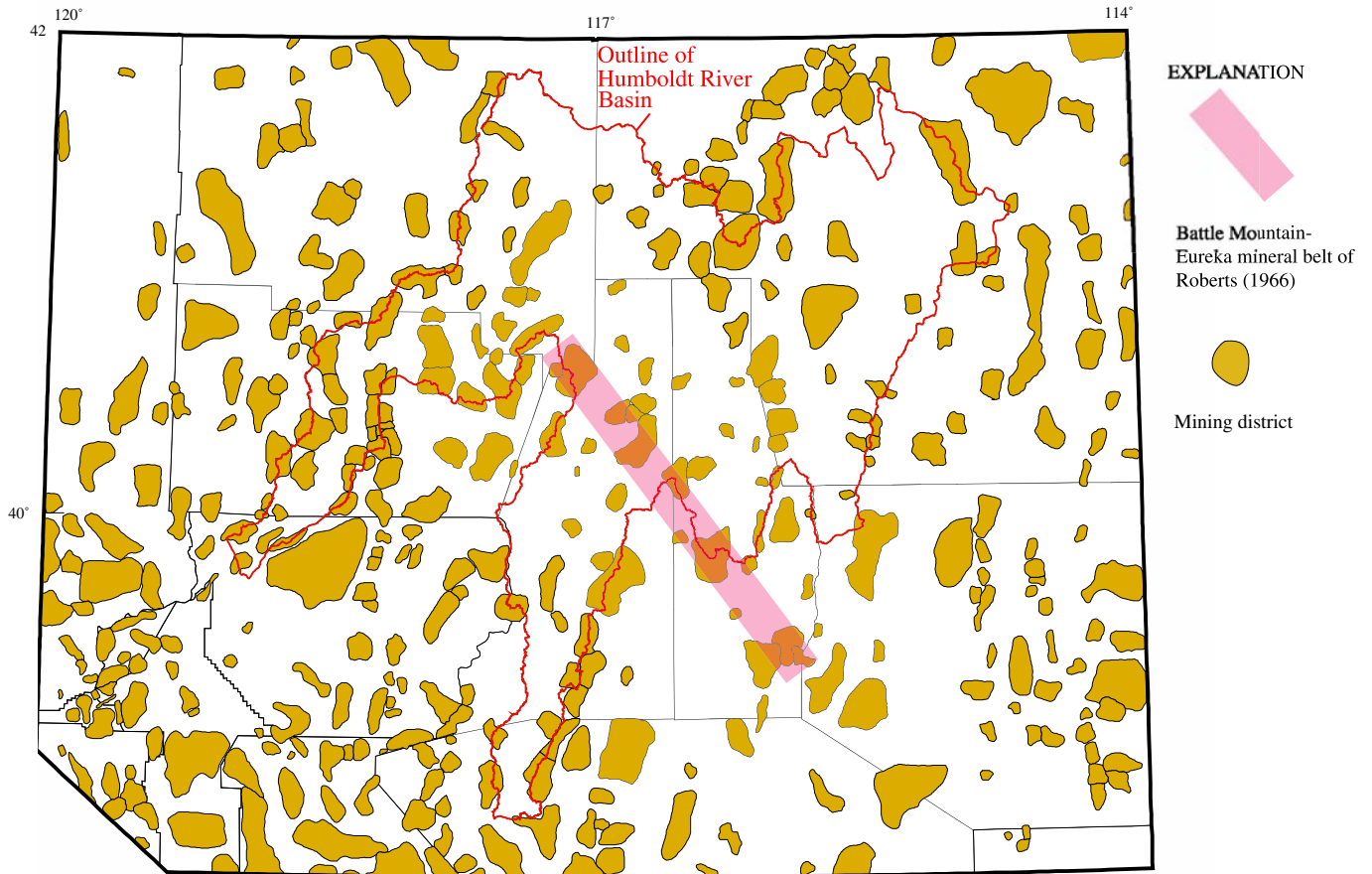
Figure 7-2. Map of northern Nevada showing outlines of mining districts (ochre) from Tingley (1992), outline of Humboldt River Basin (red line), and Battle Mountain-Eureka mineral belt (light red band).

EXPLANATION

▨	Cretaceous Thrust Belt
■	Mesozoic Batholiths
⚒	Porphyry Copper Deposit
— · —	State boundary
— ·· —	National boundary

— • — (red)	Approximate eastern limit of Cordillean Orogen
— ✕ — (blue)	Western edge of Precambian Craton
- - - - (green)	Quartz Diorite Line

▬ (blue)	San Pedro Belt
▬ (magenta)	Cananea Belt
▬ (orange)	Walker Belt
▬ (yellow)	Battle Mountain-Eureka mineral belt

Figure 7-3.   Batholiths, Cretaceous thrust belt, major cratonal features, and major porphyry Cu deposits in western North America. Modified from Hollister (1978).
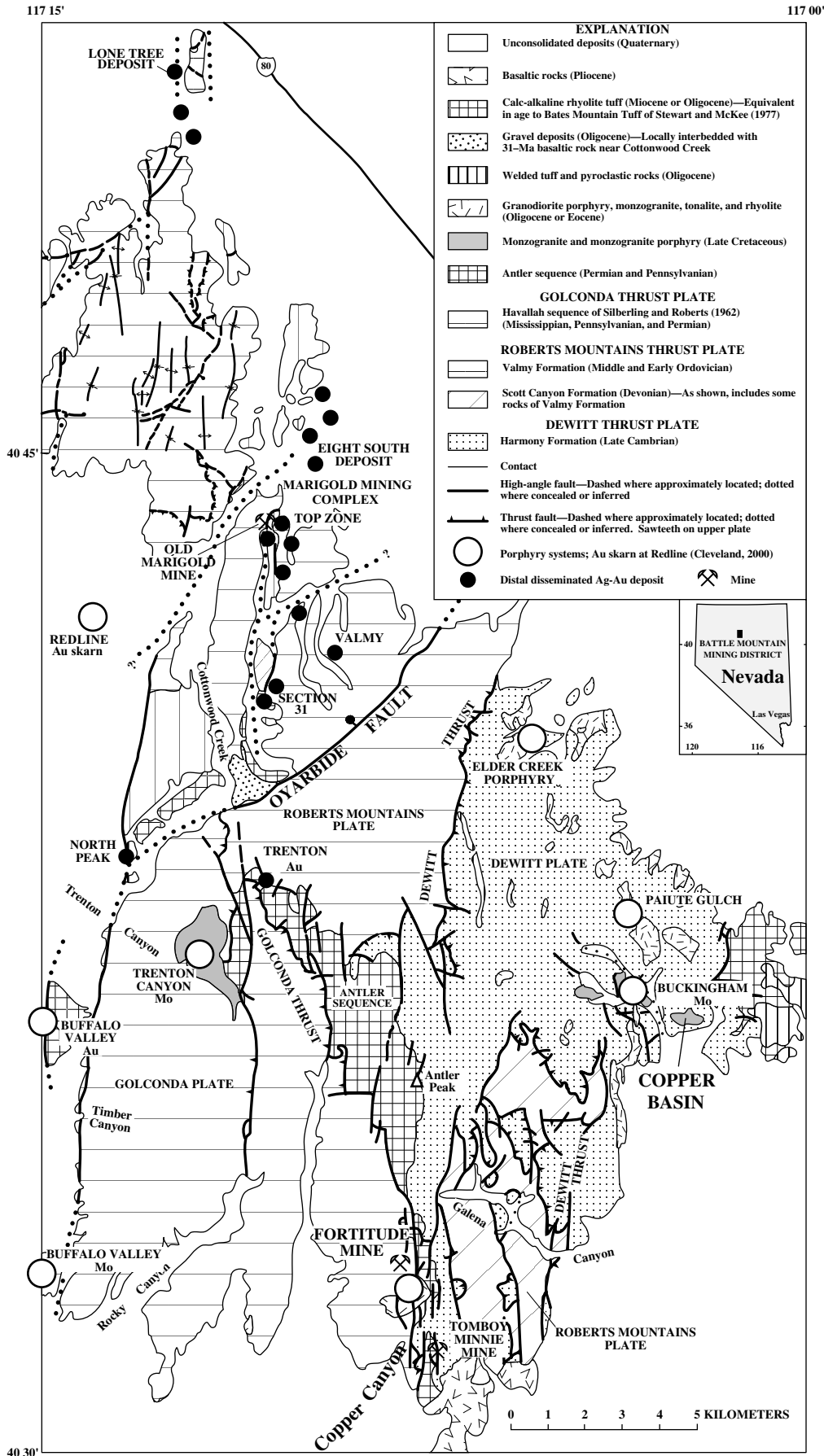
Figure 7-4. Geology of the Battle Mountain Mining District, Nevada, showing major centers of mineralized rock. Modified from Roberts (1964), Doebrich (1995), and Theodore (2000).
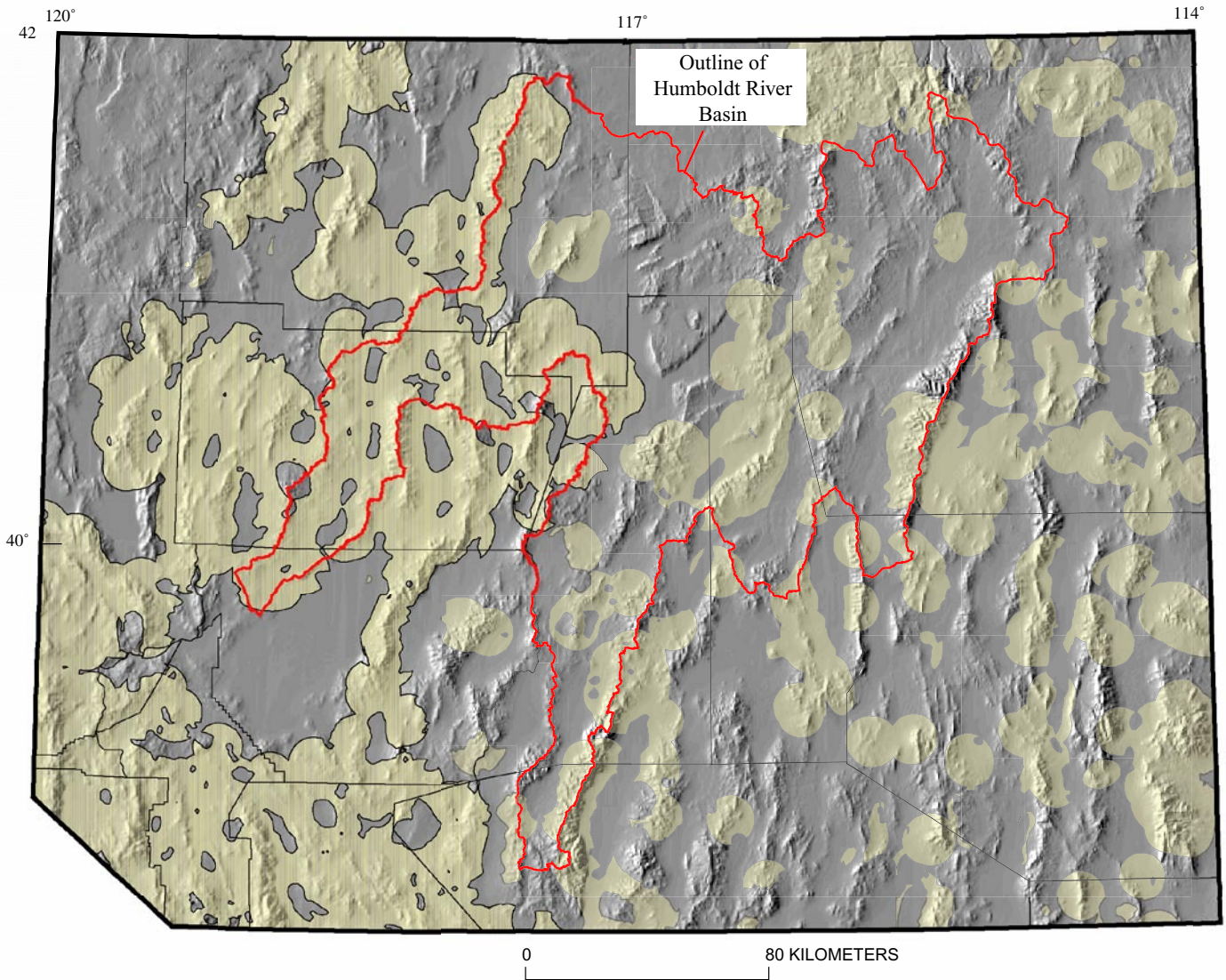
Figure 7-5. Digital elevation model of northern Nevada showing in pale yellow areas permissive for pluton-related deposits. Permissive areas defined as being within a 10–km radial buffer of plutons shown on State geologic map of Stewart and Carlson (1978) (see text). Outline of Humboldt River Basin also shown. Modified from Cox and others (1996).
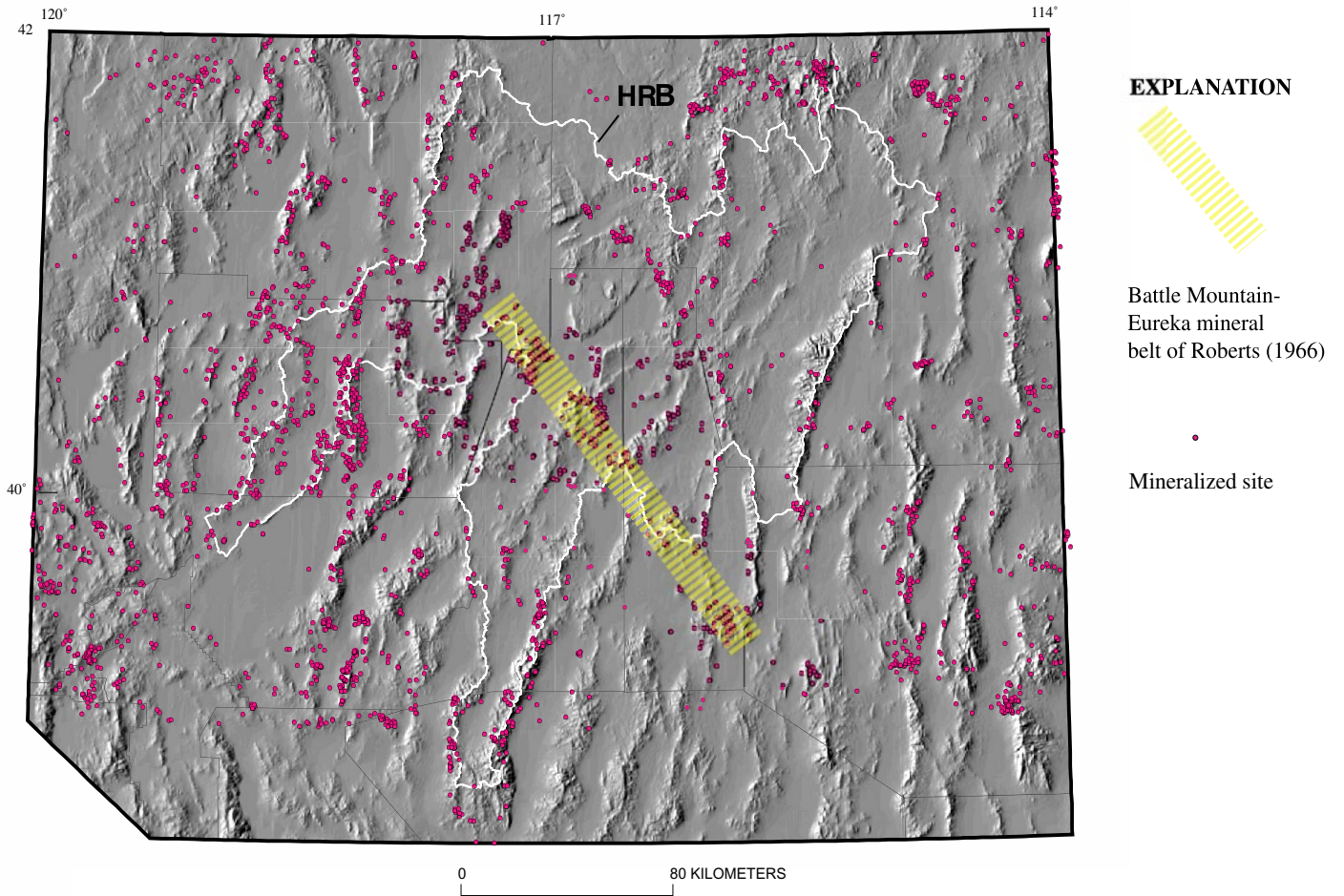
Figure 7-6.   Digital elevation model of northern Nevada showing all mineralized sites (red circles) recorded in U.S. Geological Survey Mineral Resources Data System (MRDS) and the outline of the Humboldt River Drainage System (HRB, white line).

alun = alunite
Bn = bornite
bx = breccia
Cal, cc = calcite
Chl = chlorite
Cp = chalcopyrite
Cv = covellite
Dg = digenite
Diop = diopside
En = enargite
Gl = galena
Hm = hematite
IGN = igneous
Kaol = kaolinite
MET = metamorphic
Mont = montmorillonite
Mt = magnetite
P = propylitic alteration
Po = pyrrhotite
Py = pyrite
Pyroph = pyrophyllite
Qz = quartz
S = sericitic
Ser = sericite
SED = sedimentary
Sl = sphalerite
Tn = tennantite
Trem = termolite
vn = vein
vnlt = veinlet
volc = volcanics

EXPLANATION

Breccia	MtPy (Qz Cc Chl Po)	Weak potassic alteration (PyCp)
Cp Py (Bn)	Py Qz	Ser Qz Py (CpTnSl)
Igneous	Local Skarn	Chl-Mont-Cal (PyCpTnSl)
Bn Py	Py, Sl, Gl or Hm	Alun Pyroph Kool Qz Py (BnEnSl)

Figure 7-7. Schematic vertical section through idealized porphyry Cu, skarn-related deposit showing typical alteration zonal patterns developed in limestone and calcareous siltstone protoliths adjacent to high-level mineralizing porphyry. Modified from Einaudi (1982).
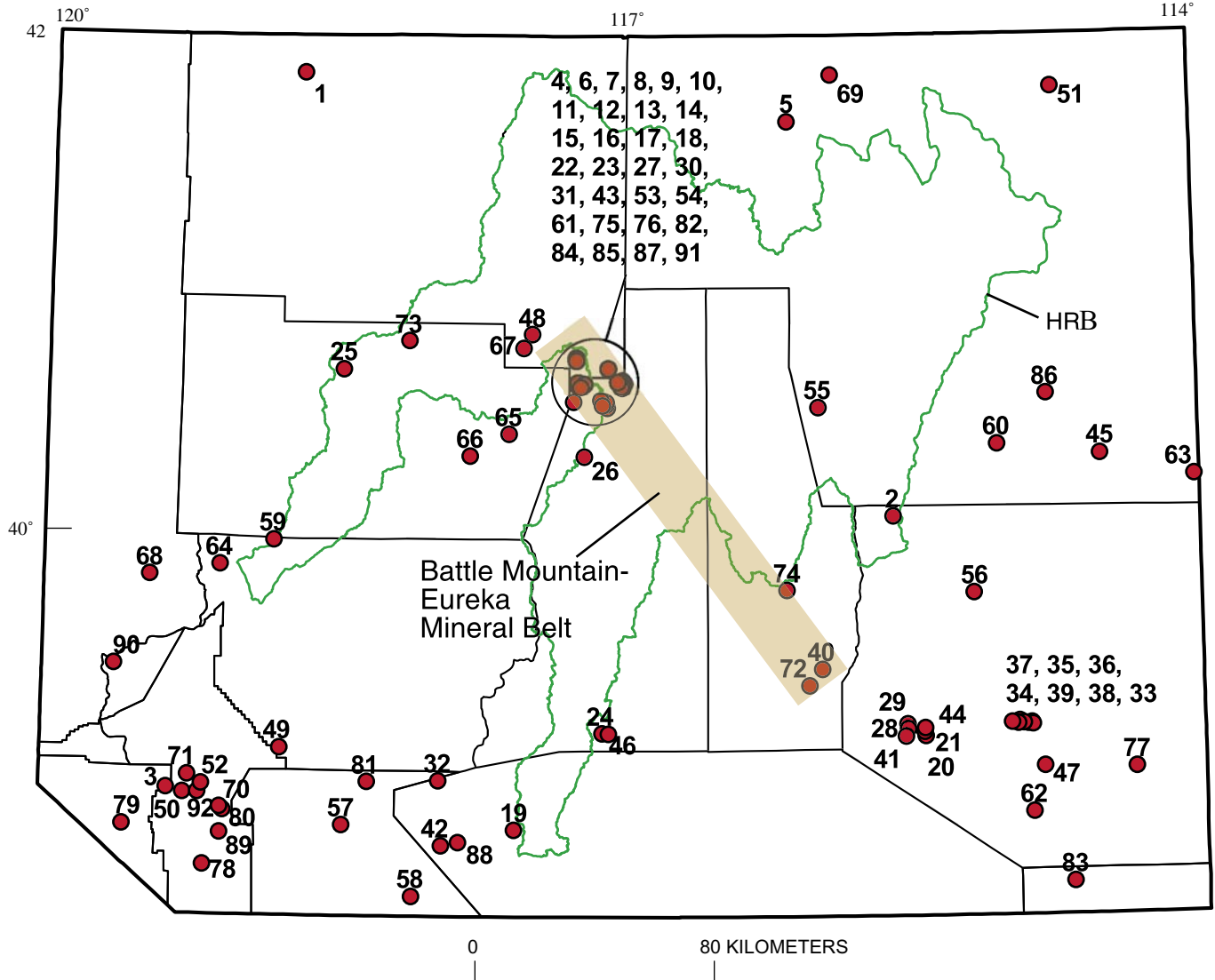
Figure 7-8. Map showing locations of 92 mineralized sites (red circles) in northern Nevada that comprise the training set for the evaluation of pluton-related favorability. Numbers same as in table 7–1. Battle Mountain-Eureka mineral belt of Roberts (1966) and boundary of Humboldt River Basin (HRB) also shown.
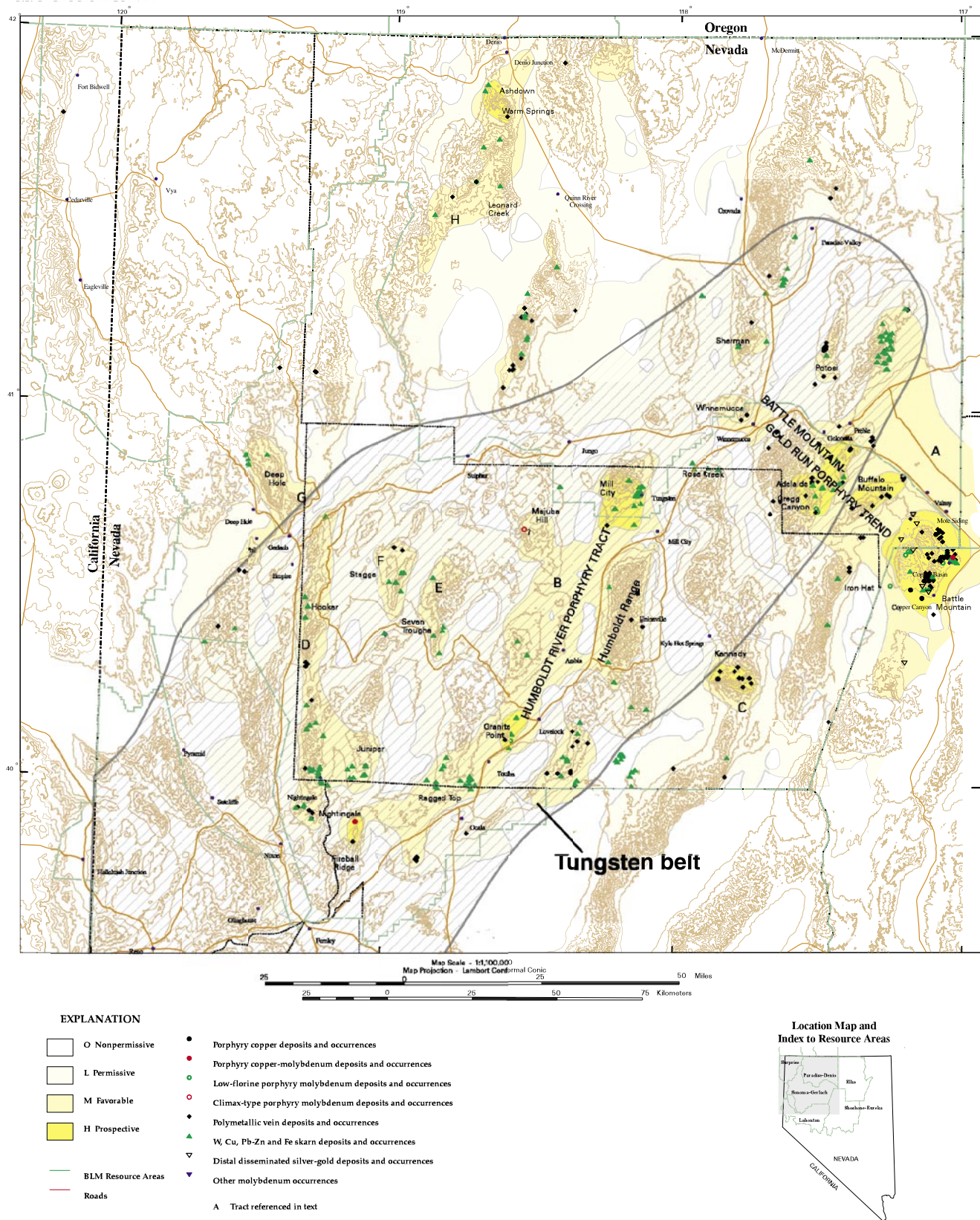
Figure 7-9. Map showing tracts for pluton-related deposits and tungsten belt in the U.S. Bureau of Land Management Winnemucca District and Surprise resource area, northwest Nevada and northeast California. Modified from Peters and others (1996) and Stager and Tingley (1988).
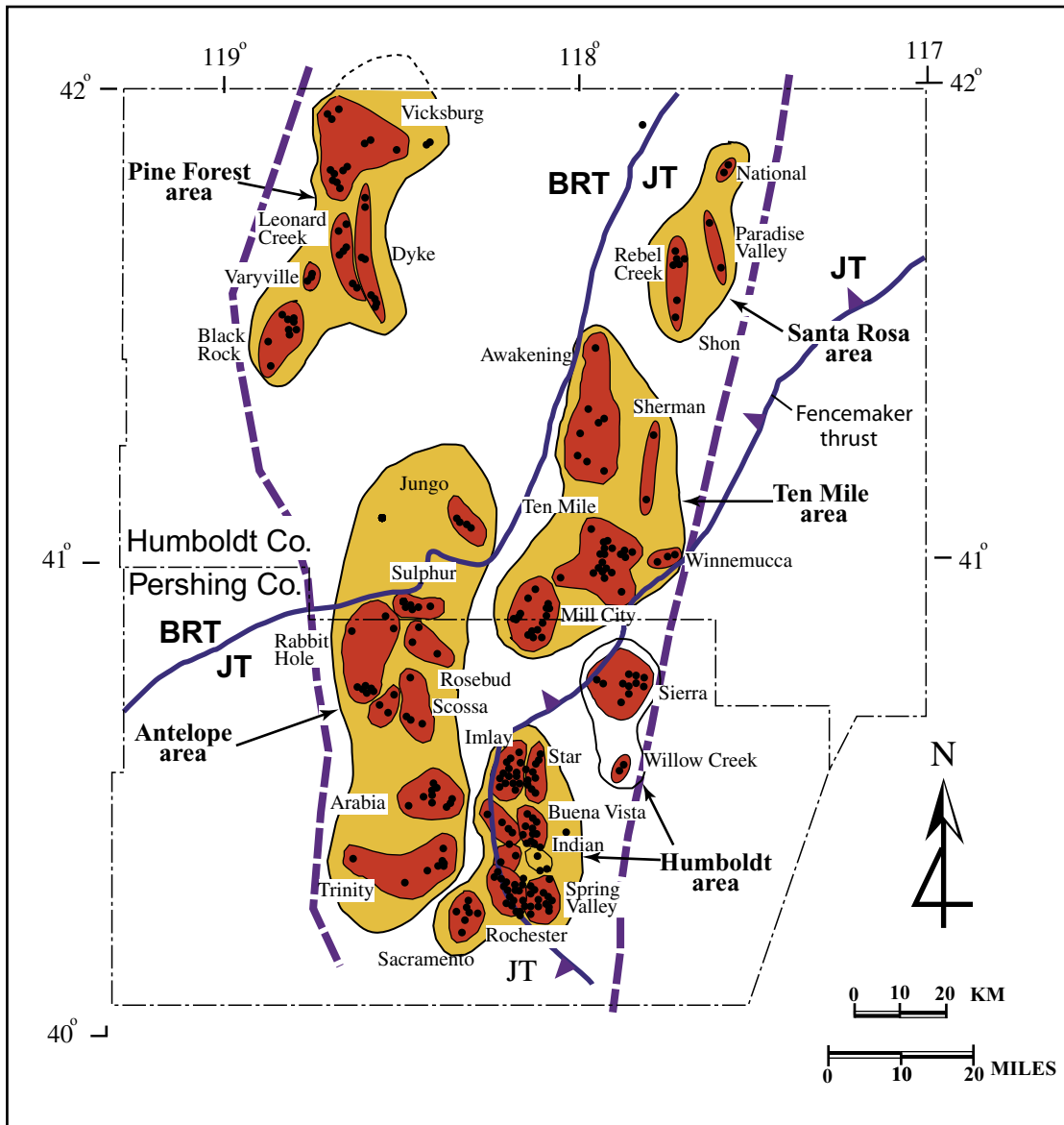
Figure 7-10. Map showing distribution of low-sulfide Au–quartz veins (dots) and mining districts in northwestern Nevada (plotted from MRDS records of U.S. Geological Survey and Peters and others, 1996). Bold dashed lines (blue) indicate boundaries of inferred regional-scale Late Cretaceous shear zone. JT, Jungo terrane; BRT, Black Rock terrane from Silberling and others (1984, 1987). Modified from Cheong and others (2000).
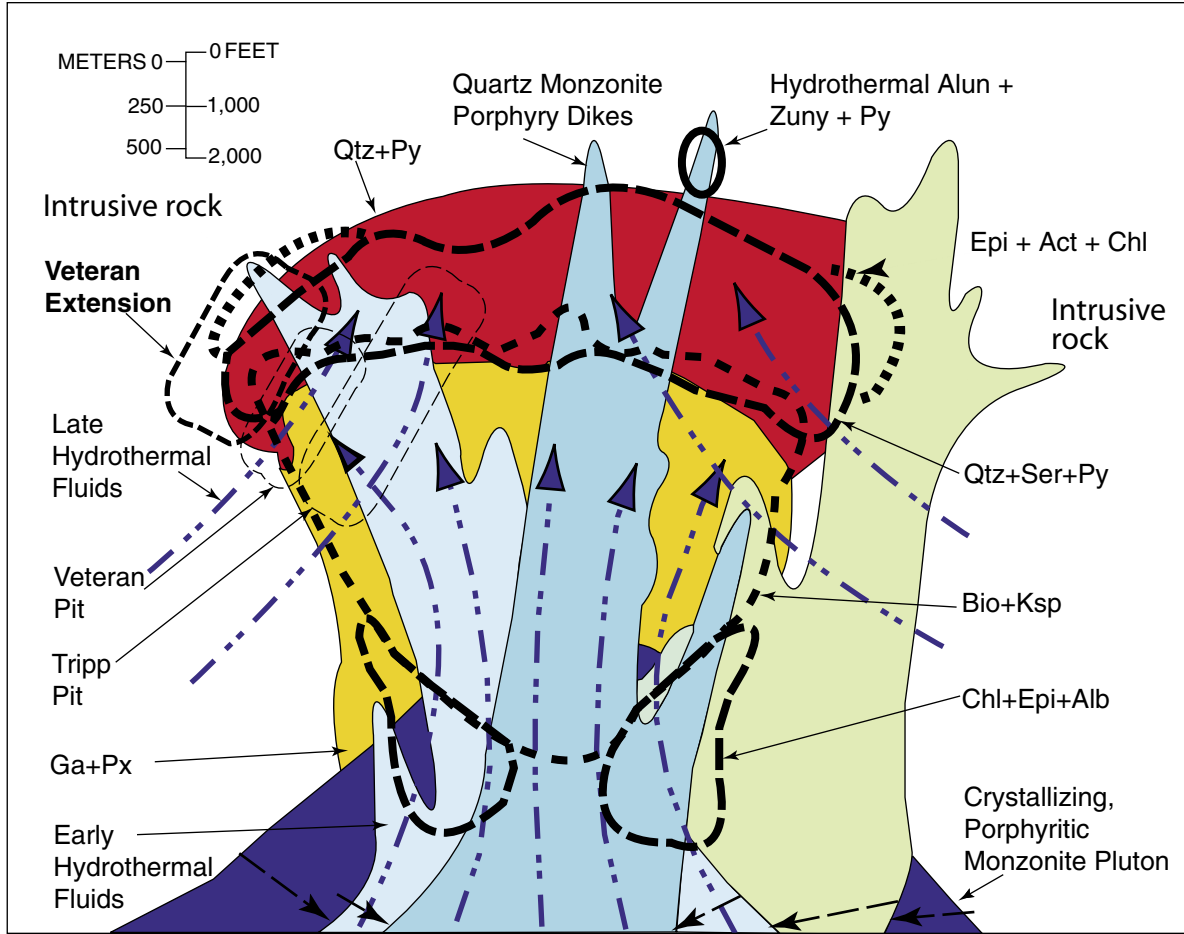
Figure 7-11.   Schematic cross-section through reconstructed Cretaceous porphyry copper system in the Robinson Mining District, Nevada. Filled areas are intrusive rocks and hydrothermal wall rock alteration. Heavy outlines show approximate extent of zones of hydrothermal alteration of porphyry. Modified from Maher (1996).
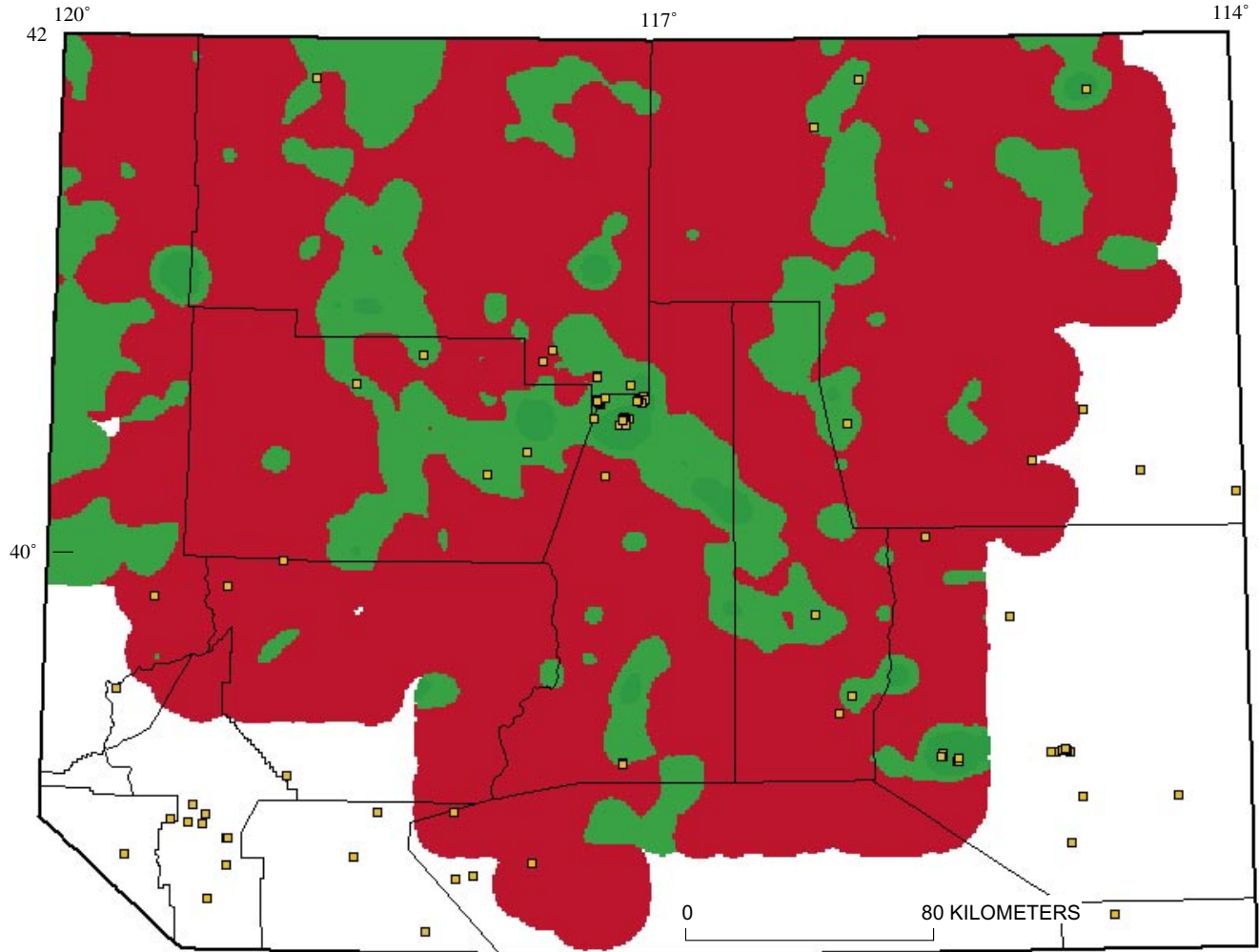
EXPLANATION

Area of strong positive association between summed Cu+Pb+Zn
 Z–scores and sites of pluton-related training set.

Area of positive association between summed Cu+Pb+Zn Z–scores
 and sites of pluton-related training set.

Area of negative association between summed Cu+Pb+Zn Z–scores
 and sites of pluton-related training set.

Pluton-related training site (same as table P–1).

Figure 7-12.   Distribution of normalized Z–score values of additive Cu+Pb+Zn (see text) in sediments (Folger, 2000) in northern Nevada. Small squares, locations of 92 sites in table 7–1 that comprise training set for pluton-related occurrences.
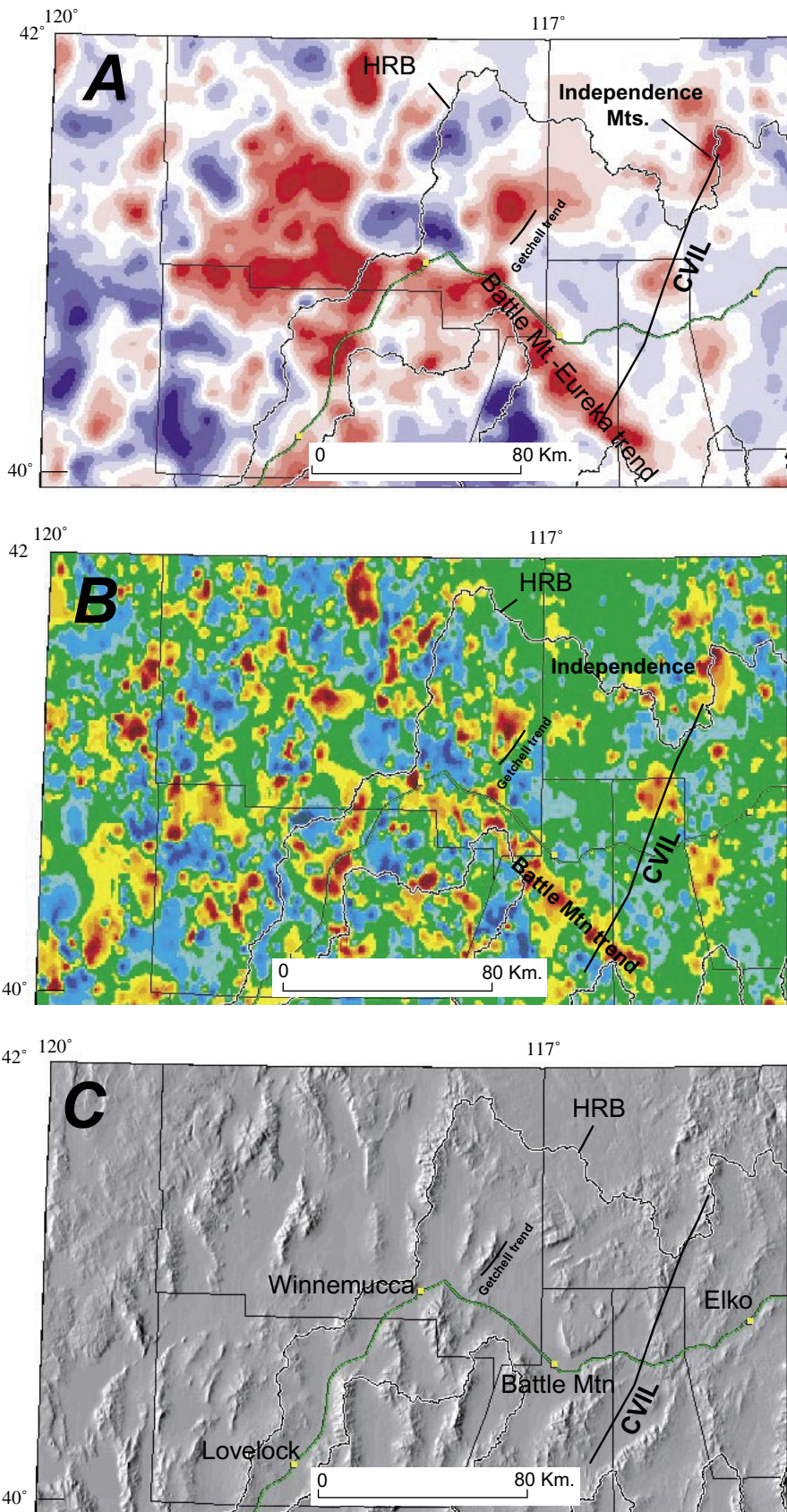
Figure 7-13. Arsenic distribution in National Uranium Resource Evaluation (NURE) sediment samples reanalyzed by Folger (2000) in the north-central part of the Humboldt River Basin (HRB), Nevada. A, Log As distributions contoured in quartile standard deviations from the mean (hotter colors represent higher deviations); B, Contoured As distributions (hotter colors represent higher contents) (S. Ludington, written commun., 2000); C, digital elevation model of north-central part of HRB. CVIL, Crescent Valley-Independence lineament of Peters (1998, 2000).

Figure 7-14. Geologic sketch map of the Jurassic Yerington Batholith as exposed beneath early Tertiary rocks. Modified from Dilles and Proffett (1995).
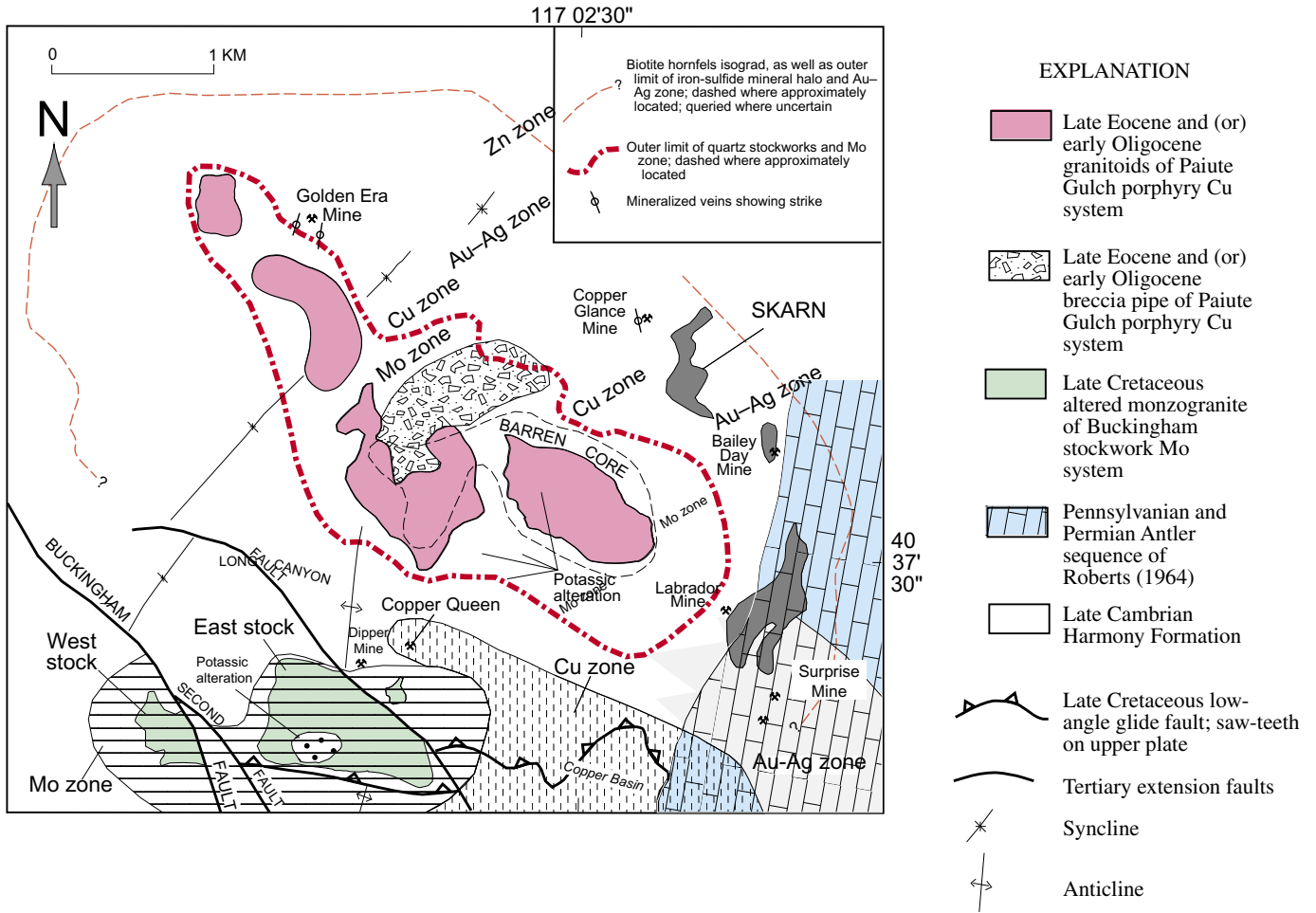
Figure 7-15. Geologic sketch map showing superposition of metal zones of late Eocene and (or) Early Oligocene Paiute Gulch porphyry Cu system onto metal zones of Late Cretaceous Buckingham low–F stockwork Mo system, Battle Mountain Mining District, Nevada. Modified from Ivosevic and Theodore (1996).
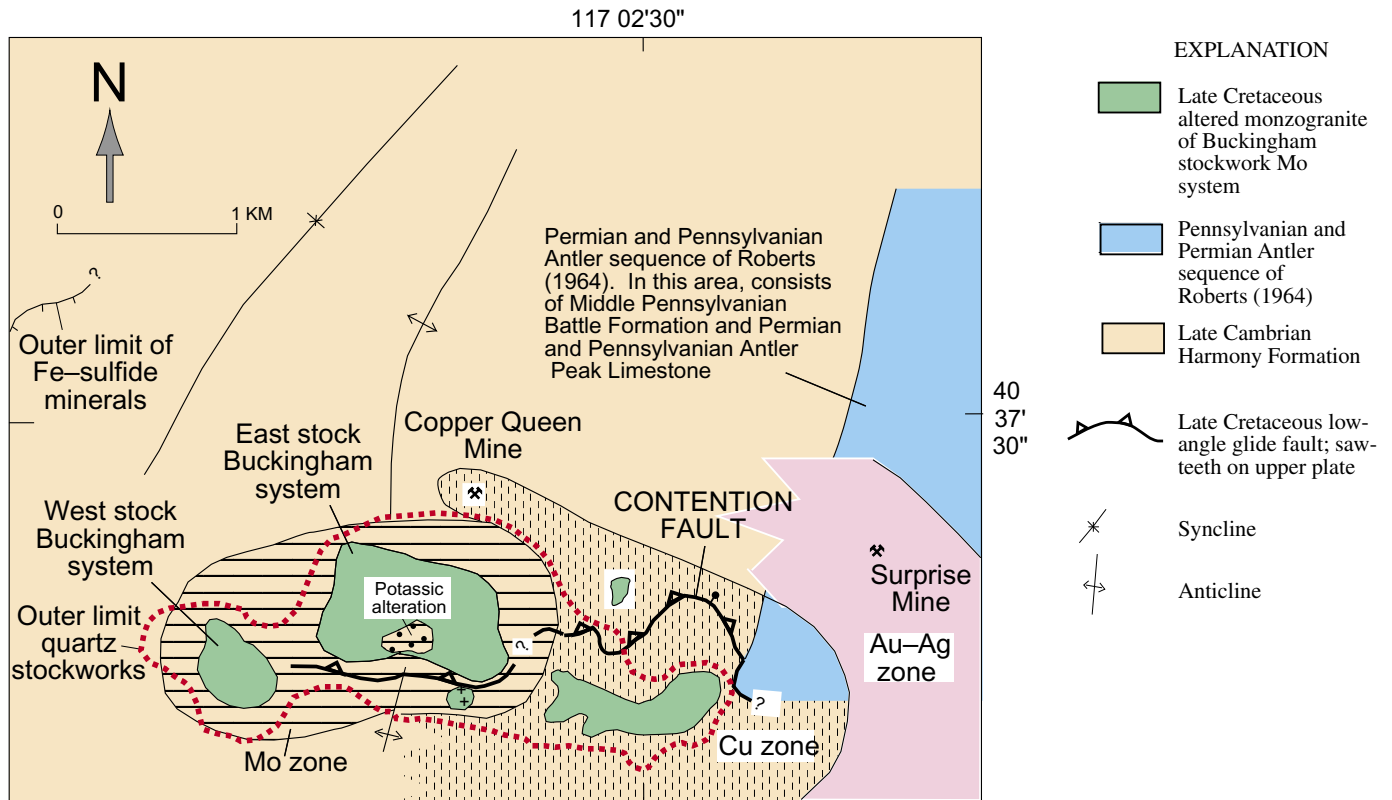
Figure 7-16.   Geologic sketch map showing reconstructed metal zones of Late Cretaceous Buckingham low–F stockwork Mo system after removal of Tertiary extension, Battle Mountain Mining District, Nevada. Modified from Ivosevic and Theodore (1996).
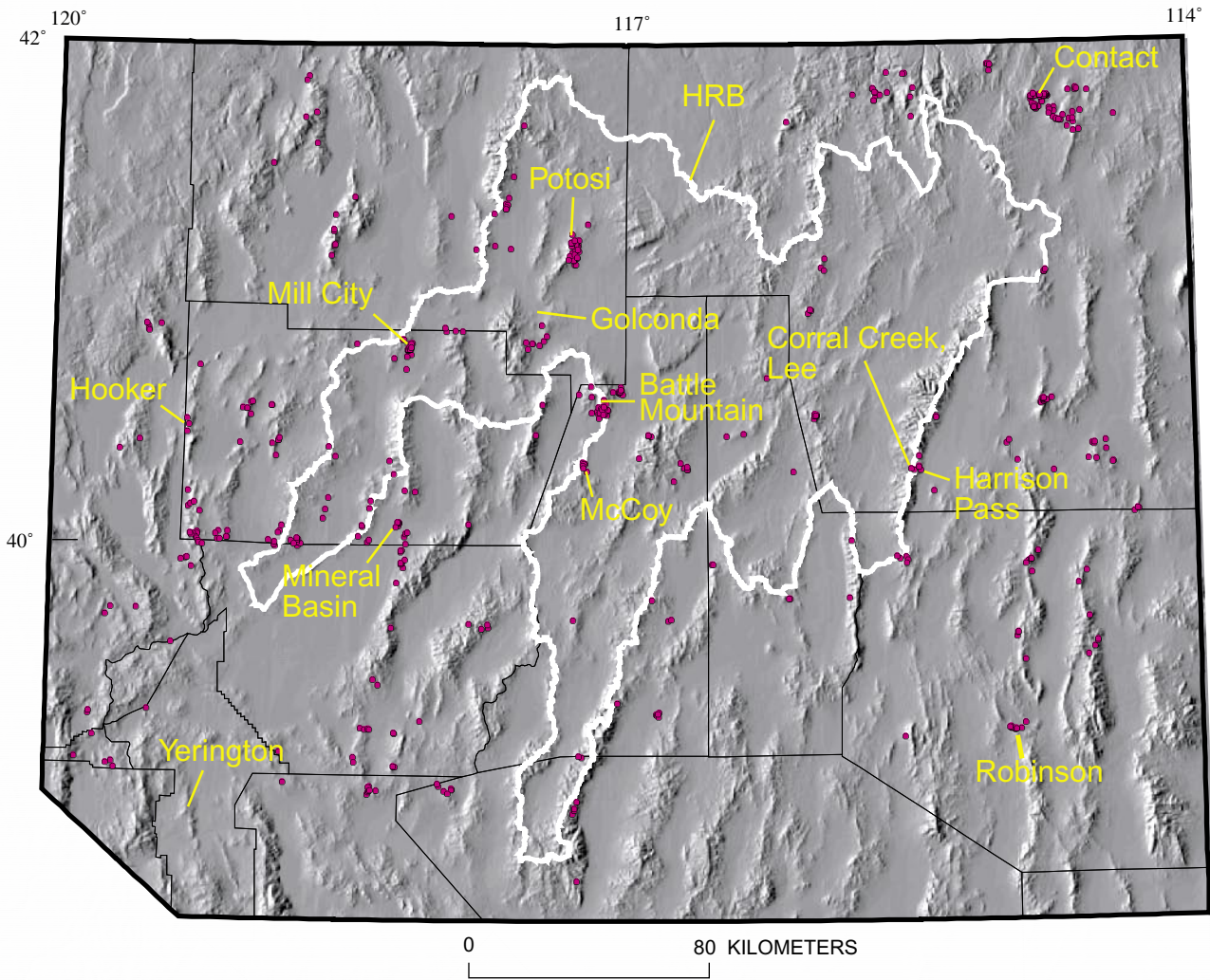
Figure 7-17. Digital elevation map of northern Nevada showing locations of W skarn; porphyry Cu, skarn related; Cu skarn; Zn–Pb skarn; and Fe skarn occurrences (red dots) in U.S. Geological Survey Mineral Resource Data System (MRDS) and outline of Humboldt River Basin (HRB). Names and locations of a number of mining districts also shown.
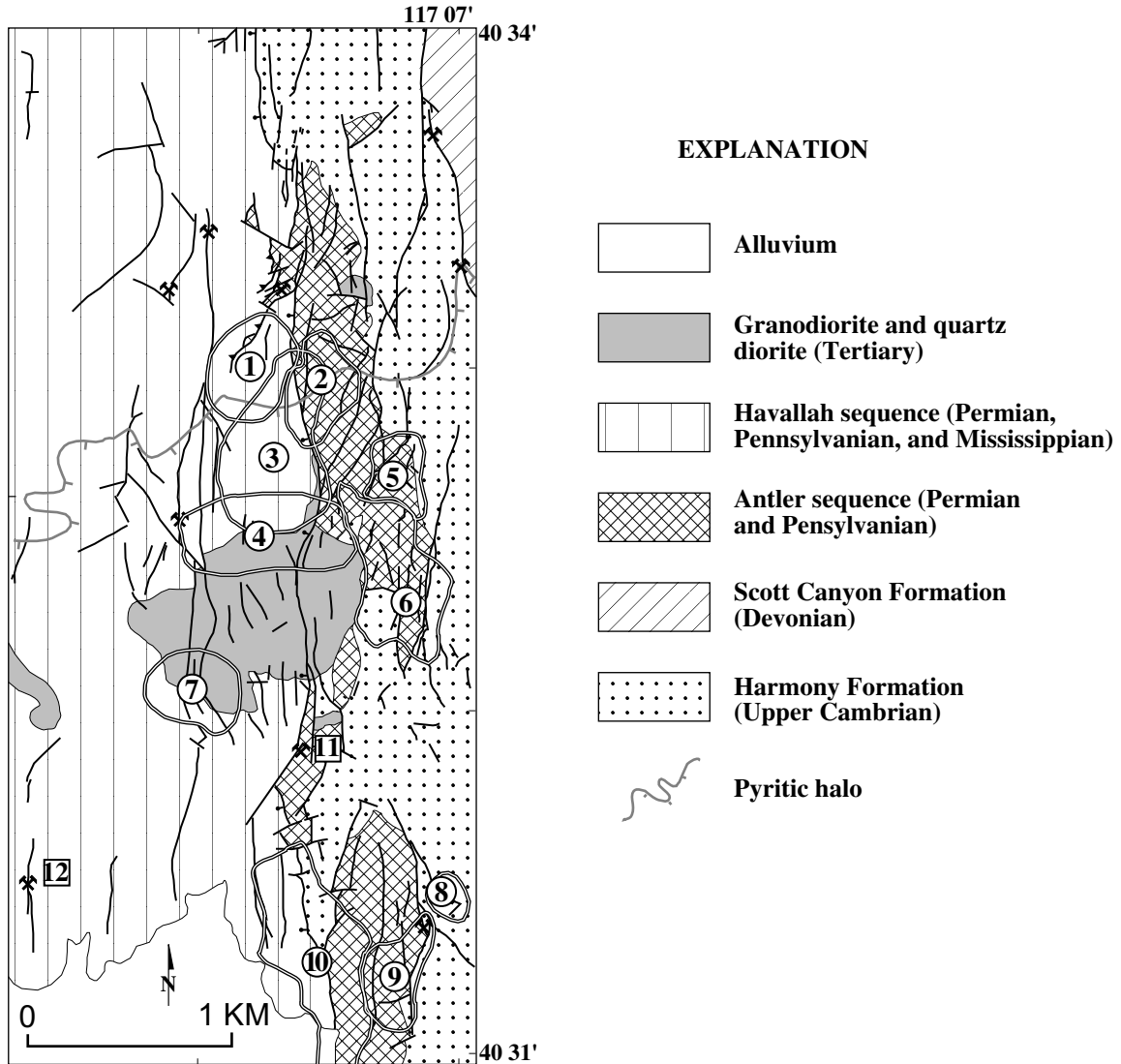
Figure 7-18. Geology of the Copper Canyon area (modified from Theodore and Blake 1975). Deposit nos. 1–12: 1, Lower Fortitude; 2, Upper Fortitude; 3, Phoenix; 4, West Orebody; 5, Northeast Extension; 6, East Orebody; 7, Reona; 8, Minnie; 9, Tomboy; 10, Midas; 11, Copper Canyon underground (Cu–Pb–Zn); 12, Wilson-Independence (Au–Ag). Deposit numbers in circles indicate large Au–Ag deposits previously mined, or scheduled to be mined in the future, by open-pit methods. Deposit numbers in squares are underground mines. Modified from Kotlyar and others (1998b).
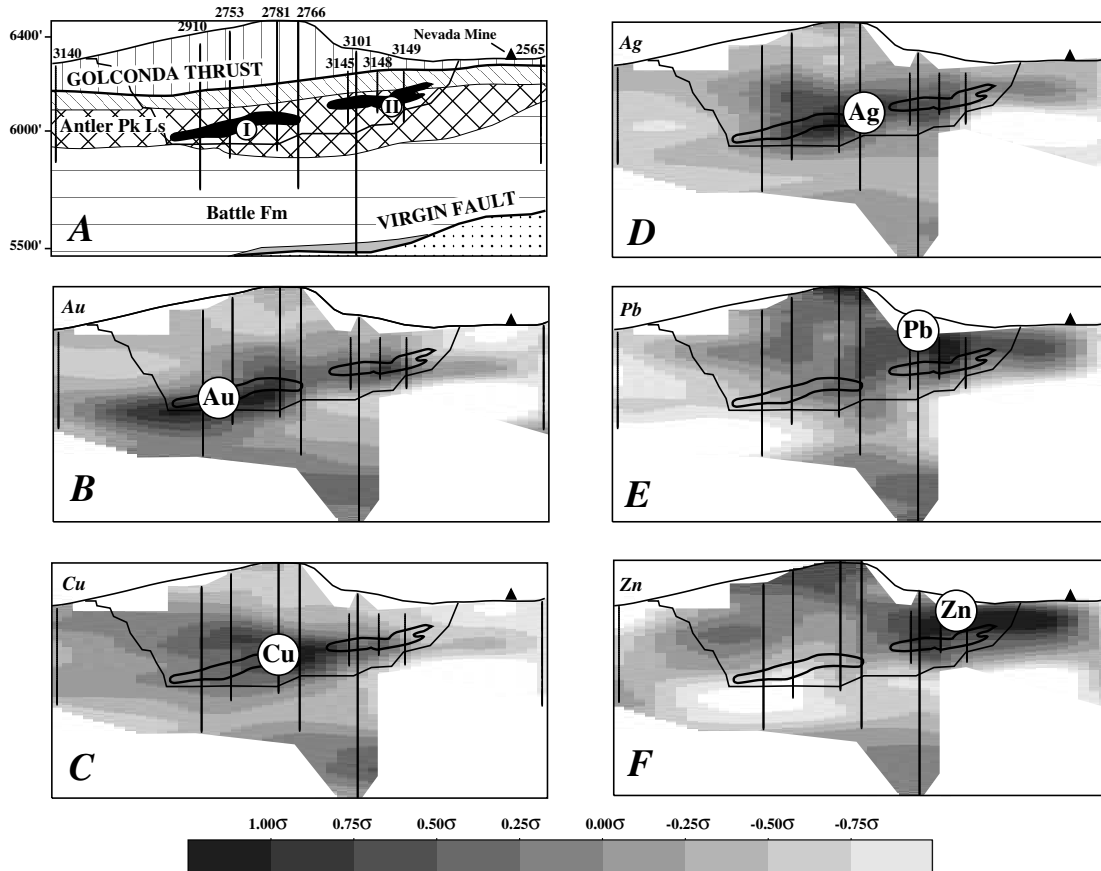
Figure 7-19.   Geology (*A*) and normalized, gridded, and filtered (see Kotlyar and others, 1998b) distributions of Au (*B*), Cu (*C*), Ag (*D*), Pb (*E*), and Zn (*F*) in north-south cross section through Lower Fortitude Au–skarn deposits, Battle Mountain Mining District, Nevada. Explanation for *A* same as figure 7-18; black, projection of ore in Lower Fortitude to plane of section. More densely shaded patterns (in *B–F*) represent higher deviations from a mean distribution. Circled chemical symbols represent respective loci for most intensely concentrated presence of proximal (Cu, Au, Ag) and distal metals (Pb, Zn). I, Southern orebody of Lower Fortitude; II, Northern orebody of Lower Fortitude. Modified from Kotlyar and others (1998b).

Figure 7-20. Map of the Phoenix project area, Battle Mountain Mining District, Nevada, showing major granodiorite stocks, the 1999 year-end pits, and the previously mined open-pits. The following are the previously mined open-pit names and metals produced: (1) Copper Canyon Underground Mine, Cu–Au–Ag; (2) West, Cu–Au–Ag; (3) East, Cu–Au–Ag; (4) Minnie, Au–Ag; (5) Tomboy, Au–Ag; (6) NE Extension, Au–Ag; (7) Fortitude, Au–Ag; (8) P1, Au–Ag; (9) P2, Au–Ag; (10) P3, Au–Ag; (11) Sunshine, Au–Ag; (12) Iron Canyon, Au–Ag. Modified from Cary and others (2000).
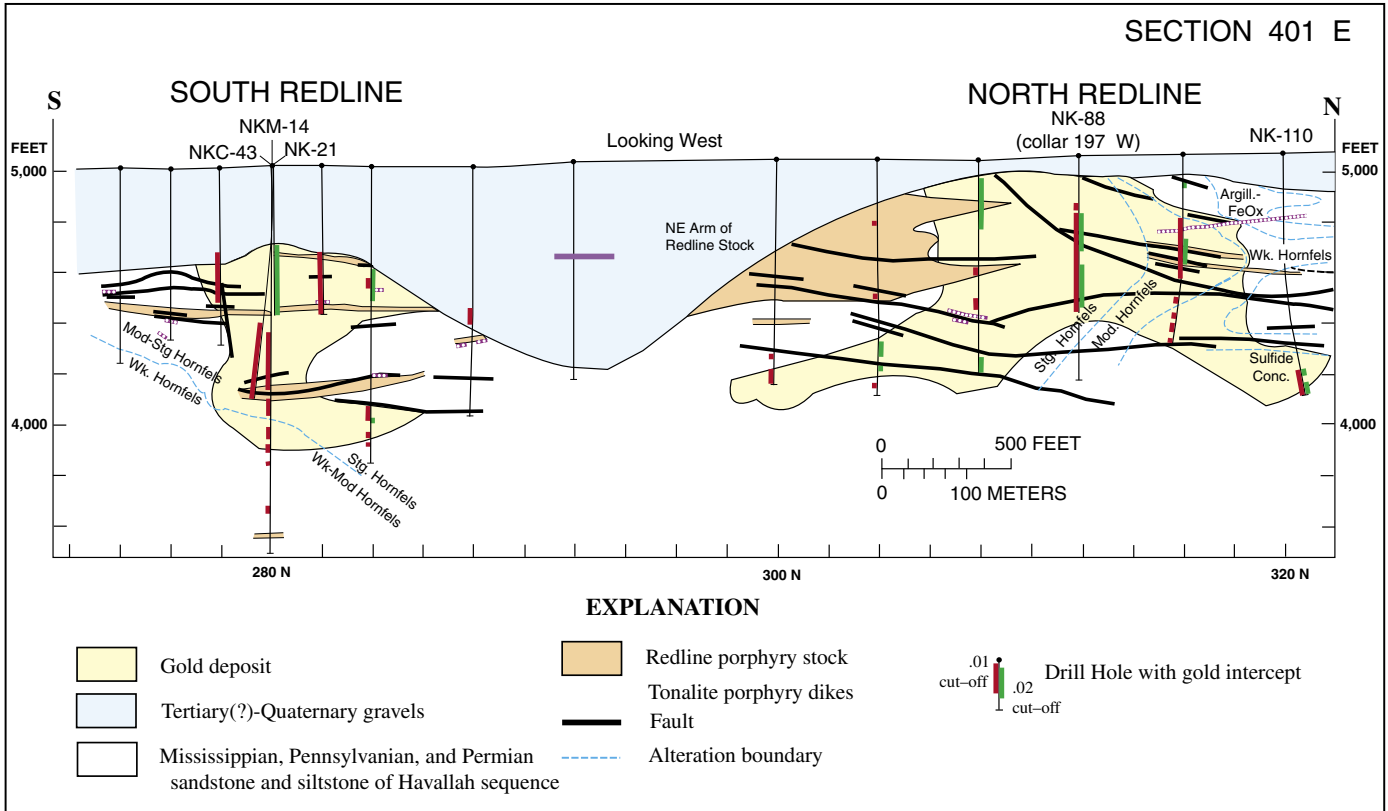
Figure 7-21.   Cross section through North and South Redline deposit, Buffalo Valley, Battle Mountain Mining District, Nevada. Modified from Cleveland (2000).
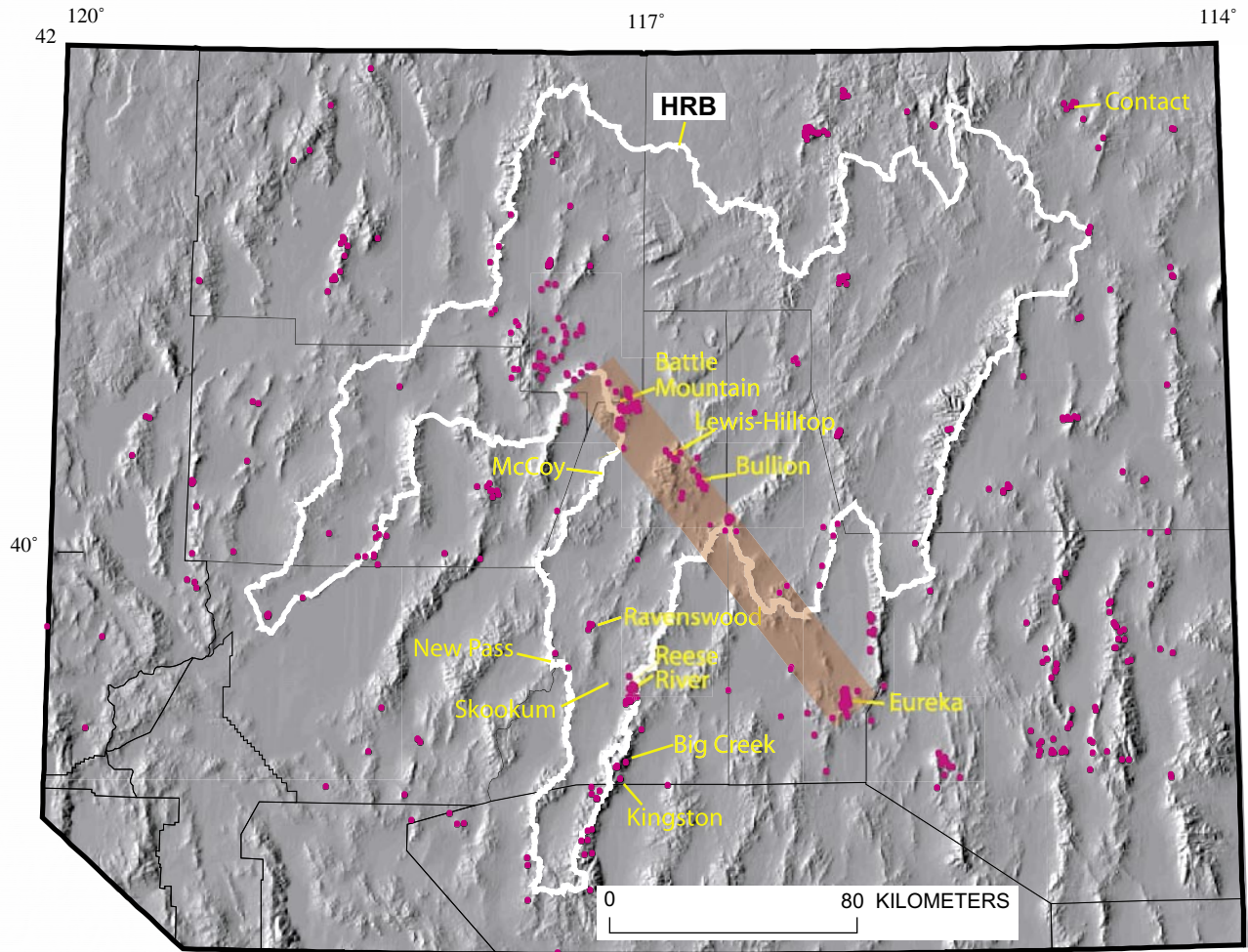
Figure 7-22. Digital elevation model of northern Nevada showing locations of polymetallic replacement, replacement Mn, and polymetallic vein mineral occurrences (red dots) in U.S. Geological Survey Mineral Resources Data System (MRDS) and outline of Humboldt River Basin (HRB). Locations of Battle Mountain, McCoy, Lewis-Hilltop, Bullion, Ravenswood, Skookum, New Pass, Big Creek, Kingston (Victorine), Reese River, Eureka, and Contact Mining Districts also shown.
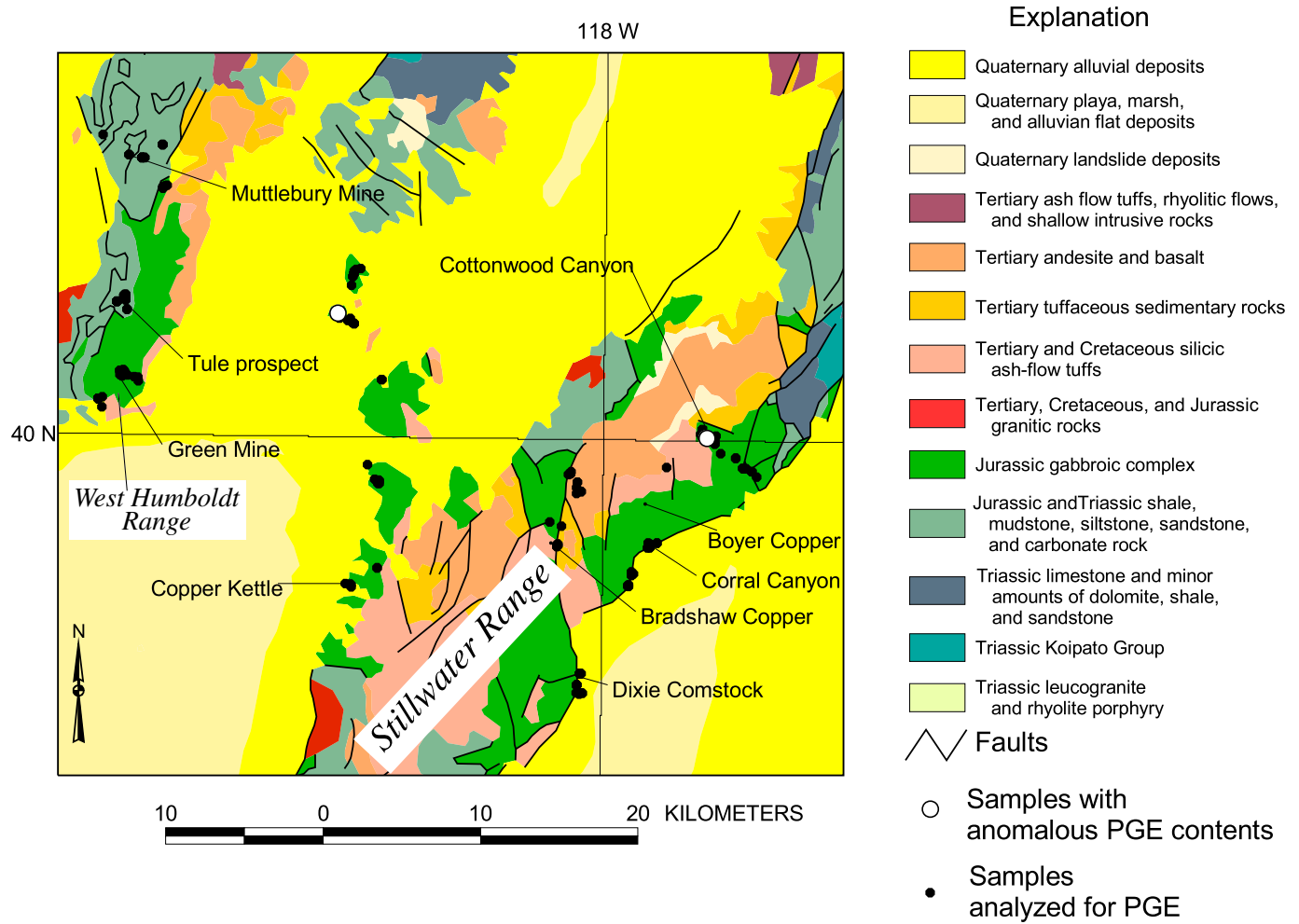
Figure 7-23. Map of parts of West Humboldt and Stillwater Ranges, Nevada, showing location of samples analyzed for platinum-group elements (PGE). Geologic base modified from Turner and others (1991).
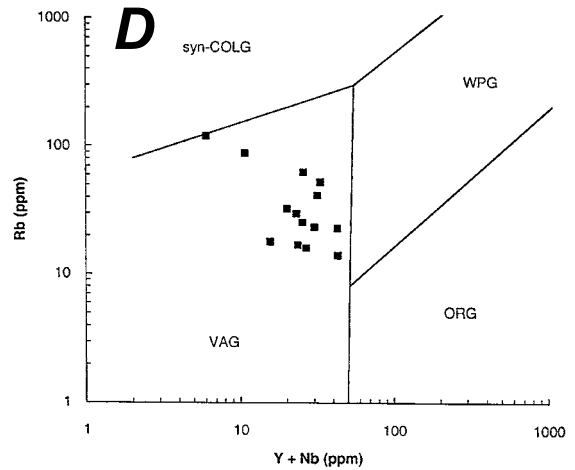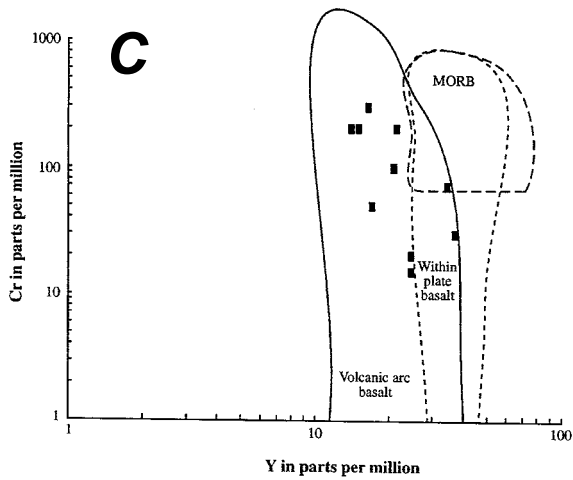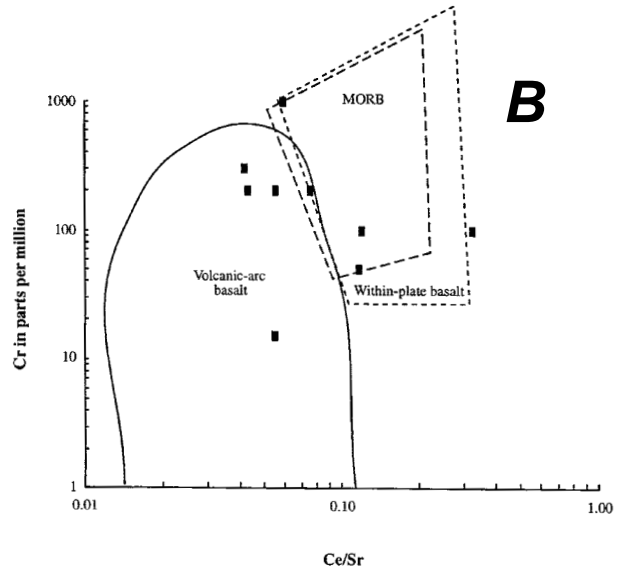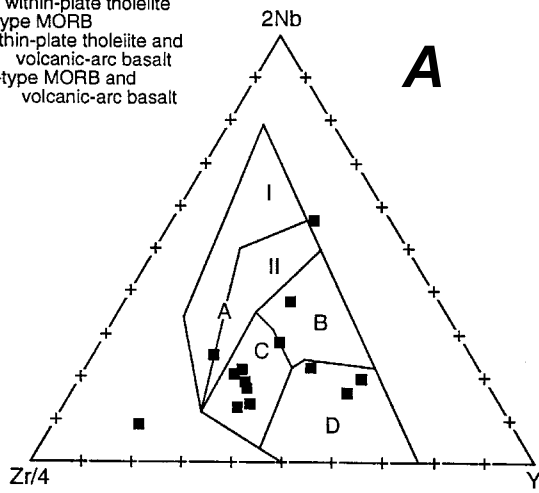
Figure 7-24.   Whole-rock trace-element data for the Humboldt mafic complex plotted on trace-element discrimination diagrams for various magmatic settings. *A*, Zr/4–2Nb–Y diagram; *B*, Cr versus Ce/Sr diagram; *C*, Cr versus Y diagram; and *D*, Rb vs. Y+Nb diagram. (*B–D*, see Pearce and Norry (1979) and Pearce (1996) for explanations of fields).
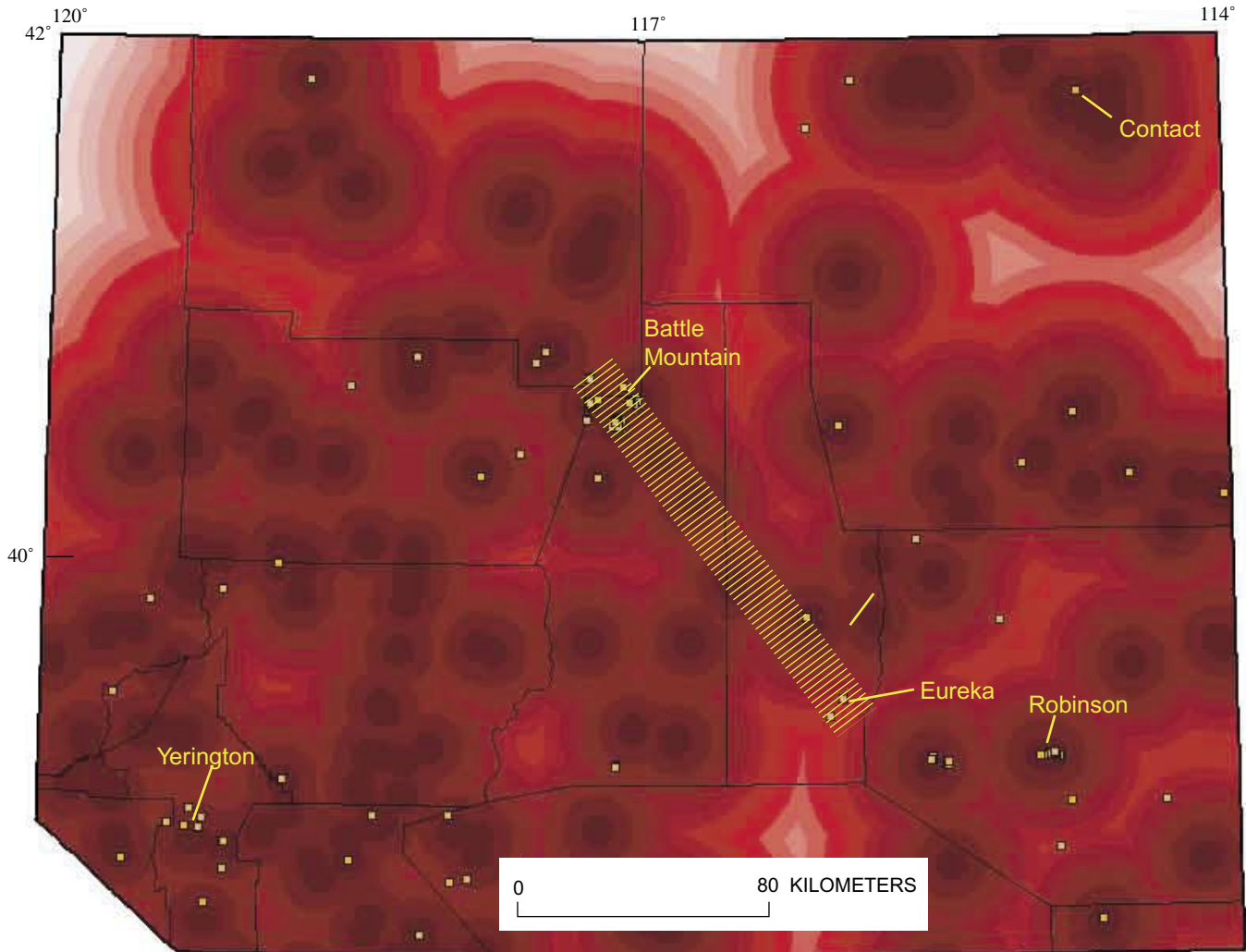
EXPLANATION

Battle Mountain- Eureka mineral belt of Roberts (1966)

Site of mineralized occurrence in MRDS used as training
set for pluton-related assessment

Figure 7-25.   Buffers around all occurrences of skarn in U.S. Geological Survey Mineral Resource Data System (MRDS) in northern Nevada compared with 92 occurrences (table P–1) that comprise training set used for evaluation. Lighter shades of red indicate increasing distance from site of skarn. Locations of Battle Mountain, Contact, Eureka, Robinson, and Yerington Mining Districts also shown.
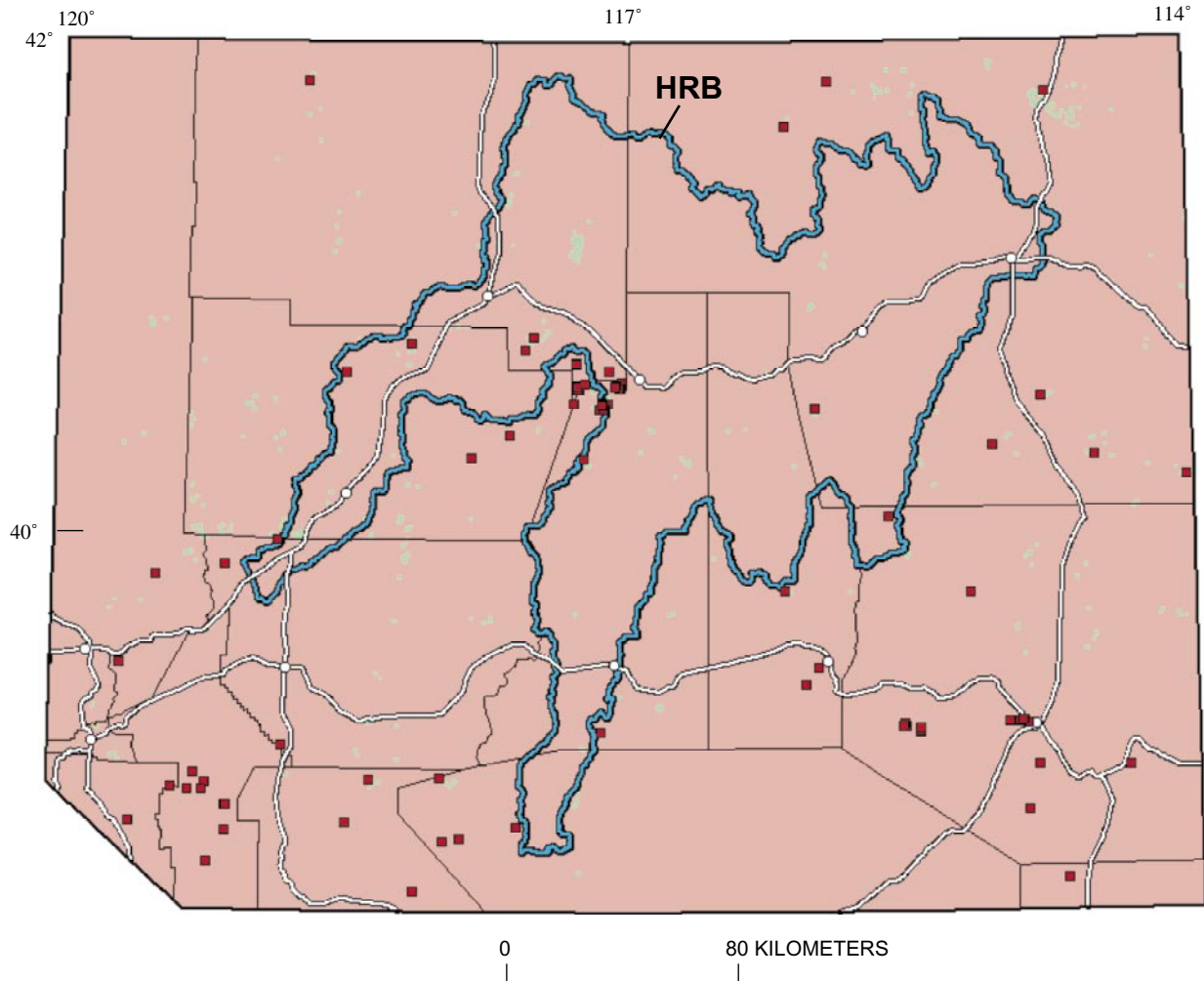
Figure 7-26. Skarn proximity evidence map of northern Nevada. Predictor pattern present, green; predictor pattern absent, red. Pluton-related deposit training sites shown as red squares. Humboldt River Basin (HRB) shown as light blue outline.
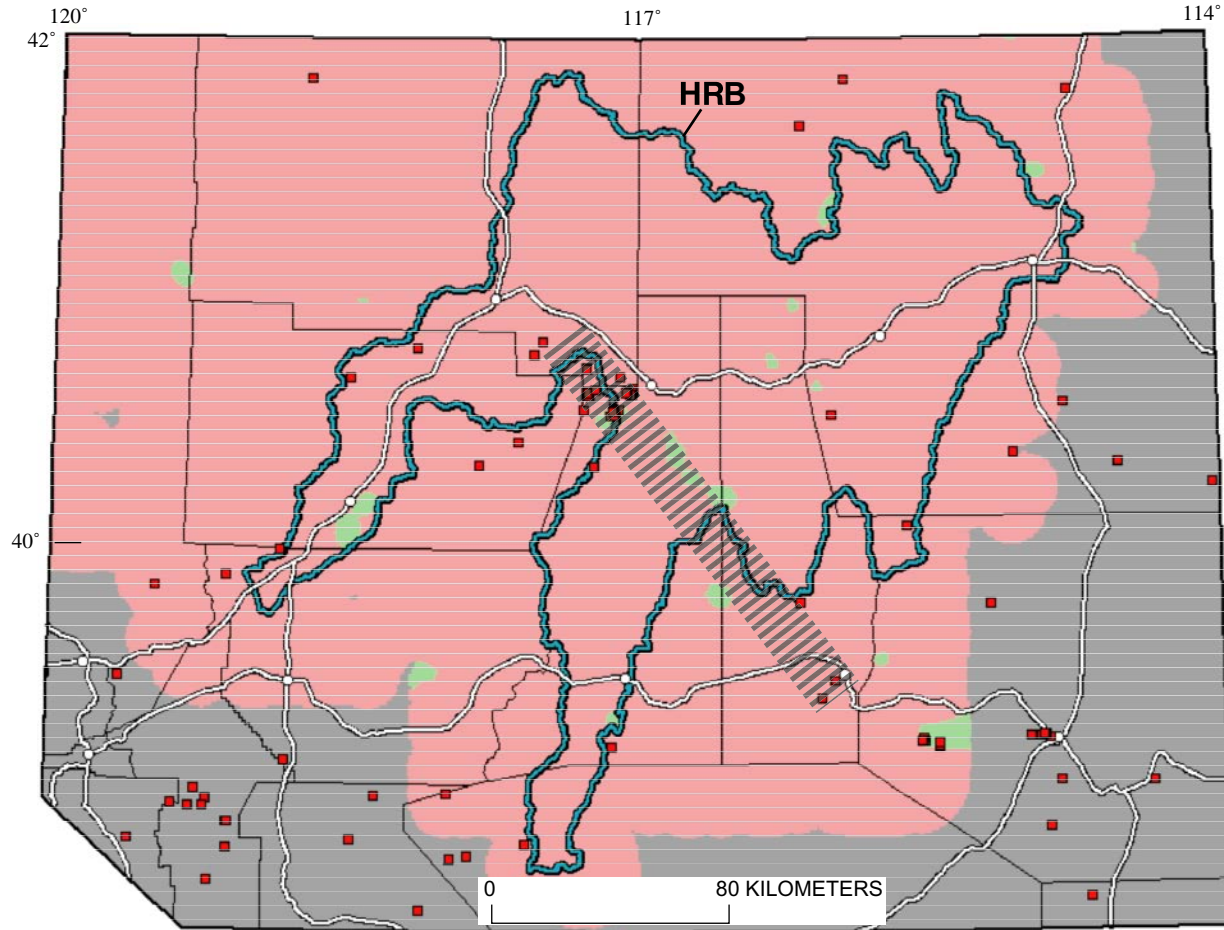
EXPLANATION

‖‖‖‖‖‖‖   Battle Mountain-Eureka mineral belt of Roberts (1966)

Figure 7-27.   Cu–Pb–Zn signature evidence map for northern Nevada from reanalyzed (Folger, 2000) National Uranium Resource Evaluation (NURE) sediment samples. Predictor pattern present, green; predictor pattern absent, red. Missing evidence map coverage shown in gray. Pluton-related deposit training sites shown as red squares. Humboldt River Basin (HRB) shown as light blue outline.
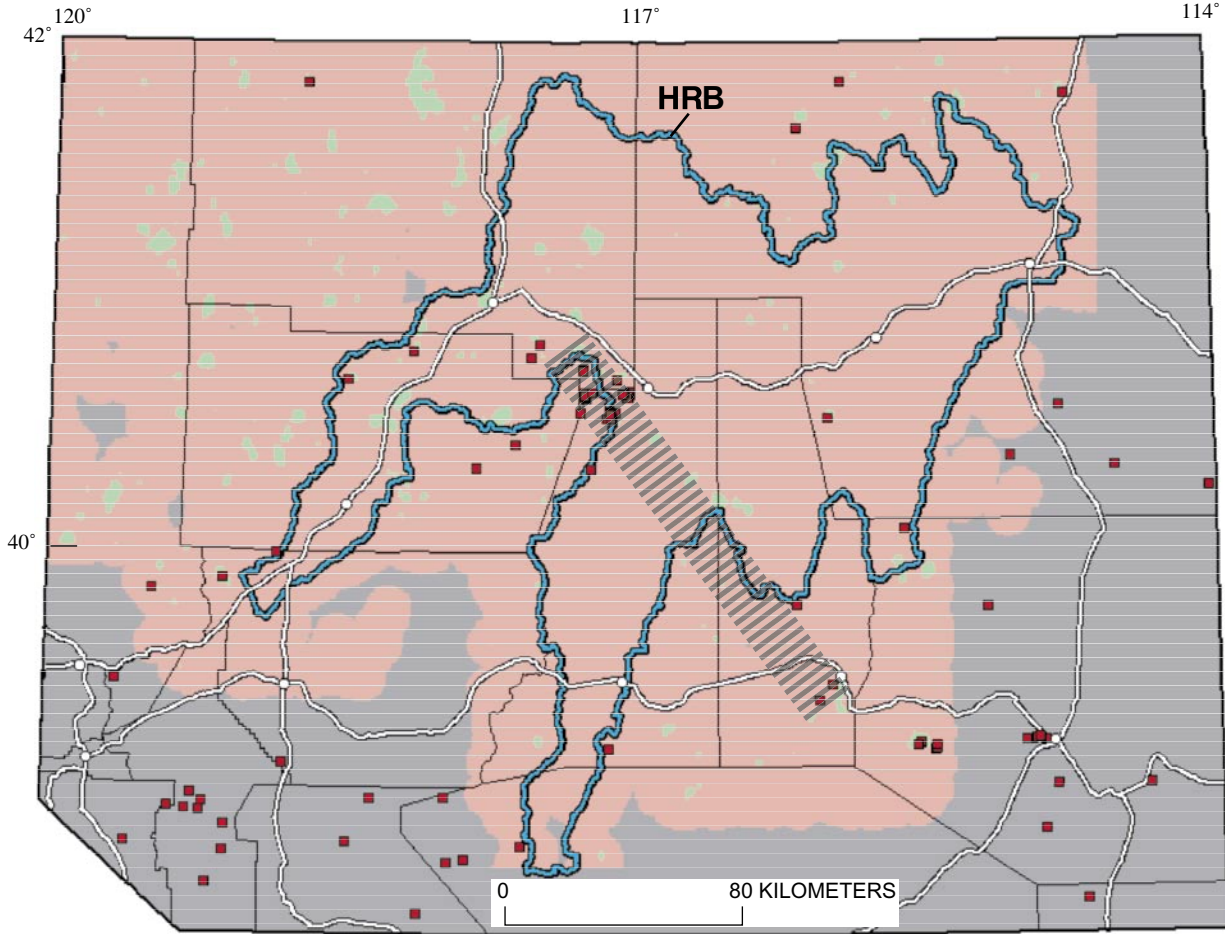
EXPLANATION

|||||||| Battle Mountain-Eureka mineral belt of Roberts (1966)

Figure 7-28.   Arsenic frequency evidence map for northern Nevada from reanalyzed (Folger, 2000) National Uranium Resource Evaluation (NURE) sediment samples. Predictor pattern present, green; predictor pattern absent, red. Missing evidence map coverage shown in gray. Pluton-related deposit training sites shown as red squares. Humboldt River Basin (HRB) shown as light blue outline.
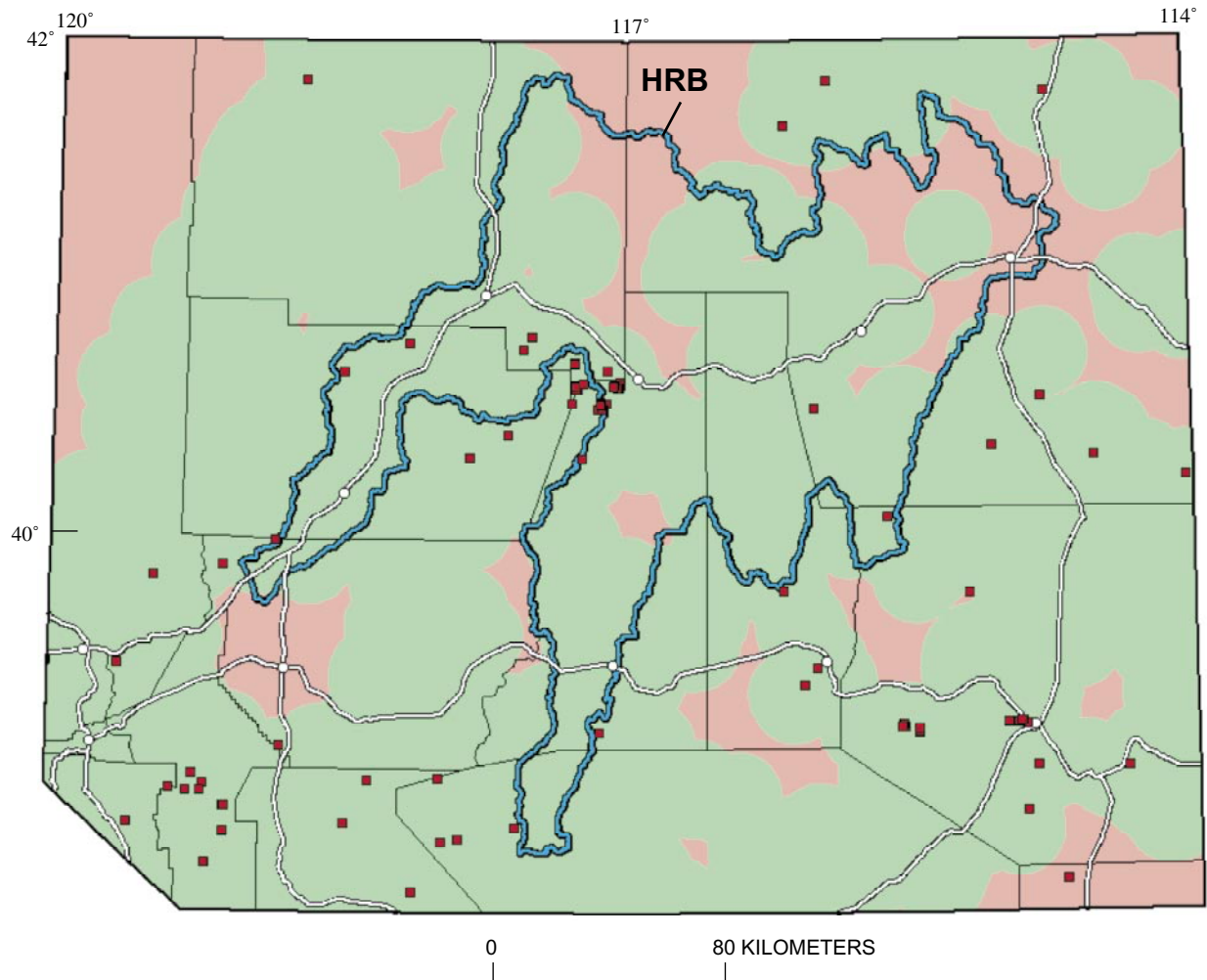
Figure 7-29.   Pluton proximity evidence map for northern Nevada. Predictor pattern present, green; predictor pattern absent, red. Pluton-related deposit training sites shown as red squares. Humboldt River Basin (HRB) shown as light blue outline.
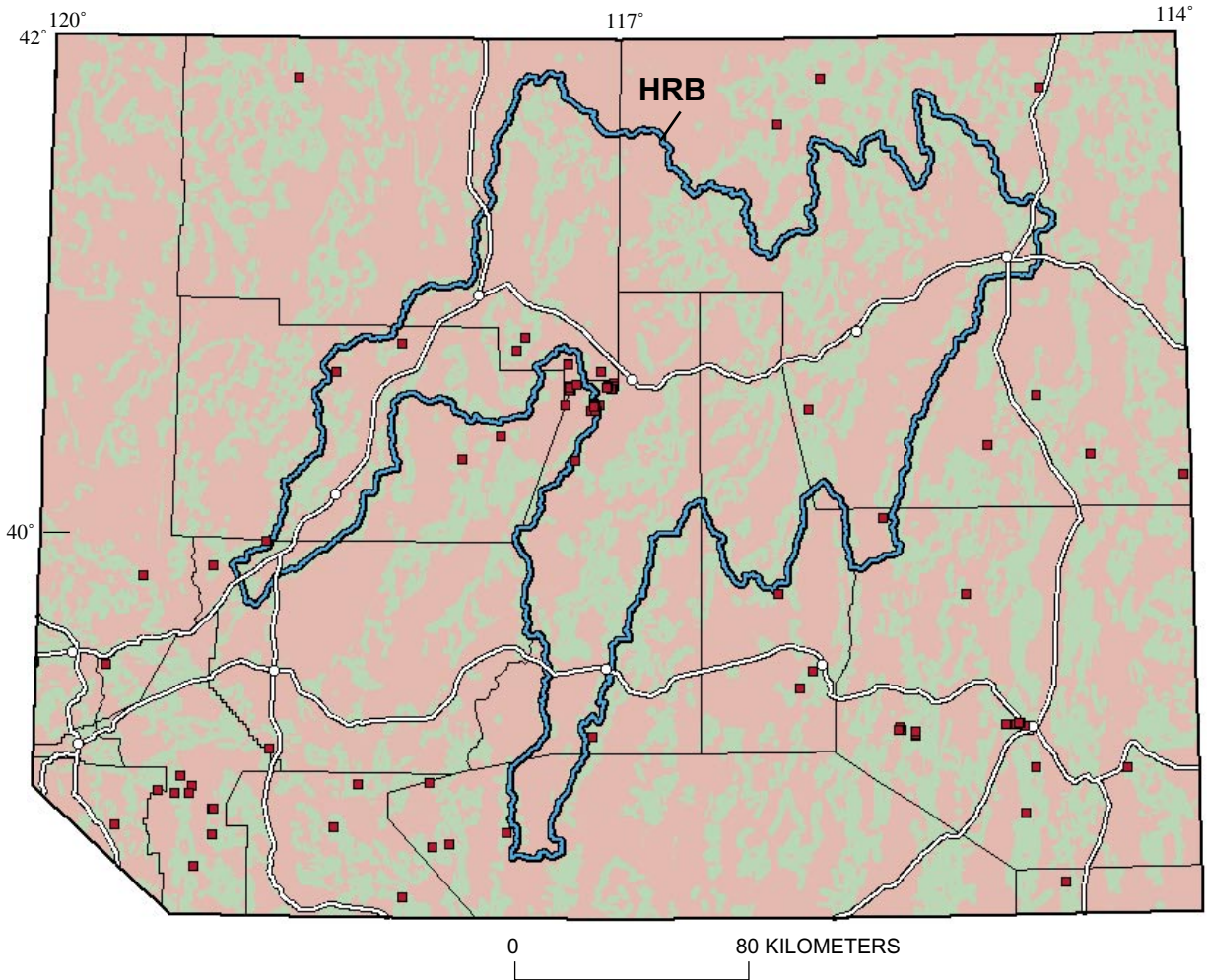
Figure 7-30.   Lithodiversity (see text) evidence map for northern Nevada. Predictor pattern present, green; predictor pattern absent, red. Pluton-related deposit training sites shown as red squares. Humboldt River Basin (HRB) shown as light blue outline.
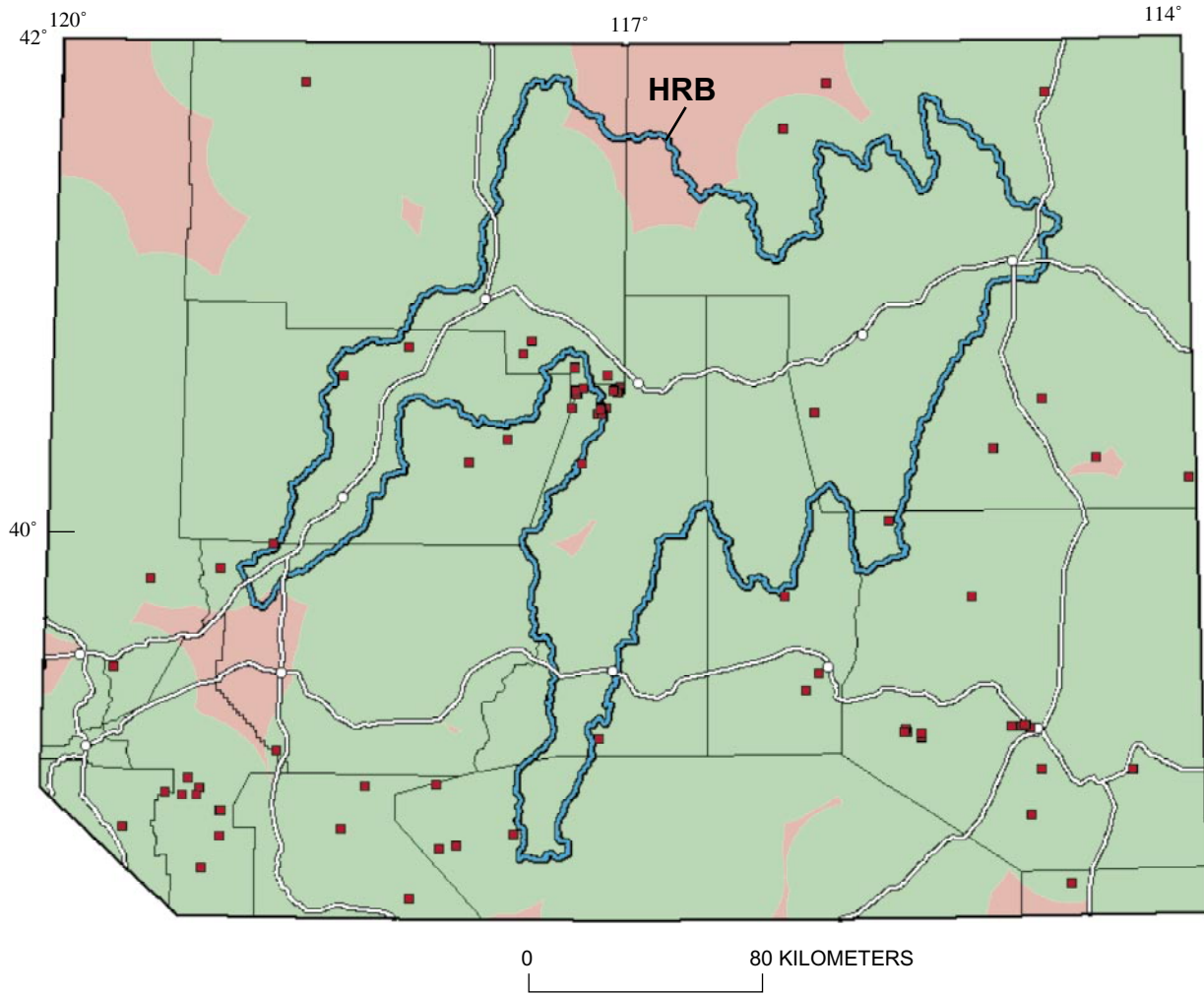
Figure 7-31.   Gravity linears (see text) proximity evidence map for northern Nevada. Predictor pattern present, green; predictor pattern absent, red. Pluton-related deposit training sites shown as red squares. Humboldt River Basin (HRB) shown as light blue outline.
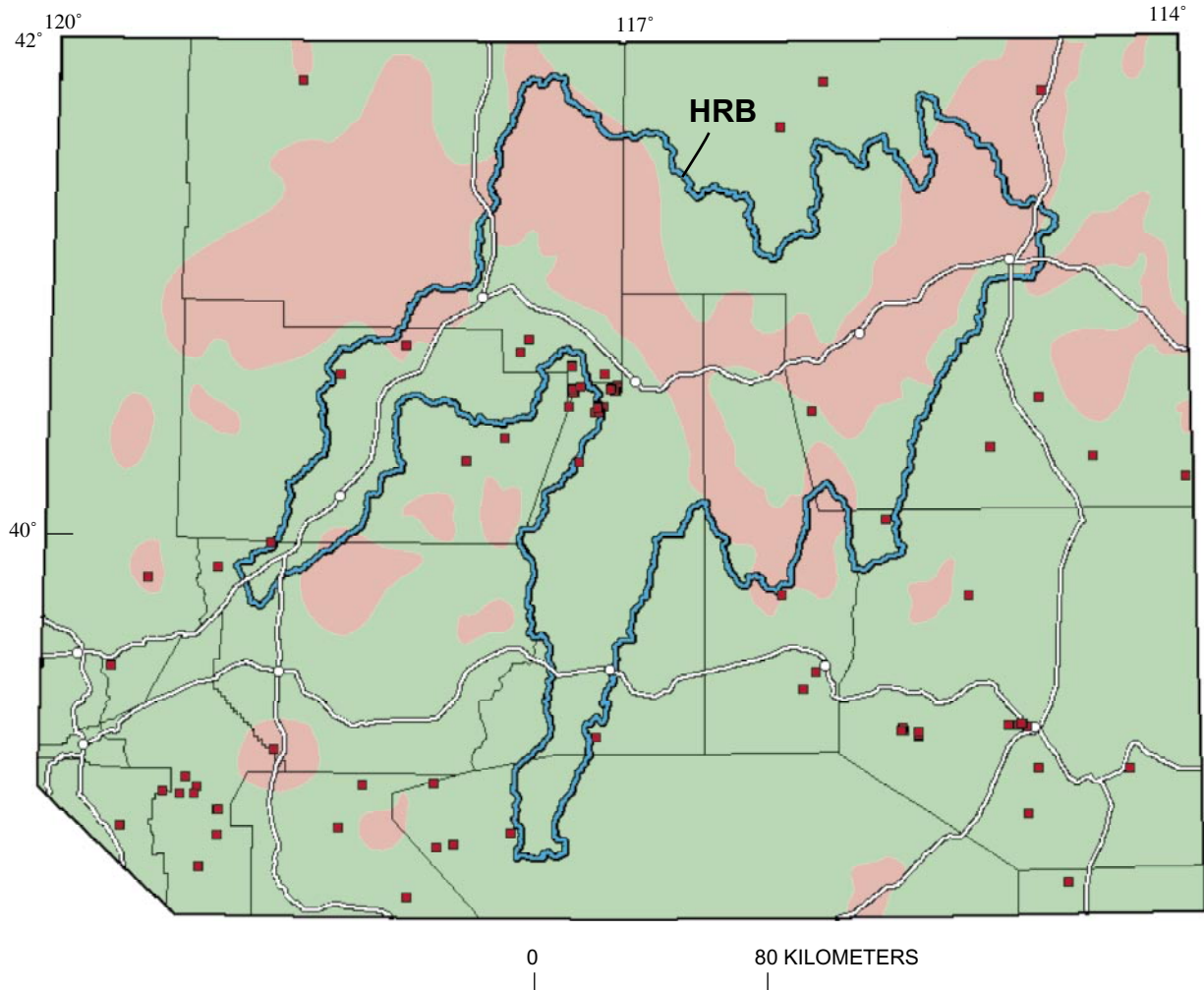
Figure 7-32.   Gravity terrane evidence map for northern Nevada. Predictor pattern present, green; predictor pattern absent, red. Pluton-related deposit training sites shown as red squares. Humboldt River Basin (HRB) shown as light blue outline.
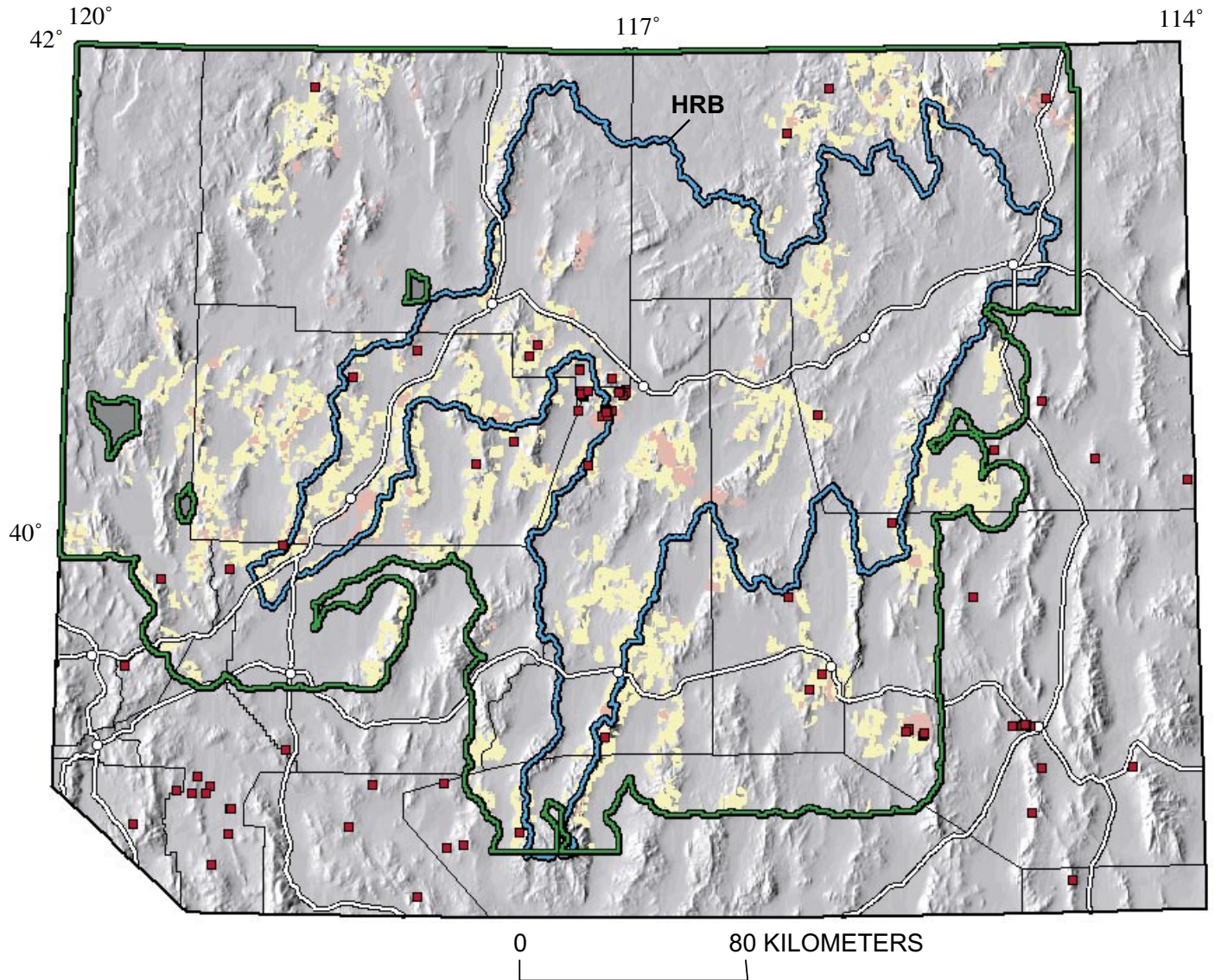
Figure 7-33.   Digital elevation map of northern Nevada showing favorability of pluton-related deposit mineral-resource assessment tracts. Prospective tracts, red; favorable tracts, yellow. Note that prospective and favorable tracts were delineated only where National Uranium Resource Evaluation (NURE) geochemical data (As frequency and Cu–Pb–Zn signature evidence) are available within light green line. Pluton-related deposit training sites shown as red squares. Humboldt River Basin (HRB) outlined in light blue; major cities and roads shown in white.
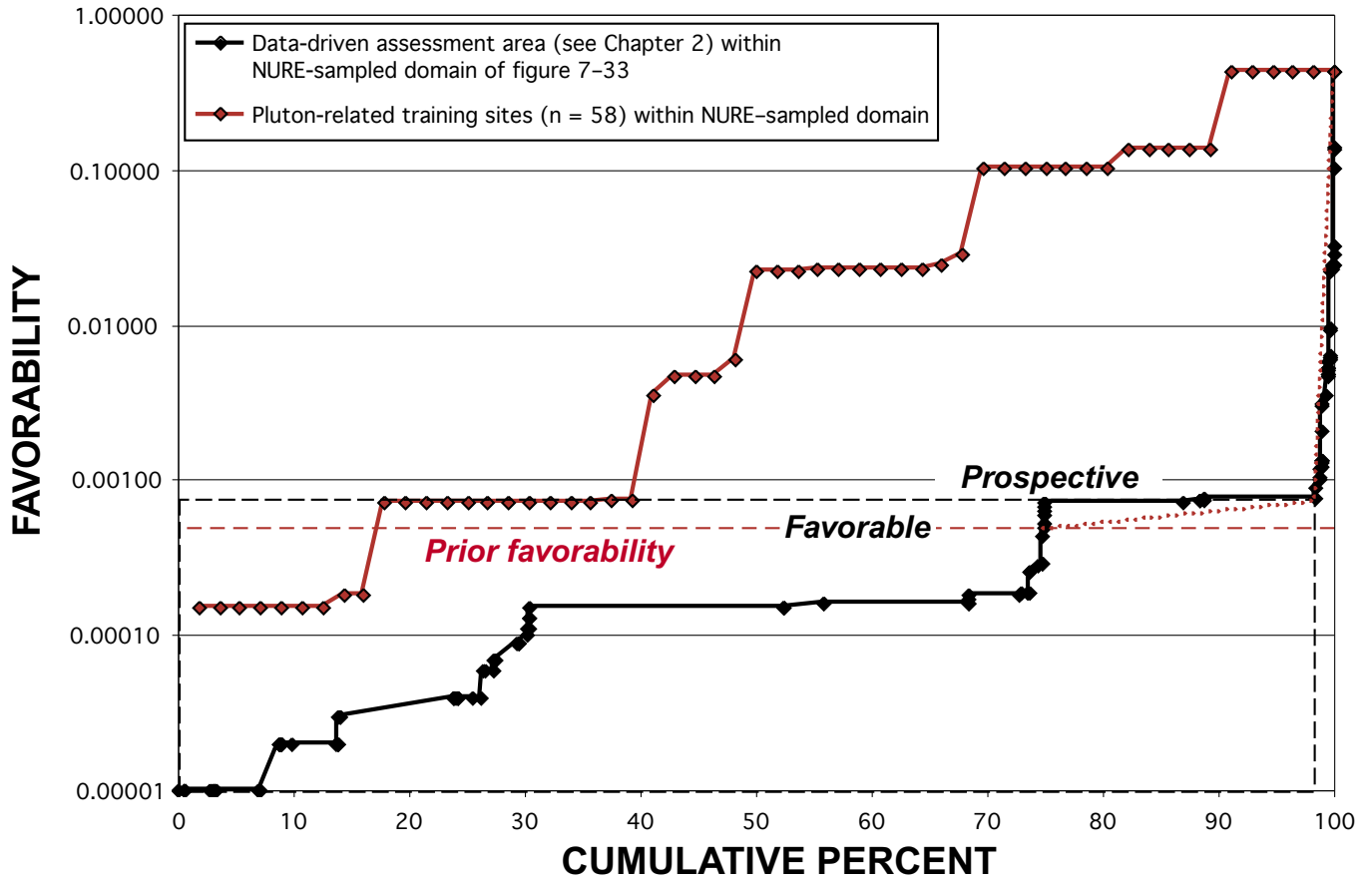
Figure 7-34. Plot showing pluton-related deposit weighted-logistic-regression (WLR) favorability versus cumulative assessment area (black) and versus cumulative training sites (red) for Humboldt River Basin study area, northern Nevada. Permissive-favorable rank boundary is defined as the prior favorability (0.0005, red dashed line). The favorable-prospective rank boundary is defined as the most prominent break-point in the cumulative assessment area above the prior favorability (0.00076, black dashed line). The favorable-prospective break-point is highlighted by the dotted red line. NURE, National Uranium Resource Evaluation.
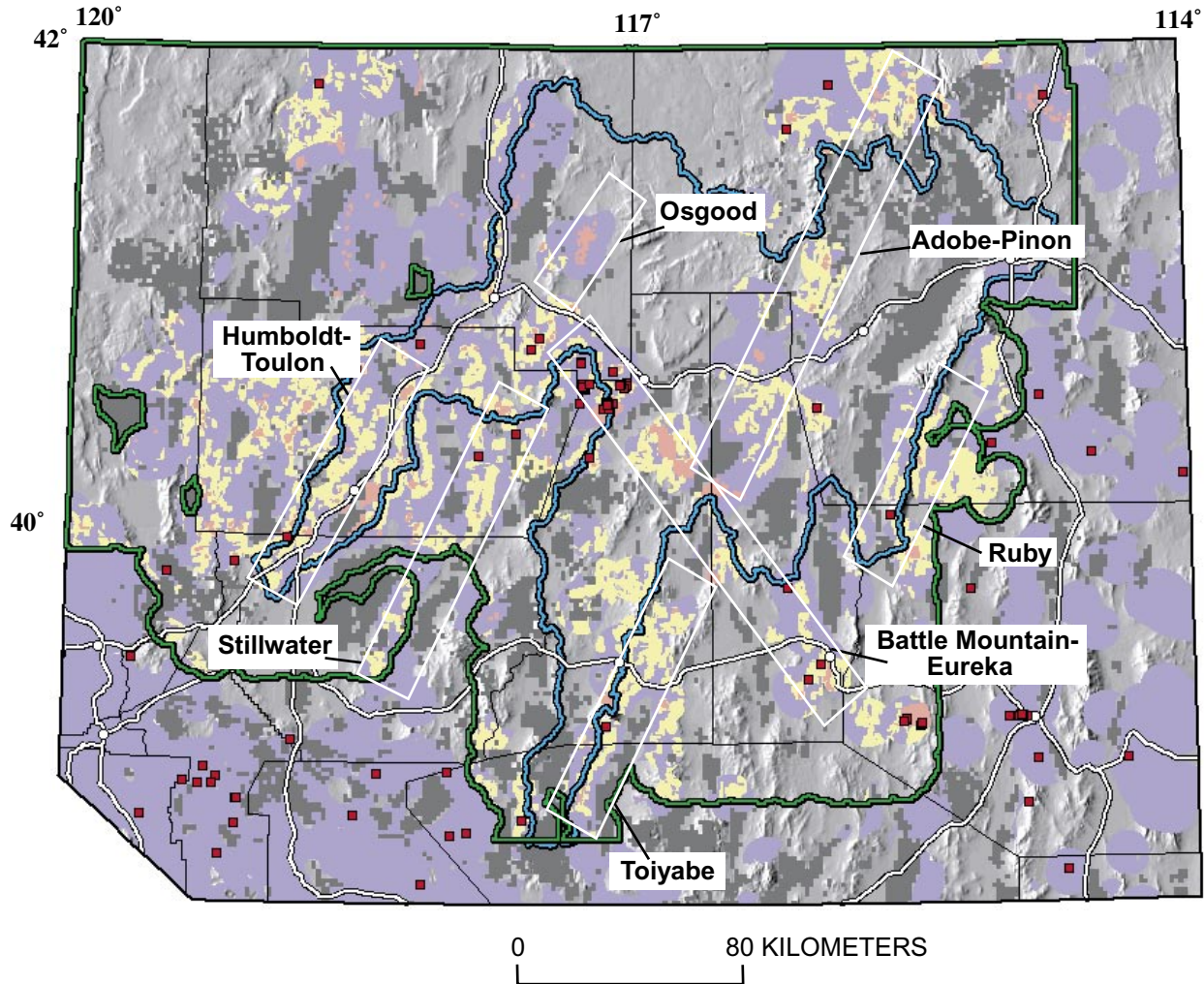
Figure 7-35.   Pluton-related mineral resource assessment map of northern Nevada showing selected belts (white rectangles) discussed in text. Training sites are shown as red squares. Humboldt River Basin (HRB) shown as pale blue outline; limit of National Uranium Resource Evaluation (NURE) geochemical data shown with green line. Occurrence favorability (see text): red, prospective; yellow, favorable; pale purple, permissive (from fig. 7-5; see also, Cox and others, 1996); uncolored, nonpermissive. Dark gray areas represent Cenozoic cover deposits that are greater than 1 km thick.

Table 7-1.   Descriptive data, including assessment rank, for 92 mineralized sites in northern Nevada used as training sites for pluton-related assessment of the Humboldt River Basin.

This table is oversize and must be viewed or printed separately from this page—click here

Table 7-2.   Historic gold-copper-silver production from the Copper Canyon area of the Battle Mountain Mining District, Nevada. Modified from Cary and others (2000).

Deposit	Years Operated	Mined Tonnes	Au (kg)	Au Grade (recovered g/t)	Ag (kg)	Ag Grade (g/t)	Cu (short t)	Cu Grade (percent)
Pre-1961 Production	Prior to 1961	N.a.	2,643	N.a.	N.a.	N.a.	N.a.	N.a.
Copper Canyon underground	1871–1954[1]	596,839	1,501	2,503	26,855	44.91	4,811	0.73
East and West Pits	1966–1978							
Mill		13,482,583	5,527	0.411	123,630	9.26	74,837	0.50
Leach		43,407,895	N.a.	N.a.	N.a.	N.a.	32,565	0.07
Tomboy	1978–1982							
Mill		2,661,681	6,406	2.4	10,951	4.11	--	--
Minnie	1978–1981							
Mill		621,490	1,496	2.4	2,557	4.11	--	--
NE Extension	1981–1989							
Mill		1,124,002	2,698	2.4	10,405	9.26	--	--
Upper Fortitude	1982–1984							
Mill		2,572,777	7,020	2.743	73,277	28.46	--	--
Lower Fortitude	1984–1993							
Mill		7,327,435	59,137	8.057	232,805	31.89	--	--
Iron Canyon	1991–1993					*in situ grade*		
Mill		180,412	786	4.354	3,155	17.49	--	--
Leach		689,292	794	1.166	12,074	17.49	--	--
Reona Leach Project[2]	1994–1997							
Leach		N.a.	7,935	N.a.	N.a.	N.a.	--	--
						in situ grade		
Midas (P1, P2, P3) Pits		20,614,251	N.a.	0.857	N.a.	N.a.	--	--
Sunshine Pit		1,690,567	N.a.	0.754	N.a.	N.a.	--	--
Copper Canyon Totals		94,969,224	95,943	1.01	495,707	5.22	112,213	--

[1] Production from 1929 to 1954
[2] Production to September 1,1999

Table 7-3.   Proven and probable ore reserves at year-end 1999 for the Phoenix Project at Copper Canyon, Battle Mountain Mining District, Nevada. Ore reserves calculated using the following prices for metals: $325 per oz gold, $5.25 per oz silver, and $0.95 per pound copper. In situ (head) grades are listed for Iron Canyon and Reona; in situ reserves are listed for Iron Canyon. Modified from Cary and others (2000).

Area		Ore (KTonnes)	Au (g/t)	Ag (g/t)	Cu (percent)	Contained Au (kg)	Contained Ag (kg)	Contained Cu (tons)
Phoenix Pit	Mill	74,416	1.408	9.924	0.145	104,779	738,486	118,550
	Leach	2,315	1.023	7.808	N.a.	2,517	18,148	N.a.
Greater Midas Pit	Mill	41,281	1.141	9.867	0.189	47,117	407,325	85,785
	Leach	10,227	1.097	9.451	N.a.	12,053	85,906	N.a.
Reona Pit	Mill	4,175	1.14	7.752	0.166	4,758	32,364	7,659
	Leach	1,782	1.07	7.412	N.a.	1,907	13,206	N.a.
Iron Canyon Pit	Mill	1,082	1.599	19.124	0.115	1,730	20,688	1,370
	Leach	137	1.96	37.548	N.a.	272	5,210	N.a.
Sunshine Pit	Leach	390	0.678	5.143	N.a.	264	2,006	N.a.
Midas Stockpile	Mill	914	1.351	6.038	N.a.	1,235	5,515	N.a.
Sub totals	Mill	121,868	1.310	9.883	0.159	159,620	1,204,378	213,364
	Leach	14,851	1.146	8.362	N.a.	17,013	124,477	N.a.
Total Project		136,719	1.292	9.72	0.159	176,633	1,328,854	213,364

Table 7-4. Examples of types of magmatic mineralization associated with various geologic environments for the occurrence of mafic and ultramafic rocks.

		Magma conduit – physical trap	Marginal sulfides	PGE reef-type sulfides	Other stratabound sulfide deposits	Magmatic breccias, discordant pegmatoids, and deuterically altered rocks	PGE - enriched chromitites, sulfide)	PGE –enriched chromitites, alloy)	Podiform chromitite
Plutonic rocks associated with large igneous provinces - intraplate magmatism (Mahoney and Coffin, 1997)	**Large ultramafic to mafic layered stratiform intrusions, composite mafic layered intrusions, and alkaline layered mafic-ultramafic complexes** (Hatton and von Gruenewaldt, 1990); Vermaak and von Gruenewaldt, 1986)		**Mouat deposit, Stillwater Complex** (Zientek, 1993); **Konttijarvi, Portimo area** (Alapieti and others, 1989); **Marathon, Coldwell** (Watkinson and others, 1983); **Duluth Complex** (Listerud and Meineke, 1977)	**Merensky Reef, Bushveld Complex** (Naldrett and others, 1987); **J-M Reef, Stillwater Complex** (Todd and others, 1982); **Main sulfide zone, Great Dyke** (Prendergast and Wilson, 1989); **Platreef, Bushveld Complex** (Gain and Mostert, 1982)	**Picket Pin, Stillwater Complex** (Boudreau and McCallum, 1986); **Bird River sill** (Scoates and others, 1987); **Platinova Reef, Skaegaard intrusion** (Andersen and others, 1998)		**UG2, Bushveld Complex** (Gain, 1985); **A/B chromitite, Stillwater Complex** (Zientek, 1993)		
	Mafic differentiated sills associated with continental flood basalts	**Noril'sk-Talnakh** (Naldrett and Lightfoot, 1999)							
Massif anorthosites (Anderson, 1983; Emslie, 1985)	**Large anorthosite-dominated intrusions that are associated with mangerite-charnokites and rapakivi granites**	**Voisey's Bay, Nain province** (Lightfoot and Naldrett, 1999)							
Calc-alkaline to alkaline magmatism at convergent plate margins	**Small mafic - ultramafic plutonic complexes that display close temporal and spatial association with calc-alkaline plutonic rocks** (Regan, 1985)		See Page (1986c) and Singer (1986b)		**Lake Owens Complex, Wyoming** (Loucks, 1991)	**Lac des Iles, Ontario** (MacDonald and others, 1989)			
	Alaskan ultramafic complexes (Irvine, 1974; Findlay, 1969; Smirnov, 1977; Mertie, 1969)							**Nizhney-Tagil, Russia; Tulameen, B.C.** (Page, 1986a)	
Ophiolites (fragments of oceanic crust and lithosphere formed at accreting plate margins; Coleman, 1977)	**Tectonized harzburgite and dunite, cumulate ultramafic and gabbroic rocks, noncumulate gabbros, sheeted dikes, and pillowed lavas and flows**								See Albers, (1986); Singer and Page, (1986); and Singer and others, (1986a)

Table 7-5. Sulfur isotopic values determined for samples near Humboldt mafic complex, Nevada.

Field number /material analyzed	Sample field description	$\delta^{34}S$
BDSW3 / PY	Bradshaw Copper -hematite stained altered mafic volcanic rock	2.5
BDSW1 / PY	Bradshaw Copper - altered mafic volcanic rock with disseminated sulfide minerals	3.9
BCU11 / PY	Bradshaw Copper - altered volcanic breccia	4.1
BCU10B / PY	Bradshaw Copper - volcanic breccia with disseminated pyrite and chalcopyrite	4.3
BCUl0A / PY	Bradshaw Copper - volcanic breccia with disseminated pyrite and chalcopyrite	7.3
COTCN4 / PY	Cottonwood Canyon – nickel-enriched silicate mineral vein	9.3
COTCN1 / PY	Cottonwood Canyon - quartzite with Fe oxide and disseminated sulfide minerals	9.8
COTCN1 A / PY	Cottonwood Canyon - quartzite with Fe oxide and disseminated sulfide minerals	10.5
COTCN8 / PY	Cottonwood Canyon - layered gabbro	10.6
COTCN1 B / PY	Cottonwood Canyon - quartzite with Fe oxide and disseminated sulfide minerals	11
86HLZDC10 / PY	Dixie Comstock -jasperoid (silicified gabbro with disseminated pyrite)	5.1
DXC13 / PY	Dixie Comstock - very fine-grained to medium-grained silicified, vuggy gabbro	8.9
DXC14 / PY	Dixie Comstock - gabbro with elongate plagioclase and amphibole; carbonate alteration	15.9
86HLZ62 / PY	Green mine - Fine-grained, altered Jgi with disseminated pyrite	5.5
86HLZ63 / PY	Green mine - Altered Jgi with clots of pyrite	7.8
86HLZ72 / PY	Green mine - Quartz vein with Fe oxide after sulfide in altered gabbro	9.4
86HLZ71 / PY	Green mine - Quartz vein with Fe oxide after sulfide in altered gabbro	9.8
86HLZ81 / PY	Green mine – Quartz vein with-Fe oxide after sulfide in altered gabbro	10.1
86HLZ30 / SL	Jqd with disseminated, interstitial sulfide near Bradshaw Copper	14.6
86HLZ89 / PY	Jgk with disseminated sulfide minerals	17.1
86HLZ32(2) / gp	Muttlebury Formation, gypsum	11.4
86HLZ33 / gp	Muttlebury Formation, gypsum	14.5
86HLZ32 Vein #2 / gp	Muttlebury Formation, gypsum	20.7
86HLZ32 Vein #3 / gp	Muttlebury Formation, gypsum	21.1
86HLZ32 Vein #1 / gp	Muttlebury Formation, gypsum	21.2
86HLZ37 / gp	Muttlebury Formation, gypsum	22.3
MTLBRY11 / PY	Muttlebury mine – pyrite in quartz vein	1.2
86HLZ12 / PY	Near Corral Canyon - quartz vein containing weathered pyrite (vuggy boxwork)	3.9
86HLZ3 / PY	Prospect south of Dixie Comstock - altered gabbro with disseminated pyrite, magnetite (pink carbonate)	11.7
86HLZ2 / PY	Prospect south of Dixie Comstock - altered gabbro with disseminated pyrite	14.9
86HLZ5 / PY	Prospect south of Dixie Comstock - altered vein cutting altered gabbro with disseminated sulfide	15.4
86HLZ2 / SL	Prospect south of Dixie Comstock - altered gabbro with disseminated pyrite	15.6
86HLZ51 A	Tule deposits - massive sulfide	11.4
LONGSECT34-1 / PY	Tule deposits – dike ? in altered shale	15
86HLZ51 B / SL	Tule deposits - massive sulfide	15.9
86HLZ51 U / PY	Tule deposits - massive sulfide	16.2
86HLZ51 B	Tule deposits - massive sulfide	16.3
86HLZ50 / PY	Tule deposits - massive sulfide	17.7
86HLZ48 / PY	Tule deposits - very fine grained altered dike?, abundant sulfide minerals.	17.8
LONGSECT34-7 / PY	Tule deposits – altered dike ?	19.8

Table 7-6. Summary of sulfur isotope results for samples collected within and adjacent to the Humboldt mafic complex, Nevada.

What and where	Alteration	Sulfide/oxide minerals	Sulfur isotope results
Magmatic (volcanic source) of sulfur			
Muttlebury mine		Pyrite associated with antimony ore	1.2‰
Altered volcanic rocks, Bradshaw Copper mine	Clay after plagioclase accompanied by chlorite, carbonate, and tourmaline, with locally developed quartz-kaolinite-muscovite	Chalcopyrite	2.5‰ and 4.3, with one value as high as 7.3‰.
Mixed igneous-sedimentary source of sulfur – alteration characteristic of volcanic related epithermal system			
Jasperoid (strongly silicified gabbro), Dixie Comstock Mine	Quartz plus kaolinite with only traces of epidote and without carbonate	Pyrite	5.1‰
Cobalt-nickel mineralization developed in ankeritic carbonate in the Cottonwood Canyon			9.3
Altered quartzite and gabbro, Cottonwood Canyon area			9.8 to 11.0
Altered plagioclase-rich diabasic or gabbroic rocks, Green Mine	Altered gabbros contain albite, carbonate, muscovite, quartz, apatite, and tourmaline. Quartz veins in these rocks contain abundant tourmaline.	Pyrite is the dominant sulfide, but some samples contain minor amounts of a sulfosalt mineral tentatively identified as boulangerite	Sulfur isotopes from samples of the quartz vein range from 9.4‰ to 10.1‰; the associated altered diabase samples gave values of 5.5‰ and 7.8‰.
Sedimentary source of sulfur			
Diabasic rocks **near the Tule iron prospect**	Relatively fresh to extensively altered. The diabases are plagioclase rich and show varying degrees of albitization with minor sericite. Mafic minerals also vary from relatively fresh to extensively altered with replacement by amphibole, epidote, chlorite ± calcite, and sphene	Disseminated and fracture-controlled pyrite with minor amounts of pyrrhotite and chalcopyrite	Sulfur isotope values range from 15.0‰ to 19.8‰
Fine-grained plagioclase-rich gabbro, several km south of **Tule iron prospect**	Similar to above but with more carbonate, including a vein of coarse ankerite plus minor pyrite		17.1‰.
Massive sulfide in coarse-grained gabbro **near the Tule iron prospect**	Gangue to the massive sulfide is dominantly albite, tremolite, and sphene, with coarse-grained scapolite in some samples	Dominantly pyrrhotite with some chalcopyrite and pyrite	11.4‰ to 17.7‰
Altered gabbro, Bradshaw Copper mine			14.6‰
Gypsum-bearing rocks of the Early to Middle Jurassic Muttlebury Formation			11.4‰ to 22.3‰.

Table 7-7. Compositional data for samples anomalous in PGE and for a sample of hydrothermal Ni–Co arsenide ore in the general area of the Humboldt mafic complex, Nevada.

Lab number	M174668	M186651	M174672
Field number	3HLP86	BVH-26	8HLP86
Locality	Cottonwood Canyon; between Lovelock and Nickel mine	Buena Vista Hills; northwest of Buena Vista mine	Cottonwood Canyon; between Lovelock and Nickel mine
Map unit from Speed (1976).	Jvs (volcanic rocks, chiefly stratified)	Jgs (scapolitite)	
Field description	Copper oxide-stained mafic volcanic rock	Coarse-grained elongate scapolite with amphibole. Sparse magnetite.	Ni-Co arsenide ore sample
Fe, %-s	3.7	5	1.1
Ag, ppm-s	27	N 0.5	13
As, ppm-s	6300	N 200	32000
Au, ppm	N 0.002	0.006	N 0.002
Ba, ppm-s	190	2000	--
Co, ppm-s	479	50	1240
Cu, ppm-s	35800	30	447
Ni, ppm-s	472	50	46000
Pt, ppb	340	69	< 2
Pd, ppb	930	640	< 3
Rh, ppb	30	22	< 2
Ru, ppb	4	2.9	18
Ir, ppb	< 2	1.1	< 2

Table 7-8. Whole rock analyses of massive sulfide minerals associated with altered igneous rock, Tule Iron prospects, West Humboldt Range, Nevada.

Lab number	Field number	Fe, %s	Co, ppm-s	Cu, ppm-s	Ni, ppm-s	Au, ppm	Pt, ppb	Pd, ppb	Rh, ppb	Ru, ppb	Ir, ppb
M183473	86HLZ 50	> 20	30	1000	30	< 0.05	<2	5.6	2	<2	<2
M183474	86HLZ 51	20	50	1500	30	< 0.05	<1	<1	<1	<1	<1
M183475	86HLZ 52	20	100	700	30	< 0.05	<1	<1	<1	<1	<1

Table 7-9. Evidence maps, prediction criteria, and spatial associations with respect to 92 pluton-related deposit training sites in northern Nevada listed in order of descending strength of spatial association. Prediction criteria were determined by data-driven means (see Chapter 2).

Evidence Map	Prediction Criteria	Spatial Associations (W^+, W^-, C, Studentized C)			
		Predictor Present	Predictor Absent	Strength	Significance
Skarn Proximity	within 1 km	4.1889	-0.4905	4.6794	21.6969
Cu-Pb-Zn Signature	signature value = 1 (see section M.xx)	3.3338	-0.3230	3.6568	12.7084
As-Frequency	$\geq$ 18 ppm	2.8749	-0.4289	3.3038	12.0608
Pluton Proximity	within 19 km of Tri, Tmi, Ti, Tr2, Tr1, TJgr, Tgr, Mzgr, Kgr, KJd, Jgr, TRgr, and TRlgr	0.1828	-2.7852	2.9680	2.9518
Lithodiversity	$\geq$ 3 lithologic units per 6.25 km^2	0.8514	-1.3144	2.1659	7.8730
Basement Gravity Lineaments	within 29 km	0.0717	-1.9878	2.0596	2.0483
Basement Gravity Terranes	outside of terranes of anomaly highs	0.1858	-1.3736	1.5594	3.3906

Table 7-10. Proportion of areas for various assessment ranks of pluton-related deposits in northern Nevada. Area and training site proportions are relative to that part of the study area covered by As–frequency and Cu–Pb–Zn geochemical evidence maps (see figs. 7-27 and 7-28).

Assessment Rank	Area (127,920 km^2)	Training Sites (n = 58)
Prospective	2%	59%
Favorable	12%	22%
Permissive	28%	17%
Non-Permissive	58%	2%

Chapter 8

Assessment for Sedimentary Rock-Hosted Au–Ag Deposits

By Stephen G. Peters, Mark J. Mihalasky, and Ted G. Theodore

Introduction

North-central Nevada contains many sedimentary rock-hosted Au–Ag deposits of several types and sizes. The region is well known for its large Au mines, most of which are sedimentary rock-hosted deposits, and many of which are either in or peripheral to the Humboldt River Basin (HRB). Gold is the main metal mined from sedimentary rock-hosted Au–Ag deposits in northern Nevada, although some deposits contain significant amounts of As, Ag, Sb, and Hg and lesser amounts of Cu, Pb, and Zn. The large, locally high-grade, sedimentary rock-hosted Au–Ag deposits in northern Nevada are a significant contributor to the United States' resource-based economic base, and they have made a large contribution to the economy of Nevada. Exploration by drilling, geophysical, and geochemical prospecting methods continued at a high rate in the HRB in the 1980s and 1990s (fig. 8-1). In 1998, Nevada produced 74 percent of the Nation's Au and 40 percent of the Nation's Ag and has ranked first in the United States' Au production since 1981, the majority coming from Carlin-type deposits, the economically most important of the sedimentary rock-hosted Au–Ag deposits. This has made Nevada the second leading producer of Au in the world (Nevada Bureau of Mines and Geology, 2000). Announced Au reserves of the Carlin-trend deposits alone are 70,000,000 ounces Au (Teal and Jackson, 1997a,b).

The region of the HRB is exceptionally well endowed with respect to economic resources of Au and Ag (U.S. Geological Survey Minerals Team, 1996). The region contains well over 100 million ounces of Au resources and produces over 8 million ounces Au or more per year, most from sedimentary rock-hosted Au–Ag deposits (Teal and Jackson, 1997a,b; Nevada Bureau of Mines and Geology, 2000). Mining since the mid-1800s was intermittent and of relatively low level in many main mining districts that a century later would be recognized as having sedimentary rock-hosted Au–Ag deposits (Hill, 1912; Lincoln, 1923; Couch and Carpenter, 1943; Bergendahl, 1964; Koschman and Bergendahl, 1968; Schilling, 1976; and Johnson, 1992), such as the Carlin trend and the Independence, Getchell (Potosi), Cortez-Pipeline, Battle Mountain, Bald Mountain–Alligator Ridge, and Eureka (White Pine, Antelope) Mining Districts (see also, U.S. Geological Survey and Nevada Bureau of Mines, 1964; Wong, 1982; Tingley, 1992a,b) (fig. 8-2).

Mining increased in scale during the 1970s and 1980s when it was finally recognized that these deposits could be economically mined from open pits using bulk-tonnage methods and that the ore could be processed with carbon-in-pulp or heap-leaching, cyanide-based technologies (Schafer and others, 1988). Metallurgical analysis and mining of recent discoveries of sulfide-bearing sedimentary rock-hosted Au–Ag ores from below the oxide zone have proven that such ores also can be processed profitably with large capital investments using roasters and autoclaves. Exploration between 1975 and 2000 discovered a number of large- (~>1 tonne Au) and super-large (~>10 tonne Au) deposits. Exploitation of the sulfidic, deep ores, however, has necessitated extensive surface disturbances and dewatering of large aquifers, which has caused concern about discharges into the HRB and its adjacent aquifers. The economic significance of these deposits and their accompanying potential environmental impact are important reasons for estimating the potential for and location of further discoveries in the HRB.

The present mineral assessment of sedimentary rock-hosted Au–Ag deposits in the HRB applies known geologic features of these deposits to available digital geologic data bases in order to estimate areas where new discoveries are likely to be made. In order to provide an accurate assessment of a mineral deposit type, it is necessary to classify and define the physical and geologic characteristics of the deposits (U.S. Bureau of Mines, 1980; Taylor and Steven, 1983; Bliss, 1992). The Carlin-type of sedimentary rock-hosted Au–Ag deposits is referred to as Carlin-type deposits and these deposits have been considered economically significant and geologically distinct since the early 1960s. Similar deposits have been discovered in China, Australia, Dominican Republic, Spain, Russia, Malaysia, Philippines, Yugoslavia, and Greece (Li and Peters, 1998; Peters, 2002), in addition to the Great Basin of Nevada. These deposits have similar characteristics that can be understood in terms of geologic processes, which allow analysis of regional geologic data bases for the present mineral assessment process. The distal-disseminated (porphyry-related) type of sedimentary rock-hosted Au–Ag deposits have slightly different characteristics, and generally are smaller deposits, but they also are a significant deposit type in the HRB.

Limestone, siltstone, argillite, shale, and quartzite are hosts for sedimentary rock-hosted Au–Ag deposits. Gold

in hypogene ores usually is micron-size, mainly associated with disseminated As-rich pyrite and marcasite (Hofstra and Cline, 2000). One traditional exploration method for lode Au deposits is prospecting by tracing Au placers back to their source. This has not worked in exploration for the sedimentary rock-hosted Au–Ag deposits, because the Au particles are so small that they do not readily concentrate by panning and also do not concentrate in streambeds and therefore do not form Au placers downstream from the sources. However, they can be found by analysis of As and Sb contents in stream-sediments (Theodore and others, 1999). Because sedimentary rock-hosted Au–Ag deposits have become so important economically and have provided a major source of Au over the last 40 years, it has become important to understand their origin, which, in turn, allows us to accurately assess the potential for future discoveries.

Although the origin of sedimentary rock-hosted Au-Ag deposits is incompletely understood, a number of features, including field relations at all scales, age relations, and geochemical and isotopic characteristics, enhance our understanding of these deposits to allow adequate resource assessments to be made. Previous genetic models were developed from observations made during mining of the oxidized or weathered (supergene) parts of these deposits in Nevada during the 1960s to 1980s. However, the recent exploitation and exposure of sulfide (hypogene) parts of these orebodies have significantly increased our knowledge of their genesis because primary textures and geochemical signatures of the ores are not obscured by oxidation.

A previous U.S. Geological Survey (USGS) quantitative mineral assessment of the Bureau of Land Management's Winnemucca-Surprise Resource Areas included the western part of the HRB assessment area. That assessment considered sedimentary rock-hosted Au–Ag deposits (Carlin-type), as well as distal-disseminated Au–Ag deposits, a subtype of these deposits (Doebrich and others, 1994; Doebrich, 1996; Peters and others, 1996; U.S. Bureau of Mines, 1996). These two subtypes (Carlin-type and distal-disseminated) of sedimentary rock-hosted Au deposits were considered separately in the quantitative Winnemucca-Surprise assessment because the deposits contain distinct grade-tonnage curves—Carlin-type deposits are generally larger and of higher grade than the distal-disseminated Ag–Au deposits. The two subtypes also were considered separately in an assessment of the State of Nevada (Cox and others, 1996). In the present assessment, we have included both of these two subtypes of deposits together in the assessment of sedimentary rock-hosted Au–Ag deposits in the HRB because (1) the assessment does not estimate the number of undiscovered deposits of the two subtypes, and (2) these subtypes share many geologic features that can be conveniently assessed spatially and qualitatively using the weighted logistical regression (WLR) methodology (see chapter 2).

The current assessment is timely because extensive, modern, and detailed mineral exploration has been conducted for these deposits during the last 10 years in, and proximal to, the HRB. Therefore, much of the exposed bedrock, as well as

some areas covered by post-mineralization Tertiary and Quaternary alluvium and volcanic rocks, have been tested to various degrees. Current exploration programs and this assessment focus on deep and hidden targets in known districts, "trends," or relatively unexplored areas. The following discussion outlines the geologic parameters and approach used in conducting the present assessment for sedimentary rock-hosted Au–Ag deposits. Geologic setting, deposit type modeling, level of exposure, data bases, and the large relevant mining districts are discussed with respect to their importance to the present assessment process of the HRB area.

Geologic Setting

The geologic history that directly affects distribution of sedimentary rock-hosted Au–Ag deposits in northern Nevada involves early and middle Paleozoic, deep-water, siliciclastic sedimentary and volcanic rocks that initially were thrust eastward approximately 75 to 200 km during the Late Devonian to Early Mississippian Antler orogeny (Roberts and others, 1958; Stewart, 1980; see chapter 4). These rocks compose the approximately 5–km-thick Roberts Mountains allochthon (Oldow, 1984; Madrid and others, 1992), which was thrust over coeval shallow-water, carbonate-rich rocks of the continental platform and age-equivalent rocks of the autochthonous slope (fig. 8-3). The Roberts Mountains thrust fault separates two litho-stratigraphic packages of rocks, the upper and lower plates. The majority of sedimentary rock-hosted Au–Ag deposits are located beneath the Roberts Mountains fault in lower-plate rocks and in many places are covered by upper plate rocks (fig. 8-3) (see also, Prihar and others, 1996).

The Golconda allochthon (Silberling and Roberts, 1962; Silberling, 1975) consists of uppermost Devonian to lower Upper Permian carbonate-rich turbiditic sandstone and basinal strata. The allochthon was thrust on top of the continental margin and parts of the Roberts Mountains allochthon along the Golconda thrust during the latest Permian and early Triassic (fig. 8-3; see chapter 4). These Paleozoic rocks lie above the boundary between continental and oceanic crust that is composed of Proterozoic to Cambrian detrital rocks, which in turn, overlie Achaean crystalline crust (fig. 8-3). Paleozoic and Mesozoic tectonic events produced crustal thickening marked by deformation above this older crustal boundary.

Mesozoic and Tertiary igneous activity produced plutons and Tertiary volcanic rocks in the surrounding region (Blake and others, 1979; Barton, 1990) (see chapters 7 and 9). Many known areas of sedimentary rock-hosted Au–Ag deposits are devoid of direct links to magmatic activity (Ilchik and Barton, 1997). However, early Tertiary igneous activity may have had a direct role in the genesis of some of these mineral deposits (Henry and Ressel, 2000a,b; Ressel and others, 2000a,b). Sedimentary rock-hosted Au–Ag deposits along the Carlin trend and in most of north-central Nevada are interpreted to be either Late Cretaceous or late Eocene (Arehart and others, 1993b; Goff, 1997; Teal and Jackson, 1997a,b; Henry and oth-

ers, 1998; Hofstra and others, 1999; Tretbar and others, 2000; Ressel and others, 2000a). This indicates that Au deposition in these deposits was synchronous with or closely followed magmatic activity and heat flow in the region during or shortly after the Sevier-Laramide tectonic event (see also, Seedorff, 1991; Cox and others, 1991; Maher and others, 1993).

Regional geologic setting of many sedimentary rock-hosted Au–Ag deposits in north-central Nevada indicates that Au–bearing hydrothermal fluids were transported along regional-scale conduits—an hypothesis offered on the basis of the petrology of some rocks in the ore deposits and their apparently associated fluid conduits that are of regional extent (Peters, 2000). Ore assessment methodology for the sedimentary rock-hosted Au–Ag deposits heavily relies on the interpretation of these regional structures with respect to the Paleozoic, Mesozoic, and Cenozoic geologic history and the spatial expression of this interpretation in the available data sets.

General Description of Deposit Type

Characteristics of specific deposits allow them to be classified and separated into distinct deposit types that can be assessed as a group. The characteristics of a deposit type also suggest genetic processes that can be linked to local- and regional-scale geologic parameters in the assessment process. Sedimentary rock-hosted Au–Ag deposits have many styles; they may be stratabound, structurally controlled, and complex (fig. 8-4), as noted along the Carlin trend by Christensen (1993, 1996). They generally are characterized by relatively uniform, low Au grades they are exploited by surface, bulk-mining methods (Arehart, 1996; Hofstra and Cline, 2000). Some hypogene deposits contain high-grade oreshoots, which are zoned complexly in three dimensions (fig. 8-5) and allow exploitation by underground methods (Peters, 1996, 1997b; Peters and others, 1998).

Geologic investigations of sedimentary rock-hosted Au–Ag deposits in northern Nevada have been numerous (Teal and Jackson, 1997a,b), but the origin of these deposits is still debated (see also, Radtke and Dickson, 1974; Radtke and others, 1980; Bagby and Berger, 1985; Kuehn, 1989; Hofstra and others, 1991b; Ilchik and Barton, 1997; Arehart, 1996; Hofstra, 1997; Vikre and others, 1997; Hofstra and Rye, 1998; Henry and others, 1998; Tosdal, 1998; Hofstra and Cline, 2000). Genetic hypotheses call for: (1) possible connections to igneous activity at depth, (2) complex evolution of tectonothermal events, (3) inherent host rock permeabilities, and (4) evolved meteoric or metamorphic fluids, oil brines, or orogenic fluids, as well as many other factors (see also, Peters, 2001a).

Classification of sedimentary rock-hosted Au–Ag deposits is controversial, and even the age of Carlin-type deposits, including those that have been investigated intensely for as many as 30 years, remains enigmatic. This mineral-resource assessment of the HRB recognizes two main types of sedimentary rock hosted Au–Ag deposits: (1) the Carlin-type or

sediment-hosted Au–Ag deposit model (model 26a of Cox and Singer, 1986; Mosier and others, 1992), and (2) distal-disseminated, or pluton-related Ag–Au deposit model (model 19c of Cox and Singer, 1992). These two classifications have been made on the basis of mineralogy, geochemistry, host rock type, and other geologic characteristics in individual deposits. The Carlin-type deposits in the sedimentary rock-hosted Au–Ag training set (table 8-1) were further subdivided into a "north-type" and a "south-type" on the basis of geographic location, size, tenor, mineralogy and host rock type (fig. 8-2). These subtype classifications of the general group of sedimentary rock-hosted Au–Ag deposits in north-central Nevada and HRB were made so that subjective variation and ranking decisions could be discussed with respect to the final mineral-resource assessment map.

The type of sedimentary rock-hosted Au-Ag deposit, either distal-disseminated—as we use the term—or classic Carlin-type deposit, inferred to be present in an area is critical for overall exploration methodology, but it is less important for regional-scale assessment methodology (see also Roberts and Sheehan, 1988; Singer and Cox, 1988; Barton, 1990, 1993; Bliss, 1992, Singer, 1993; Cox, 1993; Kirkham and others, 1993; Ludington and others, 1993). We recognize that Carlin-type systems may be: (1) the products of far-traveled fluids that ultimately owe their origins to magma (Sawkins, 1983; Sillitoe, 1988; Sillitoe and Bonham, 1990), (2) the products of metamorphic fluids derived from devolatilization reactions at deeper levels driven by heat supplied by magma, or (3) products of convecting meteoric waters also driven by magmatism (see also, Sverjensky, 1984; Hofstra and others, 1999; Hofstra and Cline, 2000). We suggest, however, that if classic Carlin-type deposits were products of far-traveled magmatic fluids (scenario (1) above), then they most likely would be present "outboard" of the distal-disseminated Ag–Au deposits, which formed relatively close to the magmatic source. The complex geologic setting of most sedimentary rock-hosted Au–Ag districts in the HRB, however, do not provide this definitive spatial link.

Ore fluid characteristics also may have some similarities in both the Carlin-type and distal-disseminated deposits. Boiling indicators in fluid-inclusions are not documented in most fluid-inclusion studies in either deposit type. Ore-stage fluid salinities also are low in both deposit types (Kuehn, 1989; Johnson, 2000), although higher salinities are common in the magmatic parts of the systems in the distal-disseminated deposits (Hitchborn and others, 1996; Theodore, 2000). Dilute (mostly 0.5 to ≤ 10 weight percent NaCl equivalent) hydrothermal fluids dominantly formed probably from evolved meteoric water in many Carlin-type deposits (Hofstra and others, 1991a; 1991b). An exception is the Getchell trend area (Cline and Hofstra, 1996), where magmatic sources of fluid are indicated, similar to the distal-disseminated deposits (Peters and others, 1996; Theodore, 2000). On the basis of fluid-inclusion studies, main-stage ore-forming events in the Carlin-type deposits probably were between 200 to 250°C and 400 to 800 bars, whereas distal-disseminated deposits may

have formed at these or higher temperatures (see also Rytuba, 1985; Woitsekhowskaya and Peters, 1998). Gold-associated minerals in Carlin-type deposits have a wide range of ^{34}S, from –5 to +20 per mil. The source of sulfur may be either magmatic or from the enclosing sedimentary rocks in some distal-disseminated deposits (see also, Hitchborn and others, 1996).

Comparative quantitative and qualitative estimates of Au endowments in parts of north-central Nevada for similar numbers of distal-disseminated Ag–Au and Carlin-type deposits indicate approximately three times as much Au in Carlin-type deposits (Peters and others, 1996; Theodore, 2000). Individual deposits used in the present assessment are tabulated in a "training set" for the weights-of-evidence analysis on table 8-1 and shown on figure 8-2. Nonetheless, assessment and favorability maps were drawn to reflect all types of sedimentary rock-hosted Au–Ag deposits, regardless of sub-classifications summarized above and discussed in more detail below.

The following discussion outlines the characteristics of the two main subtypes of sedimentary rock-hosted Au–Ag deposits used in the present assessment. Classification is not perfect for these large and important deposits, and more detailed mineral-resource assessment maps, if available, would take into account further differences in deposit type. During the present assessment process, differences in spatial association with available data bases between the north and south Carlin-type deposits and between the Carlin-type deposits and distal-disseminated deposits were considered small enough to allow all sedimentary rock-hosted Au–Ag deposits to be considered together for the present mineral-resource assessment using the data-driven methodology.

Sediment-hosted Au–Ag (Carlin-type) Deposits (Model 26a of Cox and Singer, 1986)

The sediment-hosted Au–Ag deposits (Carlin-type) for the HRB mineral assessment were subdivided into north and south Carlin-type deposits (fig. 8-2, table 8-1), on the basis of differing characteristics in the deposits in the region. Therefore, most deposits along the Getchell and Carlin trends, and in the Cortez-Pipeline and Independence Mountains Mining Districts belong to the north Carlin-type, whereas deposits in the Bald Mountain and Alligator Ridge area are south Carlin-type deposits. The north Carlin-type deposits are larger and have a greater abundance of As minerals, and are generally hosted in middle Paleozoic Silurian and Devonian sedimentary rocks, with the exception of the Getchell trend deposits that mainly are hosted in lower Paleozoic sedimentary and volcanic rocks. The south Carlin-type deposits are smaller and of lesser Au grade, and they are hosted either in lower Paleozoic or upper Paleozoic rocks. Both north and south types share many other general characteristics.

Characteristics considered for Carlin-type deposits in general are similar to those indicated by Berger (1996), Peters and others (1996), Arehart (1996), and Hofstra and Cline (2000).

These characteristics commonly include submicron-sized Au, generally in the crystal structure of disseminated pyrite or marcasite (fig. 8-6). The host rocks are variably silicified, decalcified, and argillized (Hausen and Kerr, 1966; Tooker, 1985; Berger, 1986; Arehart and others, 1993a), and the host lithologies include calcareous or siliceous sedimentary rocks, skarn, mafic metavolcanic rocks, and felsic intrusive rocks. The most abundant host rocks are thin-bedded, flaggy, mixed carbonate-siliciclastic rocks (fig. 8-4B). Deposition of ore minerals was at moderated depths of approximately ~1 to 3 km or possibly deeper (Rytuba, 1985; Juehn and Rose, 1985; Kuehn, 1989), in contrast to the more shallow paleodepths for the epithermal gold-silver deposits (see chapter 9).

Mineralogy in ore zones of Carlin-type deposits includes Au–bearing arsenian pyrite (fig. 8-6), marcasite, stibnite, realgar, orpiment, cinnabar, Tl-sulfide minerals, rare Ag–Sb and Pb–Sb sulfosalt minerals, Hg-rich sphalerite, and Ni sulfide minerals (Ferdock and others, 1997; Peters and others, 1998) (figs. 8-5 and 8-6). The northern Carlin-type deposits have an abundance of these minerals, whereas the southern deposits generally lack abundant As sulfide minerals. Total sulfide mineral content in all Carlin-type deposits usually ranges from less than 1 volume percent to local massive accumulations of pyrite (Bagby and Berger, 1985; Percival and others, 1988; Berger and Bagby, 1991). Barite and calcite also are present. This mineralogy is well expressed in the regional-scale stream-sediment geochemistry of As and Sb, as well as the ratio (see chapter 5)

Alteration types associated with Au–mineralized rocks in the north and south Carlin-type deposits is argillization (illite-clay), and silicification (jasperoid development), similar to alteration types described by Radtke (1985), Bakken and Einaudi (1986), Kuehn and Rose (1992), Drews-Armitage (1996), and Arehart (1996). A widespread characteristic of these deposits is the tremendous increase in porosity and permeability that accompanied early stage decalcification. Such porous rocks have much lower volumes and tensile strengths than their prealteration equivalents. Pre–Au alteration assemblages include syngenetic or diagenetic minerals in Paleozoic sedimentary rocks, as well as contact metamorphic and metasomatic minerals associated spatially with local contact metamorphic aureoles of small stocks. Post–Au alteration effects are related to supergene processes and locally to Miocene hot spring-related events associated with regional extension and basin and range faulting. Carbonation, as pre- and syn-Au carbon, forms in large masses of black, sooty sedimentary rocks that surround and are present in orebodies, and carbon commonly is associated with most Carlin-type deposits (see Radtke and Scheiner, 1970a,b; Kuehn, 1989). Much of this pre-ore carbon is considered to be relict from heated petroleum (Armstrong and others, 1997, 1998). Although hydrothermal alteration is an important and diagnostic constituent of the sedimentary rock-hosted Au–Ag deposits, silicification, argillization, decalcification, and carbonation are poorly represented in the regional-scale data bases available to the present mineral assessment.

The main geochemical elements associated with Carlin-type deposits are As, Sb, Hg, Zn, and Ba (see also, Lawrence, 1963, Papke, 1984; King, 1996; King and others, 1996). Trace amounts of Tl, Pb, Cu, Co, Ni, P, and some rare-earth elements locally are present as well (Erickson and others, 1964; Ressel and others, 2000). High Fe and S are associated with most of these ores as pyrite or other sulfide minerals. Thallium is anomalously high in some Carlin-type deposits, but minor to absent in others. Tellurium and Bi usually are absent to extremely low in Carlin-type deposits but may be elevated in distal-disseminated deposits (Hill and others, 1986; Albino, 1993, 1994). Base metals usually are at background levels. Locally in some deposits, such as Gold Quarry (Hausen and others, 1982; Rota, 1987), or in some distal-disseminated deposits (Johnson, 2000), base metals attain concentrations in the thousands of parts per million, although they do not contribute to the overall economic value of the deposits. The geochemical signature of the Carlin-type deposits is typically Au—gold/silver ratios generally are <1 (that is, Ag is not of significant economic value)—As, Sb, and Hg. Many of these ratios, however, were determined in oxidized Carlin-type deposits wherein Ag may have been removed during the process of protracted oxidation. Silver concentrations generally are much higher in the distal-disseminated deposits (Theodore, 2000), as well as in some deposits near the north parts of the Carling tend (Dobak and others, 2001).

Distal-disseminated Ag-Au Deposits (Model 19c of Cox and Singer, 1990, 1992)

Distal-disseminated Ag–Au (pluton-related) deposits have some distinctions from the Carlin-type deposits, but they are considered to be part of the sedimentary rock-hosted Au–Ag deposits for the present assessment. They are directly related to porphyry systems and contain Ag and Au in disseminations and (or) replacements and stockworks of narrow quartz-sulfide veinlets and (or) Fe oxide-stained fractures in sedimentary rock. They contain some diagnostic trace elements—specifically Pb, Zn, Mn, Cu, and Bi—that suggest that the deposits may be pluton-related (Cox and Singer, 1990, 1992). In addition, stable-isotope studies indicate that the fluids involved in the formation of the distal-disseminated Ag–Au deposits in the northern part of the Battle Mountain Mining District (fig. 8-2) included a significant magmatic component (Howe and others, 1995; Norman and others, 1996). In addition to some extensions to the southeast of the Battle Mountain Mining District along the Battle Mountain-Eureka mineral belt, other important districts for pluton-related deposits include parts of the Bald Mountain and the Eureka Mining districts (fig. 8-2).

A major distinction between distal-disseminated Ag-Au deposits and Carlin-type sediment-hosted Au–Ag deposits is that several distal-disseminated deposits show significant K metasomatism (Bloomstein and others, 1993, 2000), which is comparatively rare in the Carlin-type deposits, a notable exception being the Twin Creeks deposit in the Getchell trend.

In addition, many distal-disseminated Ag–Au deposits contain more Ag and base metals than most Carlin-type sediment-hosted Au–Ag deposits. The Cove deposit in the McCoy Mining District is one of the largest producers of Ag in the United States; in 1995, the McCoy-Cove deposits produced approximately 12 million oz Ag (372,000 kg Ag). Echo Bay, which has been mining the deposits, ceased production in March, 2002. At Cove, Ag–rich base-metal mineral assemblages are superimposed on the Carlin-type mineral assemblage (Nevada Division of Minerals, 2000; Johnson, 2000).

The association of distal-disseminated Ag–Au deposits with porphyry systems is significant. Porphyry systems generally consist of large volumes of rock that are characterized by disseminated concentrations of pyrite, chalcopyrite ($CuFeS_2$), bornite (Cu_5Fe_2), molybdenite (MoS_2), or Au—as well as a number of other prograde and secondary sulfide minerals—in intensely fractured rocks filled by stockwork veins or disseminated grains in hydrothermally altered porphyritic intrusions and (or) in their hydrothermally altered adjacent wall rock (Beane and Titley, 1981; Peters and others, 1996; see also, chapter 7). In the Battle Mountain Mining District, the Tertiary porphyry Cu systems contain relatively high concentrations of Au compared to many other porphyry Cu systems elsewhere in the southwestern United States, especially those present in Arizona. Much of the mineralization in these types of systems owed its origin to fluids that were expelled during the process of crystallization of a genetically associated magma. These intrusive centers represent composites of a number of closely associated igneous phases and include a number of genetically associated ore-types, such as Au skarns and polymetallic veins (fig. 8-7).

Although distal-disseminated Ag–Au deposits appear to be related genetically to porphyry systems, many deposits do not contain obvious features that would indicate this connection. An important factor is that these deposits truly are distal in nature, in many cases occurring over 1 km away from the causative intrusions. Deposits generally are of medium size, for instance approximately 1 million oz Au near the Eight South deposit, a probable 1 million oz Au in three other deposits (Trenton, Valmy, North Peak; Felder, 2000), and approximately 5 million oz Au in the Lone Tree deposits (see also, Bloomstein and others, 1993, 2000; Theodore, 2000). About 15 deposits in the Battle Mountain Mining District have many notable differences, some as described above, compared to the deposits used by Cox and Singer (1990, 1992) to construct the original distal-disseminated Ag–Au model. Due to complex tectonism and extension after mineral deposition, the deposits contain different geometric relations to the intrusive centers and also are hosted in different parts of the overall stratigraphic succession (fig. 8-7). For example, ore may be hosted by intensely fractured Ordovician quartzarenite (a relatively common relation), or it may be hosted by calcareous rocks in either the Pennsylvanian and Permian Antler sequence of Roberts (1964) or the Mississippian, Pennsylvanian, and Permian Havallah sequence (Theodore, 2000).

The distal-disseminated Ag–Au deposit model genetically belongs to the porphyry Cu or pluton-related mineral-

izing environment, and this model has a strong affiliation with upper crustal magmatism. A good example of this association is the Top deposit in the Bald Mountain Mining District where Au mineralization is superimposed over a porphyry-style system (fig. 8-8; see also, Hitchborn and others, 1996; Nutt and others, 2000). Many Carlin-type deposits, by comparison, typically cannot be definitively tied to magmatism (Ilchick and Barton, 1997), except in some isolated cases (Ressel and others, 2000). An underestimation of base-metal contents of mineralized systems, particularly from oxide ores, also has contributed to their problematic classification.

Geochemically, some sedimentary rock-hosted deposits in the HRB have high base-metal contents, chemical and physical attributes, and fluid-inclusion signatures (Theodore, 1998) that are characteristic of distal-disseminated Ag-Au deposits. Many of these deposits have elevated contents of K_2O (sericite) associated with Au–mineralized rock (Bloomstein and others, 1991). Large-scale additions of K_2O are not as common in most classic Carlin-type deposits (see also Nutt and others, 2000). Some difficulty of classifying Au deposits in the Lone Tree and Marigold areas in the north part of the Battle Mountain Mining District (fig. 8-2) involves protracted oxidation, probably lasting as long as 23 m.y., which may have altered significantly base- and precious-metal ratios from their preoxidation values.

Vertically stacked, large porphyry Cu systems contain a large number of peripheral distal-disseminated Ag–Au deposits in the northwest part of the Battle Mountain Mining District, similar to deposits elsewhere referred to as distal-epithermal Au deposits (Jones, 1992). These deposits represent the predominantly structurally controlled, high-level parts of porphyry Cu systems, commonly inboard from more common Ag–rich polymetallic vein and replacement deposits. Gold in these deposits originally was present in Au–enriched Fe sulfide minerals that comprised the pyritic halo of the porphyry Cu system. Metal zoning in the most outermost parts of these systems is complicated because absolute differences in precious-metal abundances are difficult to quantify due to intense oxidation of many of the known occurrences. Distal-disseminated Ag–Au deposits are analogous to polymetallic vein deposits (fig. 8-7), and they may be considered to be variants of them (Cox and Singer, 1990, 1992). However, distal-disseminated Ag–Au deposits differ from polymetallic veins in their disseminated nature, which make them amenable to exploitation by bulk-mining methods.

Changes in geochemical elemental ratios brought about by oxidation in distal-disseminated deposits cause high-level occurrences to have Carlin-type geochemical signatures. Indeed, Albino (1993) points out that the common enrichment of As, Sb, and Hg in both Carlin-type systems and distal-disseminated Ag–Au deposits partly results from these elements having the ability to be transported as bisulfide complexes (see also Brooks and Berger, 1978). In addition, Albino (1993) points out that many distal-disseminated Ag–Au deposits are enriched in Mn, whereas some Carlin-type deposits, in fact, may be leached of Mn.

Level of Exposure

Three parameters affecting level of exposure of sedimentary rock-hosted Au–Ag deposits have been considered in this assessment: (1) concealment by post-ore cover rocks, (2) concealment of pre-ore tectonic units, such as the upper parts of the Roberts Mountains and Golconda allochthons, and (3) depth of oxidation. Most rocks exposed in the mountain ranges in the HRB formed before Late Miocene (~6 Ma). These rocks were subjected to post–6-Ma extension, uplift, and erosion that resulted in post-ore basins that were filled with late Cenozoic sedimentary and volcanic rocks. The main mining districts (fig. 8-2) are present in and alongside the ranges. The deep parts of the basins have not had significant testing by exploration. It is likely that basins may conceal as many deposits as are exposed in the ranges (see also, Madden-McGuire and others, 1991).

Most sedimentary rock-hosted Au–Ag deposits are hosted in lower-plate rocks of the Roberts Mountains or Golconda thrusts (fig. 8-3). The deposits therefore are most likely to be exposed in areas where the tectonic windows through either of the upper plates are present, and they are most likely to be concealed where overburden covers the host rocks or where the host rocks are concealed tectonically. The Roberts Mountains and Golconda allochthons are several km thick. Because the thrust faults have shallow-dips, economically mineable deposits in their lower plates are more likely within about 10 km of the map projection of these thrust faults. These subjective concepts are not accurately represented or portrayed in the data bases available for the present mineral assessment because of the two-dimensional nature of the data.

Overall intensity of oxidation of sedimentary rock-hosted Au–Ag deposits and the thickness of oxidized rock have a direct effect on mining and milling costs and methods, as well as geologic inferences about ore genesis and environmental consequences of mining operations. Surface oxidation of some distal-disseminated Ag–Au deposits can result in bonanza Ag orebodies that are rich in Ag chloride minerals. Oxidation of Au–bearing pyrite also releases the Au chemically, which makes the Au amenable to treatment by heap-leach methods. Oxidation of the sulfide minerals allows low-cost heap-leach processing methods to be employed and also reduces blasting costs because the rocks commonly are softer. The depth of oxidation also can affect the Au concentrations in the ore and may provide structural information about the tectonic level of exposure of some deposits. In addition, oxidation may obscure many mineral textures and geochemical characteristics of sedimentary rock-hosted Au–Ag deposits that allow proper classification (see also Blake, 1992).

The apparent transition between two major types of deposits in the Battle Mountain Mining District, porphyry Cu and stockwork Mo deposits on the one hand, and distal-disseminated Ag–Au deposits on the other hand, reflects a different depth of formation (Doebrich and Theodore, 1996; Theodore, 2000). Post-mineralization faulting may have displaced ore during the last 17 to 14 m.y. The Au deposits

in the down-faulted terranes in the Battle Mountain Mining District may represent high-level parts of large mineralized hydrothermal systems, which formed either in calcareous sedimentary rocks or highly fractured siliceous sedimentary rocks near the paleosurface at the time of mineralization. The bulk of the Au mineralization in the Battle Mountain Mining District took place between 38 and 40 Ma (Theodore 1992a,b, 2000). A similar spatial transition in the Bald Mountain Mining District between distal-disseminated Ag–Au deposits in the west and Carlin-type deposits in the east also may reflect paleodepths of a single, zoned hydrothermal system or may represent the juxtaposition of two different Au-mineralizing systems (see chapter 7).

The thickness of Cenozoic deposits in the HRB (referred to as "depth to basement"; see chapters 2 and 6) was estimated for the present assessment from isostatic residual gravity data that were filtered to separate the observed gravity field into a basement component, caused by density variation within the pre-Tertiary basement, and a basin component, caused by variations in thickness of Cenozoic deposits. This filtering yielded a map of the thickness of Cenozoic deposits based on assumed variations of density with depth in these deposits (Jachens and others, 1996). The depth to basement map does not serve as an evidence map proper, but it is used as an overlay on the final mineral-resource assessment map to mask out areas that are covered by Cenozoic deposits that are greater than 1 km in thickness.

Data Bases Used for Assessment

Of the many data bases available for the Humboldt River Basin Mineral Assessment, several are particularly relevant to sedimentary rock-hosted Au–Ag deposits and the processes suspected to have formed and spatially controlled these deposits. The preliminary weights of evidence (WofE) assessments, as well as the final WLR assessment, require statistically significant intersections of the chosen data sets with the sedimentary rock-hosted Au–Ag training set. The data bases used include those from published geological literature, particularly the geologic map of the state of Nevada (Stewart and Carlson, 1978), structural and tectonic interpretive maps, Mineral Resource Data System (MRDS) records of Au deposit training sites (table 8-1), geophysical data, and regional-scale National Uranium Resource Evaluation (NURE) stream-sediment geochemical data. A training site dataset was created from the Nevada Bureau of Mines and Geology (NBMG) database (Davis and Tingley, 1999). The sedimentary rock-hosted Au–Ag deposit training site set consists of 293 deposits and occurrences (fig. 8-2, table 8-1) that include Carlin-type (northern and southern subtypes) and distal-disseminated Ag–Au ore deposit and occurrence sites. Another criteria used in the selection of the data bases was a subjective judgment of patterns in the raw data and in the predictor maps of good or bad spatial correlation with the shapes of the clustered training set points that was compatible with known geologic processes.

Geologic Map of Nevada

The training set of sedimentary rock-hosted Au–Ag deposits and occurrences were intersected with the geologic map of Nevada (Stewart and Carlson, 1978) using a 1–km radial buffer around each training site (see chapter 2). The host-rock map intersection with these training sites and the actual host rock of the deposits and occurrences are indicated on table 8-1. The host rocks mainly are sedimentary rocks of the upper and lower plates of the Roberts Mountains and Golconda thrusts, but they also include Mesozoic and Tertiary igneous rocks (table 8-2, fig. 8-9). In some cases the GIS intersection and the known host rock are the same; however, due to level of exposure and type of cover and differences with geology at large-scale near the deposits, the actual host rock commonly was different from that intersected on the digital geologic map of Nevada.

Sedimentary Rocks

Each mining district has distinct Paleozoic rock strata of that contain the bulk of the sedimentary rock-hosted Au–Ag deposits. The deposits along the Carlin trend lie in a 300–m-thick interval of favorable host stratigraphy, usually in upper units of the lower plate of the Roberts Mountain thrust (fig. 8-10). Examples are the Silurian and Devonian Roberts Mountains Formation (unit St from Stewart and Carlson, 1978)—a silty laminated dolomitic limestone, the Devonian unnamed limestone (Dc) (Evans, 1980), locally called the Popovich Formation—composed of platy, laminated, silty dolomitic and micritic limestone, and the locally recognized Devonian Rodeo Creek unit (not designated on Stewart and Carlson, 1978; see also, Christensen, 1993), which consists of laminated mudstone, siltstone, and siliciclastic and cherty rocks, with local limestone (Armstrong and others, 1997).

Upper-plate rocks locally are mineralized and include rocks of the siliceous (western) assemblage of Evans (1980), which are generally assigned to the Ordovician Vinini or Valmy Formations (unit Osv) in the area of the Carlin trend (Madrid and others, 1992), but also include Silurian and Devonian rocks (Cluer and others, 1997). The specific host units or stratigraphic horizons within these units for the sedimentary rock-hosted Au–Ag deposits cannot be represented accurately using the digital geologic map of Nevada (Stewart and Carlson, 1978) because most host rocks are hidden under younger rock units.

Sedimentary rock-hosted Au–Ag deposits in the Getchell (Potosi) area are hosted in upper Paleozoic carbonate-rich sedimentary rocks of the Mississippian Goughs Canyon Formation, the Pennsylvanian and Permian Etchart Formation, the Middle Pennsylvanian Battle Formation, and possibly the Pennsylvanian and Permian(?) Adams Peak Formation. These correspond with units of Stewart and Carlson (1978) unit MDs or Webb Formation. Deposits, especially around the Getchell Mine area, also are hosted in Lower Paleozoic clastic sedimentary rocks of the Cambrian Osgood Mountain and Preble

Formations and the Ordovician Comus Formation, which roughly correspond to units Os and Ct (Transitional Assemblage) of Stewart and Carlson (1978). These rocks are in tectonic contact with the Ordovician Vinini Formation (unit Os) and Valmy (unit Osv) in the Roberts Mountains allochthon (table 8-1). Intersections of deposits in the training set in the Getchell trend area with lithologies from the geologic map of Nevada (Stewart and Carlson, 1978) using the GIS generally are with units Os and Qa. The Qa intersections represent deposits covered by this unit and therefore unit Qa intersections were defined as "missing," in the modeling procedure and calculations. This means that the application of the lithologic data bases in the present mineral assessment in the Getchell trend and surrounding area may not be accurate.

In the Bald Mountain Mining District, sedimentary rock-hosted Au–Ag deposits are hosted by lower Paleozoic calcareous rocks (see Hitchborn and others, 1996) of the Cambrian Geddes Limestone (not on fig. 8-11; unit C of Stewart and Carlson, 1978), Dunderberg Shale (unit C), Hamburg Dolomite and Secret Canyon Shale (unit C), and Ordovician Antelope Valley Limestone (unit Oc) and Windfall Formation (unit Oc). Ore also is hosted in upper Paleozoic rocks in the Mississippian and Devonian Webb Formation (not on fig. 8-11; unit MDs), Chainman Shale (unit MDs), Diamond Peak Formation (unit MDs), Pilot Shale (unit MDs), and Joanna Limestone (unit MDs) (table 8-1, fig. 8-11). Although individual host stratigraphic horizons in the Bald Mountain Mining District area are not identifiable using the Geologic Map of Nevada (Stewart and Carlson, 1978), the host units are adequately represented in the present mineral assessment.

In the Battle Mountain Mining District, the main host rocks for ore are the Pennsylvanian and Permian Antler sequence (unit PPa) including the Middle Pennsylvanian Battle Formation (unit PPa) below the Golconda thrust and the Mississippian, Pennsylvanian, and Permian Havallah sequence (unit PMh) above the Golconda thrust (Roberts, 1964; Theodore, 2000). The inclusion of these rock types in the mineral assessment is broadly representative of their importance to ore control.

Sedimentary host rocks of most Carlin-type sedimentary rock-hosted Au–Ag deposits and some distal-disseminated deposits also contain sedimentary collapse breccia, as well as other breccias, which served as host rocks for most of the large orebodies, as conduits for migrating fluids, and as host rocks for other orebodies in most of north-central Nevada (Peters and others, 1997). These important host rock lithologies were not well represented as specific geologic elements in the data bases available for the present mineral assessment.

Igneous and Metamorphic Rocks

Close spatial association exists between some sedimentary rock-hosted Au–Ag deposits and Mesozoic plutons (Silberman and others, 1974; Blake and others, 1979), particularly in the Getchell, Battle Mountain, Carlin trend, and Bald Mountain areas (Peters and others, 1998) (figs. 8-2,

8-12). Tertiary intrusive rocks also may be directly related to some distal-disseminated Ag–Au deposits, but are not as common in many Carlin-type deposits. Proximity to plutonic and intrusive rocks (referred to as "pluton proximity"; see chapters 2 and 7) was prepared from the 1:500,000 scale geologic map of Nevada (Stewart and Carlson, 1978). Plutonic rocks that were selected range in age from Middle-Late Triassic to late Miocene and were buffered at distance intervals of 1 km (fig. 8-12). A 21–km radial buffer was used around plutons in the WofE analysis for intersection of this data layer with the sedimentary rock-host Au–Ag deposit training set (table 8-1, fig. 8-12). Size of the radial buffer was selected on the basis of statistical constraints used in the WLR methodology. This radial buffer is not representative of known or inferred geological processes, which typically are confined to a radius if <2 km from a pluton (see chapter 7).

Lithodiversity

Structure, stratigraphy, and intrusive activity are important factors controlling the mineralization process of sedimentary rock-hosted Au–Ag deposits. Tectonism also plays an important role exposing orebodies at the surface. In the HRB, the degree of lithologic complexity or "lithodiversity" that is represented on geologic maps reflects the structural, stratigraphic, and intrusive relations in each area. For example, faults distort, dismember, and rotate structural blocks, disrupt the continuity of units, and juxtapose unrelated rocks. The greater the number and more intricate these relations, the more complex an area appears on a geologic map. In addition, the process that created the lithodiversity may represent ground preparation for district- or regional-scale fluid flow. It then follows that lithologically diverse areas may show a higher degree of spatial association with sedimentary rock-hosted Au–Ag deposits.

This proposition is supported by the research of Griffiths and Smith (1992) and Mihalasky and Bonham-Carter (2000). Griffiths and Smith (1992) demonstrated that a simple linear relation among geologic diversity and the mineral-resource diversity is present where areas with relatively high diversity are favorable hosts for metallic ores. This is demonstrated in most of the counties in Nevada (12 of 17), which have a high diversity and are prolific producers of base- and precious metals. Our assumption is that this also is applicable to sedimentary rock-hosted Au–Ag deposits because lithodiversity spatially emphasizes a degree of complexity of processes necessary for the formation of these deposits (fig. 8-13).

Spatial association between sedimentary rock-hosted Au–Ag deposits and lithodiversity is assumed to increase with increasing lithodiversity, such that areas with more than four geological map units per 25 km2 contain more of these deposits than would be expected due to chance (see also, Mihalasky and Bonham-Carter, 2000). High lithologic diversity on figure 8-13 likely reflects the presence of complex structural, stratigraphic, and intrusive relationships that are thought to control, focus, localize, and expose both the Carlin-type and pluton-

related distal-disseminated sedimentary rock-hosted Au–Ag deposits.

Structural Geology and Tectonic Elements

The overall assessment methodology adopted for the sedimentary rock-hosted Au–Ag deposits involved identifying available regional-scale data sets that adequately reflect structural control of deposits. In addition, the data sets were required to be compatible with genetic processes that controlled distribution of both subclassifications of the deposits.

Regional- and specific district-scale ore controls are an important constraint for assessment of sedimentary rock-hosted Au–Ag deposits. Generally, first-order control at regional scales is defined by "trends" or areas (Roberts, 1966; Shawe and Stewart, 1976; Rowan, 1979; Shawe, 1991; Peters, 2000) that commonly are associated with tectonic windows through the upper plates of thrust faults in the region (fig. 8-2). Second-order control is displayed by more local, district-scale, steep-dipping normal faults, which may be subparallel to the overall first-order "trends" (Madrid and Roberts, 1991). Structures in Proterozoic basement that can be discerned through geophysical data also may be important localizers of deposits and districts (Grauch, 1986; Grauch and others, 1995; Teal and James, 2000). Local control can be either typically structural (see also, Peters, 1996; Peters and others, 1996) or stratigraphic. Specific stratigraphic intervals or zones within them when adjacent to specific structures are considered to be significant factors in localizing Au in sedimentary rock-hosted Au–Ag deposits.

Sedimentary rock-hosted Au–Ag deposits classified as distal-disseminated Ag–Au deposits are strongly concentrated in the Battle Mountain Mining District, which is near the northwestern terminus of the Battle Mountain-Eureka mineral belt (fig. 8-2). This remarkable concentration of pluton-related mineralized systems results from a number of district- and regional-scale metallotects (Doebrich and Theodore, 1996; Peters and others, 1996). In addition, other clusters of these types of deposits are concentrated in the Bald Mountain and Robinson Mining Districts (see chapter 7).

Northwest-striking Jurassic or older faults also control the location of the distal-disseminated type of sedimentary rock-hosted Au–Ag deposits, particularly in the Battle Mountain Mining District and the Carlin trend (Evans and Theodore, 1978), as well as in the Bald Mountain Mining District (Hitchborn and others, 1996). In the Battle Mountain Mining District, most centers of widespread mineralized rock are controlled by intersection of northwest-striking faults and (or) dikes with north-striking faults (Doebrich and others, 1995, 1996). Shattered rocks at these broad structural intersections appear to have controlled subsequent emplacement of intrusive rocks and their genetically associated mineralized systems. Tertiary-age north-trending fabrics, however, are the predominant structural orientation throughout the Battle Mountain Mining District. This structural grain follows the orientation of hinge lines of Paleozoic and (or) early Mesozoic folds,

some of which have kilometer–wide amplitudes in the upper plates of the Roberts Mountains and Golconda thrusts. Further, the Battle Mountain Mining District probably owes its metal endowment to the presence of deep regional-scale fractures that acted as fluid conduits (see also Peters and others, 1996; Theodore, 2000). At Bald Mountain, northwest-striking faults controlled emplacement of the Jurassic pluton and were reactivated repeatedly. During Mesozoic contraction, they acted as strike-slip tear faults, and, during Tertiary extension, they controlled the rotation of district-scale blocks and the uplift of the mountain range (Nutt and others, 2000).

Many sedimentary rock-hosted Au–Ag deposits in northern Nevada are hosted in, or spatially associated with, district-scale north-northwest- and northeast-striking, medium- to high-angle faults. In addition, several west-northwest–striking, medium- to shallow- northeast-dipping shear zones and shear folds have been recognized in some districts (Peters, 1997a,b,c, 2000). These shear zones contain evidence of fluid transport, dissolution, and coeval deformation (fig. 8-14), which suggests that they acted as district- and regional-scale conduits for hydrothermal fluids. The Carlin, Getchell, and Battle Mountain-Eureka mineral trends are examples of aligned mineral occurrences along regional-scale lineaments (see also, Roberts, 1966) that contain textural evidence of fluid flow and deformation (fig. 8-14) (Evans and Theodore, 1978; Peters, 2000). Faults shown on the geologic map Nevada (Stewart and Carlson, 1978) differ in age, and most faults represented there are late Miocene and younger. Therefore, the geologic map of Nevada does not adequately differentiate ore-controlling faults from younger faults for this assessment.

Many well-known and other regional-scale lineaments, including district-scale faults and shear zones, appear to have been active before, during, and after the Au mineralization event that formed the bulk of the sedimentary rock-hosted Au–Ag deposits (figs. 8-14, 8-15). Besides northwest- and north-striking mineral belts and their accompanying folds and faults, examples of probable regional-scale conduits are: (1) permeable early Paleozoic stratigraphic units in the lower plate of the Roberts Mountains thrust; (2) the Roberts Mountains thrust zone and parallel thrusts; and (3) the northeast-trending Crescent Valley Independence lineament and associated faults (figs. 8-14, 8-15, 8-16, 8-17, 8-18).

A northeast-trending lineament, the Crescent Valley-Independence lineament (CVIL), is interpreted by Peters (1998) and by Theodore and Peters (1999) to have been active from the Late Paleozoic to the Middle Cenozoic, which also overlaps the Au–mineralizing time estimates of many sedimentary rock-hosted Au–Ag deposits (figs. 8-14, 8-15). The CVIL is defined by deformed rocks, igneous intrusions, and hydrothermal activity of several ages along a zone that extends for about 90 km southwest from near the Independence Mining District to near the Cortez Mine in the north part of Crescent Valley (figs. 8-15, 8-16). Because the CVIL traverses through three large sedimentary rock-hosted (Carlin-type) Au districts with similar characteristics, it may have served as a common regional fluid conduit for these districts (Peters, 2000). Cres-

cent Valley-Independence (CVIL) and Getchell lineaments (referred to as "NE linears"; see chapter 2) were constructed for this present assessment to represent two corridor regions that envelop the CVIL (Peters, 1998; Theodore and Peters, 1999) and the Getchell trend by use of LANDSAT MSS and shaded relief of topography and known faults and other structural features (fig. 8-16).

Lithotectonic map terrane units, referred to as "lithotectonic terrane" (see chapter 2), were selected using lithotectonic terrane boundaries from Lahren and others (1996), spatially tied to lithologic unit patterns on the 1:500,000–scale geologic map of Nevada (Stewart and Carlson, 1978) (fig. 8-17). Proximity to autochthon-allochthon and structural window thrust contacts, referred to as "thrust proximity" (see chapter 2), were prepared from the 1:500,000–scale lithotectonic terrane map (fig. 8-17). Contacts of thrust surfaces were extracted and buffered at a distance interval of 2 km (fig. 8-18), on the basis of statistical constraints in the WofE methodology (see chapter 2). The buffer distance is compatible with presumed fluid flow distances interpreted for sedimentary rock-hosted Au–Ag deposits in the HRB area (see also, Peters, 1998, 2000).

Fluids may have traversed more than 10 km along some permeable or structurally prepared horizons, especially in or adjacent to district-scale tectonic lineaments that cross many lithostratigraphic terranes (figs. 8-7, 8-18). Fluid flow along or beneath the Roberts Mountain or Golconda thrusts, or other thrusts, that separate or cross the lithostratigraphic terranes, produced jasperoidal rocks, silicified breccia, gouge, and phyllonite along or adjacent to these thrust planes. Quartz veining and additional jasperoid development was localized above the thrust planes, especially adjacent to district-scale structures. Multiple thrusting events during and after the Antler Orogeny (see Ketner and others, 1993; Theodore and Peters, 1999; Theodore and others, 1998; 1999) provided shallow-dipping faults or fractures that served as conduits for regional- and district-scale fluid migration. Commonly, thrust planes are overlain by impermeable mudstone, shale, chert, and other siliciclastic rocks that are certainly much less permeable than calcareous rocks in the lower plate (fig. 8-16).

Geophysical Data

Geophysical data were used to analyze deep structures and terranes in assessment of sedimentary rock-hosted Au–Ag deposits in the HRB. Also, much of the region, and therefore many undiscovered deposits, are covered by Tertiary and Quaternary alluvium, colluvium, and volcanic units and by the Roberts Mountains and Golconda allochthons. The geophysical data were used to identify features beneath this cover. A number of geophysical data bases and interpretations are important for assessing sedimentary rock-hosted Au–Ag deposits, including airborne radiometric K data (Grauch and Bankey, 1991; Pitkin, 1991), isostatic gravity (Gilluly and Harold, 1965; Grauch and others, 1995), depth to basement,

basement anomaly, and aeromagnetic maps (Grauch, 1986; Hoover and others, 1991, 1992; Teal and James, 2000), as well as electromagnetic methods (Pierce and Hoover, 1991). In addition, geophysical data have been used to interpret deep crustal structures that may influence location of the sedimentary rock-hosted Au–Ag deposits, such as magnetotelluric (MT) data (Rodriguez, 1997, 1998) and two-dimensional (2–D) resistivity modeling to help determine basin-fill thickness (Jachens and Moring, 1990; Jachens and others, 1996). These studies helped provide a better understanding of: (1) the role of crystal structure during fluid migration, (2) possible sources of metals, and (3) the spatial distribution of mineral deposits. These latter interpretations were not directly or fully reflected in the current assessment because the data bases were not used.

The only geophysical data base directly used for the present assessment of sedimentary rock-hosted Au–Ag deposits was a buffer of lineaments interpreted from a derivative basement gravity map (fig. 8-19). This data base contains interpreted regions of crustal highs and lows, referred to as "gravity terrane" (see chapter 2), where broad regions of generally high and low value were delineated from the basement gravity anomaly and are portrayed as lineaments (see also, chapter 6). From this basement gravity anomaly, a proximity to interpreted lineament features was intersected with the sedimentary rock-hosted Au–Ag deposit training set (table 8-1). This geophysical data base was deemed important because sharp changes in gravity gradient are inferred to represent major breaks in the crust that acted as conduits for hydrothermal ore fluids, which in turn could have formed the sedimentary rock-hosted Au–Ag deposits (fig. 8-19). This geophysical data base provides a subsurface evidence component to the present assessment.

Geochemical Data

Geochemically, Carlin-type deposits bear some similarities to distal-disseminated Ag–Au (pluton-related) deposits (Cox and Singer, 1990, 1992). The latter are directly attributable to fluids emanating from porphyry Cu systems and have some base-metal and Ag geochemical signatures similar to porphyry systems as well as a number of igneous isotopic signatures. Ore-forming fluids responsible for most Carlin-type deposits do not show isotopic and chemical evidence for a relationship to porphyry-type systems (Seedorff, 1991), although some recent data suggest that some deposits (Twin Creeks, Getchell) may have been generated from fluids involving a significant magmatic component (Norman and others, 1996; Hofstra and Cline, 2000).

Arsenic, Ba, and Na were used in the assessment for sedimentary rock-hosted Au–Ag deposits (figs. 8-20, 8-21). Arsenic is one of the most useful pathfinder elements for sedimentary rock-hosted Au–Ag deposits because it is associated strongly with Carlin-type deposits and some distal-disseminated Au–Ag deposits. A high Ba/Na ratio in NURE

samples (fig. 8-21) spatially coincides with the distribution of known Carlin-type deposits. The Ba/Na ratio functions as a proxy for the upper-plate rocks of the Roberts Mountains allochthon, which spatially are related to and overlie many Carlin-type Au-Ag deposits. It also may reflect regional-scale alteration associated with the passage of hydrothermal fluids and alteration related to the formation of sedimentary rock-hosted Au–Ag deposits (Mihalasky, 2000, 2001; see also, Papke, 1984, Orris, 1986). In general for most Carlin-type deposits, the Ba/Na ratio should increase as Na is depleted and Ba is introduced (see Hofstra, 1994; also see Barnes and Rose, 1998, who indicate that Na is removed from host rocks to become a major solute in hydrothermal fluids). The Ba/Na ratio is not a perfect indicator of all sedimentary rock-hosted Au deposits in northern Nevada, as Na commonly is introduced in distal-disseminated Ag–Au deposits, and lower-plate carbonate rocks generally have original low Na concentrations. Despite ambiguous processes, the pattern of the Ba/Na ratio was helpful in defining areas of favorability in the data-driven modeling.

NURE As data were processed in the spatial domain (referred to as "As-spatial"; see chapter 2). The local surface was interpolated using a fixed sampling radius of 15 km and a distance-decay rate that diminishes with the square of the distance, and is taken to represent the local-scale variation of As. This radius was helpful in the WLR assessment method, but is too large to have geological or geochemical meaning. The regional surface generated from this radius, however, was then interpolated using a fixed sampling radius of 100 km and a distance-decay rate that diminishes with square of the distance, and is taken to represent the broad, regional-scale variation of As. The regional surface was subtracted from the local to yield a third surface, the residual local-scale anomaly, which was used in the WLR method to represent the departure from the background variation to produce the evidence map (fig. 8-20). NURE Ba and Na data, treated as the ratio Ba/Na, also were processed in the spatial domain in the same way (fig. 8-21).

Descriptions of Specific Mining Areas

The main areas of mining that contain the largest clusters and largest deposits of sedimentary rock-hosted Au–Ag deposits are the Carlin trend, the Getchell tend, the Independence Mountains, Battle Mountain, and Bald Mountain Mining District (fig. 8-2). The Carlin trend, Getchell trend, Independence Mountains, and Cortez-Pipeline Mining Districts contain Carlin-type Au–Ag deposits, whereas the Battle Mountain-Eureka mineral trend mainly contains distal-disseminated Ag–Au deposits. The Bald Mountain Mining District contains both types of deposits. The White Pine and Antelope Mining Districts and many other smaller districts (see Tingley, 1992a,b; and also chapter 7) contain pluton-related and distal-disseminated Ag–Au deposits.

Carlin Trend Area

The Carlin trend is a 65–km-long alignment of sedimentary rock-hosted Au–Ag deposits in northwestern Nevada, northwest and southeast of the town of Carlin, Nevada (fig. 8-2) (McFarlane, 1991; Christensen, 1993). The principle commodities produced are Au, with lesser Ba, Ag, and As. From 1965 to 1999, the district produced more than 660 tonnes (21 million troy oz) Au to 1997 and over 50 million tonnes Au total (Teal and Jackson, 1997a,b). Production in 2001 is forecast to exceed 3.8 million ounces Au, from several companies mining from more than eight mines (see also, Nevada Bureau of Mines and Geology, 2000) (figs. 8-22, 8-23, table 8-1). Mining is done by both open-pit and underground methods. The large size of several of the mining operations is emphasized by the large volume of rock involved daily from the Goldstrike open pit mine that approximates 500,000 tpd moved, of which approximately 40,000 tpd is ore—all accomplished by 24–hour operations (see also Bettles and Lauha, 1991; Leonardson and Rahn, 1996). The large Gold Quarry mine also has had similar production volumes, whereas the small open pit mines and underground mines produce less volume. Ore is exploited from about six underground operations, mostly declines, but also three major deep shafts. Processing is by heap leach and carbon-in-pulp for oxide ores and by autoclave and roaster for sulfide ores. Approximately 75 million to 100 million oz Au constitute the reserve base, and an additional 50 million oz Au are in resource categories. Most mines have relatively low grades (approx. 0.040 oz/t Au), but some deep mines have high grades (0.5-0.9 oz/t Au) (see also, table 8-1) (Clode, 1995).

Sedimentary rock-hosted disseminated Au-Ag deposits along the Carlin trend are associated spatially with tectonic windows through the Roberts Mountains allochthon or with structural highs beneath the allochthon (Roberts, 1960; 1966; Thorman and Christensen, 1991; Peters, 1997a,b,c; 1999). The Carlin trend is a northwest-trending belt of Au deposits near these windows (fig. 8-22) in lower-plate rocks (Bagby and Berger, 1985; Madrid and Bagby, 1986; Baschuk, 2000). Gold-mineralized rocks along the Carlin trend are concentrated along a series of NNW– and NE–striking, medium- to high-angle district-scale shear zones and faults (figs. 8-22, 8-23). In addition, several WNW–ESE-striking, medium to shallow, NE–dipping shear zones and shear folds also have been recognized (Peters, 1997a,b,c; 1999).

Getchell Trend Area

The area of the Getchell trend includes the Twin Creeks Mine area, the Getchell Mine area, and the Pinson and Preble mine areas (fig. 8-24). The deposits are in the Potosi (Getchell) Mining District, which lies on the east flank of the Osgood Mountains (figs. 8-2 and 8-24). This area recently has emerged as a major Au district, but it has had a long history since the discovery and mining of the Getchell Mine in

1934 (Erickson and others, 1964). Deep hypogene discoveries at Getchell and at Twin Creeks Mines have encouraged additional exploration for deep sulfide ore in the Pinson and Preble areas. The orebodies have characteristics typical of Carlin-type deposits (Berger, and Tingley, 1985; Berger, 1985; Bagby and Cline, 1991; Stenger and others, 1998; Bowell and others 1999; Hofstra and Cline, 2000) and they are particularly well known for massive, coarse crystalline realgar and orpiment lodes in the Getchell Mine.

The geologic history of the Getchell trend area is the result of accretion of Paleozoic terranes that have been faulted and deformed near a major terrane boundary along the Getchell fault (Grauch and Bankey, 1991; Hoover and others, 1991; Hotz and Willden, 1964; Crafford, 2000a,b). These rocks were intruded by a large Cretaceous (85 –94 Ma, Silberman and others, 1974; Groff, 1996) granodiorite stock (see also, Joralemon, 1975). Gold deposits are hosted in early and late Paleozoic sedimentary rocks (fig. 8-24).

The Twin Creeks Mine is the third largest primary Au–producing mine in North America and includes the Mega, Vista, and West Pits. In May 1997, Santa Fe Pacific Gold combined with Newmont Mining Corporation to operate the property. In 1999, the mine produced 760,574 oz Au from an oxide and sulfide milling and oxide leaching operation (Thoreson and others, 2000). Oxide ores at Twin Creeks Mine are processed at a rate of 28,000 tpd on three leach pads. Sulfide ores are processed through the Sage Mill that feeds two 4,000 tpd autoclaves. Production of sulfide ore from the Twin Creeks operation to 2000 is approximately 4.05 million oz Au, about 59 percent of the total reserves. Ore from other Newmont properties also is trucked to and processed at the Twin Creeks operations (Thoreson and others, 2000).

Gold orebodies at the Twin Creeks Mine are present at the intersection of the north-northeast-striking Getchell trend and the north end of the north-striking Valmy trend. Twin Creeks orebodies are present in the Early Ordovician Comus Formation, which is composed of distal carbonate slope to basinal plain sequences with intercalated fine-grained siliciclastic rocks, silty carbonate rocks, and fine-grained lapilli-sized basaltic tuffs that are intruded by mafic to ultramafic sills. The Ordovician Valmy Formation was emplaced structurally above the Comus Formation along the Roberts Mountains thrust. The upper plate rocks are overlain by the Pennsylvanian and Permian Etchart Formation that is part of the overlap assemblage of Roberts (1964) and is composed of silty limestone and calcarenite with minor bioclastic limestone, chert pebble conglomerate, calcareous quartz siltstone, and arenite (Osterberg and Guilbert, 1988, 1991; Osterberg, 1990; Thoreson and others, 2000).

The Getchell Mine property is one of the earliest open-pit oxide and sulfide Au production sites in Nevada and represents the earliest large-scale Carlin-type exploitation (Joralemon, 1959; Erickson, 1964; Berger and Tingley, 1985). Recent discovery of the Turquoise Ridge deposit and underground reserves along the Getchell fault have led to additional exploration by Placer Dome Exploration that follow up on total

proven and probable reserves of 9.4 million oz Au in 1998 (Chevillon and others, 2000).

The Getchell deposits are controlled by intersection of high- and low-angle faults and by chemically and physically favorable Paleozoic stratigraphic units. The most favorable units are the Preble Formation, Comus and Valmy Formations, and Etchart Formations. Major offset of these rocks has taken place along major north-, northeast-, and northwest-striking faults (Berger and Taylor, 1980; Berger, 1985; Chevillon and others, 2000). New understanding of the structural complexity and stratigraphic units of the Getchell Mine area has allowed additional potential in the area to be realized, and it is likely that resources will increase and underground mining activity will expand. Placer Dome stopped operation on the Getchell property and wrote off expenses in October, 2001.

The Pinson, Preble, and Kramer Hill areas lie south of the Getchell mine. From 1980 to 1999, the Pinson Mining Co. produced >1 million oz Au from oxide ores in sedimentary rock-hosted Au–Ag deposits (McLachlan and others, 2000). The Pinson Mine is hosted in carbonate rocks and argillites of the Comus Formation and exhibits stratigraphic control as well as structural control along faults (fig. 8-24). The Preble Mine is hosted in carbonaceous shale, calcareous shale, and silty limestone of the middle member of the Upper Cambrian to Lower Ordovician Preble Formation, especially along northeast-striking, southeast-dipping shear zones (Crafford, 2000). The Kramer Hill Mine is hosted in shattered shale and impure quartzite of the Twin Canyon member of the Cambrian Osgood Mountain Quartzite in the hanging wall of a north-northeast-striking, west-dipping fault (Kretschmer, 1984a,b, 1991, Foster and Kretschmer, 1991; McLachlan and others, 2000). The deposit is distinct from an epithermal vein deposit at Kramer Hill and lies along the southwest extension of the Getchell trend.

Battle Mountain Mining District

The Battle Mountain Mining District is the main and type location for distal-disseminated Ag–Au deposits and pluton-related mineral occurrences in the northern Great Basin, and it is an area of substantial recent production of Au by Battle Mountain Gold Co., Marigold Mining Co., and Newmont Mining Corp. (figs. 8-2, 8-25). The district includes four Tertiary porphyry Cu and three Cretaceous stockwork Mo systems, as well as a large number of distal-disseminated Ag–Au deposits (Doebrich and Theodore, 1996; Theodore, 2000). Historically, the Battle Mountain Mining District intermittently has produced metals over a span of about 120 years. It has yielded approximately 3.5 million oz Au since 1978, when production shifted from base and precious metals to precious metals. Prior to 1978, production of Au from large-scale mining operations, which began in 1967, was mostly as a byproduct of production of Cu from two separate porphyry systems centered at Copper Canyon and at Copper Basin. Previous investigations by the USGS in the mining district demonstrated a genetic link

between distal-disseminated Ag–Au deposits (Cox and Singer, 1992) in the northern part of the area and porphyry Cu and stockwork Mo systems in the southern part (Theodore, 2000).

About 15 precious-metal deposits in the Battle Mountain Mining District (fig. 8-2, table 8-1) are classified as distal-disseminated Ag–Au deposits (Cox and Singer, 1992). They owe their origins to relatively far-traveled, hypogene Au–bearing fluids emanating from buried porphyry Cu systems, somewhat akin to the evolution of immiscible fluids described for porphyry systems (Hedenquist and Lowenstern, 1994; Albino, 1994). The Eight South Au deposit (Graney and McGibbon, 1991, 1999; McGibbon and Wallace, 1997) was the first of these recent discoveries near the Old Marigold Mine (fig. 8-25). The distal-disseminated Ag–Au deposits in the Battle Mountain Mining District are in Paleozoic sedimentary rocks and represent mineral occurrences at various levels vertically in large magmatic-hydrothermal systems as described by Albino (1994) (fig. 8-25).

Assuming a reasonable future price for Au, a number of additional open pit operations should be brought into production during the next 10 to 15 years in the general area of the distal-disseminated Au–Ag deposits near Eight South (D.H. McGibbon, written commun., 2000). These operations would include one at the Section 31 Au-resource area, one in the adjoining Sec. 30, T.33N., R.43E., and others at the Eight North and Five North deposits on the pediment, north of the Eight South deposit (fig. 8-25). The Section 31 Au deposit includes a combined measured and indicated as well as inferred resource of approximately 1.5 million oz Au in 52 million ± tons (Glamis Gold Ltd., Press Release, Nov. 2, 2000). Furthermore, a possible Au–bearing skarn target might be present southwest of Eight South as a replacement deposit in chemically favorable rocks of the overlap assemblage below the Golconda thrust (D.H. McGibbon, written commun., 2000). The entire mining complex centered at Marigold has produced more than 1 million oz Au through Jan., 2000—which amounts to approximately 150 percent of the originally mineable reserve announced at the start up of mining operations. As of Dec. 31, 1999, economic reserves included about 19 million t at an average grade of 0.032 oz Au/t or about 613,000 oz Au (D. H. McGibbon, written commun., 2000). This latter Au reserve figure is approximately the same as the original figure announced before mining started in 1988.

Bald Mountain Mining District

Most sedimentary rock-hosted Au–Ag deposits in the Bald Mountain Mining District mostly are hosted by lower Paleozoic platform rocks in the lower plate of the Roberts Mountains thrust; these rocks include massive to thick-bedded carbonate strata and calcareous clastic units (Hitchborn and others, 1996; Nutt and others, 2000) (fig. 8-26). The west side of the district mainly contains distal-disseminated Ag–Au deposits, whereas the east side and south side, including Alligator Ridge deposits to the south (fig. 8-26),

contain Carlin-type sediment-hosted Au–Ag deposits (fig. 8-2). The distal-disseminated Ag–Au deposits are related to a single, restricted, relatively Fe–sulfide-poor system that formed sub-economic porphyry (?) Cu and W skarns. The related Au deposits are present both within and outside a 1–km-wide contact aureole surrounding a small Jurassic (159 Ma) K–feldspar-biotite-(hornblende) quartz monzonite stock (Nutt and others, 2000) (figs. 8-26 and 8-27).

Mineralization at Bald Mountain took place somewhat deeper (probably 3 to 6 km) than in the Battle Mountain Mining District. Further, polymetallic quartz veins are sparse in the Bald Mountain Mining District compared to their widespread presence in the Battle Mountain Mining District. At Bald Mountain, approximately 1.4 million oz Au have been produced from seven oxide deposits since 1983; approximately 800,000 oz Au currently (early 2000) have been blocked out as a mineable reserve, and the likelihood of additional discoveries is excellent (Nutt and others, 2000). The Bald Mountain Mining District has produced mainly oxide ores that are processed by cyanide heap leach methods. Considerable potential exists for deep sulfide orebodies below known oxide ores and elsewhere in the area.

Independence Mining District

Independence Mining District contains clusters of sedimentary rock-hosted Au–Ag deposits of the northern Carlin type at the northeast end of the CVIL (figs. 8-2, 8-15, 8-16, 8-28). The district-scale cluster of orebodies in the Independence Mining District defines a 6.5– to 8–km-wide, northeast-trending zone of complex tectonic windows through the upper-plate rocks of the Roberts Mountains thrust (Peters and others, 2003) (fig. 8-28). Production from 1869 to 1989 was 2.3 million oz Au, 7,559 oz Ag and 41,980 lbs Sb. Barite also was produced from small mines in upper plate rocks (>70,000 tons) (LaPointe and others, 1991). Exploration for sedimentary rock-hosted Au–Ag deposits began in the 1970s, and a large deposit was discovered in the Jerritt Canyon area (fig. 8-28). These and subsequently discovered deposits were developed as a number of large open pit mines through joint venture operations with the Independence Mining Co. Underground mining began in the late 1990s in a number of locations for high-grade sulfide ores, and Anglo American, Ltd., began to operate most properties in 1999. Production between 1981 and 1999 was approximately 6 million oz Au with production rates at about 300,000 oz Au per year. Reserves in 1999 were 1.5 million oz Au and resources 3.8 million oz Au (Nevada Bureau of Mines and Geology, 2000).

The Au deposits in the Independence Mountains Mining District contain host-rock lithologies and mineralogical, geochemical, and structural features common to Au deposits along the Carlin trend area (Hofstra and others, 1991a; Peters and others, 2002). Host rocks are lower-plate rocks that have been multiply thrust, dismembered, and repeated, and Au deposition favors the lower tectonic slices of the Silurian and Ordovician

Hanson Creek (unit St of Stewart and Carlson, 1978) and Silurian and Devonian Roberts Mountains Formation (unit St) (Daly and others, 1991; LaPointe and others, 1991) (fig. 8-28). Northeast-striking faults cross cut tectonic windows through the upper plate of the Roberts Mountains thrust or associated structural highs below the thrust. The Au deposits in the Independence Mining District have a geochemical signature of elevated As, Sb, Tl, and Hg contents. The orebodies are structurally controlled, many by northeast-striking faults (Birak and Hawkins, 1985; Coats, 1987; Bratland, 1991; Daly and others, 1991; LaPointe and others, 1991). This northeastern elongation of faults, orebodies, and windows also is interpreted here as the expression of the north part of the CVIL (fig. 8-28). The structural complexity and mountainous terrane has hindered exploration in the Independence Mountains Mining District, but significant potential exists there on the basis of comparison to similar northern Carlin-type systems elsewhere in the HRB.

Cortez-Pipeline Mining District

The Cortez-Pipeline Mining District, also called the Cortez-Bullion-Hilltop area and Central Battle Mountain trend, is located in the Bullion district and includes the Gold Acres, Pipeline, South Pipeline, Horse Canyon, and Cortez Mines, which are hosted in lower-plate rocks, and the Hill Top Mine, which is hosted in upper-plate rocks of the Roberts Mountains allochthon (figs. 8-2, 8-29). Recent discoveries include the Pediment and Crossroads deposits. The deposits are of the northern Carlin type of sedimentary rock-hosted Au–Ag deposits. Mining began in the area in 1862 and was intermittent until the formation of the Cortez Joint Venture in 1964. The Cortez Joint Venture now includes the Pipeline complex, operated by Placer Dome U.S. Inc., and Au mining and production has steadily increased with new discoveries and application of new mining and processing technologies. Between 1942 and 1984, the area produced 5.2 million tons of ore from the Cortez and Little Gold Acres areas that graded about 0.1 oz/t Au. In 1988 and 1989, production rose to about 40,000 oz Au per year and included mining at Horse Canyon (fig. 8-29). The Cortez mine contributed about 50,000 oz Au per year between 1990 and 1993. The discovery of the Pipeline and South Pipeline deposits has increased production from 1.8 million oz Au between 1995 and 1998 to 1.3 million oz Au in 1999. Reserves are 189.4 million tons grading 0.050 oz/t Au, and resources are 119.1 million tons grading 0.035 oz/t Au. The potential of additional increases in resources in the area is good.

Ore controls in the Cortez-Pipeline Mining District are both stratigraphic and structural (Kelson and others, 2000). The main hosts are the lower-plate rocks to the Roberts Mountains thrust, including the Roberts Mountains Formation and Wenban Limestone, and upper-plate rocks Valmy Formation rocks; quartz porphyry dikes are present locally. Structural control is both by northwest-striking faults and other structures along the Battle Mountain-Eureka mineral belt

(fig. 8-29) and northeast-striking faults, particularly the Fence fault in the Pipeline deposit (see also, Foo and others, 1996a,b) and the Gold Acres and Island faults in the Gold Acres deposit (Hays and others, 1991), which are part of the CVIL (Peters, 1998). Fold axial planes in the windows trend west or west-northwest and are cut by a set of northeast-striking faults, which lie in the general trend of the Au deposits (fig. 8-29). Tertiary basin fill or the upper plate of the Roberts Mountains thrust covers most areas of Au potential. Modern exploration techniques have proven effective in identifying targets below and penetrating this cover, which suggests that additional large discoveries are likely in the area.

Rationale for Assessment

The HRB contains abundant sedimentary rock-hosted Au–Ag deposits. Some are small, and others are of world-class size. Innumerable studies have been done on the various deposits, as well as on the regional geologic setting of the deposits. These studies lead to several empirical conclusions that provide the basis of the present mineral assessment:

(1) Sedimentary rock-hosted Au–Ag deposits commonly are hosted by sedimentary rocks, mostly Paleozoic marine carbonate strata and shale, whose overall porosity and permeability have been enhanced by authigenic conversion of magnesian calcite to dolomite (A.K. Armstrong, oral commun., 1996). Some deposits (Twin Creeks) are hosted, in places, by Paleozoic basaltic rocks, whereas others—particularly the distal-disseminated Ag–Au type in the Battle Mountain Mining District—are hosted by densely fractured and altered Paleozoic quartzarenite. These host rocks provide the lithology evidence layer for the present assessment (fig. 8-9, table 8-2). A large permissive terrane of host rocks capable of containing sedimentary rock-hosted Au–Au deposits from Cox and others (1996) is the best documented expression of the rocks in the HRB that have potential for hosting the sedimentary rock-hosted Au–Ag deposits (fig. 8-31).

(2) Many sedimentary rock-hosted Au mining districts lie along northwest-trending belts (Roberts, 1960, 1966; Thorman and Christensen, 1991) and regional-scale lineaments (Shawe, 1991). Belts and lineaments are compatible with genetic theories of ore genesis, which call for deep-seated, over-pressured fluids and associated conduits (Kuehn and Rose, 1995; Lamb and Cline, 1997). Alignment of these and other Au ore deposits and their inherent structural control associated with the lineaments has been suggested by Shawe (1991) to be an important factor in producing the large number of sedimentary rock-hosted Au–Ag deposits in Nevada. Prominent district-scale, steeply-dipping, deep-seated structural conduits were permissive zones for the accumulation or formation of solid cryptocrystalline carbon, and deformation and dissolution textures, as well as other

products of alteration such as jasperoid and illite-clay. The conduits also may display anomalous geochemical concentrations of As, Sb, Hg, and other pathfinder elements. Many regional-scale trends that control sedimentary rock-hosted Au–Ag deposits are spatially manifested in a number of geochemical, geophysical, and geologic data bases used in the present assessment (table 8-2).

(3) The Carlin-type deposits and some distal-disseminated deposits generally contain sub-micron sized particles of Au in the lattice of arsenical pyrite or marcasite (Hofstra and Cline, 2000; Johnson, 2000). Carlin-type deposits commonly contain orpiment and realgar, whereas these minerals are rare in the distal-disseminated deposits, although As values are elevated in these deposits. However, most distal-disseminated deposits and some Carlin-type deposits contain free Au dispersed in gangue minerals or associated with sulfide minerals. In both deposit types, the geochemical association of Au is with (1) As (strong positive correlation between Au and As), (2) Sb (Sb generally later than the bulk of the Au), and (3) Hg. The ratios Au/Ag roughly are ≥ 1; and Sb/Au ≈ 50. Regional-scale As in NURE stream sediment samples provides an approximate spatial representation of the associations (fig. 8-20, table 8-2), and it is an important evidence layer in the present assessment.

(4) Ore-forming fluid produced large areas of hydrothermally altered rock in and around Carlin-type deposits. These areas are characterized by dissolution of carbonate minerals and presence of silicified rocks and clay minerals. These also are common features in many distal-disseminated, pluton-related sedimentary rock-hosted Au–Ag deposits, and the features are indistinguishable in the oxide zones of many deposits of both types. Brecciated rocks, many resulting from collapse and dissolution by abundant flow of hydrothermal solutions through them, commonly host or are associated with ore in both the Carlin-type and distal-disseminated deposits. Although alteration products are not directly represented in the data bases used for the present assessment, Ba/Na ratio (fig. 8-21, table 8-2) and spatial As geochemistry (fig. 8-20) proxy for large altered areas. In addition, the pathway of the hydrothermal fluids can be approximated by use of structural data sets, such as northeast lineaments (fig. 8-16), lithostratigraphic terranes (fig. 8-17), thrusts (fig. 8-18), and deep crustal lineaments interpreted from gravity (fig. 8-19). Local structural pathways and fluid traps also can be roughly simulated with lithodiversity (fig. 8-13).

(5) Pre-ore Mesozoic igneous dikes and stocks are common near or in most Carlin-type deposits, except at Alligator Ridge, Twin Creeks, and Gold Bar. Tertiary stocks and dikes locally are mineralized in Carlin-type systems (Ressel and others, 2000) and are a documented direct link to ore genesis in the distal-disseminated deposits (Theodore, 2000). Proximity to plutons of all ages can be

used as an evidence layer to provide a coarse approximation of these associations (fig. 8-12, table 8-2).

Results of Assessment

A mineral-resource assessment map for sedimentary rock-hosted Au–Ag deposits was created using a combination of knowledge- and data-driven modeling techniques (fig. 8-31). The sedimentary rock-hosted Au–Ag deposit WLR model was generated from nine evidence maps, summarized in table 8-2, using a unit cell size of 1 km^2, and a significance level of 1.282 (90 percent confidence, tabled Student–t value. Four assessment ranks (nonpermissive, permissive, favorable, and prospective) are derived from the model favorabilities (fig. 8-31) on the basis of break points in the cumulative assessment area curve (fig. 8-30). The area of each assessment rank and the number of training sites in each rank are given in table 8-3. These ranks differ in derivation and meaning than those in the assessment of the Winnemucca-Surprise assessment area (Peters and others, 1996) in the northwest part of the HRB. Expert knowledge was used to identify permissive and nonpermissive tracts defined by Cox and others (1996). Expert knowledge also was used to select evidence maps for data-driven preliminary WofE analysis, but not for WLR modeling (see chapter 2). WofE analysis was used to analyze the spatial associations among the training sites and evidence maps and to optimize the evidence maps for prediction. WLR modeling was used to combine the optimized evidence maps and to delineate prospective and favorable tracts within the expert-delineated permissive tract. The evidence map criteria used for prediction were determined by data-driven means (see chapter 2).

The mineral-resource assessment map of sedimentary rock-hosted Au–Ag deposits in the HRB (fig. 8-31) was created by (1) superimposing the data-driven favorability map onto expert-delineated tracts that are permissive for sedimentary rock-hosted Au–Ag deposits (fig. 8-31) (plate 12-3 of Cox and others, 1996) and (2) superimposing the depth-to-basement map (see chapters 2 and 6) onto the combined response and expert-delineated permissive tract map. On the final map, shown in figure 8-31, all sedimentary rock-hosted Au–Ag deposit training sites fall within permissive areas.

Geochemical, tectonic-related, and lithologic evidence are the strongest predictors for the presence of sedimentary rock-hosted deposits, followed by geophysical evidence, proximity to plutonic rocks, and lithodiversity (table 8-3). Most evidence maps, particularly As–spatial, serve to exclude areas unlikely to host sedimentary rock-hosted Au–Ag deposits, and they were characterized in the WofE analysis by extensive predictor patterns with W$^-$ magnitudes that are significantly larger than W$^+$ where the predictor pattern is absent. The NE linears evidence map (fig. 8-16), and particularly the thrust proximity map (fig. 8-18), serve to include areas that host sedimentary rock-hosted Au–Ag deposits. These two maps are character-

ized by a restrictive predictor pattern with a W⁺ magnitude that is significantly larger than W⁻ where the pattern is present. The Ba/Na and lithodiversity predictor patterns (figs. 8-21, 8-13) are roughly balanced between inclusive and exclusive evidence, as indicated by similar W⁺ and W⁻ magnitudes (table 8-2).

In comparison to the pluton and gravity linears proximity evidence maps (figs 8-12, 8-19), the thrust proximity predictor pattern is narrow (2 km, as opposed to 17 to 21 km for other evidence layers; table 8-2). Although many important training sites lie outboard of 2 km (the distal-disseminated ore deposits of the Battle Mountain Mining District and the southern Carlin-type ore deposits of the Bald Mountain Mining District), a larger number of sites close to, or within, the thrust fronts and structural windows that are represented in this dataset (for example, the northern and southern Carlin trend deposits, the Independence Mountains Mining District deposits, and the Cortez-Pipeline Mining District, fig. 8-13). The result is a measure of point-density that decreases rapidly with increasing distance from these structural features, which is consistent with the structural and tectonic setting of the northern Carlin-type deposits.

The tracts are derived from the WLR model favorabilities and based on break-points in the cumulative assessment area curve (fig. 8-30). The prior favorability was used to delineate the permissive–favorable rank boundary. The most prominent break-point in the curve above the prior favorability was used to delineate the favorable–prospective rank boundary (see blue dotted line on fig. 8-30).

Permissive areas for sedimentary rock-hosted Au-Ag deposits in the HRB region generally are areas of pre-Tertiary sedimentary and metasedimentary rocks within the area covered by tectonically thickened crust due to Paleozoic and Mesozoic thrust faulting (see also Cox and others, 1996). These permissive areas exclude post-accretionary plutons larger than 100 km², but they include local areas of late Paleozoic overlap assemblage rocks that have been further categorized as belonging to favorable and (or) prospective tracts. The permissive area for sediment-hosted Au-Ag deposits includes most of the Golconda and Roberts Mountains allochthons, as well as Paleozoic miogeosynclinal or platformal rocks (see also, Peters and others, 1996; Doebrich, 1996).

Favorable areas include known sedimentary rock-hosted Au–Ag deposits near the western projection of the Roberts Mountains allochthon beneath the sole of the Golconda thrust. The Prospective areas in the HRB specifically include areas in and adjacent to the Carlin trend, Getchell trend, Battle Mountain-Eureka mineral belt and Independence and Bald Mountain Mining Districts (fig. 8-31). The prospective tract areas for sedimentary rock-hosted Au–Ag deposits also reflects in the influence of the distal-disseminated Ag–Au deposits in and around the Battle Mountain Mining District. Distal-disseminated Ag–Au deposits are present in or near mining districts that contain major porphyry-related skarn, replacement, and base-metal vein ores (see chapters 2 and 7).

The overall regional-scale distribution of the favorable and prospective assessment ranks delineates the major sedimentary rock-hosted ore deposit mineral trends and alignments (Battle Mountain-Eureka, Carlin, Getchell, and Independence). An area west of Getchell in the Hot Springs Range was identified from As geochemistry, proximity to gravity lineaments, favorable lithology, proximities to plutons and to thrusts, and high lithodiversity. The area contains the Poverty Peak Hg deposits and Dutch Flat polymetallic vein deposits, and therefore may have potential for both Carlin-type and distal-disseminated deposits (also, see discussion of these districts in chapter 9). In addition, large favorable and prospective areas are identified in areas not in these trends or minerals belts and are designated by letters A through E on figure 8-31. These areas are summarized below:

(A) Sonoma-East and Tobin Range area.—This area lies to the southwest of the extension of the Getchell trend and includes the Harmony, Gold Run, and Washiki polymetallic deposit clusters in the Sonoma Range, the Willow Creek and Goldbanks Hg–Au–Ag–Sb deposits in the East Range, and the polymetallic deposits in the north Tobin Range. The area contains elevated As geochemistry, high Ba/Na geochemistry, high lithodiversity, and favorable lithology, and it is close in proximity to plutons, thrust faults, and basement gravity lineaments. These characteristics are suggestive of distal-disseminated Ag–Au deposits, although few occurrences are known.

(B) Northumberland, north Monitor, and Toquima Range area.—This area also includes the northernmost part of the Antelope Range. The tracts include the Spencer Hot Spring, Northumberland, and Dobbin Summit precious-metal and polymetallic deposits, and the area contains characteristics of both distal-disseminated Ag–Au and Carlin-type deposits. The high favorability is due to high As and Ba/Na geochemistry and proximity to basement gravity lineaments, plutons, and favorable thrusts. The area also contains high lithodiversity and favorable lithology—it is located near favorable lithotectonic stratigraphic terranes of the Golconda and Roberts Mountains allochthons and contains lower-plate, carbonate-bearing lithologies. These characteristics may be favorable for both Carlin-type deposits and for distal-disseminated Ag-Au deposits.

(C) Bull Run, Copper, and Jarbidge Mountains area.—This area contains the Jarbidge, Wood Gulch and Doby George precious-metal, low-sulfidation epithermal deposits and polymetallic replacement and vein deposits in the west Bull Run Mountains, including occurrences in the Edgemont, Aura, Charleston, and Mountain City Mining Districts. The tracts are constructed on the basis of high As and Ba/Na geochemistry, lithodiversity, favorable lithology, and proximity to plutons and to thrusts. Locally basement gravity lineaments are present. The most likely deposit type present is distal-dis-

seminated Ag–Au deposits in the favorable lithologic horizons. Proximity to the Independence Mountains to the south may imply that Carlin-type deposits also could be present.

(D) North Adobe Range.—This area contains the Coal Mine District and the Garamendi Mine and Canyon Property, and it has potential for future discoveries of polymetallic deposits, oil shale, barite, and phosphate deposits. The tracts were constructed on the basis of high As and Ba/Na geochemistry, lithodiversity, favorable lithology, and

proximity to plutons and thrusts. The lithostratigraphic terrane includes the upper and lower plates of the Roberts Mountains thrust and has potential for Carlin-type and distal-disseminated deposits.

(E) North Pequop Mountains area.—The area contains the Pequop polymetallic district. Tracts were constructed with all favorable evidence layers except the northeast-striking (CVIL–type) lineaments. This area has potential for both Carlin-type and distal-disseminated Ag–Au deposits.
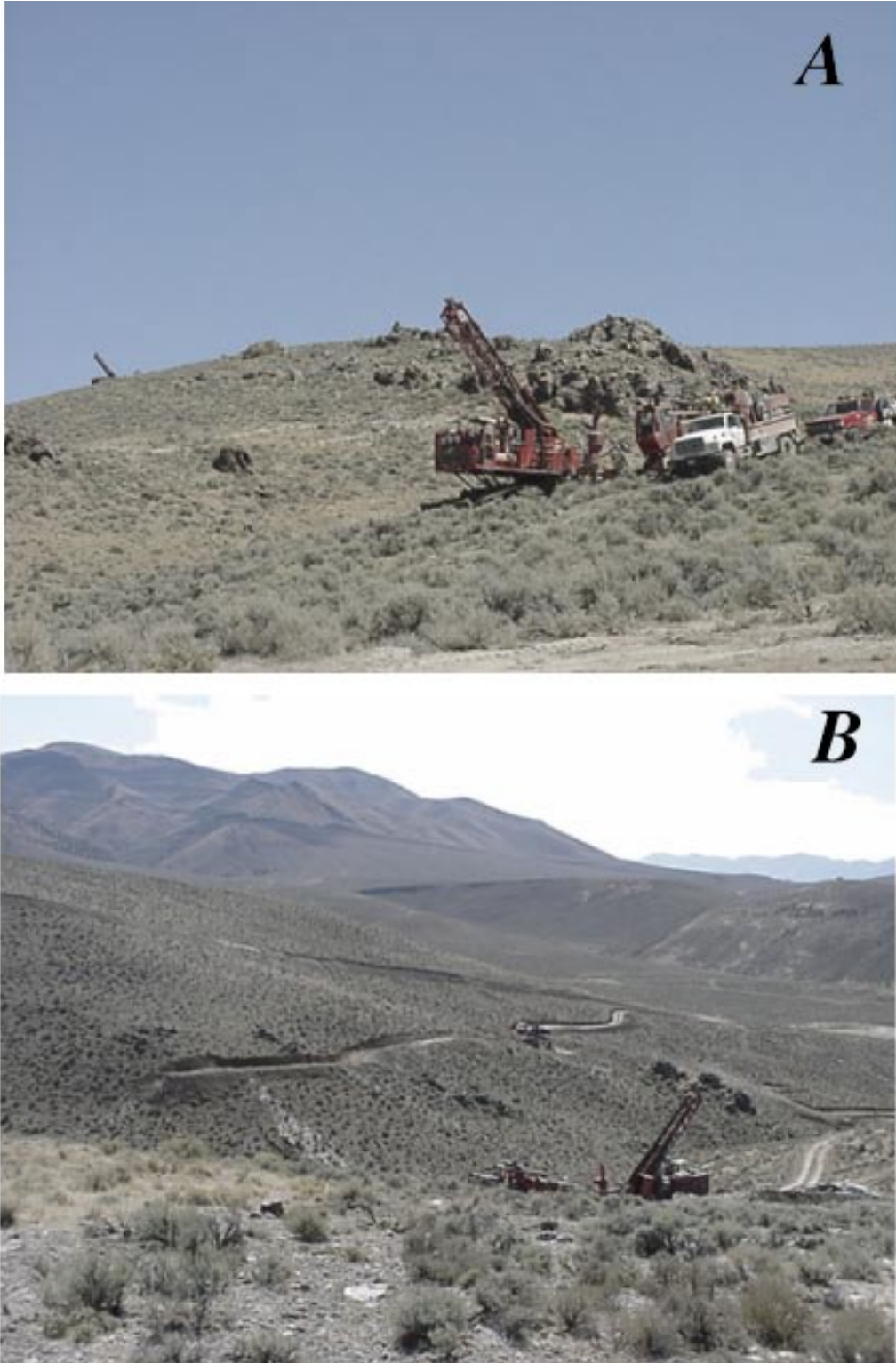
Figure 8-1. Photographs showing drill rigs operating during 2000 at Section 31 distal-disseminated Ag–Ag deposit, Battle Mountain Mining District, Nevada. *A*, View to north showing drill in foreground below bold outcrop of quartz arenite of Ordovician Valmy Formation. *B*, View to southwest showing main drainage of Trenton Canyon in middle ground.
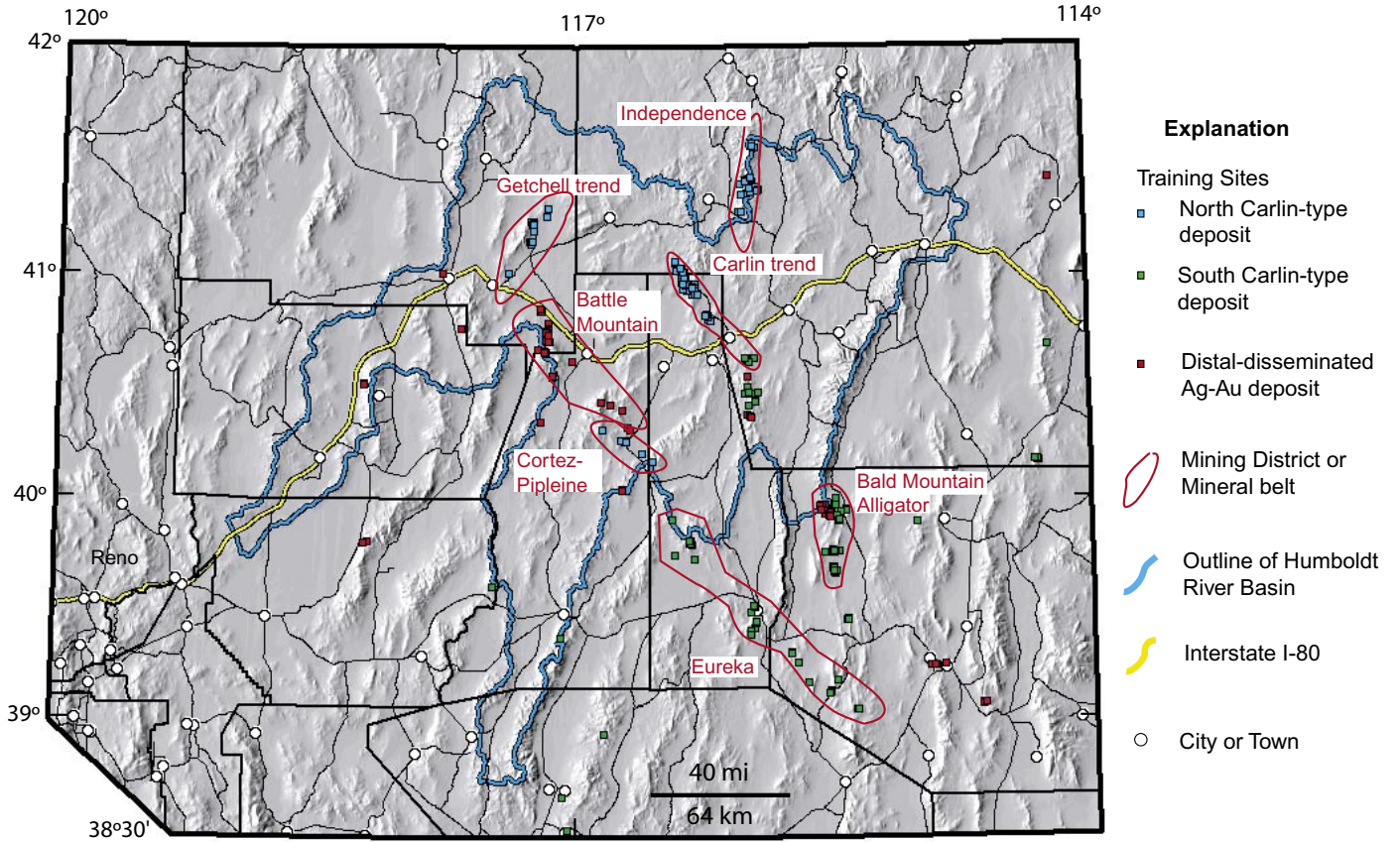
Figure 8-2.   Index map showing spatial distribution of training sites for sedimentary rock-hosted Au–Ag deposits shown on table 8-1 and major mining areas discussed in text.
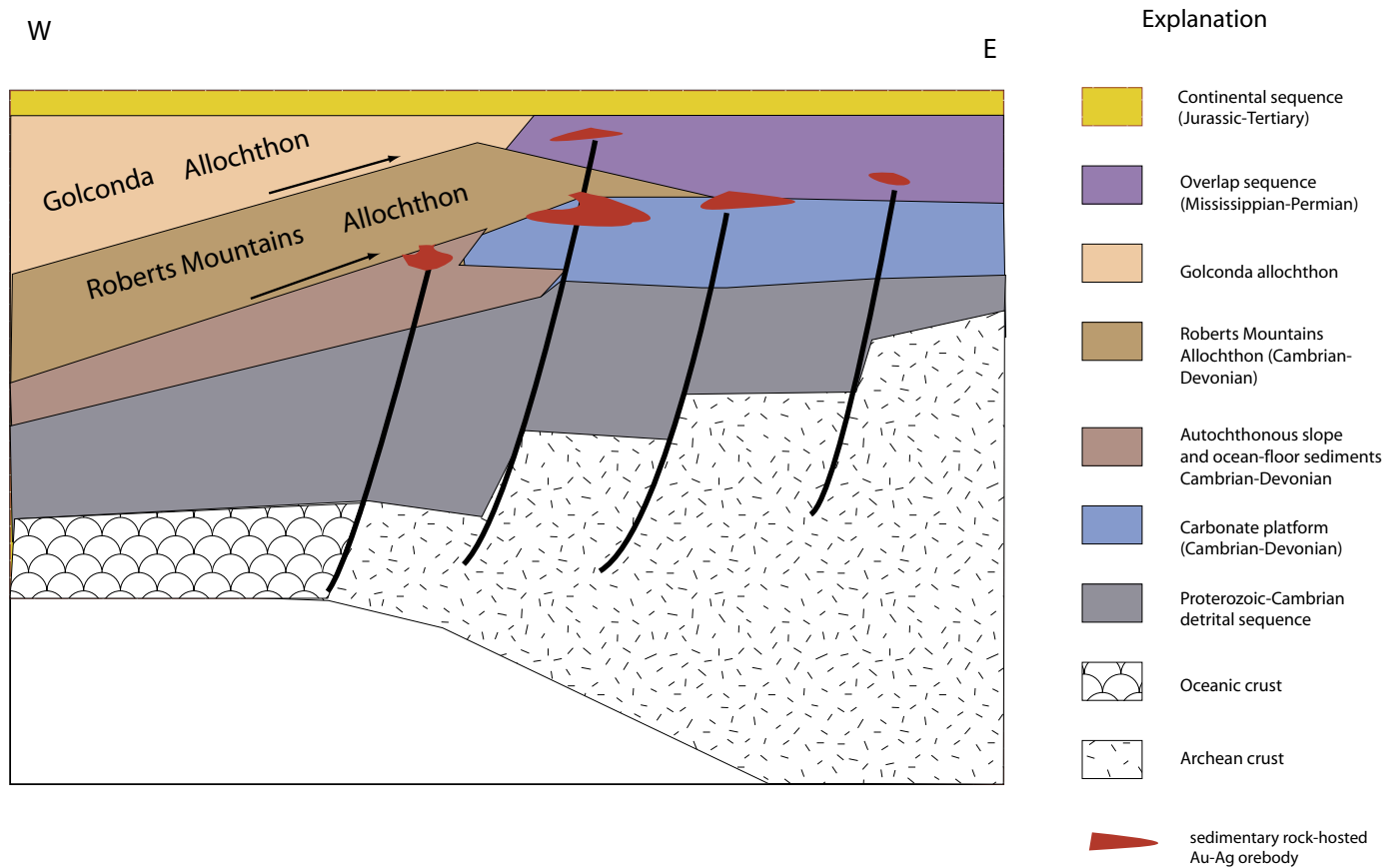
Figure 8-3.   Schematic east-west cross section of northern Nevada and northwestern Utah, showing Achaean crust, oceanic crust, overlying stratigraphic and tectonic sequences, fault zones, and location of sedimentary rock-hosted Au–Ag deposits (adapted from Hofstra and Cline, 2000).
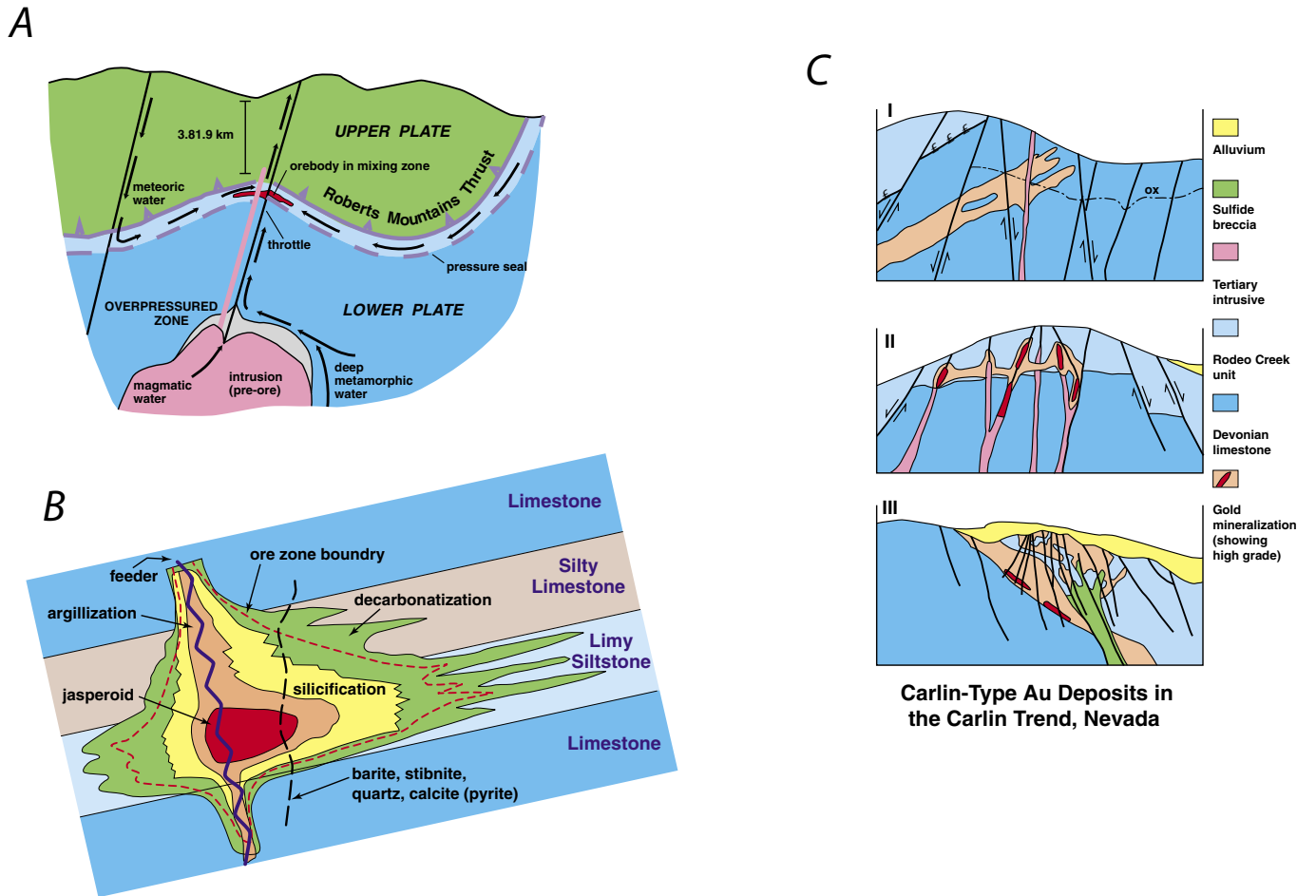
Figure 8-4. Models and styles of mineralization in Carlin-type deposits in Nevada. *A*, Pressure and fluid mixing model, adapted from Kuehn and Rose (1995). *B*, Model of typical sedimentary rock-hosted Au–Ag deposit, adapted from Arehart (1996). *C*, Three styles of Carlin-type deposit, stratabound (I), structural (II) and complex (breccia) (III), adapted from Christensen (1993, 1996).
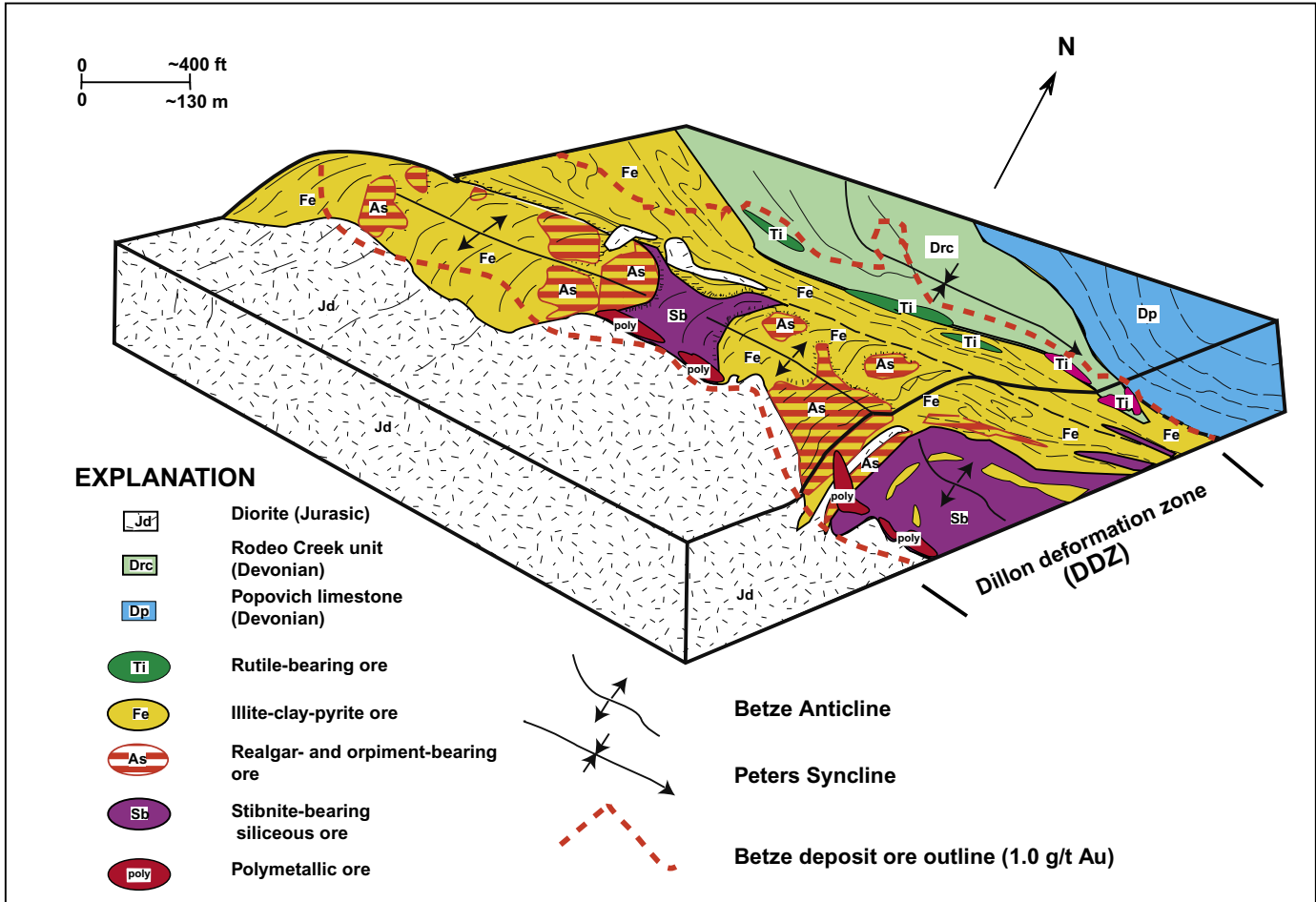
Figure 8-5. Diagrammatic block diagram of the Betze Au orebody, Goldstrike Mine, Carlin trend area at about 4,600 to 5,000 ft elevation. Shows the spatial distribution and zoning of types of ore and their relation to structures and local geology. Adapted from Peters and others (1998).
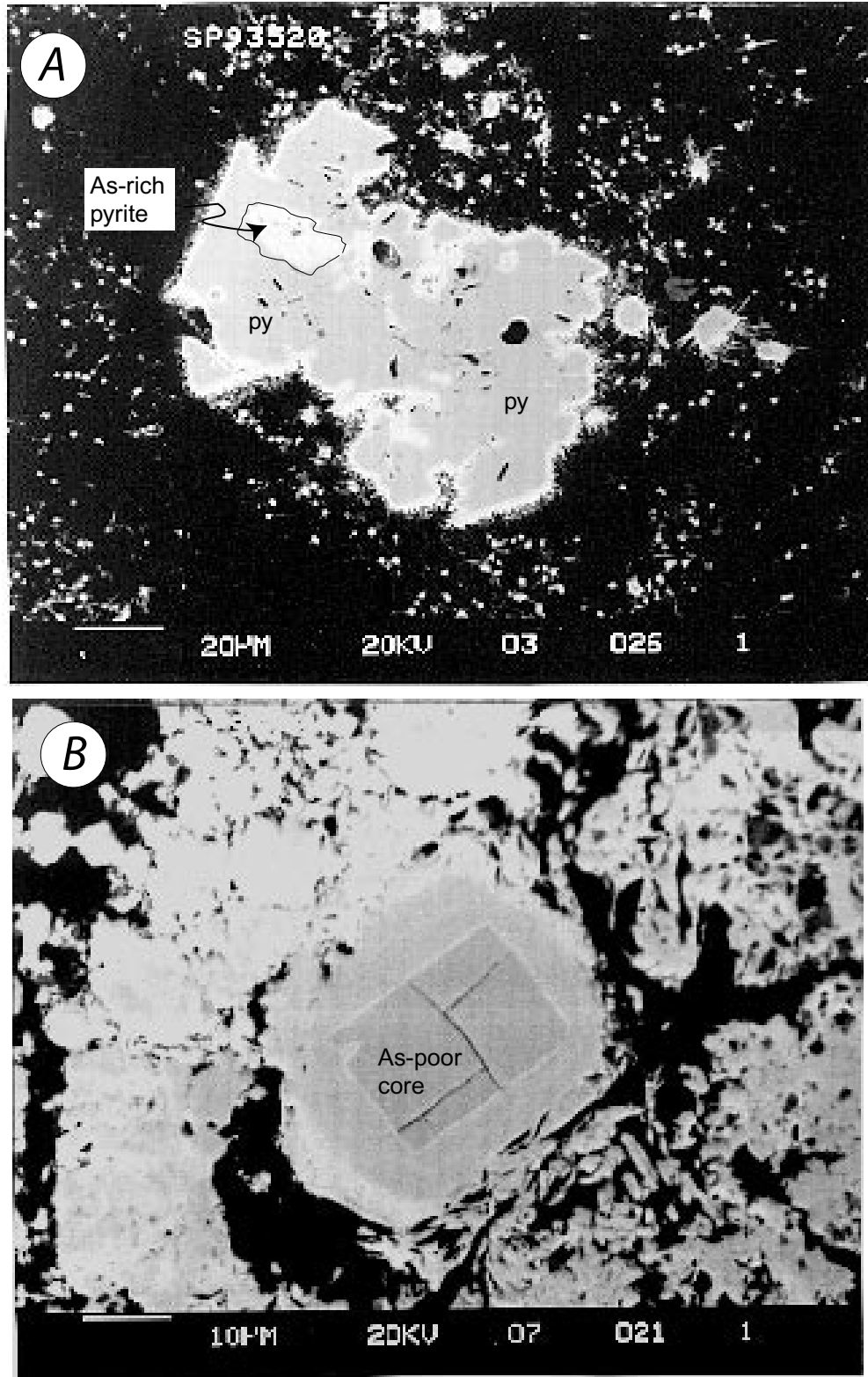
Figure 8-6.   Scanning electron microscope backscatter images of examples of zoned, rimmed arsenical pyrite around or inside As-poor pyrite. *A*, As-rich pyrite rimming and as inclusions in As-poor pyrite. *B*, Multiply zoned pyrite; darker colors are As-poor, lighter colors are As-rich. These pyrite textures are very common and diagnostic in the Carlin-type sedimentary rock-hosted Au–Ag deposits in the Humboldt River Basin. Most of the Au is contained in or associated with these arsenical pyrites.
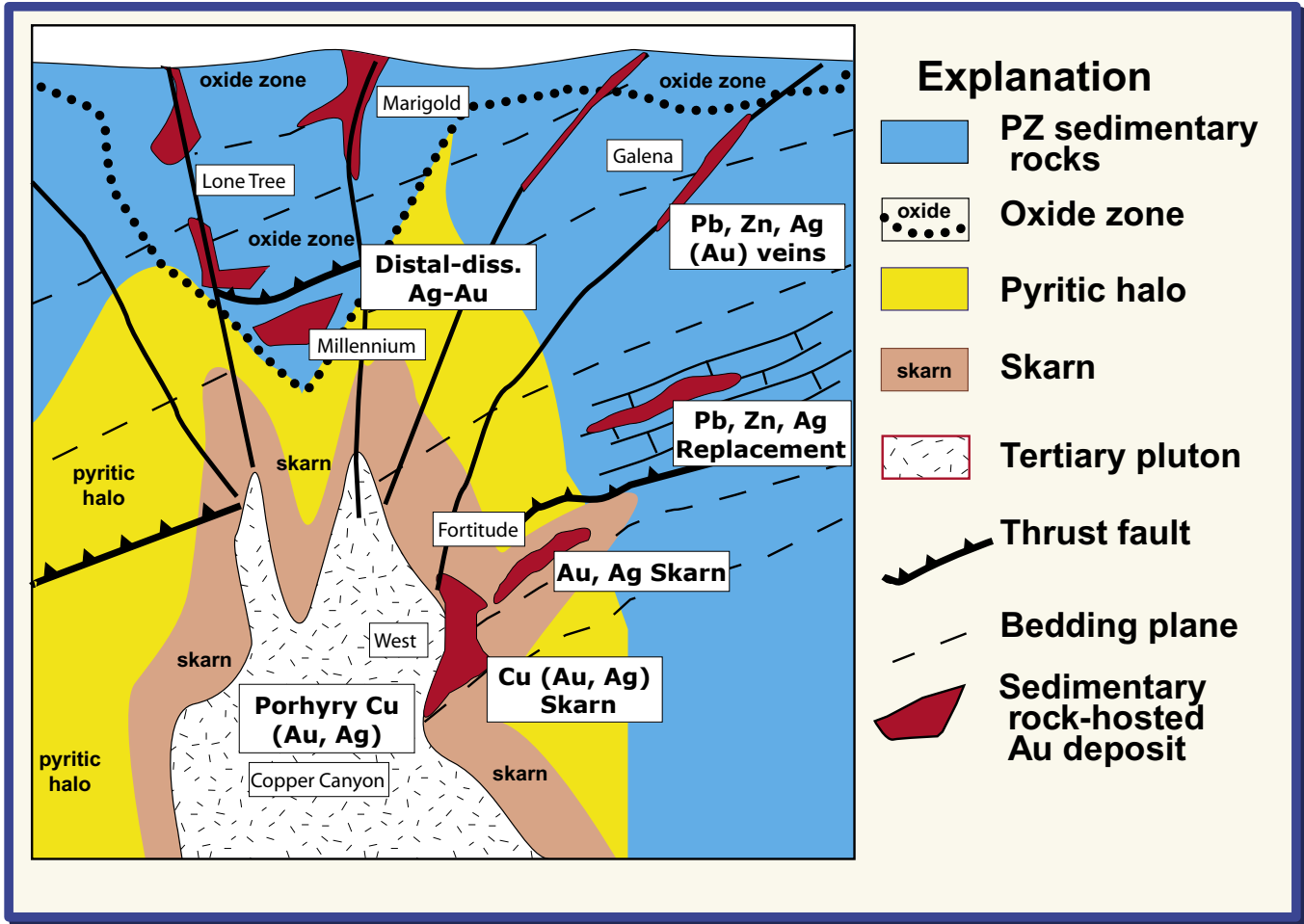
Figure 8-7. Diagrammatic model of geologic setting of distal-disseminated Ag–Au deposits and associated deposits in the HRB. Adapted from Sawkins (1984), Sillitoe and Bonham (1990), and Theodore (2000).
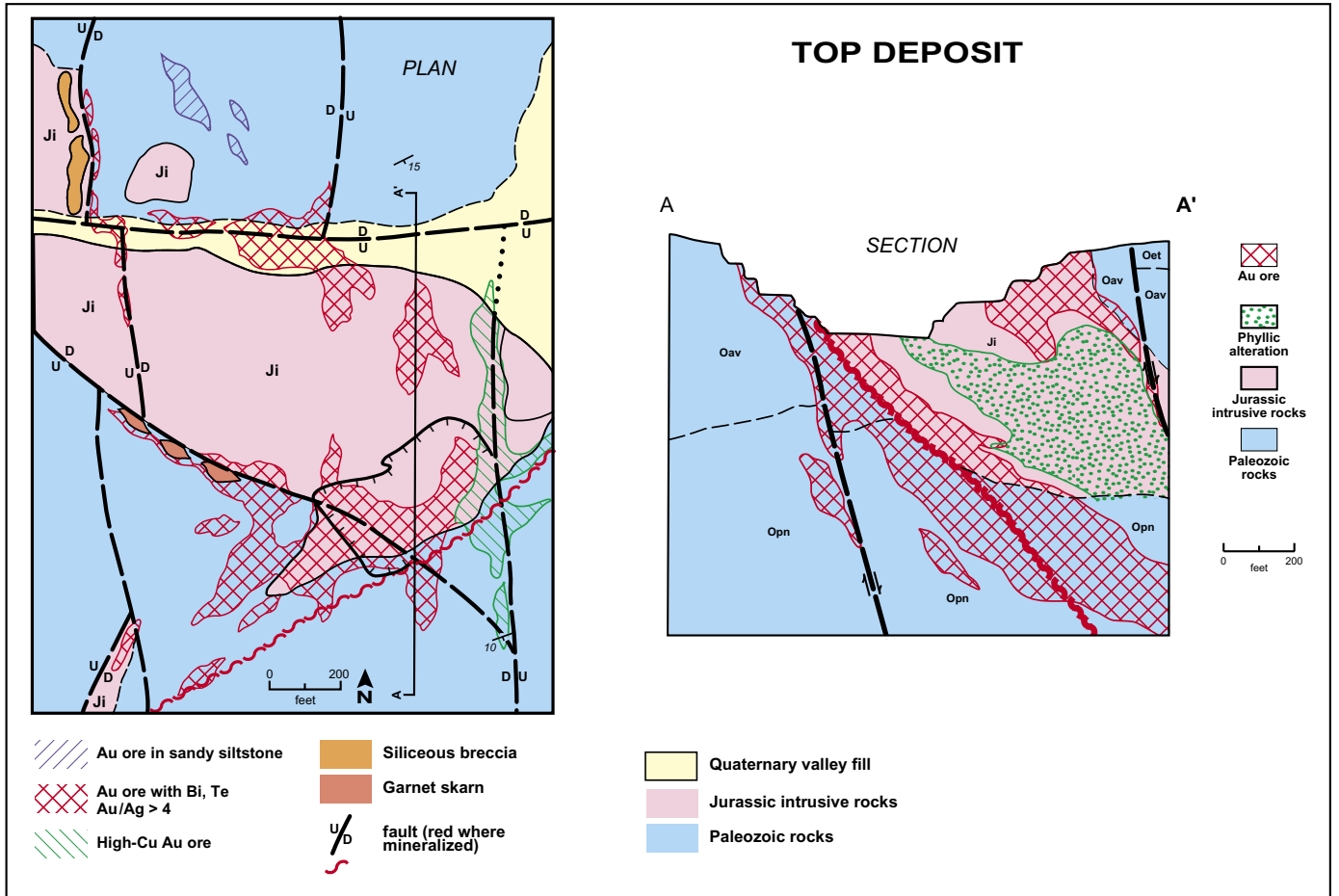
Figure 8-8. Example of a distal-disseminated Ag–Au type sedimentary rock-hosted Au–Ag deposit at the Top deposit in the Bald Mountain Mining District.
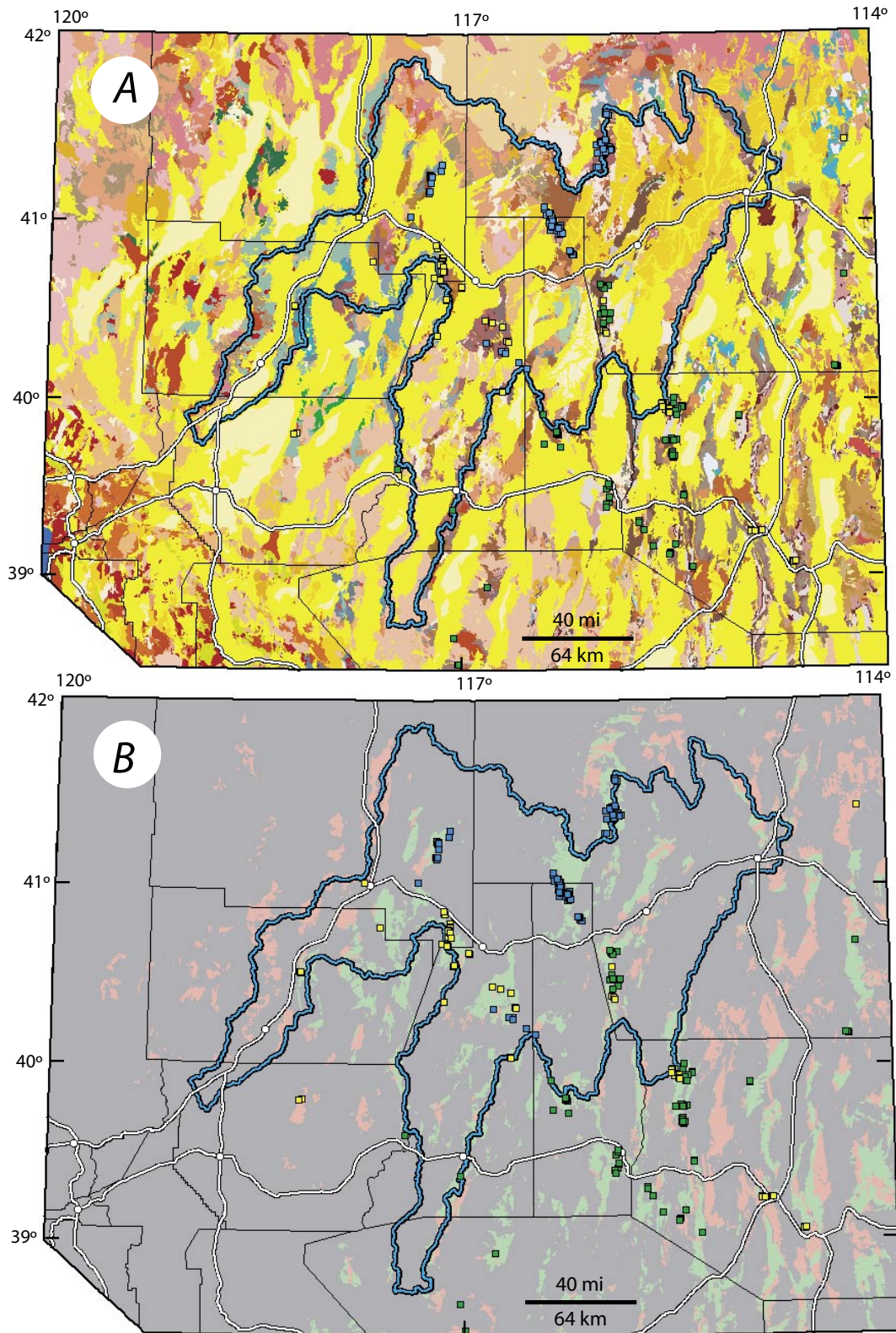
Figure 8-9. Lithology evidence and predictor maps. *A*, Lithology from Stewart and Carlson (1978) (see chapter 2 for explanation). *B*, Predictor map; predictor pattern present, green; predictor pattern absent, red; missing evidence map coverage shown in gray. Sedimentary rock-hosted Au-Ag deposit training sites shown as blue (north Carlin-type), green (south Carlin-type), and yellow (distal-disseminated Ag-Au) squares. Humboldt River Basin shown as light blue outline.
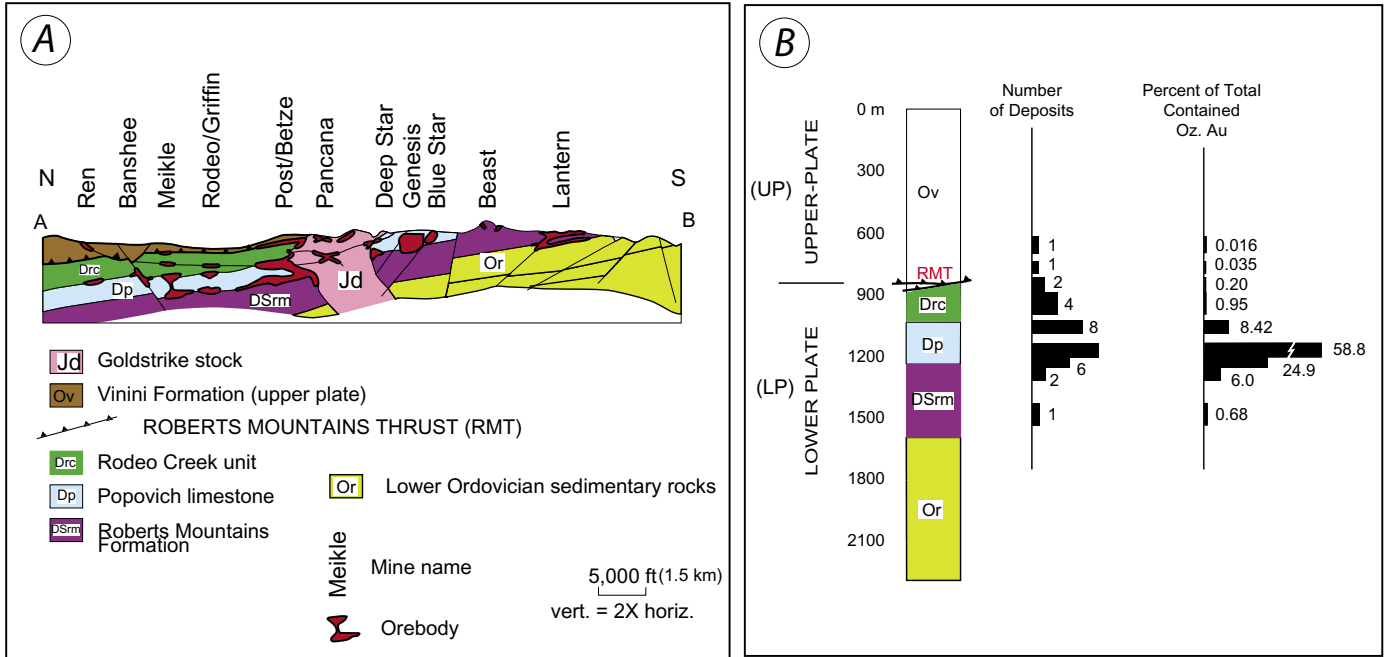
Figure 8-10. Stratigraphic control of ore in the Carlin trend area. *A*, Diagrammatic cross section showing stratigraphic control along the Upper Paleozoic units. *B*, Number of deposits and percent of total contained Au in stratigraphic units (adapted from Peters and others, 1998; see also Teal and Jackson, 1997a,b).
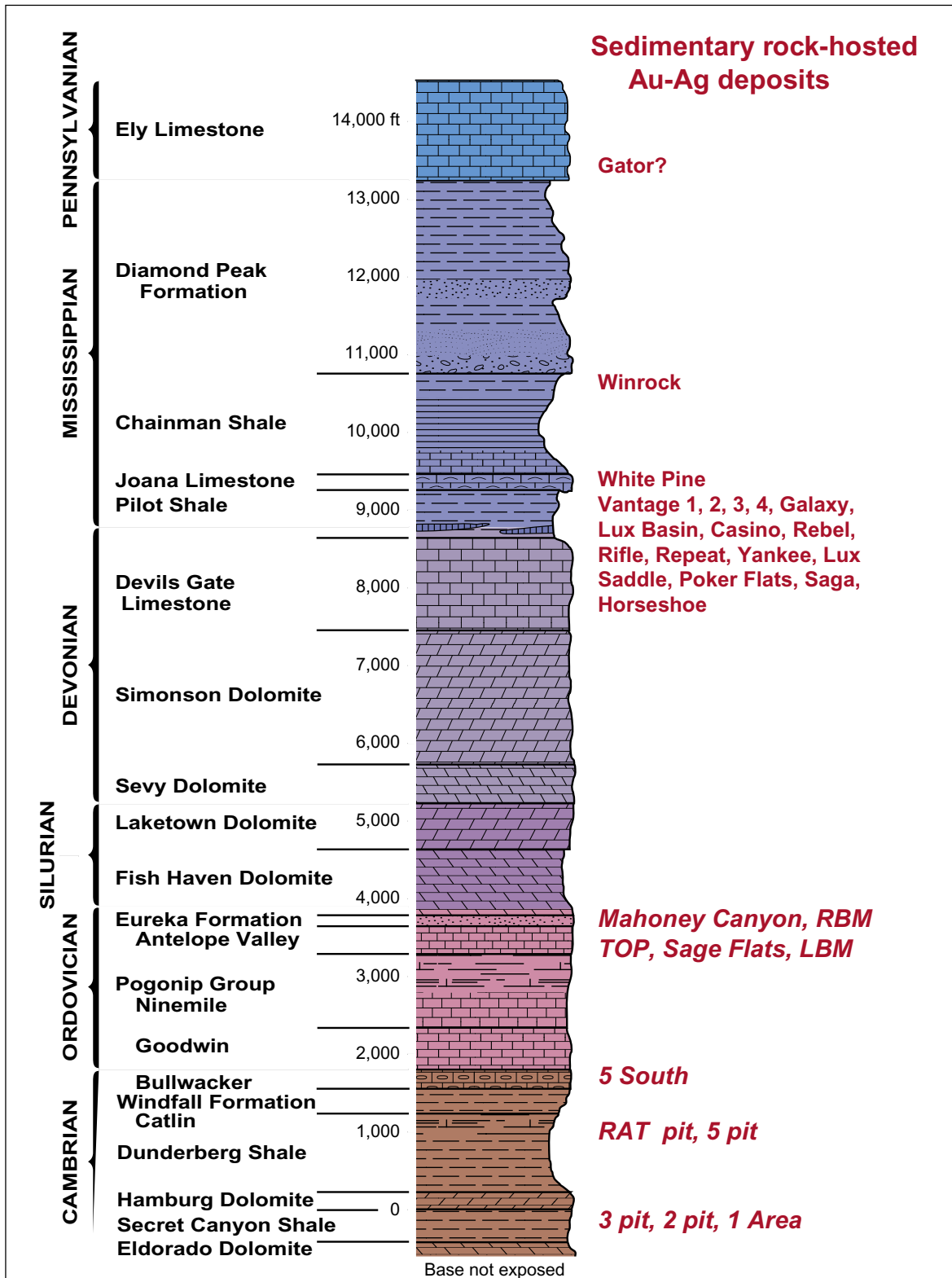
Figure 8-11. Stratigraphic control of both types of sedimentary rock-hosted Au-Ag deposits in the Bald Mountain Mining District. Both Carlin-type and distal-disseminated-type deposits are hosted together in specific units of the stratigraphic section (modified from Hitchborn and others, 1996).
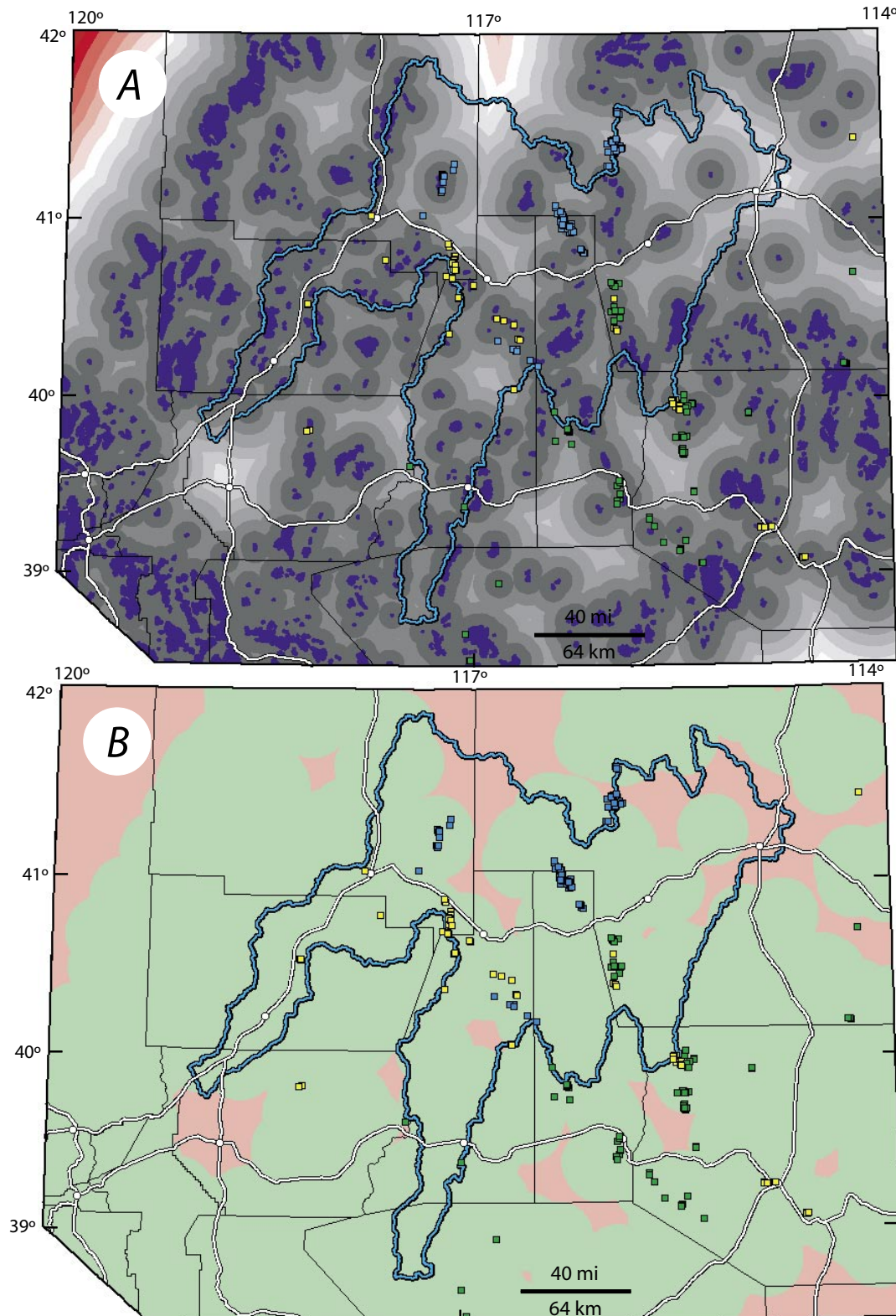
Figure 8-12. Pluton proximity evidence and predictor maps. *A*, Pluton proximity evidence map; see chapter 2 for explanation of patterns. *B*, Predictor map; predictor pattern present, green; predictor pattern absent, red. Sedimentary rock-hosted Au-Ag deposit training sites shown as blue (north Carlin-type), green (south Carlin-type), and yellow (distal-disseminated Ag-Au) squares. Humboldt River Basin shown as light blue outline.
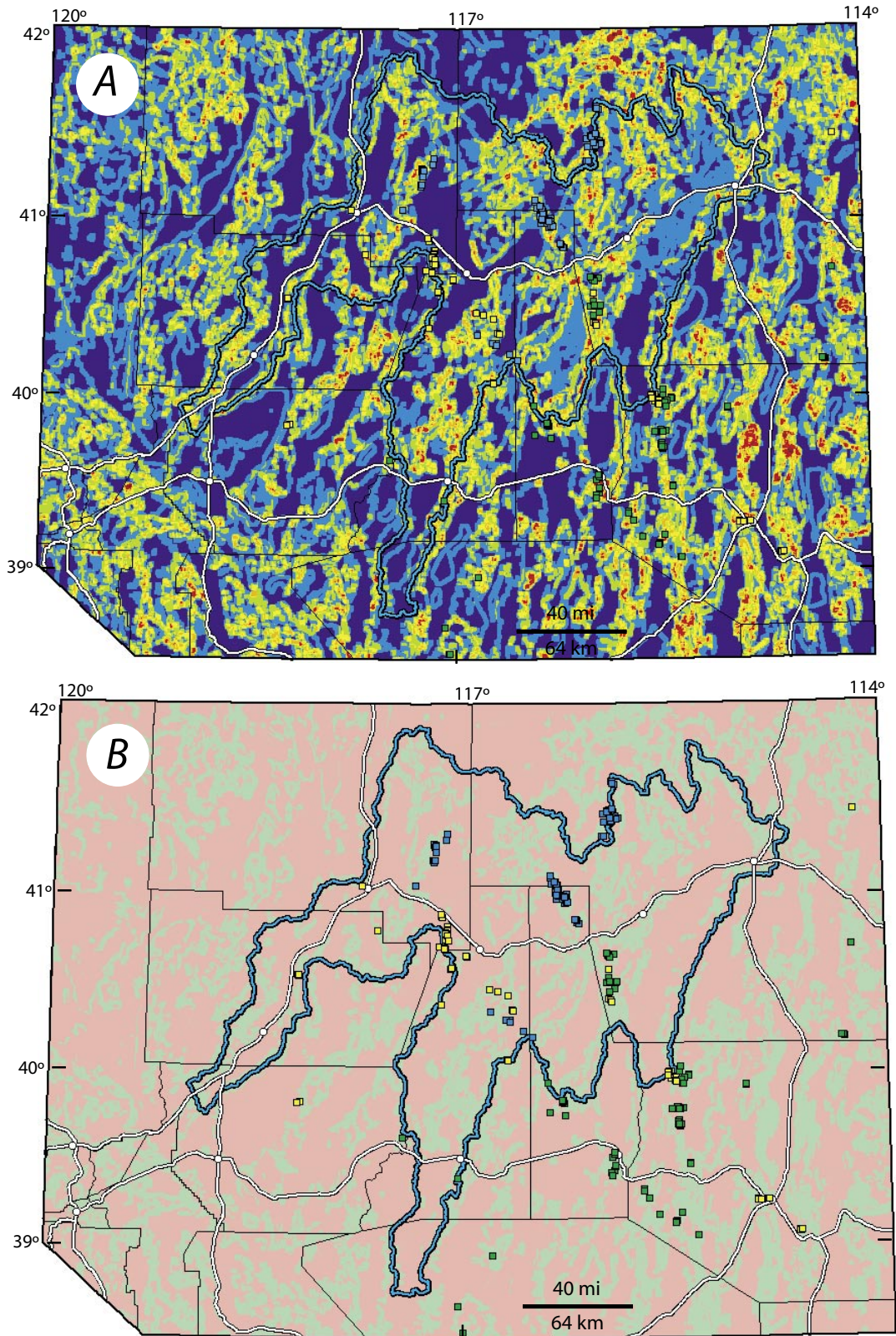
Figure 8-13. Lithodiversity evidence and predictor maps. *A*, Lithodiversity evidence map; see chapter 2 for explanation of patterns. *B*, Predictor map; predictor pattern present, green; predictor pattern absent, red. Sedimentary rock-hosted Au-Ag deposit training sites shown as blue (north Carlin-type), green (south Carlin-type), and yellow (distal-disseminated Ag-Au) squares. Humboldt River Basin shown as light blue outline.
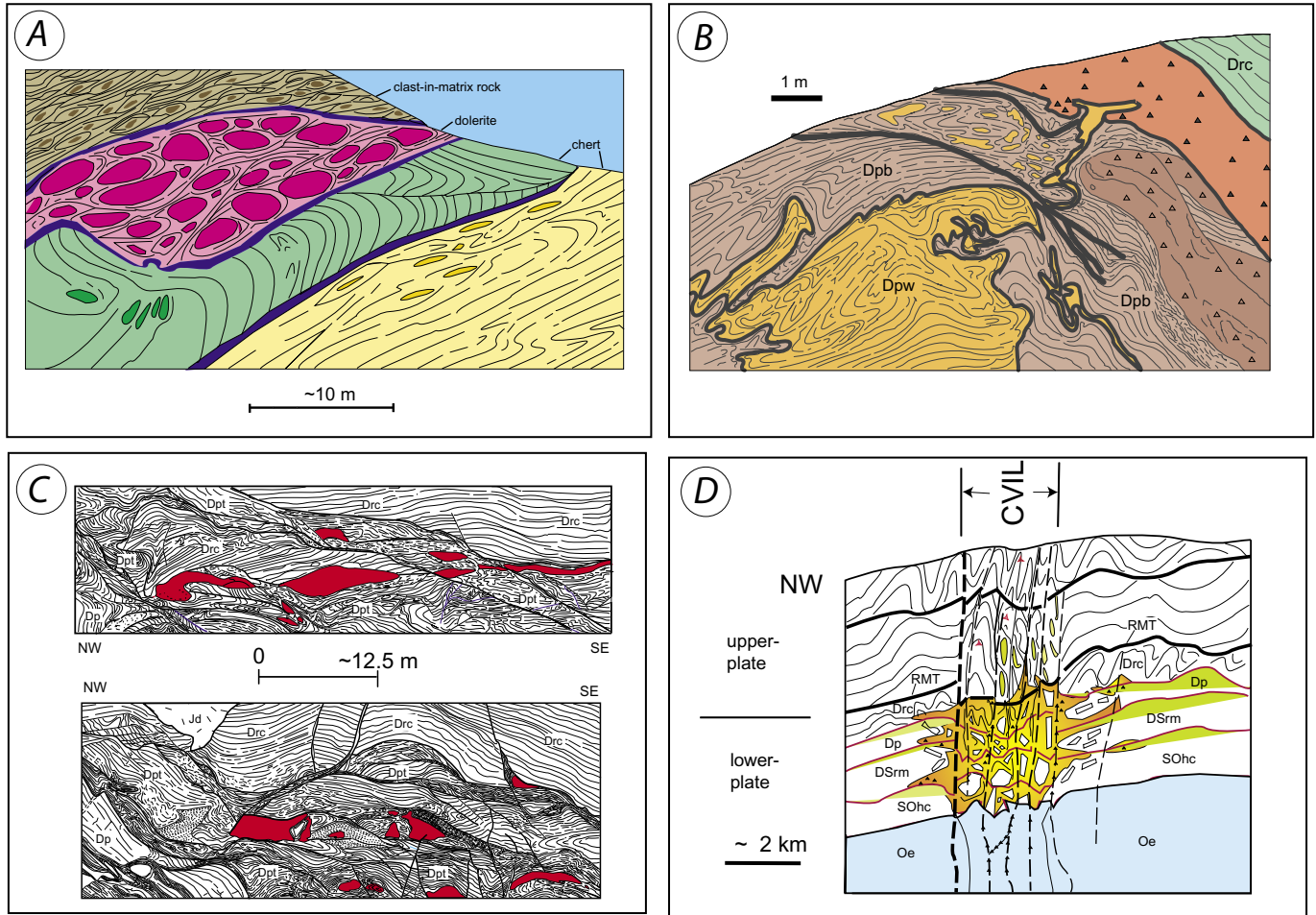
Figure 8-14.   Examples of ore deposit- and conduit-scale deformation textures in sedimentary rock-hosted Au-Ag deposit areas resulting from dissolution. *A*, Mélange textures in upper plate rocks, Carlin Mine area. *B*, Contact between Popovich limestone and Rodeo Creek unit, Betze Mine. *C*, Contact between Popovich Formation and Rodeo Creek unit, Betze orebody, Goldstrike Mine. *D*, Idealized cross section through the Crescent Valley-Independence lineament (CVIL) at about 42° latitude (see Peters and others, 1998; Peters, 2000).
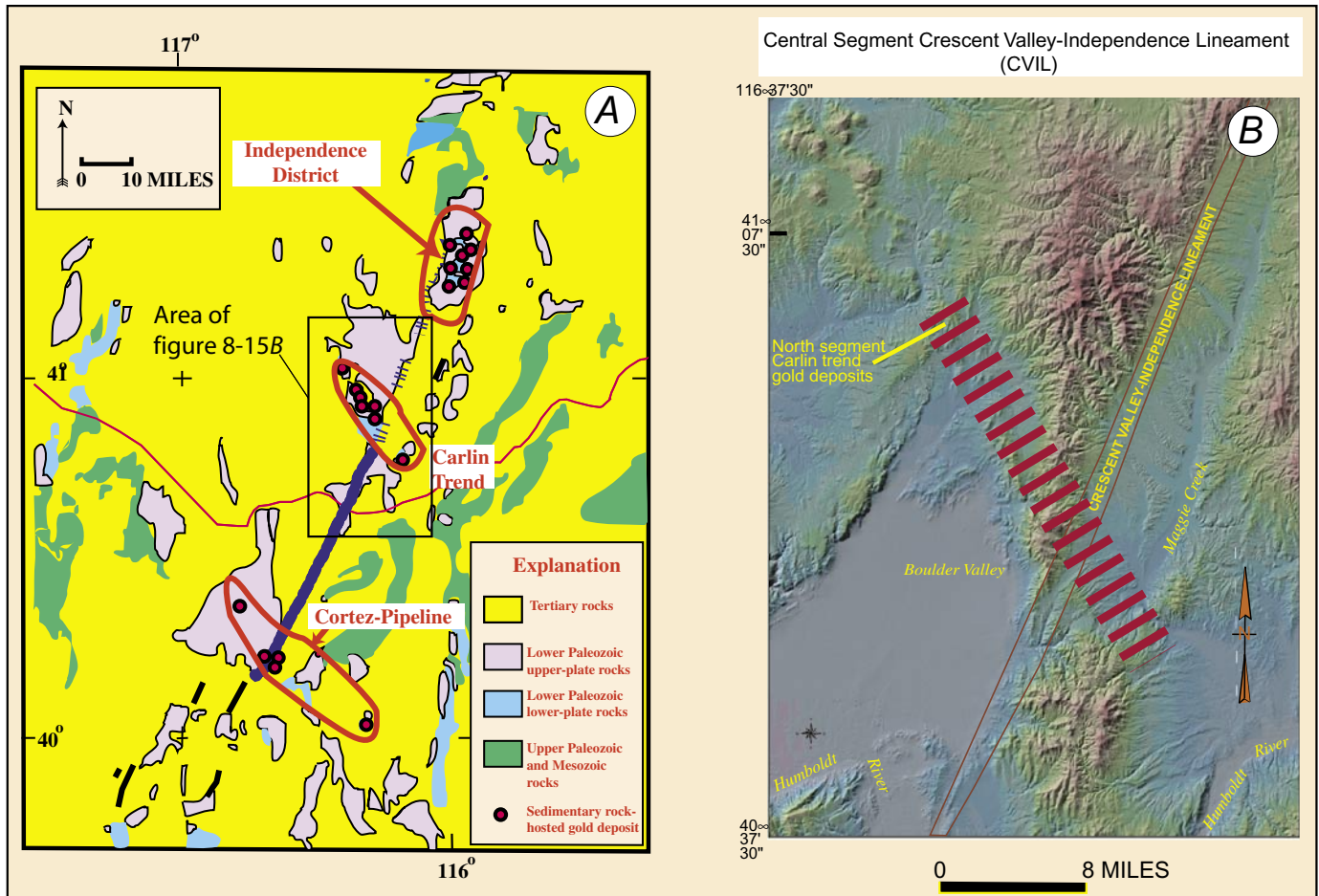
Figure 8-15. Relation of Crescent Valley-Independence lineament (CVIL) to sedimentary rock-hosted Au-Ag, Carlin-type, deposits in north-central Nevada. The CVIL has geologic expression in structural, geochemical, and geophysical data sets, and strands of the lineament are ore-controlling structures in the three mining districts shown. *A*, Simplified geology and mining districts. *B*, Landsat expression of CVIL. The CVIL and the parallel Getchell trend to the west (fig. 8-2) contain the north Carlin-type sedimentary rock-hosted Au–Ag deposits in the Humboldt River Basin.
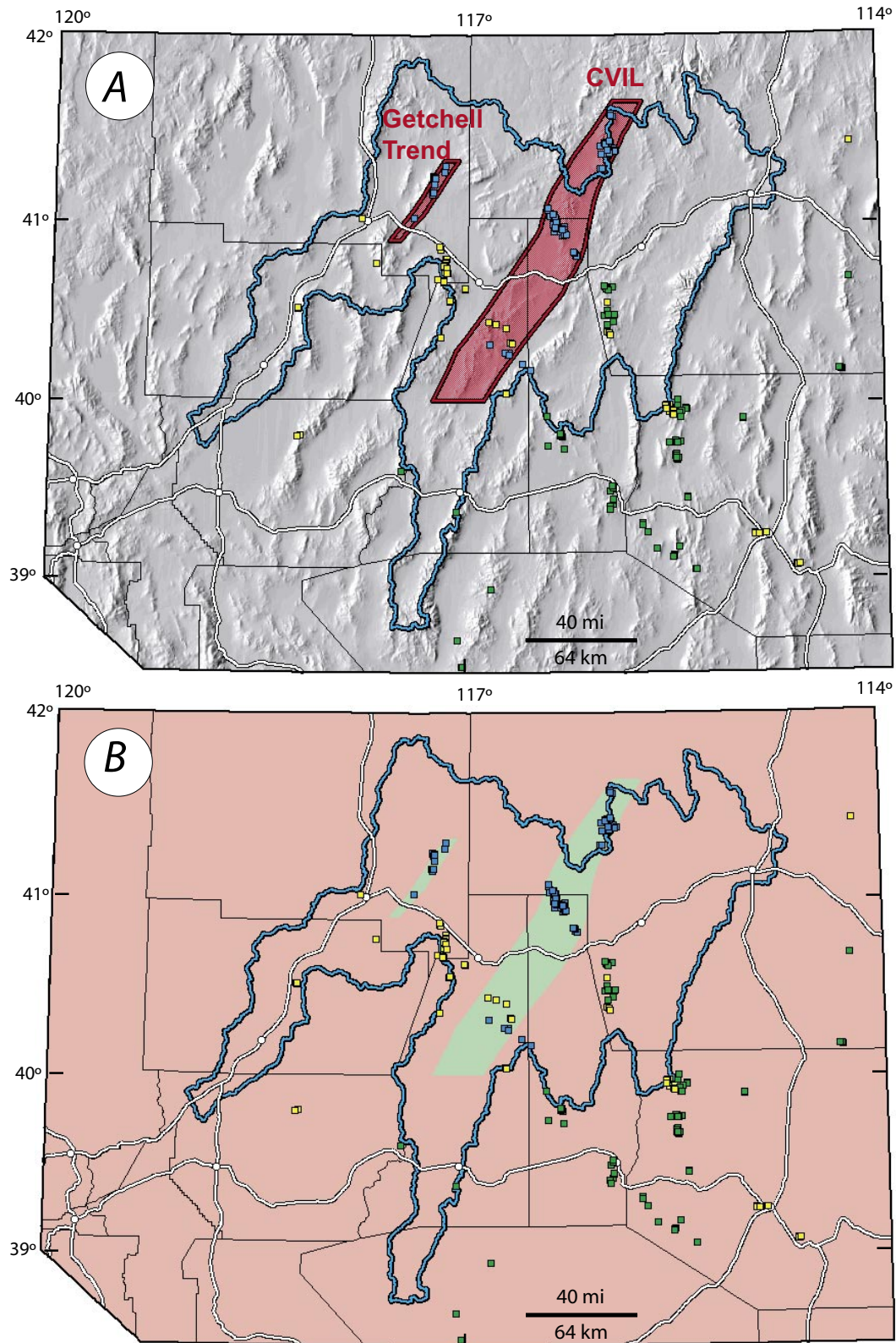
Figure 8-16.   Northeast-striking lineament evidence and predictor maps. *A*, Evidence map, showing major northeast-striking lineaments and trends (red polygons) in northern Nevada; evidence map of CVIL includes a number of strands of the fault and therefore is wider than single strand shown in figure 8-15. *B*, predictor map; predictor pattern present, green; predictor pattern absent, red. Sedimentary rock-hosted Au–Ag deposit training sites shown as blue (north Carlin-type), green (south Carlin-type), and yellow (distal-disseminated Ag-Au) squares. Humboldt River Basin shown as light blue outline.
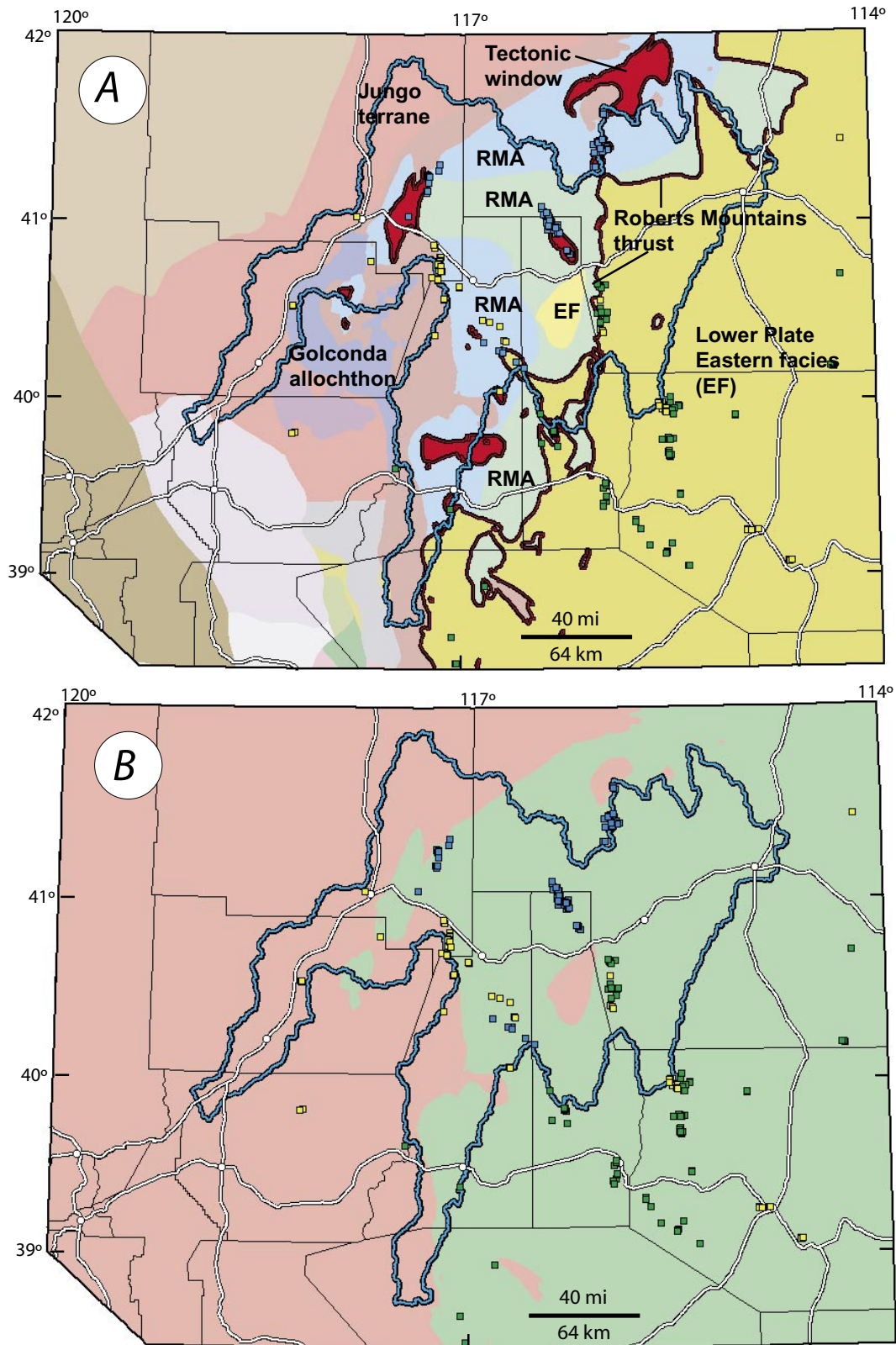
Figure 8-17. Lithotectonic terrane evidence and predictor maps. *A*, Evidence map from Lahren and others (1996) (see chapter 2 for explanation; see also, Silberling and others, 1984, 1987; Silberling, 1991). *B*, Predictor map; predictor pattern present, green; predictor pattern absent, red. Sedimentary rock-hosted Au–Ag deposit training sites shown as blue (north Carlin-type), green (south Carlin-type), and yellow (distal-disseminated Ag-Au) squares. Humboldt River Basin shown as light blue outline.
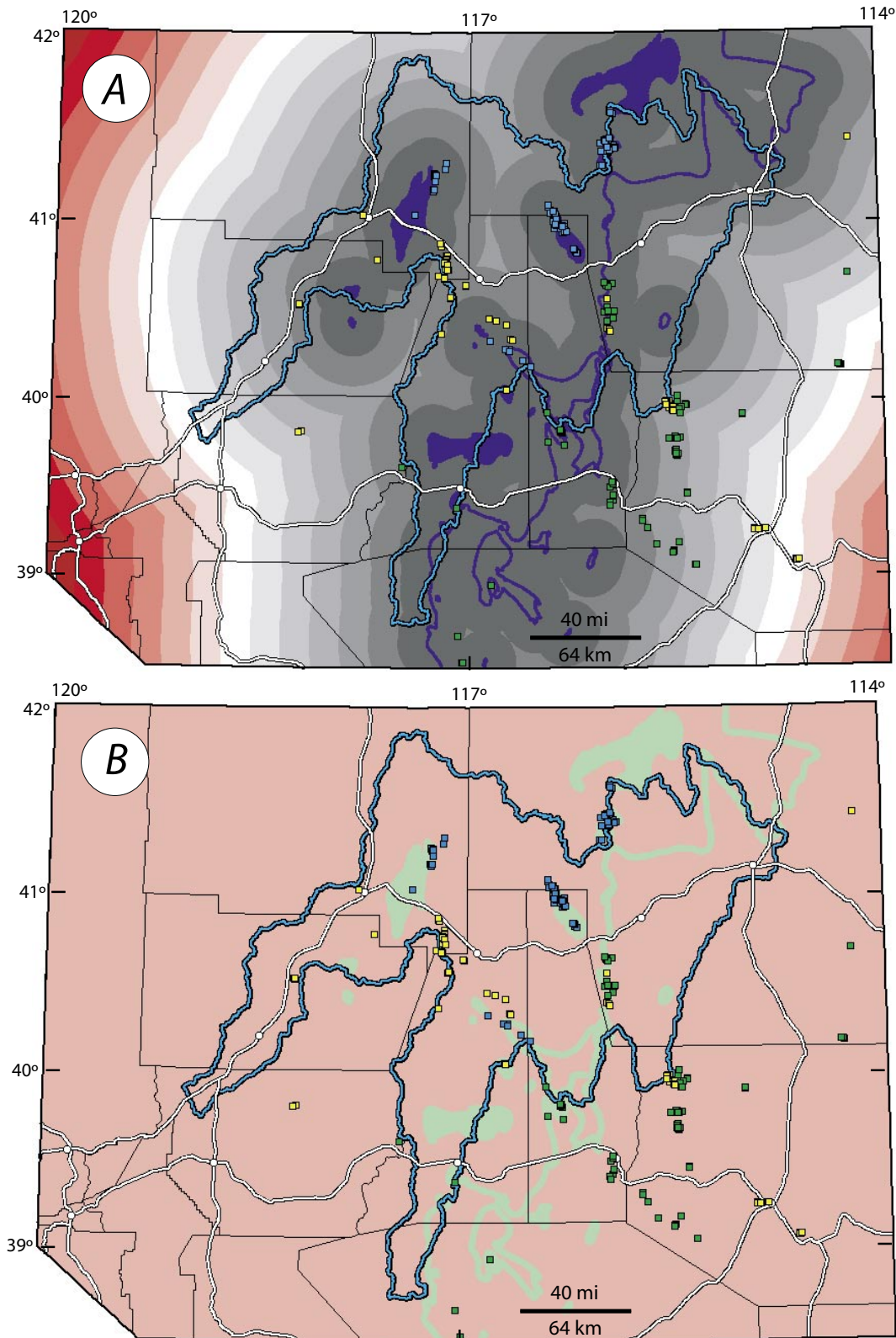
Figure 8-18.   Thrust proximity evidence and predictor maps. *A*, Thrust proximity evidence map; see chapter 2 for explanation. *B*, Thrust proximity predictor map; predictor pattern present, green; predictor pattern absent, red. Sedimentary rock-hosted Au–Ag deposit training sites shown as blue (north Carlin-type), green (south Carlin-type), and yellow (distal-disseminated Ag-Au) squares. Humboldt River Basin shown as light blue outline.
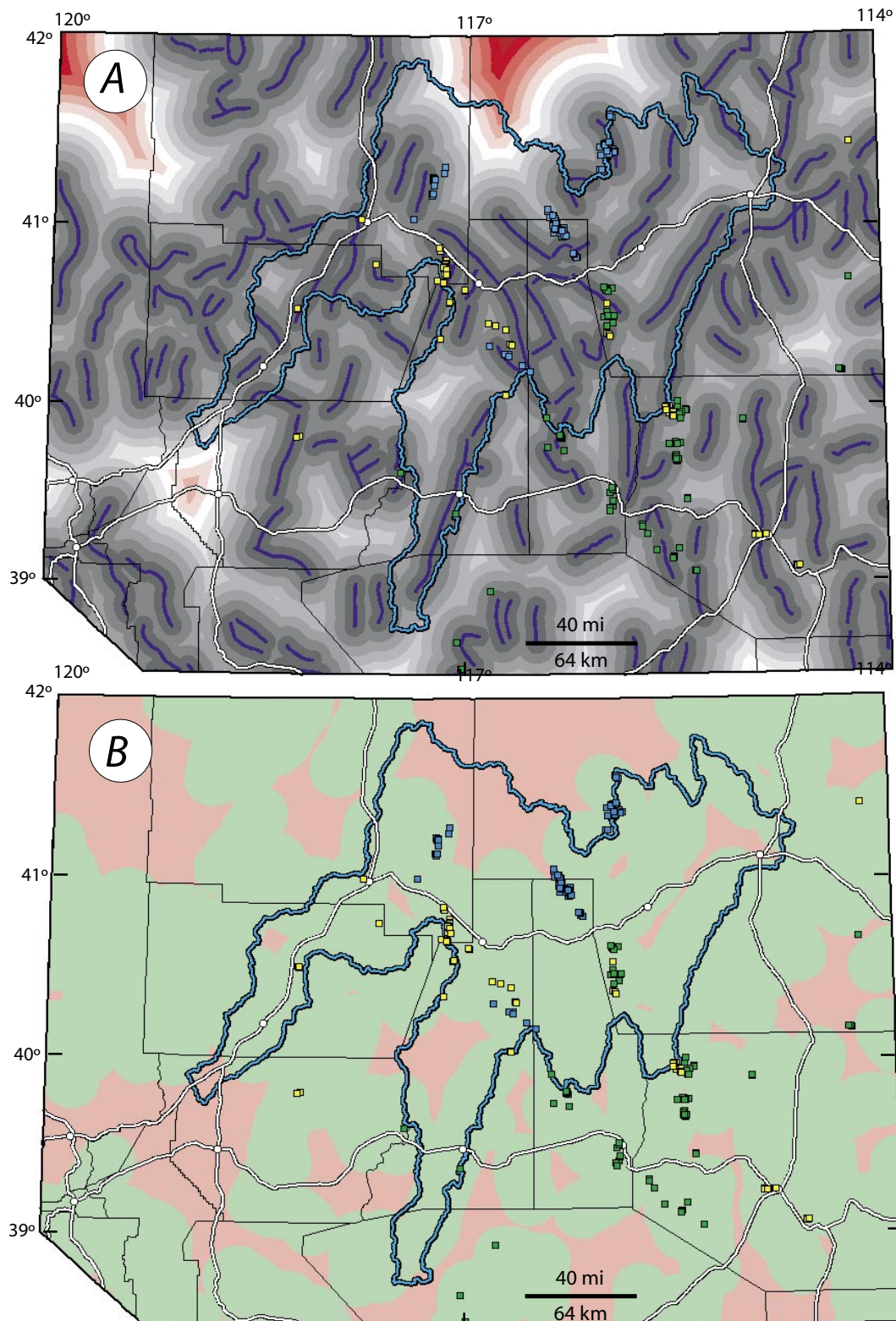
Figure 8-19. Gravity lineaments proximity evidence and predictor maps. *A*, Lineaments interpreted from basement gravity anomaly shown in dark blue; see chapter 2 for explanation of patterns. *B*, Gravity lineament proximity evidence map; predictor pattern present, green; predictor pattern absent, red. Sedimentary rock-hosted Au–Ag deposit training sites shown as blue (north Carlin-type), green (south Carlin-type), and yellow (distal-disseminated Ag-Au) squares. Humboldt River Basin shown as light blue outline.
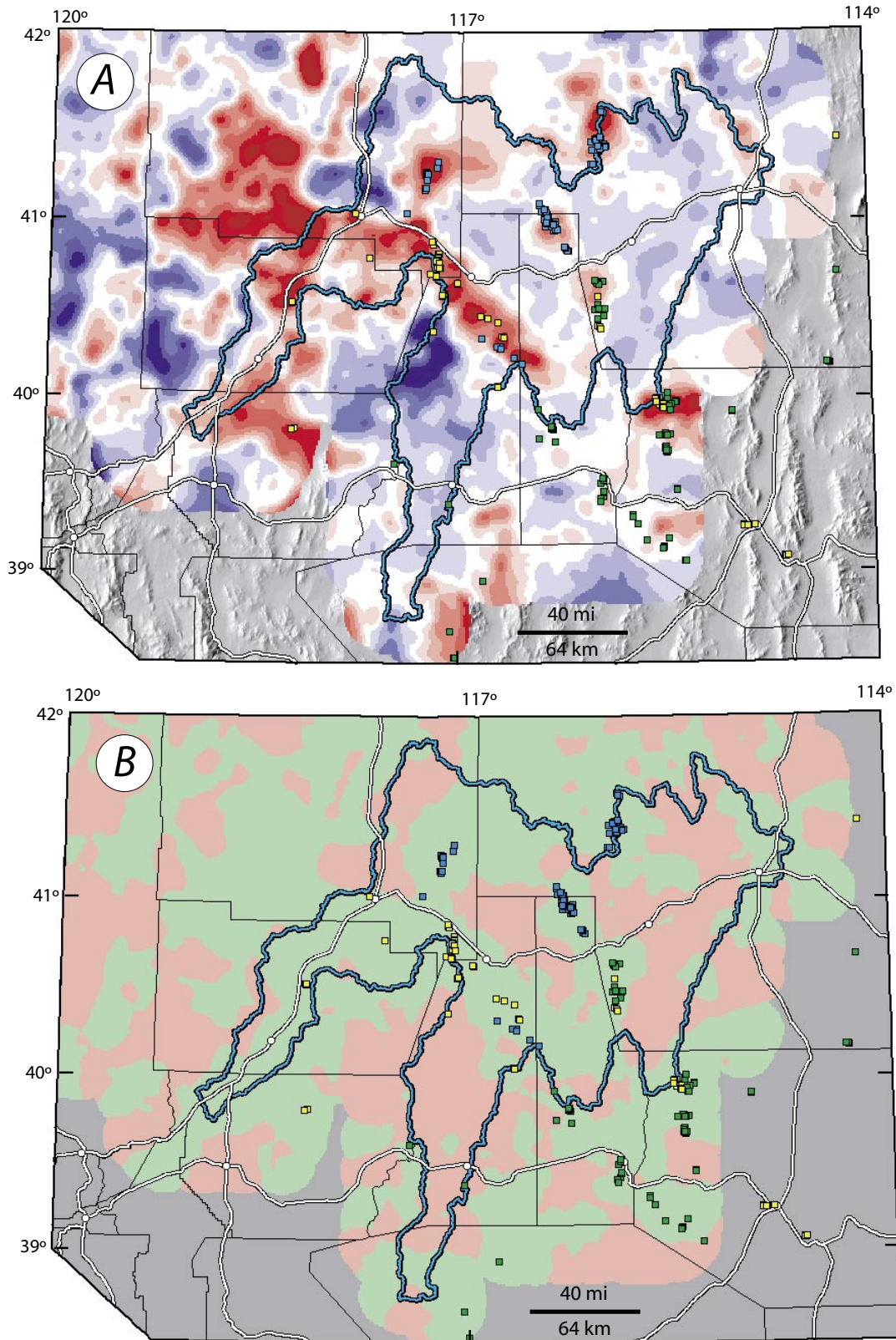
Figure 8-20.   As-spatial evidence and predictor maps. *A*, As-spatial evidence map; see chapter 2 for explanation of patterns. *B*, Predictor map; predictor pattern present, green; predictor pattern absent, red. Missing evidence map coverage shown in gray. Sedimentary rock-hosted Au–Ag deposit training sites shown as blue (north Carlin-type), green (south Carlin-type), and yellow (distal-disseminated Ag-Au) squares. Humboldt River Basin shown as light blue outline.
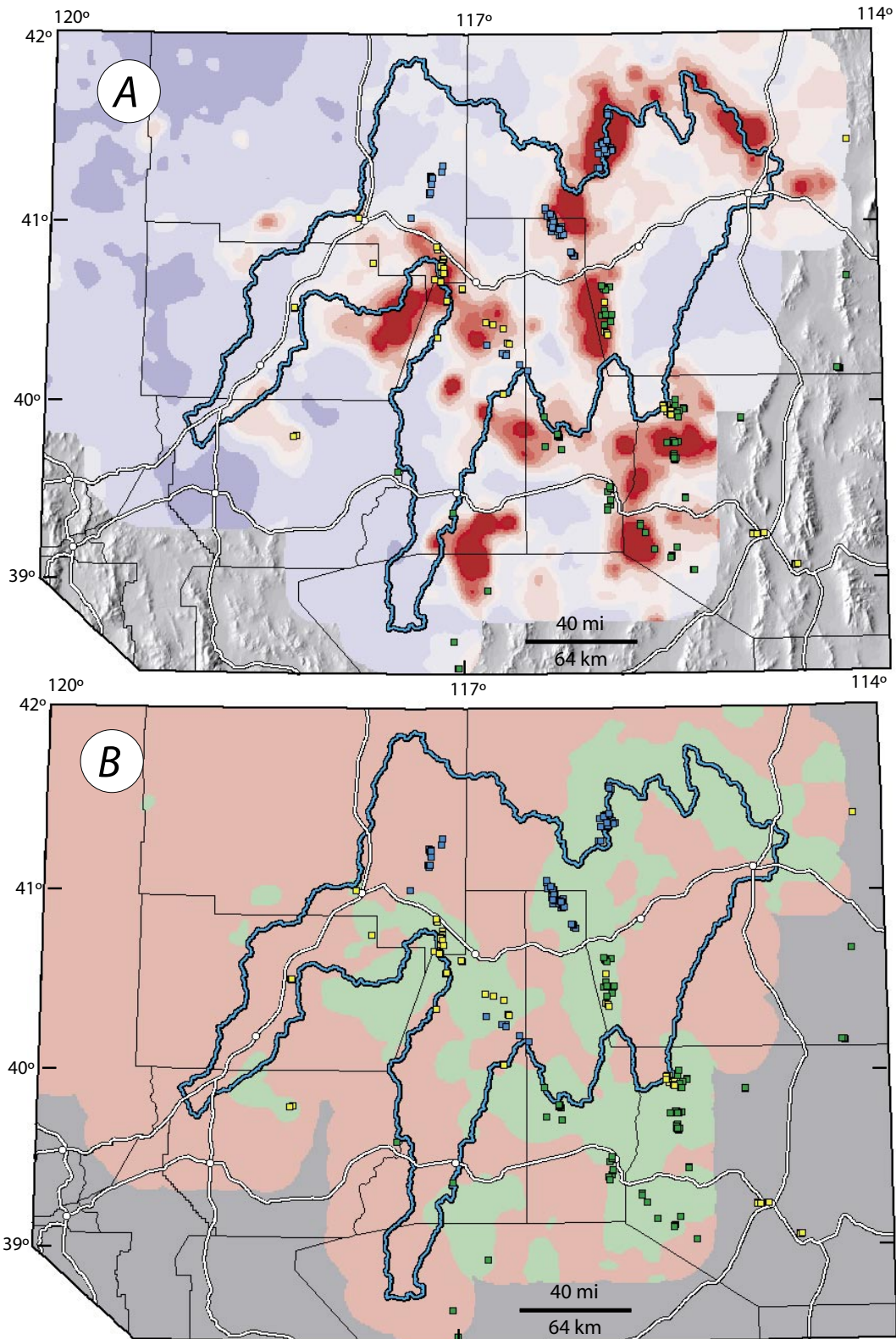
Figure 8-21.   Ba/Na geochemistry evidence and predictor maps. *A*, Ba/Na evidence map; see chapter 2 for explanation. *B*, Predictor map; predictor pattern present, green; predictor pattern absent, red. Missing evidence map coverage shown in gray. Sedimentary rock-hosted Au–Ag deposit training sites shown as blue (north Carlin-type), green (south Carlin-type), and yellow (distal-disseminated Ag-Au) squares. Humboldt River Basin shown as light blue outline.

116°00'

EXPLANATION

Q	Alluvium (Quaternary)
Ts	Sedimentary rocks (Tertiary)
Tv	Volcanic rocks (Tertiary)
Ti	Intrusive rocks (Tertiary)
KJi	Intrusive rocks (Cretaceous-Jurassic)
Jvs	Volcanic and sedimentary rocks (Jurassic)
OLA	Overlap assemblage (Mississippian-Permian)
MA	Miogeoclinal assemblage (Ordovician-Devonian)
RMA	Roberts Mountains allochthon (Ordovician-Devonian) Includes some overlap assemblage (OLA)

✗GQ Mine

⚊ ⚊ Boundaries of regional lineaments
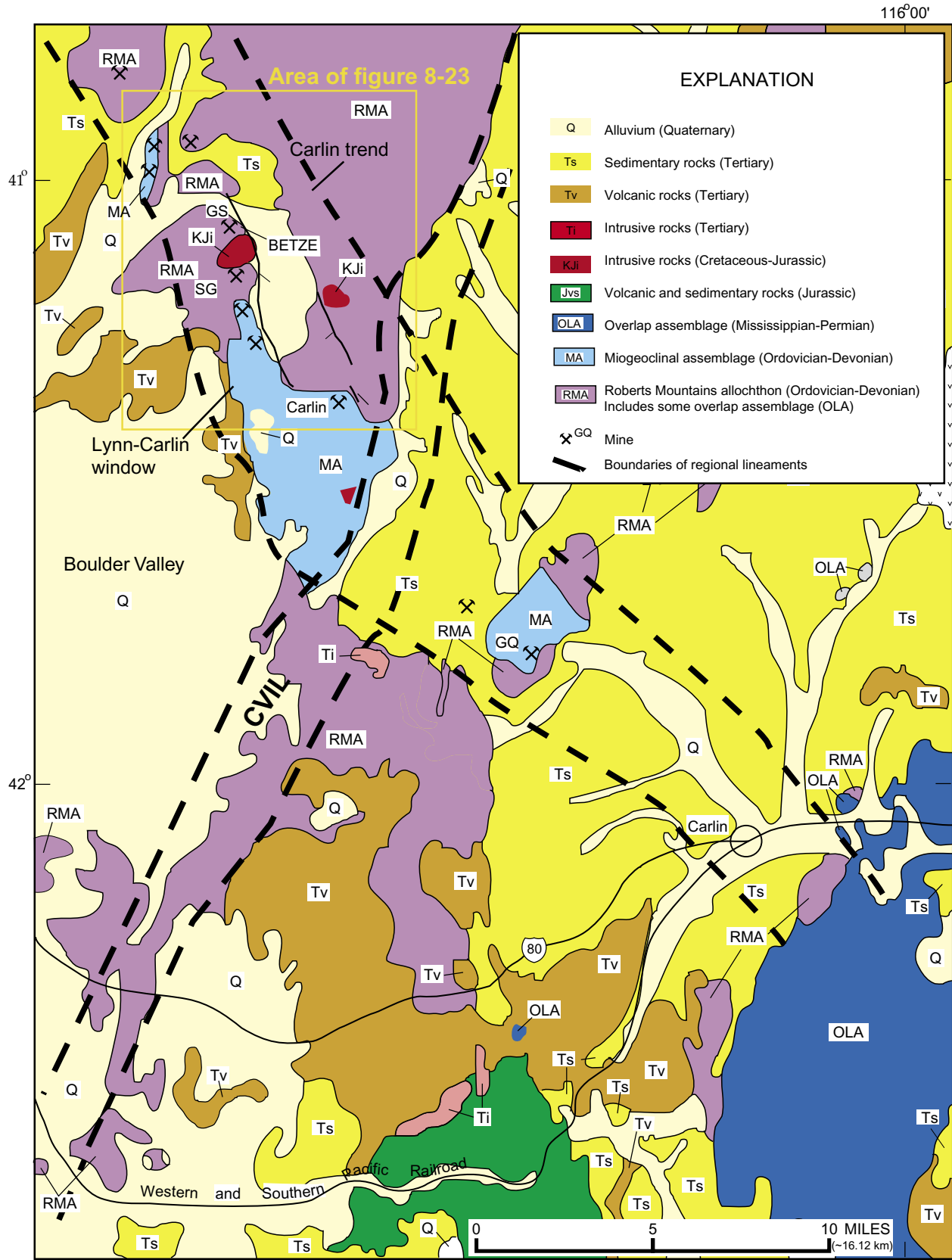
Figure 8-22. Geology of the Carlin trend area showing the distribution of allochthons and tectonic windows. The Carlin trend lies along the Lynn-Carlin and other tectonic windows through the Roberts Mountains allochthon that exposed Au deposits. Modified from Stewart and Carlson (1976).
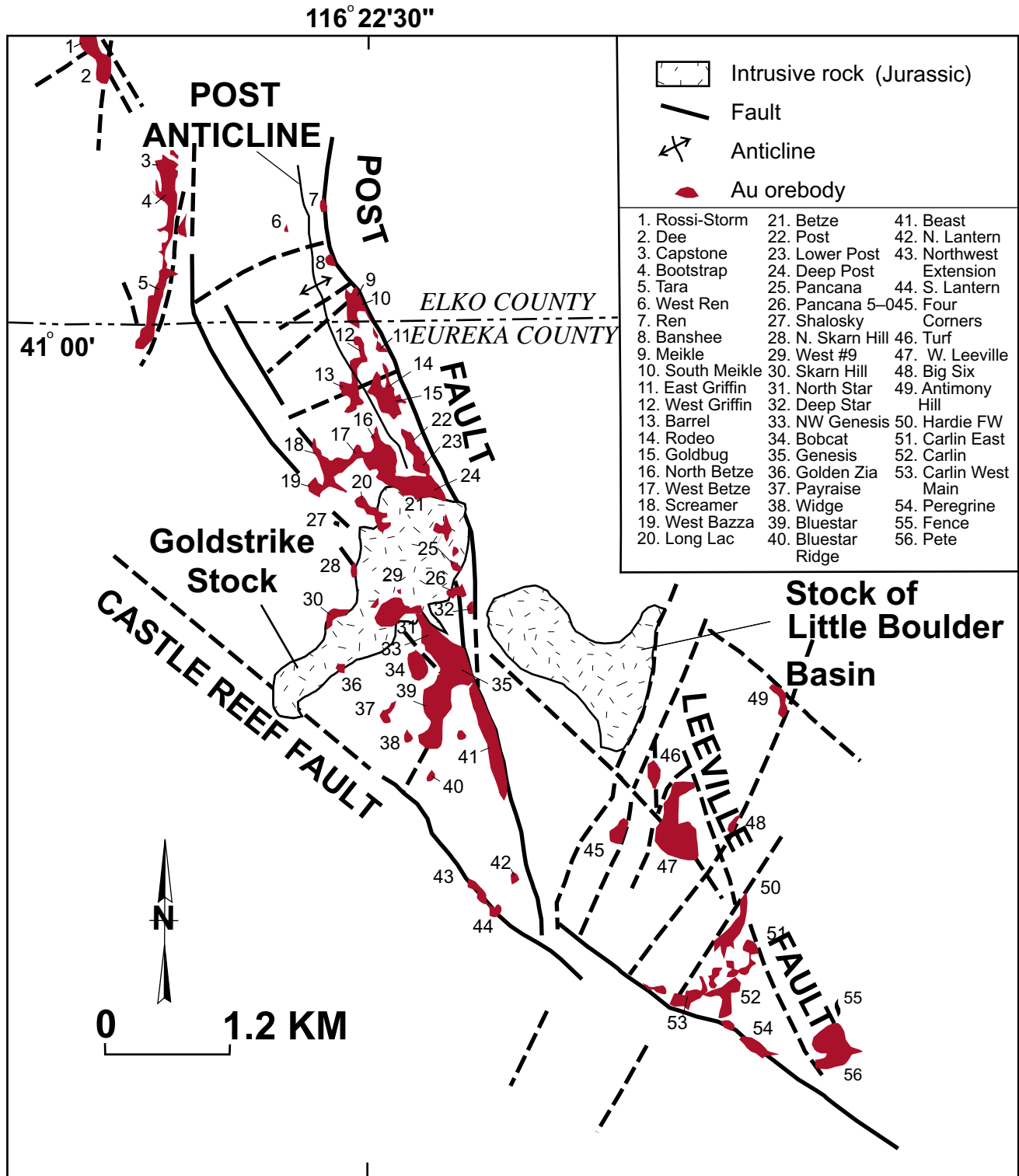
Figure 8-23.   Gold ore deposits and structural features of the main Carlin trend, northern Nevada. Adapted from Teal and Jackson (1997). For location, see figure 8-22.
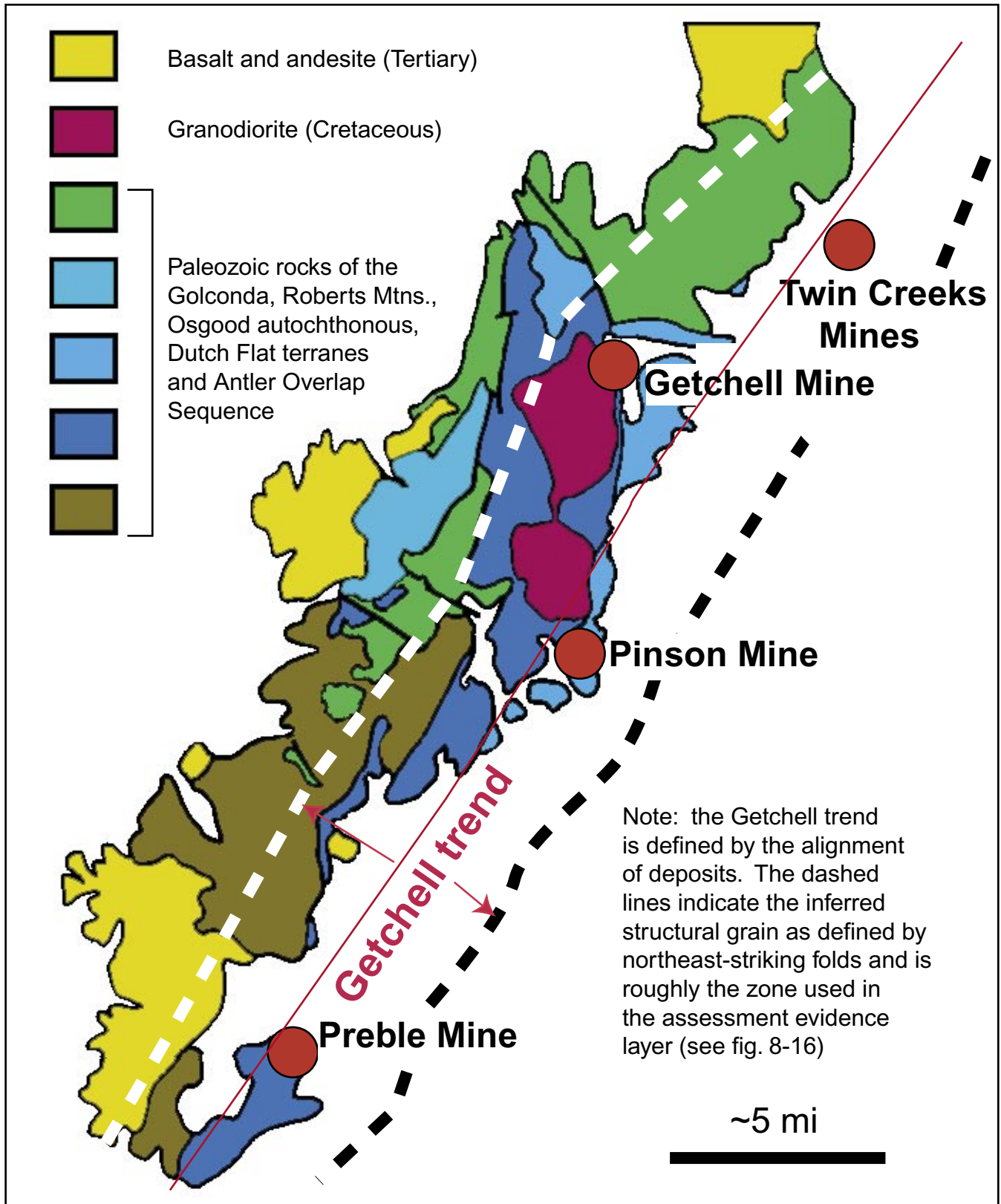
Figure 8-24. Simplified geologic map of the Osgood Mountains showing locations of mines along the Getchell trend. Geology modified from Hotz and Willden (1964) and Stewart and Carlson (1976). See figure 8-2 for location.

Explanation

Unconsolidated deposits (Quaternary)

Basaltic rocks (Pliocene)

Calc-alkaline rhyolite tuff (Miocene or Oligocene)—Equivalent in age to Bates Mountain Tuff of Stewart and McKee (1977)

Gravel deposits (Oligocene)—Locally interbedded with 31–Ma basaltic rock near Cottonwood Creek

Welded tuff and pyroclastic rocks (Oligocene)

Granodiorite porphyry, monzogranite, tonalite, and rhyolite (Oligocene or Eocene)

Monzogranite and monzogranite porphyry (Late Cretaceous)

Antler sequence (Permian and Pennsylvanian)

GOLCONDA THRUST PLATE

Havallah sequence of Silberling and Roberts (1962) (Mississippian, Pennsylvanian, and Permian)

ROBERTS MOUNTAINS THRUST PLATE

Valmy Formation (Middle and Early Ordovician)

Scott Canyon Formation (Devonian)—As shown, includes some rocks of Valmy Formation

DEWITT THRUST PLATE

Harmony Formation (Late Cambrian)

——— Contact

——— High-angle fault—Dashed where approximately located; dotted where concealed or inferred

▲—▲ Thrust fault—Dashed where approximately located; dotted where concealed or inferred. Sawteeth on upper plate

● Porphyry systems; Au skarn at Redline (Cleveland, 2000)

● Distal-disseminated Ag-Au deposit

⚒ Mine

Figure 8-25. Geology of the Battle Mountain Mining District, Nevada, showing locations of major sedimentary rock-hosted Au–Ag deposits of the distal-disseminated type and their relation to porphyry systems. Modified from Roberts (1964), Doebrich (1995), and Theodore (2000).
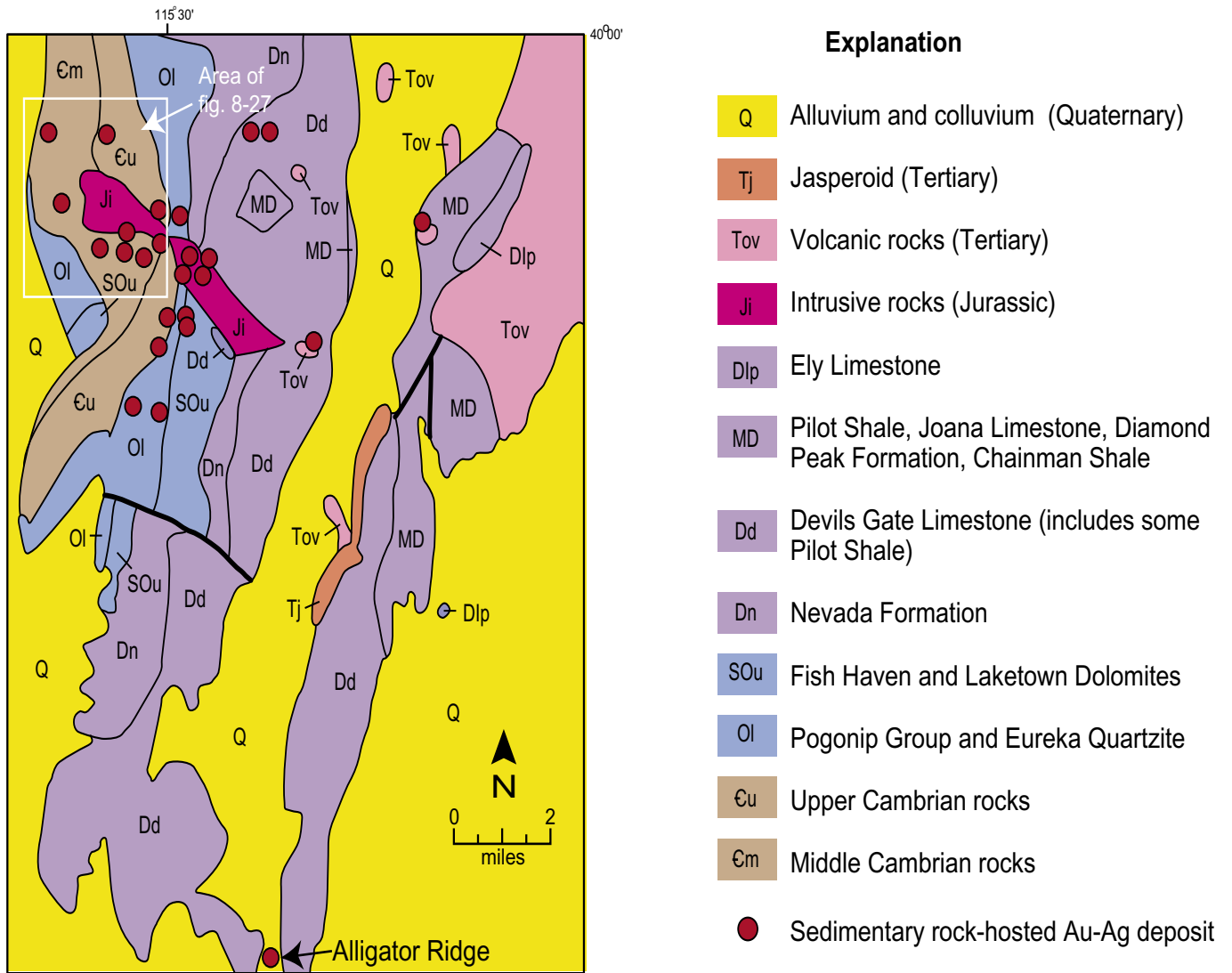
Figure 8-26. Sedimentary rock-hosted Au-Ag deposits of the Bald Mountain Mining District. Adapted from Hitchborn and others (1996). For location see figure 8-2. Detailed lithology of figure 8-11. Area of figure 8-27 is where distal-disseminated Ag-Au deposits are present. Other deposits are considered to be Carlin-type Au deposits.
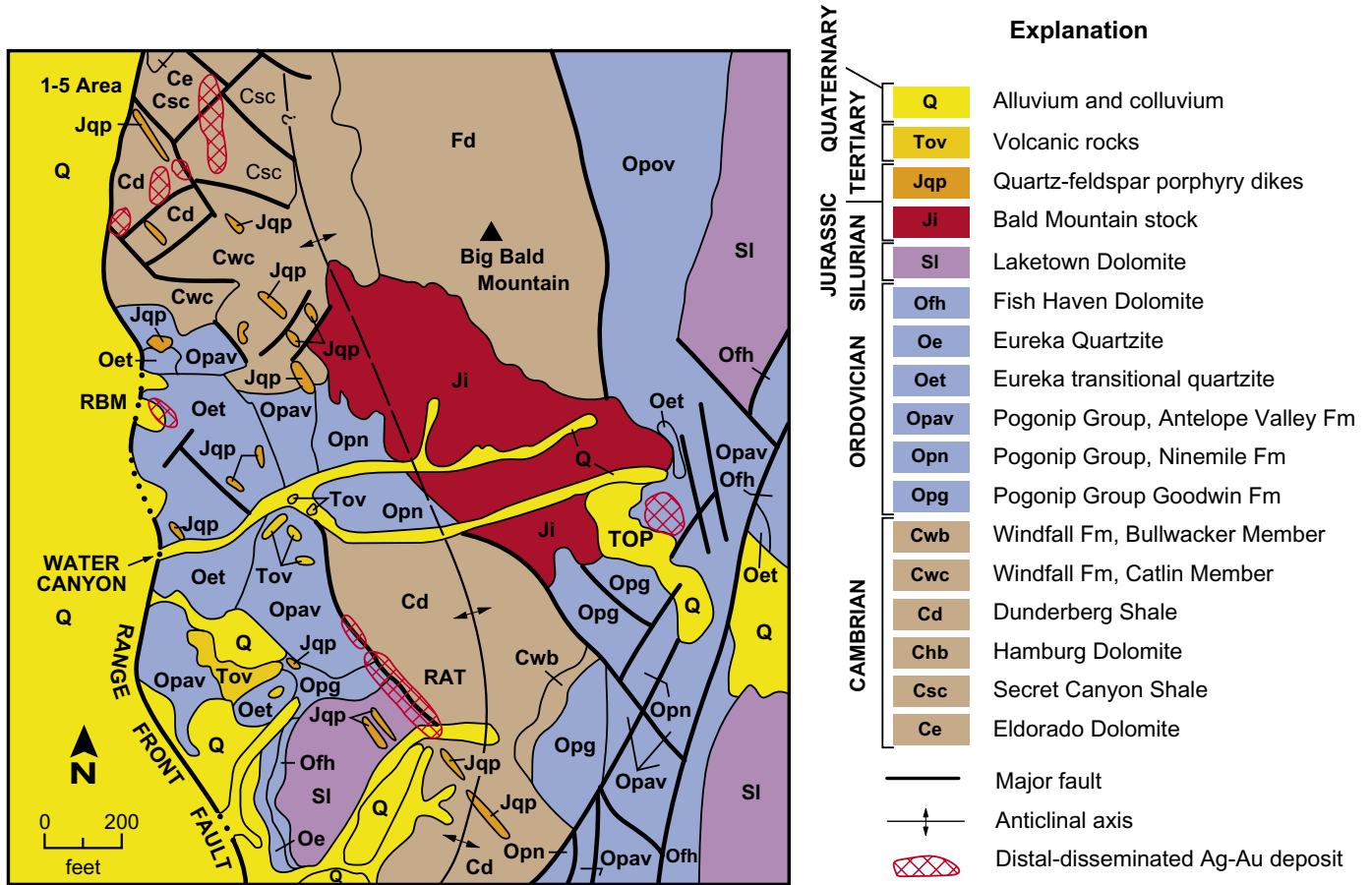
Figure 8-27.   Geology of the Little Bald Mountain mining area showing distal-disseminated Ag–Au deposits of the Bald Mountain Mining District from Hitchborn and others (1996). See figure 8-26 for location.
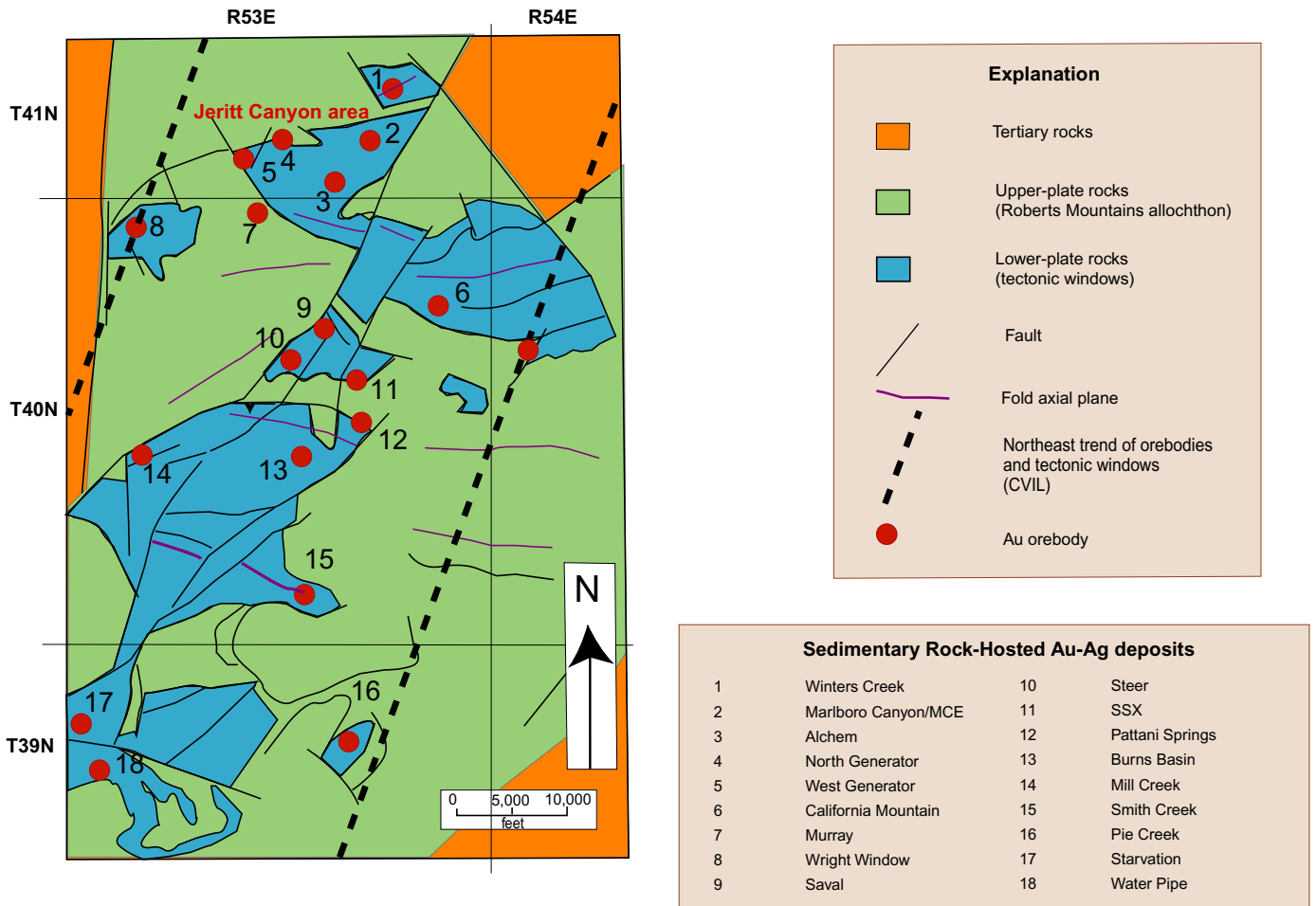
Figure 8-28. Geology and distribution of Carlin-type sedimentary rock-hosted Au–Ag deposits in the Independence Mining District (and Jerritt Canyon), northern Nevada, showing northeast trend of tectonic windows and associated faults and orebodies (adapted from Daly and others, 1991; LaPointe and others, 1991). Dark dashed lines are northwest and southeast margins of northeast-trending Crescent Valley-Independence lineament.
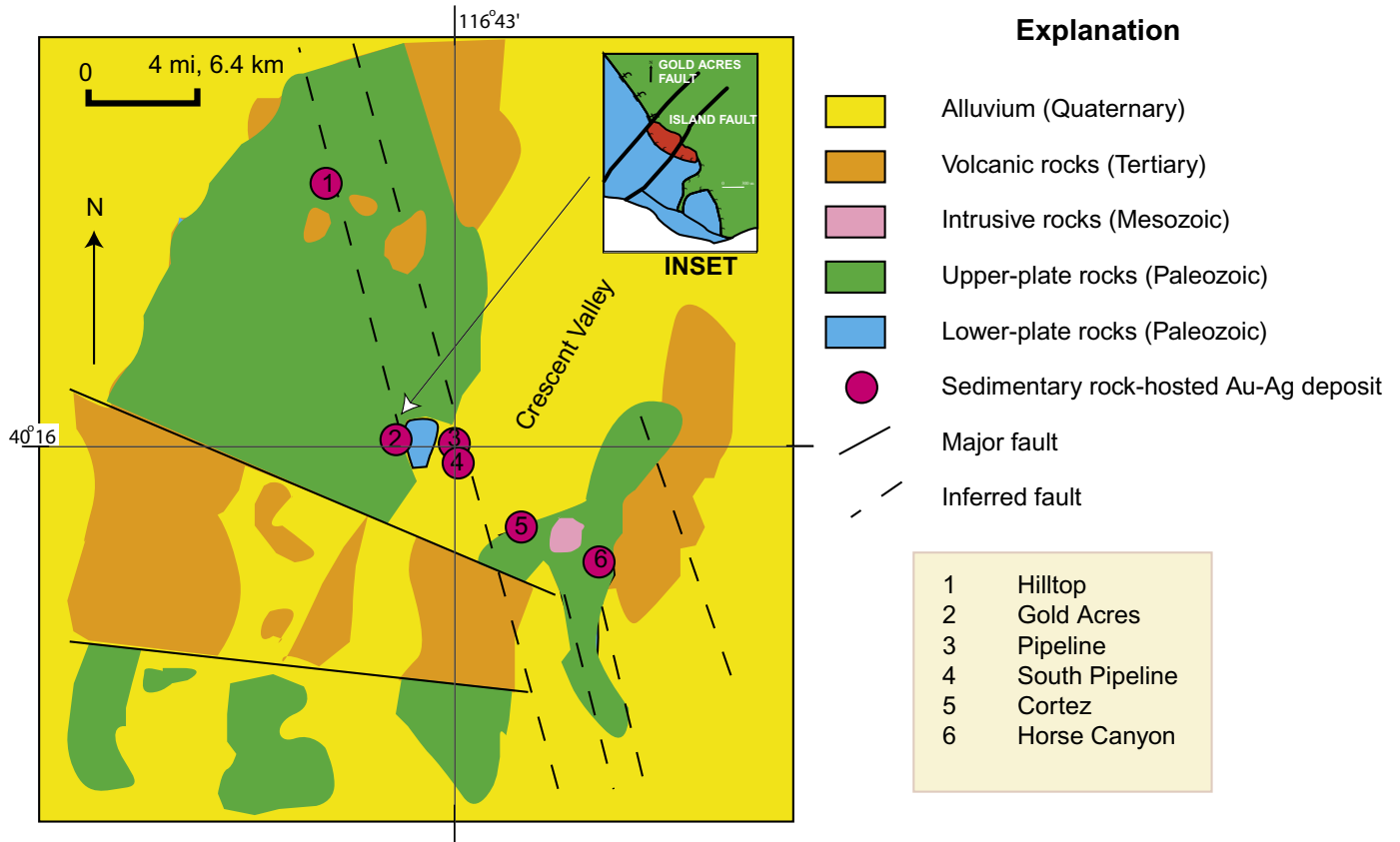
Figure 8-29.   Map of sedimentary rock-hosted Au–Ag deposits of the Carlin-type in the Cortez-Pipeline Mining District that show examples of northeast- and northwest-striking faults and trends in the southern parts of the CVIL. Inset, Gold Acres sedimentary rock-hosted Au-Ag deposit (in red) showing control by northeast-striking Gold Acres and Island Faults (adapted from Hays and Foo, 1991).
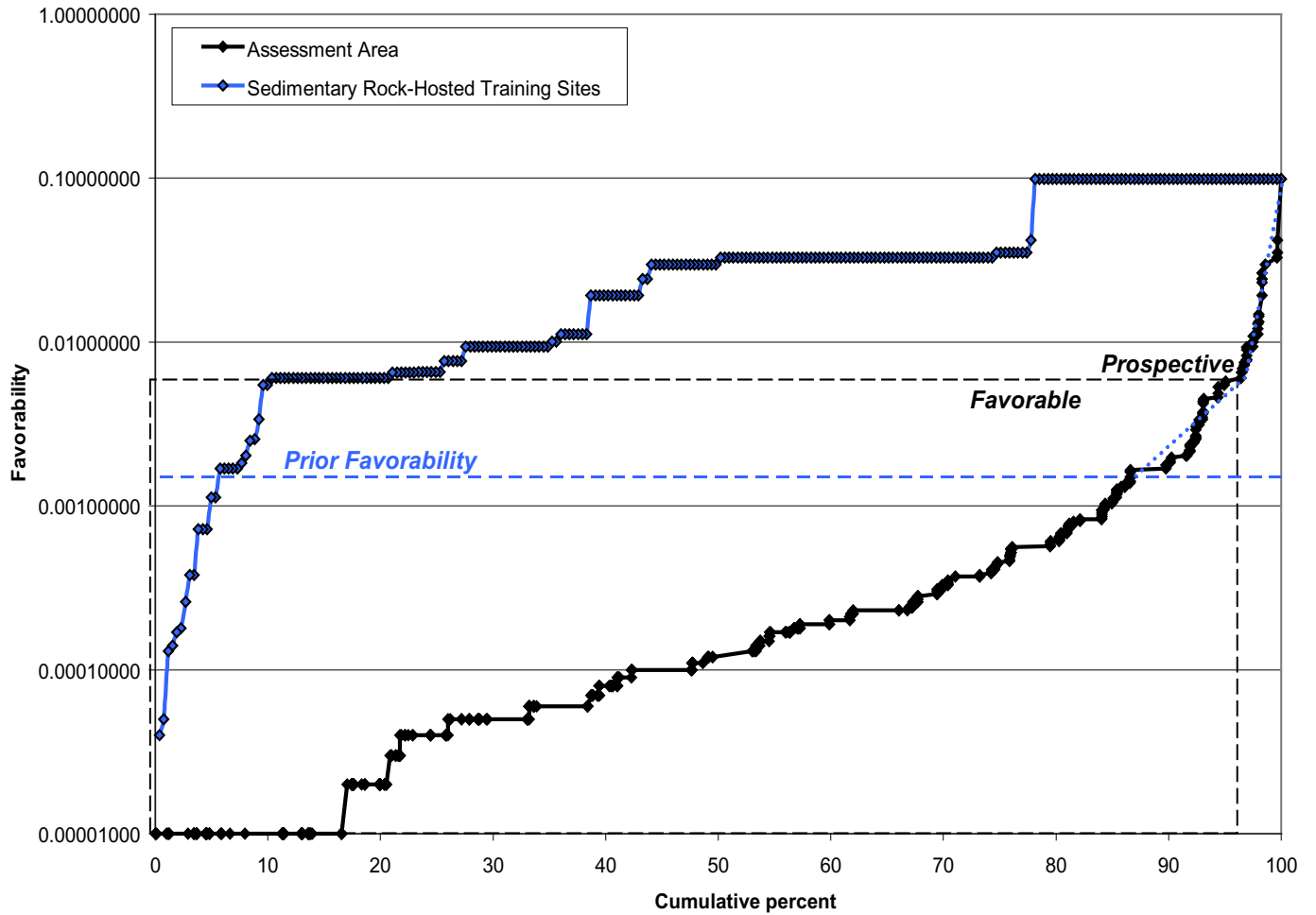
Figure 8-30. Sedimentary rock-hosted Au–Ag deposit weighted logistic regression (WLR) favorability plotted against cumulative assessment area (black) and against cumulative training sites (blue). The permissive–favorable rank boundary is defined as the prior favorability (0.0015, blue dashed line). The favorable–prospective rank boundary is defined as the most prominent break point in the cumulative assessment area above the prior favorability (0.006, black dashed line). The favorable–prospective break point is highlighted by a blue dotted trend-line.
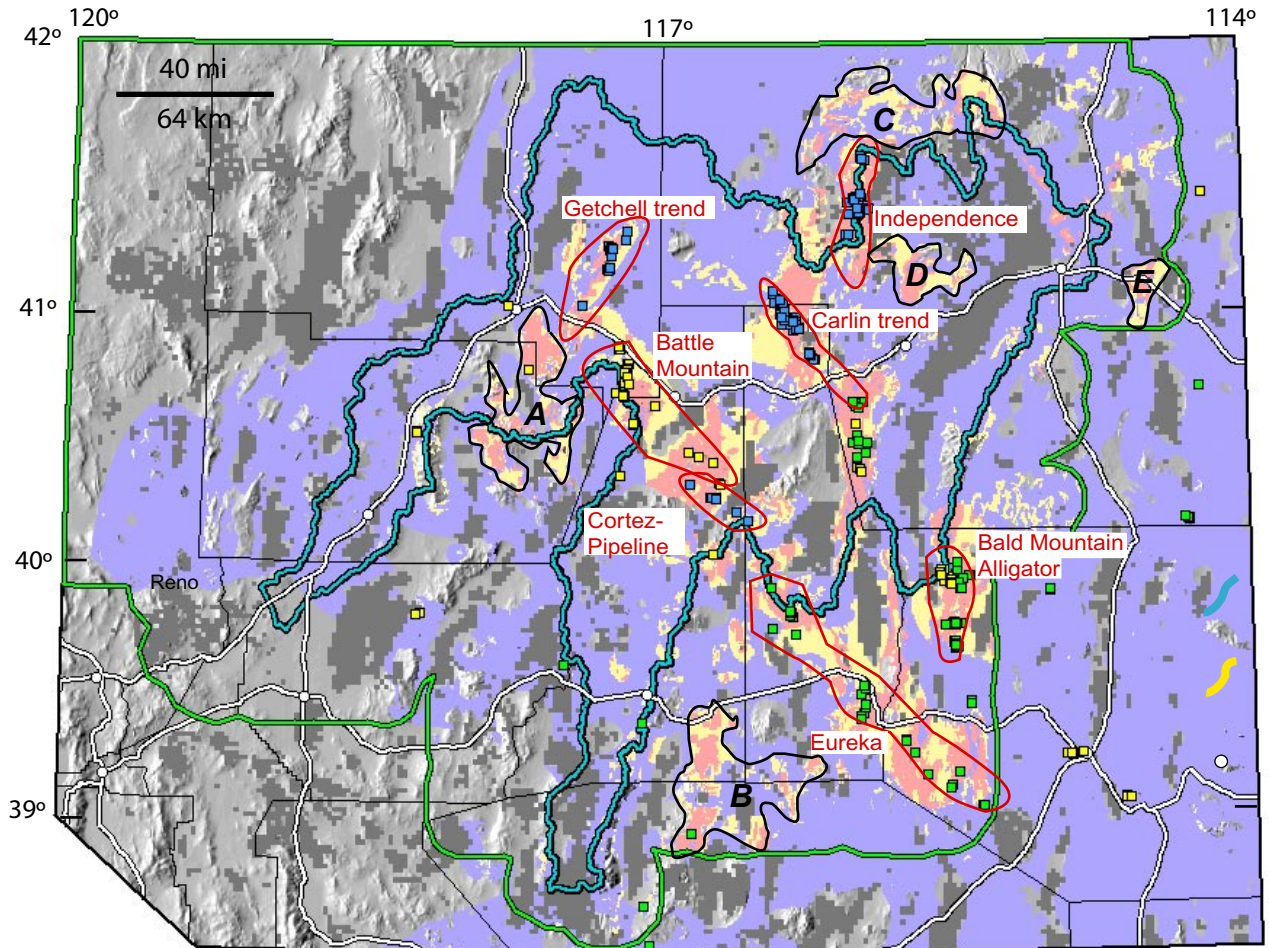
Figure 8-31. Sedimentary rock-hosted Au–Ag deposit mineral resource assessment map, showing prospective (red), favorable (yellow), permissive (blue), and nonpermissive (uncolored) tracts. Note that prospective and favorable tracts were delineated only where National Uranium Resource Evaluation (NURE) geochemical data is available (As-spatial and Ba/Na evidence, within the light green line). Darker gray areas represent Cenozoic cover deposits that are greater than 1 km thick. Sedimentary rock-hosted Au–Ag deposit training sites shown as blue (north Carlin-type), green (south Carlin-type), and yellow (distal disseminated) squares. The Humboldt River Basin is outlined in light blue. Major cities and roads are shown in white. Features are plotted on a background of shaded relief of topography. Main mining districts are outlined in red (see also fig. 8-1 and text). Areas outlined in black are areas that were prospective and favorable in the model and are discussed in text as (*A*), Sonoma-East and Tobin Range area; (*B*), Northumberland, north Monitor, and Toquima Range area; (*C*), Bull Run, Copper, and Jarbidge Mountains area; (*D*), North Adobe Range; and (*E*), North Pequop Mountains area.

Table 8-1.   Training set of sedimentary rock-hosted Au–Ag deposits

This table is oversize and must be viewed or printed separately from this page—click here

Table 8-2. Evidence maps, prediction criteria, and spatial associations

[Evidence maps listed in order of descending strength of spatial association. Prediction criteria were determined by data-driven means. W+, positive weight; W-, negative weight; C, strength of association; Studentized C, significance of C (see chapter 2). Training sites = 293]

Evidence Map	Prediction Criteria	Spatial Associations (W+, W-, C, Studentized C)			
		Predictor Present	Predictor Absent	Strength	Significance
As-Spatial	≥ 0.95 ppm	0.5045	-2.6266	3.1311	8.7214
NE Linear Features	within corridor area	2.5836	-0.4791	3.0627	25.5168
Lithologic Units	Osv, PMh, Cc, Oc, PPa, Pcd, St, Os, MDs, Ct, Dc, Ch, SOc, TRc, Dsl, Tbr, OCc	0.5732	-2.4525	3.0257	8.8905
Ba/Na	≥ 1/4 standard deviations above mean	1.2317	-1.7670	2.9987	16.3253
Lithotectonic-Terrane Units	Roberts Mountains, Vinini, North America (includes structural windows)	0.6056	-2.1821	2.7877	10.8404
Thrust Proximity	within 2 km	2.0789	-0.5180	2.5969	21.9686
Basement Gravity Lineaments	within 17 km	0.2402	-1.9520	2.1922	6.8119
Pluton Proximity	within 21 km	0.1339	-1.8117	1.9456	5.0851
Lithodiversity	≥ 4 lithologic units per 6.25 km^2	0.7971	-1.0871	1.8843	13.3189

Table 8-3.   Sedimentary rock-hosted Au–Ag deposit response map assessment rank areas and training sites.

[Area and training site proportions are relative to the part of the study area covered by geochemical data (As-spatial and Ba/Na evidence maps)]

Assessment Rank	Area (139,580 km^2)	Training Sites (n = 267)
Prospective	6%	88%
Favorable	7%	5%
Permissive	46%	5%
Non-Permissive	41%	2%

Chapter 9

Assessment of Epithermal Au-Ag Deposits and Occurrences

By Alan R. Wallace, Mark J. Mihalasky, David A. John, and David A. Ponce

Introduction

Northern Nevada, and the Humboldt River Basin (HRB) in particular, contains abundant epithermal mineral deposits that formed in a wide variety of geologic host rocks and environments. Historical mining in the region since the mid-1800s exploited many of these deposits, and exploration from 1975 to the present has discovered several large deposits (fig. 9-1). Some of these recent discoveries were in historic epithermal districts, including the Ken Snyder deposit (Midas district), Sleeper (Awakening), Hollister (Ivanhoe), Florida Canyon (Imlay), and Rosebud (Rosebud). Other deposits, such as Mule Canyon, were discovered in areas outside of known epithermal centers.

Metals extracted from epithermal deposits in northern Nevada include Au, Ag, Hg, U, and Mn. The Winnemucca-Surprise assessment of northwestern Nevada (Peters and others, 1996) evaluated each epithermal deposit type separately, using mineral deposit models defined in Cox and Singer (1986). For the present assessment, near-surface hot-spring and deeper epithermal vein deposits were assessed collectively as a system because they commonly represent a vertical continuum and formed during the same mineralizing event. Barring major global economic changes, only deposits that contain significant amounts of Au or Ag likely will be mined in the next ten years. Thus, this assessment focused on those epithermal deposits of the quartz-adularia-sericite ("low-sulfidation") type (Heald and others, 1987; John and others, 2000b; Hedenquist and others, 2000) that are mined primarily for Au and/or Ag. These include shallowly formed hot-spring Au-Ag deposits (model 25a of Cox and Singer, 1986) and epithermal vein deposits (Comstock epithermal vein: quartz-sericite-adularia, models 25c and 25d; and Sado-type, model 25d). Although not assessed per se, the other types of deposits were used as indicators of epithermal mineralizing processes. Important quartz-alunite ("high-sulfidation") epithermal Au-Ag deposits (model 25e; Heald and others, 1987; Hedenquist and others, 2000) are found elsewhere in Nevada (for example, Goldfield and Fairplay (Paradise Peak deposit) districts). However, with the minor exception of a small zunyite deposit in Oligocene rocks northeast of Midas (LaPointe and others, 1991), good evidence for the igneous environments required for the formation of high-sulfidation deposits is absent in or near the HRB (John and others, 1999;

John, 2000). Therefore, this type of deposit was not considered in the assessment of the HRB.

Extensive and detailed mineral exploration, some primitive and some sophisticated, has pursued these deposits since the mid 1800s, and the increased price of Au since 1973 has been a recent economic incentive. Virtually all exposed bedrock, as well as some areas concealed by Quaternary alluvium, have been scrutinized in great detail. Thus, most exposed or obvious targets have been evaluated and either mined or dismissed as subeconomic. Current exploration programs are focusing on deep targets in known epithermal districts, an exploration concept proven successful in the Midas district; in shallow to deep areas outside of conventional epithermal districts, such as the Mule Canyon area; and in areas with a thin cover of surficial sediments, such as at Sleeper.

General Description of Deposit Type

Low-sulfidation epithermal mineral deposits generally form at depths of less than 1-2 km and are related to hot, circulating ground water. Near-surface magmatic systems, such as volcanic or shallow intrusive centers, typically provide the heat that drives the system, and most deposits therefore are present in or near volcanic or shallow intrusive rocks. However, virtually any type of rock, including unconsolidated alluvium, can host an epithermal deposit. The hydrothermal fluids that form the deposits largely are meteoric in origin. The water penetrates to depths of several kilometers along fractures and through permeable rocks, is heated, and then ascends along faults and through permeable units. Low-sulfidation epithermal systems have variable but generally very low contributions of magmatic fluids and (or) metals (Hedenquist and others, 2000), and the ore-forming metals and other elements largely are scavenged from the country rocks during fluid migration. As temperature and pressure decrease upward, the hydrothermal fluids lose their ability to carry the metals and ore and gangue minerals precipitate from the fluids. The fluids also react with the surrounding wall rocks, producing minor to extensive alteration zones in the host rocks and local ore deposition. Mineral deposition along open fault and breccia zones creates vein deposits, and lateral migration of the fluids into permeable rocks produces tabular, stratabound deposits.

Hot-spring deposits form at or just below the Earth's surface, where hot water is in contact with the atmosphere (fig. 9-2).

Several geologic processes can modify or destroy an epithermal ore deposit after it forms. As the hydrothermal system wanes and (or) the water table declines, cool, oxidized surface water is drawn down into the mineralized zone, and supergene minerals replace the primary hydrothermal minerals. If the deposit is exposed at the surface at some later time, both chemical and mechanical weathering can change the composition and mineralogy of the deposit. Various processes can transport elements and fragments of the exposed orebody downhill and downstream. This produces placer deposits and stream sediments that contain elements and minerals characteristic of the weathered orebody. In extreme cases, some of which are described later, tectonic uplift and erosion can completely destroy an epithermal deposit, especially hot-spring deposits that formed at the paleosurface.

In northern Nevada, low-sulfidation epithermal deposits have a wide variety of hosts and forms. Most deposits are in volcanic rocks or nearby epiclastic sedimentary units, although pre-Tertiary rocks host some deposits, such as at Florida Canyon (Hastings and others, 1988) and Relief Canyon (Wallace, 1989). Both regional and local fracture systems were important in the formation of the deposits. For example, several epithermal systems (Midas, Ivanhoe, Rock Creek, Mule Canyon, Fire Creek, and Buckhorn) formed along the regionally extensive northern Nevada rift, a deep-seated, middle Miocene fracture zone (John and others, 2000b; John and Wallace, 2000). However, the style of mineralization varies considerably from deposit to deposit, ranging from hot-spring sinter deposits at Ivanhoe (Bartlett and others, 1991; Wallace, 2003) to deep, high-grade veins at Midas (Goldstrand and Schmidt, 2000). Most of the known deposits and occurrences in northern Nevada are in veins or are fracture controlled, such as at Jarbidge, Sleeper, Midas, and Buckskin-National. Other deposits formed along the margins of dike swarms (Mule Canyon; John and others, 2000a) or are disseminated in permeable tuffaceous sedimentary units (Ivanhoe, Wind Mountain, Buckhorn). Hot-spring deposits are common in the region and include McDermitt, Hycroft/Sulphur, Ivanhoe, Dixie Comstock, and Goldbanks. The full spectrum of deposits can be seen in the Buckskin-National area, where surficial hot-spring sinters, near-surface replacement Hg deposits, and deeper high-grade Au-Ag veins are exposed (Vikre, 1985).

The surface expressions of epithermal deposits range from obvious to none (Sillitoe, 2002). In northern Nevada, hydrothermal alteration zones vary from extensive to minor. This is due to variations in the chemistry of the hydrothermal fluids, the amount of magmatic fluids that mixed with the meteoric fluids, the structural setting, the compositions and physical properties of the host rocks, and the duration and depth of mineralization (Hedenquist and others, 2000; John, 2001). At one extreme, widespread and pervasive alteration surrounds the Round Mountain gold deposit in south-central Nevada (Sander and Einaudi, 1990) and the Comstock Lode near Reno (which contains alteration related to more than one mineralizing event; Whitebread,

1976; Castor and others, 2002). At the other extreme, most alteration in the Midas district is confined to narrow zones around the high-grade veins (Leavitt and others, 2000). Thus, the intensity and volume of alteration in an epithermal system is not necessarily proportional to the size or grade of the mineral deposit. Other surficial expressions of deposits can be equally variable. Sinter deposits at some hot-spring systems, such as Buckskin Mountain and Ivanhoe, are obvious (Vikre, 1985; Bartlett and others, 1991). In contrast, the surface expression of the shallow-formed Mule Canyon Au deposit is extremely poorly expressed, and the deposit was discovered on the basis of one stream-sediment sample with anomalous Au (Thomson and others, 1993). Some high-grade deposits are not exposed at all—the Ken Snyder Au-Ag deposit at Midas was discovered when exploration drilling intersected a high-grade vein that does not extend to the surface (Casteel and others, 1999), and Quaternary alluvium concealed most of the Sleeper Au deposit (Wood and Hamilton, 1991).

Gold, Ag, and Hg are the most common elements that have been mined from epithermal mineral deposits in the Humboldt River basin. Their presence today therefore provides a tool for exploration. Other elements associated with these deposits include As, Sb, Tl, U, Mn, and Se (Silberman and Berger, 1985), and these pathfinder elements are used to explore for epithermal deposits. These elements are not unique to these deposits, but anomalous amounts or combinations of these elements in stream sediments, soils, and rocks have been used to discover epithermal deposits.

The grades and tonnages of epithermal Au–Ag deposits in northern Nevada vary widely. Historical mining used underground mines to exploit large to small high-grade veins. Recent mining has used both underground mining (Rosebud, Ken Snyder/Midas) and open-pit methods (Mule Canyon, Florida Canyon, Hog Ranch, and others), which exploit large-tonnage and (or) lower-grade deposits near the surface. Large deposits include the Comstock Lode, from which 190 million oz Ag and 8 million oz Au were produced (Bonham, 1969), Round Mountain (>3.6 million oz Au produced through 1994; 1996 reserves of 10.2 million oz Au), Sleeper (1.7 million oz Au ; Nash and Trudel, 1996), and Ken Snyder/Midas (1998 reserves of 3.04 million oz Au, 47.9 million oz Ag; Goldstrand and Schmidt, 2000). Other epithermal deposits produced moderate to significant amounts of Au and Ag in the past 20 years, including Mule Canyon, Florida Canyon, Relief Canyon, Rosebud, Hollister, Hog Ranch, Gooseberry, Rawhide, Hycroft/Sulphur, Tuscarora, and Wind Mountain. Historic epithermal districts that produced significant amounts of precious metals from underground veins include Buckskin-National, Jarbidge, Midas, Seven Troughs, Como, Ramsey, Wonder, Fairview, and Manhattan.

Databases Used for Assessment

This assessment of epithermal deposits identified processes that formed the known epithermal deposits and used

various databases as proxies for expressing those processes spatially at a regional scale. Published descriptions define the characteristics of known epithermal deposits, and regional databases suggest where those features may occur elsewhere in the region. Thus, the assessment iterated between detailed and regional data sources. Several databases, described below, are particularly relevant to epithermal deposits in northern Nevada. Three of those databases—volcanic rock assemblages, As NURE geochemistry, and aeromagnetic anomalies—were utilized in the final data-driven assessment described later in the chapter. Individually, the databases reflect systems or processes that may or may not be related to mineralization, but the combination shows areas of overlap that might define areas where mineralization took place.

Most of the epithermal deposits, as well as many other mineralized and unmineralized areas, were visited during the Winnemucca-Surprise and HRB assessments and as part of other ongoing U.S. Geological Survey (USGS) projects. Data from those field studies were incorporated into the databases and the final resource assessment.

Geologic Map of Nevada

The state geologic map of Nevada (Stewart and Carlson, 1978) was used as the geologic base for the assessment. The map was used to define volcanic assemblages and the level of exposure, as discussed below. At the scale of this assessment (see chapter 3), the various lithologic and time divisions are adequate for a regional evaluation. Recent geochronology studies and large-scale geologic mapping have revised the age assignments and geology in some areas. These changes are not reflected on the geologic map, but the revisions as they apply to this assessment are noted elsewhere in this chapter.

High-angle faults are an important component of epithermal deposits because they focus and localize flow of ascending and descending hydrothermal and supergene fluids. Large-scale geologic mapping in many parts of northern Nevada shows that faults are extremely common in virtually all areas with exposed bedrock. This high fault density is not reflected in regional fault compilations (Stewart and Carlson, 1978; Dohrenwend and others, 1996). As a result, many faults are not shown on those compilations, and those maps under-represent the high and equally distributed fault density in the exposed bedrock. In addition, fluid flow takes place along open or conductive fractures and faults, and the "openness" of a fault depends upon the regional stress regime at the time of fluid flow and mineralization. Thus, even with a high density of faults in an area, fluid flow might utilize only a subset of those faults, depending on fracture orientation versus regional stress directions. Therefore, this assessment assumed that the fault density is equally high and fracture orientations variable at the scale of known mineral deposits and in all areas of exposed bedrock, and faults and fault density were not considered further in this assessment.

Known Epithermal Deposits (Training Sites and MRDS)

The characteristics of the major epithermal deposits in Nevada ("training sites") are provided in table 1 and their locations shown on figures 9-1 and 9-3. As described in chapter 2, these deposits represent the major epithermal deposits that have been mined or are known through industry property evaluations in the region, and their characteristics help define the origin of epithermal deposits in the area. Mineral Resource Data System (MRDS) records include both large mines and small prospects, and they show where epithermal mineralization took place (fig. 9-3). Many MRDS sites are small prospects, but a concentration of these sites indicates a larger mineralizing system. The training sites were used in the data-driven model.

As discussed in ensuing sections, the epithermal deposits in the training set include deposits that formed at different times and in a variety of geologic environments. The data-driven component of this mineral assessment used the entire training set, rather than age- or environment-specific subsets. Two deposits – Buckskin and Gardnerville, both well outside of the HRB – were included in the data-driven model, but subsequent evaluation indicates that they are Mesozoic in age and thus not applicable to the assessment. The deposits intersect neither the volcanic nor magnetic terranes data layer, and the inclusion of the deposits therefore did not affect the data-driven model and the prospective and favorable tracts.

Geochemistry

As noted above, epithermal deposits commonly contain anomalous amounts of Au, Ag, Hg, As, Sb, Tl, U, Mn, and Se (Silberman and Berger, 1985). Element abundances and ratios vary vertically, but not always predictably, through an epithermal system, and the level of exposure can influence the geochemical signature detected at the surface. Epithermal deposits contain anomalous As at most levels of exposure (Berger and Silberman, 1985), and As data from the National Uranium Resource Evaluation (NURE) dataset were used in the data-driven model for this assessment (see further details in chapters 2 and 5). The dataset includes samples from all rock lithologies and mineral deposit types. As a result, the data are most relevant to Tertiary epithermal deposits in areas where only Tertiary volcanic or sedimentary rocks are exposed, thereby minimizing the influence of older rocks and pluton- or sedimentary rock-hosted mineral deposits that might be exposed at the surface.

Aeromagnetic Data

A modified version of the aeromagnetic map of the state of Nevada (Hildenbrand and Kucks, 1988; see also, chapter 6) was used in the data-driven model. Because most epithermal deposits are associated with volcanic rocks and most volcanic

rocks are moderately magnetic, magnetic methods are a useful tool for delineating potential host rocks. However, because volcanic rocks have a wide range in magnetic properties, it is difficult to determine their extent without the aid of detailed physical property measurements, which are limited in scope within the study area.

The magnetic anomalies shown on the modified map represent the northern Nevada rift and two parallel zones to the west that reflect deep-seated middle Miocene mafic intrusive bodies (chapter 6; see also, Blakely and Jachens, 1991). These three zones are directly related to basaltic andesite and related mafic rocks in those areas.

Volcanic and Epithermal Environments

Subaerial volcanic systems and epithermal mineral deposits have close genetic and spatial relationships, both worldwide and in Nevada (Hedenquist and others, 2000; Buchanan, 1981). Extensive field-based research on epithermal deposits in northern Nevada shows a strong genetic relationship between specific volcanic environments and types of epithermal mineral deposits (John and others, 1999; also, numerous studies on specific mineral deposits). As a result, the nature and distribution of volcanic rocks are key components for assessing epithermal deposits in northern Nevada.

Volcanic Assemblages

Most epithermal deposits in the region are related spatially and (or) genetically to one of three Tertiary igneous assemblages in northern Nevada. These include: (1) the late Eocene to late Oligocene interior andesite-rhyolite assemblage, (2) the Miocene to early Pliocene western andesite assemblage, and (3) the Miocene to Holocene bimodal basalt-rhyolite assemblage (Ludington and others, 1996). Volcanic rocks dominate the assemblages at the surface, although each assemblage contains related shallow intrusive rocks. Each volcanic suite has genetic and physical attributes that affected the types and styles of related mineralization. These assemblages are described briefly below and their distributions shown in figure 9-4; more detail is provided in Ludington and others (1996) and John and others (1999, 2000b). Deposits related to each assemblage are given in table 1.

The interior andesite-rhyolite assemblage includes numerous large-volume calderas, silicic ash-flow tuffs that were erupted from the calderas, smaller-volume rhyolitic intrusive bodies, and andesitic-dacitic lava flows and breccias. The silicic tuffs originally covered wide areas in Nevada, and they are preserved largely in the central and southern parts of the state. The earliest eruptions were in the Tuscarora area at about 43 Ma, and the volcanic activity migrated southwestward, eventually producing widespread ash-flow tuff fields in central and southern Nevada after about 30 Ma (fig. 9-5). Igneous activity formed volcanic and intrusive centers from which the tuffs were dispersed.

The western andesite assemblage formed a northwest-trending zone in western Nevada, extending into adjacent parts of northeastern California. The zone coincides with the Walker Lane structural belt, and it continues northwest into the Cascade Mountains (fig. 9-5). Volcanism in western Nevada began in the early Miocene and continued through the late Miocene. The dominant volcanic forms were stratovolcanoes consisting of intermediate-composition flows, lahars, domes, intrusions, and minor tuffs, with adjacent sedimentary basins. In many areas of western Nevada, the volcanic rocks of this assemblage were erupted on top of rocks of the interior andesite-rhyolite assemblage. The resulting volcanic terranes were complex, with a wide variety of ages, morphologies, and compositions. The western andesite and interior andesite-rhyolite assemblages had similar compositions, although the interior andesite-rhyolite assemblage contains more rhyolite.

The bimodal basalt-rhyolite assemblage is the most widely exposed volcanic suite in northern and northwestern Nevada, and related volcanic rocks were erupted throughout western Nevada. The bimodal assemblage began to form during west-southwest extension at about 17 Ma (fig. 9-5), and it continues weakly to the present time; the major pulse of magmatism in northern Nevada was between 17 and 13 Ma. As the name implies, both mafic and felsic rocks comprise the assemblage. The more mafic component includes basalt to andesite flows, dikes, and tuffs. Some mafic feeder zones penetrated the entire crust along >100-km fracture zones or rifts to form extensive but narrow dike swarms, such as the northern Nevada rift (fig. 9-5). The felsic component of the assemblage includes rhyolite to rhyodacite domes, flows, and tuffs. Dacite flows and tuffs are common in some areas, such as along the northern Nevada rift (John and others, 2000). This assemblage includes some calderas, many of them in southeastern Oregon and southwestern Idaho, although overall they are less common than in the interior andesite-rhyolite assemblage.

Ages of Mineralization

The known ages of epithermal mineral deposits in northern Nevada largely mimic the ages of the volcanic rocks, and they mostly are middle Miocene (17-10 Ma; table 9-1). Epithermal deposits related to the interior andesite-rhyolite assemblage range in age from 39 Ma at Tuscarora in the north to 26 Ma at Round Mountain in the south. Most deposits associated with the western andesite and bimodal assemblages are middle Miocene in age, similar to the related volcanic rocks (John, 2001). A few deposits are very young, including Wind Mountain (Wood, 1991) and Hycroft (Ebert and Rye, 1997), which are Pliocene or younger, and Dixie Comstock, which is Quaternary in age (Vikre, 1994). As described later, these young deposits reflect the high regional geothermal gradient and related hydrothermal convection in much of northern Nevada (Lachenbruch and Sass, 1978).

Many epithermal deposits have not been dated. The ages of some deposits have been inferred from the ages of associ-

ated volcanic rocks, which are more extensively dated than the mineral deposits, and from the geologic relations between the volcanic rocks and the mineral deposits. Some epithermal deposits are significantly younger than the volcanic host rocks, such as at Rosebud, where ~26–Ma volcanic rocks host ~15–Ma epithermal Au-Ag vein deposits (R. Vance and C. Henry, written commun., 2000). The ages of epithermal deposits hosted by pre-Tertiary rocks generally are known only where the deposit itself has been dated, such as the middle Miocene Adelaide and Ten Mile districts (Silberman and others, 1973).

Epithermal Environments

Epithermal deposits in northern Nevada formed in several specific environments related to the three volcanic assemblages (tables 9-1, 9-2). These include calderas, rhyolite domes and flows, stratovolcanoes, rifts, hot springs, and areas of high heat flow. In most cases, volcanic, subvolcanic, and nearby volcaniclastic rocks host the deposits. Pre-Tertiary rocks proximal to the volcanic systems also host some deposits. This is especially true of the fine-grained Mesozoic sedimentary rocks of the Jungo terrane, which was a host rock in at least fourteen Miocene epithermal systems. Table 9-1 summarizes the relation between volcanic environments and epithermal deposits in northern Nevada. Generalized epithermal environments in Nevada are given in table 9-2.

Calderas

Calderas are present in both the interior andesite-rhyolite assemblage, in which more than 50 calderas have been identified (Best and others, 1989; Ludington and others, 1996), and the bimodal assemblage. A few small postulated calderas are present in the western andesite assemblage. The calderas formed when large volumes of silicic to intermediate magma were erupted to form ash-flow tuffs, leaving a semi-circular collapse feature along arcuate ring fractures at the site of the eruption. Intermediate- to felsic-composition flows, domes, and plutons, formed both before and after the eruption, creating an igneous complex at the surface. Styles of mineralization include veins along ring faults and in nearby volcanic rocks (including domes erupted along the ring faults), disseminations in nearby permeable volcanic and volcaniclastic units, fractures and breccias along intrusive margins, and breccias in and near eruptive centers. Despite the large number of calderas in Nevada, surprisingly few of them have related epithermal mineral deposits. In northern Nevada, caldera-related epithermal deposits include those at McDermitt, Wonder, Atlanta, Fairview, Round Mountain, and Tonopah. Other deposits, such as at Tuscarora, formed close to calderas and at about the same time as caldera formation, but they are not necessarily related to the caldera itself. The ash-flow tuff sheets extend great distances from the source calderas, but they rarely were mineralized by the igneous systems that formed them. More commonly, mineralization in an ash-flow tuff unit is related to

a younger caldera or other igneous event. On the state geologic map (Stewart and Carlson, 1978), units Tt_1, Tt_2, Tr_1, Tr_2, Ta_1, and Ta_2 represent the caldera-related igneous centers and outflow tuffs.

Rhyolite Flows and Domes

Rhyolite flows and domes are common parts of the bimodal and interior andesite-rhyolite assemblages, and they form a minor component in the western andesite assemblage. The volcanic stratigraphy in areas underlain by these rhyolitic units can be complex. The flows and domes commonly were erupted while airfall tuffs and epiclastic and lacustrine sediments were being deposited nearby. Local and regional faulting usually accompanied the volcanic activity. Where these volcanotectonic relations have been studied in some detail, such as at Hog Ranch (Bussey, 1996), Buckskin-National (Vikre, 1985), Sleeper (Nash and others, 1995), and Ivanhoe (Bartlett and others, 1991; Wallace, 2003), the various igneous and sedimentary units are intimately interbedded and were deposited relatively rapidly during active faulting. The rhyolitic magmas induced convective circulation of heated meteoric water along faults, contacts, and permeable zones in the rhyolites, sediments, and adjacent older Tertiary and pre-Tertiary volcanic and sedimentary units. Epithermal deposits related to this environment include Hog Ranch, Seven Troughs, Jessup, Buckskin-National, Sleeper, Goldbanks, Ivanhoe, Jarbidge, Kramer Hill, Adelaide, Midas, Bruner, and Mina Gold. On the state geologic map (Stewart and Carlson, 1978), units Tri, Tr_1, Tr_2, Tr_3, and Tt_3 represent the rhyolite flows and domes and related pyroclastic units; units Tts, Ts_1, Ts_2, Ts_3 represent coeval tuffaceous sedimentary rocks.

Stratovolcanoes

Stratovolcanoes typified the western andesite volcanic environment of western Nevada (fig. 3; John and others, 1999). Low-sulfidation epithermal deposits related to this assemblage include those in the Comstock, Gooseberry, Ramsey, Como, and Talapoosa districts. Many volcanoes formed during strike-slip faulting along the northwest-trending Walker Lane belt (fig. 9-5), creating complex volcanic and structural relations. The deposits are linked closely to both the magmatic systems, which provided heat and metals, and to the active high-angle faults, which controlled the flow of hydrothermal fluids and continually provided open spaces to form veins. Thus, most of the epithermal deposits are along faults in and near igneous centers. Some deposits, such as at Washington Hill east of Reno, are directly related to intrusive rocks and thus are more characteristic of porphyry environments (see chapter 7). On the state geologic map (Stewart and Carlson, 1978), unit Ta_3 represents the stratovolcanoes, although Ta_3 in some areas of northernmost Nevada includes basaltic rocks related to rift environments (see following section).

Rifts and Basalt Flows

Middle Miocene (~17-14 Ma) mafic magmas of the bimodal assemblage invaded faults and deep fractures during middle Miocene extension and faulting (Zoback and Thompson, 1978; John and others, 2000b; Ponce and Glen, 2002). Some of these fault-controlled zones were narrow, deep crustal structures, termed "rifts," which appear as pronounced to subtle linear anomalies on aeromagnetic surveys (fig. 9-6; Blakely and Jachens, 1991). The most prominent of these is the northern Nevada rift, which extends southeastward from the Oregon-Nevada border into east-central Nevada (figs. 9-5, 9-6). Two similar zones are present west of the northern Nevada rift (fig. 9-6; additional information in chapter 6), and Ponce and Glen (2002) have identified other, less-obvious zones based on aeromagnetic data. The magmas formed closely spaced dike swarms that fed abundant basalt, basaltic andesite, and less abundant dacite flows at the surface. High-angle faulting accompanied volcanism, producing a complex, fault-controlled volcanic and volcaniclastic stratigraphy. The magmatic heat induced circulation of meteoric waters, and epithermal Au-Ag deposits formed along or near faults and dike margins in the volcanic and related volcaniclastic and sedimentary rocks. These systems formed at or very close to the paleosurface, with vein-dominated systems grading upward into hot-spring environments. Epithermal deposits that formed in this environment include Mule Canyon, Fire Creek, Buckhorn, and possibly part of Florida Canyon. On the state geologic map (Stewart and Carlson, 1978), unit Tba includes the mafic-dominated rift and related flow unit environments. This map unit, however, includes mafic volcanic rocks erupted between 34 and 4 Ma (Stewart and Carlson, 1978), many of which are not related to the mafic volcanism described here.

As discussed in the later section entitled "Level of Exposure," variable uplift and erosion of the middle Miocene paleosurface has exposed relatively deeper levels of rift environments in some areas. This is evident along the southern part of the northern Nevada rift and the related rift zones to the west. There, erosion removed the mafic flows and exposed the underlying dike swarms. These levels comprise the deeper epithermal environment, where faults, fractures, and other fabrics in pre-Tertiary rocks controlled epithermal mineralization, and where mineral textures and mineralogies indicate somewhat deeper and hotter depositional environments. Deposits of this type include epithermal veins in the Ten Mile district and possibly part of the Florida Canyon Au deposit.

High Heat Flow

During the past 6 m.y., shallow underplating of the crust by mafic magmas related to the bimodal assemblage has produced an anomalously high heat flow throughout much of northern Nevada (fig. 9-7; Lachenbruch and Sass, 1978). The region also has been seismically active during that period, especially along range fronts, creating abundant faults in units

of all ages. The combined high heat flow and fault activity generated numerous hot springs and geothermal systems in the region (Garside and Schilling, 1979; Shevenell and others, 2000). Several epithermal Au–Ag–Hg deposits in northern Nevada formed in Pliocene and Quaternary hot-spring environments related to high heat flow or geothermal activity (fig. 9-6). These include Hycroft/Sulphur, Wind Mountain, Golconda, and Dixie Comstock, and likely part of Florida Canyon. Some sinters at modern hot springs, such as Beowawe and Steamboat Springs, contain anomalous amounts of metals and may be forming modern epithermal mineral deposits.

Classification of Rock Units for Data-Driven Assessment

Using the criteria outlined above, units shown on the state geologic map (Stewart and Carlson, 1978) were combined into five units (epithermal units 1-5) to form the epithermal lithology evidence map (table 9-4). The units were defined on the basis of their relative roles in epithermal mineralization. The highest category (epithermal unit 1; table 9-4) represents the Tertiary igneous units that most likely were responsible for epithermal mineralization. These units contributed heat and, in some places, metals and water to the mineralizing process. Epithermal unit 2 includes Tertiary igneous rocks that are that were significant host rocks in epithermal systems but whose roles during mineralization are unknown. Sedimentary rocks of the Jungo terrane comprise epithermal unit 3; as discussed above, these rocks are important pre-Tertiary host rocks for epithermal deposits. Rock units in epithermal unit 5 include all Quaternary (Q) and Quaternary-Tertiary (QT) map units. These units are younger than all but the high-heat-flow epithermal deposits and thus are non-permissive for Miocene epithermal deposits. Epithermal unit 4 includes all other rock units of Miocene or older age; these units can host deposits but are not, by themselves, significant exploration targets in the absence of a known igneous-driven mineralizing system (represented by epithermal unit 1). Deep-seated igneous magmas that may have produced the high late Cenozoic heat flow and related epithermal deposits are not exposed and thus are not represented by any geologic units (see discussion of these deposits in later section entitled "Deposits related to high regional heat flow").

Geophysical Data

An aeromagnetic map of the state of Nevada (Hildenbrand and Kucks, 1988) was used as an aid to assess the potential for undiscovered epithermal Au-Ag deposits within the HRB in north-central Nevada. Because of the regional scale of the investigation and the nature of data-driven assessment techniques, magnetic data were transformed by visual inspection into polygons that represent different magnetic terranes. Some polygons, such as those associated with

the northern Nevada rift and the two similar anomalies to the west (fig. 9-6), probably represent zones of middle Miocene mafic intrusive bodies. These zones are directly related to the basaltic andesite and related mafic rocks in those areas, which in turn are prospective units for bimodal assemblage epithermal deposits of middle Miocene age. Basaltic andesite flow (Tba, Stewart and Carlson, 1978) and rhyolite flow and dome (Tr$_3$, Stewart and Carlson, 1978) units outside of these zones are equally prospective, but they are difficult to trace geophysically because of their highly variable magnetic properties. Thus, the magnetic terrane map outside of these zones was assigned neutral evidence in the data-driven assessment.

Early to middle Tertiary tuffs (units Tt$_1$ and Tt$_2$, Stewart and Carlson, 1978) do not readily distinguish igneous centers and have highly variable magnetic properties. As discussed in chapter 6, most Eocene-Oligocene igneous centers cannot be distinguished readily by the aeromagnetic map. Thus, the magnetic terrane map is not useful to the assessment of Eocene-Oligocene (interior andesite-rhyolite assemblage) epithermal deposits.

The prospective unit for epithermal deposits in the western andesite assemblage is Ta$_3$ (fig. 9-4; Stewart and Carlson, 1978). This unit and magnetic highs shown on the magnetic map of Hildenbrand and Kucks (1988) (fig. 6-5) correlate extremely well. The Pine Nut Mountains and the related Como district are notable exceptions and may reflect coeval volcanic rocks with different magnetic properties or widespread hydrothermal alteration. Thus, the magnetic map is a useful dataset for identifying areas underlain by unit Ta$_3$.

Very recent work by D. Ponce and J. Glen (2002), done after the assessment modeling was completed, has identified additional aeromagnetic anomalies in northern Nevada. As discussed by Ponce and Glen (2002), these anomalies likely are related to the northern Nevada rift and other anomalies. These anomalies were not used in the data-driven assessment, but the implications of these anomalies towards epithermal deposits is discussed in a later section.

Level of Exposure

By definition, epithermal deposits form near the Earth's surface at the time of mineralization (the "paleosurface"). Epithermal deposits in northern Nevada generally formed during the late Eocene and Oligocene and the early to middle Miocene. Thus, presence or absence of the Eocene-Oligocene and middle Miocene paleosurfaces is a broad indication if Tertiary epithermal deposits of those ages may have been preserved or destroyed.

Eocene-Oligocene and middle Miocene volcanic and sedimentary rocks were deposited on and thus demark the paleosurface at the time of deposition. Figure 9-8, derived from units shown by Stewart and Carlson (1978), shows several broad areas where one or both of the Tertiary volcanic

and sedimentary suites are absent, and other areas where both groups overlie the pre-Tertiary basement. The presence of either an early or late Tertiary volcanic and sedimentary suite in an area indicates that the related paleosurface and related epithermal deposits may have been preserved. The absence of one or both of the Tertiary suites suggests that one or two major erosional episodes—one between the middle Oligocene and middle Miocene, and the other after the middle Miocene—may have affected the area. The abundant Quaternary units that filled structural basins indicate significant late Miocene and younger uplift and erosion of horsts adjacent to the basins. The original distribution of early Tertiary units largely is unknown in many areas, and their current absence does not necessarily mean that they were deposited and then eroded. In some areas, such as in central Nevada, ash-flow tuffs are widely preserved; elsewhere, such as in western Nevada near the California border, many tuffs were preserved only in paleochannels (Davis and others, 2000). Miocene eruptions generally were less explosive, but their eruptive centers were widespread, so units of this age were extensive; Miocene sediments, on the basis of modern exposures and depositional environments, also were widespread. Quaternary units occupy broad topographic depressions, including basins between modern mountain ranges, and they represent major depocenters related to late Cenozoic uplift and erosion.

Specific Areas Shown in Figure 9-8 Include:

- **Northwesternmost Nevada (Area A).** Middle Miocene volcanic rocks form an almost continuous blanket across this area, and any underlying older volcanic rocks are not exposed except along the southeastern margin. The widespread blanket of Miocene rocks and the relatively thin Quaternary deposits indicates minimal post-middle Miocene erosion. Accordingly, any middle Miocene epithermal deposits that formed in this area still should be present.

- **Northeastern Nevada (Area B).** Miocene volcanic and sedimentary rocks are widespread in this area. Early Tertiary volcanic rocks are exposed in the western part of the area, but their presence beneath Miocene rocks in the eastern part of area is unknown. The presence of both Tertiary suites and the relatively small amounts of Quaternary deposits indicate that this area has not undergone significant erosion in the Cenozoic. The exception is the Independence Mountains horst, which is flanked on all sides by Tertiary volcanic and sedimentary rocks. Field evidence shows that exposure of most pre-Tertiary rocks through the Tertiary paleosurface is shallow and thus does not represent deep erosion. Therefore, epithermal deposits of both ages are likely to be preserved in most of this area except in the basement-cored parts of the Independence Mountains.

- **Northern Nevada rift (Area C).** Miocene rocks in the northernmost part of this area rest on both early Tertiary volcanic rocks and the pre-Tertiary basement, indicating minimal middle Tertiary erosion. The Miocene rocks in the southern three-quarters of the rift rest directly on pre-Tertiary rocks despite the presence of early Tertiary volcanic units to the east and west, suggesting middle Tertiary removal of most earlier Tertiary units. John and others (2000b) and John and Wallace (2000) show post-middle Miocene northward tilting of the zone and progressively deeper erosion and exposure to the south. Thus, early Tertiary and Miocene epithermal deposits are more likely to be preserved to the north, and middle Miocene epithermal deposits in the south end of the zone would have formed at deeper levels or not at all, considering the shallow origin of epithermal deposits.

- **Central Nevada (Area D).** Eocene and Oligocene tuff units are preserved in this area, but Miocene units largely are absent. Either the Miocene units originally were limited in extent, or they were removed by post-middle Miocene uplift and erosion. The extensive Quaternary units indicate major basin subsidence and deposition of eroded materials. Thus, early Tertiary epithermal deposits (largely Oligocene in this area) likely were preserved along with the volcanic rocks, but any Miocene epithermal deposits may have been removed by erosion or buried beneath Quaternary units. Evidence in the Battle Mountain area shows that the middle Tertiary (~34 Ma) paleosurface extended only a few hundred meters above the ~38 Ma Battle Mountain plutonic center and surrounding Paleozoic rocks, showing that erosion into the older rocks was not significant (Theodore and Blake, 1975).

- **Northwestern Nevada (Area E).** Tertiary units of any age are limited in this area. Eocene volcanic rocks are not known in this area, although not all units have been dated. The only dated Oligocene igneous centers are the Kennedy stock (30.1 Ma; Thurber, 1982) and Majuba Hill intrusive complex (24-25 Ma; MacKenzie and Bookstrom, 1976), as well as local volcanic rocks of unknown derivation at Rosebud (~26 Ma; R. Vance and C. Henry, written commun., 2000). Pre-26 Ma volcanic rocks either may have had limited original extents or were largely removed by erosion; local post-volcanic erosion extended to shallow plutonic depths. Miocene sedimentary and volcanic units are sparse in comparison to surrounding areas. Quaternary deposits fill wide, deep basins throughout this area, indicating substantial late Cenozoic extension, uplift, and erosion. Thus, the limited Tertiary volcanic rocks and related paleosurfaces suggest that epithermal deposits in this area are either localized in known volcanic centers or represent the deeper parts of volcanic-related epithermal systems.

- **Western Nevada (Area F).** This area is part of the northwest-trending Walker Lane, which contains both strike-slip and high-angle normal faults. The strike-slip fault movement has caused significantly more lateral offset than in other areas in northern Nevada, and amounts and levels of exposure differ as a result. Extensively exposed middle Miocene volcanic rocks in this area overlie both Oligocene ash-flow tuffs erupted from outside the area and pre-Tertiary rocks. Thus, the middle Miocene paleosurface and epithermal environment was preserved in many parts of this area.

- **Eastern Nevada (Area G).** Tertiary units are sparse in this region, and pre-Tertiary basement and Quaternary deposits are the most common units. Most of the limited Tertiary rocks are early to middle Tertiary rhyolite and andesite flow units, and only scattered remnants of late Eocene to Oligocene ash-flow tuffs are preserved in this area. The extensive Quaternary basin fill and the basement-cored mountain ranges reflect substantial uplift and erosion during the Tertiary. Any epithermal deposits present would be related to the few preserved volcanic centers. Most exposed mineral deposits, however, likely formed in deeper, non-epithermal environments.

- **Alluvium-filled basins.** Tertiary volcanic rocks and related epithermal deposits are preserved beneath sediment-filled basins that separate the mountain ranges throughout northern Nevada. Pediments outboard from range fronts may be covered by thin to thick alluvial deposits. Gravity data show that the deepest parts of the basins in the HRB vary from less than a kilometer east of the Osgood Mountains to more than 6 km in Pine Valley southwest of Elko (chapter 6; Blakely and Jachens, 1991). The gravity data show that the basal morphologies of basins can be complex, with shallow to deep margins and concealed basement topographic highs and lows within the basin.

Updates to Specific Areas

Large-scale geologic mapping and new geochronology in several areas containing epithermal deposits indicate that the State geologic map (Stewart and Carlson, 1978) does not correctly represent the geology and ages of rocks in those areas. Some of these areas include:

Ivanhoe District

The State map shows that early and middle Tertiary units are the primary host rocks for the Ivanhoe Au-Hg deposits. New mapping shows that the host rocks in the district are middle Miocene in age, and that mineralization took place during rhyolite volcanism at about 15.1 Ma (Wallace, 2003).

Recently discovered veins also are present in Ordovician sedimentary rocks directly beneath the Miocene rocks; the veins also formed at about 15.1 Ma. The Hollister Au mine training site is shown to be in middle Tertiary tuffs (Tt_2). However, the actual host rocks are middle Miocene basaltic andesite flows (Tba) and tuffaceous sedimentary rocks (Tts), and ~15 Ma rhyolite porphyry flows (Tr_3) provided the heat that drove the hydrothermal system.

Goldbanks

The state map shows that pre-Tertiary rocks host the Au-Hg deposits, with nearby Miocene basaltic andesite flows (Tba). Recent work (Stone and others, 2000) demonstrates that the deposit is related to and in part hosted by middle Tertiary felsic and mafic volcanic rocks (Tts). New $^{40}Ar/^{39}Ar$ dating gives a 14.1–Ma age for mineralization (Connors and others, 1999).

Sleeper (Awakening District)

Quaternary alluvium concealed most of the Sleeper deposit before mining. A 16.3–Ma rhyolite contributed heat to the mineralizing system and is the host rock for the deposit (Conrad and McKee, 1996); this rhyolite which is part of the Tr_3 suite. Tertiary volcanic rocks exposed nearby (1–4 km) are shown as Tba, some of which are Miocene rhyolite (Tr_3; Nash and others, 1995). Thus, the most important mineralizing unit, when exposed by mining, was Tr_3, with both Tr_3 and Tba exposed in the vicinity of the deposit.

Poverty Peak/Dutch Flat Districts

Two volcanic units—Tba and Tr_3—are shown in the Poverty Peak district south of the Little Humboldt River. New data indicate that Tba in the Hot Springs Range could include mafic volcanic rocks ranging from a 22–Ma andesite that is older than the bimodal assemblage (Jones, 1997; Wallace and McKee, 1994) to ~15.8 Ma andesite flows (A. Wallace, unpubl. data, 2002). The unit shown as Tr_3 has been dated at 40 Ma and thus should be included in unit Tt_1 (A. Wallace, unpubl. data, 2000). The only Tertiary volcanic units that are related spatially to both the Poverty Peak and Dutch Flat districts are the early to middle Miocene andesites, and all epithermal occurrences are in Paleozoic sedimentary units (Jones, 1997).

Rosebud District

The host unit at Rosebud is shown as Miocene rhyolite (Tr_3). New age data indicate that part of the volcanic sequence is late Oligocene (~26 Ma) and that the ore deposit formed in the middle Miocene (~15 Ma; R. Vance and C. Henry, written commun., 2000). Middle Miocene volcanic rocks may be present in the host-rock sequence, but most volcanic rocks at Rosebud have not been dated.

Jessup District

As shown on the state map, host rocks at Jessup include Mesozoic metasedimentary rocks (JTRs), Mesozoic granite (Mzgr), and Miocene andesites (Ta_3). The county report (Willden and Speed, 1974) reports an association between the mineral deposits and small rhyolite intrusions that cut the other units; these rhyolites are not shown on the state geologic map. The Reno CUSMAP assessment (John and others, 1993) associated the deposit with the bimodal assemblage, which is supported by unpublished USGS data cited in John and others (1993).

Jackson District

Most deposits in the Jackson district are base-metal-rich veins in Permian volcaniclastic rocks. Many veins parallel Tertiary rhyolite dikes of unknown age that cut middle Tertiary tuffs elsewhere in the district (Kleinhampl and Ziony, 1984). Thus, the Jackson district contains a small intrusive center unrelated to the ash-flow tuffs and not shown on the state map.

Ten Mile District

The Ten Mile district contains a variety of mineral deposit types, including low-sulfide Au–quartz veins, polymetallic veins, and epithermal veins (Nash, 1972; Peters and others, 1996; A. Wallace, unpub. data, 2000). The epithermal deposits are in Mesozoic plutonic and metasedimentary rocks, and they contain abundant quartz-adularia gangue. Small rhyolite dikes (unit Ti) that are not shown on the county map (Willden, 1964) are closely associated with the veins (A. Wallace, unpub. data, 2000) and may have been responsible for mineralization.

Results of Mineral Resource Assessment

The following assessment for epithermal deposits in northern Nevada and the HRB combines the empirical data described in previous sections with data-driven modeling methods.

Data-Driven Assessment Model

Methods

The favorable and prospective tracts for epithermal deposits in the HRB were created using data-driven modeling techniques (see chapter 2). As described in chapter 2, the per-

missive and nonpermissive areas used in this assessment were defined by Cox and others (1996) using expert knowledge. Expert knowledge also was used to create, modify, and select the evidence maps for the data-driven weights of evidence (WofE) analysis and weighted logistic regression (WLR) modeling. WofE analysis was used to analyze the spatial associations among the training sites and evidence maps and to optimize the evidence maps for prediction. WLR modeling was used to combine the optimized evidence maps and to delineate prospective and favorable tracts within the expert-delineated permissive tract. The evidence map criteria used for prediction was determined by data-driven means (see also chapter 2).

The prospective and favorable tracts were modeled using three evidence maps (geochemistry, lithology, and magnetic terranes; figs. 9–10-12; table 9-4), a unit cell size of 1 km^2, and a significance level of 1.282 (90 percent confidence, tabled Student–t value). The evidence map criteria used for prediction were determined by data-driven means (see also chapter 2). The lithology and magnetic terranes are described briefly below, with additional information elsewhere in this chapter. The geochemical data are described briefly in chapter 5, and the relation between As geochemistry and epithermal deposits is discussed elsewhere in this chapter.

Discussion of Data-Driven Results

Arsenic geochemistry (anomalies) and lithology, followed by magnetic terranes, are the strongest predictors for epithermal deposits. The geochemical and, in a more limited geographic area, magnetic terrane maps include areas that are likely to host epithermal occurrences and deposits. The permissive-Jungo predictor pattern of the epithermal lithology evidence map (unit 3) also is a predictor layer in areas of pre-Tertiary exposure. These predictor patterns, particularly As-frequency, are characterized by narrowly-defined predictor patterns with W$^+$ magnitudes that are significantly larger than W$^-$. On the other hand, the permissive-medium and prospective-high predictor patterns (units 2 and 1, respectively; table 9-3) of the epithermal lithology evidence map provide approximately equal amounts of inclusive and exclusive evidence (fig. 9-11).

In the expert-ranked epithermal-lithologic units evidence map (chapter 2; table 9-3), epithermal units 1 and 2 (permissive-high and -medium, respectively), due to their spatial and, in places, genetic relation to mineralizing systems, were given a higher "expert" rank than the Jungo terrane (epithermal unit 3). The WofE analysis, however, ranks the Jungo terrane rocks higher than both units because the terrane has a substantially higher density of training sites than the other two units. It should be noted that seven of the ten training sites that are in Jungo terrane rocks are in the small Willard district. If the Willard district were represented by only one training site, which would be more reasonable given its very small size, then the Jungo terrane would have only four training sites and a lower predictive rank than both epithermal units 1 and 2 (see later discussion under "Northwestern Nevada").

In the data-driven modeling, the magnetic terranes map (fig. 9-12) was trained with the full epithermal training set to identify favorable and prospective areas. Some deposits along the aeromagnetic anomalies are related genetically to the middle Miocene mafic rocks that produced the anomalies; these include Buckhorn, Fire Creek, Mule Canyon, and Rock Creek. Other deposits along the anomalies, such as Sleeper, Midas, and possibly Goldbanks, are similar in age to the mafic rocks along the anomalies, but they are genetically related to rhyolite domes and flows of the cogenetic bimodal assemblage. Other deposits along the anomalies are late Miocene to Quaternary in age and are not genetically related to the mafic rocks that produced the anomalies; these include Relief Canyon, Dixie Comstock, and possibly Florida Canyon. Therefore, the favorable and prospective tracts that were defined in part by the aeromagnetic evidence map are most applicable to epithermal deposits related to the mafic rocks that produced the aeromagnetic anomalies.

The data-driven epithermal deposit favorability map delineates prospective and favorable tracts and is shown in figure 9-13. The tracts are derived from the WLR model favorabilities and are based on break-points in the cumulative assessment area curve (fig. 9-14). The prior favorability was used to delineate the permissive–favorable rank boundary. The most prominent break-point in the curve above the prior favorability was used to delineated the favorable–prospective rank boundary (see orange dotted line on fig. 9-14).

The epithermal mineral-resource assessment map combines the data-driven favorable-prospective favorability map with the expert-delineated permissive tract of Cox and others (1996), and areas with unconsolidated basin fill greater than 1 km are masked out (fig. 9-15; see fig. 9-9 and chapter 2). The area of each assessment tract and the number of training sites in each tract are given in table 9-5, and the rank of each training site is given in table 9-1. The most prominent prospective and favorable areas within the HRB, as defined by the data-driven methods, are in the northeastern, north-central, and northwestern parts of the HRB. Prospective and favorable areas also are present in the southwestern and southern parts of the basin near the northeastern edge of the Walker Lane, which may have been an important structural control on the formation and regional-scale distribution of epithermal ore deposits in western and southwestern Nevada (Cox and others, 1991, Ludington and others, 1993).

Discussion of Mineral Potential of Subregions

Epithermal mineral deposits in northern Nevada and the Humboldt River Basin are related to three Tertiary volcanic assemblages (bimodal, western andesite, and interior andesite-rhyolite), and the deposits formed in specific volcanic environments described above. Tertiary and Quaternary uplift and erosion have variably preserved, destroyed, exposed, and concealed the volcanic rocks and related epithermal deposits. The following sections describe the potential for undiscovered epithermal deposits in six subregions of northern Nevada,

shown in figure 9-15 as subregions A-G, five of which include parts of the HRB.

Northwesternmost Nevada (Subregion A)

This subregion is entirely outside of the HRB, but it contains mineralizing environments similar to those found within the Basin. Miocene basalt flows, rhyolite flows and domes, and tuffaceous sedimentary rocks directly underlie most of this subregion, and Oligocene volcanic rocks are exposed along the eastern margin. Although abundant high-angle normal faults cut the volcanic rocks, dissection and differential uplift have not been sufficient to expose rocks older than middle Miocene. As a result, the presence, depth, and type of pre-Miocene rocks and epithermal deposits beneath the Miocene volcanic rocks in this area is unknown.

Exposed middle Tertiary volcanic rocks include Oligocene andesite and rhyolite flows and tuffs (Bonham, 1969; Noble and others, 1970). The only known mineralized area in these volcanic rocks consists ~ 3 km^2 of altered volcanic rocks, which contain pre-Miocene Pb–Ag–Zn veins of the Leadville deposit near the Hog Ranch training site (Bonham, 1969). The veins probably are related to Oligocene magmatism and may not be epithermal (Peters and others, 1996), but relatively little is known about the volcanic rocks or the deposit. Because of exposure, the presence of similar Oligocene mineralizing systems in the rest of the subregion is unknown.

Extensive Miocene volcanic units in this subregion include ~17–15-Ma mafic volcanic flows; ~16.5–14-Ma rhyolite tuffs, flows, and domes and tuffaceous sedimentary rocks; and <10-Ma basalt flows. The older mafic rocks are part of a widespread suite of rocks that elsewhere in northern Nevada contain coeval epithermal deposits (for example, Mule Canyon, Buckhorn). This suite therefore is prospective for epithermal deposits. This subregion has several small As anomalies in Miocene volcanic rocks (fig. 9-10), and these areas are shown as prospective on the data-driven favorability map (fig. 9-13). The known epithermal Au deposits in the subregion are associated with the rhyolite units, which are prospective for epithermal deposits, and related sedimentary rocks, which are favorable for epithermal deposits in proximity to the rhyolites. The Hog Ranch Au deposits (Bussey, 1996) are the only significant deposits of this type in the subregion, but similar volcanic environments, some with As anomalies, are present throughout the rhyolite terrane. The Mountain View deposit in the Deephole district, which underlies Quaternary sediments, is in a rhyolite flow-dome complex that overlies middle Miocene basalts (Margolis and Marlowe, 1996). Caldera-related hot-spring Hg and U deposits, such as in the Virgin Valley and McDermitt districts, formed in Miocene rhyolites and sedimentary rocks related to several caldera complexes (Castor and Henry, 2000; Rytuba and Glanzman, 1979). Rhyolite-hosted Au anomalies related to these complexes have been identified north of the HRB in the Double H Mountains near the Nevada-Oregon border (Platoro West Inc., press release, 2001). These anomalies occur in areas shown as prospective on figure 9-15.

Northeastern Nevada (Subregion B)

Both Eocene and middle Miocene volcanic rocks are exposed in this subregion. Important volcanic centers include the late Eocene Tuscarora and Emigrant Pass volcanic fields and the middle Miocene Jarbidge Rhyolite. Extensive areas are underlain by middle Miocene sedimentary rocks, which overlie middle Miocene and Eocene volcanic rocks and pre-Tertiary units. Late Tertiary uplift exposed pre-Tertiary rocks in several mountain ranges, but the relatively small amount of Quaternary alluvium indicates that the accompanying basins are small and shallow. Only one As anomaly is present in this subregion (fig. 9-10), and it most likely is related to sedimentary rock-hosted mineralization in the northern Independence Range (chapter 8).

The distribution of known epithermal deposits indicates that the Tuscarora and Jarbidge volcanic centers are prospective for these types of deposits. The Tuscarora epithermal deposits are related to the late Eocene volcanic center in that area, which includes at least one caldera and several other eruptive centers (Henry and others, 1998). The volcanic field also hosts several other smaller mineral occurrences, primarily vein deposits. The Jarbidge district is related to rhyolite domes and flows of the middle Miocene Jarbidge Rhyolite, and the rhyolite-hosted Au–Ag veins in the district are about the same age as the volcanic activity (LaPointe and others, 1991). The Doby George and Wood Gulch deposits at the north end of the Independence Mountains are epithermal deposits in and adjacent to late Eocene dacite volcanics of unknown source. The Trout Creek epithermal resource is near middle Miocene rhyolite flows, but little is known about that prospect beyond resource data released by industry. Epithermal deposits are not known to be present in the Emigrant Pass volcanic field (Henry and Faulds, 1999), which includes a series of intermediate-composition flows.

The extensive cover of Miocene sedimentary rocks may conceal late Eocene and middle Miocene epithermal deposits in many parts of this subregion. However, the thickness of many of these sedimentary units is unknown. Relatively few Eocene volcanic rocks have been identified in the eastern part of this subregion, and they include both distally derived tuffs and locally derived andesitic flow units (Brooks and others, 1995). Small windows of middle Miocene rhyolite flows are exposed through the Miocene sedimentary cover, and those and adjacent areas are prospective for epithermal deposits, such as at the Trout Creek prospect.

Extensive 13– to 9–Ma volcanic rocks of unknown thickness conceal all older rock units in the northwestern part of the subregion. All known mineralizing events in the region are older than these rocks, and any mineralized zones that may be present in older rocks are concealed.

Northern Nevada Rift (Subregion C)

This subregion contains primarily middle Miocene volcanic rocks, and minor Eocene units are exposed beneath

the Miocene rocks in the northern half of the subregion. On the basis of present exposures, most of the Miocene units were erupted onto pre-Tertiary rocks. This indicates either nondeposition of Eocene and Oligocene volcanic rocks in those areas or middle Tertiary erosion of some or all of the volcanic rocks. Deep-sourced middle Miocene mafic intrusive rocks form a pronounced aeromagnetic anomaly (the northern Nevada rift) that reflects a relatively narrow feeder zone for surface flows. Middle Miocene, synvolcanic extension created abundant north-northwest-striking high-angle faults that influenced volcanism, clastic sedimentation, and epithermal mineralization. Late Miocene to Quaternary northwest-directed extension segmented the subregion into east-northeast-trending horsts and grabens. Also, post-volcanic northward tilting of the subregion exposed progressively deeper levels from north to south.

The subregion contains several significant epithermal Au-Ag-Hg deposits, including those at Buckskin-National, Midas, Ivanhoe, Rock Creek, Mule Canyon, Fire Creek, and Buckhorn. Buckskin-National, Midas, and Ivanhoe are related to 15– to 16–Ma rhyolite flows and domes; Mule Canyon, Rock Creek, Fire Creek, and Buckhorn are related to 15– to 16–Ma basaltic andesite activity of the northern Nevada rift. Numerous prospects related to both volcanic environments have been identified and drilled throughout the subregion. Arsenic anomalies are sparse in this subregion. The largest is in Paleozoic sedimentary rocks west of the Buckhorn district, and it may be related to mineralization at or near the Horse Canyon sedimentary rock-hosted deposit (chapter 8).

The southern half of the subregion is prospective for epithermal deposits related to basaltic andesite volcanism. Where preserved, the mafic flows may host the deposits, such as at Mule Canyon and Buckhorn. In areas to the south where uplift and erosion removed the flows, deeper-formed epithermal deposits may be near and related to exposed feeder dikes. The absence of early and middle Tertiary volcanic and intrusive rocks indicates that the Eocene-Oligocene paleosurface has been removed and that igneous centers of that age did not form in this area.

The northern half of the subregion is prospective for middle Miocene epithermal deposits related to both basaltic andesite volcanism and rhyolite flows and domes. The known deposits are related to rhyolites, but mafic rocks related to the rift are present throughout this area. Based on the 15– to 15.5–Ma ages of known mineralization for both types, and on extensive, slightly younger (15– 13–Ma) unmineralized rhyolite flows and tuffs, mineralized areas may be concealed in some areas. The Eocene rocks that are exposed in this area are welded tuffs; some tuffs were derived from the Tuscarora volcanic field, and others have no known source. One small aeromagnetic anomaly north of the Osgood Mountains coincides with tuff of possible Eocene age that is exposed in windows through Miocene units, but it is not known if the anomaly also represents a concealed igneous center. Therefore, this subregion has an unknown probability of containing Eocene epithermal deposits.

Central Nevada (Subregion D)

This subregion contains widespread early to middle Tertiary (largely Oligocene) volcanic rocks of the interior andesite-rhyolite assemblage that overlie pre-Tertiary basement rocks. The area has many known or inferred Oligocene calderas and igneous centers that produced extensive ash-flow tuff units (Ludington and others, 1996). The Miocene paleosurface, as well as Miocene volcanic and sedimentary rocks, is poorly preserved in this area. Late Cenozoic faulting created numerous horsts and grabens, and Quaternary basin-filling sediments are abundant. Some ranges have nearly continuous exposures of Oligocene volcanic rocks, and others have little or no Tertiary cover above the pre-Tertiary rocks. This in part may be due to preferential preservation of tuffs in paleovalleys, as described by Davis and others (2000). Thus, any epithermal mineral deposits exposed in the mountain ranges likely are older than Miocene, and Quaternary sediments possibly conceal mineralizing centers.

The Reese River subbasin of the HRB bisects this subregion, and all but one of the significant epithermal deposits are outside of the basin. However, the regional geologic setting suggests that similar mineralizing environments may be present within the HRB. The principal epithermal deposits in this southern part of the study area include Round Mountain, Manhattan, and Wonder. Host rocks for most of the deposits are welded tuffs, andesite flows, and local breccias and intrusions, and the deposits principally are fault-controlled veins, stockworks, and disseminations along caldera margins. Detailed studies of some districts identify felsic intrusive bodies that are too small to show on the state map, and some of these small plutons and dikes may have been responsible for local mineralization. Many of these small intrusive bodies are included in welded tuff unit (Tt_2) on the state geologic map (Stewart and Carlson, 1978). At the scale of this assessment, all middle Tertiary felsic volcanic and intrusive rocks are prospective for epithermal deposits. Underlying Tertiary andesites are favorable hosts for deposits, but only in proximity to felsic igneous centers. The Manhattan epithermal deposits are in Cambrian quartzites, but most other mineral deposits in pre-Tertiary rocks, such as the pluton-related deposits of the Battle Mountain area, largely formed at subvolcanic and deeper levels.

Northwestern Nevada (Subregion E)

Fault-bounded mountain ranges separated by wide basins filled with Quaternary sediments typify this subregion. As described earlier, relatively minor early Tertiary (Eocene and Oligocene) volcanic rocks have been identified in the ranges, although relatively few isotopic dates on volcanic rocks in this subregion are available. Most early Tertiary igneous rocks are subvolcanic or somewhat more deeply emplaced plutons, such as the Kennedy and Majuba Hill intrusive systems. For the most part, the early Tertiary paleosurface, volcanic rocks, and epithermal environments, if present, are not readily apparent in this subregion. This subregion contains few As anomalies

(fig. 9-10). Only one of these anomalies, near Goldbanks, has a clear connection with epithermal mineralization, and the remainder are in pre-Tertiary rocks and may be related to other mineralizing environments.

Miocene rocks include rhyolite flows and tuffs, basaltic andesite flows and mafic dikes of the rift environment, and tuffaceous sedimentary rocks. Where these units are preserved, they directly overlie the pre-Tertiary basement. Most of these rocks are exposed in a north-trending belt that includes the Kamma Mountains, the Seven Troughs Range, and the central and southern parts of the Trinity Range. Isolated occurrences of Miocene rocks are present in most, but not all, of the other ranges in the subregion.

Most of the known epithermal deposits are associated with middle Miocene rhyolitic volcanic and shallow intrusive rocks and nearby tuffaceous sedimentary rocks. These deposits include Sleeper, Adelaide, Seven Troughs, and Jessup, as well as prospects and small quartz-adularia-Au veins throughout the area. Thus, Miocene rhyolitic flows and tuffs are prospective for epithermal deposits. Small rhyolitic bodies that are too small to show on the state geologic map (Stewart and Carlson, 1978) in places were included in tuffaceous units, and the tuffaceous rocks, although not genetically related to the volcanic systems, served as host rocks at a number of districts. These units are permissive to favorable for epithermal deposits.

The two north-trending, bifurcating aeromagnetic anomalies (Northern Nevada Rift West (NNRW) of chapter 6) associated with deep-seated mafic intrusive rocks and scattered dikes are analogous to the northern Nevada rift, which has several epithermal deposits associated with mafic volcanic rocks (see chapter 6; also, John and others, 2000; John and Wallace, 2000). Several epithermal deposits hosted by pre-Tertiary rocks are along or near these mafic zones, including Ten Mile, Florida Canyon, Standard, and Relief Canyon. Ten Mile has been dated at 16.7 Ma, similar to the regional age of mafic igneous activity, and basaltic andesite flows are present in the district. The ages of Florida Canyon, Standard, and Relief Canyon are unknown, although indirect evidence suggests that parts or all of both deposits could be late Miocene in age and related to late Cenozoic high heat flow (Wallace, 1989; Thomason, 2002; Larson, 2002; see ensuing section on "Deposits of uncertain origin"). The 14.1–Ma Goldbanks Au-Hg deposits are along the eastern of the two mafic zones, and host rocks include Miocene and pre-Tertiary rocks. The deposits are younger than the associated mafic volcanic rocks and thus are spatially, but not genetically, related to the mafic rocks. Ponce and Glen (2002) identified another magnetic anomaly west of these two anomalies. On the basis of the analogous northern Nevada rift and the association of several epithermal deposits in this subregion, the north-trending zones of mafic rocks are favorable for epithermal deposits, and associated tuffaceous units are permissive for these deposits.

Ponce and Glen (2002) identified another magnetic anomaly west of the two bifurcating anomalies and suggested that deep-seated mafic intrusive rocks produced the anomaly, similar to the other magnetic anomalies. Several rhyolite-related epithermal deposits (Hycroft, Rosebud, Seven Troughs, Velvet, and Jessup) are along this anomaly. Although the rhyolite volcanism and related mineralization are somewhat younger than the mafic activity, Ponce and Glen (2002) proposed that the deep structure that controlled the mafic intrusive activity also might have localized later hydrothermal fluids.

Mesozoic sedimentary rocks of the Jungo terrane (JTRs) host a disproportionately large number of small- to medium-size epithermal deposits in this subregion. Rocks of this terrane host roughly 90 percent of the training sites and MRDS deposits in pre-Tertiary rocks in this subregion. Larger deposits in rocks of the Jungo terrane include Willard, Wind Mountain (in part), and Florida Canyon; small deposits are in the Antelope Springs, Rose Creek, Awakening, and Ten Mile districts. Most Jungo-hosted deposits are along or adjacent to the aeromagnetic anomalies and related Miocene mafic dikes, and epithermal deposits are sparse in the Jungo terrane away from the aeromagnetic anomalies. The data-driven model reflects this correlation between lithology, magnetic anomaly, and epithermal mineral deposits (fig. 9-13). As noted in the section on level of exposure, this subregion has undergone significant uplift and erosion since the middle Miocene. The deposits along the anomalies may be analogous to the southern end of the northern Nevada rift, where differential uplift has exposed deeper magmatic and epithermal environments. Thus, Miocene magmatism that formed the dikes and aeromagnetic anomalies likely mineralized the Jungo terrane rocks in some areas, and uplift has exposed these more deeply formed deposits. In relative comparison to other pre-Tertiary lithologic packages, sedimentary rocks of the Jungo terrane are favorable hosts for epithermal mineral deposits, especially near known or inferred igneous centers.

Western Nevada (Subregion F)

Volcanic rocks as mapped in this subregion include Miocene andesite and dacite flows, breccias, tuffs, and intrusive rocks of the western andesite assemblage that formed in stratovolcanoes and domes that covered much of the area. These units overlie and intrude discontinuous Oligocene ash-flow tuff units, which were erupted from other subregions and preserved in paleovalleys (Davis and others, 2000), and various pre-Tertiary sedimentary and igneous rocks. Mafic lava flows of the bimodal assemblage locally overlie the andesitic volcanic rocks, primarily in the northeastern part of the subregion. The area is part of the northwest-trending Walker Lane, which is composed of abundant strike-slip and normal faults, and both early Tertiary and Miocene paleosurfaces largely have been preserved. Quaternary sediments fill small to extensive basins that formed during late Cenozoic faulting.

This subregion is almost entirely outside of the HRB. The types of mineralizing environments that are prospective in this subregion, such as high-sulfidation epithermal systems (as defined in Hedenquist and others, 2000), generally are not found in the HRB. Also, most of this area is outside of the NURE geochemical data coverage used for this assessment (chapters 2, 5) and is not included in the data-driven model. Most of the known epithermal mineral deposits in this subre-

gion formed in Miocene stratovolcano environments along or in proximity to coeval high-angle faults. Significant deposits of this type include those in the Comstock Lode, Como, Ramsey, and Talapoosa districts, where host rocks include andesite and dacite and, locally, underlying tuff and pre-Tertiary units near andesitic volcanic centers (John and others, 1999). As a result, Miocene andesitic volcanic rocks in this subregion are prospective for epithermal mineral deposits. The Rawhide deposits are an exception, as they are associated with rhyolites and sedimentary rocks. The basaltic andesite environment may be prospective for epithermal deposits, as it is throughout much of northern Nevada, but no deposits are known to be related to this volcanic suite in this subregion. The Olinghouse Au-Ag deposits are in basaltic andesite flows, but they are related to dacite dikes of the western andesite assemblage.

Eastern Nevada (Subregion G)

Most of this subregion is outside of the HRB and the area of NURE geochemical coverage (chapters 2, 5). Tertiary volcanic rocks are extremely sparse in eastern Nevada, and pre-Tertiary rocks are the only exposed rocks in most mountain ranges. Thick Quaternary alluvial deposits fill the numerous intermontane basins, indicating substantial uplift. The few Tertiary units here include early Tertiary ash-flow tuff and rhyolite; Miocene rocks are mostly sedimentary with a few rhyolitic units. Epithermal deposits are notably absent, and only four prospects are described (briefly and perhaps erroneously) in MRDS records as being epithermal in origin. Overall, this subregion is not favorable for Tertiary epithermal deposits. However, to be consistent with the data-driven assessment of the rest of northern Nevada, early Tertiary ash-flow tuff is shown to be prospective for epithermal deposits, and coeval andesite is shown to be favorable. Similarly, Miocene rhyolite is shown as prospective and tuffaceous rock as favorable.

Deposits Related to High Regional Heat Flow

Much of northern Nevada, including the HRB, has a high geothermal gradient or heat flow (fig. 9-7; Lachenbruch and Sass, 1978). This heat flow has produced hot springs and geothermal areas throughout the region (Shevenell and others, 2000; Garside and Schilling, 1979), similar to the environment at the tops of older epithermal deposits. This heat flow anomaly has been present for several million years, and hot springs related to it have formed small to large epithermal deposits at Hycroft/Sulphur, Warm Springs, Golconda, Dixie Comstock, and the younger parts of Florida Canyon. These deposits are along late Miocene to Quaternary range-front faults that are widespread throughout much of the study area (Dohrenwend and others, 1996). These deposits can be present in rocks of any age, and no unit shown on the State geologic map (Stewart and Carlson, 1978) represents the high heat-flow environment. However, many deposits and geothermal areas are in Quaternary or late Tertiary sedimentary units or at the fault contact

between these and older units (Shevenell and others, 2000), reflecting the young age and shallow level of mineralization. Favorable areas for young hot-spring deposits include areas where late Miocene and younger faults (Dohrenwend and others, 1996) and high heat flow are coincident. This includes a substantial part of northern Nevada.

Concealed Deposits

Post-mineralization sedimentary and volcanic rocks can cover and conceal epithermal mineral deposits. Also, some young volcanic rocks in places cover placer Au deposits derived from the epithermal deposits. Quaternary and Pliocene alluvial deposits were deposited above older rocks in the many basins in northern Nevada as adjacent mountains were eroded. These deposits can range from thin veneers on mountain-front pediments to thick, basin-filling deposits, such as in Pine Valley southwest of Elko, where they are >6 km thick. Thin alluvial deposits can conceal mineral deposits, as shown at Sleeper and at several sedimentary rock-hosted Au-Ag deposits (Lone Tree, Marigold, Twin Creeks, Pipeline, Turquoise Ridge), and epithermal deposits undoubtedly are present beneath the extensive alluvium-filled basins in the region. Also, post-mineralization volcanic and sedimentary rocks can conceal prospective areas, such as in the Snowstorm Mountains and northern Shoshone Range, where extensive volcanic flows blanket most of the prospective 15– to 16–Ma volcanic rocks (Wallace, 1991, 1993; John and others, 2000a). However, once a concealed deposit is discovered, the thickness of the cover units and the cost of removing or mining through that unmineralized material influences the decision to mine the deposit.

This regional assessment is based heavily on specific types of volcanic systems and volcanic units. Due to the nature of their formation and to subsequent faulting and erosion, these units are not predictably continuous in any direction, as is clearly evident in areas where they are exposed. Thus, the projection of any particular volcanic unit or suite beneath extensive younger units is even more unpredictable. For this assessment, favorable host units were not extrapolated beneath younger units due to the lack of information at the working scale of this study, and the mineral-resource assessment maps (figs. 9-13, 16) therefore do not reflect favorable or prospective host rocks beneath Quaternary cover. However, site-specific exploration, such as that at Sleeper and other epithermal deposits, could identify areas where favorable volcanic rocks, and perhaps epithermal deposits, are present beneath thin cover units. As a result, all basins where the Quaternary cover is less than 1 km thick are permissive for epithermal mineral deposits (fig. 9-15; Cox and others, 1996).

Deposits of Uncertain Origin

Several deposits and districts in northern Nevada have characteristics of epithermal deposits, but their ages and origins are ambiguous or unknown. These include the deposits

in the Poverty Peak and Dutch Flat districts, and the Willard, Relief Canyon, Standard, and Florida Canyon Au-Ag deposits in the Humboldt and West Humboldt Ranges. Pre-Tertiary sedimentary rocks host all of these deposits, and nearby or temporally related volcanic rocks are either absent or too distant to be realistic heat sources. These deposits provide evidence that not all epithermal mineral deposits fit neatly into general models of regional ore formation, and that all pre-Tertiary rocks permissively may host epithermal deposits, regardless of the apparent presence or absence of related volcanic systems.

Adularia from the Willard district was dated by K-Ar methods at 6.1±0.3 Ma (Noble and others, 1987), and geologic relations at Relief Canyon suggest an equal if not younger age of formation (Wallace, 1989). The Standard deposit, based on very limited evidence, was included in the assessment of sedimentary rock-hosted Au-Ag deposits (see chapter 8). However, work published after this assessment was completed indicates that the Standard deposit formed during the late Miocene to Pliocene, similar to Relief Canyon (Larson, 2002). As such, Willard, Relief Canyon, and Standard are younger than the main middle Miocene pulse of the bimodal assemblage, but older than or perhaps the earliest-formed of the deposits related to high regional heat flow. The age of mineralization at Florida Canyon is unknown. Field observations by USGS, university, and industry geologists suggest that as many as four episodes of mineralization took place at this location, ranging from Late Cretaceous low-sulfide Au-quartz vein formation at the 1800s Florida Canyon mine to modern geothermal mineralization at and near the modern open-pit mine. Most geologists feel that the gold deposit being mined formed in a late Cenozoic, likely late Miocene and younger, epithermal environment (Pruess, 1998; Hastings and others, 1988; Thomason, 2002).

As noted earlier, the only volcanic rocks near the epithermal Poverty Peak and Dutch Flat Hg districts are 22 Ma andesites (Jones, 1997), which, by analogy with the Rosebud district, may be spatially coincidental but not genetically related. The mineralogies and textures of these deposits are similar to those formed under deep epithermal conditions (A. Wallace, unpub. data, 2000), and they may have formed in environments such as those along the western magnetic anomalies and the southern part of the northern Nevada rift. Alternatively, the cinnabar-stibnite veins at Poverty Peak also are similar to those that form in the distal and somewhat cooler parts of low-sulfide Au-quartz vein systems (Goldfarb and others, 1998; see chapter 7). The Hg-bearing epithermal deposits at Dutch Flat are adjacent to a Cretaceous intrusive and skarn system, but the relation, if any, between the two types of systems is unknown (Willden, 1964). Little additional information is available on these deposits.

Comparison to Other Assessments

The region covered by this assessment (fig. 9-15) includes areas that were evaluated during two regional

assessments for epithermal deposits: the Winnemucca-Surprise (Peters and others, 1996) and Nevada (Singer, 1996) assessments. The Winnemucca-Surprise study focused on the northwestern part of Nevada and a small part of northeastern California, and the resulting assessment map is shown in figure 9-16. The Nevada assessment covered the entire state; the northern part of that study area is shown in figure 9-9.

As discussed in chapter 2, the assessment methodologies and the terms used to define areas that may contain undiscovered mineral resources differ somewhat among the Nevada, Winnemucca-Surprise, and the present assessments. All three assessments used volcanic assemblages and the locations of known epithermal deposits as the key determining factors. Both this and the Winnemucca-Surprise assessments support the general result of the Nevada assessment (Cox and others, 1996): virtually all exposed bedrock and Quaternary deposits permissively host epithermal deposits. As a result, the conclusions of the three assessments are similar in their areas of overlap. The shapes and sizes of the favorable and prospective areas differ in detail, however, largely due to the different assessment methodologies. For example, the boundaries of prospective areas in the Winnemucca-Surprise assessment were adjusted to eliminate areas that were known to not contain deposits or evidence of mineralizing processes, or to include areas that did contain these features. In the present assessment, the consistent use of criteria across the entire study area, such as a particular volcanic lithology, likely caused unmineralized areas to be included in the favorable or prospective regions.

Summary of Epithermal Mineral Assessment

This assessment for undiscovered epithermal mineral deposits in the HRB builds upon the permissive tracts defined in the Nevada assessment (Cox and others, 1996). It defines areas within those permissive tracts that, based upon the criteria used in this assessment (volcanic systems, As geochemistry, and magnetic terranes), may be relatively more favorable or prospective for epithermal deposits. The assessment is based on the close genetic relationship between Cenozoic igneous (largely volcanic) systems and epithermal deposits. Heat provided by these igneous systems produced convective hydrothermal systems that, in some places, formed epithermal Au-Ag mineral deposits. Some deposits formed in or close to the related volcanic system, and others, such as those related to young high heat flow, formed in nonvolcanic environments. In general, most of the western and central parts of the HRB are at least permissive for having undiscovered epithermal deposits, as previously described in the Nevada assessment (Cox and others, 1996). Favorable and prospective areas shown on the final assessment maps (figs. 9-13, 9-15), as defined by both expert-based and data-driven methods, are aligned closely with specific volcanic and subvolcanic igneous environments.

Post-mineralization volcanic and sedimentary units cover a considerable part of northern Nevada. Many of these units are sediments that fill deep inter-montane basins, but post-mineralization cover in other areas is not as thick. Current exploration and economic constraints lower the potential for undiscovered deposits in many of these covered areas. However, changes in metal prices and exploration and mining methods may make these areas more attractive targets in the future.

This assessment considered epithermal deposits of all Cenozoic ages and related volcanic environments, and it therefore represents a general overview assessment of the region. Some features that are specific to one age or igneous system, such as the aeromagnetic anomalies related to middle Miocene mafic dikes or volcanic units related to early to middle Tertiary caldera eruptions, were evaluated with the data-driven methods for the entire study area and training set. In part, this led to data-driven results that, in places, may under- or overestimate the relative favorability of a specific area. However, on the basis of empirical data and criteria used for the assessment, all areas shown as favorable or prospective are more likely to contain epithermal deposits than areas shown as permissive. A more detailed assessment of epithermal deposits related to each of the three volcanic systems and the young high heat-flow environment would be possible with additional data on the ages of mineralization and volcanism in a number of districts. Evaluations of specific areas within the HRB, such as a mountain range or mining district, would require more focused assessments that utilized commensurately more detailed data than were used for this assessment.
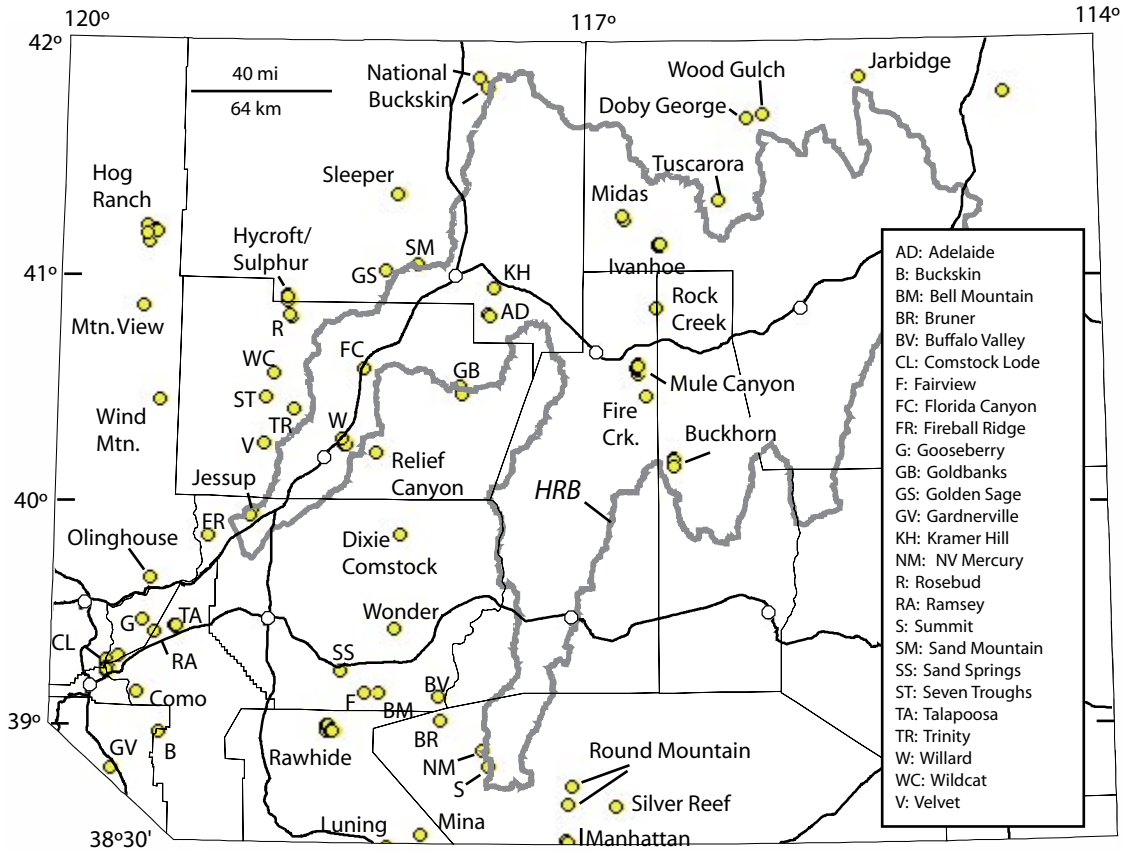
Figure 9-1.   Map showing locations of epithermal training sites in northern Nevada. Some named areas have more than one training site. Buckskin (B) and Gardnerville (GV) are Mesozoic and not thus related to Tertiary epithermal assessment (see text for discussion). Humboldt River Basin (HRB) shown by heavy gray line. County boundaries (light lines), highways (dark lines), town locations (open circles) as in figure 1-1.
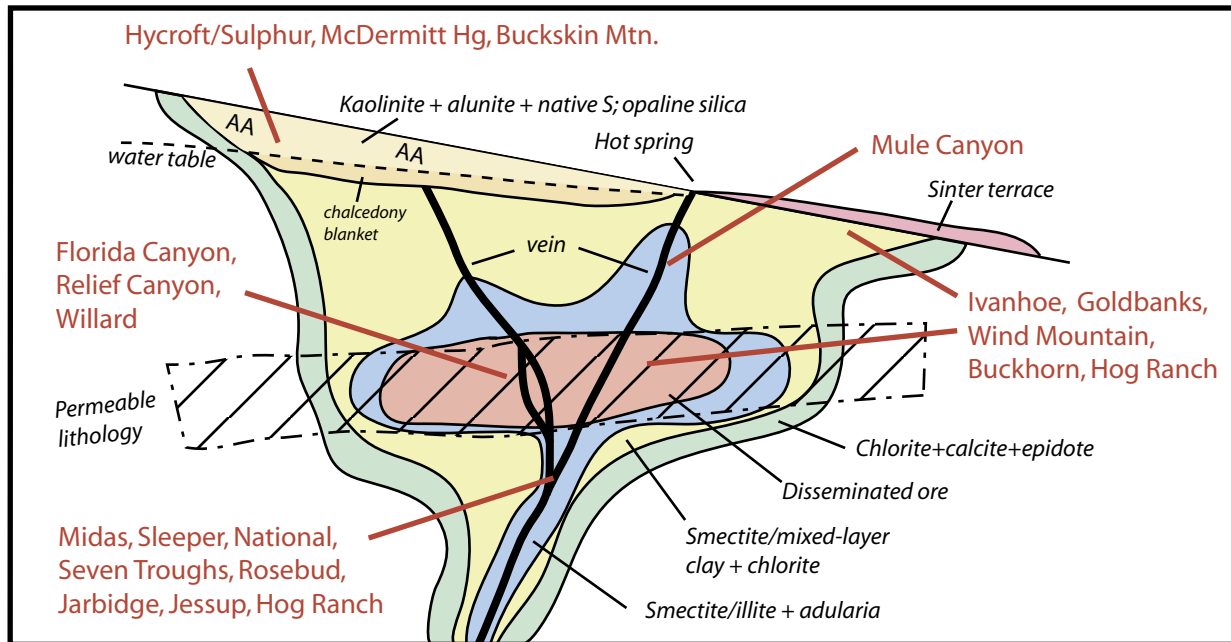
Figure 9-2. Schematic cross-section of low-sulfidation epithermal mineral deposits, showing general depositional environment of representative epithermal deposits in northern Nevada. Cross-section from Hedenquist and others (2000). AA, advanced argillic alteration.
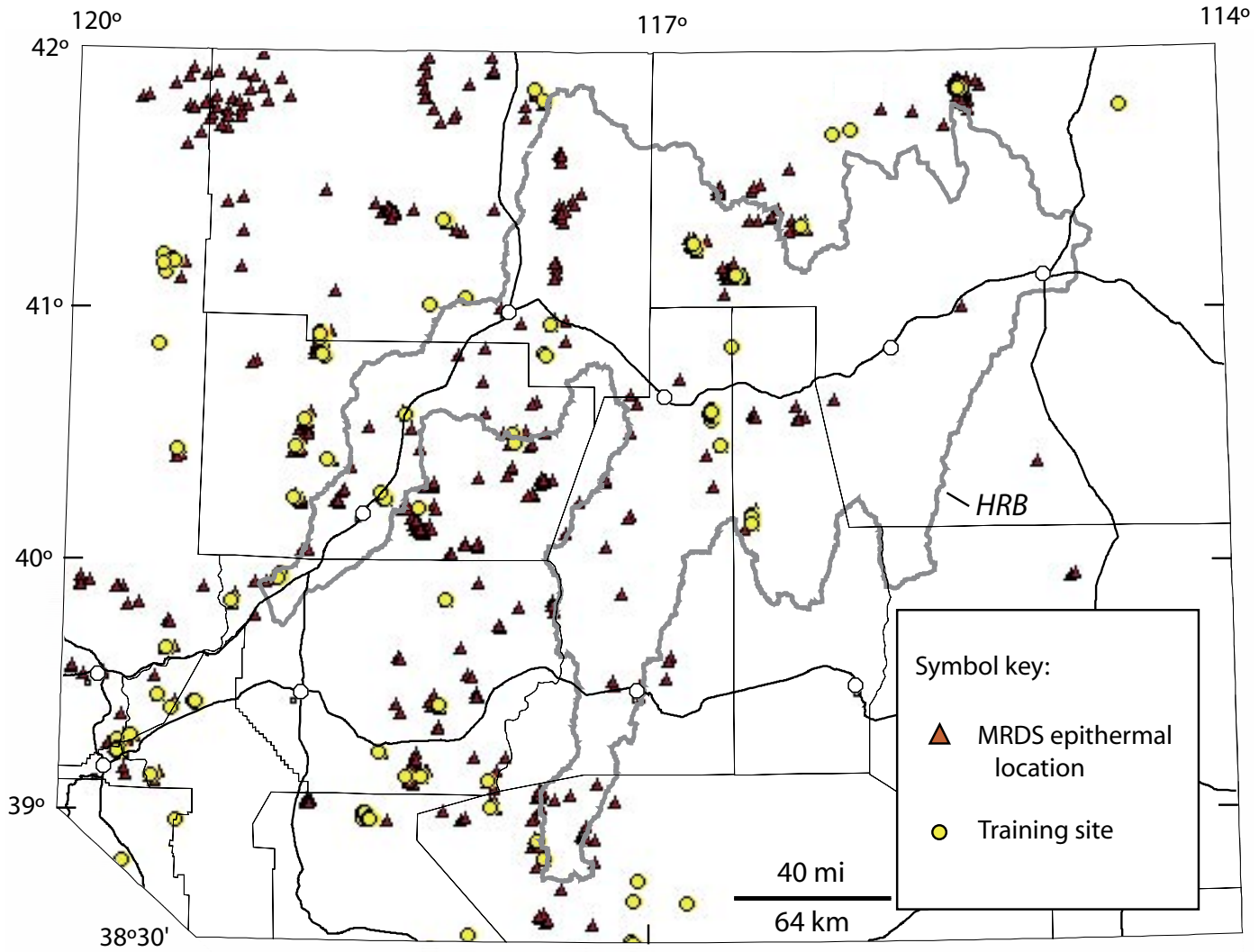
Figure 9-3.   Map showing locations of epithermal sites (red triangles) from Mineral Resource Data System (MRDS) database. Includes all deposit types (Cox and Singer, 1986) that formed in epithermal environments. Training sites from Figure 9-1 shown in yellow circles. Humboldt River Basin (HRB) shown by heavy gray line. County boundaries (light lines), highways (dark lines), town locations (open circles) as in figure 1-1.
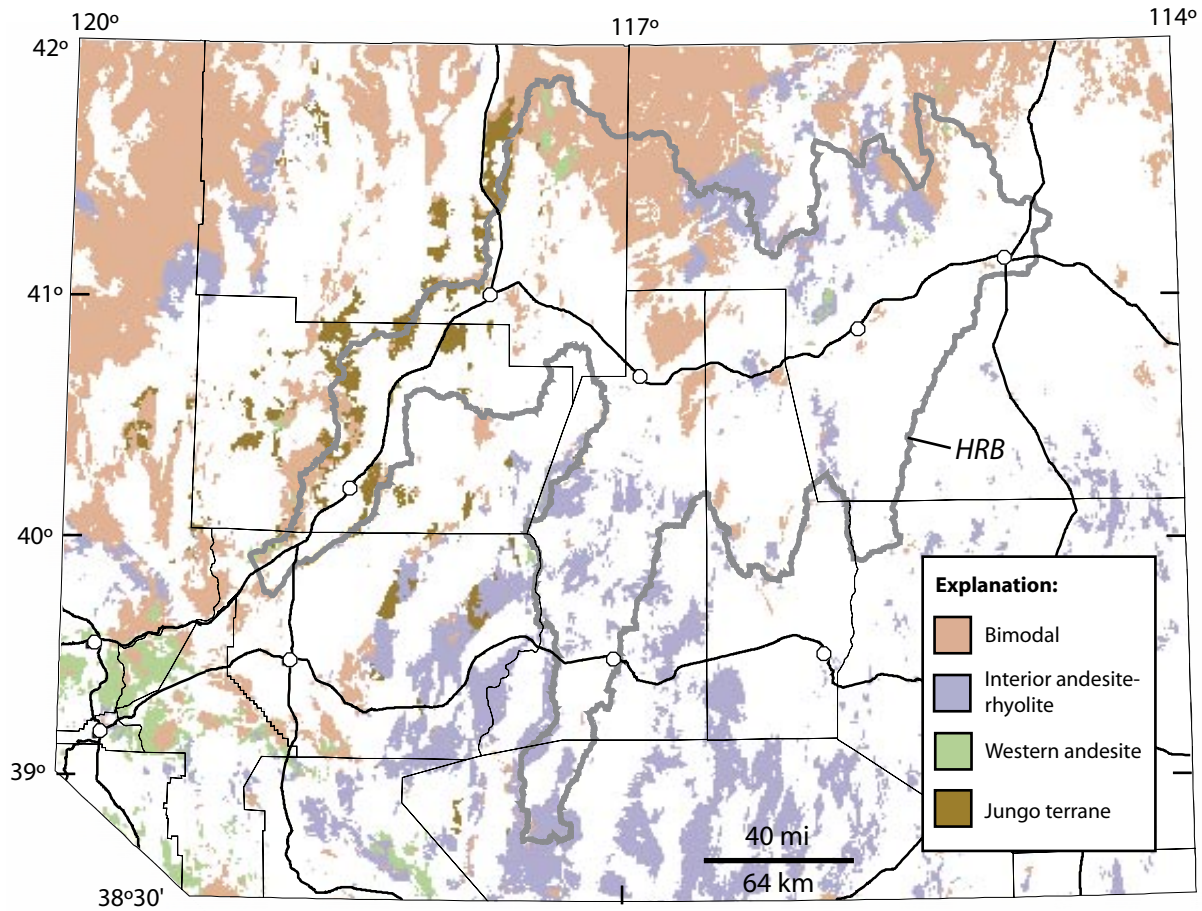
Figure 9-4.   Map showing the general distribution of Cenozoic volcanic assemblages in northern Nevada. Jungo terrane (Mesozoic sedimentary rocks; see text) shown in brown. Humboldt River Basin (HRB) shown by heavy gray line. County boundaries (light lines), highways (dark lines), town locations (open circles) as in figure 1-1.
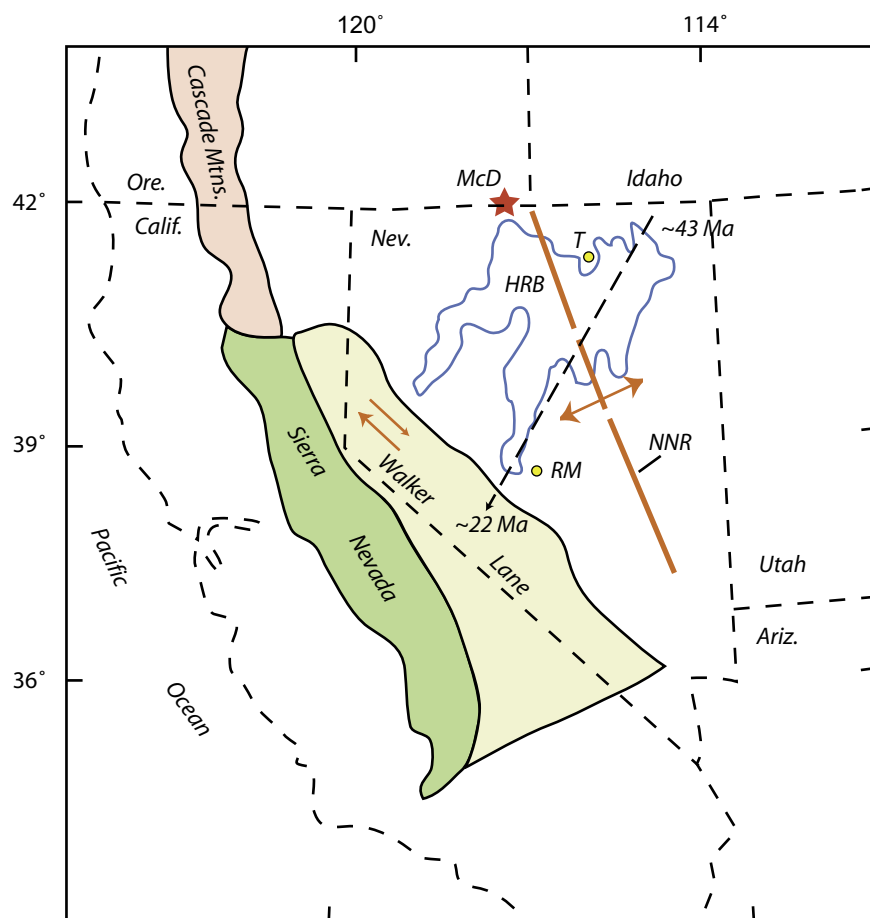
Figure 9-5.   Major igneous and structural features in Nevada and surrounding areas. Western andesite volcanic assemblage is coincident with Walker Lane and extends northwest into Cascade Mountains; arrows in Walker Lane show right-lateral fault movement along zone. Dashed southwest-trending line shows general age progression of interior andesite-rhyolite volcanic events; related epithermal deposits: T, Tuscarora district; RM, Round Mountain mine. NNR, northern Nevada rift, showing directions of regional extension at 16-15 Ma. McD (star), McDermitt caldera (middle Miocene). HRB, Humboldt River Basin shown by blue outline. Modified from John and others (2000).
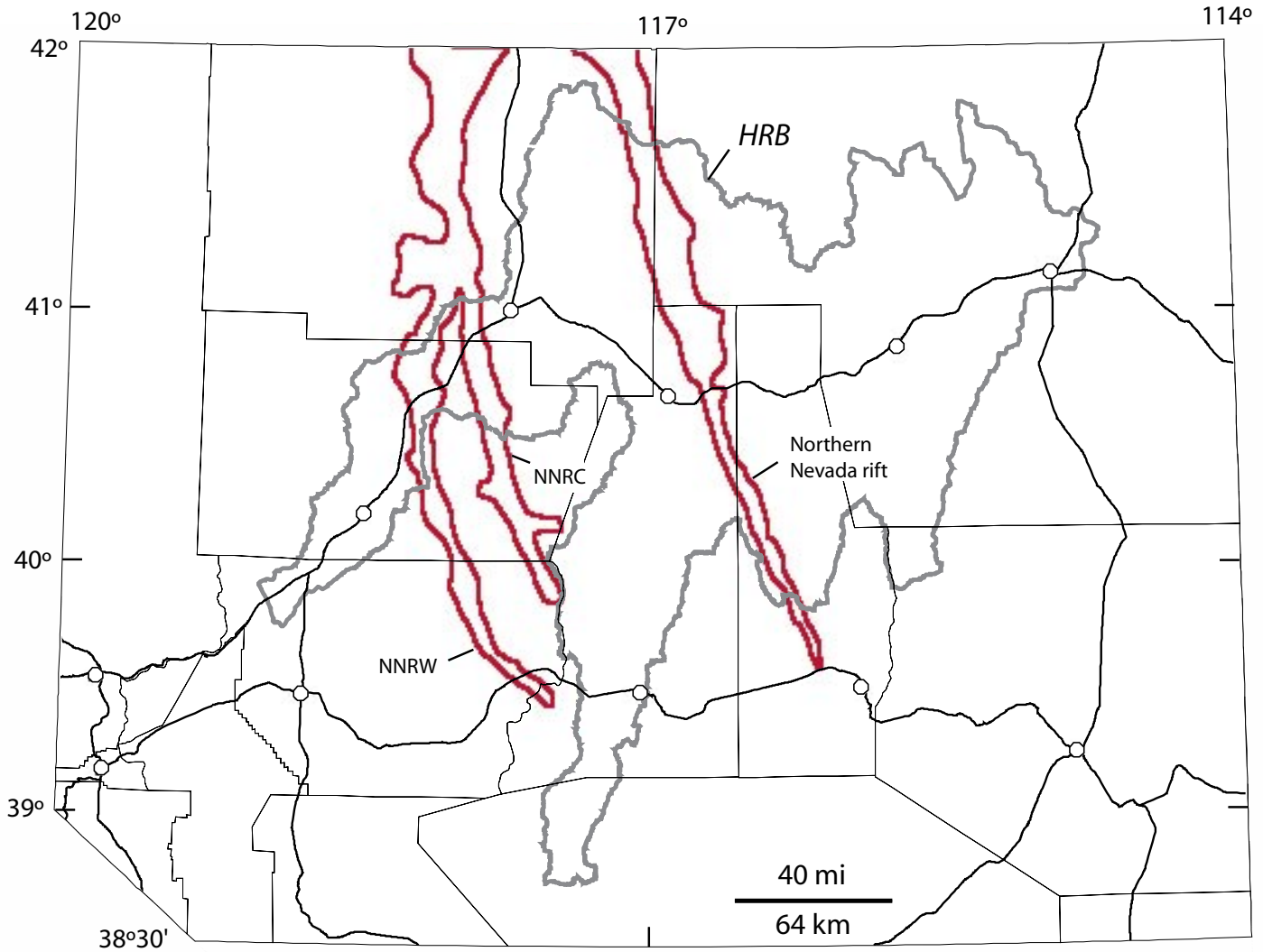
Figure 9-6.   Map showing northern Nevada rift and parallel magnetic highs (NNRC, NNRW, see chapter 6 for explanation) related to known and inferred mafic intrusive zones. Aeromagnetic data from Hildenbrand and Kucks (1988). See chapter 6 for discussion of aeromagnetic anomalies. Humboldt River Basin (HRB) shown by heavy gray line. County boundaries (light lines), highways (dark lines), town locations (open circles) as in figure 1-1.
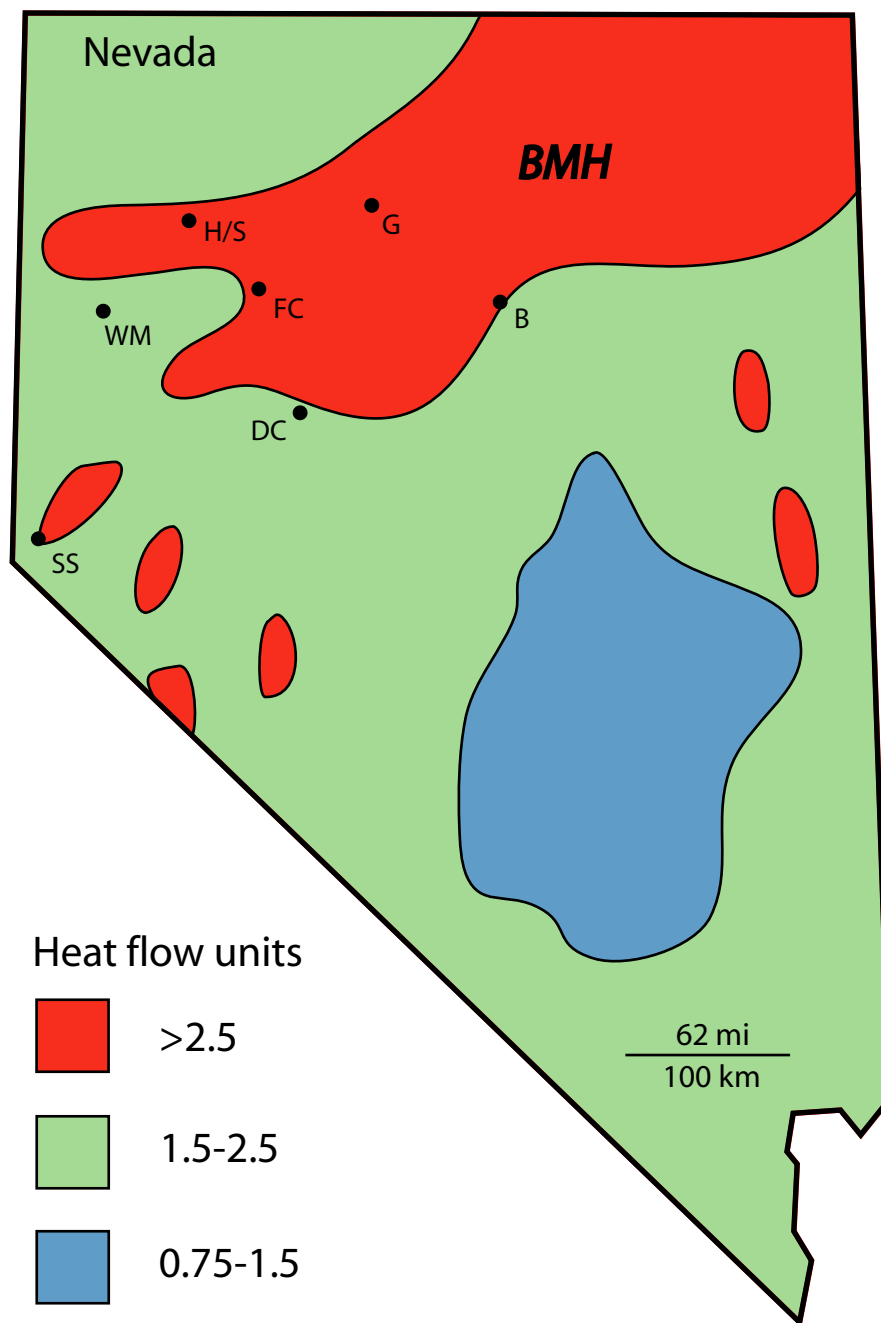
Figure 9-7.   Generalized heat flow map of Nevada showing regions of high heat flow (>2.5 heat flow units). BMH, Battle Mountain geothermal high. From small-scale heat flow map of western United States (Lachenbruch and Sass, 1978). Epithermal deposits related to high heat flow: DC, Dixie Comstock; FC, Florida Canyon (part); H/S, Hycroft/Sulphur; WM, Wind Mountain. Modern hot-spring systems mentioned in text: B, Beowawe; G, Golconda; SS, Steamboat Springs. Locations of epithermal deposits and hot springs very approximate due to original small scale of heat-flow figure.
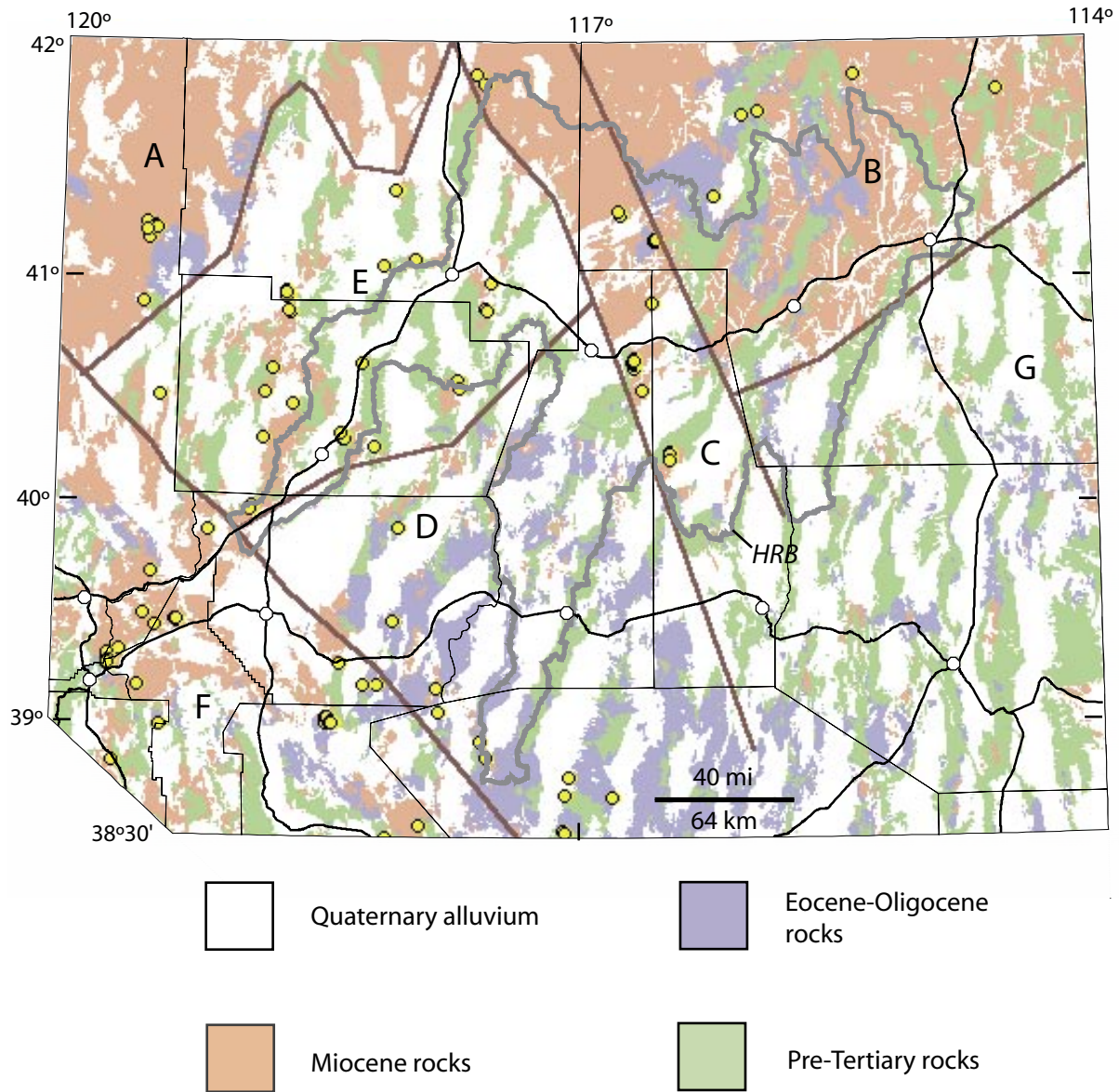
Figure 9-8. Map showing levels of exposure of Eocene-Oligocene and Miocene paleosurfaces in northern Nevada, as represented by rock units of those ages. Also shown are areas with no Tertiary exposures and areas covered by extensive Quaternary deposits. Letters keyed to areas discussed in text. Training sites from figure 9-1 shown in yellow circles. Boundaries between areas are approximate and were drawn to show obvious regional differences in exposed Tertiary volcanic and sedimentary rocks. County boundaries (light lines), highways (dark lines), town locations (open circles) as in figure 1-1. Humboldt River Basin (HRB) shown by heavy gray line.
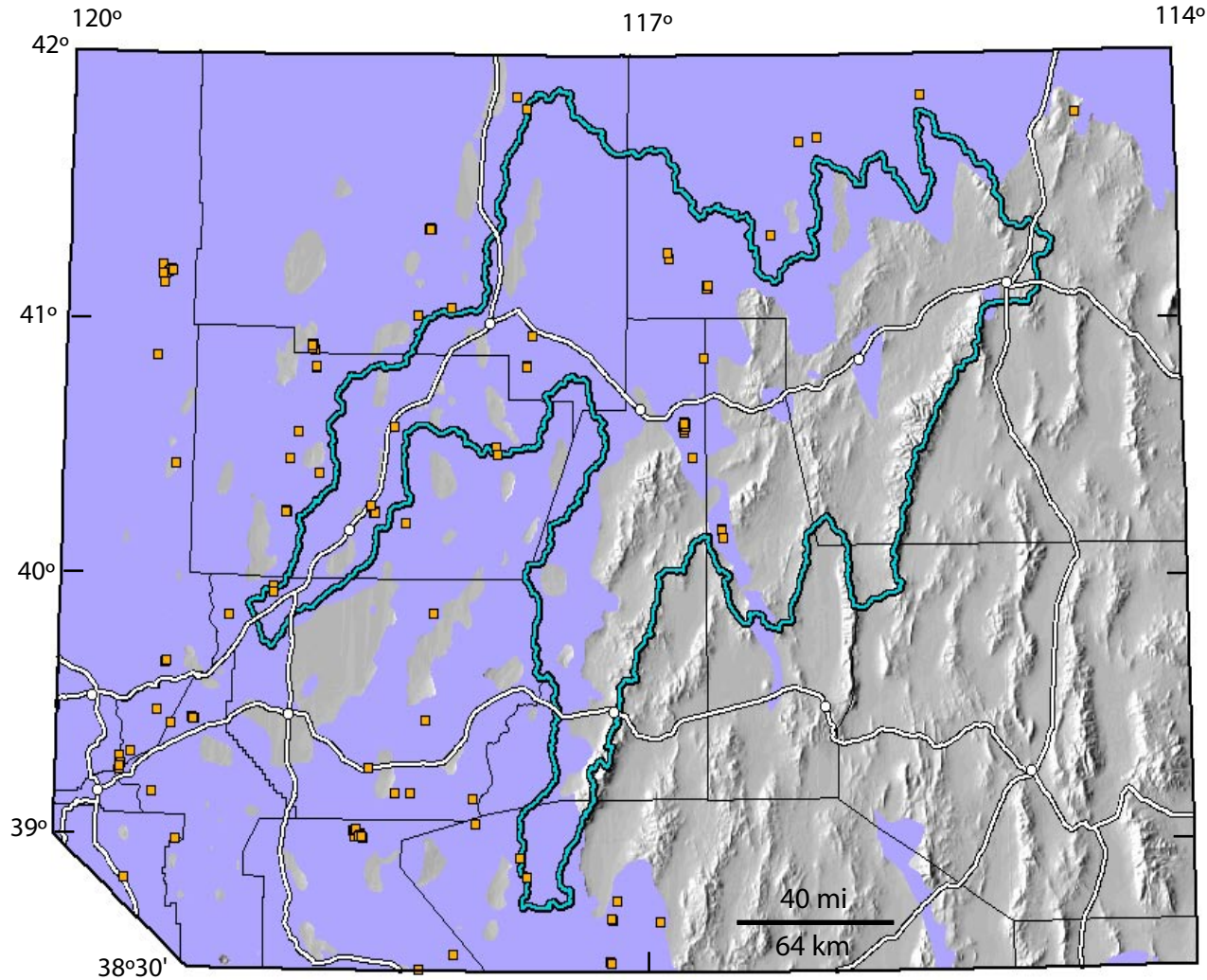
Figure 9-9. Tracts permissive for epithermal deposits, as delineated by Cox and others (1996, plate 12-2). Epithermal deposit training sites are shown as orange squares. The HRB is outlined in light blue. County boundaries (light lines), highways (dark lines), town locations (open circles) as in figure 1-1. Features are plotted on a background of shaded relief of topography.
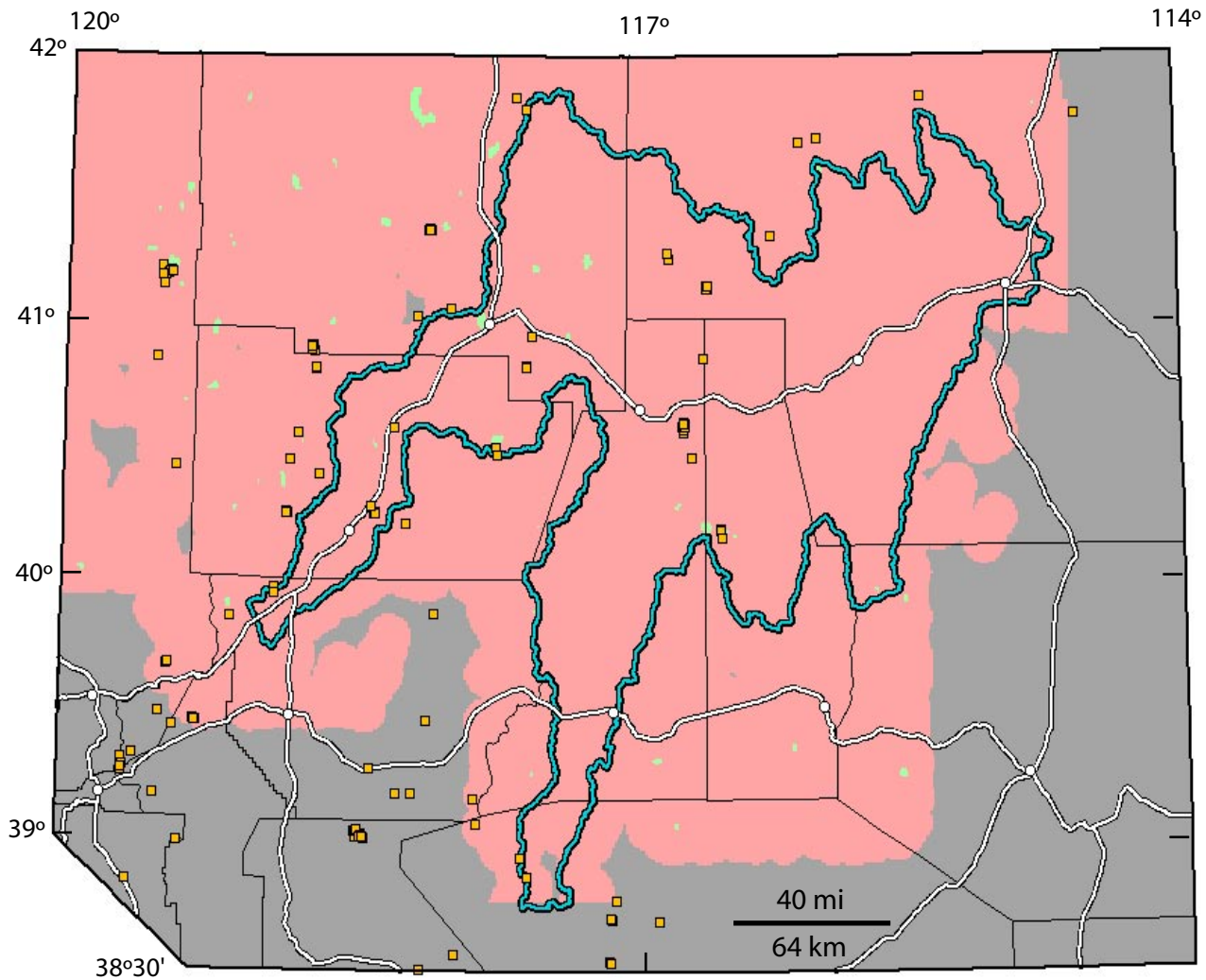
Figure 9-10.   As-frequency evidence map. Predictor pattern present: green. Predictor pattern absent: red. Missing evidence map coverage is shown in gray. Epithermal deposit training sites are shown as orange squares. The HRB is outlined in light blue. County boundaries (light lines), highways (dark lines), town locations (open circles) as in figure 1-1.
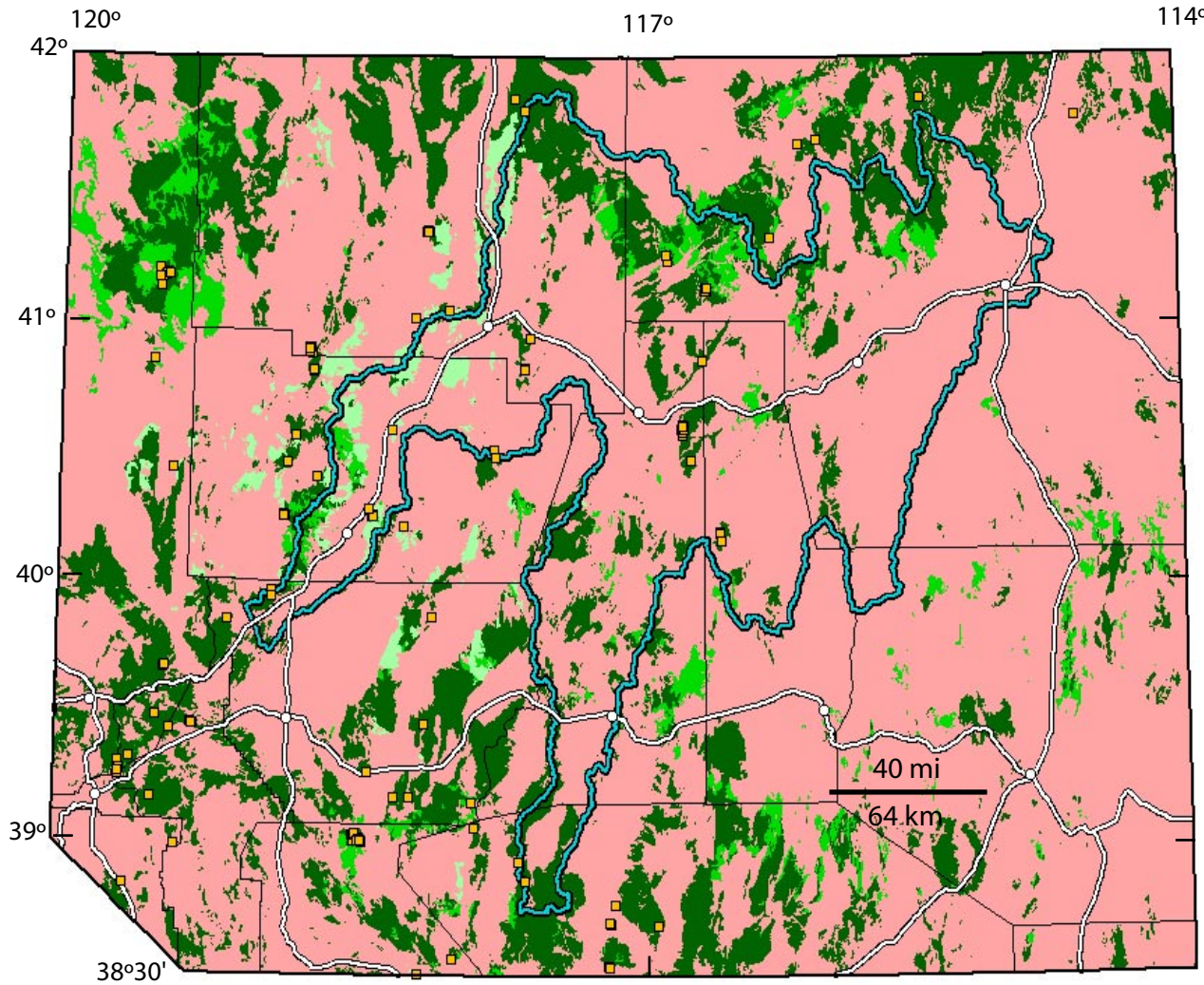
Figure 9-11. Epithermal lithologic units evidence map. Predictor pattern present: dark green (present-high), medium green (present-medium), and light green (present-Jungo). Predictor pattern absent: red. Epithermal deposit training sites are shown as orange squares. The HRB is outlined in light blue. County boundaries (light lines), highways (dark lines), town locations (open circles) as in figure 1-1.
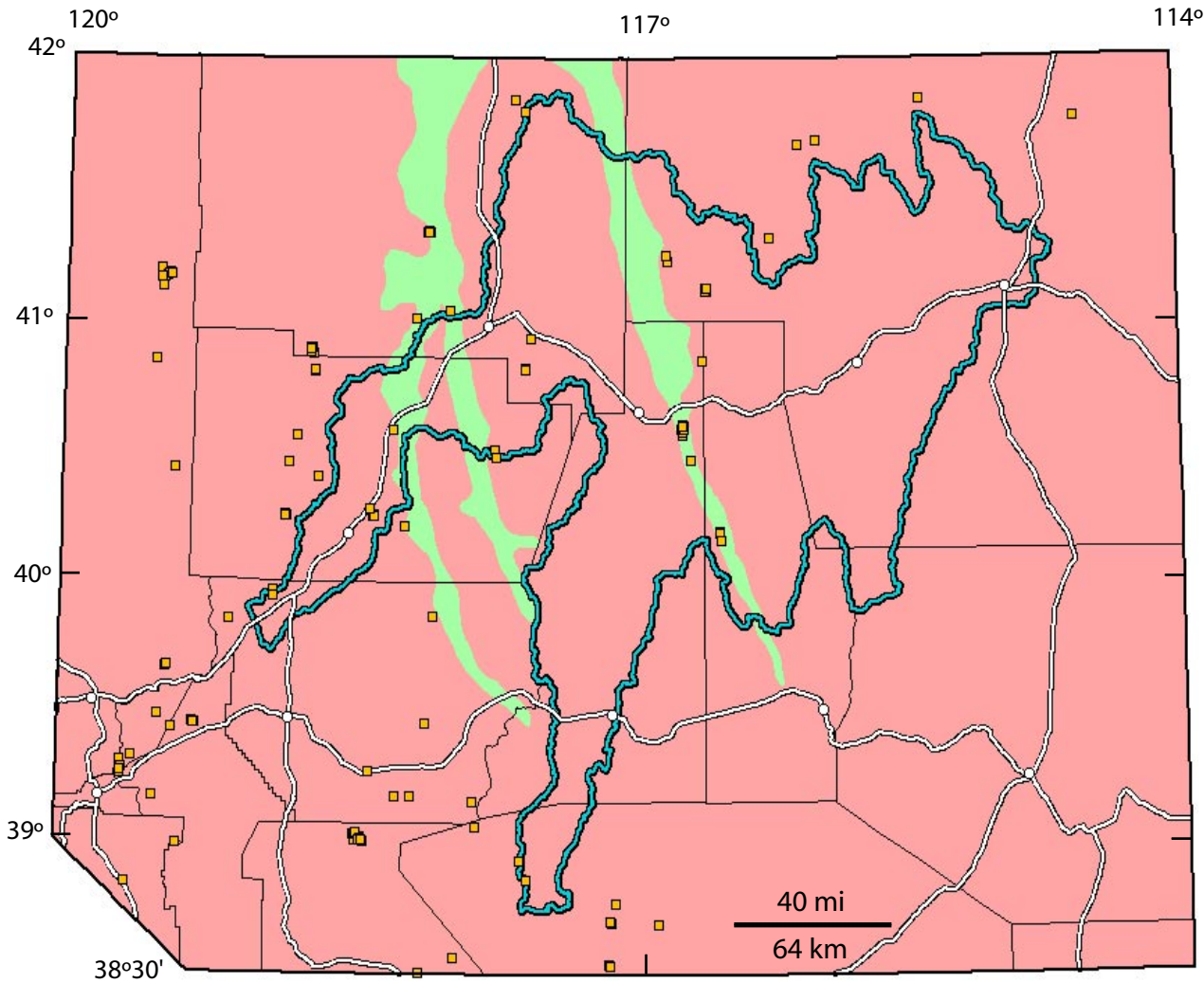
Figure 9-12.   Magnetic terranes evidence map (only the northern Nevada rift-related terranes were selected; compare to figure 2-21). Predictor pattern present: green. Predictor pattern absent: red. Epithermal deposit training sites are shown as orange squares. The HRB is outlined in light blue. County boundaries (light lines), highways (dark lines), town locations (open circles) as in figure 1-1.
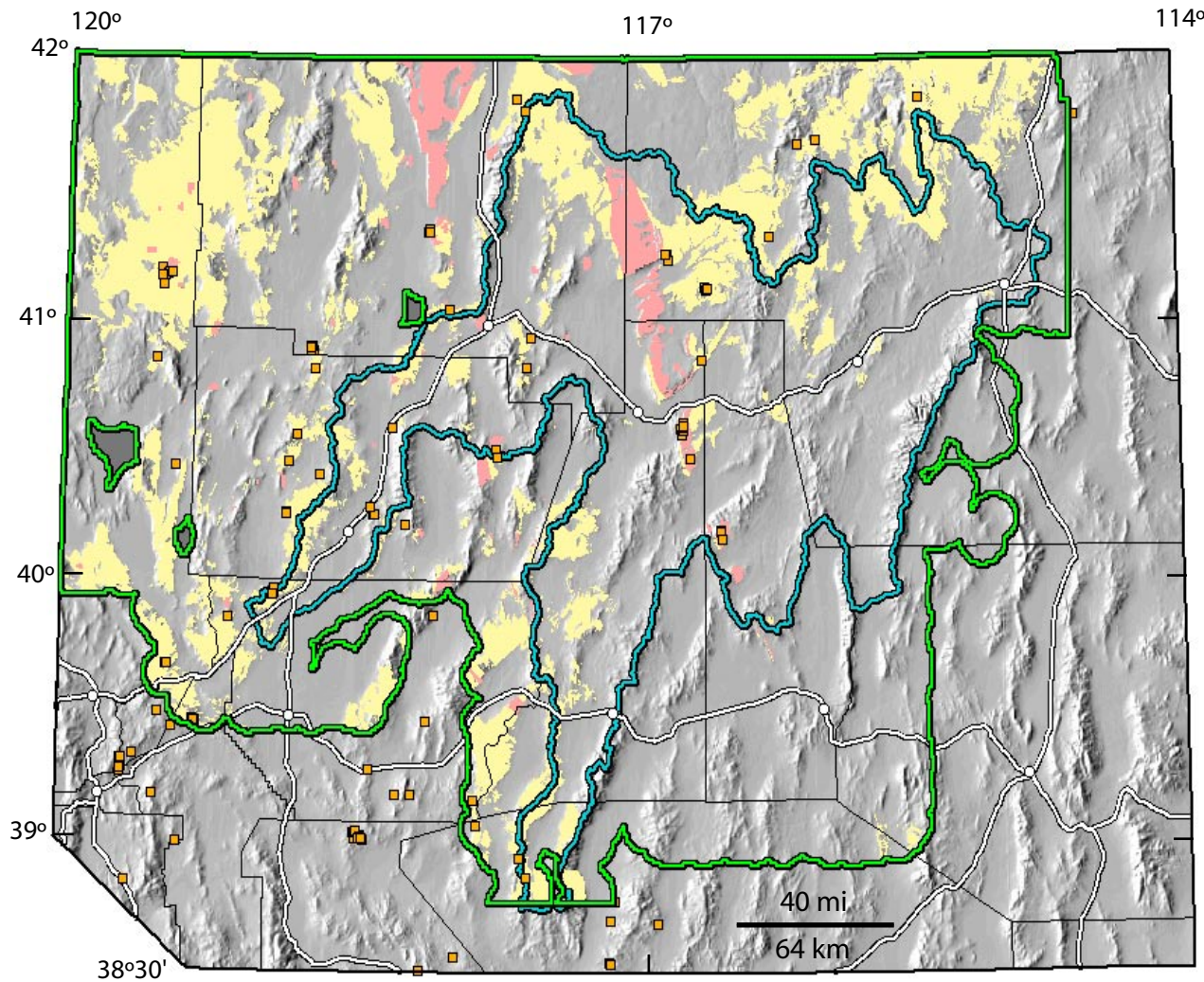
Figure 9-13.   Epithermal Au-Ag deposit favorability map, showing prospective (red) and favorable (yellow) mineral resource assessment tracts. Note that prospective and favorable tracts were delineated only where NURE geochemical data are available (As-frequency evidence, within the light green line). Epithermal deposit training sites are shown as orange squares. The HRB is outlined in light blue. County boundaries (light lines), highways (dark lines), town locations (open circles) as in figure 1-1. Features are plotted on a background of shaded relief of topography.
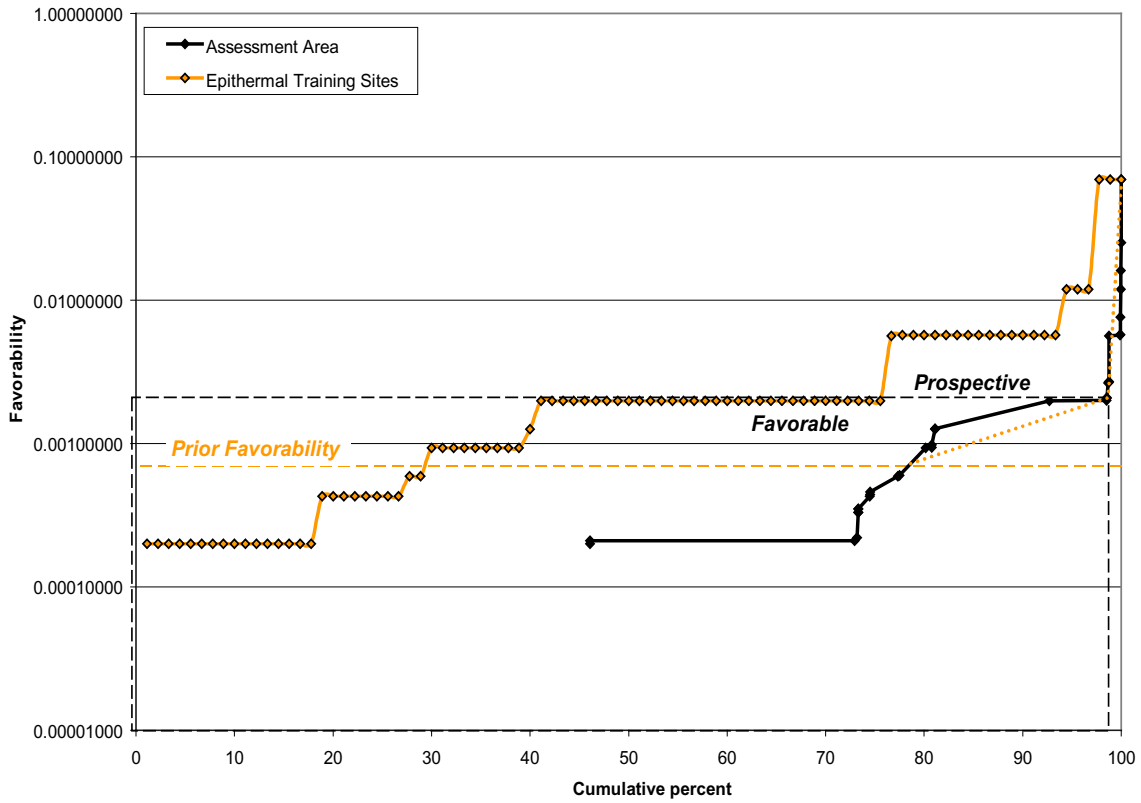
Figure 9-14.   Epithermal deposit weighted-logistic-regression (WLR) favorability plotted against cumulative assessment area (black) and against cumulative training sites (orange). The permissive–favorable rank boundary is defined as the prior favorability (0.0007, orange dashed line). The favorable–prospective rank boundary is defined as the most prominent break-point in the cumulative assessment area above the prior favorability (0.002, black dashed line). The favorable–prospective break-point is highlighted by an orange dotted trend-line.
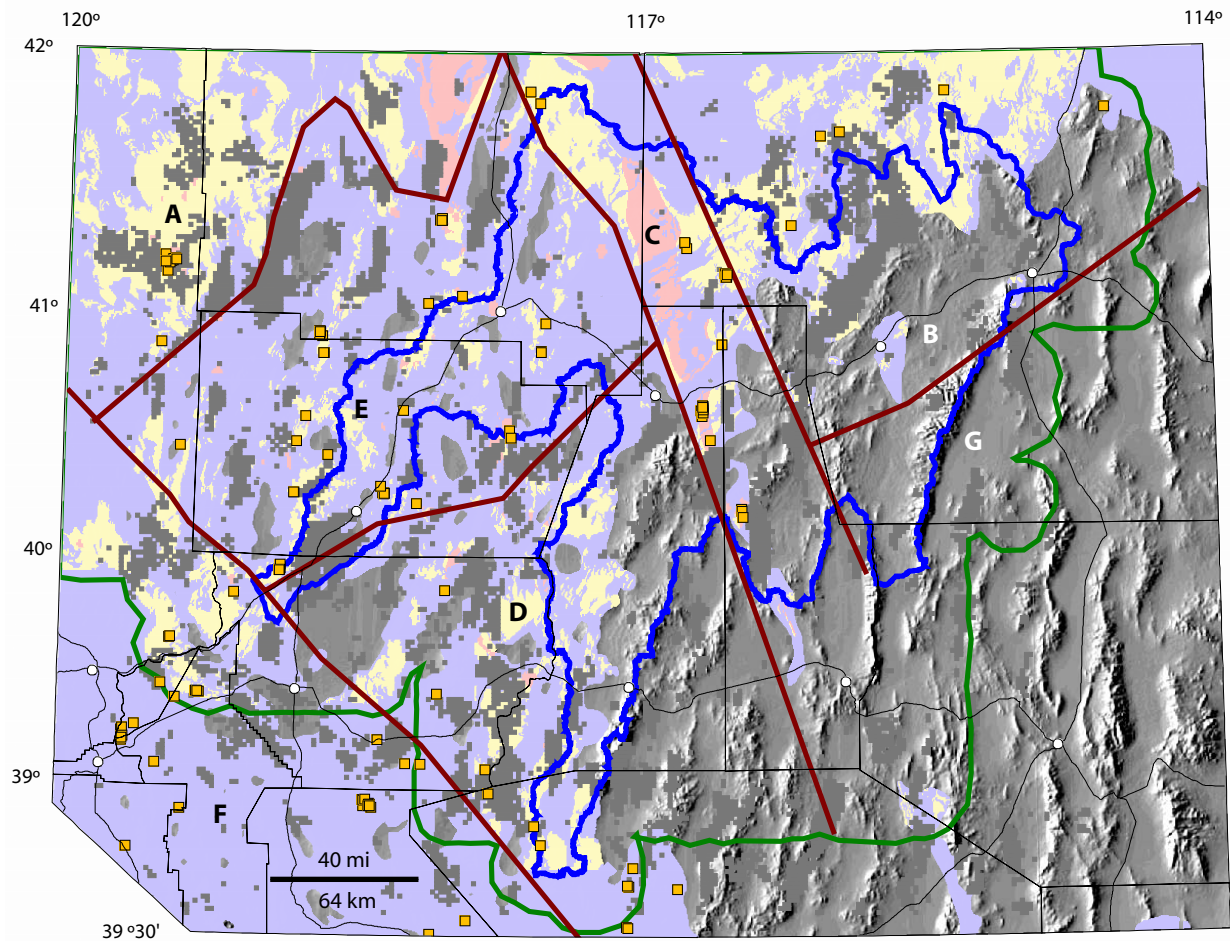
Figure 9-15.   Epithermal Au-Ag deposit mineral resource assessment map, showing prospective (red), favorable (yellow), permissive (blue), and nonpermissive (uncolored) tracts. Note that prospective and favorable tracts were delineated only where National Uranium Resource Evaluation (NURE) geochemical data are available (As-frequency evidence, within the light green line). Darker gray areas represent Cenozoic cover deposits that are greater than 1 km thick (see chapter 6). Epithermal deposit training sites are shown as orange squares. Areas of differing exposure levels are shown in brown lines (from fig. 9-8). Letters A-G refer to subregions described in text. The Humboldt River Basin (HRB) is outlined in light blue. County boundaries (light lines), highways (dark lines), town locations (open circles) as in figure 1-1. Features are plotted on a background of shaded relief of topography.
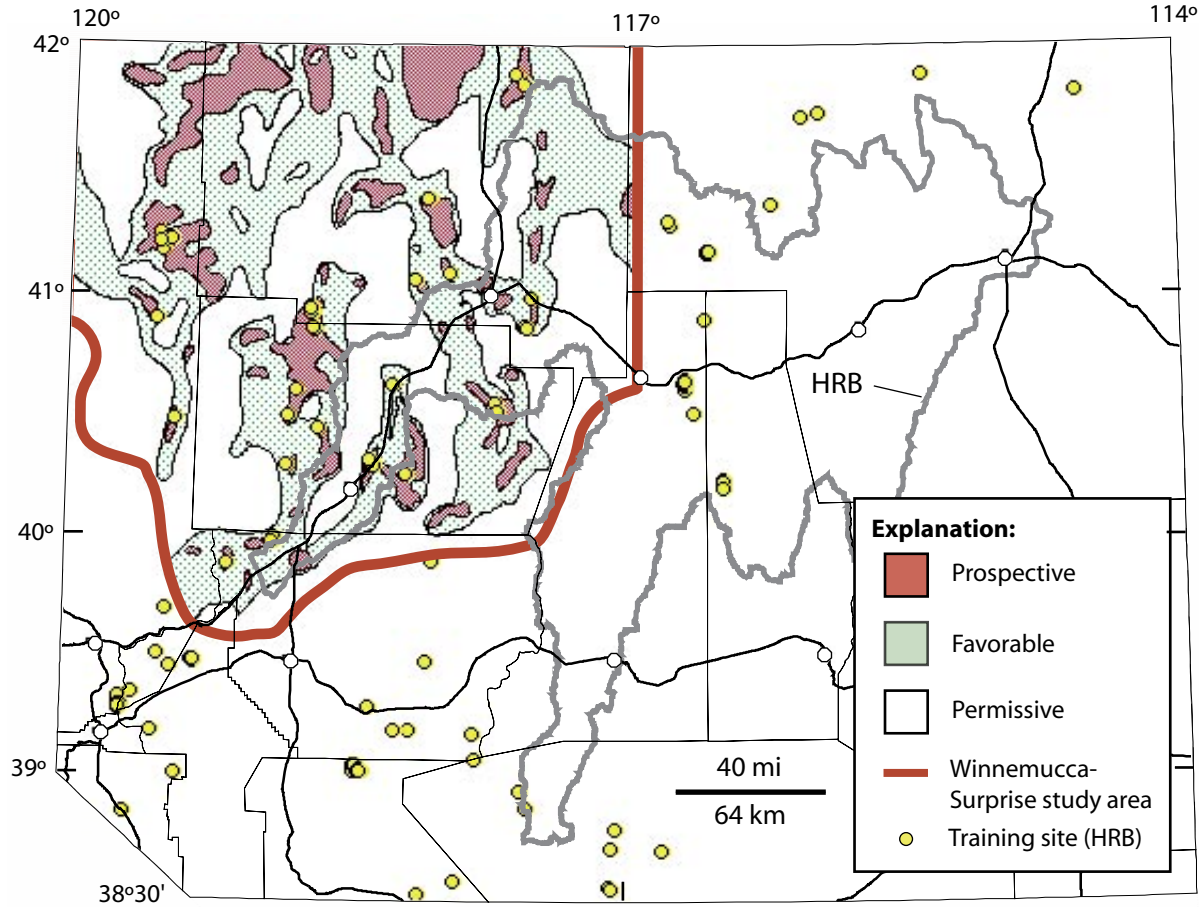
Figure 9-16.   Map showing prospective, favorable, and permissive areas for undiscovered epithermal mineral deposits, from Winnemucca-Surprise mineral assessment (Peters and others, 1996). Training sites used for the Humboldt River Basin assessment shown by yellow circles. County boundaries (light lines), highways (dark lines), town locations (open circles) as in figure 1-1. Heavy gray line outlines Humboldt River Basin (HRB). Nevada part of Winnemucca-Surprise study area shown in heavy red line.

Table 9-1.   Major epithermal deposits in northern Nevada

[host rock, age, production, etc., from training site spreadsheet]

This table is oversize and must be viewed or printed separately from this page—click here

Table 9-2. Volcanic environments and representative low-sulfidation epithermal deposits in northern Nevada

Igneous Environment	Representative Epithermal Deposits
Caldera margin	McDermitt, Round Mountain, Manhattan[1], Wonder
Rhyolite flow and dome	Hog Ranch, Sleeper, Jessup, Midas, Rawhide, National, Ivanhoe (deep veins), Jarbidge, Rosebud, Spring Creek, Adelaide
Stratovolcano	Comstock, Ramsey, Como, Talapoosa
Rift-related mafic magmatism	Mule Canyon, Fire Creek, Buckhorn, Ten Mile, Florida Canyon[2]
Hot spring (Miocene)	Ivanhoe (Hollister mine), Buckhorn, Goldbanks, Florida Canyon[2], Buckskin Mountain
Regional heat flow (Pliocene-Quaternary)	Dixie Comstock, Wind Mountain, Hycroft/Sulphur, Beowawe, Florida Canyon[2]
Uncertain	Relief Canyon, Willard, Standard, Poverty Peak, Dutch Flat (epithermal part)

[1] Manhattan is along a caldera margin, but it is 10 m.y. younger than the caldera.

[2] Florida Canyon possibly formed during several episodes of mineralization; see text for details.

Table 9-3.   Lithologic classifications used for the epithermal model.

["Units" column refers to units shown on state geologic map (Stewart and Carlson, 1978). "High," "medium," "low," and "nonpermissive" refer to expert rank of non-Jungo rock units. See text for discussion and rationale]

Epithermal Unit	Included Units	Comments
1 (high)	Tri, Ti, Tt_3, Tr_3, Ta_3, Tba, Tt_2,Tr_2, Tt_1, Tr_1	Major mineralizing units for epithermal deposits
2 (medium)	Tmi, Trt, Tts, Ta_2, Ta_1	Significant host units and minor mineralizing centers
3 (Jungo)	JTRs	Jungo terrane units
4 (low)	All other units	Tertiary sedimentary and basalt cover; pre-Tertiary rocks other than Jungo terrane
5 (nonpermissive)	Qa, Qp, Qls, Qm, QToa, QTr, Qta, QTb, QTs	Quaternary and Tertiary surficial units

Table 9-4. Evidence maps, prediction criteria, and WofE spatial associations with respect to epithermal deposit training sites (listed in order of descending strength of spatial association).

[Prediction criteria were determined by data-driven means (see chapter 2). Training sites = 127]

Evidence Map	Prediction Criteria	Spatial Associations (W+, W-, C, Studentized C)					
		Predictor Present			Predictor Absent	Strength	Significance
As-Frequency	≥ 200 ppm	3.0238			-0.0772	3.1009	7.8265
Epithermal-Lithologic Units	(1) permissive-Jungo, (2) permissive-medium, (3) prospective-high	(1) 1.6168	(2) 1.0966	(3) 1.1941	-1.3170	2.9338	7.8748
Magnetic Terranes	inside of terranes	1.2943			-0.1344	1.4286	5.9748

Table 9-5. Epithermal deposit mineral resource assessment map areas and training sites.

[Area and training site proportions are relative to the part of the study area covered by geochemical data (As-frequency evidence map, see fig. 9-10)]

Assessment Rank	Area ($127{,}920$ km^2)	Training Sites ($\underline{n} = 90$)
Prospective	2%	24%
Favorable	19%	47%
Permissive	44%	29%
Nonpermissive	35%	0%

References Cited

Adams, Opal, Coyner, A.R., Cuffney, R., Atkinson, R., and Buffa, R., 1991, Roadside geology and precious-metal mineralization, I–80 corridor, Reno to Elko, Nevada, *in* Buffa, R.H., and Coyner, A.R., eds., Geology and ore deposits of the Great Basin, Field Trip Guidebook Compendium, p. 1,085–1,123.

Agterberg, F.P., 1974, Automatic contouring of geological maps to detect target areas for mineral exploration: Journal of Mathematic Geology, v. 6, p. 373–395.

Agterberg, F.P., 1989, LOGDIA—FORTRAN 77 program for logistic regression with diagnostics: Computers and Geosciences, v. 15, p. 599–614.

Agterberg, F.P., 1992, Combining indicator patterns in weights of evidence modeling for resource evaluation: Nonrenewable Resources, v. 1, p. 39–50.

Agterberg, F.P., Bonham-Carter, G.F., Cheng, Q., and Wright, D.F., 1993, Weights of evidence modeling and weighted logistic regression for mineral potential mapping, *in* Davis, J.C., and Herzfeld, U.C., eds., Computers in Geology, 25 Years of Progress: Oxford, England, Oxford University Press, p. 13–32.

Agterberg, F.P., Bonham-Carter, G.F., Wright, D.F., 1990, Statistical pattern integration for mineral exploration, *in* Gaál, G., and Merriam, D.F., eds., Computer Applications in Resource Estimation Prediction and Assessment of Metals and Petroleum: New York, Pergamon Press, p. 1–12.

Alapieti, T.T., Lahtinen, J.J., Huhma, Hannu, Hänninen, Esko, Piirainen, T.A., and Sivonen, S.J., 1989, Platinum-group element-bearing Cu–Ni sulphide mineralization in the marginal series of the early Proterozoic Suhanko-Konttijärvi layered intrusion, northern Finland, *in* Prendergast, M.D., and Jones, M.J., eds., Magmatic sulphides—the Zimbabwe volume: London, The Institution of Mining and Metallurgy, p. 177–189.

Albers, J.P., 1986, Descriptive model of podiform chromite, *in* Cox, D.P., and Singer, D.A., eds., Mineral deposit models: U.S. Geological Survey Bulletin 1693, p. 34.

Albino, G.V., 1993, Application of metal zoning to gold exploration in porphyry copper systems by B.K. Jones—Comments: Journal of Geochemical Exploration, v. 48, no 3, p. 359–366.

Albino, G.V., 1994, Geology and lithogeochemistry of the Ren gold prospect, Elko County, Nevada: The role of rock sampling in exploration for deep Carlin type deposits: Journal of Geochemical Exploration, v. 51, no. 1, p. 37–58.

Andersen, J.C.O., Rasmussen, Henrik, Nielsen, T.F.D., and Ronsbo, Jorn, 1998, The triple group and the Platinova gold and palladium reefs in the Skaergaard intrusion: Stratigraphic and petrographic relations: Economic Geology, v. 93, p. 488–509.

Anderson, J.L., 1983, Proterozoic anorogenic granite plutonism of North America: Geological Society of America Memoir 161, p. 133–154.

Arehart, G.B., 1996, Characteristics and origin of sediment-hosted gold deposits: a review: Ore Geology Reviews, v. 11, p. 383–403.

Arehart, G.B., Chryssoulis, S. L., and Kessler, S. E., 1993a, Gold and arsenic in iron sulfides from sediment–hosted gold deposits: Implications for depositional processes: Economic Geology, v. 88, p. 172–185.

Arehart, G.B., Foland, K.A., Naeser, C.W., And Kesler, S.E., 1993b, ^{40}Ar/^{39}Ar, K/Ar, and fission track geochronology of sediment–hosted disseminated Au deposits at Post–Betze, Carlin trend, northeastern Nevada: Economic Geology, v. 88, p. 622–646.

Armstrong, A.K., Theodore, T.G., Kotlyar, B.B., Lauha, E.G., Griffin, G.L., Lorge, D.L., and Abbott, E.W., 1997, Preliminary facies analysis of Devonian autochthonous rocks that host Au along the Carlin trend, Nevada, *in* Vikre, Peter, Thompson, T.B., Bettles, K., Christensen, Odin, and Parratt, R., eds., Carlin–Type Au Deposits Field Conference: Economic Geology Guidebook Series, vol. 28, p. 53–74.

Armstrong, A.K., Theodore, T.G., Oscarson, R.L., Kotlyar, B.B., Harris, A.G., Bettles, K.H., Lauha, E.A., Hipsley, R.A., Griffin, G.L., Abbott, E.W., and Cluer, J.K., 1998, Preliminary facies analysis of Silurian and Devonian autochthonous rocks that host gold along the Carlin trend, Nevada, *in* Tosdal, R.M., ed., Contributions to the Au metallogeny of the northern Great Basin: U.S. Geological Survey Open–File Report 98–338, p. 38–68.

Audétat, Andreas, Günther, Detlef, and Heinrich, C.A., 2000, Causes for large-scale metal zonation around mineralized plutons: Fluid inclusion LA–ICP–MS evidence from the Mole Granite, Australia: Economic Geology, v. 95, no. 8, p. 1,563–1,581.

Baedecker, P.A., Grossman, J.N., and Buttleman, K.P., 1998, National geochemical database; PLUTO geochemical database for the United States: U.S. Geological Survey DDS–0047, 1 disc.

Bagby, W.C., and Berger, B.R., 1985, Geological characteristics of sediment-hosted, disseminated precious–metal deposits in the western United States: Society of Economic Geologists, Reviews in Economic Geology, v. 2, p. 169–202.

Bagby, W.C., and Cline, J.S., 1991, Constraints on the pressure of formation of the Getchell gold deposit, Humboldt County Nevada, as interpreted from secondary fluid–inclusion data, *in* Raines, G.L., Lisle, R.W., Schafer, R.W., and Wilkinson, W. H., eds., Geology and Ore Deposits of the Great Basin, Symposium Proceedings: Reno, Nevada, Geological Society of Nevada, v. 2, p. 793–804.

Bakken, B.M., and Einaudi, M.T., 1986, Spatial and temporal relations between wall–rock and Au mineralization, main pit, Carlin Au Mine, Nevada, *in* Macdonald, A.J., Gold '86, Willowdale, Ontario: Konsult International Inc., p. 388–403.

Baranov, V. and Naudy, H., 1964, Numerical calculation of the formula of reduction to the magnetic pole: Geophysics, v. 29, p. 67-79.

Baranov, V., 1957, A new method for interpretation of aeromagnetic maps: pseudo-gravimetric anomalies: Geophysics, v. 22, p. 359-383.

Barnes, H.L., and Rose, A.W., 1998, Origins of hydrothermal ores: Science, v. 279, no. 5359, p. 2064-2065.

Barnes, S.-J., and Maier, W.D., 1999, The fractionation of Ni, Cu and the noble metals in silicate and sulphide liquids, *in* Keays, R.R., Lesher, C.M., Lightfoot, P.C., and Farrow, C.E.G., eds., Dynamic processes in magmatic ore deposits and their application in mineral exploration: Geological Association of Canada Short Course Notes volume 13, p. 69–106.

Barringer Resources, Inc., 1982, Geochemical and geostatistical evaluation of wilderness study areas, Winnemucca district, northwest Nevada, 5 vols.: Golden, Colorado, available from NTIA, U.S. Commerce Department, Springfield, VA 22161.

Bartlett, M.W., Enders, M.S., and Hruska, D.C., 1991, Geology of the Hollister gold deposit, Ivanhoe district, Elko County, Nevada, *in* Raines, G.L., Lisle, R.E., Schafer, R.W., and Wilkinson, W.H., eds., Geology and ore deposits of the Great Basin, Symposium Proceedings: Geological Society of Nevada, p. 957-978.

Barton, M.D., 1990, Cretaceous magmatism, metamorphism, and metallogeny in the east-central Great Basin: Geological Society of America Memoir 174, p. 293–302.

Barton, M.D., 1996, Granitic magmatism and metallogeny of southwestern North America: Geological Society of America Special Paper 315, p. 261–280.

Barton, M.D., Battles, D.A., Bebout, G.E., Capo, R.C., Christensen, J.N., Davis, S.R., Hanson, R.B., Michelson, C.J., and Trim, H.E., 1988, Mesozoic contact metamorphism in the western United States, Rubey Volume VII, *in* Ernst, W.G., ed., Metamorphism and crustal evolution of the western United States: Englewood Cliffs, N.J., Prentice-Hall, p. 110–178.

Barton, P.B., Jr., 1986, User–friendly mineral deposit models, *in* Cargill, S.M., and Green, S.B., eds., Prospects for mineral resource assessment on Public lands: Proceedings of the Leesburg Workshop: U.S. Geological Survey Circular 980, p. 94–110.

Barton, P.B., Jr., 1993, Problems and opportunities for mineral deposit models, *in* Kirkham, R.V., Sinclair, W.D., Thorpe, R.I., and Duke, J.M., eds., Mineral Deposit Modeling: Geological Association of Canada Special Paper, p. 7–14.

Baschuk, G.J., 2000, Lithologic and structural ore controls within the upper zone of Barrick's Rodeo Deposit, Eureka County, *in* Cluer, J. K., Price, J. G., Struhsacker, E. M., Hardyman, R. F., and Morris, C. L., eds., Geology and Ore Deposits 2000: The Great Basin and Beyond: Geological Society of Nevada symposium Proceedings, May 15–18, 2000, p. 989–1001.

Bates, R.L., and Jackson, J.A., eds., 1987, Glossary of Geology, 3rd edition: Alexandria, VA, American Geological Institute, 788 p.

Battles, D.A., and Barton, M.D., 1989, Na–Ca hydrothermal alteration in the Western Great Basin: Eos, Transactions of the American Geophysical Union, v. 70, p. 1382.

Beane, R. E., and Titley, S.R., 1981, Porphyry copper deposits, Part II, Hydrothermal alteration and mineralization: Economic Geology Seventy-Fifth Anniversary Volume, p. 235–269.

Benedetto, K.M.F., Dean, D.A., and Durgin, D.C., 1991, Roadside geology and precious-metal mineralization along US 50, Reno to Ely, Nevada, *in* Buffa, R.H., and Coyner, A.R., eds., Geology and ore deposits of the Great Basin, Field Trip Guidebook Compendium, p. 1,124–1,140.

Bergendal, M.H., 1964, Gold in mineral and water resources of Nevada: Nevada Bureau of Mines Bulletin 65, p. 87–100.

Berger, B.R., 1985, Geological and geochemical relationships at the Getchell mine and vicinity, Humboldt County, Nevada, *in* Hollister, V.F.M, ed., Case histories of mineral discoveries, Volume I, Discoveries of epithermal precious metal deposits: New York, New York, Society of Mining Engineers of the American Institute of Mining, Metallurgical and Petroleum Engineers, Inc., p. 51–60.

Berger, B.R., 1986, Descriptive model of carbonate-hosted Au–Ag, *in* Cox, D. P., and Singer, D. A., eds., Mineral deposit models: U.S. Geological Survey Bulletin 1693, p. 175.

Berger, B.R., and Bagby, W. C., 1991, The geology and origin of Carlin type deposits, *in* Foster, R.P., ed., Gold exploration and metallogeny: London, Blackie and Sons, p. 210–248.

Berger, B.R., and Silberman, M.L., 1985, Relationships of trace-element patterns to geology in hot-spring-type precious-metal deposits, *in* Berger, B.R., and Bethke, P.M., eds., Geology and geochemistry of epithermal systems: Society of Economic Geologists, Reviews in Economic Geology, v. 2, p. 233-247.

Berger, B.R., and Taylor, B.E., 1980, Pre–Cenozoic normal faulting in the Osgood Mountains, Humboldt County, Nevada: Geology, v. 8, p. 594–598.

Berger, B.R., and Tingley, 1985, History of discovery, mining, exploration of the Getchell mine, Humboldt County, Nevada, *in* Hollister, V.F., ed., Case Histories of Mineral Discoveries, Volume I, Discoveries of epithermal precious metal deposits: New York, New York, Society of Mining Engineers of the American Institute of Mining, Metallurgical and Petroleum Engineers, Inc., p. 49–50.

Berger, V.I., Theodore, T.G., Tosdal, R.M., and Oscarson, R.L., 2000, Implications of celsian in the Ruby Mountains, Nevada, *in* Cluer, J.K., Price, J.G., Struhsacker, E.M., Hardyman, R.F., and Morris, C.L., eds., Geology and ore deposits 2000: The Great Basin and beyond: Geological Society of Nevada Symposium Proceedings, May 15–18, 2000, p. 325–347.

Bettles, K.H., and Lauha, E.A., 1991, Gold deposits of the Goldstrike Mine, Carlin Trend, Nevada, in World Gold '91, *in* Peters, S.G., Williams, C.L., Volk, J., (leaders), Structural Geology of the Carlin Trend: Geology and Ore Deposits of the American Cordillera (1995), Trip B (reprinted), Geological Society of Nevada, p. 251–257.

Birak, D.J., and Hawkins, R.B., 1985, The geology of the Enfield Bell Mine and the Jerritt Canyon District, Elko County, Nevada, *in* Tooker, E.W., ed., Geologic characteristics of sediment- and volcanic-hosted disseminated Au deposits—search for an occurrence model: U.S. Geological Survey Bulletin 1646, p. 95–105.

Blake, D.W., 1992, Supergene copper deposits at Copper Basin, *in* Theodore, T.G., Blake, D.W., Loucks, T.A., and Johnson, C.A., Geology of the Buckingham stockwork molybdenum deposit and surrounding area, Lander County, Nevada: U.S. Geological Survey Professional Paper 798–D, p. D154–D167.

Blake, D.W., Theodore, T.G., Batchelder, J.N., and Kretschmer, E.L., 1979, Structural relations of igneous rocks and mineralization in the Battle Mountain Mining District, Lander County, Nevada, *in* Ridge, J.D., ed., Papers on mineral deposits of western North America: International Association on the Genesis of Ore Deposits Symposium, 5th, Snowbird–Alta, Utah, 1978, Proceedings: Nevada Bureau of Mines and Geology Report 33, p. 87–99.

Blake, D.W., Wotruba, P.R., and Theodore, T.G., 1984, Zonation in the skarn environment at the Tomboy-Minnie gold deposits, Lander County, Nevada, *in* Wilkins, Joe, Jr., ed., Gold and silver deposits of the Basin and Range province, western U.S.A.: Arizona Geological Society Digest, v. 15, p. 67–72.

Blakely, R.J., 1988, Curie temperature isotherm analysis and tectonic implications of aeromagnetic data from Nevada: Journal of Geophysical Research, v. 93, no. B10, p. 11817-11832.

Blakely, R.J., 1995, Potential theory in gravity and magnetic applications: Cambridge University Press, 441 p.

Blakely, R.J., and Jachens, R.C., 1991a, Concealed mineral deposits in Nevada—Insights from three-dimensional analysis of gravity and magnetic anomalies, *in* Raines, G. L., Lisle, R. E., Schafer, R. W., and Wilkinson, W. H., eds., Geology and Ore Deposits of the Great Basin, Symposium Proceedings Volume 1: Geological Society of Nevada, Reno/Sparks, Nevada, p. 185–192.

Blakely, R.J., and Jachens, R.C., 1991b, Regional study of mineral resources in Nevada--Insights from three-dimensional analysis of gravity and magnetic anomalies: Geological Society of America Bulletin, v. 103, p. 795-803.

Blakely, R.J., and Simpson, R.W., 1986, Approximating edges of source bodies from gravity or magnetic data: Geophysics, v. 51, p. 1494-1498.

Bliss, J.D., ed., 1992, Developments in mineral deposit modeling: U.S. Geological Survey Bulletin 2004, 168 p.

Bloomstein, E., Braginton, B., Owen, R., Parrat, R., Raabe, K., and Thompson, W., 1993, Geology and geochemistry of the Lone Tree gold deposit, Humboldt County, Nevada: Society for Mining, Metallurgy and Exploration, Preprint 93–205, 23 p.

Bloomstein, E.I., Braginton, B.L., Owen, R.O., Parratt, R.L., Raabe, K.C., and Thompson, W.F., 2000, Lone Tree gold deposit, *in* Theodore, T.G., Geology of pluton–related gold mineralization at Battle Mountain, Nevada: Tucson, Arizona, University of Arizona and U.S. Geological Survey Center for Mineral Resources, Monograph 2, p. 186–219.

Bloomstein, E.I., Massingill, G.L., Parratt, R.L., and Peltonen, D.R., 1991, Discovery, geology, and mineralization of the Rabbit Creek gold deposit, Humboldt County, Nevada, *in* Raines, G.L., Lisle, R.E., Schafer, R.W., and Wilkinson, W.H., eds., Geology and ore deposits of the Great Basin, Symposium Proceedings: Reno, Nevada, Geological Society of Nevada, p. 821–843.

Bonham, H.F., 1969, Geology and mineral deposits of Washoe and Storey Counties, Nevada, with a section on Industrial rock and mineral deposits by K.G. Papke: Nevada Bureau of Mines and Geology Bulletin 70, 107 p.

Bonham, H.F., Jr., Garside, L.J., Jones, R.B., Papke, K.G., Quade, J., and Tingley, J.V., 1985, A mineral inventory of the Paradise-Denio and Sonoma-Gerlach resource areas, Winnemucca District, Nevada: Nevada Bureau of Mines and Geology Open-File Report 85-35, 218 p.

Bonham-Carter, G.F., 1994, Geographic Information Systems for Geoscientists: Modelling with GIS (Computer Methods in the Geosciences Volume 13): Tarrytown, New York, Pergamon Press/Elsevier Science Publications, 398 p.

Bonham-Carter, G.F., Agterberg, F.P., and Wright, D.F., 1989, Weights of evidence modelling: A new approach to mapping mineral potential, *in* Agterberg, F.P., and Bonham-Carter, G.F., eds., Statistical Applications in the Earth Science: Geological Survey of Canada, Paper 89–9, p. 171–183.

Boudreau, A.E., and McCallum, I.S., 1986, Investigations of the Stillwater Complex: III. The Picket Pin Pt/Pd deposits: Economic Geology, v. 81, p. 1,953–1,975.

Bowell, R. J., Bauman, M., Gingrich, M., Tretbar, D., Perkins, w. F., and Fisher, P. C., 1999, The occurrence of gold at the Getchell Mine, Nevada: Journal of Geochemical Research, v. 67, p. 127–143.

Bowes, W.A., Kutina, Jan, Fredrikson, Kurt, and Golightly, D.W., 1982, A porphyry Mo–Cu discovery at Granite Mountain, Nevada: Predictions based on mineralogical and geochemical study of zoning: Global Tectonics and Metallogeny, v. 1, no. 4, p. 402–439.

Boyd, R., Barnes, S.-J., and Grønlie, A., 1988, Noble metal geochemistry of some Ni–Cu deposits in the Sveconorwegian and Caledonian orogens in Norway, *in* Prichard, H.M., Potts, P.J., Bowles, J.F.W., and Cribb, S.J., eds., Geo-platinum 87: New York, Elsevier Applied Science, p. 145–158.

Boyd, R., McDade, J.M., Millard, H.T., Jr., and Page, N.J, 1987, Platinum metal geochemistry of the Bruvann nickel-copper deposit, Rana, North Norway: Norsk Geologisk Tidsskrift, v. 67, p. 205–213.

Boyd, R., and Nixonk, F., 1985, Norwegian nickel deposits: A review, *in* Papunen, H., and Gorbunov, G.I., eds., Nickel-copper deposits of the Baltic shield and Scandinavian Caledonides: Geological Survey of Finland, Bulletin 333, p. 363–394.

Branham, Alan, and Arkell, Brian, 1995, The Mike gold-copper deposit, Carlin trend, Nevada, *in* Hagni, R.D., ed., Process mineralogy XIII: Applications to beneficiation problems, pyrometallurigical products, advanced mineralogical techniques, precious metals, environmental concerns, ceramic materials, hydrometallurgy, and minerals exploration: Warrendale, Pennsylvania, The Minerals, Metals, and Materials Society, p. 203–211.

Bratland, C.T., 1991, Geology of the Winters Creek gold deposit, Independence Mountains, Elko County, Nevada, *in* Raines G.L., Lisle, R.E., Schafer, R.W., and Wilkinson, W.H., eds., Geology and Ore Deposits of the Great Basin, Geologic Society of Nevada Symposium Proceedings, Reno/Sparks, Nevada, April, 1990, v. 1, p. 607–618.

Brew, D.A., and Morrell, R.P., 1983, Intrusive rocks and plutonic belts of southeastern Alaska, U.S.A.: Geological Society of America, Memoir 159, p. 171–193.

Briggs, I.C., 1974, Machine contouring using minimum curvature: Geophysics, v. 39, p. 39-48.

Briggs, P.H., 1990, Elemental analysis of geologic materials by inductively coupled plasma-atomic emission spectrometry, *in* Arbogast, B.F., ed., Quality Assurance Manual for the Branch of Geochemistry: U.S. Geological Survey Open-File Report 90-668, p. 83-91.

Brooks, J.W., Meinert, L.D., Kuyper, B.A., and Lane, M.L, 1991, Petrology and geochemistry of the McCoy gold skarn, Lander County, Nevada, *in* Raines, G.L., Lisle, R.E., Schafer, R.W., and Wilkinson, W.H., eds., Geology and ore deposits of the Great Basin, Symposium Proceedings: Reno, Nevada, Geological Society of Nevada, p. 419–442.

Brooks, R.A., and Berger, B.R., 1978, Relationship of soil-mercury values to soil type and disseminated gold mineralization, Getchell mine area, Humboldt County, Nevada: Journal of Geochemical Exploration, v. 9, p. 186–194.

Buchanan, L.J., 1981, Precious metal deposits associated with volcanic environments in the Southwest: Arizona Geological Society Digest, v. 14, p. 237-262.

Burke, D.B., and McKee, E.H., 1979, Mid-Cenozoic volcano-tectonic troughs in central Nevada: Geological Society of America Bulletin, v. 90, no. 2, p. 1181–1184.

Burt, D.M., 1972, Mineralogy and geochemistry of Ca–Fe–Si skarn deposits: Cambridge, Massachusetts, Harvard University, Ph.D. Dissertation, 256 p.

Burt, D.M., 1977, Mineralogy and petrology of skarn deposits: Societa Italiana Minerologia Petrologia Rendiconti, v. 33, p. 859–873.

Bussey, S.D., 1996, Gold mineralization and associated rhyolitic volcanism at the Hog Ranch district, northwest Nevada, *in* Coyner, A.R., and Fahey, P.L., eds., Geology and ore deposits of the American cordillera: Geological Society of Nevada Symposium Proceedings, Reno/Sparks, Nevada, April 1995, p. 181-207.

Buttl, J.B., 1945, Unique Golconda deposit yields its tungsten: Engineering and Mining Journal, v. 146, no. 8, p. 79–81.

Cabri, L.J., and Naldrett, A.J., 1984, The nature of the distribution and concentration of platinum-group elements in various geological environments: Proceedings of the 27th International Geological Congress, v. 10, Mineralogy, p. 17–46.

Cameron, E.N., 1939, Geology and mineralization of the northeastern Humboldt Range, Nevada: Geological Society of America Bulletin, v. 50, p. 563–634.

Carten, R.B., Walker, B.M., Geraughty, E.P., and Gunow, A.J., 1988, Comparison of field-based studies of the Henderson porphyry molybdenum deposit, Colorado, with experimental theoretical models of porphyry systems, *in* Taylor, R.P., and Strong, D.F., eds., Recent advances in the geology of granite-related mineral deposits: Canadian Institute of Mining and Metallurgy, Special Volume 39, p. 351–366.

Carten, R.B., White, W.H., and Stein, H.J., 1993, High-grade granite-related molybdenum systems: classification and origin, *in* Kirkham, R.V., Sinclair, W.D., Thorpe, R.I., and Duke, J.M., eds. Mineral deposit modeling: Geological Association of Canada Special Paper 40, p. 521–554.

Cary, Jeff, Johnson, Todd, Nicholes, Jeff, Campo, Art, Felling, Rick, Slayton, Jim, Lappin, Steve, Mohn, Pat, Moss, Ken, Lane, Chuck, and Kennedy, Larry, 2000, Geology, skarn alteration, and Au–Cu–Ag mineralization of the Phoenix Project (Battle Mountain Mining District), Lander County, Nevada, *in* Cluer, J.K., Price, J.G., Struhsacker, E.M., Hardyman, R.F., and Morris, C.L., eds., Geology and ore deposits 2000: The Great Basin and beyond: Geological Society of Nevada Symposium Proceedings, May 15–18, 2000, p. 1,021–1,045.

Casteel, M.V., Schmidt, K., Goldstrand, P., Bernard, J., and Sandberg, J., 1999, Geologic setting of the Ken Snyder gold and silver mine, Elko County, Nevada, *in* Kizis, J.A., Jr., ed., Low-sulfidation gold deposits in northern Nevada: Geological Society of Nevada, 1999 Spring Field Trip Guidebook, Special Publication No. 29, p. 213-220.

Castor, S.B., Garside, L.J., Henry, C.D., Hudson, D.M., McIntosh, W.C., and Vikre, P.G., 2002, Multiple episodes of magmatism and mineralization in the Comstock district, Nevada: Geological Society of America, Abstracts with Programs, v. 34, no. 6, p. 185.

Castor, S.B., and Henry, C.D., 2000, Geology, geochemistry, and origin of volcanic rock-hosted uranium deposits in northwestern Nevada and southeastern Oregon, USA: Ore Geology Reviews, v. 16, no. 1-2, p. 1-40.

Cheng, Q., 1999, Spatial and scaling modelling for geochemical anomaly separation: Journal of Exploration Geochemistry, v. 65, p. 175–194.

Cheng, Q, Agterberg, F.P., and Ballantyne, S.B., 1994, The separation of geochemical anomalies form background by fractal methods: Journal of Geochemical Exploration, v. 51, p. 109-130.

Cheng, Q., Agterberg, F.P. and Bonham-Carter, G.F., 1996, Spatial analysis method for geochemical anomaly separation: Journal of Exploration Geochemistry, v. 56, p. 183–195.

Cheong, Sangwon, 1999, Structural setting and fluid characteristics of metamorphic gold-quartz veins in northwestern Nevada: Reno, Nevada, University of Nevada, Reno, Ph.D. dissertation, 344 p.

Cheong, Sangwon, Peters, S.G., and Iriondo, Alexander, 2000, Summary of structural setting and fluid characteristics of low-sulfide Au–quartz veins in northwestern Nevada, *in* Cluer, J.K., Price, J.G., Struhsacker, E.M., Hardyman, R.F., and Morris, C.L., eds., Geology and ore deposits 2000: The Great Basin and beyond: Geological Society of Nevada Symposium Proceedings, May 15–18, 2000, p. 473–506.

Chevillon, Vic, Berentsen, Eric, Gingrich, Mark, Harold, Bill, and Zbinden, Elizabeth, 2000, Geologic overview of the Getchell gold mine geology, exploration and ore deposits, Humboldt county, Nevada, *in* Crafford, A.E.J., ed., Geology and ore deposits of the Getchell Region Humboldt county, Nevada: Geological Society of Nevada Symposium 2000 Field Trip Guidebook No. 9, p. 113–122.

Christensen, O.D., 1993, Carlin Trend Geologic Overview, *in* Christensen, O.D., ed., Au deposits of the Carlin Trend, Nevada: Society of Economic Geologists Guidebook Series, v. 18, P. 3–26.

Christensen, O.D., 1996, Carlin trend geologic overview, *in* Peters, S.G., Williams, C.L., and Volk, Jeff, Field trip guidebook for Trip B–Structural geology of the Carlin trend, *in* Green, S.M., and Struhsacker, Eric, eds., Field Trip Guidebook Compendium: Reno, Nevada, Geological Society of Nevada, Geology and Ore Deposits of the American Cordillera, p. 147–156.

Christiansen, E.H., Sheridan, M.F., and Burt, D.M., 1986, The geology and geochemistry of Cenozoic topaz rhyolites from the Western United States: Geological Society of America Special Paper 205, 82 p.

Christiansen, R.L., and Yeats, R.S., 1992, Post-Laramide geology of the U.S. Cordilleran region, with contributions by S.A. Graham, W.A. Niem, A.R. Niem, and P.D. Snavely, Jr.: Geological Society of America, The Cordilleran Orogen, Conterminous U.S., v. G-3, p. 261-406.

Chung, C.F., 1978, Computer program for the logistic model to estimate the probability of occurrence of discrete events: Geological Survey of Canada Paper 78–11, 23 p.

Chung, C.F., and Agterberg, F. P., 1980, Regression models estimating mineral resources from geological map data: Mathematical Geology, v. 12, p. 473–488.

Claypool, G.E., Holser, W.T., Kaplan, I.R., Sakai, H., and Zak, I., 1980, The age curves of sulfur and oxygen isotopes in marine sulfate and their mutual interpretation: Chemical Geology, v. 28, p. 199–260.

Cleveland, Gaylord, 2000, Geology of the Redline gold skarn deposits, Converse project, Humboldt County, Nevada, *in* Cluer, J.K., Price, J.G., Struhsacker, E.M., Hardyman, R.F., and Morris, C.L., eds., Geology and ore deposits 2000: The Great Basin and beyond: Geological Society of Nevada Symposium Proceedings, May 15–18, 2000, p. 1047–1068.

Cline, J.S., and Hofstra, A.H., 2000, Ore fluid evolution at the Getchell Carlin-type gold deposit, Nevada, USA: European Journal of Mineralogy, v. 12, p. 195–212.

Clode, C.H., 1995, Geology of the Deep Star Gold Deposit, Eureka County, Nevada, *in* Peters, S.G., Williams, C.L., Volk, J., (leaders), Structural Geology of the Carlin Trend: Geology and Ore Deposits of the American Cordillera, Field Trip Guidebook, Trip B, Geological Society of Nevada, Reno, Nevada, 5 p.

Cluer, J. K, Cellura, B.R., Keith, S.B, Finney, S.C., And Bellert, S.J., 1997, Stratigraphy and structure of the Bell Creek nappe (Antler Orogen), Ren property, northern Carlin trend, Nevada, *in* Perry, A..J., and Abbott, E.W., eds., The Roberts Mountains Thrust, Elko and Eureka Counties, Nevada: Nevada Petroleum Society 1997 Field Trip Guidebook, Reno, Nevada, p. 41–54.

Cluer, J.K., Price, J.G., Struhsacker, E.M., Hardyman, R.F., and Morris, C.L., eds., 2000, Geology and Ore Deposits 2000: The Great Basin and Beyond: Geological Society of Nevada Symposium Proceedings, May 15-18, 2000, 1176 p. (2 vols.).

Coats, R.R., 1987, Geology of Elko County, Nevada: Nevada Bureau of Mines and Geology Bulletin 101, 112 p.

Coleman, R.G., 1977, Ophiolites: Berlin, Springer-Verlag, 229 p.

Connors, K.A., Noble, D.C., Brake, S.S., Thomas, W.D., and Fleck, R.J., 1999, Gold and mercury mineralization associated with middle Miocene bimodal volcanism and faulting in the Goldbanks district, Pershing County, Nevada [abs.]: American Geophysical Union Spring meeting, v. 80, no. 17, p. S372.

Connors, R.A., Robinson, M.L., Bukofski, J.F., Meyer, W.T., and Howarth, R.J., 1982, Geochemical and geostatistical evaluation of wilderness study areas, Winnemucca District, northwestern Nevada: Golden, Colorado, Barringer Resources, Inc., U.S. Bureau of Land Management, Contract no. YA-553-CTI-1096, Open-File Report 1-5.

Conrad, J.E., ed., 1990, Mineral summaries for Nevada Bureau of Land Management wilderness study areas: U.S. Geological Survey Open-File Report 90-638, 373 p.

Conrad, J.E., and McKee, E.H., 1996, High-precision $^{40}Ar/$ ^{39}Ar ages of rhyolitic host rock and mineralized veins at the Sleeper deposit, Humboldt County, Nevada, *in* Coyner, A.R., and Fahey, P.L., eds., Geology and ore deposits of the American cordillera: Geological Society of Nevada Symposium Proceedings, Reno/Sparks, Nevada, April 1995, p. 257-262.

Coope, J.A., 1991, Carlin trend exploration history: Discovery of the Carlin deposit: Nevada Bureau of Mines and Geology, Special Publication 13, 16 p.

Couch, B. F., and Carpenter, J. A., 1943, Nevada's Metal and Mineral Production: Nevada Bureau of Mines and Geology Bulletin, v. 38, P. 65–70.

Cox, D.P, 1992, Descriptive and grade and tonnage models of distal–disseminated Ag–Au, *in* Bliss, J.D., ed., Developments in deposit modeling: U.S. Geological Survey Bulletin 2004, p. 19–22.

Cox, D.P., 1986a, Descriptive model of W skarn deposits, *in* Cox, D.P., and Singer, D.A., eds., Mineral deposit models: U.S. Geological Survey Bulletin 1693, p. 55.

Cox, D.P., 1986b, Descriptive model of Fe skarn deposits, *in* Cox, D.P., and Singer, D.A., eds., Mineral deposit models: U.S. Geological Survey Bulletin 1693, p. 94.

Cox, D.P., 1986c, Descriptive model of porphyry Cu, *in* Cox, D.P., and Singer, D.A., eds., Mineral deposit models: U.S. Geological Survey Bulletin 1693, p. 76.

Cox, D.P., 1986d, Descriptive model of porphyry Cu-Mo, *in* Cox, D.P., and Singer, D.A., eds., Mineral deposit models: U.S. Geological Survey Bulletin 1693, p. 115.

Cox, D.P., 1986e, Descriptive model of porphyry Cu- skarn-related deposits, *in* Cox, D.P., and Singer, D.A., eds., Mineral deposit models: U.S. Geological Survey Bulletin 1693, p. 82.

Cox, D.P., 1986f, Descriptive model of porphyry Cu-Au, *in* Cox, D.P., and Singer, D.A., eds., Mineral deposit models: U.S. Geological Survey Bulletin 1693, p. 110.

Cox, D.P., 1986g, Descriptive model of Zn-Pb skarn deposits, *in* Cox, D.P., and Singer, D.A., eds., Mineral deposit models: U.S. Geological Survey Bulletin 1693, p. 90.

Cox, D.P., 1993, The development and use of mineral deposit models in the United States Geological Survey, *in* Kirkham, R.V., Sinclair, W.D., Thorpe, R.I., and Duke, J.M., eds., Mineral deposit modeling: Geological Association of Canada Special Paper 40, p. 15–20.

Cox, D.P., and Bagby, W.C., 1986, Descriptive model of W veins, *in* Cox, D.P., and Singer, D.A., eds., Mineral deposit models: U.S. Geological Survey Bulletin 1693, p. 64.

Cox, D.P., Barton, P.B., and Singer, D., 1986, Introduction, *in* Cox, D.P., and Singer, D.A., eds., Mineral deposit models: U.S. Geological Survey Bulletin 1693, p. 1-10.

Cox, D.P., Berger, B.R., Ludington, Steve, Moring, B.C., Sherlock, M.G., Singer, D.A., and Tingley, J.V., 1996, Delineation of mineral resource assessment tracts and estimation of number of undiscovered deposits in Nevada, *in* Singer, D.A., ed., An analysis of Nevada's metal-bearing mineral resources: Nevada Bureau of Mines and Geology Open-File Report 96–2, Chapter 12, p.12.1–12.25, 3 sheets, scale 1:1,000,000, [ftp://ftp.nbmg.unr.edu/NBMG/ofr962/index.htm].

Cox, D.P., Ludington, S., Sherlock, M.J., Singer, D.A., Berger, B.R., and Tingley, J.V., 1991, Mineralization patterns in time and space in the Great Basin of Nevada, *in* Raines, G.L., Lisle, R.E., Schafer, R.W., and Wilkinson, W.H., eds., Geology and Ore Deposits of the Great Basin: Reno, Nevada, Geological Society of Nevada, Symposium Proceedings, p. 193–198.

Cox, D.P., and Singer, D.A., eds., 1986, Mineral deposit models: U.S. Geological Survey Bulletin 1693, 379 p.

Cox, D.P., and Singer, D.A., 1990, Descriptive and grade-tonnage models for distal-disseminated Ag–Au deposits: A supplement to U.S. Geological Survey Bulletin 1693: U.S. Geological Survey Open–File Report 90–282, 7 p.

Cox, D.P., and Singer, D.A., 1992, Grade and tonnage model of distal disseminated Ag–Au, *in* Bliss, J.D., ed., Developments in mineral deposit modeling: U.S. Geological Survey Bulletin 2004, p. 20–22.

Cox, D.P., and Theodore, T.G., 1986, Descriptive model of Cu skarns, *in* Cox, D.P., and Singer, D.A., eds., Mineral deposit models: U.S. Geological Survey Bulletin 1693, p. 86.

Crafford, E.J., ed., 2000a, Geology and ore deposits of the Getchell region Humboldt County, Nevada: Geological Society of Nevada Symposium 2000 Field Trip Guidebook No. 9, 153p.

Crafford, E.J., 2000b, Overview of regional geology and tectonic setting of the Osgood Mountains Region, Humboldt County, Nevada, *in* Crafford, A.E.J., ed. Geology and ore deposits of the Getchell region Humboldt County, Nevada: Geological Society of Nevada Symposium 2000 Field Trip Guidebook No. 9, p. 69–85.

Czamanske, G.K., Haffty, Joseph, and Nabbs, S.W., 1981, Pt, Pd, and Rh analyses and beneficiation of mineralized mafic rocks from the La Perouse layered gabbro, Alaska: Economic Geology, v. 76, no. 7, p. 2,001–2,011.

Daly, W.E., Doe, T.C., and Loranger, R.J., 1991, Geology of the Northern Independence Mountains, Elko County, Nevada, *in* Raines, G.L., Lisle, R.W., Schafer, R.W., and Wilkinson, W. H., eds., Geology and Ore Deposits of the Great Basin, Reno: Geological Society of Nevada, Symposium Proceedings, v. 2, p. 583–352.

Davis, D.A., and Tingley, J.V., 1999, Gold and silver resources in Nevada: Nevada Bureau of Mines and Geology Map 120, scale 1:1,000,000.

Davis, D.A., Henry, C.H., Garside, L.J., Faulds, J.E., and Goldstrand, P.M., 2000, Eocene-Oligocene paleovalleys cross the Sierra Nevada-Basin and Range boundary, western Nevada and eastern California: Geological Society of America, Abstracts with Programs, v. 32, no. 7, p. A-167.

Dickinson, W.R., 2001, Tectonic setting of the Great Basin through geologic time: Implications for metallogeny, *in* Shaddrick, D.R., Zbinden, Elizabeth, Mathewson, D.C., Prenn, Camille, eds., Regional tectonics and structural control of ore: The major gold trends of northern Nevada: Geological Society of Nevada, Special Publication no. 33, p. 27–53.

Dilek, Yildirim, and Moores, E.M., 1995, Geology of the Humboldt igneous complex, Nevada, and tectonic implications for the Jurassic magmatism in the Cordilleran orogen, *in* Miller, D.M., and Busby, Catherine, eds., Jurassic magmatism and tectonics of the North American Cordillera: Geological Society of America Special Paper 299, R.L. Armstrong Memorial Volume, p. 229-248.

Dilek, Yildirim, Moores, E.M., and Erskine, M.C., 1988, Ophiolitic thrust nappes in western Nevada: Implications for the Cordilleran Orogen: Journal of the Geological Society, London, v. 145, p. 969–975.

Dilles, J.H., Einaudi, M.T., Proffett, John, and Barton, M.D., 2000a, Overview of the Yerington porphyry copper district: Magmatic to nonmagmatic sources of hydrothermal fluids: Their flow paths and alteration effects on rocks and Cu–Mo–Fe–Au ores, *in* Dilles, J.H., Barton, M.D., Johnson, D.A., Proffett, J.M., and Einaudi, M.T., eds., Contrasting styles of intrusion-associated hydrothermal systems, Part 1: Society of Economic Geologists, Guidebook Series, v. 32, p. 55–66.

Dilles, J.H., Farmer, G.L., and Field, C.W., 1995, Sodium-calcium alteration by non-magmatic saline fluids in porphyry copper deposits: Results from Yerington, Nevada, *in* Thompson, J.F. H., ed., Magmas, fluids, and ore deposits: Victoria, British Columbia, Mineralogical Association of Canada, Short Course v. 23, p. 309–338.

Dilles, J.H., and Proffett, J.M., 1995, Metallogenesis of the Yerington batholith, Nevada, *in* Pierce, F.W., and Bolm, J,.G., eds., Porphyry copper deposits of the American Cordillera: Arizona Geological Society Digest 20, p. 306–315.

Dilles, J.H., Proffett, John, and Einaudi, M.T., 2000b, Magmatic and hydrothermal features of the Yerington batholith with emphasis on the porphyry Cu (Mo) deposit in the Ann-Mason area, *in* Dilles, J.H., Barton, M.D., Johnson, D.A., Proffett, J.M., and Einaudi, M.T., eds., Contrasting styles of intrusion-associated hydrothermal systems, Part 1: Society of Economic Geologists, Guidebook Series, v. 32, p. 67–89.

Dobak, P.J., Arbonies, D., Hipsley R., and Visher, M., 2001, Geology of the Storm gold deposit, northern Carlin trend, Nevada: Society of Mining Engineers, Annual Meeting, February 26-28, Denver, Colorado, Preprint 01–167, 7 p.

Dobrin, M.B., and Savit, C.H., 1988, Introduction to Geophysical Prospecting (4th ed.): New York, McGraw-Hill, 867 p.

Doebrich, J.L., 1995, Geology and mineral deposits of the Antler Peak 7.5-minute quadrangle, Lander County, Nevada: Nevada Bureau of Mines and Geology Bulletin 109, 44 p.

Doebrich, J.L., 1996, Resource Assessment of the Bureau of Land Management's Winnemucca District and Surprise Resource Area, northwest Nevada and California–Geology, and its relation to resource genesis: U. S. Geological Survey Open–File Report 96–30, 33 p.

Doebrich, J.L., Albino, G.V., Barker, C.E., Duffield, W.A., Dunn, V.C., Hanna, W.F., McFarlan, J.P., McGuire, D.J., Miller, M.S., Peters, S.G., Plouff, D., Raines, G.L., Sawatzky, D.L., and Spanski, G.T., 1994, Resource assessment of the Bureau of Land Management's Winnemucca District and Surprise Resource Area, northwest Nevada and northeast California: U.S. Geological Survey Open–File Report 94–712, 101 p.

Doebrich, J.L., and Theodore, T.G., 1995, Geology and ore deposits of the Battle Mountain mining district, Nevada: an overview [abs.], in Geology and Ore Deposits of the American Cordillera, A symposium: Reno, Nevada, Nevada Geological Society, Program with Abstracts, p. 24.

Doebrich, J.L., and Theodore, T.G., 1996, Geologic history of the Battle Mountain Mining District, Nevada, and regional controls on the distribution of mineral systems, in Coyner, A.R., and Fahey, P.L., eds., Geology and ore deposits of the American Cordillera: Reno, Nevada, Geological Society of Nevada, Symposium Proceedings, Reno/Sparks, Nevada, April, 1995, p. 453–483.

Doebrich, J.L., Wotruba, P.R., Theodore, T.G., McGibbon, D.H., and Felder, R.P., 1995, Field guide for geology and ore deposits of the Battle Mountain Mining District, Humboldt and Lander Counties, Nevada, Field Trip H: Reno, Nevada, Geological Society of Nevada, Geology and Ore Deposits of the American Cordillera, A Symposium, 92 p.

Doebrich, J.L., Wotruba, P.R., Theodore, T.G., McGibbon, D.H., and Felder, R.P., 1996, Field trip guidebook for Trip H–Geology and ore deposits of the Battle Mountain Mining District, in Green, S.M., and Struhsacker, Eric, eds., Field Trip Guidebook Compendium: Reno, Nevada, Geological Society of Nevada, Geology and Ore Deposits of the American Cordillera, p. 327–388.

Dohrenwend, J.C., Schell, B.A., Menges, C.M., Moring, B.C., and McKittrick, M.A., 1996, Reconnaissance photogeologic map of young (Quaternary and late Tertiary) faults in Nevada, in Singer, D.A., ed., An analysis of Nevada's metal-bearing mineral resources: Nevada Bureau of Mines and Geology Open-file Report 96-2, p. 9-1–9-12.

Drew, L.J., and Berger, B.R., 2002, Application of the porphyry copper/polymetallic vein kin deposit system to mineral-resource assessment in the Mátra Mountains, northern Hungary, in Fabbri, A.G., Gaál, G., and McCammon, R.B., eds., Deposit and Geoenvironmental Models for Resource Exploitation and Environmental Security: Boston, Kluwer Academic Publishers, p. 171-186.

Drews–Armitage, S.P., Romberger, S.B., Whitney, C.G., 1996, Clay alteration and gold deposition in the Genesis and Blue-star deposits, Eureka County, Nevada: Economic Geology, v. 91, p. 1383–1393.

Eaton, G.P., Wahl, R.R., Prostka, H.J., Mabey, D.R., and Kleinkopf, M.D., 1978, Regional gravity and tectonic patterns: Their relation to late Cenozoic epeirogeny and lateral spreading in the western Cordillera, in, Smith, R.B., and Eaton, G.P., eds., Cenozoic Tectonics and Regional Geophysics of the Western Cordillera: Geological Society of America Memoir 152, p. 51–91.

Ebert, S.W., and Rye, R.O., 1997, Secondary precious metal enrichment by steam-heated fluids in the Crofoot-Lewis hot spring gold-silver deposit and relation to paleoclimate: Economic Geology, v. 92, p. 578-600.

Eckstrand, O.R., 1984, 12.2 Gabbroid-associated nickel, copper, platinum group elements, in Eckstrand, O.R., ed., Canadian mineral deposit types: A geological synopsis: Geological Survey of Canada Economic Geology Report 36, p. 41–42.

Einaudi, M.T., 1982, Description of skarns associated with porphyry copper plutons, southwestern North America, in Titley, S.R., ed., Advances in geology of the porphyry copper deposits: Tucson, Arizona, The University of Arizona Press, p. 139–183.

Einaudi, M.T., 2000, Skarns of the Yerington District, Nevada: A trip log and commentary, in Dilles, J.H., Barton, M.D., Johnson, D.A., Proffett, J.M., and Einaudi, M.T., eds., Contrasting styles of intrusion-associated hydrothermal systems, Part 1: Society of Economic Geologists, Guidebook Series, v. 32, p. 101–126.

Einaudi, M.T., and Burt, D.M., 1982, Introduction—terminology, classification, and composition of skarn deposits: Economic Geology, v. 77, p. 745–754.

Einaudi, M.T., Meinert, L.D., and Newberry, R.S., 1981, Skarn deposits, in Skinner, B.J., ed., Seventy-Fifth Anniversary Volume: Economic Geology Publishing Co., p. 317–391.

Emslie, R.F., 1985, Proterozoic anorthosite massifs, *in* Tobi, A.C., and Touret, J.L.R., eds., The deep Proterozoic crust in the North Atlantic Provinces: Dordrecht, D. Reidel Publishing Co., p. 39–60.

Erickson, R.L., and Marsh, S.P., 1974a, Geologic quadrangle map of the Iron Point quadrangle, Humboldt County, Nevada: U. S. Geological Survey Geologic Quadrangle Map GQ-1175, scale 1:24,000.

Erickson, R.L., and Marsh, S.P., 1974b, Geologic map of the Golconda quadrangle, Humboldt County, Nevada: U.S. Geological Survey Geologic Quadrangle Map GQ-1174, scale 1:24,000.

Erickson, R. L., and Marsh, S. P., 1974c, Geochemical, areomagnetic, and generalized geologic maps showing distribution and abundance of tungsten and bismuth, Brooks Springs Quadrangle, Humboldt and Lander Counties, Nevada: U.S. Geological Survey Miscellaneous Field Studies Map MF-567.

Erickson, R.L., Marranzino, A.P., Uteana, O., and Janes, W.W., 1964, Geochemical exploration near the Getchell Mine, Humboldt County, Nevada: U.S. Geological Survey Bulletin 1198–A, 26 p.

Espenshade, G.H., 1972, Geology of the Moxie Pluton in the Moosehead Lake-Jo-Mary Mountain area, Piscataquis County, Maine: U.S. Geological Survey Bulletin 1340, 40 p.

Evans, J.G., 1980, Geology of the Rodeo Creek NE and Welches Canyon quadrangles, Eureka County, Nevada: U.S. Geological Survey Bulletin, 1473, 81 p., 1 sheet [1:24,000].

Evans, J.G., and Theodore, T.G., 1978, Deformation of the Roberts Mountains allochthon in north–central Nevada: U.S. Geological Survey Professional Paper 1060, 18 p.

Felder, R.P., 2000, Geology, mineralization, and exploration history of the Trenton Canyon project, *in* Theodore, T.G., Geology of pluton–related gold mineralization at Battle Mountain, Nevada: Tucson, Arizona, University of Arizona and U.S. Geological Survey Center for Mineral Resources, Monograph 2, p. 240–246.

Ferdock, G.C., Castor, S.B., Leonardson, R.W., And Collins, T., 1997, Mineralogy and paragenesis of ore stage mineralization in the Betze Au deposit, Goldstrike Mine, Eureka County, Nevada, *in* Vikre, Peter, Thompson, T.B., Bettles, K., Christensen, Odin, And Parratt, R., eds., Carlin-Type Au Deposits Field Conference, Economic Geology Guidebook Series, v. 28, p. 75–86.

Ferguson, H.G., 1939, Nickel deposits in Cottonwood Canyon, Churchill County, Nevada: Nevada Bureau of Mines and Geology Bulletin 33, no. 5, 21 p.

Findlay, D.C., 1969, Origin of the Tulameen ultramafic-gabbro complex, southern British Columbia: Canadian Journal of Earth Sciences, v. 6, p. 399–425.

Folger, H.W., 2000, Analytical results and sample locations of reanalyzed NURE stream-sediment and soil samples for the Humboldt River Basin mineral-environmental assessment, northern Nevada: U.S. Geological Survey Open-File Report 2000-421, 1 CD-ROM.

Foo, S.T., Hays, Jr., R.C., and McCormack, J.K., 1996b, Geology and mineralization of the Pipeline Au deposit, Lander County, Nevada, *in* Coyner, A.R., and Fahey, P.L., Eds., Geology and Ore Deposits of the American Cordillera: Geological Society Of Nevada Symposium Proceedings, Reno/Sparks, Nevada, April, 1995, p. 95–109.

Foo, S.T., Hays, R.C., Jr., and McCormack, J.K., 1996a, Geology and mineralization of the South Pipeline Au deposit, Lander County, Nevada, *in* Coyner, A.R., and Fahey, P.L., eds., Geology and Ore Deposits of the American Cordillera: Geological Society of Nevada Symposium Proceedings, Reno/Sparks, Nevada, April, 1995, p. 111–121.

Foster, J.M., and Kretschmer, E.L., 1991, Geology of the Mag deposit, Pinson Mine, Humboldt County, Nevada, *in* Raines, G.L., Lisle, R.W., Schafer, R.W., and Wilkinson, W. H., eds., Geology and Ore Deposits of the Great Basin, Reno: Geological Society of Nevada, Symposium Proceedings, v. 2, p. 845–856.

Fournier, R.O., 1967, The porphyry copper deposit exposed in the Liberty open-pit mine near Ely, Nevada, Part I: Syngenetic formation: Economic Geology, v. 62, p. 57–81.

Gain, S.B., 1985, The geologic setting of the platiniferous UG–2 chromitite layer on the Farm Maandagshoek, eastern Bushveld Complex: Economic Geology, v. 80, no. 4, p. 925–943.

Gain, S.B., and Mostert, A.B., 1982, The geological setting of the platinoid and base metal sulfide mineralization in the Platreef of the Bushveld Complex in Drenthe, North of Potgietersrus: Economic Geology, v. 77, no. 6, p. 1,395–1,404.

Garside, L.J., and Davis, D.A., 1992, A mineral inventory of the Nevada portion of the Cedarville resource area, Susanville Bureau of Land Management District, Nevada: Nevada Bureau of Mines and Geology Open-File Report, 126 p.

Garside, L.J., and Schilling, J.H., 1979, Thermal waters of Nevada: Nevada Bureau of Mines and Geology Bulletin 91, 163 p.

Gehrels, G.E., and Dickinson, W.R., 2000, Detrital zircon geochronology of the Antler overlap and foreland basin assemblages, Nevada, *in* Sorgehan, M.J., and Gehrels, G.E., eds., Paleozoic and Triassic paleogeography and tectonics of western Nevada and northern California: Geological Society of Nevada Special Paper 347, p. 57-63.

Gehrels, G.E., Dickinson, W.R., Riley, B.C.D., Finney, S.C., and Smith, M.T., 2000, Detrital zircon geochronology of the Roberts Mountains allochthon, Nevada, *in* Sorgehan, M.J., and Gehrels, G.E., eds., Paleozoic and Triassic paleogeography and tectonics of western Nevada and northern California: Geological Society of Nevada Special Paper 347, p. 19-42.

Gilluly, James, and Masursky, Harold, 1965, Geology of the Cortez quadrangle, Nevada, with a section on Gravity and aeromagnetic surveys by D.R. Mabey: U.S. Geological Survey Bulletin 1175, 117 p.

Gleason, J.D., Barton, M.D., Marikos, M.A., and Johnson, D.A., 1994, Nd–Sr isotopic study of REE–rich Fe–oxide mineralization in the Great Basin: Evidence for REE sources and mobility in contrasting mid-Jurassic magmatic-hydrothermal systems [abs.]: Supplement to Eos, Transactions, American Geophysical Union, 1994 Fall Meeting, v. 75, no. 44, p. 738.

Glen, J.M.G., and Ponce, D.A., 2000, Large-scale geologic patterns point to the birth of a hotspot in the northwest U.S. [abs]: Eos (Transactions, American Geophysical Union), v. 81, no. 48, p. F1217.

Godson, R.H., and Plouff, Donald, 1988, BOUGUER version 1.0, a microcomputer gravity-terrain-correction program: U.S. Geological Survey Open-File Report 88-644-A, Documentation, 22 p.; 88-644-B, Tables, 61 p., 88-644-C, 5 1/4-inch diskette.

Goff, J. A., Heizler, M. T., McIntosh, W. C., and Norman, D. I., 1997, $^{40}Ar/^{39}Ar$ dating and mineral paragenesis for Carlin–type gold deposits along the Getchell trend: evidence for Cretaceous and Tertiary gold mineralization: Economic Geology, v. 92, p. 601–622.

Goldfarb, R.J., Phillips, G.N., and Nokleberg, W.J., 1998, Tectonic setting of synorogenic gold deposits of the Pacific Rim: Ore Geology Reviews, v. 13, p. 185-218.

Goldstrand, P.M., and Schmidt, K.W., 2000, Geology, mineralization, and ore controls at the Ken Snyder gold-silver mine, Elko County, Nevada, *in* Cluer, J.K., Price, J.G., Struhsacker, E.M., Hardyman, R.F., and Morris, C.L., eds., Geology and ore deposits 2000: The Great Basin and Beyond: Geological Society of Nevada Symposium Proceedings, May 15-18, 2000, p. 265-287.

Gostyayeva, Natalya, Theodore, T.G., and Lowenstern, J.B., 1996, Implications of fluid-inclusion relations in the Elder Creek porphyry copper system, Battle Mountain Mining District, Nevada: U.S. Geological Survey Open-File Report 96–268, 60 p.

Graney, J.R., and McGibbon, D.H., 1991, Geological setting and controls on gold mineralization in the Marigold Mine area, Nevada, *in* Raines, G.L., Lisle, R.W., Schafer, R.W., and Wilkinson, W. H., eds., Geology and Ore Deposits of the Great Basin. Reno: Geological Society of Nevada, Symposium Proceedings, v. 2, p. 865–874.

Grauch, V.J.S., 1986, Regional aeromagnetic and gravity data of northern Nevada: Relation to tectonics and disseminated gold deposits: Terra Cognita, v. 6, no. 3, p. 496–497.

Grauch, V.J.S., 1998, Crustal structure and its relation to gold belts in north-central Nevada: Overview and progress report, *in* Tosdal, R.M., ed., Contributions to the gold metallogeny of the northern Great Basin: U.S. Geological Survey Open-File Report 98–338, p. 34–37.

Grauch, V.J.S., and Bankey, Viki, 1991, Preliminary results of aeromagnetic studies of the Getchell disseminated gold deposit trend, Osgood Mountains, North central Nevada, *in* Raines, G.L., Lisle, R.W., Schafer, R.W., and Wilkinson, W. H., eds., Geology and Ore Deposits of the Great Basin: Reno, Geological Society of Nevada, Symposium Proceedings, v. 2, p. 781–791.

Grauch, V.J.S., Jachens, R.C., and Blakely, R.J., 1995, Evidence for a basement feature related to the Cortez disseminated gold trend and implications for regional exploration in Nevada: Economic Geology, v. 90, p. 203-207.

Grauch, V.J.S., Klein, D.P., and Rodriguez, B.D., 1998, Progress on understanding the crustal structure near the Battle Mountain-Eureka mineral trend from geophysical constraints, *in* Tosdal, R.M., ed., Contributions to the gold metallogeny of northern Nevada: U.S. Geological Survey Open-File Report 98-338, p. 8-14.

Greene, R.C., 1976, Volcanic rocks of the McDermitt caldera, Nevada-Oregon: U.S. Geological Survey Open-File Report 76-753, 80 p.

Greene, R.C., 1984, Geologic appraisal of the Charles Sheldon Wilderness Study Area, Nevada and Oregon: U.S. Geological Survey Bulletin 1538-A, p. 13-34.

Greene, R.C., and Plouff, D., 1981, Location of a caldera source for the Soldier Meadow Tuff, northwestern Nevada, indicated by gravity and aeromagnetic data: Geological Society of America Bulletin, Part I, v. 92, p. 4-6 and Part II, v. 92, p. 39-56.

Griffiths, J.C., and Smith, C.M., Jr., 1992, Mineral resources versus geologic diversity in small areas: Computers and Geosciences, v. 18, p. 477–486.

Gustafson, L.B., Einaudi, M.T., and Dilles, J.H., 1999, Porphyry Cu–Mo–Au deposits; geologic understanding and discovery [abs.]: Geological Society of America, Abstracts with Programs, v. 31, no. 7, p. 22.

Hallof, P.G., 1982, Reconnaissance and detailed geophysical results, Granite Mountain area, Pershing County, Nevada: Global Tectonics and Metallogeny, v. 1, no. 4, p. 374–400.

Hammer, Sigmund, 1939, Terrain corrections for gravimeter stations: Geophysics, v. 4, p. 184-194.

Hastings, J.S., Burkart, T.H., and Richardson, R.W., 1988, Geology of the Florida Canyon gold deposit, Pershing County, Nevada, *in* Schafer, R.W., Cooper, J.J., and Vikre, P.G., eds., Bulk mineable precious metal deposits of the western United States, Symposium Proceedings, Reno: Geological Society of Nevada, p. 433-452.

Hatton, C.J., and Von Gruenewaldt, Gerhard, 1990, Early Precambrian layered intrusions, *in* Hall, R.P., and Hughes, D.J., eds., Early Precambrian basic magmatism: London, Blackie & Son Ltd., p. 56–82.

Haughton, D.R., Roeder, P.L., and Skinner, B.J., 1974, Solubility of sulfur in mafic magmas: Economic Geology, v. 69, p. 451–467.

Hausen, D.M., and Kerr, P.F., 1966, Fine gold occurrence at Carlin, Nevada: Economic Geology, v. 61, no. 8, p. 1468–1469.

Hayford, J.F., and Bowie, William, 1912, The effect of topography and isostatic compensation upon the intensity of gravity: U.S. Coast and Geodetic Survey Special Publication no. 10, 132 p.

Hays, R.C., Jr., and Foo, S.T., 1991, Geology and mineralization of the Gold Acres deposit, Lander County, Nevada, *in* Raines, G.L., Lisle, R.E., Schafer, R.W., and Wilkinson, W.H., eds., Geology and Ore Deposits of the Great Basin: Geologic Society of Nevada Symposium Proceedings, Reno/Sparks, Nevada, April, 1990, p. 677–685.

Heald, P., Foley, N.K., and Hayba, D.O., 1987, Comparative anatomy of volcanic-hosted epithermal deposits; acid-sulfate and adularia-sericite types: Economic Geology, v. 82, p. 1-26.

Hedenquist, J.W., and Lowenstern, J.B., 1994, The role of magmas in the formation of hydrothermal ore deposits: Nature, v. 370, p. 519–527.

Hedenquist, J.W., Arribas R., A., and Gonzalez-Urien, E., 2000, Exploration for epithermal gold deposits, *in* Hagemann, S.G., and Brown, P.E., eds., Gold in 2000: Society of Economic Geologists, Reviews in Economic Geology, v. 13, p. 245-277.

Henry, C.D., and Faulds, J.E., 1999, Geologic map of the Emigrant Pass quadrangle, Nevada: Nevada Bureau of Mines and Geology Open-File Report 99-9, scale 1:24,000.

Henry, C.D., and Ressel, M.W., 2000a, Eocene magmatism of northeastern Nevada: the smoking gun for Carlin-type gold deposits, *in* Cluer, J.K., Price, J.G., Struhsacker, E.M., Hardyman, R.F., and Morris, C.L., eds., Geology and Ore Deposits 2000: the Great Basin and Beyond: Geological Society of Nevada Symposium Proceedings, May 15–18, 2000, p. 365–388.

Henry, C.D., and Ressel, M.W., 2000b, Interpretation of Eocene magmatism, extension, and Carlin–type gold deposits in northeastern Nevada, *in* Lageson, D.R., Peters, S.G., and Lahren, M.M., eds., Great Basin and Sierra Nevada: Boulder, Colorado, Geological Society of America Field Guide 2, p. 165–187.

Henry, C.D., Boden, D.R., and Castor, S.B., 1998, Geology and mineralization of the Eocene Tuscarora volcanic field, Elko County, Nevada, *in* Tosdal, R.M., ed., Contributions to the gold metallogeny of northern Nevada: U.S. Geological Survey Open-File Report 98-338, p. 279-290.

Hess, F.L., 1911, Tungsten: U.S. Geological Survey Mineral Resources of the United States, 1909, Part I, p. 579–580.

Hess, F.L., and Larson, E.S., 1921, Contact-metamorphic tungsten deposits of the United States: U.S. Geological Survey Bulletin 725–D, p. D245–D309.

Hess, F.L., 1917, Tungsten minerals and deposits: U.S. Geological Survey Bulletin 652, p. 1–85.

Hildenbrand, T.G., Berger, Byron, Jachens, R.C., and Ludington, Steve, 2000, Regional crustal structures and their relationship to the distribution of ore deposits in the western United States based on magnetic and gravity data: Economic Geology, v. 95, no. 8., p. 1583–1603.

Hildenbrand, T.G., Berger, Byron, Jachens, R.C., and Ludington, Steve, 2001, Utility of magnetic and gravity data in evaluating regional controls on mineralization: Examples from the western United States, *in* Richards, J.P., and Tosdal, R.M., eds., Structural controls on ore genesis: Reviews in Economic Geology, v. 14, p. 75–109.

Hildenbrand, T.G., and Kucks, R.P., 1988, Total intensity magnetic anomaly map of Nevada: Nevada Bureau of Mines and Geology Map 93A, scale 1:750,000.

Hill, J.M., 1912, The mining districts of the western United States: U.S. Geological Survey Bulletin 507, 309 p.

Hill, R.H., Adrian, B.M., Bagby, W.C., Bailey, E.A., Goldfarb, R.J., and Pickthorn, W.J., 1986, Geochemical data for rock samples collected from selected sediment-hosted disseminated precious metal deposits in Nevada: U.S. Geological Survey Open–File Report 86–107, 30 p.

Hitchborn, A.D., Arbonies, D.G., Peters, S.G., Connors, K.A., Noble, D.C., Larson, L.T., Beebe, J.S., and McKee, E.H., 1996, Geology and gold deposits of the Bald Mountain Mining District, White Pine County, Nevada, *in* Coyner, A.R., and Fahey, P.L., eds., Geology and Ore Deposits of the American Cordillera, Symposium Proceedings, Geological Society of Nevada, Reno/Sparks, Nevada, April, 1995, p. 505–546.

Hobbs, S.W., and Clabaugh, S.E., 1946, Tungsten Deposits of the Osgood Range, Humboldt County, Nevada: Nevada Bureau Mines and Geology Bulletin 44, 32 p.

Hobbs, S.W., and Elliott, J.E., 1973, Tungsten: U.S. Geological Survey Professional Paper 820, p. 667–678.

Hofstra, A.H., 1994, Geology and genesis of the Carlin-type gold deposits in the Jerritt Canyon district, Nevada: Boulder, University of Colorado, Ph.D. dissertation, 719 p.

Hofstra, A.H., 1997, Isotopic composition of sulfur in Carlin–type gold deposits: implications for genetic models, *in* Vikre, Peter, Thompson, T.B., Bettles, K., Christensen, Odin, And Parratt, R., eds., Carlin-Type Gold Deposits Field Conference, Economic Geology Guidebook Series, v. 28, p. 119–131.

Hofstra, A.H., and Cline, J.S., 2000, Characteristics and models for Carlin-type gold deposits, *in* Hagemann, S.G., and Brown, P.E., eds, Gold in 2000: Society of Economic Geology, Reviews in Economic Geology, v. 13, p. 163–220.

Hofstra, A.H., and Rye, R.O., 1998, δD and δ^{18}O data from Carlin–type Au deposits–implications for genetic models, *in* Tosdal, R.M., ed., Contributions to the Au Metallogeny of Northern Nevada: U.S. Geological Survey Open–File Report 98–338, p. 202–210.

Hofstra, A.H., Daly, W.E., Birak, D.J., and Doe, T.C., 1991a, Geologic framework and genesis of Carlin–type gold deposits in the Jerritt Canyon District, Nevada, USA, *in* Ladeiro, E.A., ed., Brazil gold '91; the economics, geology, geochemistry, and genesis of gold deposits: Rotterdam, Netherlands, A.A. Balkema, Proceedings, p. 77–87.

Hofstra, A.H., Leventhal, J.S., Northrop, H.R., Landis, G.P., Rye, R.O., Birak, D.J., and Dahl, A.R., 1991b, Genesis of sediment-hosted disseminated-Au deposits by fluid mixing and sulfidization: chemical-reaction-path modeling of ore-depositional processes documented in the Jerritt Canyon District, Nevada: Geology, v. 19, p. 36–40.

Hofstra, A.H., Snee, L.W., Rye, R.O., Folger, H.W., Phinesey, J.D., Loranger, R.J., Dahl, A.R., Naeser, C.W., Stein, H.J., and Lewchuk, M., 1999, Age constraints on Jerritt Canyon and other Carlin-type gold deposits in the western United States–Relationship to mid-Tertiary extension and magmatism: Economic Geology, v. 94, no. 6, p. 769–794.

Hollister, V.F., 1978, Geology of the porphyry copper deposits of the western hemisphere: New York, Society of Mining Engineers, 219 p.

Hoover, D.B., Grauch, V.J.S., Pitkin, J.A., Krohn, D., and Pierce, H.A., 1991, Getchell trend airborne geophysics–an integrated airborne geophysical study along the Getchell Trend of gold deposits, north central Nevada, *in* Raines, G.L., Lisle, R.W., Schafer, R.W., and Wilkinson, W. H., eds., Geology and Ore Deposits of the Great Basin: Reno, Geological Society of Nevada, Symposium Proceedings, v. 2, p. 739–758.

Hoover, D.B., Heran, W.D., and Hill P.L., eds., 1992, The geophysical expression of selected mineral deposit models: U.S. Geological Open–File Report 92–557, 128 p.

Hose, R.K., Blake, M.C., Jr., and Smith, R.M., 1976, Geology and mineral resources of White Pine County, Nevada: Nevada Bureau of Mines and Geology Bulletin 85, 105 p.

Hotz, P.E., and Willden, Ronald, 1964, Geology and mineral deposits of the Osgood Mountains quadrangle, Humboldt County, Nevada: U.S. Geological Survey Professional Paper 431, 128 p.

Houston, R.S., Duebendorfer, E.M., Karlstrom, K.E., and Premo, W.R., 1989, A review of the geology and structure of the Cheyenne belt and Proterozoic rocks of southern Wyoming, *in* Grambling, J.A., and Tewksbury, B.J., eds., Proterozoic geology of the southern Rocky Mountains: Geological Society of America Special Paper 235, p. 1–12.

Howard, K.A., 1966, Structure of the metamorphic rocks of the northern Ruby Mountains, Nevada: New Haven, Connecticut, Yale University, Ph.D. dissertation, 170 p.

Howard, K. A., 1980, Metamorphic infrastructure in the northern Ruby Mountains, Nevada, *in* Crittenden, M. D., Jr., Coney, P. J., and Davis, G. H., eds., Cordilleran metamorphic core complexes: Geological Society of America Memoir 153, p. 335-347.

Howard, K.A., Kistler, R.W., Snoke, A.W., and Wilden, R., 1979, Geologic map of the Ruby Mountains: U.S. Geological Survey Miscellaneous Investigations Series Map I-1136, scale 1:125,000.

Howe, S.S., Theodore, T.G., and Arehart, G.B., 1995, Sulfur and oxygen isotopic composition of vein barite from the Marigold Mine and surrounding area, north-central Nevada Application to gold exploration [abs.]: Geological Society of Nevada, Geology and ore deposits of the American Cordillera, Symposium Program with Abstracts, p. 39.

Hulbert, L.J., Duke, J.M., Eckstrand, O.R., Lydon, J.W., Scoates, R.F.J., Cabri, L.J., and Irvine, T.N., 1988, Geological environments of the platinum group elements: Geological Survey of Canada Open–File Report 1440, 148 p.

Ilchik, R.P., and Barton, M.D., 1997, An amagmatic origin of the Carlin-type gold deposits: Economic Geology, v. 92, p. 269–288.

International Union of Geodesy and Geophysics, 1971, Geodetic reference system 1967: International Association of Geodesy Special Publication no. 3, 116 p.

Irvine, T.N., 1974, Petrology of the Duke Island Ultramafic Complex, southeastern Alaska: Geological Society of America Memoir 138, 240 p.

Irvine, T.N., 1987, Appendix II. Processes involved in the formation and development of layered igneous rocks, *in* Parsons, Ian, ed., Origins of Igneous Layering: Dordrecht, D. Reidel Publishing Company, p. 649-656.

Irvine, T.N., Keith, D.W., and Todd, S.G., 1983, The J–M platinum-palladium reef of the Stillwater Complex, Montana: II. Origin by double diffusive convective magma mixing and implications for the Bushveld Complex: Economic Geology, v. 78, p. 1287–1334.

Ivosevic, S.W., and Theodore, T.G., 1996, Weakly developed porphyry system at upper Paiute Canyon, Battle Mountain Mining District, Nevada, *in* Coyner, A.R., and Fahey, P.L., eds., Geology and ore deposits of the American Cordillera, Symposium Proceedings, Geological Society of Nevada, Reno/Sparks, Nevada, April, 1995, v. 3, p. 1573–1594.

Jachens, R.C., Moring, B.C., and Schruben, P.G., 1996, Chapter 2 – Thickness of Cenozoic deposits and the isostatic residual gravity over basement, *in* Singer, D.A., ed., An analysis of Nevada's metal-bearing mineral resources: Nevada Bureau of Mines and Geology Open-File Report 96–2, [ftp://ftp.nbmg.unr.edu/NBMG/ofr962/index.htm].

Jachens, R.C., Simpson, R. W., Blakely, R. J., and Saltus, R. W., 1989, Isostatic residual gravity and crustal geology of the United States, *in* Pakiser, L.C., and Mooney, W.D., eds., Geophysical Framework of the Continental United States: Geological Society of America Memoir 172, p. 405–424.

Jachens, R.C., and Moring, B.C., 1990, Maps of the thickness of Cenozoic deposits and the isostatic residual gravity over basement for Nevada: U.S. Geological Survey Open-File Report 90-404, 15 p.

Jachens, R.C., and Moring, B.C., 1990, Maps of the thickness of Cenozoic deposits and the isostatic residual gravity over basement for Nevada: U.S. Geological Survey Open–File Report 90–404, 15 p.

Jachens, R.C., Moring, B.C., and Schruben, P.G., 1996, Thickness of Cenozoic deposits and the isostatic residual gravity over basement for Nevada, *in* Singer, D.A., ed., An analysis of Nevada's metal-bearing mineral resources: Nevada Bureau of Mines and Geology Bulletin Open-file Report 96-2, p. 2-1 to 2-22, 1 sheet, scale 1:1,000,000.

Jachens, R.C., and Roberts, C.W., 1981, Documentation of a FORTRAN program, 'isocomp', for computing isostatic residual gravity: U.S. Geological Open-File Report 81-574, 26 p.

James, L.P., 1976, Zoned alteration in limestone at porphyry copper deposits, Ely, Nevada: Economic Geology, v. 71, p. 488–512.

Jensen, E.P., and Barton, M.D., 2000, Gold deposits related to alkaline magmatism, *in* Hagemann, S.G., and Brown, P.E., eds, Gold in 2000: Society of Economic Geology, Reviews in Economic Geology, v. 13, p. 279–314.

John, D.A., 2000, Magmas and Miocene low-sulfidation Au-Ag deposits in the northern Great Basin [abs.]: Geological Society of America, Abstracts with Programs, v. 32, no. 7, p. 250.

John, D.A., 2001, Miocene and Early Pliocene epithermal gold-silver deposits in the northern Great Basin, western USA: Characteristics, distribution, and relationship to magmatism: Economic Geology (in press, December 2001 issue).

John, D.A. and Bliss, J.D., 1994, Grade and tonnage model of tungsten skarn deposits, Nevada: U.S. Geological Survey Open-File Report 94–005, 35 p.

John, D.A., Brummer, J.E., Saderholm, E.C., and Fleck, R.J., 2000a, Geology of the Mule Canyon gold-silver deposit, Lander County, Nevada, *in* Wallace, A.R., and John, D.A., eds., Volcanic history, structure, and mineral deposits of the north-central northern Nevada rift: Field Trip Guidebook No. 8, Geological Society of Nevada Symposium 2000, The Great Basin and Beyond, p. 119-134.

John, D.A., Garside, L.J., and Wallace, A.R., 1999, Magmatic and tectonic setting of late Cenozoic epithermal gold-silver deposits in northern Nevada, with an emphasis on the Pah Rah and Virginia Ranges and the northern Nevada rift, *in* Kizis, J.A., Jr., ed., Low-sulfidation gold deposits in northern Nevada: Geological Society of Nevada, 1999 Spring Field Trip Guidebook, Special Publication No. 29, p. 64-158.

John, D.A., and Sherlock, M.G., 1991, Map showing mines and prospects in the Reno 1° x 2° quadrangle, Nevada and California: U.S. Geological Survey Miscellaneous Field Studies Map MF–2154–B, 14 p.

John, D.A., Stewart, J.H., Kilburn, J.E., Silberling, N.J., and Rowan, L.C., 1993, Geology and mineral resources of the Reno 1° x 2° quadrangle, Nevada and California: U.S. Geological Survey Bulletin 2019, 65 p.

John, D.A., and Wallace, A.R., 2000, Epithermal gold-silver deposits related to the northern Nevada rift, *in* Cluer, J.K., Price, J.G., Struhsacker, E.M., Hardyman, R.F., and Morris, C.L., eds., Geology and Ore Deposits 2000: The Great Basin and Beyond: Geological Society of Nevada Symposium Proceedings, May 15-18, 2000, p. 155-175.

John, D.A., Wallace, A.R., Ponce, D.A., Fleck, R.J., and Conrad, J.E., 2000, New perspectives on the geology and origin of the northern Nevada rift, *in* Cluer, J.K., Price, J.G., Struhsacker, E.M., Hardyman, R.F., and Morris, C.L., eds., Geology and Ore Deposits 2000: The Great Basin and Beyond: Geological Society of Nevada Symposium Proceedings, Reno/Sparks, May 15-18, 2000, p. 127-154.

Johnson, A.C., and Benson, W.T., 1963, Tungsten Deposits of Nevada: U.S. Bureau Mines, Open-File Report, 198 p.

Johnson, D.A., and Barton, M.D., 2000, Time-space development of an external brine-dominated, igneous-driven hydrothermal system: Humboldt mafic complex, western Nevada, *in* Dilles, J.H., Barton, M.D., Johnson, D.A., Proffett, J.M., and Einaudi, M.T., eds., Contrasting styles of intrusion-associated hydrothermal systems, Part 1: Society of Economic Geologists, Guidebook Series, v. 32, p. 127–143.

Johnson, K.M., Ludington, Steve, and Gray, K.M., 1986, A peraluminous tungsten-mineralized stock at New York Canyon, Pershing County, Nevada [abs.]: Geological Society of America, Abstracts with Programs, v. 18, no. 2, p. 122.

Johnson, M.G., 1973, The mining districts of Nevada: Economic Geology, v. 24, p. 115–148.

Johnson, M.G., 1977, Geology and mineral deposits of Pershing County, Nevada: Nevada Bureau of Mines and Geology, Bulletin 89, 115 p.

Johnson, T.W., 2000, Metal and mineral zoning at the greater Midas Au–Cu–Ag skarn deposit (Battle Mountain District), Lander County, Nevada, *in* Cluer, J.K., Price, J.G., Struhsacker, E.M., Hardyman, R.F., and Morris, C.L., eds., Geology and ore deposits 2000: The Great Basin and beyond: Geological Society of Nevada Symposium Proceedings, May 15–18, 2000, p. 1083–1106.

Johnson, V.Y., and Keith, J.D., 1991, Petrology and geochemistry of the Springer scheelite skarn deposit, Mill City Nevada, *in* Raines, G.L., Lisle, R.W., Schafer, R.W., and Wilkinson, W. H., eds., Geology and Ore Deposits of the Great Basin, Symposium Proceedings: Reno, Nevada, Geological Society of Nevada, v. 1, p. 553–578.

Johnston, M.K., 2000, Hypogene alteration and ore characteristics at the Cove gold–silver deposit, Lander County, *in* Cluer, J. K., Price, J. G., Struhsacker, E. M., Hardyman, R. F., and Morris, C. L., eds., Geology and Ore Deposits 2000: The Great Basin and Beyond: Geological Society of Nevada Symposium Proceedings, May 15–18, 2000, p. 621–641.

Jones, B.K., 1992, Application of metal zoning to gold exploration in porphyry copper systems: Journal of Geochemical Exploration, v. 43, no. 2, p. 127–155.

Jones, E.L., 1997, Geologic map of the Hot Springs Peak quadrangle and the southeastern part of the Little Poverty quadrangle, Nevada: Nevada Bureau of Mines and Geology Field Studies Map 14, scale 1:24,000.

Jones, R.B., 1983, Lead deposits and occurrences in Nevada: Nevada Bureau of Mines and Geology Map 78, scale 1: 1,000,000.

Jones, R.B., 1984a, Zinc deposits and occurrences in Nevada: Nevada Bureau of Mines and Geology Map 85, scale 1: 1,000,000.

Jones, R.B., 1984b, Hog Ranch gold area: Unpublished Nevada Bureau of Mines and Geology Report, 1 p.

Jones, R.B., 1985, Directory of Nevada mine operations active during 1984, in The Nevada Mineral Industry—1983: Nevada Bureau of Mines and Geology Special Publication MI–1983, 32 p.

Joralemon, Peter, 1951, The occurrence of gold at the Getchell Mine, Nevada: Economic Geology, v. 46, p. 267–310.

Joralemon, Peter, 1975, K–Ar relations of granodiorite emplacement and tungsten and gold mineralization near the Getchell mine, Humboldt County: Economic Geology, v. 70, no. 2, p. 405–406.

Juhas, A.P., 1982, Preliminary geology of the Kennedy porphyry molybdenum-copper district, Pershing County, Nevada: Global Tectonics and Metallogeny, v. 1, no. 4, p. 356–372.

Kaban, M.K., and Mooney, W.D., 2001, Density structure of the lithosphere in the southwestern United States and its tectonic significance: Journal of Geophysical Research, v. 106, no. B1, p. 721–739.

Kane, M.F., and Godson, R.H., 1989, A crust/mantle structural framework of the conterminous United States based on gravity and magnetic trends, *in* Pakiser, L.C., and Mooney, W.D., eds., Geophysical Framework of the Continental United States: Geological Society of America Memoir 172, p. 383–403.

Kelly, W.C., and Rye, R.O., 1979, Geologic, fluid inclusion, and stable isotope studies of the tin-tungsten deposits of Panasqueira, Portugal: Economic Geology, v. 74, no. 8, p. 1721–1822.

Kelson, C.R., Keith, J.D., Christiansen, E.H., and Meyer, P.E., 2000, Mineral paragenesis and depositional model of the Hilltop gold deposit, Lander County, Nevada, *in* Cluer, J.K., Price, J.G., Struhsacker, E.M., Hardyman, R.F., and Morris, C.L., eds., Geology and ore deposits 2000: The Great Basin and beyond: Geological Society of Nevada Symposium Proceedings, May 15–18, 2000, p. 1107–1132.

Kemp, L.D., Bonham-Carter, G.F., Raines, G.L. and Looney, C.G., 2001, Arc-SDM: Arcview extension for spatial data modelling using weights of evidence, logistic regression, fuzzy logic and neural network analysis, [http://ntserv.gis.nrcan.gc.ca/sdm/].

Kepper, J.C., Lugaski, T.P., and Aymard, W., 1991, Precious metal deposits, structural blacks and volcanism in the central structural zone, *in*, Raines, G.L., Lisle, R.E., Schafer, R.W., and Wilkinson, W.H., eds., Geology and Ore Deposits of the Great Basin, Symposium Proceedings Volume 1: Geological Society of Nevada, Reno/Sparks, Nevada, p. 213–234.

Kerr, P.F., 1934, Geology of tungsten deposits near Mill City, Nevada: Nevada Bureau of Mines and Geology Bulletin 21, 46 p.

Kerr, P.F., 1940, Tungsten-bearing manganese deposit at Golconda, Nevada: Geological Society America Bulletin, v. 51, p. 1,359–1,390.

Kerr, P.F., 1946, Tungsten mineralization in the United States: Geological Society of America Memoir 15, 241 p.

Ketner, K.B., 1977, Late Paleozoic orogeny and sedimentation, southern California, Nevada, Idaho, and Montana, *in* Stewart, J.H., Stevens, C.H., and Fritsche, A.E., eds., Paleozoic Paleogeography of the western United States: Pacific Section, SEPM, p. 363-369.

Ketner, K.B., Murchey, B.L., Stamm, R.G., and Wardlaw, B.R., 1993, Paleozoic and Mesozoic rocks of Mount Icabod and Dorsey Canyon, Elko County, Nevada—evidence for post–Early Triassic emplacement of the Roberts Mountains and Golconda allochthons: U.S. Geological Survey Bulletin 1988–D, 12 p.

King, H.D., 1996, Interpretation of reconnaissance geochemical data from the Bureau of Land Management's Winnemucca District and Surprise Resource Area, northwest Nevada and northeast California: U.S. Geological Survey Open–File Report 96–533, 36 p.

King, H.D., Feyl, D.L., Motooka, J.M., Knight, R.J., Roushey, B.H., and McGuire, D.J., 1996, Analytical data and sample locality map of stream-sediment and soil samples from the Winnemucca-Surprise Resource Assessment Area, northwest Nevada and northeast California, U.S. Geological Survey Open-file Report 96-062-A (paper version) and -B (diskette version).

King, W.H., and Holmes, G.H., Jr., 1950, Investigation of Nevada-Massachusetts tungsten deposits, Pershing County, Nevada: U.S. Bureau of Mines Report of Investigations 4634, p. 3–4.

Kirkham, R.V., Sinclair, W.D., Thorpe, R.I., and Duke, J.M., eds., 1993, Mineral deposit modeling: Geological Association of Canada, Special Paper 40, 770 p.

Kistler, R.W., and Peterman, Z.E., 1978, Reconstruction of crustal blocks of California on the basis of initial strontium isotopic compositions of Mesozoic granitic rocks: U.S. Geological Survey Professional Paper 1071, 17 p.

Kistler, R.W., and Speed, R.C., 2000, $^{40}Ar/^{39}Ar$, K–Ar, Rb–Sr whole-rock and mineral ages, chemical composition, strontium, oxygen, and hydrogen isotopic systematics of Jurassic Humboldt Lopolith and Permian (?) and Triassic Koipato Group rocks, Pershing and Churchill Counties, Nevada: U.S. Geological Survey Open-File Report 00–0217, 14 p.

Kleinhampl, F.J., and Ziony, J.I., 1984, Mineral resources of northern Nye County, Nevada: Nevada Bureau of Mines and Geology Bulletin 99-B, 243 p.

Klepper, M.R., 1943, Tungsten deposits of the Mill City district, Eugene Mountains, Pershing County, Nevada: U.S. Geological Survey unpublished report, 33 p.

Klopstock, Paul, 1913, The Kennedy mining district, Nevada: American Institute of Mining Engineers Bulletin, v. 77, p. 1041–1046.

Kornhauser, B.A., and Stafford, P.T., 1978, Tungsten: U.S. Bureau of Mines Mineral Commodity Profiles MCP-21, 22 p.

Koschmann, A.H., and Bergendahl, M.H., 1968, Principal gold–producing districts of the United States: U.S. Geological Survey Professional Paper 610, 283 p.

Kotlyar, B.B., Singer, D.A., Jachens, R.C., and Theodore, T.G., 1998a, Regional analysis of the distribution of gold deposits in northeast Nevada using NURE arsenic data and geophysical data, *in* Tosdal, R.M., ed., Contributions to the gold metallogeny of the northern Great Basin: U.S. Geological Survey Open-File Report 98–338, p. 234–242.

Kotlyar, B.B., Theodore, T.G., Singer, D.A., Moss, Ken, Campo, A.M., and Johnson, S.D., 1998b, Geochemistry of the gold skarn environment at Copper Canyon, Nevada, *in* Lentz, D.R., ed., Mineralized intrusion-related skarn systems, Mineralogical Association of Canada Short Course Series, v. 26, p. 415–443.

Kretschmer, E.L., 1984a, Guidebook geology of the Pinson Mine, Humboldt County, Nevada, *in* Slavik, Greta, ed., Geological Society of Nevada 1984 Field Trip Guide: Reno, Nevada, Geological Society of Nevada, 8 p.

Kretschmer, E.L., 1984b, Geology of the Pinson mine, Humboldt County, Nevada, *in* Tingley, J.V., and Bonham, H.F., eds., Sediment-hosted precious-metal deposits of northern Nevada: Nevada Bureau of Mines and Geology, Report 40, p. 52–55.

Kretschmer, E.L., 1991, Geology of the Kramer Hill gold deposit, Humboldt County, Nevada, *in* Raines, G.L., Lisle, R.W., Schafer, R.W., and Wilkinson, W.H., eds., Geology and ore deposits of the Great Basin: Reno, Geological Society of Nevada, Symposium Proceedings, v. 2, p. 857–863.

Kucha, Henryk, 1982, Platinum-group metals in the Zechstein copper deposits, Poland: Economic Geology, v. 77, p. 1578–1591.

Kucha, Henryk, 1983, Precious metal bearing shale from Zechstein copper deposits, Lower Silesia, Poland: Institute of Mining and Metallurgy Transactions, Sec. B, p. B72–B79.

Kuehn, C.A., 1989, Studies of disseminated gold deposits near Carlin, Nevada: Evidence for a deep geologic setting of ore formation: State College, Pennsylvania State University, unpublished Ph.D. dissertation, 395 p.

Kuehn, C.A., And Rose, A.W., 1992, Geology and geochemistry of wall rock alteration at the Carlin Au deposit, Nevada: Economic Geology, v. 87, p. 1697–1721.

Kuehn, C.A., and Rose, A.W., 1995, Carlin Au deposits, Nevada: origin in a deep zone of mixing between normally pressured and over pressured fluids: Economic Geology, v. 90, p. 17–36.

Kutina, Jan, and Bowes, W. A., 1982, Structural criteria defining the Granite Mountain area in NW–Nevada as a target for mineral exploration: Global Tectonics and Metallogeny, v. 1, no. 4, p. 336–354.

Kuyper, B.A., 1988, Geology of the McCoy gold deposit, Lander County, Nevada, *in* Schafer, R.W., Cooper, J.J., and Vikre, P.G., eds., Bulk mineable precious metal deposits of the western United States, Symposium Proceedings: Reno, Nevada, Geological Society of Nevada, April 6–8, 1987, p. 173–185.

Kuyper, B.A., Mach, L.E., Streiff, R.E., and Brown, W.A., 1991, Geology of the Cove gold-silver deposit: Preprint, 1991 Society of Mining Engineers Annual Meeting, 20 p.

Lachenbruch, A.H., and Sass, J.H., 1978, Models of an extending lithosphere and heat flow in the Basin and Range province, *in* Smith, R.B., and Eaton, G.P., eds., Cenozoic tectonics and regional geophysics of the western Cordillera: Geological Society of America Memoir 152, p. 209-250.

Lahren, M.M., Schweickert, R.A., and Connors, K.A., in press, Preliminary map of allochthonous tectonic units in Nevada and eastern California: U.S. Geological Survey Map, scale 1:750,000.

Lahren, M.M., Schweickert, R.A., Connors, K.A., and Ludington, S., 1995, Allochthonous tectonic units of the central and western Great Basin: Geology and Ore Deposits of the America Cordillera, Reno/Sparks, Nevada, 1995, Program with Abstracts, p. A45.

Lamb, J.B., and Cline, J.M., 1997, Depths of formation of the Meikle and Betze/Post deposits, *in* Vikre, P., Thompson, T.B., Bettles, K., Christensen, O, and Parratt, R., eds., Carlin–Type Au Deposits Field Conference: Economic Geology Fieldbook Series, v. 28, p. 101–108.

Lang, J.R., and Baker, Timothy, 2001, Intrusion-related gold systems: The present level of understanding: Mineralium Deposita, v. 36, p. 477–489.

Langel, R.A., IGRF, 1991 revision: Eos, v. 73, no. 16, p. 182. [IGRF, International Geomagnetic Reference Field]

LaPointe, D.D., Tingley, J.V., and Jones, R.B., 1991, Mineral resources of Elko County, Nevada: Nevada Bureau of Mines and Geology Bulletin 106, 236 p.

Larsen, R.K., 2002, Geology and mineralization of the Standard mine, Pershing County, Nevada, *in* Wendt, C., ed., Gold deposits of the Humboldt Range: New discoveries in an old district: Geological Society of Nevada, Special Publication No. 36, p. 73-94.

Lawrence, E.F., 1963, Antimony deposits of Nevada: Nevada Bureau of Mines and Geology Bulletin 61, 248 p.

Leavitt, E.D., Arehart, G.B., and Goldstrand, P.M., 2000, Hydrothermal alteration associated with the Colorado Grande vein, Ken Snyder mine, Elko County, Nevada [abs.]: Geological Society of America, Abstracts with Programs, v. 32, no. 7, p. 251.

LeBlanc, M., and Fischer, W., 1990, Gold and platinum group elements in cobalt-arsenide ores: Hydrothermal concentration from a serpentinite source-rock (Bou Azzer, Morocco): Mineralogy and Petrology, v. 42, p. 197–209.

Lechler, P.J., and Desilets, M.O., 1987, Determination of anions by ion chromatography—Application to pedogeochemical exploration for metallic mineralization, *in* Elliott, I.L., and Smee, B.W., eds., GEOEXPO/86: Exploration in the North American Cordillera: The Association of Exploration Geochemists, Proceedings of a symposium, Vancouver, British Columbia, May 1986, p. 202–208.

Lee, D.E., Kistler, R.W., Friedman, I., and Van Loenen, R.E., 1981, Two-mica granites of northeastern Nevada: Journal of Geophysical Research, v. 86, p. 10607-10616.

Lee, W.T., Stone, R.W., Gale, H.S., and others, 1915, Guidebook of the western United States, Part B. The Overland Route, with a side trip to Yellowstone Park: U.S. Geological Survey Bulletin 612, 251 p.

Lemmon, D.M., and Tweto, O.L., 1962, Tungsten: U.S. Geological Survey Mineral Investigations Resource Map 25.

Leonard, C.S., Mihalasky, M.J., and Peters, S.G., 2002, Chapter 6: Weights-of-evidence analysis of sedimentary rock-hosted Au deposits in the P.R. China, *in* Peters, S.G., ed., Geology, geochemistry, and geophysics of sedimentary rock-hosted Au deposits in P.R. China: U.S. Geological Survey Open-File Report 02-131, 403 p., [http: //geopubs.wr.usgs.gov/open-file/of02-131/].

Leonardson, R.W., and Rahn, J.E., 1996, Geology of the Betze–Post Au deposits, Eureka County, Nevada, *in* Coyner, A.R., and Fahey, eds., Geology and Ore Deposits of the American Cordillera: Geological Society of Nevada, Symposium Proceedings, Reno/Sparks, Nevada, April, 1995, p. 61–94.

Leszcykowski, A.M., 1985, Mineral resources of the North Fork of the Little Humboldt Study Area, Humboldt County, Nevada: U.S. Bureau of Mines Open–File Report MLA 85–47, 8 p.

Li, Zhiping, and Peters, S.G., 1998, Comparative geology and geochemistry of sedimentary- rock-hosted (Carlin-type) gold deposits in the People's Republic of China and in Nevada, USA: U.S. Geological Survey Open-File Report 98-466, (CD-ROM, v. 1.1 with data base), [http: //geopubs.wr.usgs.gov/open-file/of98-466/. (ver. 1.2 updated May, 2000)].

Lightfoot, P.C., and Naldrett, A.J., 1999, Geological and geo-chemical relationships in the Voisey's Bay Intrusion, Nain Plutonic Suite, Labrador, Canada, *in* Keays, R.R., Lesher, C.M., Lightfoot, P.C., and Farrow, C.E.G., eds., Dynamic processes in magmatic ore deposits and their application in mineral exploration: Geological Association of Canada Short Course Notes, v. 13, p. 1–30.

Lincoln, F. C., 1923, Mining districts and mineral resources of Nevada: Reno, Nevada, Newsletter Publishing Company, 265 p.

Lipske, J.L., and Dilles, J.H., 2000, Advanced argillic and ser-icitic alteration in the subvolcanic environment of the Yer-ington porphyry copper system, Buckskin Range, Nevada, *in* Dilles, J.H., Barton, M.D., Johnson, D.A., Proffett, J.M., and Einaudi, M.T., eds., Contrasting styles of intru-sion-associated hydrothermal systems, Part 1: Society of Economic Geologists, Guidebook Series, v. 32, p. 91–100.

Listerud, W.H., and Meineke, D.G., 1977, Mineral resources of a portion of the Duluth Complex and adjacent rocks in St. Louis and Lake Counties, northeastern Minnesota: Minne-sota Department of Natural Resources, Division of Miner-als, Minerals Exploration Section, Report 93, 74 p.

Loucks, R.R., 1991, Platinum-gold and vanadiferous magne-tite mineralization in the Early Proterozoic Lake Owen lay-ered mafic intrusion, Medicine Bow Mountains, Wyoming, *in* Frost, B.R., and Roberts, Sheila, eds., Mineral resources of Wyoming: Wyoming Geological Association 42nd Field Conference Guidebook, p. 37–38.

Loucks, T.A., and Johnson, C.A., 1992, Economic geology, *in* Theodore, T.G., Blake, D.W., Loucks, T.A., and John-son, C.A., 1992, Geology of the Buckingham stockwork molybdenum deposit and surrounding area, Lander County, Nevada: U.S. Geological Survey Professional Paper 798–D, p. D101–D138.

Lowe, N.T., Raney, R.G., and Norberg, J.R., 1985, Principal deposits of strategic and critical minerals in Nevada: U.S. Bureau of Mines Information Circular 9035, 202 p.

Ludington, S., 1986, Descriptive model of Climax Mo depos-its, *in* Cox, D.P., and Singer, D.A., eds., Mineral deposits models: U.S. Geological Survey Bulletin 1693, p. 73–74.

Ludington, S., Cox, D.P., Leonard, K.W., and Moring, B.C., 1996, Cenozoic volcanic geology of Nevada, *in* Singer, D.A., ed., An analysis of Nevada's metal-bearing mineral resources: Nevada Bureau of Mines and Geology Bulletin Open-file Report 96-2, p. 5-1--5-10.

Ludington, S., Cox, D.P., Singer, D.A., Sherlock, M.G., Berger, B.R., and Tingley, J.V., 1993, Spatial and temporal analysis of precious metal deposits for a mineral resource assessment of Nevada, *in* Kirkham, R.V., Sinclair, W.D., Thorpe, R.I., and Duke, J.M., eds., Mineral deposit modeling: Geological Association of Canada Special Paper 40, p. 31-40.

Ludington, S., Folger, H., Hildenbrand, T. G., and Kotlyar, B., 2000, Arsenic distribution in surficial materials of the northern Great Basin [abs.]: Geological Society of America Abstracts with Programs, v. 32, p. A–392.

Ludington, S., and Johnson, K.M., 1986, The New York Canyon tungsten vein system and the probable grade [abs.]: Geological Society of America, Abstracts with Programs, v. 18, no. 2, p. 128.

Mabey, D.R., Oliver, H.W., and Hildenbrand, T.G., 1983, Regional gravity and magnetic anomalies in the northern Basin and Range province: Geothermal Resources Council, Special Report no. 13, p. 307–315.

Macdonald, A.J., 1988, Platinum-group element mineraliza-tion and the relative importance of magmatic and deuteric processes: Field evidence from the Lac des Iles deposit, Ontario, Canada, *in* Prichard, H.M., Potts, P.J., Bowles, J.F.W., and Cribb, S.J., eds., Geo-platinum 87: London and New York, Elsevier Applied Science, p. 215–236.

Macdonald, A.J., Brügmann, G.E., and Naldrett, A.J., 1989, Preliminary results of investigations into magma mixing, fractionation, and deuteric alteration during formation of PGE–rich Ni–Cu mineralization in the Lac des Iles gabbroic complex, Ontario Canada, *in* Prendergast, M.D., and Jones M.J., eds., Magmatic sulphides—the Zimbabwe volume: The Institution of Mining and Metallurgy, p. 139–150.

MacKenzie, W.B., and Bookstrom, A.A., 1976, Geology of the Majuba Hill area, Pershing County, Nevada: Nevada Bureau of Mines and Geology Bulletin 86, 23 p.

Madden–McGuire, D.J., Smith, S.M., Botinelly, T., Silberman, M.L., and Detra, D.E., 1991, Nature and origin of alluvium above the Rabbit Creek gold deposit, Getchell gold belt, Humboldt County, Nevada, *in* Raines, G.L., Lisle, R.W., Schafer, R.W., and Wilkinson, W. H., eds., Geology and Ore Deposits of the Great Basin: Reno, Geological Society of Nevada, Symposium Proceedings, v. 2, p. 895–911.

Madrid, R.J., and Roberts, R.J., 1991, Origin of gold belts in north-central Nevada, *in* Madrid, R.J., Roberts, R.J., and Mathewson, David, eds., Stratigraphy and structure of the Battle Mountain gold belt and their relationship to gold deposits, Field Trip 15, *in* Buffa, R.H., and Coyner, A.R., eds., Geology and ore deposits of the Great Basin: Reno, Nevada, Geological Society of Nevada, Fieldtrip Guidebook Compendium, v. 2, p. 927–939.

Madrid, R.J., Roberts, R.J., Poole, F.G., and Wrucke, C.T., 1992, Rocks of the Antler orogen – The Roberts Mountain allochthon, *in* Poole, F.G., Stewart, J.H., Palmer, A.R., Sandberg, Madrid, R.J., Ross, R.J., Jr., Hintze, L.F., Miller, M.M., and Wrucke, C.T., eds., Chapter 2, latest Precambrian to latest Devonian time; Development of a continental mar-gin, *in* Burchfiel, B.C., Lipman, P.W., and Zoback, M.L., eds. The Cordilleran Orogen: Conterminous U.S., Geologi-cal Society of America, The Geology of North America, Volume G–3, p. 28–34.

Maher, B. J., Browne, Q. J., McKee, E. H., 1993, Constraints on the age of gold mineralization and metallogenesis in the Battle Mountain-Eureka mineral belt, Nevada: Economic Geology, v. 88, p. 469–478.

Maher, David, 1996, Stratigraphy, structure, and alteration of igneous and carbonate wallrocks at Veteran Extension in the Robinson (Ely) porphyry copper district, Nevada, in Coyner, A.R., and Fahey, P.L., eds., Geology and ore deposits of the American Cordillera, Symposium Proceedings: Reno, Nevada, Geological Society of Nevada, April 10–13, 1995, p. 1595–1621.

Maher, K.A., 1989, Geology of the Jackson Mountains, northwest Nevada: Pasadena, California Institute of Technology, Ph.D. dissertation, 526 p.

Mahoney, J.J., and Coffin, M.F., eds., 1997, Large igneous provinces, continental, oceanic, and planetary flood volcanism: American Geophysical Union Geophysical Monograph 100, 438 p.

Manuszak, J.D., Satterfield, J.I., and Gehrels, G.E., 2000, Detrital zircon geochronology of Upper Triassic strata in western Nevada, in Sorgehan, M.J., and Gehrels, G.E., eds., Paleozoic and Triassic paleogeography and tectonics of western Nevada and northern California: Geological Society of Nevada Special Paper 347, p. 109-118.

Margolis, J., and Marlowe, K., 1996, Middle Miocene, selenide-rich, low-sulfidation, epithermal gold mineralization, Mountain View district, northwestern Nevada [abs.]: Geological Society of America, Abstracts with Programs, v. 28., no. 7, p. A-93.

Marsh, S.P., Kropschot, S.J., and Dickinson, R.G., 1984, Wilderness Mineral Potential, Assessment of mineral-resource potential in U.S. Forest Service Lands studied 1964-1984: U.S. Geological Survey Professional Paper 1300, 1,183 p.

Mason, G.T., Jr., and Arndt, R.E., 1996, Mineral Resources Data System (MRDS): U.S. Geological Survey Digital Data Series DDS-20, 1 CD-ROM.

Massingill, Gary, 2001, A Tertiary tectonic twist for northern Nevada based on isotopic data, in Shaddrick, D.R., Zbinden, Elizabeth, Mathewson, D.C., Prenn, Camille, eds., Regional tectonics and structural control of ore: The major gold trends of northern Nevada: Geological Society of Nevada, Special Publication no. 33, p. 111–113.

McCallum, M.E., Loucks, R.R., Carlson, R.R., Cooley, E.F., and Doerge, T.A., 1975, Platinum metals associated with hydrothermal copper ores of the New Rambler mine, Medicine Bow Mountains, Wyoming: Economic Geology v. 71, p.1429–1450.

McCallum, M.E., and Orback, C.J., 1968, The New Rambler copper-gold-platinum district, Albany and Carbon Counties, Wyoming: Geological Survey of Wyoming Preliminary Report 8, 12 p.

McFarlane, D.N., 1991, Gold production on the Carlin trend, in Knutsen, G.C., Ekburg, and McFarlane, D.N., eds., Geology and mineralization of the Carlin trend, Fieldtrip 12, in Buffa, R.H., and Coyner, A.R., eds., Geology and ore deposits of the Great Basin: Reno, Nevada, Geological Society of Nevada, Fieldtrip Guidebook Compendium, v. 2, p. 841–843.

McFaul, E.J., Mason, G.T., Jr., Ferguson, W.B., and Lipin, B.R., 2000, U.S. Geological Survey mineral databases; MRDS and MAS/MILS: U.S. Geological Survey Digital Data Series, DDS–0052, 2 CD–ROMs.

McGibbon, D.H., 1999, Geology and ore deposits at the Marigold Mine, in Cunningham, Ken, ed., Geology and gold mineralization of the Buffalo Valley area, northwestern Battle Mountain trend: Geological Society of Nevada, Special Publication 31, 1999 Fall Field Trip Guidebook, p. 255–261.

McGibbon, D.H., and Wallace, A.B., 1997, Geology of the Marigold Mine area, in Theodore, T.G., ed., Geology of pluton–related gold mineralization at Battle Mountain, Nevada: Tucson, Arizona, University of Arizona and U.S. Geological Survey Center for Mineral Resources, Monograph 2, p. 222–238.

McGrew, J. C., Jr., and Monroe, C. B., 1993, Statistical problem solving in geography: Dubuque, Iowa, Wm. C. Brown Publishers, 305 p.

McKee, E.H., 1970, Fish Creek Mountains Tuff and volcanic center: U.S. Geological Survey Professional Paper 681, 17 p.

McKee, E.H., 1992, Potassium argon and ^{40}Ar/^{39}Ar geochronology of selected plutons in the Buckingham area, in Theodore, T.G., Blake, D.W., Loucks, T.A., and Johnson, C.A., Geology of the Buckingham stockwork molybdenum deposit and surrounding area, Lander County, Nevada: U.S. Geological Survey Professional Paper 798–D, p. D36–D40.

McKee, E.H., 2000, Potassium-argon chronology of Cretaceous and Cenozoic igneous activity, hydrothermal alteration, and mineralization, in Theodore, T.G., ed., Geology of pluton-related gold mineralization at Battle Mountain, Nevada: Tucson, Arizona, University of Arizona and U.S. Geological Survey Center for Mineral Resources, Monograph 2, p. 121–126.

McLachlan, C.D., Struhsacker, E.M., and Thompson, W.F., 2000, the gold deposits of Pinson Mining Company: a review of the geology and mining history through 1999, Humboldt County, Nevada, in Crafford, A.E.J., ed., Geology and ore deposits of the Getchell Region Humboldt county, Nevada: Geological Society of Nevada Symposium 2000 Field Trip Guidebook No. 9, p. 123–147.

McMillan, W.J., and Panteleyev, A., 1988, Porphyry copper deposits, in Roberts, R.G., and Sheahan, P.A., eds., Ore Deposit Models: Geoscience Canada, Reprint Series 3, p. 45–58.

Meinert, L.D., 1989, Gold skarn deposits—geology and exploration criteria, *in* Keays, R.R., Ramsey, W.R.H., and Groves, D.I., eds., The geology of gold deposits, The perspective in 1988: Economic Geology Monograph 6, p. 537–552.

Meinert, L.D., 1993, Igneous petrogenesis and skarn deposits, *in* Kirkham, R.V., Sinclair, W.D., Thorpe, R.I., and Duke, J.M., eds., Mineral deposit modeling: Geological Association of Canada Special Paper 40, p. 569–584.

Meinert, L.D., 1998, A review of skarns that contain gold, *in* Lentz, D.R., ed., Mineralized intrusion-related skarn systems: Mineralogical Association of Canada, Short Course, v. 26, p. 359–414.

Meinert, L.D., 2000, Gold in skarns related to epizonal intrusions, *in* Hagemann, S.G., and Brown, P.E., eds, Gold in 2000: Society of Economic Geology, Reviews in Economic Geology, v. 13, p. 347–376.

Menzie, W.D., and Singer, D.A., 1990, A course on mineral resource assessment: Proceedings of International Symposium on Mineral Exploration: The Use of Artificial Intelligence, 1990, Tokyo, p. 172-182.

Menzie, W.D., and Theodore, T.G., 1986, Grade and tonnage model of porphyry Mo, low–F, *in* Cox, D.P., and Singer, D.A., eds., Mineral deposit models: U.S. Geological Survey Bulletin 1693, p. 120–122.

Mertie, J.B., Jr., 1969, Economic geology of the platinum metals: U.S. Geological Survey Professional Paper 630, 120 p.

Meschede, Martin, 1986, A method for discriminating between different types of mid-ocean ridge basalts and continental tholeiites with the Nb–Zr–Y diagram: Chemical Geology, v. 56, p. 207–218.

Mihalasky, M.J., 2000, The northern Nevada geochemical "V"-trend [abs.]: Geological Society of America Abstracts with Programs, v. 32, p. A–392.

Mihalasky, M.J., 2001, Mineral potential modelling of gold and silver mineralization *in* the Nevada Great Basin—A GIS-based analysis using weights of evidence: U.S. Geological Survey Open-File Report 01-291, 448 p., [http://geopubs.wr.usgs.gov/open-file/of01-291/].

Mihalasky, M.J., and Bonham-Carter, G.F., 1999, The spatial relationship between mineral deposits and lithologic diversity in the Nevada Great Basin, *in* Lippard, S.J., Naess, A., and Sinding-Larsen, R., eds., Proceedings of IAMG'99, Trondheim, Norway, 6–11 August 1999, p. 369–374.

Mihalasky, M.J., and Bonham-Carter, G.F., 2001, The spatial association between metallic mineral sites and lithodiversity in Nevada: Natural Resources Research, v. 10, no. 3, p. 209-226.

Mihalasky, M.J., and Moyer, L.A., 2004, Spatial databases of the Humboldt Basin mineral resource assessment, northern Nevada: U.S. Geological Survey Open-File Report 2004-1245, 17 p., [http://pubs.usgs.gov/of/2004/1245].

Miller, M.S., 1993, Minerals in the Emigrant Trail Study Area, Pershing, Humboldt and Washoe Counties, Nevada: U.S. Bureau of Mines MLA Open-File Report, 132 p.

Moore, Lyman, 1971, Economic evaluation of California-Nevada iron resources and iron ore markets: Bureau of Mines Information Circular 8511, 207 p.

Morelli, Carlo, ed., 1974, The International Gravity Standardization Net 1971: International Association of Geodesy Special Publication no. 4, 194 p.

Morris, H.T., 1986, Descriptive model of polymetallic replacement deposits, *in* Cox, D.P., and Singer, D.A., eds., Mineral deposit models: U.S. Geological Survey Bulletin 1693, p. 99.

Morrison, G., Kary, G., and Handfield, R., 1999, Intrusion-alteration-mineralisation relationships in the Frieda River igneous complex, PNG, *in* Weber, Graeme, ed., PACRIM '99 Congress, proceedings: Australasian Institute of Mining and Metallurgy, v. 4–99, p. 527–537.

Mosier, D.L., 1986a, Descriptive model of replacement Mn, *in* Cox, D.P, and Singer, D.A., eds., Mineral deposit models: U.S. Geological Survey Bulletin 1693, p. 105.

Mosier, D.L., 1986b, Descriptive model of epithermal Mn, *in* Cox, D.P, and Singer, D.A., eds., Mineral deposit models: U.S. Geological Survey Bulletin 1693, p. 165.

Mosier, D.L., and Page, N.J, 1987, Descriptive and grade-tonnage models of volcanogenic manganese deposits in oceanic environments—a modification: U.S. Geological Survey Bulletin 1811, 63 p.

Mosier, D.L., Singer, D.A., Bagby, W.C. and Menzie, W.D., 1992, Grade and tonnage model of sediment–hosted Au, *in* Bliss, J.D. ed., Developments in Mineral Deposit Modeling: U.S. Geological Survey Bulletin 2004, p. 26–28.

Motooka, J.M., 1990, Organometallic halide extraction applied to the analysis of geologic materials for 10 elements by inductively coupled plasma-atomic emission spectrometry, *in* Arbogast, B.F., ed., Quality Assurance Manual for the Branch of Geochemistry: U.S. Geological Survey Open-File Report 90-668, p. 92-96.

Muffler, L.J.P., 1964, Geology of the Frenchie Creek quadrangle, north-central Nevada: U.S. Geological Survey Bulletin 1179, 99 p.

Muller, S.W., Ferguson, H.G., and Roberts, R.J., 1951, Geology of the Mount Tobin quadrangle, Nevada: U.S. Geological Survey Geologic Quadrangle Map GQ-7.

Muntean, J.L., and Einaudi, M.T., 2000, Porphyry gold deposits of the Refugio District, Maricunga Belt, northern Chile: Economic Geology, v.95, no. 7, p. 1445–1472.

Muntean, J.L., Tarnocai, Charles, Coward, Michael, Rouby, Delphine, and Jackson, Andy, 2001, Styles and restorations of Tertiary extension in north-central Nevada, *in* Shaddrick, D.R., Zbinden, Elizabeth, Mathewson, D.C., Prenn, Camille, eds., Regional tectonics and structural control of ore: The major gold trends of northern Nevada: Geological Society of Nevada, Special Publication no. 33, p. 55–69.

Mutschler, F.E., Larson, E.E., and Gaskill, D.L., 1992, The fate of the Colorado Plateau—A view from the mantle: Unpublished manuscript, Department of Geology, Eastern Washington University, Cheney, Washington, 14 p.

Mutschler, F.E., Wright, E.G., Ludington, Steve, and Abbot, J.T., 1981, Granite molybdenite systems: Economic Geology, v. 76, p. 874–897.

Myers, G.L., 1994, Geology of the Copper Canyon-Fortitude skarn system, Battle Mountain, Nevada: Pullman, Washington State University, Ph.D. dissertation, 338 p.

Myers, G.L., and Meinert, L.D., 1991, Alteration, mineralogy, and gold distribution in the Fortitude gold skarn, *in* Raines, G.L., Lisle, R.E., Schafer, R.W., and Wilkinson, W.H., eds., Geology and ore deposits of the Great Basin: Reno, Nevada, Geological Society of Nevada, Symposium Proceedings, p. 407–417.

Naldrett, A.J., 1981, Nickel sulfide deposits: Classification, composition, and genesis: Economic Geology 75th Anniversary Volume, p. 628–685.

Naldrett, A.J., 1989, Magmatic sulfide deposits: New York, Oxford University Press, Oxford Monographs on Geology and Geophysics no. 14, 186 p.

Naldrett, A.J., Asif, M., Gorbachev, N.S., Kunilov, V. Ye., Stekhin, A.I., Fedorenko, V.A., and Lightfoot, P.C., 1994, The composition of the Ni–Cu ores of the Oktyabr'sky deposit, Noril'sk region, *in* Lightfoot, P.C., and Naldrett, A.J., eds., Proceedings of the Sudbury-Noril'sk Symposium: Ontario Geological Survey Special Volume 5, p. 357–371.

Naldrett, A.J., Cameron, G., von Gruenewaldt, Gerhard, and Sharge, M.R., 1987, The formation of statiform PGE deposits in layered intrusions, Chapter 10, *in* Parsons, Ian, ed., Origins of Igneous Layering: Dorcherdt, D. Reidel Publishing Company, p. 313–397.

Naldrett, A.J., and Lightfoot, P.C., 1999, Ni–Cu–PGE deposits of the Noril'sk region, Siberia: Their formation in conduits for flood basalt volcanism, *in* Keays, R.R., Lesher, C.M., Lightfoot, P.C., and Farrow, C.E.G., eds., Dynamic processes in magmatic ore deposits and their application in mineral exploration: Geological Association of Canada Short Course Notes, v. 13, p. 195–250.

Naldrett, A.J., Pessaran, R., Asif, M. and Li, C., 1994, Compositional variation in the Sudbury ores and prediction of the proximity of footwall copper–PGE orebodies, *in* Lightfoot, P.C., and Naldrett, A.J., eds., Proceedings of the Sudbury-Noril'sk Symposium: Ontario Geological Survey Special Volume 5, p. 133–143.

Nash, J.T., 1972, Fluid-inclusion studies of some gold deposits in Nevada: U.S. Geological Survey Professional Paper 800-C, p. C-15--C19.

Nash, J.T., and Trudel, W.S., 1996, Bulk mineable gold ore at the Sleeper mine, Nevada--importance of extensional faults, breccia, framboids, and oxidation, *in* Coyner, A.R., and Fahey, P.L., eds., Geology and ore deposits of the American cordillera: Geological Society of Nevada Symposium Proceedings, Reno/Sparks, Nevada, April 1995, p. 235-256.

Nash, J.T., Utterback, W.C., and Trudel, W.S., 1995, Geology and geochemistry of Tertiary volcanic host rocks, Sleeper gold-silver deposit, Humboldt County, Nevada: U.S. Geological Survey Bulletin 2090, 63 p.

National Research Council, 2001, Future roles and opportunities for the U.S. Geological Survey: Washington, D.C., National Academy Press, 179 p.

Neeham, A.B., 1942, Rambler mine, Albany County, Wyoming: U.S. Bureau of Mines War Minerals Report 17, 7 p.

Neuerburg, G.J., 1966, Distribution of selected accessory minerals in the Osgood Mountains stock Humboldt County, Nevada: U.S. Geological Survey Miscellaneous Geologic Investigations Series Map I–471.

Nevada Bureau of Mines and Geology, 2000, The Nevada Mineral Industry/1999: Nevada Bureau of Mines and Geology Special Publication MI–1999, 60 p.

Nichols, K.M., and Silberling, N.J., 1977, Stratigraphy and depositional history of the Star Peak Group (Triassic), northwestern Nevada: Geological Society of America Special Paper 108, 73 p.

Noble, D.C., McKee, E.H., and Larson, L.T., 1987, Late Miocene hydrothermal activity at the Willard and Scossa mining districts, Pershing County, northwestern Nevada: Isochron/West, no. 48, p. 8-9.

Norby, J.W., and Orobono, M.J.T., 2000, Contact metamorphic, epithermal, and supergene mineralization at the Mike deposit, Eureka County, Nevada, *in* Griffin, Lane, ed., Giant sedimentary rock-hosted mineral systems of the Carlin trend: Gold Quarry and Betze/Post deposits: Geological Society of Nevada Symposium 2000, Guidebook Fieldtrip 7, p. 107–108.

Norman, D.I., Groff, John, Camalli, Cem, Musgrave, John and More, J.N., 1996, Gaseous species in fluid inclusions: Indicators of magmatic input into ore forming geothermal systems [abs.]: Geological Society of America, Abstracts with Programs, v. 28, no. 7, p. A–401.

Nutt, C. J., Hofstra, A. H., Hart, K. S., and Mortensen, J. K., 2000, Structural setting and genesis in the Bald Mountain–Alligator Ridge area, east-central Nevada, *in* Cluer, J. K., Price, J. G., Struhsacker, E .M., Hardyman, R. F., and Morris, C. L., eds., Geology and Ore Deposits 2000: The Great Basin and Beyond: Geological Society of Nevada symposium Proceedings, May 15–18, 2000, p. 513–537.

Oldow, J.S., 1984, Evolution of a late Mesozoic back-arc fold and thrust belt, western Great Basin, U.S.A.: Tectonophysics, v. 102, p. 245–274.

Oldow, J.S., 1984, Spatial variability in the structure of the Roberts Mountains allochthon, western Nevada: Geological Society of America Bulletin, v. 95, p. 174–185.

O'Leary, R.M., Crock, J.G., and Kennedy, K.R., 1990, Determination of mercury in geologic materials by continuous flow-cold vapor-atomic absorption spectrophotometry, *in* Arbogast, B.F., ed., Quality Assurance Manual for the Branch of Geochemistry: U.S. Geological Survey Open-File Report 90-668, p. 60-67.

O'Leary, R.M., and Meier, A.L., 1990, Determination of gold in samples of rock, soil, stream sediment, and heavy-mineral-concentrate by flame and graphite furnace atomic absorption spectrophotometry following dissolution by HBr-Br2, *in* Arbogast, B.F., ed., Quality Assurance Manual for the Branch of Geochemistry: U.S. Geological Survey Open-File Report 90-668, p. 46-51.

Oppliger, G.L., Murphy, J.B., and Brimhall, G.H., Jr., 1997, Is the ancestral Yellowstone hotspot responsible for the Tertiary Carlin mineralization in the Great Basin of Nevada?: Geology, v. 25, no. 7, p. 627–630.

Orris, G.J., 1986, Descriptive model of bedded barite, *in* Cox, D.P., and Singer, D.A., eds., Mineral deposit models: U.S. Geological Survey Bulletin 1693, p. 216.

Osterberg, M.W., 1989, Geology and geochemistry of the Chimney Creek gold deposit, Humboldt County, Nevada: Tucson, Arizona, University of Arizona, Ph.D. dissertation, 145 p.

Osterberg, M.W., and Guilbert, J.M., 1988, Chimney Creek, Nevada: A Carlin subtype sediment-hosted gold deposit: 28th International Geologic Congress, v. 12, p. 558.

Osterberg, M.W., and Guilbert, J.M., 1991, Geology, wall–rock alteration and new exploration techniques at the Chimney Creek sediment-hosted gold deposit, Humboldt County, Nevada, *in* Raines, G.L., Lisle, R.W., Schafer, R.W., and Wilkinson, W. H., eds., Geology and Ore Deposits of the Great Basin: Reno, Nevada, Geological Society of Nevada, Symposium Proceedings, v. 2, p. 805–819.

Page, B.M., 1965, Preliminary geologic map of a part of the Stillwater Range, Churchill County, Nevada: Nevada Bureau of Mines and Geology Map 28, scale 1:125,000, 1 sheet.

Page, N.J, 1986a, Descriptive model of Alaskan PGE, *in* Cox, D.P., and Singer, D.A., eds., Mineral deposit models: U.S. Geological Survey Bulletin 1693, p. 49.

Page, N.J, 1986b, Descriptive model of komatiitic Ni–Cu, *in* Cox, D.P., and Singer, D.A., eds., Mineral deposit models: U.S. Geological Survey Bulletin 1693, p. 18.

Page, N.J, 1986c, Descriptive model of synorogenic-synvolcanic Ni–Cu, *in* Cox, D.P., and Singer, D.A., eds., Mineral deposit models: U.S. Geological Survey Bulletin 1693, p. 28.

Page, N.J, Foose, M.P., and Lipin, B.R., 1982, Characteristics of metallic deposits associated with ultramafic and mafic rocks, *in* Erickson, R.L., compiler, Characteristics of Mineral Deposit Occurrences: U.S. Geological Survey Open-File Report 82–795, p. 1–12.

Paktunc, A.D., 1989, Petrology of the St. Stephen intrusion and the genesis of related nickel-copper sulfide deposits: Economic Geology, v. 84, p. 817–840.

Paktunc, A.D., 1990, Comparative geochemistry of platinum-group elements of nickel-copper sulfide occurrences associated with mafic-ultramafic intrusions in the Appalachian Orogen: Journal of Geochemical Exploration, v. 37, p. 101–111.

Palmer, W.S., 1918, The occurrences of tungsten in manganese ores: Engineering and Mining Journal, v. 105, no. 17, p. 780.

Papke, K. G., 1984, Barite in Nevada: Nevada Bureau of Mines and Geology Bulletin 98, 125 p.

Pardee, J.T., and Jones, E.L., 1920, Deposits of manganese ore in Nevada: U.S. Geological Survey Bulletin 710–F, p. 209–248.

Parsons, T., Thompson, G. A., and Sleep, N. H., 1994, Mantle plume influence on the Neogene uplift and extension of the U. S. western Cordillera?: Geology, v. 22, p. 83–86.

Pearce, J.A., 1996, A user's guide to basalt discrimination diagrams, *in* Wyman, D.A., ed., Trace element geochemistry of volcanic rocks: Applications for massive sulfide exploration: Geological Association of Canada, Short Course Notes, v. 12, p. 79–113.

Pearce, J.A., and Norry, M.J., 1979, Petrogenetic implications of Ti, Zr, Y, and Nb variations in volcanic rocks: Contributions to Mineralogy and Petrology, v. 69, p. 33–47.

Penrose, R.A.F., Jr., 1893, A Pleistocene manganese deposit near Golconda: Journal of Geology, v. 1, p. 275–282.

Percival, T.J., Bagby, W.C., and Radtke, A.S., 1988, Physical and chemical features of precious–metal deposits hosted by sedimentary rocks in the western United States, *in* Schafer, R. W., Cooper, J.J., and Vikre, P.G., eds., Bulk mineable precious metal deposits of the western United States: Reno, Nevada, Geological Society of Nevada, Symposium Proceedings, p. 11–34.

Peters, S.G, 1996, Delineation of the Carlin trend using orientation of regional fold axes and applications to ore control and zoning in the central Betze orebody, Betze–Post Mine, northeastern Nevada, *in* Peters, S.G., Williams, C.L., Volk, J., leaders, Structural Geology of the Carlin Trend: Reno, Nevada, Geological Society of Nevada, Symposium Geology and Ore Deposits of the American Cordillera, Field Trip Guidebook, Trip B, 52 p.

Peters, S.G., 1997a, Structural transect across the southern Carlin Trend, Eureka County, Nevada: U.S. Geological Survey Open–File Report 97–0347, 27 p., 2 sheets [scale 1: 500].

Peters, S.G., 1997b, Structural transect across the north–central Carlin Trend, Eureka County, Nevada: U.S. Geological Survey Open–File Report 97–83, 41 p., 6 sheets [scale 1: 500].

Peters, S.G., 1997c, Structural transect across the central Carlin Trend, Eureka County, Nevada: U.S. Geological Survey Open–File Report 97–55, 40 p., 2 sheets [scale 1:6,000].

Peters, S.G., 1998, Evidence for the Crescent Valley-Independence Lineament, north-central, Nevada, *in* Tosdal, R.M., ed., Contributions to the Au metallogeny of northern Nevada: U.S. Geological Survey Open-File Report 98–338, p. 106-118, [http://geopubs.wr.usgs.gov/open-file/of98-338/]

Peters, S.G., 1999, Relations between the Richmond Mountain thrust, and the Crescent Valley-Independence lineament, Lynn window, Eureka County, Nevada: U.S. Geological Survey Open–File Report 99–329, 16 p,. 1 sheet [scale: 1: 6,000].

Peters, S.G., 2000, Regional- and district-scale dissolution, deformation and fluid flow in sedimentary rock-hosted gold deposits of northern Nevada, *in* Cluer, J. K., Price, J. G., Struhsacker, E. M., Hardyman, R. F., and Morris, C. L., eds., Geology and Ore Deposits 2000: The Great Basin and Beyond: Geological Society of Nevada symposium Proceedings, May 15–18, 2000, p. 661–681.

Peters, S.G., 2001, Use of structural geology in the mining of and exploration for sedimentary rock-hosted Au deposits: U.S. Geological Survey Open–File Report [Written for and reprinted in Nevada Geological Society Field Conference, Regional Tectonics and Structural Control of Ore: The Major Gold Trends of Northern Nevada, May, 2001, Battle Mountain: Geological Society of Nevada Special Publication no. 33, p. 147–182, also as U.S. Geological Survey Open–File Report 01–151, [http://geopubs.wr.usgs.gov/open-file/of01-151/] .

Peters, S.G., ed., 2002, Geology, geochemistry, and geophysics of sedimentary rock-hosted Au deposits in P.R. China: U.S. Geological Survey Open-File Report 02–131, 403 p., [http://geopubs.wr.usgs.gov/open-file/of02-131/].

Peters, S.G., Armstrong, A.K., Harris, A.G., Oscarson, R.L., and Noble, P.J., 2003, Biostratigraphy and structure of Paleozoic host rocks and their relation to Carlin-type Au deposits in the Jerritt Canyon Mining District, Nevada: Economic Geology, v. 98, p. 317-337.

Peters, S.G., Ferdock, G.C., Woitsekhowskaya, M.B., Leonardson, Robert, and Rahn, Jerry, 1998, Oreshoot zoning in the Carlin-type Betze orebody, Goldstrike Mine, Eureka County, Nevada: U.S. Geological Survey Open–File Report 98–620, 49 p.

Peters, S.G., Leonardson, R.W., Ferdock, G.C., and Lauha, E.A., 1997, Breccia types in the Betze orebody, Goldstrike Mine, Eureka County, Nevada, *in* Vikre, P., Thompson, T.B., Bettles, K., Christensen, O, and Parrat, R., eds., Carlin-Type Gold Deposits Field Conference: Economic Geology Field Book Series, v. 28, p. 87–107.

Peters, S.G., Nash, J.T., John, D.A., Spanski, G.T., King, H.D., Connors, K.A., Moring, B.C., Doebrich, J.L., McGuire, D.J., Albino, G.V., Dunn, V.C., Theodore, T.G., and Ludington, S., 1996, Metallic mineral resources in the U.S. Bureau of Land Management's Winnemucca District and Surprise Resource Area, northwest Nevada and northeast California: U.S. Geological Survey Open-File Report 96-712, 147 p.

Peters, S.G., Williams, C.L., and Volk, Jeff, 1995, Structural geology of the Carlin trend: Reno, Nevada, Geological Society of Nevada, Symposium Geology and Ore Deposits of the American Cordillera, Field Trip Guidebook, Trip B, 52 p.

Peters, W.C., 1978, Exploration and mining geology: New York, John Wiley and Sons, 696 p.

Pierce, H.A., and Hoover, D.B., 1991, Airborne electromagnetic applications mapping structure and electrical boundaries beneath cover along the Getchell Trend, Nevada, *in* Raines, G.L., Lisle, R.W., Schafer, R.W., and Wilkinson, W. H., eds., Geology and Ore Deposits of the Great Basin: Reno, Nevada, Geological Society of Nevada, Symposium Proceedings, v. 2, p. 771–780.

Pierce, K.L., and Morgan, L.A., 1992, The track of the Yellowstone hot spot: Volcanism, faulting, and uplift, *in* Link, P.K., Kuntz, M.A., and Platt, L.B., eds., Regional Geology of eastern Idaho and western Wyoming: Geological Society of America Memoir 179, p. 1-53.

Pierce, K.L., Morgan, L.A., and Saltus, R.W., 2000, Yellowstone plume head: Postulated tectonic relations to the Vancouver slab, continental boundaries, and climate: U.S. Geological Survey Open-File Report 00-498, 39 p.

Pitcher, W.S., 1982, Granite type and tectonic environment, *in* Hsü, K.J., ed., Mountain building processes: San Francisco, Academic Press, p. 19–40.

Pitcher, W.S., Atherton, M.P., Cobbing, E.J., and Beckinsale, R.D., eds., 1985, Magmatism at a plate edge—The Peruvian Andes: London, Blackie and Son Ltd., 328 p.

Pitkin, J.A., 1991, Radioelement data of the Getchell Trend, Humboldt County, Nevada–Geologic discussion and possible significance for gold exploration, *in* Raines, G.L., Lisle, R.W., Schafer, R.W., and Wilkinson, W. H., eds., Geology and Ore Deposits of the Great Basin: Reno, Nevada, Geological Society of Nevada, Symposium Proceedings, v. 2, p. 759–769.

Plouff, Donald, 1966, Digital terrain corrections based on geographic coordinates [abs.]: Geophysics, v. 31, no. 6, p. 1208.

Ponce, D.A., 1997a, Gravity data of Nevada: U.S. Geological Survey Digital Data Series DDS-42, CD-ROM, 27 p.

Ponce, D.A., 1997b, Mapping the Humboldt River basin using gravity and magnetic methods, Winnemucca 1- by 2-degree quadrangle, northern Nevada [abs.]: Geological Society of America, Abstracts with Programs, v. 29, no. 6, p. 304.

Ponce, D.A., and Glen, J.M.G., 2000, Geophysical expression of the northern Nevada rift [abs.]: Geological Society of America, Abstracts with Programs, v. 32, no. 7, Reno, Nev., 2000.

Ponce, D.A., and Glen, J.M.G., 2002, Relationships of epithermal gold deposits to large-scale fractures in northern Nevada: Economic Geology, v. 97, p. 3-9.

Ponce, D.A., and Morin, R.L., 1999, Isostatic gravity map of the Battle Mountain 30 x 60 minute quadrangle, north-central Nevada: U.S. Geological Survey Geologic Investigations Map I-2687, scale 1:100,000.

Ponce, D.A., Morin, R.L., and Plouff, Donald, 1999, Bouguer gravity map of Nevada, Lovelock sheet: Nevada Bureau of Mines and Geology Map 122, scale 1:250,000.

Ponce, D.A., and Moring, B.C., 1998, Drill-hole lithology map of the Winnemucca 1:250,000-scale quadrangle, Nevada: U.S. Geological Survey Open-File Report 98-220.

Ponce, D.A., and Plouff, Donald, 2001, Bouguer gravity map of Nevada, Vya sheet: Nevada Bureau of Mines and Geology Map M-128, scale 1:250,000.

Prendergast, M.D., and Wilson, A.H., 1989, The Great Dyke of Zimbabwe—II: Mineralization and mineral deposits, *in* Prendergast, M.D., and Jones, M.J., eds., Magmatic sulphides—the Zimbabwe volume: London, The Institution of Mining and Metallurgy, p. 21–42.

Preuss, N.E., 1998, Hydrothermal and vapor-related alteration at the Florida Canyon epithermal gold deposit, Pershing County, Nevada: Carbondale, Southern Illinois University, Master's, 51 p.

Prihar, D.W., Peters, S.G., Bourns, F.T., and Mckee, E.A., 1996, Geology and gold potential of the Goat Ridge window, Shoshone Range, Lander County, Nevada, *in* Coyner, A.R., and Fahey, P.L., eds., Geology and Ore Deposits of the American: Geological Society of Nevada Symposium Proceedings, Reno/Sparks, Nevada, April, 1995, p. 485–504.

Raab, M. and Spiro, B., 1991, Sulfur isotopic variations during seawater evaporation with fractional crystallization: Chemical Geology, v. 86, p. 323–333.

Radtke, A.S., 1985, Geology of the Carlin gold deposit, Nevada: U.S. Geological Survey Professional Paper 1267, 124 p.

Radtke, A.S., and Dickson, F.W., 1974, Genesis and vertical position of fine–grained disseminated replacement–type gold deposits in Nevada and Utah, U.S.A., in Problems of ore deposition, Volume I: Proceedings, International Association on the Genesis of Ore Deposits, Symposium, 4th, Varna, Romania, p. 71–81.

Radtke, A.S., Rye, R.O., and Dickson, F.W., 1980, Geology and stable isotope studies of the Carlin gold deposit, Nevada: Economic Geology, v. 75, p. 641–672.

Radtke, A.S., and Scheiner, B.J., 1970a, Influence of organic carbon on gold deposition at the Carlin and Cortez deposits, Nevada: Geological society of America, Abstracts, v. 2, no. 7, p. 660.

Radtke, A.S., and Scheiner, B.J., 1970b, Studies of hydrothermal gold deposition (I), Carlin gold deposit, Nevada: The role of carbonaceous materials in gold deposition: Economic Geology, v. 65, no. 2, p. 87–102.

Raines, G.L., 1999, Evaluation of weights of evidence to predict epithermal-gold deposits in the Great Basin of the western United States: Natural Resources Research, v. 8, p. 257–276.

Raines, G.L., Sawatzky, D.L., and Connors, K.A., 1996, Great Basin geoscience data base: U.S. Geological Survey Digital Data Series DDS–41, 2 CD–ROMS.

Ransome, F.L., 1909, Notes on some mining districts in Humboldt County, Nevada: U.S. Geological Survey Bulletin 414, 71 p.

Ray, G.E., and Dawson, G.L., 1994, The geology and mineral deposits of the Hedley gold skarn district, southwestern British Columbia: British Columbia Ministry of Energy, Mines, and Petroleum Resources Bulletin 87, 156 p.

Reeves, R.G., and Kral, V.E., 1955, Geology and iron deposits of the Buena Vista Hills, Churchill and Pershing County, Nevada: Nevada Bureau of Mines Bulletin 53, 34 p.

Regan, P.F., 1985, The early basic intrusions *in* Pitcher, W.S., Atherton, M.P., Cobbing, E.J., and Beckinsale, R.D., eds., Magmatism at a plate edge: The Peruvian Andes: New York, Halsted Press, John Wiley and Sons, Inc., p. 72–89.

Ressel, M.W., Noble, D.C., Heizler, M.T., Volk, J.A., Lamb, J B., Park, D.E., Conrad, J.E., and Mortensen, J.K., 2000a, Gold–mineralized Eocene dikes at Griffin and Meikle: bearing on the age and origin of deposits of the Carlin trend, Nevada, *in* Cluer, J.K., Price, J.G., Struhsacker, E.M., Hardyman, R.F., and Morris, C.L., eds., Geology and Ore Deposits 2000: the Great Basin and Beyond: Geological Society of Nevada symposium Proceedings, May 15–18, 2000, p. 79–101.

Ressel, M.W., Noble, D.C., Henry, C.D., and Trudel, W.S., 2000b, Dike-hosted ores of the Beast deposits and the importance of Eocene magmatism in gold mineralization of the Carlin Trend, Nevada: Economic Geology, v. 95, no. 7, p. 1417–1444.

Riley, B.C.D., Snyder, W.S., and Gehrels, G.E., 2000, U-Pb detrital zircon geochronology of the Golconda allochthon, Nevada, *in* Sorgehan, M.J., and Gehrels, G.E., eds., Paleozoic and Triassic paleogeography and tectonics of western Nevada and northern California: Geological Society of Nevada Special Paper 347, p. 65-75.

Ripley, E.M., 1999, Systematics of sulphur and oxygen isotopes in mafic igneous rocks and related Cu–Ni–PGE mineralization, *in* Keays, R.R., Lesher, C.M., Lightfoot, P.C., and Farrow, C.E.G., eds., Dynamic processes in magmatic ore deposits and their application in mineral exploration: Geological Association of Canada Short Course Notes, v. 13, p. 133–158.

Roberts, R.G., and Sheahan, P.A., 1988, Ore deposit models: Geoscience Canada Reprint Series 3, 194 p.

Roberts, R.J., 1960, Alignment of mining district in north central Nevada: U.S. Geological Survey Professional Paper 400–B, p. 17–19.

Roberts, R.J., 1964, Stratigraphy and structure of the Antler Peak quadrangle, Humboldt and Lander Counties, Nevada: U.S. Geological Survey Professional Paper 459-A, 93 p.

Roberts, R.J., 1966, Metallogenic provinces and mineral belts in Nevada, in Papers presented at the AIME Pacific southwest mineral industry conference, Sparks, Nevada, May 5-7, 1965: Nevada Bureau of Mines and Geology Report 13, p. 47-72.

Roberts, R.J., and Arnold, D.C., 1965, Ore deposits of the Antler Peak quadrangle, Humboldt and Lander Counties, Nevada: U.S. Geological Survey Professional Paper 459–B, 93 p.

Roberts, R.J., Hotz, P.E., Gilluly, James, and Ferguson, H.G., 1958, Paleozoic rocks in north-central Nevada: American Association of Petroleum Geologists Bulletin, v. 42, no. 12, p. 2813–2857.

Roberts, R.J., Montgomery, K.M., and Lehner, R.E., 1967, Geology and mineral resources of Eureka County, Nevada: Nevada Bureau of Mines Bulletin 64, 152 p.

Rodriguez, B.D., 1997, Deep regional resistivity structure across the Carlin trend, *in* Vikre, Peter, Thompson, T.B., Bettles, Keith, Christensen, Odin, and Parrat, Ron, eds., 1998, Carlin-type gold deposits field conference: Society of Economic Geologists Guidebook Series v. 28, p. 39–46.

Rodriguez, B.D., 1998, Regional crustal structure beneath the Carlin trend, Nevada, based on deep electrical geophysical measurements, *in* Tosdal, R.M., ed., Contributions to the gold metallogeny of northern Nevada: U.S. Geological Survey Open-File Report 98-338, 15-19, [http://geopubs.wr.usgs.gov/open-file/of98-338/].

Rowan, L.C., and Wetlaufer, P.H., 1979, Geologic evaluation of major Landsat lineaments in Nevada and their relationship to ore districts: U.S. Geological Survey Open–File Report 79–544, 87 p.

Rowell, W.F., and Edgar, A.D., 1986, Platinum group element mineralization in a hydrothermal Cu–Ni sulfide occurrence, Rathbun Lake, northern Ontario: Economic Geology, v. 81, p. 1272–1278.

Rytuba, J.J., 1985, Geochemistry and hydrothermal transport and deposition of gold and sulfide minerals in Carlin type gold deposits: U.S. Geological Survey Bulletin 1646, 150 p.

Rytuba, J.J., and Cox, D.P., 1991, Porphyry gold: a supplement to U.S. Geological Survey Bulletin 1693: U.S. Geological Survey Open–File Report 91–116, 7 p.

Saltus, R. W., 1988, Regional, residual, and derivative gravity maps of Nevada: Prepared by the U. S. Geological Survey in cooperation with the Nevada Bureau of Mines and Geology, Mackay School of Mines, University of Nevada, Reno, Nevada, four 1: 1,000,000 gravity anomaly maps, two 1: 1,250,000 topography and isostatic regional gravity maps.

Sander, M.V., and Einaudi, M.T., 1990, Epithermal deposition of gold during transition from propylitic to potassic alteration at Round Mountain, Nevada: Economic Geology, v. 85, p. 285-311.

Sawkins, F.J, 1983, Metal deposits in relation to plate tectonics: New York, Springer Verlag, 325 p.

Schafer, R.W., Cooper, J.J., and Vikre, P.G., eds., 1988, Bulk–mineable precious metal deposits of the western United States: Reno, Nevada, Geological Society of Nevada, April, 1987, Symposium Proceedings, 755 p.

Schilling, J.H., 1963, Tungsten mines in Nevada: Nevada Bureau of Mines and Geology, Map 18.

Schilling, J.H., 1964, Tungsten, in Mineral and water resources of Nevada: Nevada Bureau of Mines and Geology Bulletin 65, p. 155–161.

Schilling, J.H., 1976, Metal mining districts of Nevada: Nevada Bureau of Mines and Geology Map 37.

Schilling, J.H., 1980, Molybdenum deposits and occurrences in Nevada: Nevada Bureau Mines and Geology, Map 66, 1 sheet, scale 1:1,000,000.

Scoates, R.F.J., Eckstrand, O.R., and Cabri, L.J., 1987, Inter-element correlation, stratigraphic variation and distribution of PGE in the Ultramafic Series of the Bird River Sill, Canada, *in* Prichard, H.M., Potts, P.J., Bowles, J.F.W., and Cribb, S.J., eds., Geo-platinum 87: London and New York, Elsevier Applied Science, p. 239–249.

Seedorff, Eric, 1991, Magmatism, extension, and ore deposits of Eocene to Holocene age in the Great Basin—mutual effects and preliminary proposed genetic relationships, *in* Raines, G.L., Lisle, R.E., Schafer, R.W., And Wilkinson, W.H., eds., Geology And Ore Deposits of the Great Basin, Geologic Society of Nevada Symposium Proceedings, Reno/Sparks, Nevada, April, 1990, p. 133–178.

Severinghaus, Jeff, and Atwater, Tanya, 1990, Cenozoic geometry and thermal state of the subducting slabs beneath western North America, *in* Wernicke, B.P., ed., Basin and range extensional tectonics near the latitude of Las Vegas: Geological Society of America Memoir 176, p. 1–22.

Shaver, S.A., and Jeanne, R.A., 1996, The geology and evolution of the weakly Au–(Cu)-mineralized far eastern side of the Robinson Mining District, Ely, Nevada, *in* Coyner, A.R., and Fahey, P.L., eds., Geology and ore deposits of the American Cordillera, Symposium Proceedings: Reno, Nevada, Geological Society of Nevada, April 10–13, 1995, p. 1623–1637.

Shawe, D.R., 1991, Structurally controlled gold trends imply large gold resources in Nevada, *in* Raines, G.L., Lisle, R.W., Schafer, R.W., and Wilkinson, W. H., eds., Geology and Ore Deposits of the Great Basin: Reno, Nevada, Geological Society of Nevada, Symposium Proceedings, v. 2, p. 199–212.

Shawe, F. R., Reeves, R. G., and Kral, V. E., 1962, Iron ore deposits of Nevada—part C: Iron ore deposits of northern Nevada: Nevada Bureau of Mines and Geology, Bulletin 53, p. 103–109.

Shawe, D.R., and Stewart, J.H., 1976, Ore deposits as related to tectonics and magmatism, Nevada and Utah: Society of Mining Engineers of AIME Transactions, v. 260, p. 225–231.

Sheets, R.W., and Nesbitt, Bruce, 1996, Comparative geology and mineralogy of mineralized and barren plutons of the Babine Lake igneous suite, west-central British Columbia, *in* Coyner, A.R., and Fahey, P.L., eds., Geology and ore deposits of the American Cordillera, Symposium Proceedings: Reno, Nevada, Geological Society of Nevada, April 10–13, 1995, p. 1229–1251.

Shevenell, L., Garside, L.J., and Hess, R.H., 2000, Nevada geothermal resources: Nevada Bureau of Mines and Geology Map 126, scale 1:1,000,000.

Silberling, N.J., 1975, Age relationships of the Golconda thrust fault, Sonoma Range, north–central Nevada: Geological Society of America Special Paper 163, 28 p.

Silberling, N.J., 1991, Allochthonous terranes of western Nevada—current status, *in* Raines, G.L., Lisle, R.W., Schafer, R.W., and Wilkinson, W.H., eds., Geology and Ore Deposits of the Great Basin: Reno, Nevada, Geological Society of Nevada, Symposium Proceedings, p. 101–102.

Silberling, N.J., Jones, D.L., Blake, M.C., Jr., and Howell, D.G., 1984, Lithotectonic terrane map of the western contermi-nous United States, *in* Silberling, N.J. and Jones, D.L., eds., Lithotectonic maps of the North American Cordillera: U.S. Geological Survey Open–File Report 84–523, Part C, 43 p.

Silberling, N.J., Jones, D.L., Blake, M.C., Jr., and Howell, D.G., 1987, Lithotectonic terrane map of the western conterminous United States: U. S. Geological Survey Miscellaneous Field Studies Map MF–1874–C, scale 1:2,500,000, 20 p.

Silberling, N.J., and Roberts, R.J., 1962, Pre-Tertiary stratig-raphy and structure of northwestern Nevada: Geological Society of America Special Paper 72, 58 p.

Silberling, N.J., and Wallace, R.E., 1969, Stratigraphy of the Star Peak Group, Triassic, and overlying lower Mesozoic rocks, Humboldt Range, Nevada: U.S. Geological Survey Professional Paper 592, 50 p.

Silberman, M.L., and Berger, B.R., 1985, Relationships of trace-element patterns to alteration and morphology in epithermal precious-metal deposits, *in* Berger, B.R., and Bethke, P.M., eds., Geology and geochemistry of epither-mal systems: Society of Economic Geologists, Reviews in Economic Geology, v. 2, p. 203-232.

Silberman, M.L., Berger, B.R., and Koski, P.A., 1974, K–Ar age relations of granodiorite emplacement and tungsten and gold mineralization near the Getchell mine, Humboldt County, Nevada: Economic Geology, v. 69, p. 646–656.

Silberman, M.L., Johnson, M.G., Koski, R.A., and Roberts, R.J., 1973, K-Ar ages of mineral deposits at Wonder, Seven Troughs, Imlay, Ten Mile, and Adelaide mining districts in Central Nevada: Isochron/West, no. 8, p. 31-35.

Silberman, M.L., and McKee, E.H., 1971, K–Ar ages of gra-nitic plutons in north-central Nevada: Isochron/West, no. 1, p. 15–22.

Sillitoe, R.H., 1988, Gold and silver deposits in porphyry systems, *in* Schafer, R.W., Cooper, J.J., and Vikre, P.G., eds., Bulk-mineable precious metal deposits of the western United States: Reno, Nevada, Geological Society of Nevada, April, 1987, Symposium Proceedings, p. 233–257.

Sillitoe, R.H., 1988, Gold and silver deposits in porphyry systems, *in* Schafer, R.W., Cooper, J.J., and Vikre, P.G., eds., Bulk-mineable precious metal deposits of the western United States: Reno, Nevada, Geological Society of Nevada, April, 1987, Symposium Proceedings, p. 233–257.

Sillitoe, R.H., 1999, Styles of high-sulfidation gold, silver, and copper mineralisation in porphyry and epithermal environments, *in* Weber, Graeme, ed., PACRIM '99 Congress, proceedings: Australasian Institute of Mining and Metallurgy, v. 4–99, p. 29–44.

Sillitoe, R.H., 2000a, Gold-rich porphyry deposits: Descriptive and genetic models and their role in exploration and discovery, *in* Hagemann, S.G., and Brown, P.E., eds, Gold in 2000: Society of Economic Geology, Reviews in Economic Geology, v. 13, p. 315–345.

Sillitoe, R.H., 2000b, Enigmatic origins of giant gold deposits, *in* Cluer, J.K., Price, J.G., Struhsacker, E.M., Hardyman, R.F., and Morris, C.L., eds., Geology and ore deposits 2000: The Great Basin and beyond: Geological Society of Nevada Symposium Proceedings, May 15–18, 2000, p. 1–18.

Sillitoe, R.H., 2002, Rifting, bimodal volcanism, and bonanza gold veins: Society of Economic Geologists Newsletter, no. 48, p. 24-26.

Sillitoe, R.H., and Bonham, H.F., Jr., 1990, Sediment-hosted gold deposits: Distal products of magmatic-hydrothermal systems: Geology, v. 18, p. 157–161.

Simpson, R.W., Jachens, R.C., and Blakely, R.J., 1986, A new isostatic residual gravity map of the conterminous United States with a discussion on the significance of isostatic residual gravity anomalies: Journal of Geophysical Research, v. 91, no. B8, p. 8348-8372.

Singer, D.A., 1993, Basic concepts in the three-part quantitative assessments of undiscovered mineral resources: Nonrenewable Resources, v. 2, p. 69-81.

Singer, D.A., ed., 1996, An analysis of Nevada's metal-bearing mineral resources: Nevada Bureau of Mines and Geology Open-file Report 96-2, [ftp://ftp.nbmg.unr.edu/NBMG/ofr962/index.htm].

Singer, D.A., and Cox, D.P., 1988, Applications of mineral deposit models to resource assessment: U.S. Geological Survey Yearbook 1987, p. 55–57.

Singer, D.A., and Kouda, R., 1999, A comparison of the weights-of-evidence method and probabilistic neural networks: Natural Resources Research, v. 8, p. 287–298.

Singer, D.A., Mosier, D.L., and Cox, D.P., 1986a, Grade and tonnage model of porphyry Cu, *in* Cox, D.P., and Singer, D.A., eds., Mineral deposit models: U.S. Geological Survey Bulletin 1693, p. 77–81.

Singer, D.A., and Page, N.J, 1986, Grade and tonnage model of minor podiform chromitites, *in* Cox, D.P., and Singer, D.A., eds., Ore deposit models: U.S. Geological Survey Bulletin 1693, p. 34–38.

Singer, D.A., Page, N.J, and Lipin, B.R., 1986a, Grade and tonnage model of major podiform chromitites, *in* Cox, D.P. and Singer, D.A., eds., Ore Deposit Models: U.S. Geological Survey Bulletin 1663, p. 38–44.

Singer, D.A., Page, N.J, and Menzie, W.D., 1986b, Grade and tonnage model of synorogenic-synvolcanic Ni–Cu, *in* Cox, D.P., and Singer, D.A., eds., Mineral deposit models: U.S. Geological Survey Bulletin 1693, p. 28–31.

Singer, D.A., Page, N.J, and Menzie, W.D., 1986c, Grade and tonnage model of komatiitic Ni–Cu, *in* Cox, D.P., and Singer, D.A., eds., Ore deposit models: U.S. Geological Survey Bulletin 1693, p. 18–23.

Singer, D.A., Theodore, T.G., and Mosier, D.L., 1986b, Grade and tonnage model of Climax Mo deposits, *in* Cox, D.P., and Singer, D.A., eds., Mineral deposit models: U.S. Geological Survey Bulletin 1693, p. 73–75.

Smailbegovic, A., 2002, Structural and lithologic constraints to mineralization *in* Aurora, NV and Bodie, CA mining districts observed with aerospace geophysical data: Reno, University of Nevada, Reno, Ph.D. dissertation, 300 p.

Smirnov, V.I., 1977, Ore deposits of the U.S.S.R., v. III: London, Pitman Publishing, 492 p.

Smith, J.G., McKee, E.H., Tatlock, D.B., and Marvin, R.F., 1971, Mesozoic granitic rocks in northwestern Nevada: A link between the Sierra Nevada and Idaho Batholiths: Geological Society of America Bulletin, v. 82, p. 2935–2944.

Smith, S.M., 2000, National Geochemical Database — Reformatted Data from the National Uranium Resource Evaluation (NURE) Hydrogeochemical and Stream Sediment Reconnaissance (HSSR): U.S. Geological Survey Open-File Report 97-0492, v. 1.20, [http://greenwood.cr.usgs.gov/pub/open-file-reports/ofr-97-0492/].

Snoke, A.W., and Miller, D.M., 1988, Metamorphic and tectonic history of northeastern Great Basin, *in* Ernst, W.G., ed., Metamorphic and tectonic evolution of the western United States: Englewood Cliffs, N.J., Prentice-Hall, p. 606-648.

Snyder, W.S., 1977, Origin and exploration for ore deposits in upper Paleozoic chert-greenstone complexes of northern Nevada: Stanford, Calif., Stanford University, Ph.D. dissertation, 159 p.

Speed, R.C., 1962, Scapolitized gabbroic complex, West Humboldt Range, Nevada: Stanford, Calif., Stanford University, Ph.D. dissertation, 156 p.

Speed, R.C., 1963, Layered picrite-anorthositic gabbro sheet, West Humboldt Range, Nevada: Mineralogical Society of America Special Paper 1, p. 69–77.

Speed, R.C., 1974, Evaporite-carbonate rocks of the Jurassic Lovelock Formation, West Humboldt Range, Nevada: Geological Society of America Bulletin, v. 85, p. 105–118.

Speed, R.C., 1976, Geologic map of the Humboldt lopolith and surrounding terrane, Nevada: Geological Society of America Map and Chart Series MC–14, scale 1:81,000, 1 sheet.

Spiegelhalter, D.J., and Knill-Jones, R.P., 1984, Statistical and knowledge-based approaches to clinical decision-support systems, with an application in gastroenterology: Journal of the Royal Statistical Society, A, Part 1, p. 35–77.

Stager, H.K., 1977, Mineral deposits, in Geology and mineral deposits of Lander County, Nevada: Nevada Bureau of Mines and Geology Bulletin 88, p. 60–102.

Stager, H.K., and Tingley, J.V., 1988, Tungsten deposits of Nevada: Nevada Bureau of Mines and Geology Bulletin 105, 256 p.

Stenger, D.P., Kesler, S.E., Peltonene, D.R., and Tapper, C.J., 1998, Deposition of gold in Carlin-type deposits: the role of sulfidation and decarbonation at Twin Creeks, Nevada: Economic Geology, v. 98, p. 201–215.

Stewart, J.H., 1972, Initial deposits of the Cordilleran geosyncline: Evidence of a late Pre-Cambrian (850 m.y.) continental separation: Geological Society of America Bulletin, v. 83, p. 1345-1360.

Stewart, J.H., 1980, Geology of Nevada: Nevada Bureau of Mines and Geology Special Publication 4, 136 p.

Stewart, J.H., 1988, Tectonics of the Walker Lane belt, western Great Basin: Mesozoic and Cenozoic deformation in a zone of shear, in Ernst, W.G., ed., Metamorphism and crustal evolution of the western United States: Englewood Cliffs, New Jersey, Prentice Hall, Rubey v. 11, p. 683-713.

Stewart, J.H., and Carlson, J.E., 1977, Million-scale geologic map of Nevada: Nevada Bureau of Mines and Geology Map 57, scale 1:1,000,000.

Stewart, J.H., and Carlson, J.E., 1978, Geologic map of Nevada: U.S. Geological Survey and Nevada Bureau of Mines and Geology Map, scale 1:500,000.

Stewart, J.H., Gehrels, G.E., Barth, A.P., Link P.K., Christie-Blick, N., Wrucke, C.T., 2001, Detrital zircon provenance of Mesoproterozoic to Cambrian arenites in the western United States and northwestern Mexico: Geological Society of America Bulletin, v. 113 , p. 1343–1356.

Stewart, J.H., and McKee, E.H., 1977, Geology and mineral deposits of Lander County, Nevada; part I, geology: Nevada Bureau of Mines and Geology Bulletin 88, 59 p.

Stewart, J.H., and Poole, F.G., 1974, Lower Paleozoic and uppermost Precambrian Cordilleran miogeocline, Great Basin, western United States, *in* Dickinson, W.R., ed., Tectonics and Sedimentation: Tulsa, Society of Economic Petrologists and Mineralogists, p. 27-57.

Stone, B., Thomas, D., Snider, L., McDermott, R., and Nyman, M., 2000, The Goldbanks deposit, a recent discovery of disseminated gold in Tertiary volcaniclastics, Pershing County, Nevada: Geological Society of Nevada, Geology and Ore Deposits 2000--The Great Basin and Beyond, Program with Abstracts, p. 78.

Strauss, Harald, 1999, Geological evolution from isotope proxy signals; sulfur: Chemical Geology, v. 161, p. 89-101.

Sverjensky, D.A., 1984, Oil field brines as ore–forming solutions: Economic Geology, v. 79, p. 38–49.

Swick, C.H., 1942, Pendulum gravity measurements and isostatic reductions: U.S. Coast and Geodetic Survey Special Publication no. 232, 82 p.

Szumigala, D.J., 1996, Gold mineralization related to Cretaceous-Tertiary magmatism in west-central Alaska—a geochemical model and prospecting guide for the Kuskokwim region, *in* Coyner, A.R., and Fahey, P.L., eds., Geology and ore deposits of the American Cordillera, Symposium Proceedings, Geological Society of Nevada, Reno/Sparks, Nevada, April, 1995 , p. 1,317–1,340.

Taylor, B.E., 1976, Origin and significance of C–O–H fluids in the formation of Ca–Fe–Si skarn, Osgood Mountains, Humboldt County, Nevada: Stanford, Calif., Stanford University, Ph.D. dissertation, 285 p.

Taylor, R.B., and Steven, T.A., 1983, Definition of mineral resource potential: Economic Geology, v. 78, no. 6, p. 1268–1270.

Teal, Lewis, and Jackson, Mac, 1997a, Geologic overview of the Carlin trend Au deposits and descriptions of recent deep discoveries, *in* Vikre, P., Thompson, T.B., Bettles, K., Christensen, O, and Parrat, R., eds., Carlin-Type Au Deposits Field Conference: Economic Geology Field Book Series, vol. 28, p. 3–38.

Teal, Lewis, and Jackson, Mac, 1997b, Geologic overview of the Carlin trend gold deposits: Society of Economic Geology Newsletter, no. 31, p. 13–25.

Teal, Lewis, and Wright, James, 2000, Geologic and geophysical overview of the Carlin Trend, Nevada, *in* Cluer, J. K., Price, J. G., Struhsacker, E. M., Hardyman, R. F., and Morris, C. L., eds., Geology and Ore Deposits 2000: the Great Basin and Beyond: Geological Society of Nevada symposium Proceedings, May 15–18, 2000, p. 567–570.

Telford, W.M., Geldart, L.P., Sheriff, R.E., and Keys, D.A., 1976, Applied geophysics: Cambridge, Cambridge University Press, 860 p.

Theodore, T.G., 1986, Descriptive model of porphyry Mo, low–F, *in* Cox, D.P., and Singer, D.A., eds., Mineral deposit models: U.S. Geological Survey Bulletin 1693, p. 120.

Theodore, T.G., 1996, Geology and implications of silver/gold ratios in the Elder Creek porphyry copper system, Battle Mountain Mining District, Nevada, *in* Coyner, A.R., and Fahey, P.L., eds., Geology and ore deposits of the American Cordillera, Symposium Proceedings, Geological Society of Nevada, Reno/Sparks, Nevada, April, 1995 , p. 1557–1571.

Theodore, T.G., 1998a, Pluton-related Au—an overview, *in* Tosdal, R.M., ed., Contributions to the Au metallogeny of the northern Great Basin: U.S. Geological Survey Open–File Report 98–338, p. 251–252, [http://geopubs.wr.usgs.gov/open-file/of98-338/].

Theodore, T.G., 1998b, Large distal–disseminated precious–metal deposits, Battle Mountain Mining District, Nevada, *in* Tosdal, R.M., ed., Contributions to the Au metallogeny of the northern Great Basin: U.S. Geological Survey Open–File Report 98–338, p. 253–258, [http://geopubs.wr.usgs.gov/open-file/of98-338/].

Theodore, T.G., 2000, Geology of pluton-related gold mineralization at Battle Mountain, Nevada, with a section on Potassium-argon chronology of Cretaceous and Cenozoic igneous activity, hydrothermal alteration, and mineralization by E.H. McKee, and a section on Lone Tree gold deposit by E.I. Bloomstein, B.L. Braginton, R.W. Owen, R.L. Parrat, K.C. Raabe, and W.F. Thompson, and a section on Geology of the Marigold Mine area by D.H. McGibbon and A.B. Wallace, and a section on Geology, mineralization, and exploration history of the Trenton Canyon project by R.P. Felder: Tucson, Arizona, University of Arizona and U.S. Geological Survey Center for Mineral Resources, Monograph 2, 271 p.

Theodore, T.G., and Blake, D.W., 1975, Geology and geochemistry of the Copper Canyon porphyry copper deposit and surrounding area, Lander County, Nevada: U.S. Geological Survey Professional Paper 798–B, p. B1–B86.

Theodore, T.G., and Blake, D.W., 1978, Geology and geochemistry of the West ore body and associated skarns, Copper Canyon porphyry copper deposits, Lander County, Nevada, with a section on Electron microprobe analyses of andradite and diopside by N.G. Banks: U.S. Geological Survey Professional Paper 798–C, p. C1–C85.

Theodore, T.G., Armstrong, A.K., Harris, A.G., Stevens, C.H., and Tosdal, R.M., 1998, Geology of the northern terminus of the Carlin trend, Nevada: links between crustal shortening during the late Paleozoic Humboldt orogeny and northeast-striking faults, *in* Tosdal, R.M., ed., Contributions to the Au Metallogeny of Northern Nevada: U.S. Geological Survey Open–File Report 98–338, p. 69–105.

Theodore, T.G., Blake, D.W., Loucks, T.A., and Johnson, C.A., 1992, Geology of the Buckingham stockwork molybdenum deposit and surrounding area, Lander County, Nevada: U.S. Geological Survey Professional Paper 798–D, p. D1–D307.

Theodore, T.G., Howe, S.S., Blake, D.W., and Wotruba, P.R., 1986, Geochemical and fluid zonation in the skarn environment at the Tomboy-Minnie gold deposits, Lander County, Nevada: Journal of Geochemical Exploration, v. 25, p. 99–128.

Theodore, T.G., Kotlyar, B. B., Berger, V. I., Moring, B. C., and Singer, D. A., 2000, Implications of stream–sediment geochemistry in the northern Carlin trend, Nevada, *in* Cluer, J. K., Price, J. G., Struhsacker, E. M., Hardyman, R. F., and Morris, C. L., eds., Geology and Ore Deposits 2000: The Great Basin and Beyond: Geological Society of Nevada symposium Proceedings, May 15–18, 2000, p. 929–958.

Theodore, T.G., and Menzie, W.D., 1984, Fluorine-deficient porphyry molybdenum deposits in the cordillera of western North America, *in* Janelidze, T.V., and Tvalchrelidze, A.G., eds., International Association on the Genesis of Ore Deposits Quadrennial Symposium, 6th, Tbilisi, U.S.S.R., 1982, Proceedings: Stuttgart, E. Schweizerbart'sche Verlagsbuchhandlung, v. 1, p. 463–470.

Theodore, T.G., Orris, G.J., Hammarstrom, J.M., and Bliss, J.D., 1991, Gold-bearing skarns: U.S. Geological Survey Bulletin 1930, 61 p.

Theodore, T.G., and Peters, S.G., 1998, Links between crustal shortening during Late Paleozoic Humboldt orogeny, northeast-striking faults, and Carlin-type Au deposits in Nevada [abs.]: Geological Society of America Abstracts with Programs, v. 30, p. A–76.

Theodore, T.G., and Peters, S.G., 1999, Late Paleozoic crustal shortening, northeast–striking faults, and Carlin-type Au deposits in Nevada [abs.]: Geological Society of America Program with Abstracts, Toronto, p. A–76.

Theodore, T.G., Silberman, M.L., and Blake, D.W., 1973, Geochemistry and K–Ar ages of plutonic rocks in the Battle Mountain mining district, Lander County, Nevada: U.S. Geological Survey Professional Paper 798–A, 24 p.

Thomas, T.J., 1985, Geology of the Buffalo Valley prospect, Lander County, Nevada: Reno, University of Nevada-Reno, M.S. thesis, 118 p.

Thomason, R.E., 2002, Geology and mineralization of the Florida Canyon mine, Pershing County, Nevada, *in* Wendt, C., ed., Gold deposits of the Humboldt Range: New discoveries in an old district, Geological Society of Nevada, Special Publication No. 36, p. 61-69.

Thompson, J.F.H., 1984, Acadian synorogenic mafic intrusions in the Maine Appalachians: American Journal of Science, v. 284, p. 462-483.

Thompson, J.F.H., and Naldrett, A.J., 1984, Sulfide-silicate reactions as a guide to Ni–Cu–Co mineralization in central Maine, U.S.A., *in* Buchanan, D.L., and Jones, M.J., Sulphide deposits in mafic and ultramafic rocks: Third Nickel Sulphide Field Conference, Perth, Western Australia, May 23-25, 1982: United Kingdom, The Institution of Mining and Metallurgy, p. 103–113.

Thompson, J.F.H., and Newberry, R.J., 2000, Gold deposits related to reduced granitic intrusions, *in* Hagemann, S.G., and Brown, P.E., eds., Gold in 2000: Society of Economic Geology, Reviews in Economic Geology, v. 13, p. 377–400.

Thomason, R.E., 2002, Geology and mineralization of the Florida Canyon mine, Pershing County, Nevada, *in* Wendt, C., ed., Gold deposits of the Humboldt Range: New discoveries in an old district: Geological Society of Nevada, Special Publication No. 36, p. 61-69.

Thomson, K., Brummer, J.E., Caldwell, D.A., McLachlan, C.D., and Schumacher, A.L., 1993, Geology and geochemistry of the Mule Canyon gold deposit, Lander County, Nevada: Society for Mining, Metallurgy, and Exploration, Inc., Preprint 93-271, p. 10.

Thoreson, R.F., Jones, M.E., Breit, F.J., Doyle–Kunkel, M.A., and Clarke, L.J., 2000, The geology and gold mineralization of the Twin Creeks gold deposits, Humboldt County, Nevada, *in* Crafford, A.E.J., ed., Geology and ore deposits of the Getchell region, Humboldt County, Nevada: Geological Society of Nevada Symposium 2000 Field Trip Guidebook No. 9, p. 85–111.

Thorman, C.H., and Christensen, O.D., 1991, Geologic settings of gold deposits in the Great Basin, western United States, *in* Ladiera, E.A, ed., Proceedings of the symposium Brazil Gold '91: Rotterdam, Bakema, p. 65–75.

Thurber, J.E., 1982, Petrology and Cu-Mo mineralization of the Kennedy stock, East Range, Pershing County, Nevada: Fort Collins, Colorado State University, M.S. thesis, 101 p.

Thy, P., 1983, Cumulate chemistry and its bearing on the origin of layering: evidence from the Fongen-Hyllingen Basic Complex, Norway: Tschermaks Mineralogische und Petrographishe Mitteilungen, v. 32, p. 1–24.

Tingley, J.V., 1992a, Mining Districts of Nevada: Nevada Bureau of Mines and Geology, Mackay School of Mines, Nevada Bureau of Mines and Geology Map 43, scale 1: 1,000,000.

Tingley, J.V., 1992b, Mining districts of Nevada: Nevada Bureau of Mines and Geology Report 47, 124 p.

Tingley, J.V., 1995, Metals, in The Nevada Mineral Industry—1994: Nevada Bureau of Mines and Geology, Special Publication MI–1994, p. 11–22.

Titley, S.R., 1993, Characteristics of porphyry copper occurrence in the American southwest, *in* Kirkham, R.V., Sinclair, W.D., Thorpe, R.I., and Duke, J.M., eds., Mineral deposit modeling: Geological Association of Canada Special Paper 40, p. 433–464.

Titley, S.R., and Beane, R.E., 1981, Porphyry copper deposits, Part I, Geologic settings, petrology and tectogenesis: Economic Geology, Seventy-fifth Anniversary Volume, p. 214–234.

Todd, S.G., Keith, D.W., LeRoy, L.W., Schissel, D.J., Mann, E.L., and Irvine, T.N., 1982, The J–M platinum-palladium reef of the Stillwater Complex, Montana: I. Stratigraphy and Petrology: Economic Geology, v. 77, no. 6, p. 1454–1480.

Tooker, E.W., ed., 1985, Geologic characteristics of sediment and volcanic–hosted disseminated gold deposits—search for an occurrence model: U.S. Geological Survey Bulletin 1646, 150 p.

Tosdal, R.M., and Richards, J.P., 2001, Magmatic and structural controls on the development of porphyry Cu±Mo±Au deposits, *in* Tosdal, R.M., and Richards, J.P., eds., Structural controls on ore genesis: Reviews in Economic Geology, v. 14, p. 157-181.

Tosdal, R.M., ed., 1998, Contributions to the Au Metallogeny of Northern Nevada: U.S. Geological Survey Open–File Report 98–338, 290 p., [http://geopubs.wr.usgs.gov/open-file/of98-338/].

Tretbar, D.R., Arehart, G.B., and Christensen, J.N., 2000, Dating gold deposition in a Carlin-type gold deposit using Rb/Sr methods on the mineral galkhaite: Geology, v. 28, no. 10, p. 947–950.

Tukey, J. W., 1972, Discussion of paper by F.P. Agterberg and S.C. Robinson: International Statistical Institute Bulletin, v. 44, p. 596.

Turner, R.M., Bawiec, W.J., Ambroziak, R.A., 1991, Geology of Nevada; a digital representation of the 1978 geologic map of Nevada: U.S. Geological Survey DDS-0002.

U.S. Bureau of Mines, 1942, Rambler mine, Albany County, Wyoming: War Minerals Report 17, 7 p.

U.S. Bureau of Mines, 1996, Mineral resources of the Winnemucca–Surprise resource assessment area, Churchill, Humboldt, Lyon, Pershing, and Washoe Counties, Nevada, and Lassen and Modoc Counties, California: U.S. Bureau of Mines Administrative Report for the Bureau of Land Management, [summary document of 84 p., as well as several hundred pages of unpaginated tabular material in ten attached appendices].

U.S. Bureau of Mines and U.S. Geological Survey, 1980, Principles of a resource/reserve classification for minerals: U.S. Geological Survey Circular 831, 5 p.

U.S. Geological Survey and Nevada Bureau of Mines, 1964, Mineral and water resources of Nevada: Nevada Bureau of Mines and Geology Bulletin 65 and U.S. Senate Document Number 87, 314 p.

U.S. Geological Survey Minerals Team, 1996, Data base for a national mineral–resource assessment of undiscovered deposits of gold, silver, copper, lead, and zinc in the conterminous United States: U.S. Geological Survey Open–File Report 96–96, 1 CD–ROM.

Van Houten, F.B., 1956, Reconnaissance of Cenozoic sedimentary rocks of Nevada: American Association of Petroleum Geologists Bulletin, v. 40, p. 2801–2825.

Vanko, D.A., and Bishop, F.C., 1982, Occurrence and origin of marialitic scapolite in the Humboldt Lopolith, N.W. Nevada: Contributions to Mineralogy and Petrology, v. 81, p. 277–289.

Vermaak, C.F,. and von Gruenewaldt, Gerhard, 1986, Introduction to the Bushveld Complex, *in* Anhaeusser, C.R., and Maske, S., eds., Mineral Deposits of Southern Africa, v. II: Geological Society of South Africa, Johannesburg, p. 1021–1029.

Vidal C., C.E., Injoque-Espinoza, Jorge, Sidder, G.B., and Mukasa, S.B., 1990, Amphibolitic Cu–Fe skarn deposits in the central coast of Peru: Economic Geology, v. 85, p. 1447–1461.

Vikre, P.G., 1981, Silver mineralization in the Rochester district, Pershing County, Nevada: Economic Geology, v. 76, p. 580-609.

Vikre, P.G., 1985, Precious metal vein systems in the National district, Humboldt County, Nevada: Economic Geology, v. 80, p. 360-393.

Vikre, P.G., 1994, Gold mineralization and fault evolution at the Dixie Comstock mine, Churchill County, Nevada: Economic Geology, v. 89, p. 707-719.

Vikre, P.G., 1998, Intrusion-related, polymetallic carbonate replacement deposits in the Eureka district, Eureka County, County, Nevada: Nevada Bureau of Mines and Geology, Bulletin 110, 52 p.

Vikre, P.G., and McKee, E.H., 1985, Zoning and chronology of hydrothermal events in the Humboldt Range, Pershing County, Nevada: Isochron/West, no. 44, p. 17–24.

Vikre, Peter, Thompson, T.B., Bettles, Keith, Christensen, Odin, and Parrat, Ron, eds., 1998, Carlin-type gold deposits field conference: Society of Economic Geologists Guidebook Series v. 28, 287 p.

Vila, T., and Sillitoe, R.H., 1991, Gold-rich porphyry systems in the Maricunga belt, northern Chile: Economic Geology, v. 86, p. 1238–1260.

Wallace, A.R., 1977, Geology and ore deposits, Kennedy mining district, Pershing County, Nevada: Boulder, University of Colorado, M.S. thesis, 87 p.

Wallace, A.R., 1978, Relationship between the Kennedy stock and mid-Cenozoic fault troughs [abs.]: Geological Society of America, Abstracts with Programs, v. 10, no. 3, p. 152.

Wallace, A.R., 1989, The Relief Canyon gold deposit, southern Humboldt Range, Nevada–A mineralized solution breccia: Economic Geology, v. 84, p. 279-290.

Wallace, A.R., 1991, Effect of late Miocene extension on the exposure of gold deposits in north-central Nevada, *in* Raines, G.L., Lisle, R.E., Schafer, R.W., and Wilkinson, W.H., eds., Geology and ore deposits of the Great Basin: Geological Society of Nevada, Symposium Proceedings, p. 179-183.

Wallace, A.R., 1993, Geologic map of the Snowstorm Mountains and vicinity, Elko and Humboldt Counties, Nevada: U.S. Geological Survey Miscellaneous Investigations Series Map I-2394, scale 1:50,000.

Wallace, A.R., 2003, Geology of the Ivanhoe Hg-Au district, northern Nevada: Influence of Miocene volcanism, lakes, and active faulting on epithermal mineralization: Economic Geology, v. 98, p. 409-424.

Wallace, A.R., and McKee, E.H., 1994, Implications of Eocene through Miocene ages for volcanic rocks, Snowstorm Mountains and vicinity, northern Nevada: U.S. Geological Survey Bulletin 2081, p. 13-18.

Wallace, R.E., Silberling, N.J., Irwin, W.P., and Tatlock, D.B., 1969a, Geologic map of the Buffalo Mountain quadrangle, Pershing and Churchill Counties, Nevada: U.S. Geological Survey Geologic Quadrangle Map GQ-821, scale 1:62,500.

Wallace, R.E., Tatlock, D.B., Silberling, N.J., and Irwin, W.P., 1969b, Geologic map of the Unionville quadrangle, Pershing County, Nevada: U.S. Geological Survey Geologic Quadrangle Map GQ-820, scale 1:62,500.

Watkinson, D.H., Whittaker, P.J., and Jones, P.J., 1983, Platinum-group elements in the eastern gabbro, Coldwell Complex, northwestern Ontario: Ontario Geological Survey Miscellaneous Paper 113, p. 183–191.

Webring, M.W., 1981, MINC—A gridding program based on minimum curvature: U.S. Geological Survey Open File Report 81-1224, 43 p.

Wendt, C.J., and Albino, G.V., 1992, Porphyry copper and related occurrences in Nevada: Nevada Bureau of Mines and Geology Map 100, 1 sheet.

Westra, Gerhard, and Keith, S.B., 1981, Classification and genesis of stockwork molybdenum deposits: Economic Geology, v. 76, no. 4, p. 844–973.

White, W.H., Bookstrom, A.A., Kamilli, R.J., Ganster, M.W., Smith, R.P., Ranta, D.E., and Steininger, R.C., 1981, Character and origin of Climax-type molybdenum deposits, *in* Skinner, B.J., ed., Economic Geology, Seventy-fifth Anniversary Volume, 1905–1980: New Haven, Connecticut, Economic Geology Publishing Co., p. 270–316.

Whitebread, D. B., and Sorensen, M. L., 1980, Preliminary geologic map of the Granite Mountain quadrangle, and SE/4 of Kyle Hot Springs quadrangle, Pershing County, Nevada: U.S. Geological Survey Open-File Report 80–715.

Whitebread, D.H., 1976, Alteration and geochemistry of Tertiary volcanic rocks in parts of the Virginia City quadrangle, Nevada: U.S. Geological Survey Professional Paper 936, 43 p.

Willden, R., 1964, Geology and mineral deposits of Humboldt County, Nevada: Nevada Bureau of Mines and Geology Bulletin 59, 154 p.

Willden, R., and Hotz, P.E., 1955, A gold-scheelite-cinnabar placer in Humboldt County, Nevada: Economic Geology, v. 50, p. 661–668.

Willden, R., and Speed, R.C., 1974, Geology and mineral deposits of Churchill County, Nevada: Nevada Bureau of Mines and Geology Bulletin 83, 95 p.

Wilson, J.R., and Larsen, S.B., 1985, Two-dimensional study of a layered intrusion—the Hyllingen Series, Norway: Geological Magazine, v. 122, p. 97–124.

Woitsekhowskaya, M., and Peters, S.G., 1998, Geochemical modeling of alteration and Au deposition in the Betze deposit, *in* Tosdal, R.M., ed., Contributions to the gold metallogeny of Northern Nevada: U.S. Geological Survey Open–File Report 98–338, p. 211–222, [http://geopubs.wr.usgs.gov/open-file/of98-338/].

Wong, George, 1982, Preliminary map of mineralized areas in the Basin and Range of Nevada: U.S. Geological Survey Open–File Report 82–1100, 22 p.

Wood, J.D., 1991, Geology of the Wind Mountain gold deposit, Washoe Co., Nevada, *in* Raines, G.L., Lisle, R.E., Schafer, R.W., and Wilkinson, W.H., eds., Geology and ore deposits of the Great Basin, Symposium Proceedings: Geological Society of Nevada, p. 1051-1061.

Wood, J.D., and Hamilton, S.K., 1991, The Sleeper gold-silver deposit: discovery through feasibility, *in* Hutchinson, R.W., and Grauch, R.I., eds., Mineral deposits--case histories and historical perspectives of genetic concepts: Society of Economic Geologists Monograph 8, p. 289-299.

Wooden, J.L., Kistler, R.W., and Tosdal, R.M., 1998, Pb isotopic mapping of crustal structure in the northern Great Basin and relationships to Au deposit trends, *in* Tosdal, R.M., ed., Contributions to the gold metallogeny of northern Nevada: U.S. Geological Survey Open-File Report 98-338, p. 20-33.

Wotruba, P.R., Benson, R.G., and Schmidt, K.W., 1988, Geology of the Fortitude gold-silver skarn deposit, Copper Canyon, Lander County, Nevada, *in* Schafer, R.W., Cooper, J.J., and Vikre, P.G., eds., Bulk mineable precious metal deposits of the western United States: Reno, Nevada, Geological Society of Nevada, Symposium Proceedings, p. 159–171.

Wright, D.F., 1996, Evaluating volcanic hosted massive sulphide favourability using GIS-based spatial data integration models, Snow Lake area, Manitoba: Ottawa, University of Ottawa, Ph.D. dissertation, 344 p.

Wright, D.F., and Bonham-Carter, G.F., 1996, VHMS favourability mapping with GIS-based integration models, Chisel Lake-Anderson Lake area, *in* Bonham-Carter, G.F., Galley, A. G., and Hall, G. E. M., eds., EXTECH I: A Multidisciplinary Approach to Massive Sulphide Research in the Rusty Lake-Snow Lake Greenstone Belts, Manitoba: Geological Survey of Canada Bulletin 426, p. 339–376, 387–401.

Wyld, S.J., 2000, Triassic evolution of the arc and backarc of northwestern Nevada, and evidence for extensional tectonism, *in* Sorgehan, M.J., and Gehrels, G.E., eds., Paleozoic and Triassic paleogeography and tectonics of western Nevada and northern California: Geological Society of Nevada Special Paper 347, p. 185-207.

Zharikov, V.A., 1970, Skarns: International Geology Review, v. 12, p. 541–559, 619–647, 760–775.

Zientek, M.L., 1993, Mineral resource appraisal for locatable minerals: the Stillwater Complex, *in* Hammarstrom, J.M., Zientek, M.L., and Elliott, J.E., eds., Mineral resource assessment of the Absaroka-Beartooth study area, Custer and Gallatin National Forests, Montana: U.S. Geological Survey Open-File Report 93–207, p. F1–F83.

Zientek, M.L., Likhachev, A.P., Kunilov, V.E., Barnes, S.-J., Meier, A.J., Carlson, R.R., Briggs, P.H., Fries, T.L., and Adrian, B.M., 1994, Cumulus processes and the composition of magmatic ore deposits: examples from the Talnakh district, Russia, *in* Lightfoot, P.C. and Naldrett, A.J., eds., Proceedings of the Sudbury-Noril'sk Symposium: Ontario Geological Special Volume 5, p. 373–392.

Zoback, M.L., 1978, Mid-Miocene rifting in north-central Nevada: A detailed study of Late Cenozoic deformation in the northern Basin and Range: Stanford, Calif., Stanford University, Ph.D. dissertation, 247 p.

Zoback, M.L., McKee, E.H., Blakely, R.J., and Thompson, G.A., 1994, The northern Nevada rift: Regional tectonomagmatic relations and middle Miocene stress direction: Geological Society of America Bulletin, v. 106, p. 371-382.